

DESIGN AND OPTIMIZATION OF IC ENGINE'S EXHAUST VALVE

T.Vasanthadevi¹

¹M.Tech (Thermal Engineering)Department of mechanical engineering vaagdevi college of engineering (ugc autonomous) approved by AICTE & permanent affiliation to jntuh, hyderabad.p.o, bollikunta, Warangal urban- 506005.

Dr.sanjeev kumar Sajjan²

²Assistant Professor Department of mechanical engineering vaagdevi college of engineering (UGC autonomous) approved by AICTE & permanent affiliation to jntuh, hyderabad. p.o, bollikunta, Warangal urban- 506005.

ABSTRACT: Exhaust valve is termed as essential component of an IC engine as it provides path to expel out the exhaust gases generated after combustion of the fuel in the combustion chamber. If there is improper design of exhaust valve then it indirectly affects its reliability i.e.

An Exhaust valves are subjected to the axial stresses due to exhaust gas pressure, cyclic stresses due to return spring load, thermal stresses due to very high temperature inside the combustion chamber and inertia force arising on the account of valve assembly. The result of which maximum stress concentration is at the junction of fillet and valve stem of exhaust valve.

In this project, IC engine's exhaust valve is designed by selecting suitable fillet radius to reduce the stress and temperatures further best alternative material is recommended through finite element analysis in order to increase the working life of exhaust valve

1.INTRODUCTION TO IC ENGINE VALVE

Valves Train Components for Internal Combustion Engines, which include

1. Inlet and Exhaust Valves
2. Valve Guides
3. Tappets
4. Camshafts

What does an engine do?

- It generates the power required for moving the vehicle or any other specific purpose.
- It converts the energy contained in fuel to useful mechanical energy, by burning the fuel inside a combustion chamber.
- An engine contains number of parts like Valves and other Valve train components, Piston, camshaft, Connecting rod, Cylinder block, Cylinder head etc., from which REVL supplying some of the valve train components to engine manufacturers

Types of Engines

From the basic concept there are 2 major types of engine which are subdivided further based on their working principle.

1. Internal Combustion Engines (IC Engines)
 - a) 2 Stroke Engines
 - b) 4 Stroke Engines
2. External combustion Engines (EC Engines)
 - a) Steam engines (Eg. Locomotives)
 - b) Turbine engines (Eg. Aircraft)

Types of Engines

Based on the Fuel Used, IC Engines can be classified as follows

1. Diesel Engines (CI Engines)
 - a) DI / IDI / CRDI
 - b) NA / Turbo Charged
2. Petrol Engines (SI Engines)
 - a) Carburetor Engines
 - b) SPFI / MPFI Engines
3. Gas Engines
 - a) LPG
 - b) CNG

Types of Engines

Based on the Application, IC Engines can be classified as follows

1. Automotive Engines
 - a) On road Vehicles
 - b) Off road Vehicles
 - c) Marine Applications
 - d) Racing Vehicles
2. Stationary Engines
 - a) Generators
 - b) Power Plants

Types of Engines

Automotive Applications can be further subdivided as follows

1. On road Vehicles
 - a) 2 Wheelers
 - b) Passenger cars
 - c) Multi Utility Vehicles
 - b) Light Commercial Vehicles
 - d) Heavy Commercial Vehicles

- 2. Off road Vehicles
 - a) Tractors & Farm Equipments
 - b) Earth Moving Equipments

What is a Valve Train?

- It is the set of components in a 4-stroke engine, responsible for smooth functioning of the inlet and exhaust valve
- It makes the valve to open and close as per the timing required for the correct functioning of the engine
- The performance of the engine is severely depends proper functioning of valve train. Any malfunctioning in the valve train system could even lead to severe damage to the engine

Typical Valve Train Assembly

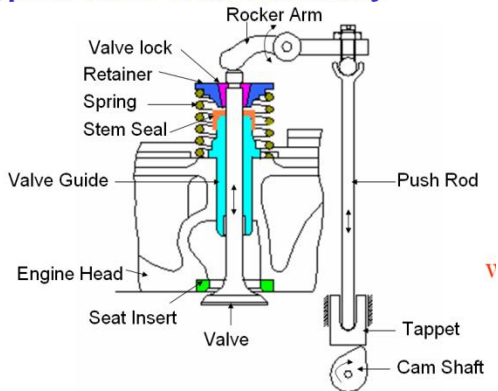


Figure.1.2

About Valves:

Engine Valve is one of the main parts which are used in all IC Engines. Each cylinder in the engine has one inlet and one exhaust valve. Now a days engine are designed with multi valves viz., two inlet and one exhaust or Two inlet and Two exhaust valves which prevents air pollution and improves engine efficiency.

Function of Inlet Valve: The inlet which operates by the action of Tappet movement, allows air and fuel mixture into the cylinder.

Function of Exhaust valve: The exhaust valve allows burnt gases to escape from the cylinder to atmosphere.

Valve Efficiency: Depends on the following characteristics like Hardness, Face roundness and sliding properties capable to withstand high temperature etc. As compared to inlet, exhaust valve operates at high temperature as exhaust gases (around 800 Deg C) escape through it. As it resulting in early ways and gets corrosion, austenitic steel is used for manufacture of exhaust valve and martensitic steel is

used for manufacture of inlet valve. The manufacturing process involves upset and forging, heat treatment and machining (turning and grinding) and special processes like TIG welding, Projection Welding, PTA Welding, Friction Welding, Induction Hardening and Nitriding.

VALVE DIMENSIONS:

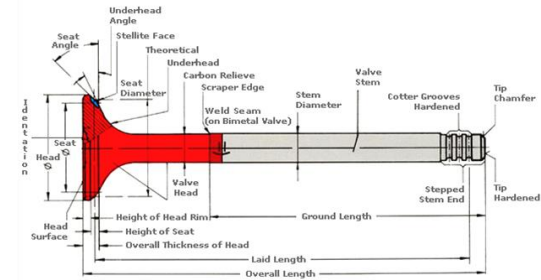


Figure.1.3

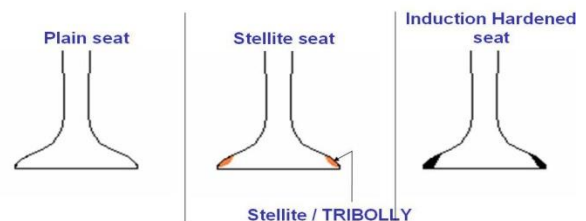
Working Requirements for Valves

1. Inlet Valve
 - a) Allow incoming charge into the engine
 - b) Seal the port with out leak for remaining period
 - c) Resistance to wear at the mating surfaces
 - d) Good sliding surface for seizure resistance
2. Exhaust Valve
 - a) Allow gases go out of the engine
 - b) Seal the port with out leak for remaining period
 - c) Strength to with stand high temperatures
 - d) Resistance to wear at the mating surfaces
 - e) Good sliding surface for seizure resistance

Important Features on the valve



Seat Features on Valves



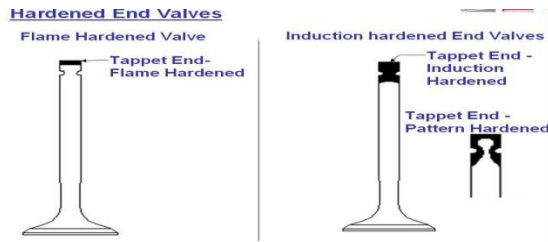
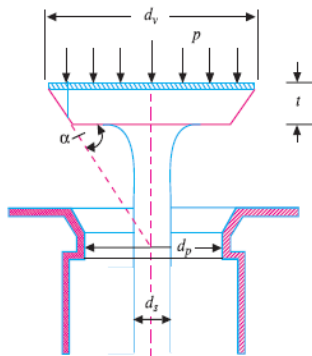


Figure.1.7

DESIGN CALCULATIONS OF EXHAUST VALVE



DESIGN OF OUTLET VALVE

a. Size of valve port

$$a_p v_p = aV$$

$$V = 90\text{m/s} = 90000\text{mm/s}$$

$$a_p = \frac{3802.66 \times 10933.33}{90000} = 462\text{mm}$$

$$a_p = \frac{\pi}{4} (d_p)^2$$

$$(d_p)^2 = \frac{462 \times 4}{\pi} = 588.53 \quad \Rightarrow \quad d_p = 24.25\text{mm}$$

b. Thickness of valve disc

$$t = K d_p \sqrt{\frac{p}{\sigma_b}}$$

$$t = 0.42 \times 24.25 \sqrt{\frac{10.936}{100}} =$$

$$3.36\text{mm}$$

c. Maximum lift of the valve

$$h = \text{lift of the valve}$$

$$h = \frac{d_p}{4 \cos \alpha} = \frac{24.25}{4 \cos 30^\circ} = \frac{24.25}{3.46} = 7\text{mm}$$

d. Valve steam diameter

$$d_s = \frac{24.25}{8} + 6.35 \quad \text{or}$$

$$d_s = 3.03 + 6.35$$

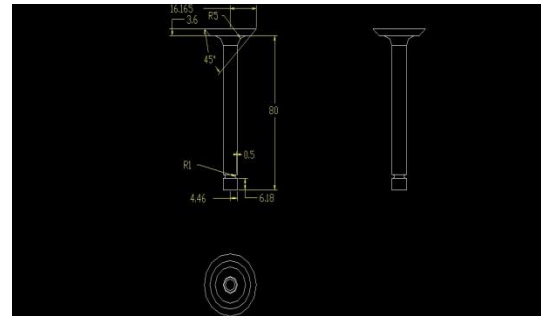
$$d_s = 9.38 \quad (\text{or}) \quad 1403\text{mm}$$

$$\tan \alpha = \frac{2(h + t)}{\left(\frac{d_v}{2}\right)} = \frac{2(h + t)}{d_v}$$

$$\tan 30 = \frac{2(3.36 + 7)}{d_v}$$

$$d_v = \frac{20.72}{0.577} = 35.9\text{mm} = 36\text{mm}$$

2D DRAWING



2. LITERATURE REVIEW

Sanoj. T et al. [1] proposed the Thermo Mechanical Analysis of Engine Valve. In this thermal and structural analysis of valve with different materials (Nimonic 80A and Nimonic 105A) were used for valve analysis. The different works are performed on the exhaust valve for different parameters in recent years.

Lucjan Witek [2] work on "Failure and thermo-mechanical stress analysis of the exhaust valve of diesel engine" In this work the failure analysis of the exhaust valve of diesel engine was performed. In order to explain the reason of premature valve damage, the non-linear finite element analysis was utilized. The results of stress analysis performed for the valve with the carbon deposit showed, that in the valve stem a high bending stresses were occurred.

Kum-Chul, et al. [3] presented "A Study of Durability Analysis Methodology for Engine Valve Considering Head Thermal Deformation and

Dynamic Behavior the authors describe the problem of exhaust valve fracture of gasoline engines. From the results, it was found that the maximum stress occurred at the stem region and that stem region is the same region at which higher temperature occurred. The stress at the valve head is similar to the stress under the combustion pressure condition, but the stress on the valve neck goes up to high level where the failure occurred.

Yuvraj K Lavhale et al. [4] had studied the overview of failure trends of inlet and exhaust valve. There are different causes for the failure of the exhaust valve such as fatigue failure, wear, thermal.

GAP IN LITERATURE REVIEW

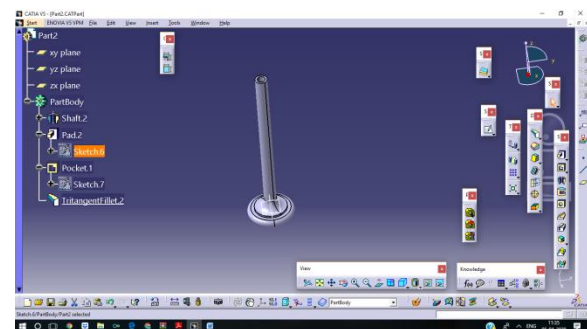
From the literature review it is seen that most of the studies on exhaust valve design had focused on fatigue behavior, wear behavior, deformation mechanisms in metallic materials. However, very less research is done in design of exhaust valve based on optimization of its any parameter.

Therefore this study is conducted to design the exhaust valve by optimizing the fillet radius and to recommend the best alternative material for valve through analytical validation in order to increase the working life of exhaust valve.

METHODOLOGY

- 1) Study the basics of valve and different modes of failure in exhaust valve
- 2) Design the valve as per the specification and model it in CATIA and analyze it in ANSYS software.
- 3) Study the different valve materials and recommend the best alternative material for valve with stress and weight as a selection criterion
- 4) Conduct the static and thermal analysis to find stress and temperatures with help of ANSYS software.

3D MODEL OF EXHAUST VALVE



INTRODUCTION TO FEA

Finite element analysis is a method of solving, usually approximately, certain problems in engineering and science. It is used mainly for problems for which no exact solution, expressible in some mathematical form, is available. As such, it is a numerical rather than an analytical method. Methods of this type are needed because analytical methods cannot cope with the real, complicated problems that are met with in engineering.

INTRODUCTION TO ANSYS

ANSYS is general-purpose finite element analysis (FEA) software package. Finite Element Analysis is a numerical method of deconstructing a complex system into very small pieces (of user-designated size) called elements. The software implements equations that govern the behaviour of these elements and solves them all; creating a comprehensive explanation of how the system acts as a whole.

CALCULATIONS TO DETERMINE PROPERTIES OF FLUID BY CHANGING VOLUME FRACTIONS

Volume fraction=0.2, 0.4, 0.6 & 0.8

MATERIAL PROPERTIES

Methane

Density = 3880 kg/m³

Thermal conductivity =40 W/m-k

Specific heat = 910J/kg-k

Viscosity =

Ethane

Density = 4930 kg/m³

Thermal conductivity =330 W/m-k

Specific heat = 711 J/kg-k

Viscosity =

NOMENCLATURE

ρ_{nf} = Density of nano fluid (kg/m³)

ρ_s = Density of solid material (kg/m³)

ρ_w = Density of fluid material (water) (kg/m³)

ϕ = Volume fraction

C_{pw} = Specific heat of fluid material (water) (j/kg-k)

C_{ps} = Specific heat of solid material (j/kg-k)

μ_w = Viscosity of fluid (water) (kg/m-s)

μ_{nf} = Viscosity of Nano fluid

(kg/m-s)

K_w = Thermal conductivity of fluid material (water)

(W/m-k)

K_s = Thermal conductivity of solid material

(W/m-k)

NANO FLUID CALCULATIONS

ALUMINUM OXIDE

DENSITY OF NANO FLUID

$$\rho_{nf} = \phi \times \rho_s + [(1-\phi) \times \rho_w]$$

SPECIFIC HEAT OF NANO FLUID

$$C_{p\text{ nf}} = \frac{\phi \times \rho_s \times C_{ps} + (1 - \phi) (\rho_w \times C_{pw})}{\phi \times \rho_s + (1 - \phi) \times \rho_w}$$

VISCOSITY OF NANO FLUID

$$\mu_{\text{nf}} = \mu_w (1 + 2.5\phi)$$

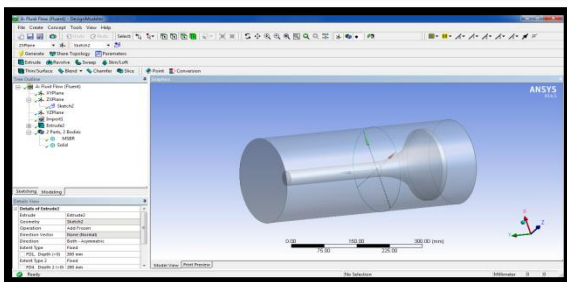
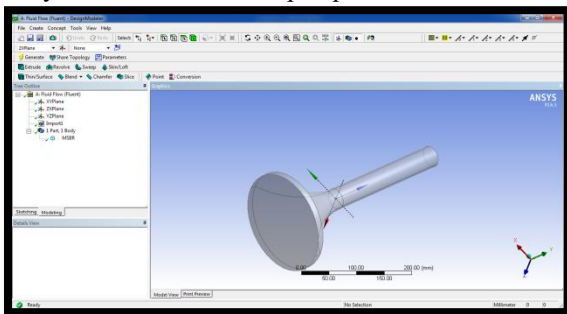
THERMAL CONDUCTIVITY OF NANO FLUID

$$K_{\text{nf}} = \frac{K_2 + 2K_1 - 2\phi(K_1 - K_2)}{K_2 + 2K_1 + (K_1 - K_2)2k_2} \times k_1$$

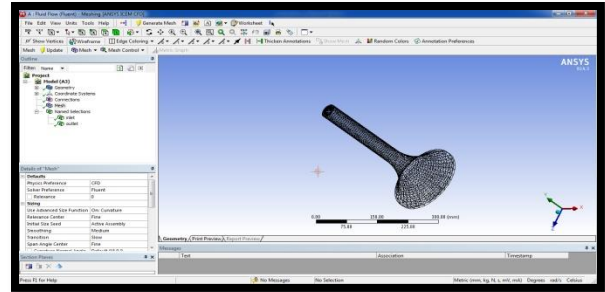
Volume fraction	Density(ρ)	Specific heat (Cp)	Thermal conductivity (w/m-k)	Viscosity (kg/m-s)
0.2	0.9276	1674.76	0.01901	0.000111
0.4	1.1982	1655.9904	0.02073	0.000148
0.6	1.4688	1644.134	0.022456	0.000185
0.8	1.7394	1635.96792	0.024177	0.000222

CFD ANALYSIS OF VALVE

→→Ansys → workbench→ select analysis system
 → fluid flow fluent → double click
 →→Select geometry → right click → import geometry → select browse →open part → ok



→→ select mesh on work bench → right click →edit
 → select mesh on left side part tree → right click → generate mesh →



Select faces → right click → create named section → enter name → water inlet
 Select faces → right click → create named section → enter name → water outlet

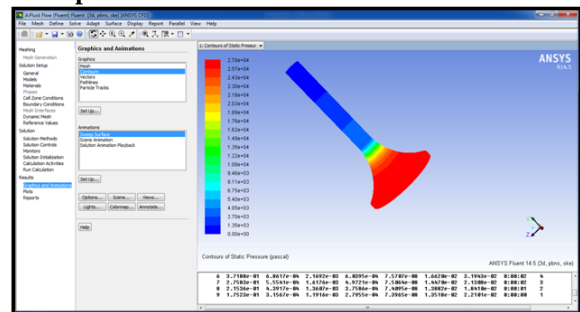
Model → energy equation → on.
 Viscous → edit → k- epsilon
 Enhanced Wall Treatment → ok
 Materials → new → create or edit → specify fluid material or specify properties → ok
 Select gasoline
 Boundary conditions → select fluid inlet → Edit → Enter velocity → 10m/s and Inlet Temperature –
 Solution → Solution Initialization → Hybrid Initialization →done

Run calculations → no of iterations = 50 → calculate → calculation complete

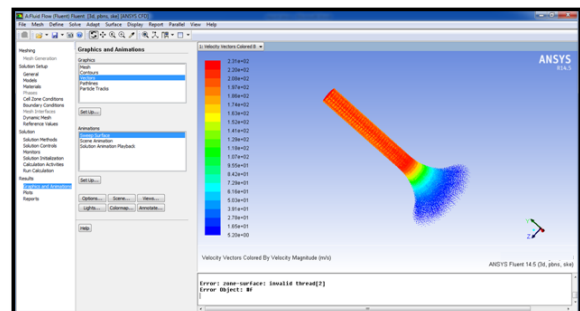
→→ **Results** → **graphics and animations** → **contours** → **setup**
Velocity = 10m/s

Volume fraction =0.2

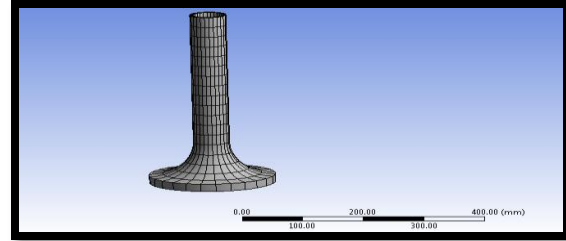
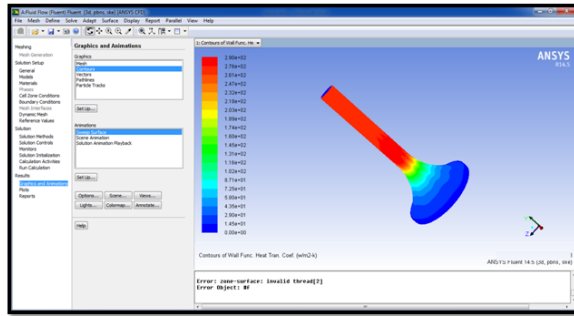
Static pressure



Velocity



Heat transfer coefficient

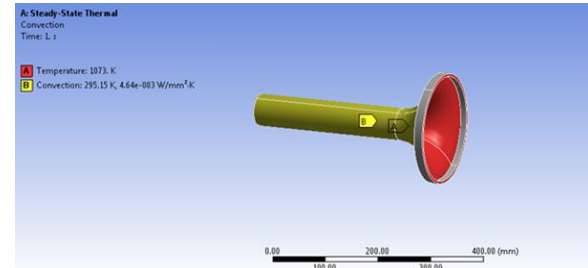


Finite element analysis or FEA representing a real project as a “mesh” a series of small, regularly shaped tetrahedron connected elements, as shown in the above fig. And then setting up and solving huge arrays of simultaneous equations. The finer the mesh, the more accurate the results but more computing power is required.

Mass flow rate

Mass Flow Rate	(kg/s)
inlet	0.24605182
interior-__msbr	15.007729
outlet	-0.24598695
wall-__msbr	0
Net	6.4864755e-05

BOUNDARY CONDITIONS



Heat transfer rate

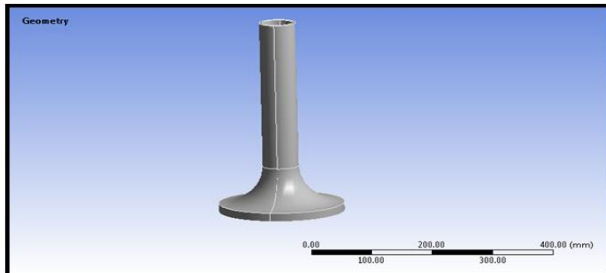
Total Heat Transfer Rate	(w)
inlet	319298.41
outlet	-319214.34
wall-__msbr	0
Net	84.0625

T = 1073K
 Select steady state thermal >right click>insert>select convection> enter film coefficient value Select steady state thermal >right click>insert>select heat flux
 Select steady state thermal >right click>solve Solution>right click on solution>insert>select temperature

THERMAL ANALYSIS OF HOLLOW EXHAUST VALVE MATERIAL-STAINLESS STEEL

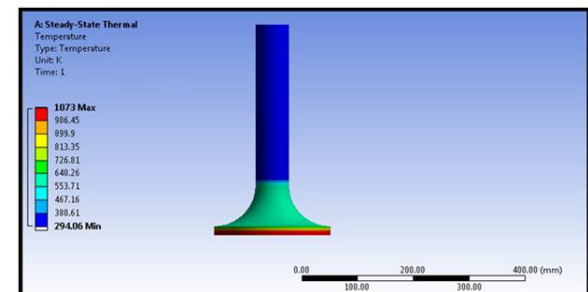
Open work bench 14.5>select **steady state thermal** in analysis systems>select geometry>right click on the geometry>import geometry>select **IGES** file>open

IMPORTED MODEL

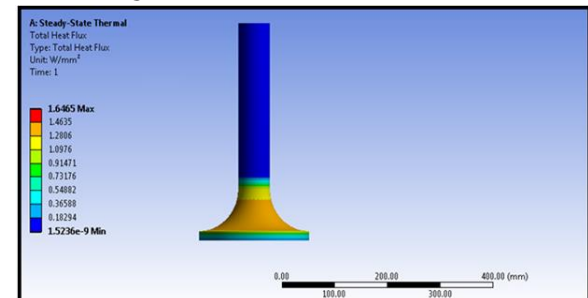


MESHED MODEL

TEMPERATURE



HEAT FLUX



RESULT TABLES

CFD RESULTS

Volume fraction	Pressure(Pa)	Heat transfer coefficient(w/m ² -k)	Mass flow rate(kg/s)	Heat transfer rate(W)
0.2	2.70e+04	2.90e+02	0.000064864	84.0625
0.4	3.48e+04	3.26e+02	0.000047415	60.375
0.6	4.26e+04	3.62e+02	0.000080376	101.9375
0.8	5.07e+04	3.97e+02	0.0000542104	68.8125

THERMAL RESULTS

Material	Temperature		Heat flux(w/mm ²)
	Min	Max	
Stainless steel	294.06	1073	1.6465
Aluminum alloy	295.15	1073	6.9237

THEORETICAL CALCULATIONS

Volume fraction (Φ) = 0.2

$$Re = \frac{\rho \times v \times L}{\mu} = \frac{0.9276 \times 10 \times 0.107}{0.000111} = 8941.72$$

$$Pr = \frac{cp \times \mu}{kw} = \frac{1674.76 \times 0.000111}{0.01901} = 9.778$$

$$Nu = 0.024 \times (Re)^{0.8} \times (Pr)^{0.4} = 0.024 \times (8941.72)^{0.8} \times (9.778)^{0.4} = 86.586$$

$$hfc = \frac{Kw \times Nu}{DH} = \frac{0.01901 \times 86.586}{0.05} = 32.919 \text{ w/m}^2\text{-k}$$

Volume fraction (Φ) = 0.4

$$Re = \frac{\rho \times v \times L}{\mu} = \frac{1.1982 \times 10 \times 0.107}{0.000148} = 8662.66$$

$$Pr = \frac{cp \times \mu}{kw} = \frac{1655.9904 \times 0.000148}{0.02073} = 11.822$$

$$Nu = 0.024 \times (Re)^{0.8} \times (Pr)^{0.4}$$

$$= 0.024 \times (8662.66)^{0.8} \times (11.822)^{0.4} = 91.0769$$

$$hfc = \frac{Kw \times Nu}{DH} = \frac{0.02073 \times 91.0769}{0.05} = 37.760 \text{ w/m}^2\text{-k}$$

Volume fraction (Φ) = 0.6

$$Re = \frac{\rho \times v \times L}{\mu} = \frac{1.4688 \times 10 \times 0.107}{0.000185} = 8495.22$$

$$Pr = \frac{cp \times \mu}{kw} = \frac{1644.134 \times 0.000185}{0.022456} = 13.544$$

$$Nu = 0.024 \times (Re)^{0.8} \times (Pr)^{0.4}$$

$$= 0.024 \times (8495.22)^{0.8} \times (13.544)^{0.4} = 94.6781$$

$$hfc = \frac{Kw \times Nu}{DH} = \frac{0.022456 \times 94.6781}{0.05} = 42.521 \text{ w/m}^2\text{-k}$$

Volume fraction (Φ) = 0.8

$$Re = \frac{\rho \times v \times L}{\mu} = \frac{1.7394 \times 10 \times 0.107}{0.000222} = 8383.59$$

$$Pr = \frac{cp \times \mu}{kw} = \frac{1635.96792 \times 0.000222}{0.024177} = 15.0219$$

$$Nu = 0.024 \times (Re)^{0.8} \times (Pr)^{0.4}$$

$$= 0.024 \times (8383.59)^{0.8} \times (15.021)^{0.4} = 97.6415$$

$$hfc = \frac{Kw \times Nu}{DH} = \frac{0.024177 \times 97.6415}{0.05} = 47.2135 \text{ w/m}^2\text{-k}$$

COMPARISON OF ANALYTICAL AND THEORETICAL

Analytical	Theoretical
Heat transfer coefficient(w/m^2-k)	Heat transfer coefficient(w/m^2-k)
2.90e+02	3.2e+02
3.26e+02	3.7e+02
3.62e+02	4.2e+02
3.97e+02	4.7e+02

CONCLUSION

In this thesis, methane fluid is mixed with ethane are calculated for their combination properties. The volume fraction 0.2, 0.4, 0.6 & 0.8. Theoretical calculations are done determine the properties for fluids and those properties are used as inputs for analysis.

In this thesis, a finite-element method is used for modeling the thermal analysis of an exhaust valve. The temperature distribution and resultant thermal stresses are evaluated. Detailed analyses are performed to estimate the boundary conditions of an internal combustion engine. In this thesis, CREO parametric is employed for modeling and ANSYS is used for analysis of the exhaust valve.

By observing the CFD analysis results the pressure and heat transfer coefficient values are increases by increasing the volume fraction and mass flow rate and heat transfer rate values are more at volume fraction 0.6. So it can be concluded the methane and ethane mixture volume fraction at 0.6 is better fluid.

By observing the thermal analysis results the more heat flux value for aluminum alloy.the extra warmness flux price for aluminum alloy.

REFERENCES

A.M.I. Bin Mamat et al. (28/08/2015) Waste heat recovery using a novel high performance low pressure turbine for electric turbocompounding in downsized gasoline engines: Experimental and computational analysis, Energy 90 218-234

F.Bengolea, S. Samuel (04/05/2016) Technology Choices for Optimizing the Performance of Racing Vehicles, Oxford Brookes University, SAE Technical Paper 2016-01-1173

S. Ziegler (04/06/2016) Aufrecht: "Ab der DTM-Saison 2018 fahren wir in Amerika", motorsport-total.com, O.P. Taylor, R. Pearson, R. Stone (04/05/2016) Reduction of CO2 Emissions through Lubricant Thermal Management During the Warm

Up of Passenger Car Engines, SAE Technical Paper 2016-01-0892

M. Trzesniowski (2014) Rennwagentechnik, Springer FachmedienWiesbaden, ISBN 978- 3-658-04919-5

I. Bamsez (2013) Cosworth's 20,000 RPM V8, Race Engine Technology, High Power Media, ISBN 977-1-740-6800050-5

D. Turner (1984) Ford Popular and the Small Sidevalves, Osprey Publishing Ltd, ISBN 1- 90308-804-6

B. Ballard (2002) "English & Australian Small Fords", Ellery Publications., ISBN 1 876 720 07 7

Chevrolet LS7 (2016) LS7 EFI Crate Engines Specifications REV 16OC14, PART NO. 19329268 P.J. Ajay,

K.A. Vikas (2014) "Evaluation and Comparative Study of ValveTrain Layouts with Different Rocker Ratio", SAE International, 2014-01-2877

K. Sakurahara (2009) Technical Review 2009, Honda F1, "Summary of Honda Formula One Engine in Third-Era Activities" ISSN 0915-3918

M. Hoshi (2009) Technical Review 2009, Honda F1, "Development of Materials during Third Formula One Era" ISSN 0915-3918

S. Hayakawa, K. Ogiyama, M. Tate (2009) , Honda F1, "Development of Vavletrain for Formula One Engine" ISSN 0915-3918

K. Kondo et al. (2009) Technical Review 2009, Honda F1, "Explanation of Honda's Third Era Formula One Engine Development" ISSN 0915-3918

DETERMINING PERFORMANCE OF GAS TURBINE BLADE WITH DIFFERENT COOLING SYSTEMS

MOGULLA SAMPATH¹

Y. UMASHANKAR²

¹M.Tech (Thermal Engineering)Department of mechanical engineering vaagdevi college of engineering (ugc autonomous) approved by AICTE & permanent affiliation to jntuh, hyderabad.p.o, bollikunta, Warangal urban-506005.

²Assistant Professor Department of mechanical engineering vaagdevi college of engineering (UGC autonomous) approved by AICTE & permanent affiliation to jntuh, hyderabad. p.o, bollikunta, Warangal urban- 506005.

ABSTRACT

A turbine blade is the individual component which makes up the turbine section of a gas turbine. The blades are responsible for extracting energy from the high temperature, high pressure gas produced by the combustor. In this paper, a turbine blade is designed and modeled in 3D modeling software Pro/Engineer. The design is modified by changing the base of the blade to increase the cooling efficiency. Since the design of turbo machinery is complex, and efficiency is directly related to material performance, material selection is of prime importance. In this project, two materials are considered for turbine blade chromium steel and stainless steel 316L. Optimization is done by varying the materials chromium steel and stainless steel 316L by performing coupled field analysis (thermal and structural) on the turbine blade for the designs (without holes, internal cooling, external cooling and internal-external cooling) .

key words:CFD,thermal and strctural.

1. INTRODUCTION

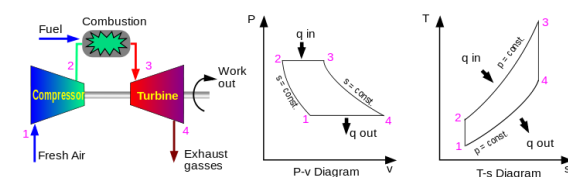
A gas turbine, also called a combustion turbine, is a type of internal combustion engine. It has an upstream rotating compressor coupled to a

downstream turbine, and a combustion chamber or area, called a combustor, in between.

The basic operation of the gas turbine is similar to that of the steam power plant except that air is used instead of water. Fresh atmospheric air flows through a compressor that brings it to higher pressure. Energy is then added by spraying fuel into the air and igniting it so the combustion generates a high-temperature flow. This high-temperature high-pressure gas enters a turbine, where it expands down to the exhaust pressure, producing a shaft work output in the process. The turbine shaft work is used to drive the compressor and other devices such as an electric generator that may be coupled to the shaft. The energy that is not used for shaft work comes out in the exhaust gases, so these have either a high temperature or a high velocity. The purpose of the gas turbine determines the design so that the most desirable energy form is maximized. Gas turbines are used to power aircraft, trains, ships, electrical generators, and tanks.

Theory of operation

In an ideal gas turbine, gases undergo four thermodynamic processes: an isentropic compression, isobaric (constant pressure) combustion, an isentropic expansion and heat rejection. Together, these make up the Brayton cycle.



2. LITERATURE REVIEW

The objective of this project is to design and stresses analyze a turbine blade of a jet engine. An investigation for the usage of new

materials is required. In the present work turbine blade was designed with two different materials named as Inconel 718 and Titanium T-6. An attempt has been made to investigate the effect of temperature and induced stresses on the turbine blade. A thermal analysis has been carried out to investigate the direction of the temperature flow which is been develops due to the thermal loading. A structural analysis has been carried out to investigate the stresses, shear stress and displacements of the turbine blade which is been develop due to the coupling effect of thermal and centrifugal loads. An attempt is also made to suggest the best material for a turbine blade by comparing the results obtained for two different materials (Inconel 718 and titanium T6). Based on the plots and results Inconel718 can be consider as the best material which is economical, as well as it has good material properties at higher temperature as compare to that of TitaniumT6.

3. INTRODUCTION TO CAD/CAE:

Computer-aided design (CAD), also known as **computer-aided design and drafting (CADD)**, is the use of computer technology for the process of design and design-documentation.

3.1. INTRODUCTION TO PRO-ENGINEER

Pro/ENGINEER Wildfire is the standard in 3D product design, featuring industry-leading productivity tools that promote best practices in design while ensuring compliance with your industry and company standards. Integrated Pro/ENGINEER CAD/CAM/CAE solutions allow you to design faster than ever, while maximizing innovation and quality to ultimately create exceptional products.

Different modules in pro/engineer

Part design, Assembly, Drawing& Sheet metal.

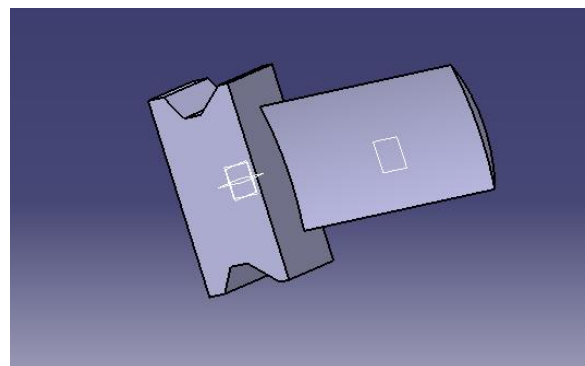
3.2. INTRODUCTION TO FINITE ELEMENT METHOD:

Finite Element Method (FEM) is also called as Finite Element Analysis (FEA). Finite Element Method is a basic analysis technique for resolving and substituting complicated problems by simpler ones, obtaining approximate solutions Finite element method being a flexible tool is used in various industries to solve several practical engineering problems. In finite element method it is feasible to generate the relative results.

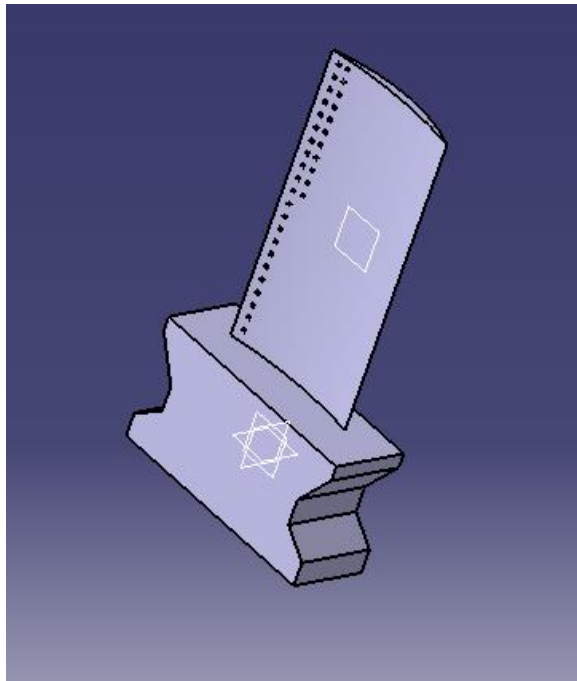
4. RESULTS AND DISCUSSIONS:

4.1. Models of pro-e wildfire 5.0:

Gas turbine blade 3D model (without holes)

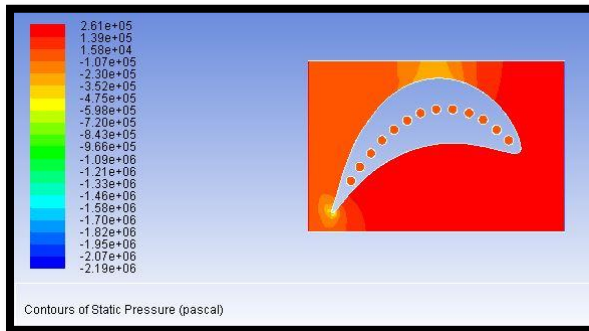


with holes

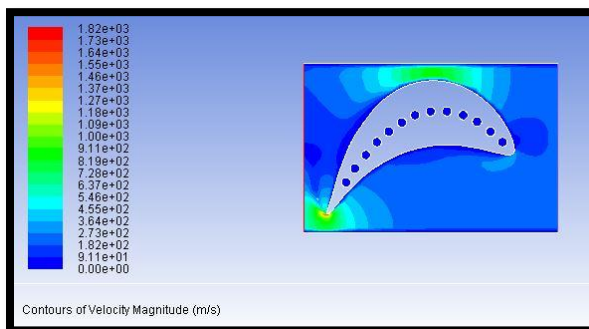


CFD ANALYSIS OF FILM COOLING TURBINE BLADE

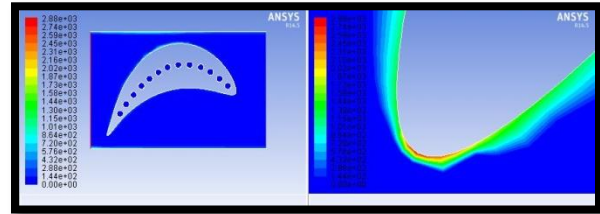
PRESSURE



VELOCITY



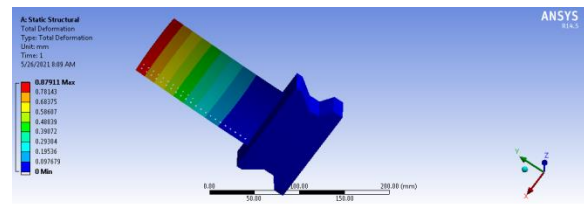
HEAT TRANSFER COEFFICIENT



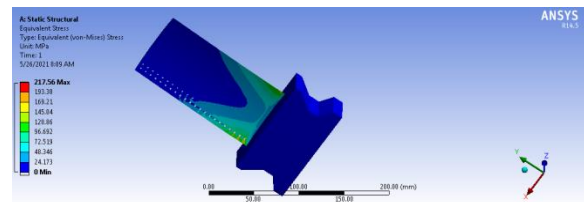
Mass Flow Rate	(kg/s)
inlet	82.889244
interior_trm_srf	501.84143
outlet	-82.707085
wall_trm_srf	0
Net	0.18215942

STATIC ANALYSIS OF GAS TURBINE BLADE

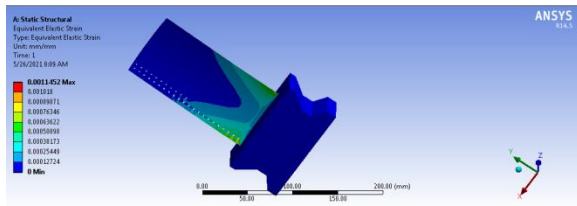
Deformation



STRESS

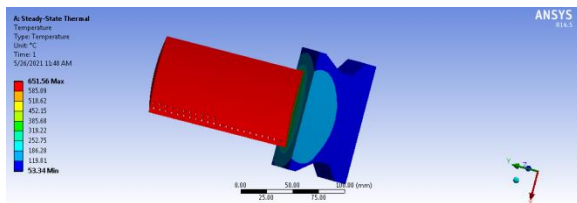


STRAIN

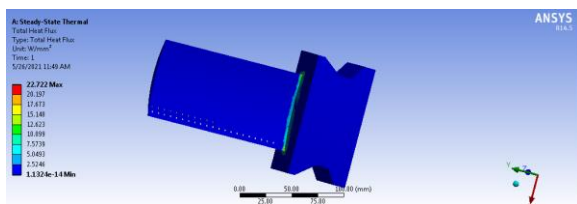


THERMAL ANALYSIS ON GAS TURBINE BLADE

TEMPERATURE



HEAT FLUX



RESULTS AND DISCUSSIONS

STATIC ANALYSIS RESULT TABLE

CASES	MATERIAL	Deformation (mm)	Stress (N/mm ²)	Strain
Without	Chromium steel	1.1897	227.16	0.0011601
	Stainless steel 316L	1.2058	225.45	0.001772
Internal	Chromium steel	1.1335	223.54	0.0011314
	Stainless steel 316L	1.1485	220.42	0.001159
External	Chromium steel	0.85002	218.22	0.0011088
	Stainless steel 316L	0.87911	217.56	0.0011452
Internal And	Chromium steel	0.78297	204.26	0.0010376
External	Stainless steel 316L	0.80993	203.55	0.0010713

THERMAL ANALYSIS RESULT TABLE

CASES	MATERIAL	Temperature (°C)	Heat flux (W/mm ²)
Without	Chromium steel	650.26	15.05
	Stainless steel 316L	650.25	19.056
Internal	Chromium steel	651.12	16.002
	Stainless steel 316L	651.04	20.685
External	Chromium steel	651.66	17.583
	Stainless steel 316L	651.56	22.722
Internal And	Chromium steel	650.45	19.805
External	Stainless steel 316L	650.42	25.594

5.CONCLUSION

In our project we have designed a turbine blade used in gas turbines and modeled in 3D modeling software PRO-E. Models are (without holes, internal cooling, external cooling and internal-external cooling).

We have done structural and thermal analysis on all the models of turbine blades using chromium steel and stainless steel 316L. By observing the analysis results, the analyzed stress values are less than their permissible stress values. So using both the materials is safe. The stress and deformation values are more for stainless steel 316L.

By observing the thermal results, thermal flux is more for stainless steel 316L and chromium steel. So using stainless steel 316L is better than chromium steel. But the main advantage is its weight.

So we can conclude that by using stainless steel 316L with internal – external cooling method is better.

REFERENCES

1. Design and Analysis of Gas Turbine Blade by Theju V, Uday P S , PLV Gopinath Reddy, C.J.Manjunath
2. Heat Transfer Analysis of Gas Turbine Blade Through Cooling Holes by K Hari Brahmaiah , M.Lava Kumar
3. The design and analysis of gas turbine blade by Pedaprolu Venkata Vinod
4. Effect Of Temperature Distribution In 10c4/60c50 Gas Turbine Blade

- Model Using Finite Element Analysis by V.Veeraragavan
5. Film Cooling on a Gas Turbine Rotor Blade by K. Takeishi, S. Aoki, T. Sato and K. Tsukagoshi
 6. Film Cooling of the Gas Turbine Endwall by Discrete-Hole Injection by M. Y. Jabbari, K. C. Marston, E. R. G. Eckert and R. J. Goldstein
 7. An advanced impingement/film cooling scheme for gas turbines – numerical study by A. Immarigeon, (Department of Mechanical and Industrial Engineering, Concordia University, Montréal, Canada), I. Hassan, (Department of Mechanical and Industrial Engineering, Concordia University, Montréal, Canada)
 8. An experimental investigation on the trailing edge cooling of turbine blades by Zifeng Yang, Hui Hu
 9. CFD Simulation on Gas turbine blade and Effect of Hole Shape on leading edge Film Cooling Effectiveness by Shridhar Paregouda, Prof. Dr. T. Nageswara Rao

DESIGN AND CFD ANALYSIS OF PISTON BOWL GEOMETRIES IN IC ENGINES

Syed Shazaan Ahmed¹

Umashankar²

Dr.P.Srinivasulu³

¹M.Tech (Thermal Engineering)Department of mechanical engineering vaagdevi college of engineering (UGC autonomous) approved by AICTE & permanent affiliation to jntuh, hyderabad.p.o, bollikunta, Warangal urban- 506005.

²Assistant Professor Department of mechanical engineering vaagdevi college of engineering (UGC autonomous) approved by AICTE & permanent affiliation to jntuh, hyderabad. p.o, bollikunta, Warangal urban- 506005.

³Professor and Head of the Department of mechanical engineering vaagdevi college of engineering (UGC autonomous) approved by AICTE & permanent affiliation to jntuh, hyderabad. p.o, bollikunta, Warangal urban- 506005.

Abstract: Two most important concerns in diesel-fuelled CI engine are NO_x and soot emissions. The improvement of air and fuel mixture will improve combustion engine performance. There are many ways to improve the air–fuel mixture inside a cylinder, and changing piston bowl geometry is one of them. Several researchers have worked on combustion chamber and different types of piston bowl geometry. This paper represents the effect of piston bowl geometry on the performance and emissions of a direct-injection diesel engine. Different piston bowl profiles, namely, hemispherical combustion chamber (HCC), shallow depth combustion chamber (SCC) and toroidal combustion chamber (TCC), have been created by using cad tool CATIA and analyzing with CAE tool ANSYS workbench. Furthermore, Karanja oil mixed with base fluid Diesel are calculated for their combination properties. The fluids are Karanja and Diesel at different volume fractions such as 0.2%, 0.3% and 0.4%. Theoretical calculations are done determine the properties for nano fluids and those properties are used as inputs for analysis. CFD analysis is done on the different geometries at different fluid volume fractions and thermal analysis is done piston bowl geometries with different composite materials (carbon fiber and armide fiber).

1. INTRODUCTION

Compression ignition engine is preferred for heavy-duty usage due to their durability and higher thermal efficiency compared to spark ignition engines [1, 2]. However, conventional diesel combustion (CDC) engines are facing significant challenges in meeting increasingly stringent emission regulations due to high oxides of nitrogen (NO_x) and particulate matter (PM) emissions [3]. Improvements in the accuracy and flexibility of common-rail injection systems [4] have allowed detailed investigation of low-temperature combustion (LTC) concepts such as, homogeneous charge compression ignition (HCCI) [5–7] and partially premixed combustion (PPC) [8,9], reactivity controlled compression ignition (RCCI) [10,11], intelligent charge compression ignition (ICCI) [12,13], diesel methanol dual fuel (DMDF) [14–16]. In these LTC engines, one fuel is usually injected directly into the cylinder during the intake/compression stroke to form a relatively lean and stratified fuel/air mixture before the onset of ignition [17]. Thus, LTC engines always require a high compression ratio (CR) (similar to the CDC engine) to ignite the lean mixture. Staged combustion is observed due to the in-cylinder mixture stratification, which offers an opportunity to simultaneously achieve high thermal efficiency and low NO_x and PM emissions without using expensive after-treatment technologies [1,5]. Compared to diesel fuel, low reactive fuels, like gasoline, have a prolonged ignition delay and

hence an improved fuel–air mixing, which shows great advantages in the load extension and knock control in direct-injection compression ignition (DICI) engines [18]. However, gasoline DICI engines suffer from high unburned hydrocarbons (UHC) and carbon monoxide (CO) emissions, and coldstart problems at low loads owing to the low fuel reactivity [19,20]. Further improvements are required for gasoline DICI engines to achieve optimized fuel distribution in the cylinder, which is strongly affected by the fuel injection system, injection strategy, injector-nozzle design parameters, fuel physical and chemical properties, combustion chamber (piston bowl) shape and operation conditions (CR, intake pressure and temperature).

2. LITERATURE REVIEW

Arumugam et.al [21] produced the rice bran oil methyl ester and test in a diesel engine using of rice bran oil methyl ester with ethanol at various proportions such as 1%, 3% and 5% by volume basis. The results showed that the increase in biodiesel concentration in the fuel blend influences CO₂ and NO_x emissions and decreases the CO and HC emissions. It is also reported that emission of ethanol-B20ROME blends, reduces CO₂ and NO_x which are the major contributors to global warming. With the addition of ethanol by 1, 3, and 5% to B20ROME.

Senthil, R., et. al [22] studied the performance, emission, and combustion characteristics of single cylinder direct injection Diesel engine Annona methyl ester as a fuel with the addition of anti oxidants such as p-phenylenediamine, a-tocopherol acetate, 1,4-dioxane, and l-ascorbic acid. Results showed that anti-oxidant additives are very effective in controlling the NO_x emission. Among different antioxidant additives, 0.010%-m concentration of p-phenylenedimine additive is optimum for NO_x emission reduction up to 42.15% when compared to that of neat biodiesel.

Mark Robert Ellis [23] studied the effective air and fuel mixing is significantly increased by modifying the combustion chamber by suitable piston bowl can significantly increased the peak pressure heat release rate.

Montajir et al [24] have attempted to achieve improvement in mixture formation by changing the combustion chamber geometry. They found that the reentrant cavity with round lip produces larger spray volumes and wider spray spreading. They found that introduction of a bottom corner radius helps to disperse the fuel accumulated at the bottom corner and the spray volume increases.

Gnanamoorthi, et. Al., [25] studied the effect of combustion chamber geometry on performance, combustion and emissions of ethanol-diesel blend in a diesel engine. It is reported that the toroidal combustion chamber creates better turbulence, squish, and swirl at high compression ratios of 19.5:1 compared to that of hemispherical cavity combustion chamber. It is also reported that the brake thermal efficiency for toroidal combustion chamber is 33% and the peak pressure in the cylinder as well as peak heat release rate is also increased. Further, it is also concluded that 60% of CO emission, 20% of HC emission, 40% of NO_x emission, and 90% in smoke emissions were reduced for toroidal combustion chamber, compared to that of hemispherical combustion chamber.

Viswanathan et.al [26] investigated the performance and emission characteristics of 20% orange oil methyl ester and 80% diesel in hemispherical combustion chamber and toroidal combustion chamber. It is reported that NO_x and HC emission is reduced in toroidal combustion chamber engine. However, smoke emission is found to be lower in hemispherical combustion chamber engine.

Rajan and Senthilkumar [27] tested the performance of a diesel engine using Jatropha methyl ester with internal jet using and reported that the BTE was improved and the exhaust gas emissions are reduced significantly at full load due to enhancement of turbulence motion of air by the internal jets.

Saito et al. [28] compared conventional combustion chambers and re-entrant combustion chambers in terms of the combustion process, engine performance, and NO_x and smoke emissions for diesel engine. It was reported that re-entrant combustion chamber, enhanced combustion because of the higher in-cylinder velocity accompanied by increased turbulence.

Li et al [29] numerically studied of the effects of piston bowl geometry on combustion and emission characteristics of a diesel engine fueled with biodiesel and its diesel blends. They reported that CO emissions were lower and NO emissions were higher for Omega combustion chamber operation with biodiesel.

Prasad et al [30] studied the effect of high swirl inducing piston to reduce exhaust emissions numerically. They found that an injection timing of 8.60 CA bTDC was found to be optimum and it leads to a 27% reduction in NO_x emissions and 85% reduction in soot levels as compared to the base engine.

Jaichandar and Annamalai [31] studied the effect of injection pressure and reentrant combustion chamber using 20% Pongamia biodiesel in a diesel engine. They reported that CO, UBHC and smoke were reduced and NO emission was increased for reentrant combustion chamber with increased injection pressure of 220bar due to improved combustion. Brake Thermal Efficiency is increased and brake specific fuel consumption decreased for biodiesel as compared to hemispherical bowl geometry of the piston for diesel engine. Hence, the objective of the research work is to investigate the combined effect of varying injection pressure and combustion chamber geometry on the performance of a 25% corn biodiesel blend in a diesel engine and the results were compared to diesel and the 25% corn biodiesel blend.

Wamankar and Murugan[32] experimentally analyzed the effect of internal jet induced piston bowl with emulsified diesel fuel. The researcher uses this piston bowl achieved a superior emission reduction through the modified piston bowl because swirl variation and fuel-air interaction. About above of paper, we can found main goal that combustion bowl profile modification can be utilized for the improvement of performance and emission behavior of diesel and biodiesel fuels.

Jaichandar and Annamalai[33] experimentally studied the toroidal and shallow depth re-entrant combustion bowl using pongamia biodiesel to power a diesel engine. So they found the reentrant bowls tended to improve the mixture formation by better fuel and air interaction resulting in the improvement of the performance characteristics.

Ramesh Bapu et al.[34] probed the consequence of a modified combustion bowl profile on a diesel engine powered by Calophyllum methyl ester. This investigation can be found that the bowl with the lower diameter to depth ratio would have superior squish flow resulting in the enhancement of the performance characteristics.

Li et al. [35] carried out the impact of piston bowl geometry use CFD tool and the fuel using biodiesel-powered diesel engine with three different combustion bowls, and the name of three bowls are Hemispherical, Shallow depth, and Omega Combustion cylinder with the same cylinder. This research can be found the Omega Combustion chamber got high-speed engines owing to superior squish motion, and the 3geometry of piston made the fuel and air complete mixture cause the engine performance improvement.

B. Harshavardhan and J. M. Mallikarjuna[36] work on “CFD analysis of in-cylinder flow and air-fuel interaction on different combustion chamber geometry in DISI Engine”. They carried the work by fixing the engine speed and crank angle. The engine speed which they took was 1500 rpm. They have concluded that flat piston has slightly high Tumble Ratio when compared to the other piston configurations i.e., dome piston with centre bowl, Pentroof Offset Bowl Piston (POBP), flat piston with centre bowl, the Turbulent Kinetic Energy (TKE) is distributed all over the combustion chamber; TKE of Flat Piston (FP) is high about 12.56% when compared to the POBP. They didn't analyze the contours of turbulent kinetic energy and turbulent intensity of all four geometries.

V. V. PrathibaBharathi and G. prasanthi[37] work on “Influence of in-cylinder air swirl on diesel engines performance and emissions” have concluded that lesser smoke can be achieved by the complete combustion, lesser carbon deposits in the combustion chamber, piston crown and exhaust system occur due to the controlled complete combustion, better fuel economy can be achieved by the improved and complete combustion, there will be raise in the cylinder pressure due to the effective combustion. But Pressure and velocity contours have not been analyzed.

Jinou song, Chunde Yao, Yike Liu and Zejun Jiang[39] work on “Investigation on flow field in simplified piston bowls for Direct Injection diesel engine” have concluded that squish flow plays an important role in the turbulence generation process near the TDC during compression, the coupling among the swirl, squish, bowl shape and turbulence is much more pronounced for the flow fields in the combustion chambers and the piston bowl configurations should be designed to coincide with the contour lines of the turbulence.

C. Morley, R. J. Price, N. P. Tait and C. R. McDonald [40] work on “Understanding how fuels behave in engines” concluded that differences in the fuel composition can sometimes play a significant role on the performance of the engine as they lead to the formation of combustion chamber deposits. Fuel components considerably differ in their deposit forming tendency, combustion chamber deposits in gasoline engines can increase NO_x and hydro carbon emissions.

2.1 PROBLEM DESCRIPTION

The objective of this project is to make a 3D model of the piston bowl geometries study the CFD and structural behavior of the Different piston bowl profiles, namely, hemispherical combustion chamber (HCC), shallow depth combustion chamber (SCC) and toroidal combustion chamber (TCC), have been created by using cad tool CATIA by performing the finite element analysis.

2.2 The methodology followed in the project is as follows:

- Study the literature review
- Create a 3D model of the piston bowl geometries using parametric software CATIA
- Convert the surface model into Para solid file and import the model into ANSYS to do analysis.
- Perform static analysis on the different geometries at different materials is to be determine the deformation, stress and strain.
- Perform Thermal analysis on the different geometries at different materials is to be determine the Temperature distribution and heat flux.
- Perform CFD analysis on the existing model of the piston bowl geometry for Velocity inlet to find out the Turbulence intensity, pressure drop and Emissions(NO_x,CO....etc).

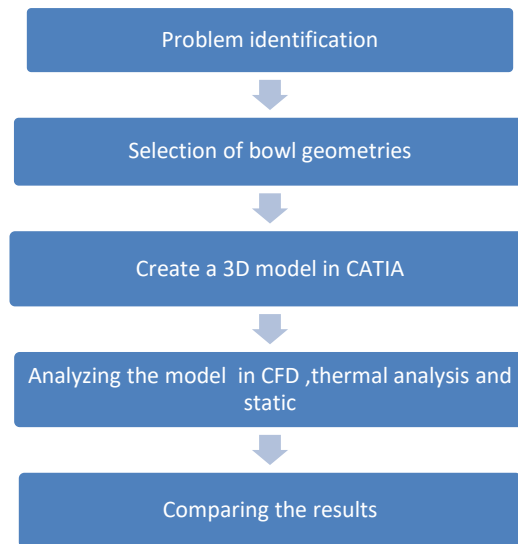


Fig: 1 Flow Chart of Work

3. MATERIALS AND METHODS

Biodiesel is produced from renewable resources like vegetable oils and animal fats. It can use as a fuel in diesel engine by blending with diesel or in pure form. Biodiesel blended diesel fuel emits less harmful gasses compare to diesel fuel. India is developing country where more than 70% of petroleum products are import. Biodiesel production from local resources provides energy security; reduce import bill, generate employment and reduced emissions of harmful gasses. Production of biodiesel from edible oil is not economical for India due to its higher price. Various non-edible oil seeds like Jatropha, Karanja, Mahua, Sal, Neem etc. are widely available in India. It is less costly compared to edible oils. Among them, Karanja has a potential to be used as a basic feedstock for the production of biodiesel. Karanja trees can grow on sides of roads, canal and boundary portion of agricultural lands with minimum care.

Table:1 Thermo Physical Properties of Fluids

Specification	Diesel	Karanja
Density(kg/m ³)	959	920
Thermal conductivity(w/m-k)	0.13	0.0168
Specific heat(j/kg-k)	2220	1572
Viscosity (kg/m-s)	0.006123	0.003831

3.1 Calculations to Determine Properties of Fluid by Changing Volume Fractions

Density Of Fluid

$$\rho_f = \Phi \times \rho_k + [(1-\Phi) \times \rho_d] \quad \text{Eq(1)}$$

Specific Heat Of Fluid

$$C_{pnf} = \frac{\Phi \times \rho_k \times C_{pk} + (1 - \Phi)(\rho_d \times C_{pd})}{\Phi \times \rho_k + (1 - \Phi) \times \rho_d} \quad \text{Eq(2)}$$

Viscosity of Fluid

$$\mu_{nf} = \mu_w (1 + 2.5\phi) \quad \text{Eq(3)}$$

Thermal Conductivity Of Fluid

$$K_{nf} = \frac{K_k + 2K_d + 2(K_k - K_d)(1 + \beta)^3 \times \Phi}{K_k + 2K_d - (K_k - K_d)(1 + \beta)^3 \times \phi} \times K_d \quad \text{Eq(4)}$$

Table 2: from Eq (1,2,3 and 4) calculating the Thermo Physical Properties of Diesel fuel mixed with karanja oil at different volume fractions

Volume fraction (ϕ)	Density (kg/m^3)	Specific heat (j/kg-k)	Thermal conductivity (w/m-k)	Viscosity (kg/m-s)
B10	951.21	2094.650	0.13944	0.00918
B15	947.3	2031.202	0.14433	0.01071
B20	943.4	1967.229	0.149349	0.01224

4. MODELING AND SIMULATION

4.1 CATIA PARAMETRIC SOFTWARE

Computer Aided Design (CAD) is the use of computer software to design a product or an object. Computer Aided Manufacturing (CAM) is the use of computer software and hardware to plan, manage and control the operations of a manufacturing plant. Computer Aided Engineering is the use of computer software to solve engineering problems and analyze products created using CAD. CATIA is an acronym for Computer Aided Three-dimensional Interactive Application. It is one of the leading 3D software used by organizations in multiple industries ranging from aerospace, automobile to consumer products. CATIA is a multi platform 3D software suite developed by Dassault Systems, encompassing CAD, CAM as well as CAE.

4.2 ANSYS

The governing equations in ANSYS Forte follow mainly the Continuity equation, Momentum equation (Navier Stokes equation) and Energy equation to solve computational fluid dynamics problem.

The conservation equation for species is given by :

$$\frac{\partial \rho}{\partial t} k + \nabla \cdot \rho k u = \nabla \cdot \rho D T \nabla \rho k \rho + \rho k c + \rho k s k = 1, \dots, K \quad (5)$$

Where: ρ is the density, subscript k is the species index, K is the total number of species, u is the flow velocity vector. Application of Fick's Law of diffusion results in a mixture-averaged turbulent diffusion coefficient DT . $\rho k c$ and $\rho k s$ are source terms due to chemical reactions and spray evaporation, respectively. The summation of Equation 1 over all species gives the continuity equation for the total fluid

$$\frac{\partial \rho}{\partial t} + \nabla \cdot (\rho \cdot u) = \rho \quad (6)$$

Steady-state thermal analyses calculate the effects of steady thermal loads on a system or component. Users often perform a steady-state analysis before doing a transient thermal analysis, to help establish initial conditions. A steady-state analysis also can be the last step of a transient thermal analysis; performed after all transient effects have diminished. ANSYS can be used to determine temperatures, thermal gradients, heat flow rates, and heat fluxes in an object that are caused by thermal loads that do not vary over time.

Computational fluid dynamics, usually abbreviated as CFD, is a branch of fluid mechanics that uses numerical methods and algorithms to solve and analyze problems that involve fluid flows. Computers are used to perform the calculations required to simulate the interaction of liquids and gases with surfaces defined by boundary conditions. With high-speed supercomputers, better solutions can be achieved. Ongoing research yields software that improves the accuracy and speed of complex simulation scenarios such as transonic or turbulent flows. Initial experimental validation of such software is performed using a wind tunnel with the final validation coming in full-scale testing, e.g. flight tests.

Designs of CFD Domains

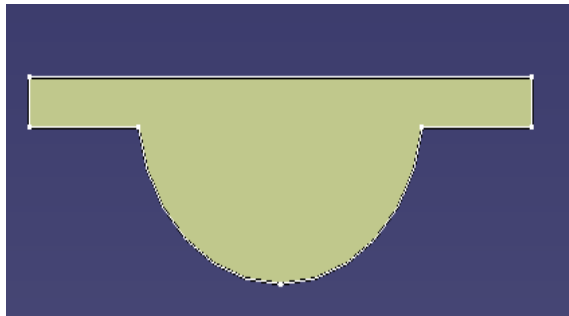


Fig: 2 hemispherical chamber

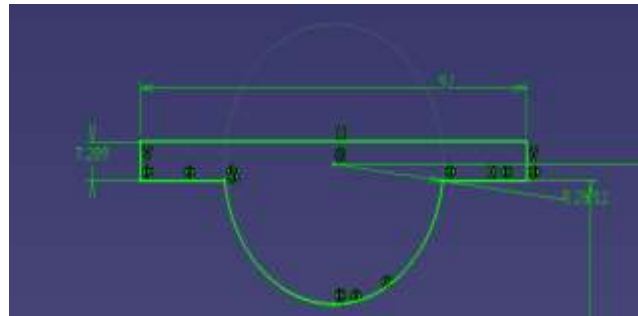


Fig: 3 2D drawing of hemispherical chamber

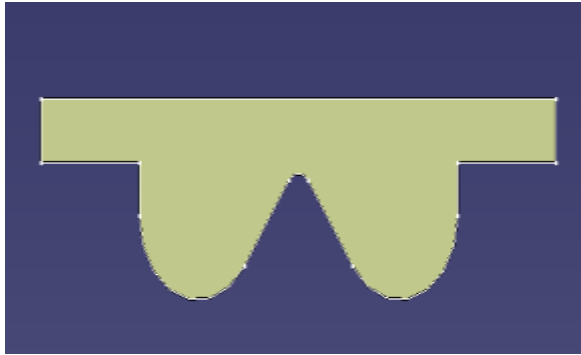


Fig: 4 Toroidal Chamber

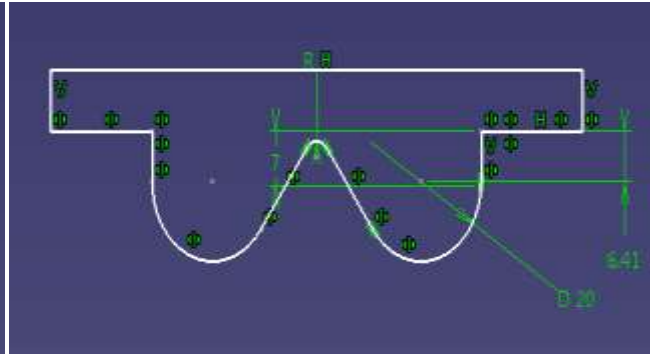


Fig: 5 2D drawing of Toroidal Chamber



Fig: 6 Shallow depth chamber

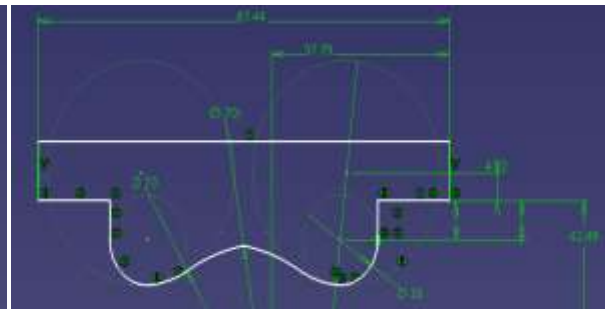


Fig: 7 2D drawing of Shallow depth chamber

3D MODEL OF PISTON BOWL GEOMETRIES



Fig: 8 hemispherical chamber

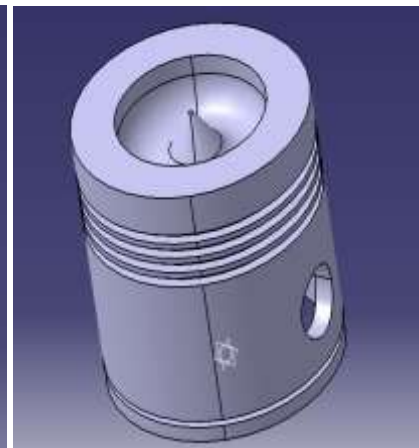


Fig:9 Toroidal Chamber

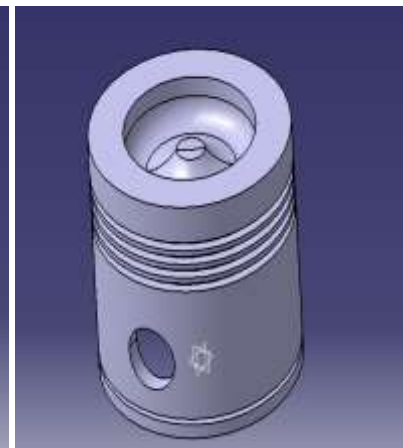


Fig: 10 Shallow depth chamber

5. RESULTS AND DISCUSSIONS

5.1 Grid models of HCC, TCC, and SCC

Grid independency is checking the result for solution is independent from different mesh types and size, result is only depend the CFD domain's Boundary conditions.

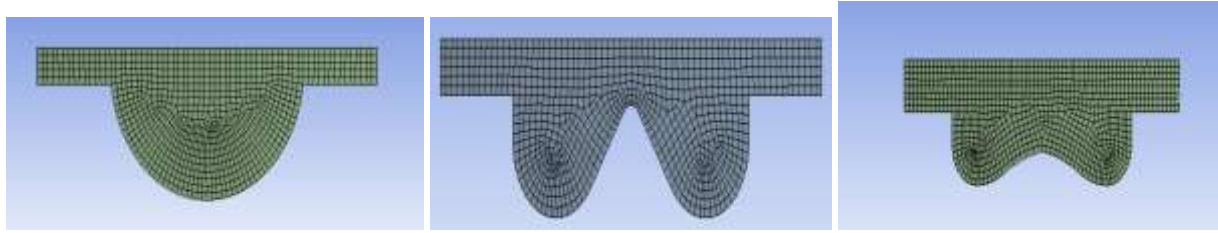
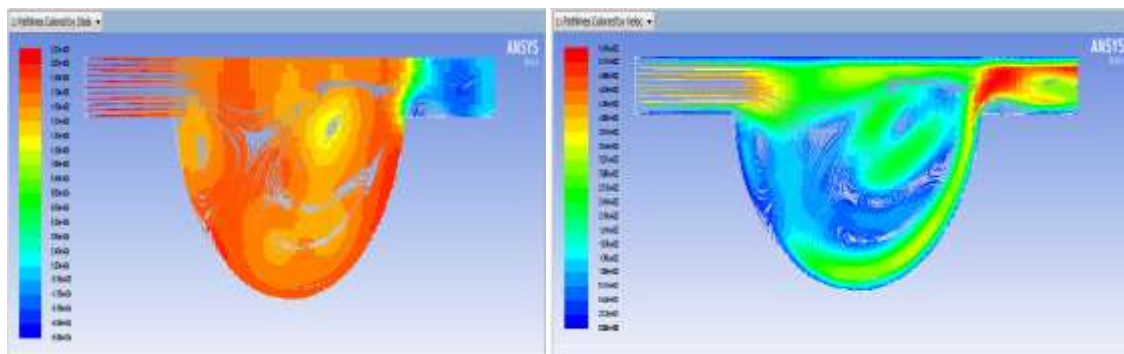


Fig: 11 meshing models of HCC, TCC and SCC piston bowl geometries

The model is designed with the help of CATIA and then import on ANSYS for Meshing and analysis. The analysis by CFD approach is used in order to calculating pressure, turbulence intensity, velocity, N_2 plots and CO_2 . For meshing, the fluid ring is divided into two connected volumes. Then all thickness edges are meshed with 360 intervals. A tetrahedral structure mesh is used. So the total number of nodes and elements is 21264 and 109297.

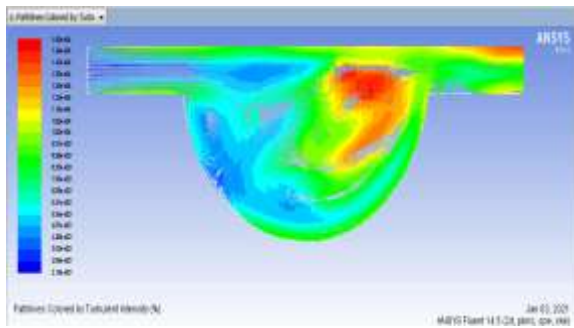
Table 4: Input parameter of CFD domain

Parameter	Magnitude
Crank shaft speed	1500
Crank radius	47
Bore	85
Stroke	85
Fuel	Diesel +B20(karanja oil)

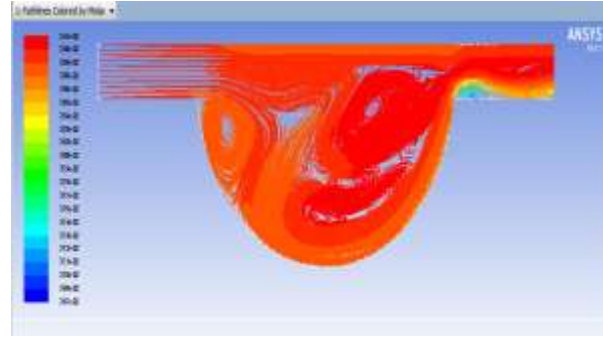


(a)

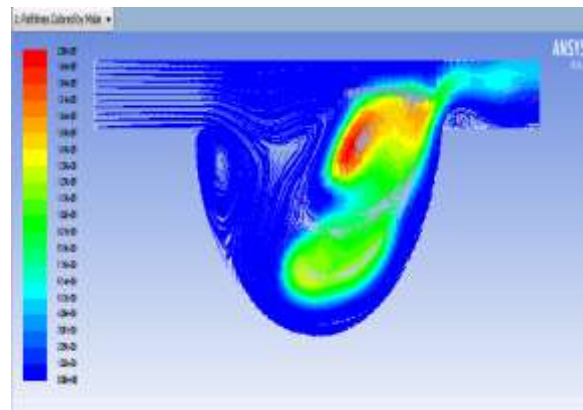
(b)



(c)

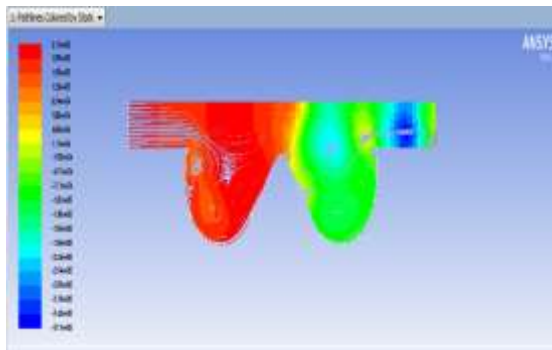


(d)

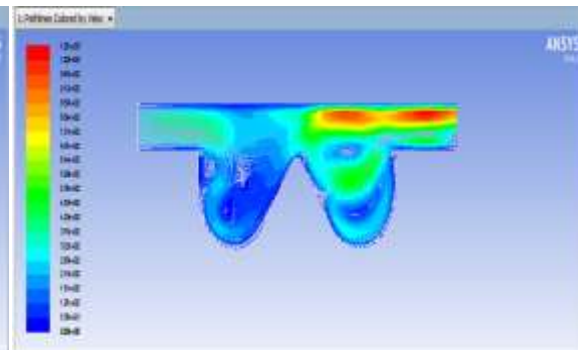


(e)

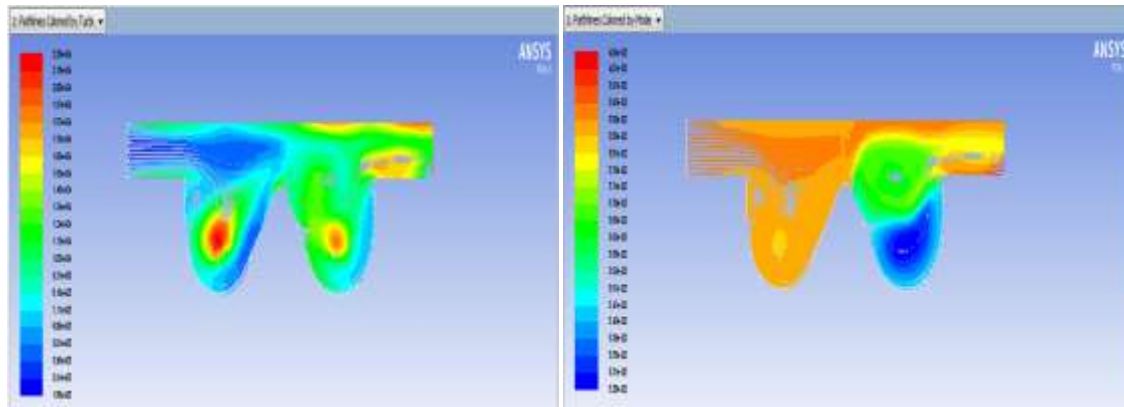
Fig: 12 The following above figures geometry is HCC at fluid diesel+B20, Path lines counter plots (a) pressure plot (b) velocity plot (c) Turbulence intensity (d)molar concentration of N₂ (e) molar concentration of CO₂



(a)

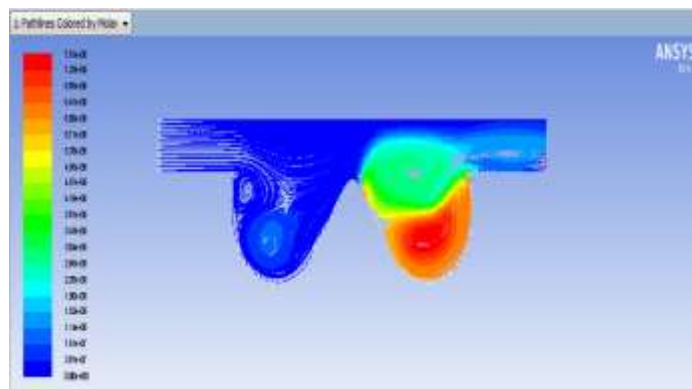


(b)



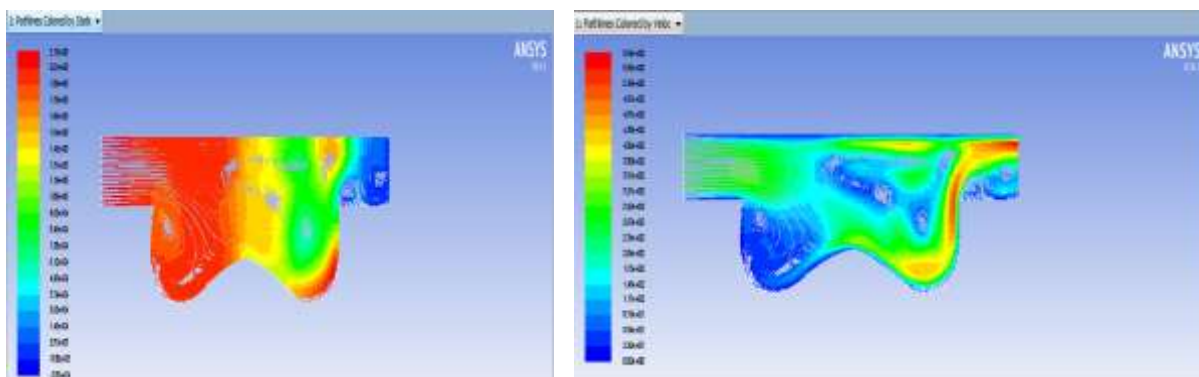
(c)

(d)



(e)

Fig: 13 The following above figures geometry is TCC at fluid diesel+B20, Path lines counter plots (a) pressure plot (b) velocity plot (c) Turbulence intensity (d)molar concentration of N₂ (e) molar concentration of CO₂



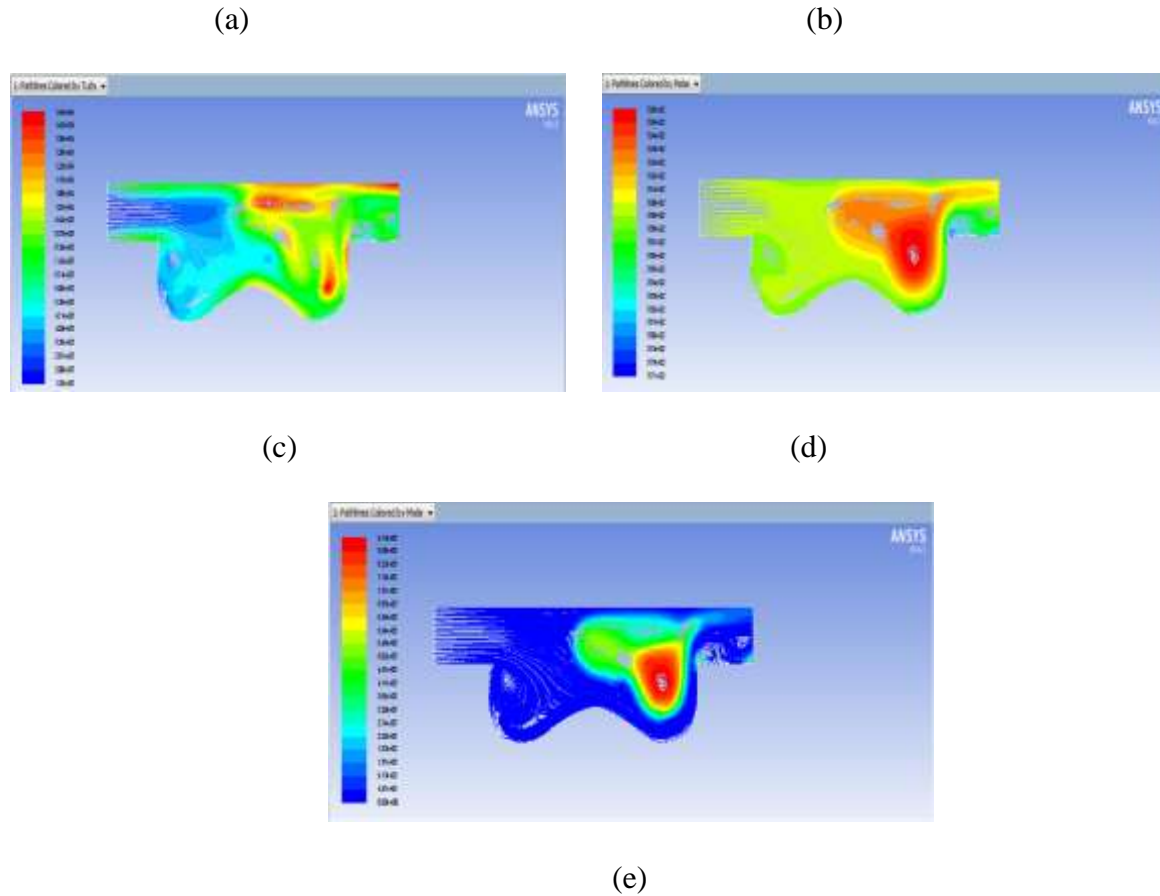


Fig: 14 The following above figures geometry is SCC at fluid diesel+B20, Path lines counter plots (a) pressure plot (b) velocity plot (c) Turbulence intensity (d)molar concentration of N₂ (e) molar concentration of CO₂

Table: 5 CFD analysis results

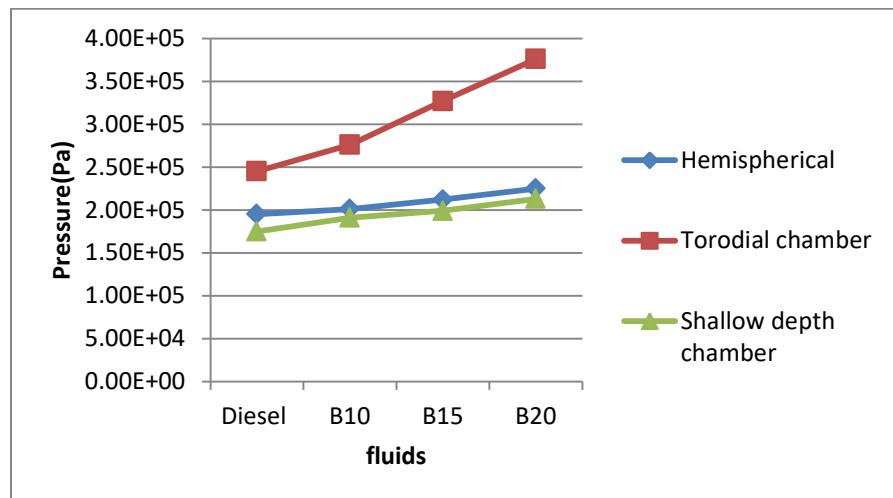
Shape of Geometry	Fluid and volume fraction (%)	Pressure (Pa)	Velocity (m/s)	Turbulence Intensity (%)	Molar concentration of N ₂	Molar concentration of CO ₂
Hemispherical	Diesel	1.95e+05	4.16	9.81e+03	0.0542	1.85e-07
	B10	2.01e+05	4.72	9.99e+03	0.0492	1.95e-07
	B15	2.12e+05	5.12	1.13e+04	0.0421	2.01e-08
	B20	2.25e+05	5.45	1.56e+04	0.0391	2.05e-08
Torodial chamber	Diesel	2.45e+05	6.83	2.13e+04	0.0611	8.91e-05
	B10	2.76e+05	8.12	2.34e+04	0.0593	8.08e-05
	B15	3.27e+05	9.16	2.56e+04	0.0445	9.07e-05

	B20	3.76e+05	10.04	2.74e+04	0.0419	4.04e-06
Shallow depth chamber	Diesel	1.75e+05	4.23	1.12e+04	0.0552	2.95e-07
	B10	1.91e+05	4.84	1.34e+04	0.0498	5.95e-07
	B15	1.99e+05	5.25	1.67e+04	0.0412	8.45e-07
	B20	2.13e+05	5.84	1.94e+04	0.0396	9.13e-08

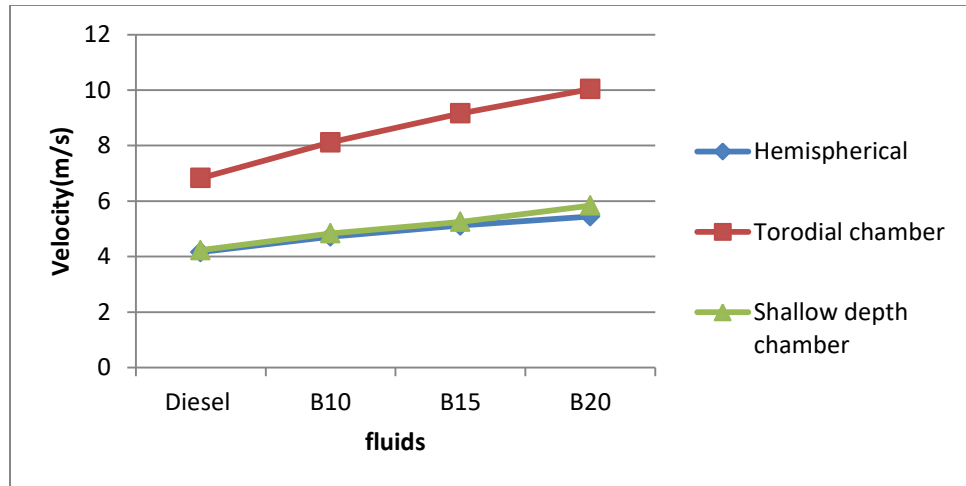
5.2 OBSERVATIONS

Following observations were made after analyzing the results of CFD analysis of hemispherical, toroidal and shallow depth piston bowl geometry.

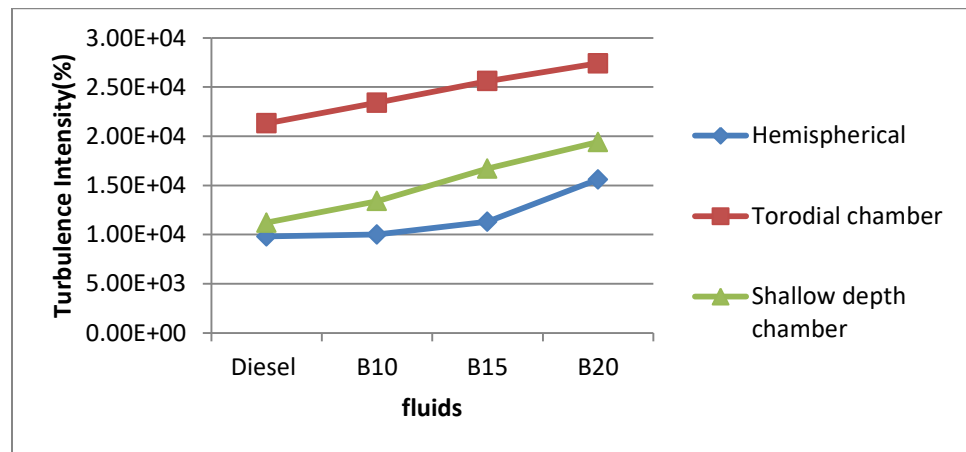
The observations were found by referring figure 12 (a,b,c,d and e) for hemispherical piston bowl. For toroidal from figure 13(a,b,c,d and e) for shallow depth shape from figure 14 (a,b,c,d and e). In analysis of hemispherical piston it was observed that air molecules were not distributed properly, pressure distribution was uneven and velocity distribution was also uneven. For toroidal piston air molecules distribution and swirl was uniform, pressure distribution was more uniform as compared to hemispherical bowl and velocity distribution was uniform but velocity of air molecules was found low. In case of shallow depth piston, air molecules distribution and swirl production was enhanced pressure distribution was enhanced, velocity distribution is more uniform and velocity of air molecules inside the cylinder was also increased.



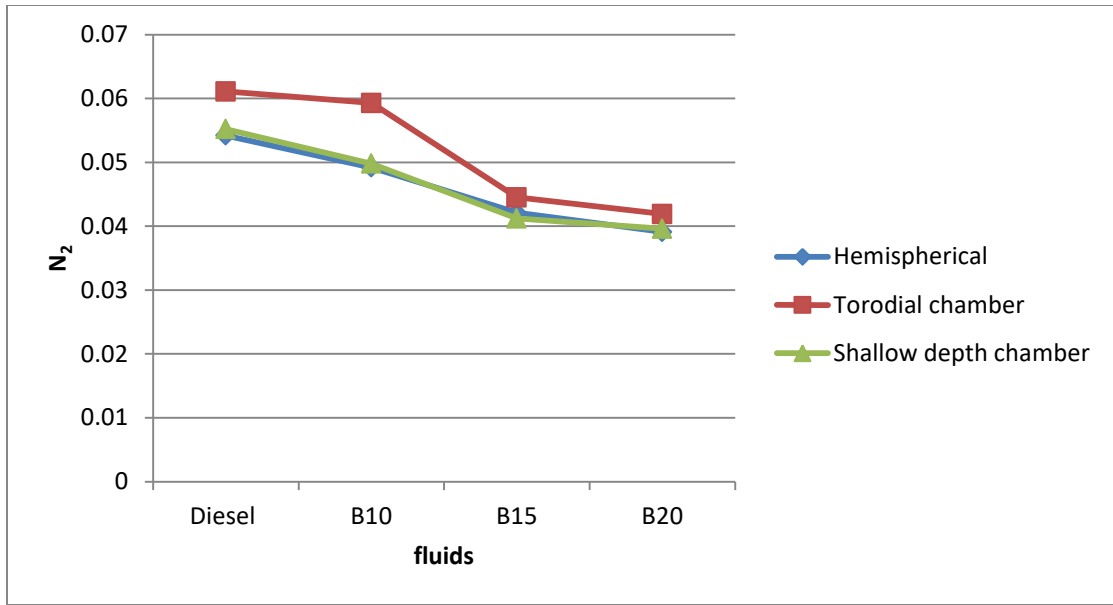
The above graph is plotted between Pressure and piston bowl geometries. The graph compares the pressure of various fuels (D100, B10, B15, and B20) used in the diesel engine. The pressure is an important parameter of an engine because it takes care of both mass flow rate and heating value of the fuel. The above graph shows that while increasing in the blend composition automatically it increases the pressure. The above graph shows that biodiesel blend B20 is higher than the diesel (D100) fuel under loading condition.



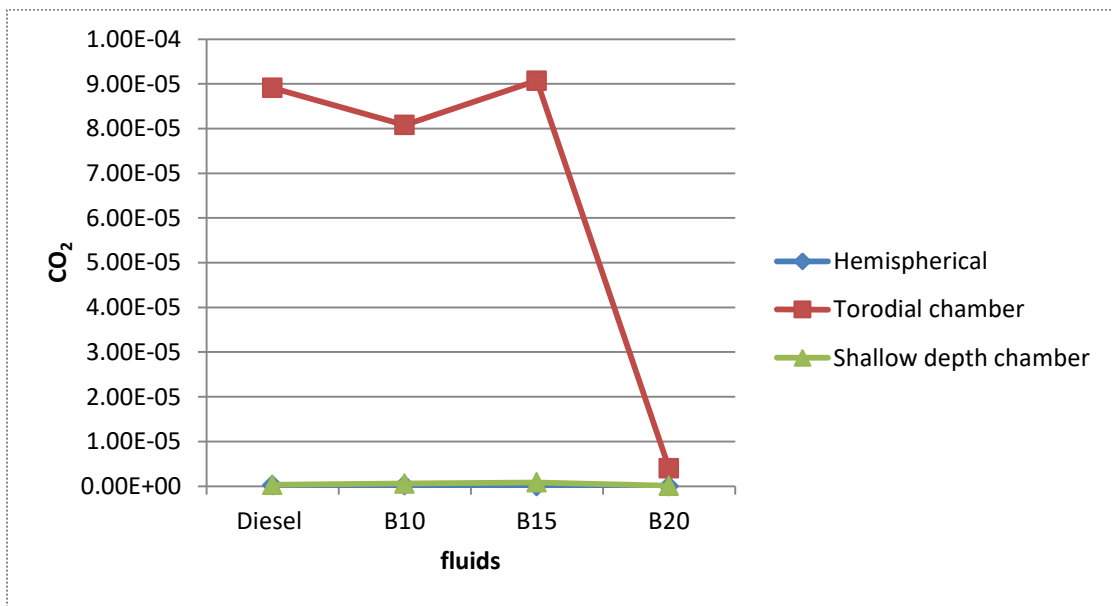
The above graph is plotted between Velocity and piston bowl geometries. The graph compares the velocity of various fuels (D100, B10, B15, and B20) used in the diesel engine. The Velocity is an important parameter of an engine because it takes care of both mass flow rate and heating value of the fuel. The above graph shows that while increasing in the blend composition automatically it increases the velocity. The above graph shows that biodiesel blend B20 is higher at torodial piston bowl than the diesel (D100) fuel under loading condition.



The above graph is plotted between turbulence intensity and piston bowl geometries. The graph compares the turbulence intensity of various fuels (D100, B10, B15, and B20) used in the diesel engine. The turbulence intensity is an important parameter of an engine because it takes care of both mass flow rate and heating value of the fuel. The above graph shows that while increasing in the blend composition automatically it increases the turbulence intensity. The above graph shows that biodiesel blend B20 is higher at torodial piston bowl than the diesel (D100) fuel under loading condition.



The above graph is plotted between fluids and N_2 . The graph compares the N_2 emissions of various fuels (D100, B10, B15, B20) used in the diesel engine. It shows that increasing in blend compositions automatically Decrease in NO_x emissions.



The above graph is plotted between fluids and CO₂. The graph compares the CO₂ emissions of various fuels (D100, B10, B15, B20) used in the diesel engine. It shows that increasing in blend compositions automatically decrease in CO₂ emissions.

Conclusion

Karanja oil mixed with base fluid Diesel are calculated for their combination properties. The fluids are Karanja and Diesel at different volume fractions such as 0.2%, 0.3% and 0.4%. Hence from 3D Modeling using CATIA and the results of CFD analysis from ANSYS of the piston bowl geometry, it was concluded that in order to achieve proper combustion to increase power output, the swirl formation can be enhanced by modifying piston bowl geometry. Turbulence intensity of various fuels (D100, B10, B15, and B20) used in the diesel engine. The turbulence intensity is an important parameter of an engine because it takes care of both mass flow rate and heating value of the fuel. While increasing in the blend composition automatically it increases the turbulence intensity. N₂ and CO₂ emissions of various fuels used in the diesel engine. It shows that increasing in blend compositions automatically decrease in NO_x emissions.

REFERENCES

- [1] Reitz R, Ogawa H, Payri, et al. IJER editorial: The future of the internal combustion engine. *Int J Engine Res* 2019;21(1):3–10.
- [2] Johnson DR, Heltzel R, Nix AC, Clark N, Darzi M. Greenhouse gas emissions and fuel efficiency of in-use high horsepower diesel, dual fuel, and natural gas engines for unconventional well development. *Appl Energy* 2017;206:739–50.
- [3] Johnson BT. Diesel engine emissions and their control. *Platinum Met Rev* 2008;52(1):23–37.
- [4] Zhao H. *Advanced direct injection combustion engine technologies and development: diesel engines*. vol. 2. Woodhead Publishing; 2009.
- [5] Lu X, Han D, Huang Z. Fuel design and management for the control of advanced compression-ignition combustion modes. *Prog Energy Combust Sci* 2011;37(6):741–83.
- [6] Yao M, Zheng Z, Liu H. Progress and recent trends in homogeneous charge compression ignition (HCCI) engines. *Prog Energy Combust Sci* 2009;35(5):398–437.
- [7] Lü X, Ji L, Zu L, Hou Y, Huang C, Huang Z. Experimental study and chemical analysis of n-heptane homogeneous charge compression ignition combustion with port injection of reaction inhibitors. *Combust Flame* 2007;149(3):261–70.
- [8] Zhang F, Yu R, Bai XS. Direct numerical simulation of PRF70/air partially premixed combustion under IC engine conditions. *Proc Combust Inst* 2015;35(3):2975–82.
- [9] Kalghatgi G, Hildingsson L, Harrison A, Johansson B. Autoignition quality of gasoline fuels in partially premixed combustion in diesel engines. *Proc Combust Inst* 2011;33(2):3015–21.
- [10] Reitz RD, Duraisamy G. Review of high efficiency and clean reactivity controlled compression ignition (RCCI) combustion in internal combustion engines. *Prog Energy Combust Sci* 2015;46:12–71.
- [11] Li Y, Jia M, Liu Y, Xie M. Numerical study on the combustion and emission characteristics of a methanol/diesel reactivity controlled compression ignition (RCCI) engine. *Appl Energy* 2013;106:184–97.
- [12] Li Z, Zhang Y, Huang G, Zhao W, He Z, Qian Y, Lu X. Control of intake boundary conditions for enabling clean combustion in variable engine conditions under intelligent charge compression ignition (ICCI) mode. *Appl Energy* 2020;274:115297.
- [13] Zhao W, Li Z, Huang G, Zhang Y, Qian Y, Lu X. Experimental investigation of direct injection dual fuel of n-butanol and biodiesel on Intelligent Charge Compression Ignition (ICCI) Combustion mode. *Appl Energy* 2020;266:114884.

- [14] Li Y, Jia M, Xu L, Bai X-S. Multiple-objective optimization of methanol/diesel dual-fuel engine at low loads: A comparison of reactivity controlled compression ignition (RCCI) and direct dual fuel stratification (DDFS) strategies. *Fuel* 2020;262:116673.
- [15] Geng P, Yao C, Wang Q, Wei L, Liu J, Pan W, et al. Effect of DMDF on the PM emission from a turbo-charged diesel engine with DDOC and DPOC. *Appl Energy* 2015;148:449–55.
- [16] Xu S, Zhong S, Pang KM, Yu S, Jangi M, Bai X-s. Effects of ambient methanol on pollutants formation in dual-fuel spray combustion at varying ambient temperatures: A large-eddy simulation. *Appl Energy* 2020;279:115774.
- [17] Pachiannan T, Zhong W, Rajkumar S, He Z, Leng X, Wang Q. A literature review of fuel effects on performance and emission characteristics of low-temperature combustion strategies. *Appl Energy* 2019;251:113380.
- [18] Manente V, Johansson B, Cannella W. Gasoline partially premixed combustion, the future of internal combustion engines? *Int J Engine Res* 2011;12(3):194–208.
- [19] Borgqvist P, Tunestal P, Johansson B. Gasoline partially premixed combustion in a light duty engine at low load and idle operating conditions. 2012, SAE 2012-01-0687.
- [20] Borgqvist P, Tunestal P, Johansson B. Comparison of negative valve overlap (NVO) and rebreathing valve strategies on a gasoline PPC engine at low load and idle operating conditions. *SAE Int J Engines* 2013;6(1):366–78.
- [21] Arumugam Krishnan, et.al., Certain investigation in a compression ignition engine using Rice Bran Methyl Ester fuel blends with ethanol additive, *Thermal Science* 21(2017), 1B, pp. 535-542.
- [22] Senthil Ramalingam, Pranesh Ganesan, and Silambarasan Rajendran, 2016. Use of antioxidant additives for NOx mitigation in compression ignition engine operated with biodiesel from annona oil, *Thermal Science*, 20(2016),S4, pp. S967-S972.
- [23] Mark Robert Ellis., Effect of Piston Bowl Geometry on Combustion and Emissions of a Direct Injected Diesel Engine, Ph.D theses, Brunel University School of Engineering and Design (1999), pp. 1-299.
- [24] Gnanamoorthi, V., et.al., Effect of Combustion Chamber Geometry on Performance, Combustion, and Emission of Direct Injection Diesel Engine With Ethanol-Diesel Blend, *Thermal Science*, 20(2016), S4, pp. S937-S946.
- [25] Montajir, R., et al., Fuel spray behavior in a small DI diesel engine: effect of combustion chamber geometry, *SAE Paper* (2000), 2000-01-0946.
- [26] Viswanathan, et al., Studies On Orange Oil Methyl Ester in Diesel Engine with Hemispherical And Toroidal Combustion Chamber, *Thermal Science*, 20 (2016), S4, pp. S981-S989.
- [27] Rajan, K., and K. R. Senthil Kumar., Performance and Emission Characteristics of Diesel Engine with Internal Jet Piston using Biodiesel, *International Journal of Environmental Studies* 67(2010), 4, pp. 557–566.
- [28] Saito, T., et al., Effects of combustion chamber geometry on diesel combustion, *SAE Paper* (1986), 861186.
- [29] Li, J., Effects of piston bowl geometry on combustion and emission characteristics of biodiesel fueled diesel engines, *Fuel* 120(2014), pp. 66–73.
- [30] Prasad, B.V.V.S.U., High swirl-inducing piston bowls in small diesel engines for emission reduction, *Applied Energy* 88 (2011), pp. 2355–2367.
- [31] Jaichandar, S., Annamalai, K., Combined impact of injection pressure and combustion chamber geometry on the performance of a biodiesel fueled diesel engine, *Energy* 55(2013), pp. 330–339.

- [32] Arun Kumar Wamankar, S. Murugan, Combustion, performance and emission characteristics of a diesel engine with internal jet piston using carbon black-water-diesel emulsion, *Energy* 91(2015)1030-1037.
- [33]. S. Jaichandar, K. Annamalai, Effects of open combustion chamber geometries on the performance of Pongamia biodiesel in a DI diesel engine, *Fuel* 98 (2012)272-279.
- [34] B.R. Ramesh Babu, L. Saravanakumar, B. Durga Prasad, Effects of combustion chamber geometry on combustion characteristics of a DI diesel engine fueled with calophylluminophyllum methyl ester, *J. Energy Inst*, (2015) 1-19.
- [35] J. Li, W. M. Yang, H. An, A. Maghbouli, S.K. Chou, Effect of piston bowl geometry on combustion and emission characteristics of biodiesel fueled diesel engines, *Fuel* 120(2014) 66-73.
- [36] B. Harshavardhan, J. M. Mallikarjuna, "CFD analysis of in-cylinder flow and air-fuel interaction on different combustion chamber geometry in DISI Engine," *I. C Engine Laboratory, IIT Madras, IJTARME*, vol. 2, Issue-3 , 2013.
- [37] V. V. Prathiba Bharathi, and G. Prasanthi, "Influence of in-cylinder flow air swirl on diesel engine performance and emission", *IJAET*, vol. 1, pp.113-118. October-December 2011
- [38] Jinou Song, Chunde Yao, Yike Liu, and Zejun Jiang, "Investigation of flow field in simplified piston bowls for DI diesel engine," *State Key Laboratory of Engines, Tianjin University, EACFM*, vol. 2, No. 3, pp. 354-365, 2008
- [39] C. Morley, R. J. Price, N. P. Trait and C. R. McDonald, "Understanding how fuels behave in engines," *Shell Research and Technology Center at Thornton, United Kingdom, The Fourth International Symposium COMODIA 98* , 2008

THERMOSTRUCTURAL AND COMPUTATIONAL FLUID DYNAMICS ANALYSIS OF STEAM BOILER USED IN POWER PLANTS

K Raveena¹ Y. Umashaker²

¹M. Tech (student) Department of Mechanical Engineering, Vaagdevi College of Engineering, Bollikunta, Warangal,506005 (UGC autonomous) approved by AICTE & permanent affiliation to JNTUH, Hyderabad.

²Assistant Professor Department of Mechanical Engineering Vaagdevi College of Engineering, Bollikunta, Warangal,506005 (UGC autonomous) approved by AICTE & permanent affiliation to JNTUH, Hyderabad.

Abstract

Steam boiler is a closed vessel in which water or other fluid is heated under pressure and the steam released out by the boiler is used for various heating applications. In this thesis the steam flow in steam boiler is modeled using SOLIDWORKS parametric design software. The thesis will focus on thermal and CFD analysis with different inlet velocities (10, 25, 35& 45m/s). In this paper, the CFD analysis to determine the heat transfer coefficient, heat transfer rate, mass flow rate, pressure drop. Thermal analysis to determine the temperature distribution, heat flux for models steam boiler with different materials such as EN 31 steel, stainless steel 316L and copper. 3D modeled in parametric software SOLIDWORKS, and analysis done in ANSYS.

Keywords: CFD analysis, SOLIDWORKS, ANSYS.

1. INTRODUCTION

A closed vessel in which the fluid(water) is heated is known as boiler. The liquid doesn't actually bubble. If the plan is not to heat up the liquid, the expression heater is frequently applied in North America. For using in warming applications or different procedures including water warming, focal warming, heater-based force age, cooking, and sanitation the disintegrated liquid or warmed liquid leaves the evaporator. Water-tube heater: In this type, the various potential arrangements are the tubes are burdened up with water and these are arranged inside a heater. Frequently the water tubes interface huge drums, water is contained in lower ones and steam along with water is contained

in upper; in different cases, The water is coursed by a siphon through a succession of curls in mono-tube heater is the example for this sort. The high steam creation rates are most part gives for this sort, however lesser capacity limit than aforementioned. The most commonly favoured in high-pressure applications are Water tube boilers can be intended to misuse any warmth source since inside little breadth pipes the high-pressure water/steam is contained. which can withstand the weight with a slenderer divider. Generally, these boilers are made set up, four-sided fit as a fiddle, and can be various levels high.

Steam Boiler

The outcome is soaked steam at the point when the water is heated up and additionally suggested to as "wet steam." Saturated steam, water smog, carries some unelaborated water as beads while comprising generally. Soaked steam is supportive for some reasons, because for cooking, warming and sanitation, however be situated alluring when steam is relied upon to clearance on verve to apparatus is the example, and a boat's impetus agenda or the "movement" of a steam train is also the example. This is on the grounds that unescapable temperature as well as weight hard luck that happens as steam ventures out from the heater to the hardware will cause some build up, fetching about fluid water being conveyed keen on the apparatus. The water entrained in the steam may harm turbine edges or on account of a responding steam motor, may cause genuine mechanical harm as of hydrostatic lock.

2. METHODOLOGY

The objective of this project is to make a 3D model of the steam boiler and study the CFD and thermal behaviour of the steam boiler by performing the finite element analysis. 3D modeling software (SOLIDWORKS) was used for designing and analysis software (ANSYS) was used for CFD and thermal analysis. The methodology followed in the project is as follows.

- Create a 3D model of the steam Boiler assembly using SolidWorks.
- Convert the surface model into Para solid file and import the model into ANSYS to do analysis.
- Perform thermal analysis on the steam Boiler assembly for thermal loads.
- Perform CFD analysis on the existing model of the surface steam boiler for Velocity inlet to find out the mass flow rate, heat transfer rate, pressure drop.

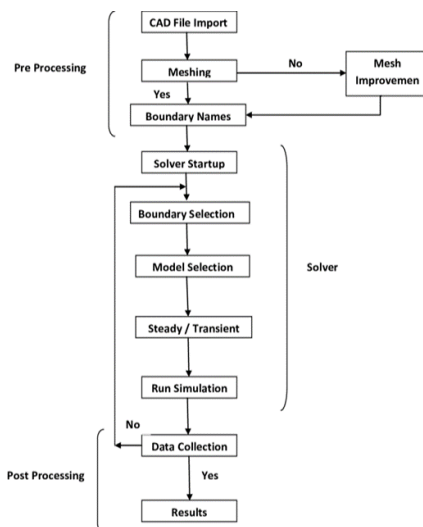


Figure.2.1 Analysis Tree

3. MODELING

To help in the creation, alteration, investigation, or upgrade of a structure computer-aided design (CAD) is used. To grow the productivity of the organizer PC supported writing computer programs were used,

through documentation to improve the idea of arrangement, improve correspondences, and to make a database for accretion. For print, machining, or other gathering assignments helped configuration yield is normally as electronic records. The word CADD (for Computer Aided Design and Drafting) is moreover used. SOLIDWORKS is a abbreviating for Computer Aided Three-Dimensional Interactive Application. Vehicle to purchaser things It is one of the vital 3D programming used by connection in different organizations stretching out from flight, vehicle. SOLIDWORKS is a multi-organize 3D programming set made by Systems, it includes CAD, CAM likewise as CAE. French structure which is Dassault was mammoth dynamic in the field of flying, 3D structures, 3D progressed bogus ups, and thing lifespan the officials (PLM) software design. 2D model of steam boiler

Modelling of Boiler

The Following Design has made using SolidWorks.

Design Dimension According to ASME Standard:

ASME standard values for

Diameter of Tubes = 0.05 m Furnace Plate Thickness = 0.016 m

Dimensions Provided Boiler main shell:

Thickness of the main shell provided = 0.05 m

Diameter of the main shell (I.D.) = 0.89 m provided

Diameter of the main shell (O.D.) = 0.94 m provided

Length of the shell provided = 2 m Fire tubes:

Diameter of the smoke tubes = 0.05 m

Thickness of the smoke tubes = 0.012 m

Length of the smoke tubes = 5 m Tube plate:

Number of the tube plates = 2

Thickness of the tube plate = 0.012 m

Diameter of the tube plate = 0.980 m Reversal

chamber dimensions:

Length of the chamber = 0.280 m Diameter of the

chamber = 0.980 m

Front chamber dimensions:

Length of the chamber = 0.280 m

Diameter of the chamber = 0.980 m

others details:

Volume of the furnace = 0.4099 m³

Volume of main shell = 10 m³

Volume of smoke tubes (30 in no.) = 0.09188 m³

Feed water quantity = 7000kg/hr.

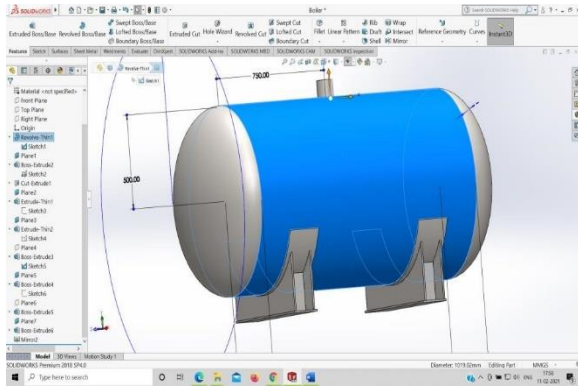


Figure.3.1 Boiler Design in SolidWorks

and Tech Plot as well as to VRML formats were used and also with emphasis on the materials process of industries POLYFLOW (And FIDAP) are also used.

4.1 CFD analysis

In the ANSYS workbench design module Steam boiler were built. It is a counter-flow Steam boiler. First, the fluid flow (fluent) module from the workbench is selected. A new window is opens by the design modeller is as the geometry is double clicked.

→→Ansys → workbench→ select analysis system → fluid flow fluent → double click →→Select geometry → right click → import geometry → select browse→ open part →ok

4. ANALYSIS

FEM/FEA

During the planning stage for the evaluation of complicated structures in a system it is more helpful. With the help of computers and FEA which justifies the cost of the analysis the strength and design of the model can be improved. The design of the structures was prominently increased by FEA that were built many years ago.

CFD

CFD is usually abbreviated as Computational Fluid Dynamics, it is a branch of fluid mechanics to solve and analyze problems that involve fluid flows that uses numerical methods and algorithms. a qualitative (and sometimes even quantitative) estimation of fluid flows was provided by Computational Fluid Dynamics (CFD) by means of Mathematical modelling (partial differential equations) Numerical methods (discretization and solution techniques) Software tools (solvers, pre- and post-processing utilities) A software package known FLUENT is a computational fluid dynamic that is used to pretend fluid flow problems. such as Fluent, Ansys CFX, ACE, these are the variety of commercial CFD software's which are available and as well as a wide range of suitable hardware and associated costs, dependent on the complication of the mesh and size of the calculation's FLUENT exports CFD's data to third-party postprocessors and visualization tools such as Insights A wide range of fields such as Field view

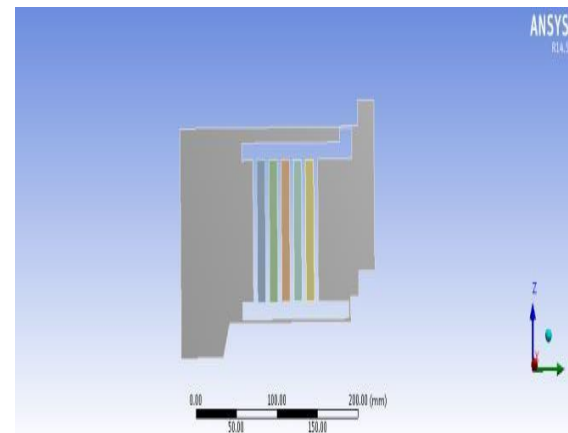


Figure.4.1.1 Surface Model

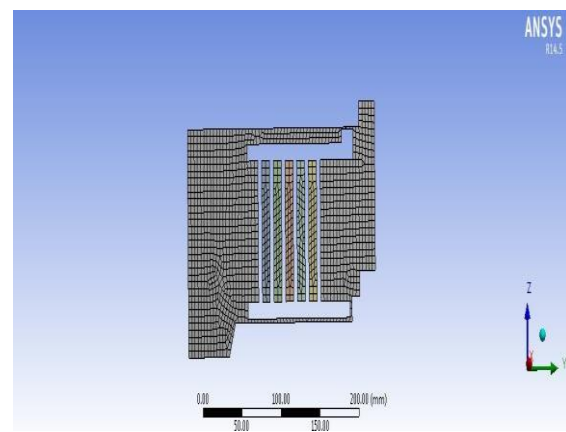


Figure.4.1.2 Meshed Model

With the help of SOLIDWORKS the model is designed and for Meshing and analysis it is imported

on ANSYS. In order to calculating pressure profile and temperature distribution the analysis of CFD is used. The fluid ring is divided into two connected volumes for meshing, then all the thickness edges were meshed with 360 intervals. The total number of nodes and elements is 6576 and 3344 for these a tetrahedral structure mesh is used
 Condition: Inlet velocity-40 m/s

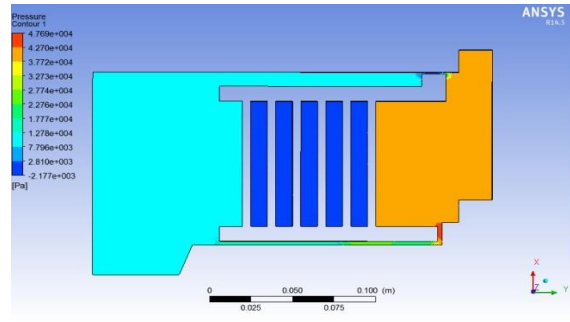


Fig.4.1.3 Pressure Contour

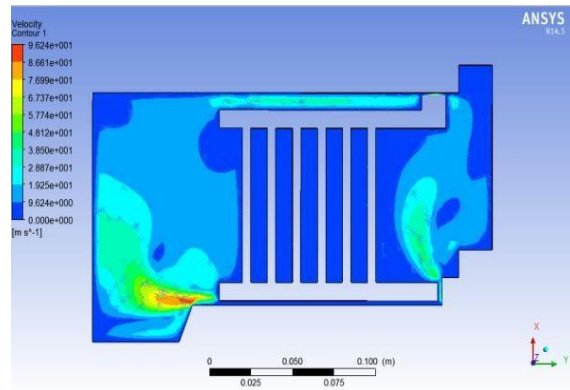


Figure.4.1.4 Velocity Contour

Total Heat Transfer Rate	(w)
steam_outlet	-143318.86
wall-fluegas	0
wall-split.2	-0.0010746096
water_inlet	224623.13
Net	81304.265

4.2 Thermal Analysis

Used Materials steel, copper, brass & stainless steel
 Copper material for tube

EN 31 Steel, brass & stainless steel 316L for boiler casing

Copper material properties

- Thermal conductivity = 385w/m-k
- Specific heat = 0.385j/g⁰C
- Density = 0.00000776kg/mm³

Steel material properties

- Thermal conductivity = 93.0w/m-k
- Specific heat = 0.669j/g⁰C
- Density = 0.0000075kg/mm³

Stainless Steel material properties

- Thermal conductivity = 34.3w/m-k
- Specific heat = 0.620j/g⁰C
- Density = 0.00000901kg/mm³

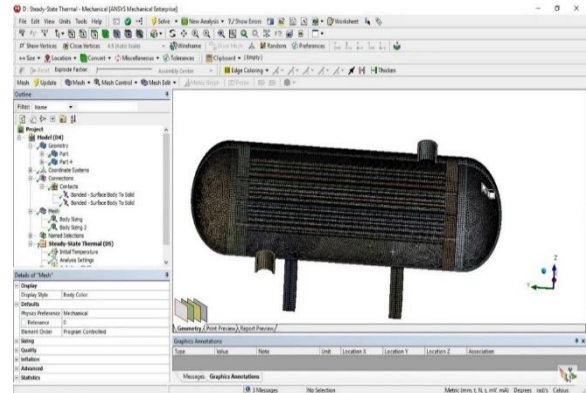


Figure.4.2.1 Meshed Model

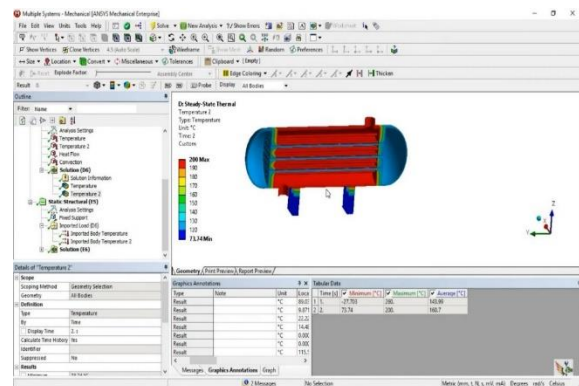


Figure.4.2.2 Temperature

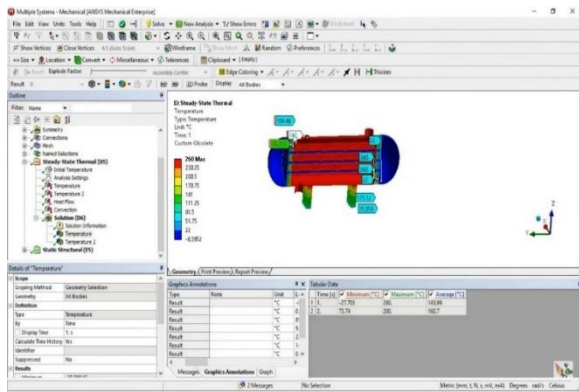


Figure.4.2.3 Heat Flux

As because of the steam passing inside of the tube the temperature distribution is maximum temperature according to the counter plot. For this reason, we are applying except inside the tubes then the temperature inside of the tube and applying the convection. Then the maximum temperature at tubes and minimum temperature at steam boiler casing.

5. RESULTS AND DISCUSSION

Velocity (m/s)	Pressure (Pa)	Velocity (m/s)	Mass flow rate (kg/s)	Heat transfer Rate(W)
20	4.53e+02	3.86e+01	0.04368	21801.56836
35	1.58e+04	5.14e+01	0.11344	5333.06641
45	3.02e+03	7.80e+01	0.15708	7213.41797
50	4.76e+03	9.62e+01	0.19678	9755.03906

Table.5.1 CFD Results

Materials	Temperature Deg C	Heat Flux
Mild Steel	103.82	7.3251
Stainless steel	104.14	19.221
Copper	104.26	50.672

Table.5.2 Thermal Results

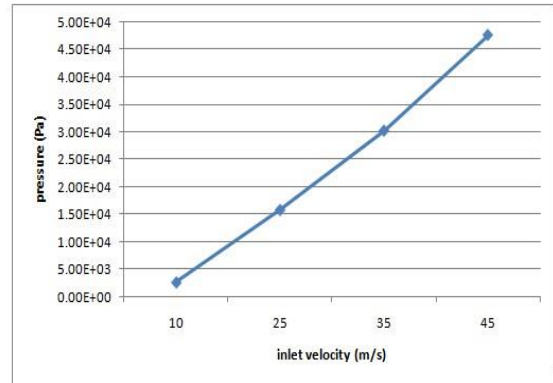


Figure.5.1 Inlet Velocity vs Pressure

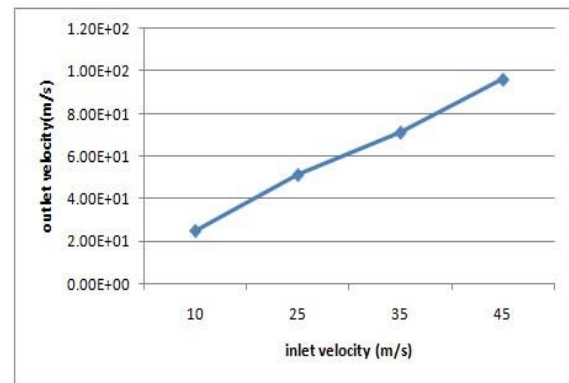


Figure.5.2 Inlet Velocity vs Outlet Velocity

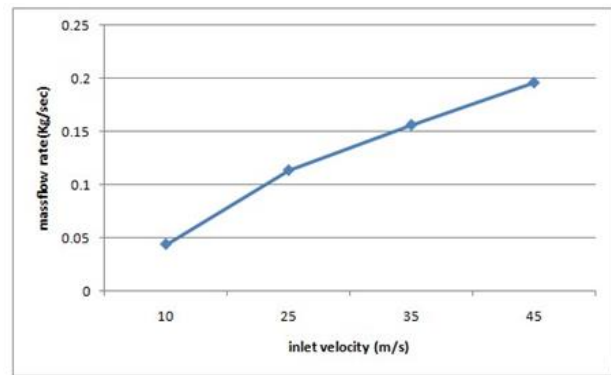


Figure.5.3 Mass Flow Rate

1. A plot between maximum pressure and velocities by FEA approach is shown in above fig.5.1 From the plot the variation of

maximum static pressure is observed. Maximum static pressure increases with increases in velocities.

2. A plot between maximum velocity and velocities by FEA approach is shown in above fig.5.2 From the plot the variation of maximum static velocity is observed. Maximum velocity increases with increases in velocities.
3. A plot between maximum mass flow rate and velocities by FEA approach is shown in above fig.5.3 From the plot the variation of maximum mass flow rate is observed. Maximum mass flow rate increases with increases in velocities.

6. CONCLUSION

In this work, the steam boiler is modelled using SOLIDWORKS design software is implemented. The thesis will focus on thermal and CFD analysis with different velocities (20, 25, 45 & 50m/s). Thermal analysis done for the steam boiler by steel, stainless steel & copper. By observing

1. In the CFD analysis the pressure drops, velocity, heat transfer coefficient, mass flow rate & heat transfer rate increases by increasing the inlet velocities.
2. In the thermal analysis, the taken heat transfer coefficient values are from CFD analysis. Heat flux value is more for copper material than steel & stainless steel.
3. According to the above contour plot, the maximum heat flux is 7.362 w/mm^2 and minimum heat flux is 0.8229 w/mm^2 .
4. Maximum velocity, Static pressure, Mass flow Rate, Heat Transfer Rate, and Heat Flux increases with increases in velocities.

REFERENCES

- [1]. A. Dehbi and H. Badreddine, "CFD prediction of mixing in a steam generator mock-up: Comparison between full geometry and porous medium approaches", *Annals of Nuclear Energy*, Volume 58, August 2013, pp 178–187
- [2]. Xinyu Wei et.al, "Primary fluid optimization in once-through steam generator", *Applied Thermal Engineering*, Volume 31, Issues 17–18, December 2011, pp 3979–3988
- [3]. Falah Alobaid et.al, "Fast start-up analyses for Benson heat recovery steam generator", *Energy*, Volume 46, Issue 1, October 2012, pp 295–309
- [4]. Xinyu Wei et.al, "Inner tube optimization of double-tube once-through steam generator", *International Journal of Heat and Mass Transfer*, Volume 59, April 2013, pp 93–102
- [5]. Sanaz Naemi et.al, "Optimum design of dual pressure heat recovery steam generator using non-dimensional parameters based on thermodynamic and thermo economic approaches", *Applied Thermal Engineering*, Volume 52, Issue 2, 15 April 2013, pp 371–384
- [6]. Emmanuelle Martelli et.al, "Numerical optimization of steam cycles and steam generators designs for coal to FT plants, *Chemical Engineering Research and Design*", Volume 91, Issue "8, August 2013, pp 1467–1482
- [7]. dipak k. sarkar, gas turbine and heat recovery steam generator, *Thermal Power Plant, Design and Operation* 2015, pp239–283
- [8]. Antonio Rovira et.al, "A model to predict the behaviour at part load operation of once-through heat recovery steam generators working with water at supercritical pressure", *Applied Thermal Engineering*, Volume 30, Issue 13, September 2010, pp 1652–1658
- [9]. Lei Chen et.al, "Multi-objective optimal design of vertical natural circulation steam generator", *Progress in Nuclear Energy*, Volume 68, September 2013, pp79–88

- [10]. Falah Alobaid et.al, “Numerical and experimental study of a heat recovery steam generator during start-up procedure”, *Energy*, Volume 64, 1 January 2014, pp 1057–1070
- [11]. Jianli Hao et.al, “Scaling modeling analysis of flow instability in U-tubes of steam generator under natural circulation”, *Annals of Nuclear Energy*, Volume 64, February 2014, pp 169–175
- [12]. Joshua Tanner Olson et.al, “Tube and shell side coupled thermal analysis of an HTGR helical tube once through steam generator using porous media method”, *Annals of Nuclear Energy*, Volume 64, February 2014, pp 67–77
- [13]. Hongcui Feng et.al, “Thermodynamic performance analysis and algorithm model of multi-pressure heat recovery steam generators (HRSG) based on heat exchangers layout”, *Energy Conversion and Management*, Volume 81, May 2014, pp 282–289
- [14]. Xinyu Wei et.al, “Study on the Structure Optimization and the Operation Scheme Design of a Double-Tube Once-Through Steam Generator”, *Nuclear Engineering and Technology*, Available online 10 March 2016

DESIGN AND HEAT TRANSFER ANALYSIS OF SOLAR POND

Divya sree Dunnala ¹

P.Raju ²

¹M.Tech (Thermal Engineering)Department of mechanical engineering vaagdevi college of engineering (UGC autonomous) approved by AICTE & permanent affiliation to jntuh, hyderabad.p.o, bollikunta, Warangal urban-506005.

²Assistant Professor Department of mechanical engineering vaagdevi college of engineering (UGC autonomous) approved by AICTE & permanent affiliation to jntuh, hyderabad. p.o, bollikunta, Warangal urban- 506005.

ABSTRACT: The use of renewable energy sources such as solar energy is the only long term solution to the present global energy crisis. This project reviews non-convective solar pond, a potential large surface area solar collector device with an additional advantage of long term storage capacity of thermal energy .It is a shallow body of water of about a 17 centimeter deep containing dissolved salts like NaCl and fresh water to generate a stable density gradient (fresh water on top and denser salt at the bottom).Part of the incident solar radiation entering the pond is absorbed leading to temperatures near 1000C without convection due to the density gradient . Here we are obtaining the temperature about 600 °C.

The hot salt water can be used to drive turbine and electric generator with the use of suitable fluids, provision of process hot water for industrial and commercial purposes, space heating, air conditioning and hot water needs of community or individual apartment.

1. INTRODUCTION

Solar pond provides thermal energy at low temperatures on continuous basis and hence is usually designed as an energy system with 100% solar traction. The pond's output depends on the quantity and quality of the energy stored which in turn depends on the depth of the storage zone (LCZ) and the collecting surface area apart from the local metrological factors and pond's operating characteristics. Earlier studies have pointed out that there is no single exact method available for the design of the pond matching the given load. However, the estimation of rate of energy collected per unit pond area based on the R N model from which the estimation of collector area matching the demand loads. The sizing of the gradient or non-convective zone (NCZ) plays an important role in the performance of the solar pond. The increase in NCZ thickness provides higher quality energy in terms of temperature stored in LCZ by reducing the top heat loss. However, increase in NCZ thickness reduces the fraction of radiation reaching LCZ thereby decreasing the quantity of energy stored. At Optimum NCZ thickness, the reduction in radiation input matches the reduced heat loss when the pond

collection efficiency will be maximum. The present study deals with the determination of optimum thickness of NCZ by matching with the fraction of insulation reaching the LCZ. Many theoretical investigations show that decrease in NCZ thickness results in increased heat loss, lower temperature and lower collection efficiency. These studies have also shown that increase in NCZ thickness from the optimum value results in lower efficiency. So it is imperative that the optimum thickness of NCZ needs to be determined for maximizing the pond collection efficiency. Apart from these, studies have shown that the optimum thickness of NCZ also depends on local available solar isolation, temperature of operation and pond clarity. Results from earlier studies both theoretical and model simulation shown that the optimum thickness of NCZ ranges from 1.0 to 1.5m. In the present work an attempt is made to fix the optimum thickness of NCZ using the one dimensional three zone pond model. The performance of a solar pond is also influenced by the daily seasonal and intermittent effects of temperature gradient, salinity gradient, ambient temperature fluctuation, solar isolation, evaporation rate, surface wind and rainfall both at the free surface as well as at its interface with the gradient zone. A thin top convective layer (UCZ) will result in unstable UCZ-NCZ boundary and a thicker UCZ will result in reduced fraction of radiation reaching the storage zone. Hence the optimum thickness of UCZ needs to be fixed based on the pond operating temperature, ambient conditions and the intensity of solar isolation available locally.

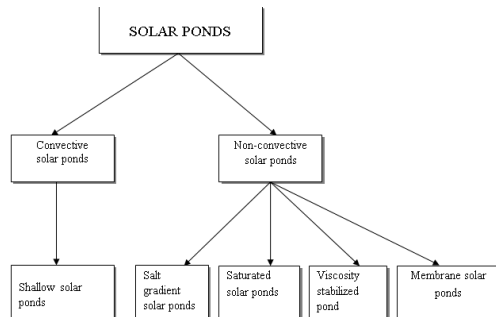


Fig 1.Types of solar pond

2. LITERATURE REVIEW

Hawllader and Brinkworth discussed on the thermal behavior of the non-convecting solar pond. They developed numerical solution for the dynamic equations, incorporating detailed representation of the losses from the surface and using the hourly meteorological data for a site in Southern England. They showed that the pond temperatures are strongly dependent on the effective extinction coefficient for solar radiation and the thermal losses from the pond bottom.

Wang and Akbarzadeh presented the optimum thickness of the density gradient layer under various conditions and also discussed on the effect of ground losses for wet soil where underground water level is high. Akbarzadeh discussed the effect of sloping walls on the salt concentration profile in solar ponds. He also obtained the general expression for salt concentration as a function of depth and presented the results for different pond configurations and also for different top and bottom salt concentration. Hillel Rubin, Barry A. Benedict and Stefan Bachu, have applied a finite difference implicit model in order to investigate the interaction among physical variables represented by various dimensionless parameters by considering that the convection currents in the pond are inhibited by salinity distribution. Hull et al modeled the ground heat losses for various perimeter insulation strategies and several pond sizes. They concluded that the un insulated sloping sidewalls are slightly more effective than insulated vertical sidewalls, except for very small ponds.

Ebtism Wilkins et. al discussed about the inherent problems encountered with the conventional salt gradient pond leading to the concept of the Solar Gel Pond in which the salt gradient is replaced by the transparent gel layer. They discussed about the relevant properties of the gel. Mehta et al. analyzed the performance of a bittern-based solar pond of an area of 1600 m² located at Bhavnagar, India. The

thermal efficiency of the pond was worked out using correlations proposed by Kooi and Hull. Newell et al. reported on the construction and operation activities at the University of Illinois salt gradient solar pond. Tabor and Dorbon reported on the design, construction and operational experiences of a 5 MWe solar pond power plant.

Ebtism Wilkins discussed the design, construction and operation of trapezoidal 400 m² and 5 m deep gel pond. The pond obtained maximum temperature of 60⁰ C with optimal gel thickness of 60 cm. Sherman and Limburger discussed on the control strategies designed to provide successful high temperature operation of a solar pond year round. They tested the Alice Springs solar pond and were able to maintain temperature in excess of 85⁰ C for several months. Zangrando discussed on the hydrodynamic issues like mass and energy balance; formation, stability, and maintenance of the gradient layer; energy extraction from the bottom mixed layer; stability of stratified fluids to shearing flows; interface dynamics; and wall effects that affect the performance of the solar pond as an energy collector and storage. Jaefarzadeh, reported on the performance of a laboratory scale salt gradient solar pond for different methods of saline injection to the bottom layer and the corresponding temperature and concentration profiles as a function of depth has been reviewed and compared with experimental results.

3. METHODOLOGY

Ponds are frequently human constructed. In the countryside farmers and villagers dig a pond in their backyard or increase the depth of an existing pond by removing layers of mud during summer season. A wide variety of artificial bodies of water are classified as ponds. Some ponds are created specifically for habitat restoration, including water treatment.

- Normal ponds receive sunlight a part of which is reflected at the surface, a part is absorbed and the remaining is transmitted to the bottom
- Due to this the lower part gets heated up and the density decreases as a result of which it rises up and convection currents are set up.
- As a result, the heated water reaches top layer and loses its heat by convection and evaporation.

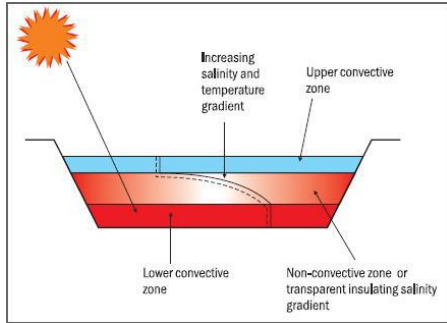


Fig 2. Different layers in Solar pond

WORKING OF SOLAR POND

A solar pond is a mass of shallow water about 1 or 2 meters deep with a large collection area, which acts as a heat trap. It contains dissolved salts to generate a stable density gradient.

Part of the incident solar radiation entering the pond surface is absorbed throughout the depth and the remainder which penetrates the pond is absorbed at the black bottom. If the pond were initially filled with fresh water, the lower layers would heat up, expand and rise to the surface. Because of the relatively low conductivity, the water acts as an insulator and permits high temperature (over 900C) to develop in the bottom layers. At the bottom of the pond, a thick durable plastic layers liner is laid. Materials used for liners include butyl rubber, black polyethylene and hypalon reinforced with nylon mesh. Salts like magnesium chloride, sodium chloride or sodium nitrate are dissolved in the water, the concentration varying from 20 to 30 percent at the bottom to almost zero at the top.



Fig 3. Construction of solar pond

INTRODUCTION TO FEA

Finite element analysis is a method of solving, usually approximately, certain problems in

engineering and science. It is used mainly for problems for which no exact solution, expressible in some mathematical form, is available. As such, it is a numerical rather than an analytical method. Methods of this type are needed because analytical methods cannot cope with the real, complicated problems that are met with in engineering.

4.ANSYS

ANSYS is general-purpose finite element analysis (FEA) software package. Finite Element Analysis is a numerical method of deconstructing a complex system into very small pieces (of user-designated size) called elements. The software implements equations that govern the behaviour of these elements and solves them all; creating a comprehensive explanation of how the system acts as a whole.

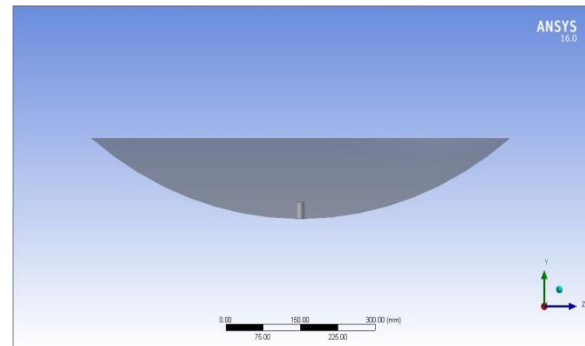


Fig 4. Design of solar pond in ANSYS Geometry

5% NaCl+Water					
Temp	Density	Sp. Heat	Thermal Conductivity	Dy Viscosity	
C	kg/m ³	kJ/kg K	W/m K	kg/m.s	
10	1040.251	3.916	0.586	0.00198	
20	1036.604	3.923	0.601	0.00124	
30	1032.650	3.930	0.615	0.00088	
40	1028.376	3.935	0.627	0.00075	
50	1023.768	3.940	0.638	0.00067	
60	1018.815	3.945	0.648	0.00062	
70	1013.502	3.951	0.656	0.00058	

10% NaCl+Water					
Temp	Density	Sp. Heat	Thermal Conductivity	Dy Viscosity	
C	kg/m ³	kJ/kg K	W/m K	kg/m.s	
10	1079.32	3.69	0.58	0.00221	
20	1075.11	3.70	0.60	0.00135	
30	1070.69	3.71	0.61	0.00096	
40	1066.04	3.72	0.62	0.00083	
50	1061.14	3.73	0.64	0.00076	
60	1055.99	3.73	0.65	0.00072	
70	1050.56	3.74	0.65	0.00070	

Fresh Water					
Temp	Density	Sp. Heat	Thermal Conductivity	Dy Viscosity	
C	kg/m ³	kJ/kg K	W/m K	kg/m.s	
10	998.609	4.191	0.580	0.00131	
20	997.115	4.189	0.598	0.00100	
30	994.637	4.188	0.615	0.00080	
40	991.282	4.188	0.630	0.00065	
50	987.147	4.189	0.643	0.00055	
60	982.317	4.190	0.654	0.00047	
70	976.867	4.193	0.663	0.00040	

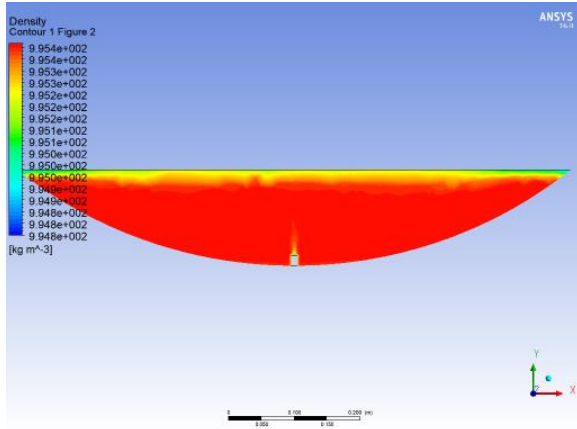
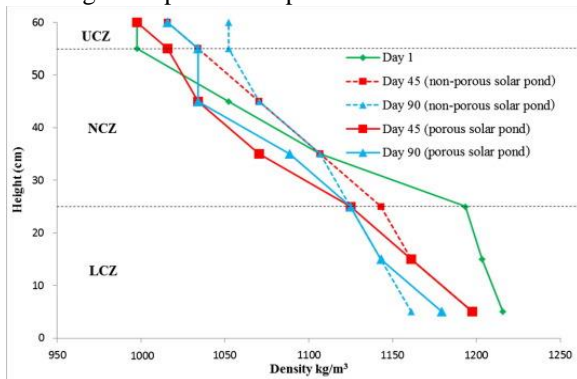


Fig 5. Density mixture in plane

The above figure shows the density variation in the salt mixture poured in the pond, as the red indicates high density and blue indicates lesser density and the remaining colors will represent their value of density.

The diagram represents in plane at middle.



Graph: Density and height variation graph

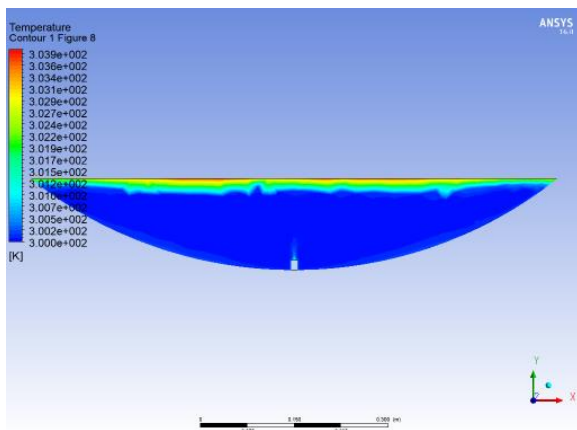


Fig 6. Temperature distribution in plane

The above figure shows the Temperature difference in the salt mixture poured in the pond, as the red indicates high temperature and blue indicates low temperature and the remaining colors will represents their value of different temperature regions.

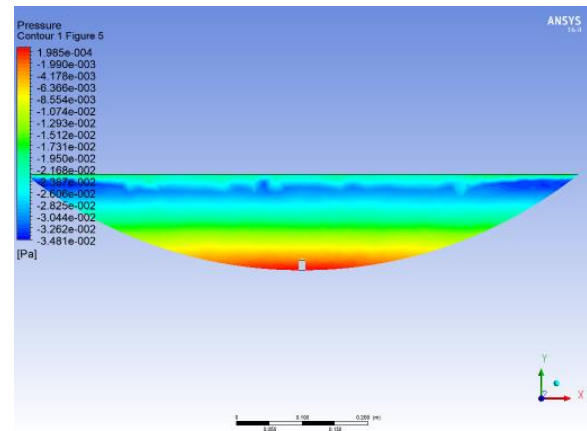


Fig 7. Pressure variation in plane

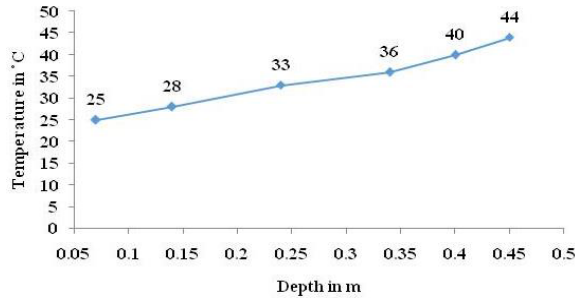
The above figure shows the pressure difference in the salt mixture poured in the pond, as the red indicates high pressure and blue indicates lesser pressure and the remaining colors will represents their value of different in pressure in regions.

5. RESULTS AND DISCUSSIONS

Temperature distribution of solar pond using salt (NaCl):

The temperature distribution of the solar pond using salt (NaCl) shows the change of temperature with time in the experiment. The temperatures are measured at 10'o clock, near the highest temperature. We can see that the temperature increases with time running and reaches steady state temperature about 5 days later and the solar pond as reached stable working conditions. The highest temperature is 62°C occurs on the 6th day may be lying on the top part of the LCZ. In general, the trend of measured temperature is well represented by the model and the temperature increased with depth and the highest temperature is appeared around the top of LCZ. The maximum temperature error is about 1.7°C which appears on the middle of UCZ. The change of temperature goes on increasing according to the time and depth of the solar pond. Temperature of the upper convective zone (UCZ) is normal to the atmospheric temperature. In the non-convective zone

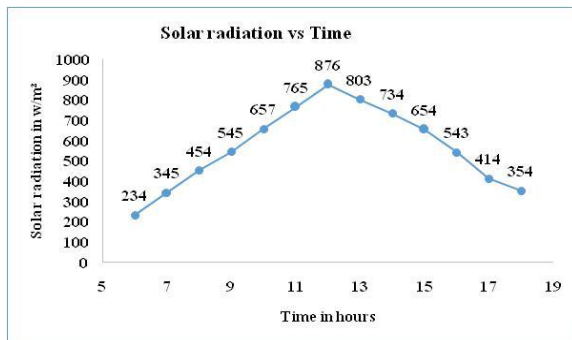
(NCZ), the temperature goes on increasing according to the time and solar radiation. In the lower convective zone (LCZ) where the high temperature is obtained is stored by the salt (NaCl) is used for further purpose



Graph: Temperature distribution vs Depth

Temperature distribution of the trapezoidal solar pond

The graph shows the result of the temperature changing with time and depth. The stimulation starts at 6'o clock in the morning and finished at 6'o clock in the evening. The overall temperature is significant increased by solar radiation. Each day, temperature will get increased mostly in 12'o clock.



Graph: Temperature distribution throughout the day

Fortunately, we can see the drop of the temperature is very small during the night, because the heat stored in the pond mainly concentrates in the LCZ due to the thermal protection function of the side wall and the isolation function of NCZ. Therefore, the solar pond can maintain good performance of heat storing even during the night. It can have been seen that temperature of solar pond does not always increase with time, because the radiation observed by the solar pond is lower than the heat loss and it led to the reduction in overall temperature. The overall temperature of the solar pond is increasing with the time running, the top temperature of each day occurs near the 12'o clock and the highest temperature

reaches to 62°C. The temperature of NCZ increases linearly with the depth. The upward trend in temperature is most obvious in the superior part of LCZ, because the heat loss caused by the low temperature surrounding limits the temperature increasing at the bottom of LCZ. We can conclude that the heat stability of the interfaces in solar pond is determined by temperature gradient.

6.CONCLUSION

This study has utilized Three-dimensional study state model to predict the performance of a salinity gradient solar pond in sunny climates. A specially designed code has been developed utilizing a predicted equation to use a single input data for calculating the solar radiation at any sunny part in the world with a good result. The monthly averaged daily solar irradiation methods have been used for these computations. Predicting the solar pond performance in a cold climate has been investigated and a comparison solar pond in terms of the input heat and the major heat loss. Coupling the salinity gradient solar pond with multi-effects desalination plant for a large pond has been studied. The following results have been concluded:

- 1.Salt gradient solar pond technology is ideally suited to arid and semi-arid areas owing to the abundance of solar radiation, the thermal energy from which can then be employed to generate power for desalination purposes. Coupling a solar pond with a desalination unit could assist in addressing the single major issue in such areas, that of providing fresh potable water to the inhabitants. This combination could also work efficiently in cold climate countries to provide space heating.
- 2.As expected, the greatest heat loss from the upper layer is a result of evaporation heat, and therefore covering the solar pond could significantly reduce this loss and may even improve the solar pond's performance. It has been found that covering an SGSP can raise the average temperature by 30%, i.e., from 76.60 C to 100 C, for example. The thickness of each of the three layers in a solar pond is critical to its performance, and must be carefully determined. It has been proved that the upper Convecting zone should be 0.2-0.3m, the non-Convecting gradient zone around 1m and the lower Convecting storage zone 0.3-1m.
- 3.The cleanliness and transparency of a solar pond is also an extremely important issue, as impurities in the saline solution may scatter the solar radiation, thereby reducing the efficiency of the storage zone, which is certain to reduce the solar pond's performance.

REFERENCES

1. IMPORTANCE OF SOLAR POND, international journal of engineering sciences & research technology, Reshmi Banerjee, Page 2-5.
2. NON CONVENTIONAL ENERGY SOURCES: SOLAR POND, International Journal of Students Research in Technology & Management , Tejas Gawade, Varun Shinde, Ketan Gawade, Page 156-158.
3. A NOTE ON SIGNIFICANCE OF SOLAR POND TECHNOLOGY FOR POWER GENERATION, International Journal of Physical and Mathematical Sciences, Donepudi Jagadish, Page 596-597.
4. PERFORMANCE OF SOLAR POND GREENHOUSE HEATING SYSTEM IN JORDAN, IOSR Journal of Mechanical and Civil Engineering, Aiman Al Alawin, Page 30-31.
5. EXPERIMENTAL INVESTIGATION ON A SOLAR GEL POND, International Journal of Innovative Research in Science, Engineering and Technology, N Sozhan, T Senthilvelan, T Kaliyappan, E Vijayakrishna Rapaka, Page 1-3.
6. EXPERIMENTAL ANALYSIS OF SALT GRADIENT SOLAR POND WITH AND WITHOUT USING A TRANSPARENT SEPARATOR (GLASS) ABOVE LOWER CONVECTIVE ZONE, SSRG International Journal of Mechanical Engineering, Gautam saini¹, Ankur agrawal², Mitesh Varshney³, Nirupam Rohatgi, Page 5-6.
7. PARAMETRIC DESIGN STUDY OF SALT GRADIENT SOLAR POND, International Journal of Scientific & Engineering Research, G. S. Gunasegarane, Page 1-4.
8. SOLAR POND TECHNOLOGY, International Journal of Engineering Research and General Science, G.M.R. ISTITUTE OF TECHNOLOGY, KARAKAVASAGOUTHAM, CHUKKASIVA KRISHNA, Page 1-3 and 9.
9. RELATIVE STUDY OF STEEL SOLAR POND WITH SODIUM CHLORIDE AND PEBBLES, Materials Science for Energy Technologies, D Sathish, S Jegadheeswaran, Pages 171 – 174.

DESIGN AND HEAT TRANSFER ANALYSIS OF PARABOLIC SHAPED SOLAR DISC COLLECTOR

Madasu Purna Chandar ¹

Dr . Sanjeev Kumar sajjan ²

¹M.Tech (Thermal Engineering)Department of mechanical engineering vaagdevi college of engineering (UGC autonomous) approved by AICTE & permanent affiliation to jntuh, hyderabad.p.o, bollikunta, Warangal urban- 506005.

²Assistant Professor Department of mechanical engineering vaagdevi college of engineering (UGC autonomous) approved by AICTE & permanent affiliation to jntuh, hyderabad. p.o, bollikunta, Warangal urban- 506005.

Abstract

Solar thermal energy collector can be described as an energy balance between the solar energy absorbed by the collector and the thermal energy removed or lost from the collector. If no alternative mechanism is provided for removal of thermal energy, the collector receiver heat loss must equal the absorbed solar Energy.

These paper will focus on thermal and CFD analysis with different fluid air, water and different solar collector's i.e flat plate and parabolic trough was modeled by using CREO design software. Thermal analysis has done one the solar collectors with different materials (aluminum & copper). These values are taken from CFD analysis. Furthermore, CFD analysis to determine the heat transfer coefficient, heat transfer rate, mass flow rate, pressure drop and thermal analysis to determine the temperature distribution, heat flux with different materials.

Key words: Flat plate, parabolic trough, CFD, CREO.

I.INTRODUCTION

A parabolic trough is a type of solar thermal energy collector. It was constructed as a long parabolic mirror (usually Coated silver or polished aluminum) with a Dewar tube running its length at the focal point. Sunlight is reflected by The mirror and concentrated on the Dewar tube. The trough is usually aligned on a north-south axis, and rotated to track the sun as it moves across the sky each day. Alternatively the trough can be aligned on an east-west axis; this reduces the overall efficiency of the collector, due to cosine loss, but only requires the trough to be aligned with the change in seasons, avoiding the need for tracking motors. This tracking method works correctly at the spring and fall equinoxes with errors in the focusing of the light at other times during the year (the magnitude of this error varies Throughout the day, taking a minimum value at solar noon). There is also an error introduced due to the daily motion of the sun across the sky, this error also reaches a minimum at solar noon. Due to these sources of error, seasonally Adjusted

parabolic troughs are generally designed with a lower solar concentration ratio.

A. Flat Plate Collectors

These collectors consist of airtight boxes with a glass, or other transparent materia, 1 cover. There are several designs on the arrangement of the internal tubing of flat plate collectors as shown in Figure 1.

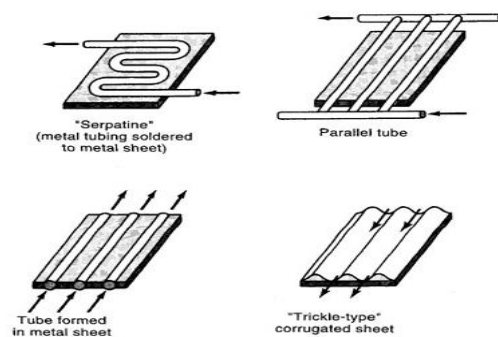


Figure 1 Internal tubing arrangement in flat plate collectors (copyright Saunders College Publishing)

Fig.1.internal tubing arrangement in flat plate collectors

Traditional collectors, like the Serpentine and Parallel tube examples above, consist

of a number of copper tubes, known as risers that are orientated vertically with respect to the collector and placed in thermal contact with a black colored, metal absorbing plate. The use of selective surfaces on absorbers improves the efficiency of solar water heaters significantly due to a very high absorbance (percentage of incoming energy that a material can absorb) and low remittance (percentage of energy that a material radiates away) of electromagnetic radiation. At the top and bottom of the metal absorbing plate, thicker copper pipes, known as headers, assist in the removal of heated water and the arrival of colder water to be heated. Insulation is placed between the absorbing plate and the external wall to prevent heat losses.

Whilst the principles of operation for flat plate collectors are fairly consistent, significant improvements in the design of systems, particularly absorber plates have occurred. Flooded plate collectors are similar to their tubed cousins, except that two metal absorbing plates are sandwiched together, allowing the water to flow through the whole plate. The increased thermal contact results in significant improvements in the efficiency of the system. In recent years, much research has been conducted on selective surfaces, which has seen significant improvements in the efficiency of solar water heaters. Today, a majority of absorber plates are composed of solar selective surfaces, made of materials that strongly absorb electromagnetic radiation (i.e. sunlight) but only weakly emit.

II. LITERATURE REVIEW

A Novel Parabolic Trough Concentrating Solar Heating for Cut Tobacco Drying System.[1] A novel parabolic trough concentrating solar heating for cut tobacco drying system was established. The opening width effect of V type metal cavity absorber was investigated. A cut tobacco drying mathematical model calculated by fourth-order Runge-Kutta numerical solution method was used to simulate the cut tobacco drying process. And finally the orthogonal test method was used to

optimize the parameters of cut tobacco drying process. The result shows that the heating rate, acquisition factor, and collector system efficiency increase with increasing the opening width of the absorber. The simulation results are in good agreement with experimental data for cut tobacco drying process.

Design, Fabrication and Experimental Testing of Solar Parabolic Trough Collectors with Automated Tracking Mechanism.[2]

This paper was concerned with an experimental study of parabolic trough collector's with its sun tracking system designed and manufactured. To facilitate rapid diffusion and widespread use of solar energy, the systems should also be easy to install, operate and maintain. In order to improve the performance of solar concentrator, different geometries and different types of reflectors were evaluated with respect to their optical and energy conversion efficiency. To assure good performance and long technical lifetime of a concentrating system, the solar reflectance of the reflectors must be high and long term stable.

Development of a Compound Parabolic Solar Concentrator to Increase Solar Intensity and Duration of Effective Temperature.[3] For efficient drying of product through indirect drying method, a compound parabolic concentrator (CPC) was installed. Six numbers of semi-cylindrical parabolic concentrators were interpolated on are Receiver plate for direct conversion of solar energy to thermal energy by trapping the maximum incident rays into metallic tubes which were placed on focus lines of the parabolas. Experiments were carried to study the comparative performance of a solar flat plate collector and compound parabolic concentrator of same size.

Dehydration of Persimmon by Concentrating Parabolic Trough Solar Air

Heater.[4] Parabolic Trough Solar (PTS) air heater was developed locally to solve the drying of persimmon with a parabolic trough and a drying box which contains a reflected steel sheet, an absorber tube, an angle iron and a fully insulated home script refrigerator. Solar irradiance results were noted for the months of Oct- Dec, 2012. Four air mass flow rates were conducted with one natural flow rate of 0.53 kg minute⁻¹ (M-1) and three convective air mass flow rates of 1.35 kg M-1, 1.87 kg M-1 and 1.97 kg M-1 respectively.

III. SOFTWARES USED IN PARABOLIC SOLAR TROUGH AND FLAT PLATE COLLECTORS

PTC CREO, formerly known as Pro/ENGINEER, is 3D modeling software used in mechanical engineering, design, manufacturing, and in CAD drafting service firms. It was one of the first 3D CAD modeling applications that used a rule-based parametric system. Using parameters, dimensions and features to capture the behavior of the product, it can optimize the development product as well as the design itself.

The name was changed in 2010 from Pro/ENGINEER Wildfire to CREO. It was announced by the company who developed it, Parametric Technology Company (PTC), during the launch of its suite of design products that includes applications such as assembly modeling, 2D orthographic views for technical drawing, finite element analysis and more.

PTC CREO says it can offer a more efficient design experience than other modeling software because of its unique features including the integration of parametric and

direct modeling in one platform.

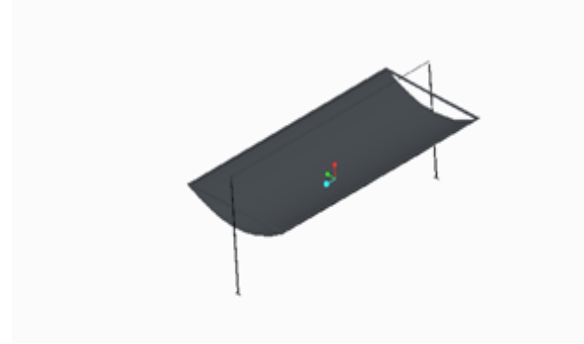


Fig:2 3D model of parabolic trough
Diameter of parabolic trough-225mm
Length -1115mm
Stand height- 400 mm

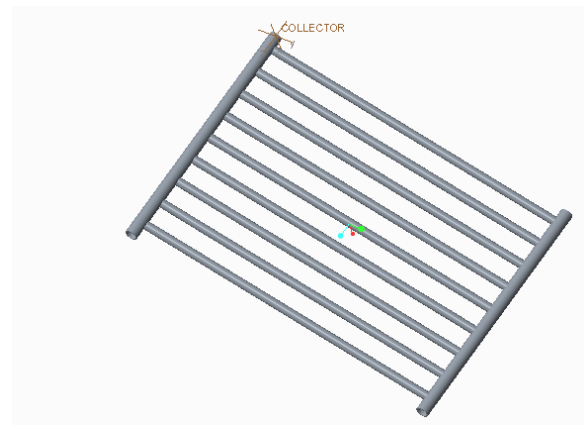


Fig: 3 3d Models of Flat plate collector

Diameter of tube-30mm
Length -1005mm
Thickness -6mm
A.ANSYS

ANSYS is capable of both steady state and transient analysis of any solid with thermal boundary conditions. Steady-state thermal analyses calculate the effects of steady thermal loads on a system or component. Users often perform a steady-state analysis

before doing a transient thermal analysis, to help establish initial conditions. A steady-state analysis also can be the last step of a transient thermal analysis; performed after all transient effects have diminished. ANSYS can be used to determine temperatures, thermal gradients, heat flow rates, and heat fluxes in an object that are caused by thermal loads that do not vary over time.

B.CFD

Computational fluid dynamics, usually abbreviated as CFD, is a branch of fluid mechanics that uses numerical methods and algorithms to solve and analyze problems that involve fluid flows. Computers are used to perform the calculations required to simulate the interaction of liquids and gases with surfaces defined by boundary conditions. With high-speed supercomputers, better solutions can be achieved. Ongoing research yields software that improves the accuracy and speed of complex simulation scenarios such as transonic or turbulent flows. Initial experimental validation of such software is performed using a wind tunnel with the final validation coming in full-scale testing, e.g. flight tests.

Refrigerant properties

R- 30 properties

Density = 1326.6 kg/m³

Specific heat = 1043.0 j/kg/k

Thermal conductivity = 0.0042 w/m-k

Viscosity = 0.000279 kg/m-s

R-160 properties

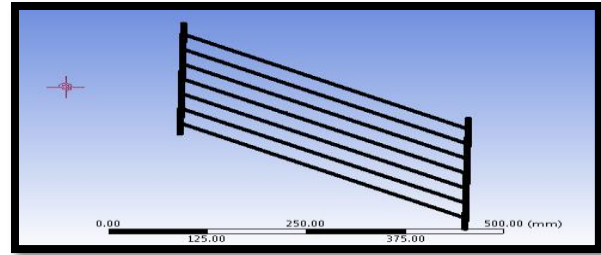
Density = 921.0 kg/m³

Specific heat = 1023.0 j/kg/k

Thermal conductivity = 0.0337 w/m-k

Viscosity = 0.00043 kg/m-s

IV. CFD ANALYSIS OF SOLAR FLATPLATE



The model is designed with the help of CREO and then import on ANSYS for Meshing and analysis. The analysis by CFD is used in order to calculating pressure profile and temperature distribution. For meshing, the fluid ring is divided into two connected volumes. Then all thickness edges are meshed with 360 intervals. A tetrahedral structure mesh is used. So the total number of nodes and elements is 6576 and 3344.

CFD Boundary conditions

Mass Flow Rate → 0.0105Kg/s and Inlet Temperature – 303K

Thermal analysis Boundary conditions

Temperature – 313K

Convection -1.80e+03

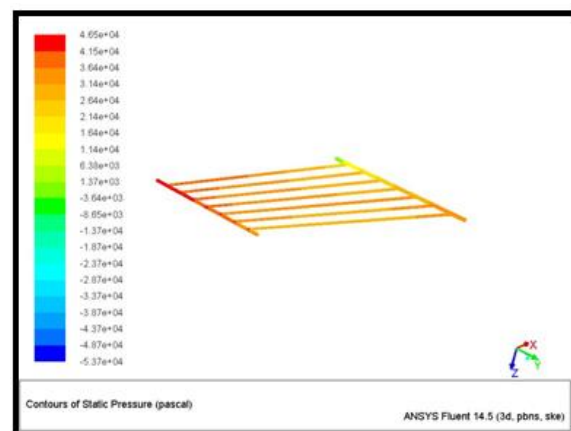


Fig 4: Static Pressure

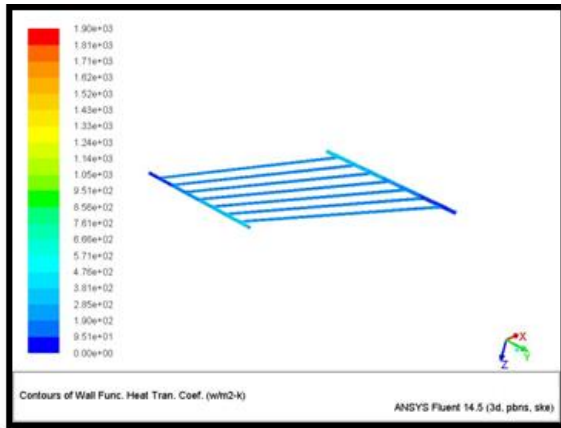


Fig 5: heat transfer coefficient

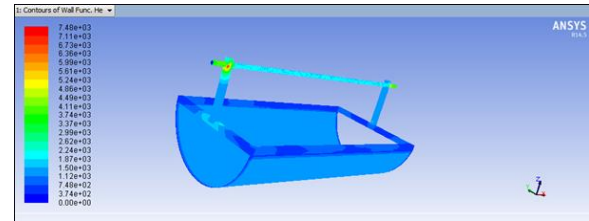


Fig 8: heat transfer coefficient

Mass Flow Rate (kg/s)	
inlet	1.4999995
interior-____msbr	-9.4357023
outlet	-1.5012258
wall-____msbr	0
Net	-0.001226306

Mass Flow Rate (kg/s)	
inlet	0.010499999
interior-partbody	0.026461512
outlet	-0.010539424
wall-partbody	0
Net	-3.9424747e-05
Total Heat Transfer Rate (w)	
inlet	790.97839
outlet	-793.94824
wall-partbody	0
Net	-2.9698486

Total Heat Transfer Rate (w)	
inlet	218614.02
outlet	-219101.16
wall-____msbr	310.48871
Net	-176.65192

A.CFD Analysis of Parabolic Solar Trough

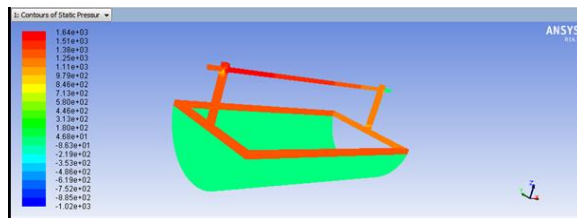


Fig 6: Static Pressure

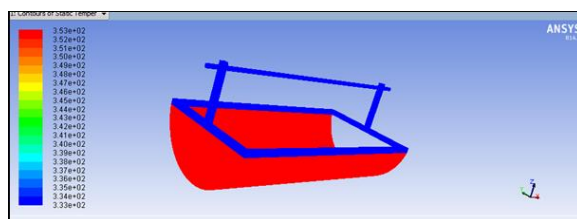


Fig 7: Temperature

B. Thermal Analysis Of Solar Parabolic Trough

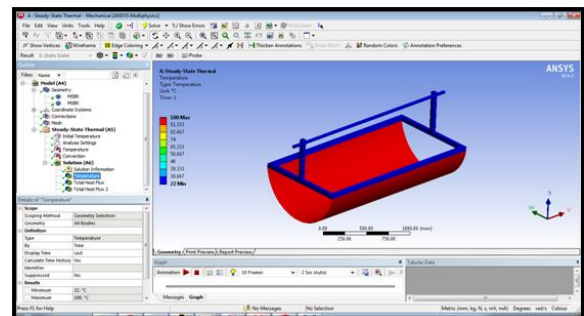


Fig 9: Temperature

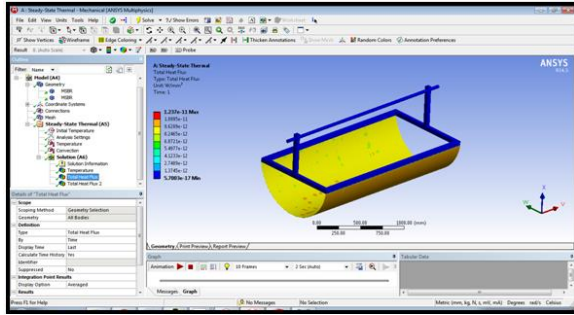


Fig 10: Heat flux

C. Thermal Analysis Solar Flat Plate Collector

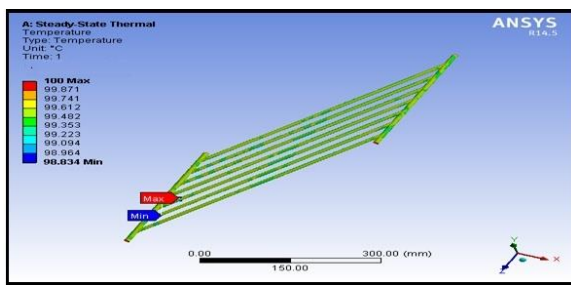


Fig 10: Temperature

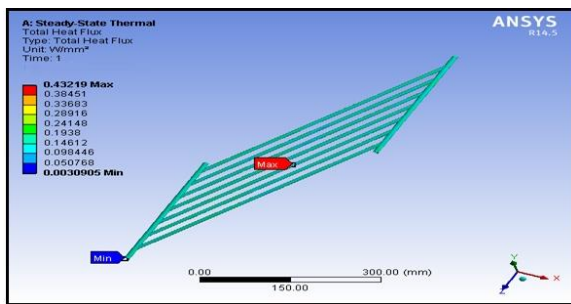


Fig 11: heat flux

V.RESULTS AND DISCUSSIONS

Table: 1 CFD Analysis results of Solar Flat Plate

Fluids	Pressure (Pa)	Heat transfer coefficient (w/m ² -k)	Mass flow rate (kg/s)	Heat transfer rate(w)
AIR	3.55e+004	1.44e+003	1.0958e-005	0.82574
WATER	4.65e+004	1.90e+003	3.9424e-005	2.9698
R30	4.68e+004	1.64e+003	2.5503e-005	1.920105
R160	3.70e+004	1.22e+003	5.0231e-005	3.1235e-005

Table: 2 CFD Analysis results parabolic trough

FLUID	PRESSURE (pa)	HEAT TRANSFER COEFFICIENT	MASS FLOW RATE	HEAT TRANSFER RATE
AIR	1.30E+06	2.11E+03	0.00412	150.8656
WATER	1.64E+03	7.48E+03	0.0012263	176.651
R 30	1.24E+03	2.87E+02	0.001788	48.89
R 160	1.79E+03	9.84E+02	0.0013078	51.32959

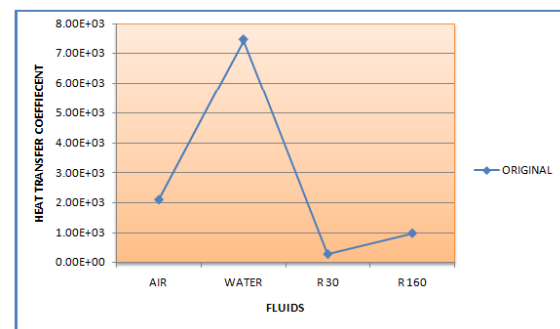
Table: 3 Thermal analysis results of parabolic trough

MATERIAL	HEAT FLUX
STEEL	1.7002E-12
ALUMINUM ALLOY	4.5574E-12
COPPER	1.237E-11

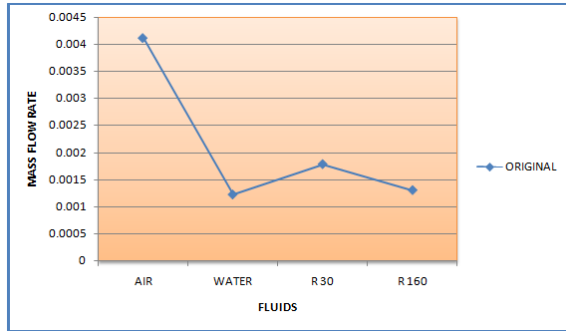
Table: 4 Thermal analysis results of solar flat plate

MATERIAL	HEAT FLUX
Aluminum alloy	0.42828
Copper alloy	0.43219

Graph:1 plotted between heat transfer coefficient and different working fluids



graph :2 plotted between mass flow rate and different working fluids



IV CONCLUSION

In this paper, the fluid flow through solar collectors (flat plate and parabolic trough) is modeled using design software. The thesis will focus on thermal and CFD analysis with different fluids air, water, R30 and R60 of the solar collectors. Thermal analysis done for the solar collectors by aluminum & copper materials.

By observing the CFD analysis the pressure drop & velocity values are more for water fluid at solar parabolic trough collectors compared with flat plate collector. The more heat transfer rate at fluid water.

By observing the thermal analysis Heat flux value is more for copper material than aluminum and steel at solar collectors

So we can conclude the copper material is better for solar collectors.

REFERENCES

- [1] D.A. Boyd, R. Gajewski, and R. Swift, "Acylindrical blackbodsolar energy receiver," *Solar Energy*, vol. 18, no. 5, pp. 395–401, 1976.
- [2] O. A. Barra and L. Franceschi, "The parabolic trough plants using black body receivers: experimental and theoretical analyses," *Solar Energy*, vol. 28, no. 2, pp. 163–171, 1982.
- [3] C. Qiaoli, G. Xinshi, C. Shuxin et al., "Numerical analysis of thermal characteristics of solar cavity receiver with absorber of a bundle of pipes," *Acta Energiæ Solaris Sinica*, vol. 16, no. 1, pp. 21–28, 1995.

[4] L. Zhang, H. Zhai, Y. Dai, and R.-Z. Wang, "Thermal analysisof cavity receiver for solar energy heat collector," *Journal ofEngineering Thermo physics*, vol. 29, no. 9, pp. 1453–1457, 2008.

[5] J. Fukuchi, Y. Ohtaka, and C. Hanaoka, "A numerical fluidsimulation for a pneumatics conveying dryer of cut tobacco,"in *Proceedings of the CORESTA Congress*, pp. 201–212, Lisbon,Portugal, 2000.

[6] Z. Pakowski, A. Druzzdel, and J. Drwiega, "Validation of amodel of an expanding superheated steam flash dryer for cuttobacco based on processing data," *Drying Technology*, vol. 22,no. 1-2, pp. 45–57, 2004.

[7] L. Huimin and M. Ming, *YC/T31-1996 Tobacco and TobaccoProducts—Preparation of Test Specimens and Determinationof Moisture Content—Oven Method*, China Standard Press,Beijing, China, 1996.

[8] X. Chengmu, L.Ming, J. Xu et al., "Frequency statistics analysisfor energy-flux-density distribution on focal plane of parabolictrough solar concentrators," *Acta Optica Sinica*, vol. 33, no. 4,Article ID 040800, pp. 1–7, 2013.

[9] R. Legros, C. A. Millington, and R. Clift, "Drying of tobaccoparticles in a mobilized bed," *Drying Technology*, vol. 12, no. 3,pp. 517–543, 1994.

[10] R. Blasco, R. Vega, and P. I. Alvarez, "Pneumatic drying withsuperheated steam: bi-dimensional model for high solid concentration,"*Drying Technology*, vol. 19, no. 8, pp. 2047–2061,2001.

[11] P. Yongkang andW. Zhong, *Modern Drying Technology*, ChemicalIndustry Press, Beijing, China, 1998.

[12] W. E. Ranz andW. R.Marshall, "Evaporation fromdrops, part I,"*Chemical Engineering Progress*, vol. 48, no. 3, pp. 141–146, 1952

ANALYTICAL INVESTIGATION OF HEAT TRANSFER ENHANCEMENT IN A MICROTUBE USING NANO FLUIDS AND INSERTS

Sandra Vijaykumar¹

Dr.Sanjeev Kumar Sajjan²

Dr.P.Srinivasulu³

¹M.Tech (Thermal Engineering)Department of mechanical engineering vaagdevi college of engineering (UGC autonomous) approved by AICTE & permanent affiliation to jntuh, hyderabad.p.o, bollikunta, Warangal urban-506005.

² Assistant Professor Department of mechanical engineering vaagdevi college of engineering (UGC autonomous) approved by AICTE & permanent affiliation to jntuh, hyderabad. p.o, bollikunta, Warangal urban- 506005.

³Professor and Head of the Department of mechanical engineering vaagdevi college of engineering (UGC autonomous) approved by AICTE & permanent affiliation to jntuh, hyderabad. p.o, bollikunta, Warangal urban-506005.

Abstract

There is a continued research to increase heat transfer rates in industrial heat exchangers. Particularly at moderate Reynolds numbers in pipe flow the augmentation methods are divided into two types viz., passive techniques and active techniques. Placing different types of inserts in tubes serve as passive techniques. Active techniques, in which external power input is used, such as power work, are less preferred.

The main aim of this thesis is to analyze the heat transfer in turbulent flow to horizontal tube using different types of inserts. The Reynolds number at 12000 and two different fluids are used such as water and water 95%+ TiC- 5%. Furthermore, the three different types of inserts used. 1) Twisted tape 2) Perforated Twisted Tape3) Double Counter Twisted Tape .The data from ANSYS is used to calculate Friction factor and Nusselt number in the presence of inserts

3D models of the horizontal tube with inserts are done in Pro/Engineer and analysis is done in ANSYS.

1. INTRODUCTION

Conventional resources of energy are depleting at an alarming rate, which makes future sustainable development of energy use very difficult. As a result, considerable emphasis has been placed on the development of various augmented heat transfer surfaces and devices. Heat transfer augmentation techniques are generally classified into three categories namely: active techniques, passive techniques and compound techniques. Passive heat transfer techniques (ex: tube inserts) do not require any direct input of external power. Hence many researchers preferred passive heat transfer enhancement techniques for their simplicity and applicability for many applications. Tube inserts present some advantages over other enhancement techniques, such as they can be installed in existing smooth tube that exchanger, and they maintain the

mechanical strength of the smooth tube. Their installation is easy and cost is low. It relatively easy to take out for cleaning operations too.

The process of improving the performance of a heat transfer system is referred as the heat transfer enhancement technique .In recent years, the high cost of energy and material has resulted in an increased effort aimed at producing more efficient heat exchange equipment .The major challenge in designing a heat transfer is to make the equipment compact and achieve a high heat transfer rate using minimum pumping power. The subject of heat transfer growth in heat exchanger is serious interest in the design of effective and economical heat exchanger. Augmentation techniques increase convective heat transfer by reducing thermal resistance in a heat exchanger. A decrease in heat transfer surface area, size, and hence weight of heat exchanger for a given heat duty and pressure drop. The heat transfer can be increased by the following different augmentation techniques. They are classified as (i) Passive Techniques (ii) Active Techniques (iii) Compound Techniques.

The various heat transfer enhancement techniques can be classified broadly as passive and active techniques. Passive techniques do not require direct input of external power, unlike active techniques. They generally use surface or geometrical modifications to the flow channel, or incorporate an insert, material, or additional device. Except for extended surfaces, which increase the effective heat transfer surface area, these passive schemes promote higher heat transfer coefficients by disturbing or altering the existing flow behavior. This, however, is accompanied by an increase in the pressure drop. In the case of active techniques, the addition of external power essentially facilitates the desired flow modification and improvement in the rate of heat transfer. The use of two or more techniques (passive and/or active) in conjunction constitutes compound augmentation techniques.

The effectiveness of any of these methods is strongly dependent on the mode of heat transfer (single-phase free or forced convection, pool boiling, forced convection boiling or condensation, and convective mass transfer), and type and process application of the heat exchanger.

Turbulent flow

The entrance lengths are much shorter for turbulent flows, because of the additional transport mechanism across the cross section. Thus, typical hydrodynamic entrance lengths in turbulent flow are 10-15 tube diameters, and the thermal entrance lengths are even smaller. Therefore, for most engineering situations where in $50 L/D \geq$, we use correlations for fully developed conditions. Correlations for turbulent flow are classified based on whether the interior wall of the tube is smooth or whether it is rough. Smooth tubes The earliest correlations for turbulent heat transfer in a smooth tube are due to Dittus and Boelter, McAdams, and Colburn. A common form to be used for fluids with $Pr > 0.5$

Reynolds Number

The value of the Reynolds number permits us to determine whether the flow is laminar or turbulent. We define the Reynolds number as follows. Reynolds number Here, D is the inside diameter of the tube (or pipe), V is the average velocity of the fluid, ρ is the density of the fluid and μ is its dynamic viscosity. It is common to use the kinematic viscosity $\nu = \mu/\rho$ in defining the Reynolds number. Another common form involves using the instead of the average velocity. The mass flow rate is related to the volumetric & mass flow rate $m = \rho$, and we can write 2&flow rate .

2. LITERATURE SURVEY

Heat Transfer Enhancement in Tube-in-Tube Heat Exchanger using Passive Techniques by Parag S. Desale, Nilesh C. Ghuge [1] The heat exchanger is an important device in almost all of the mechanical industries as in case of process industries it is key element. Thus from long time many researchers in this area are working to improve the performance of these heat exchangers in terms of heat transfer rate, keeping pressure drop in limit. This paper is a review of such techniques keeping focus on passive augmentation techniques used in heat exchangers. The thermal performance behavior for tube in tube heat exchanger is studies for wire coil inserts, twisted tape inserts and their combination.

Experimental Investigations on Augmentation of Turbulent Flow Heat Transfer in A Horizontal Tube Using Square Leaf Inserts by S. Naga Sarada, P. Ram Reddy, Gugulothu Ravi[2] The present work deals

with the results of the experimental investigations carried out on augmentation of turbulent flow heat transfer in a horizontal tube by the means of tube inserts, with air as working fluid. Experiments were carried out initially for the plain tube. Nusselt number and friction factor obtained experimentally were validated against those obtained from theoretical correlations. Secondly experimental investigations using five kinds (900, 600FW, 600

BW, 300 FW, 300 BW) of louvered square leaf inserts were carried out to estimate the enhancement of heat transfer rate for air in the presence of insert. Nusselt number and pressure drop increased, overall enhancement ratio is calculated to determine the optimum geometry of tube insert.

Heat transfer enhancement using passive enhancement technique by Vinay Kumar Patel , N. K. Sagar [3] Among many techniques (both passive and active) investigated for augmentation of heat transfer rates inside circular tubes, a wide range of inserts has been utilized, particularly when turbulent flow is considered. The inserts studied included coil wire inserts, brush inserts, mesh inserts, strip inserts, twisted tape inserts etc. Augmentation of convective heat transfer in internal flows with twisted tape inserts in tubes is a well-acclaimed technique employed in industrial practices. CFD investigations on enhancement of turbulent flow heat transfer with twisted tape inserts in a horizontal tube under forced convection with air flowing inside is carried out using ANSYS FLUNT. The variations of heat transfer coefficients; Nusselt number in the horizontal tube fitted with twisted tape is studied. A CFD investigation is conducted to study forced convection of fully developed turbulent flow through circular tube with twisted tape inserts. CFD solutions are obtained using commercial software ANSYS FLUENT v12.1. The working fluid in all cases is air. CFD analysis of heat transfer augmentation for flow through a tube using wire coil inserts by Shalini Patra The need to increase the thermal performance of heat transfer equipment (for instance, heat exchangers), thereby effecting energy, material, and cost savings as well as a consequential mitigation of environmental degradation has led to the development and use of many heat transfer enhancement techniques. These methods are referred to as augmentation or intensification techniques. This project deals with the analysis of heat transfer augmentation for fluid flowing through pipes using CFD. Using CFD codes for modeling the heat and fluid flow is an efficient tool for predicting equipment performance. CFD offers a convenient means to study the detailed flows and heat exchange processes, which take place inside the tube

Enhancement of heat transfer using varying width twisted tape inserts by S. Naga Sarada , A.V. Sita Rama Raju , K. Kalyani Radha, L. Shyam Sunder[4] The present work shows the results obtained from experimental investigations of the augmentation of turbulent flow heat transfer in a horizontal tube by means of varying width twisted tape inserts with air as the working fluid. In order to reduce excessive pressure drops associated with full width twisted tape inserts, with less corresponding reduction in heat transfer coefficients, reduced width twisted tapes of widths ranging from 10 mm to 22 mm, which are lower than the tube inside diameter of 27.5 mm are used. Experiments were carried out for plain tube with/without twisted tape insert at constant wall heat flux and different mass flow rates. The twisted tapes are of three different twist ratios (3, 4 and 5) each with five different widths (26-full width, 22, 18, 14 and 10 mm) respectively. The Reynolds number varied from 6000 to 13500. Both heat transfer coefficient and pressure drop are calculated and the results are compared with those of plain tube. It was found that the enhancement of heat transfer with twisted tape inserts as compared to plain tube varied from 36 to 48% for full width (26mm) and 33 to 39% for reduced width (22 mm) inserts. Correlations are developed for friction factors and Nusselt numbers for a fully developed turbulent swirl flow, which are applicable to full width as well as reduced width twisted tapes, using a modified twist ratio as pitch to width ratio of the tape.

2.1 GAPS IN LITERATURE

The gaps and recommendation for future research that can be concluded based on the present review are as follows:

- To reach the best modification for twisted tape, more complete simulations involving a wide range of geometry parameters need to be conducted in the future.
- Dispersion and random movement of nanoparticles due to swirl flow induced by twisted tape must be studied in order to know their effect to the overall enhancement ratio.

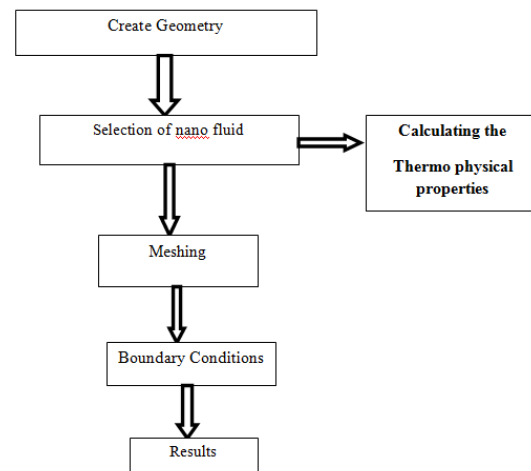
Problem Identification and objective

This project addressed an analytical investigation focused on flow patterns and heat transfer coefficient during flow boiling inside horizontal tubes for a wide range of experimental conditions. The following specific conclusions can be drawn based on the present study:

The Reynolds number at 12000 and two different fluids are used such as water and water 95%+ TiC-5%. Furthermore, the three different types of inserts used. 1) Twisted tape 2) Perforated Twisted Tape 3)

Double Counter Twisted Tape .The data from ANSYS is used to calculate Friction factor and Nusselt number in the presence of inserts

3. METHODOLOGY



3.2 MODELING AND ANALYSIS

Pro/ENGINEER Wildfire is the standard in 3D product design, featuring industry-leading productivity tools that promote best practices in design while ensuring compliance with your industry and company standards. Integrated Pro/ENGINEER CAD/CAM/CAE solutions allow you to design faster than ever, while maximizing innovation and quality to ultimately create exceptional products.

Customer requirements may change and time pressures may continue to mount, but your product design needs remain the same - regardless of your project's scope, you need the powerful, easy-to-use, affordable solution that Pro/ENGINEER provides.

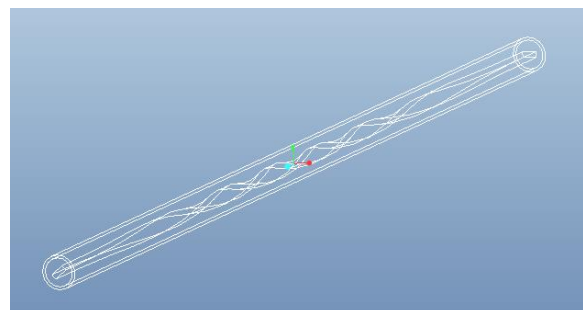


Fig : Twisted tape

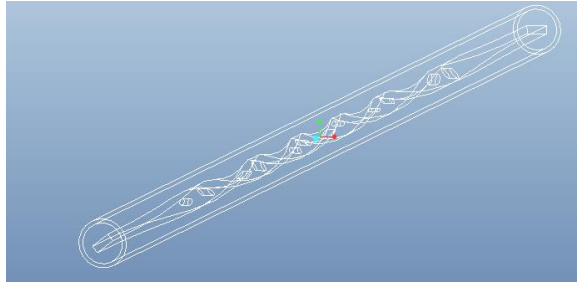


Fig: Perforated Twisted Tapes

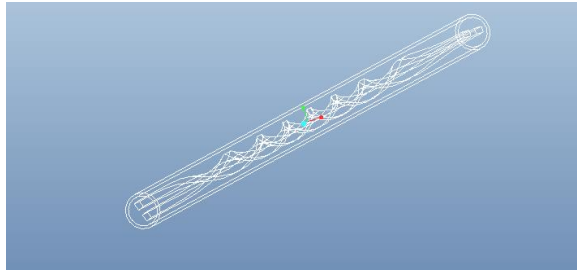


Fig :Double Counter Twisted Tapes

NANO FLUID CALCULATIONS

Density Of Nano Fluid

$$\rho_{nf} = \phi \times \rho_s + [(1-\phi) \times \rho_w]$$

Specific Heat Of Nano Fluid

$$C_{p\ nf} = \frac{\phi \times \rho_s \times C_{ps} + (1-\phi)(\rho_w \times C_{pw})}{\phi \times \rho_s + (1-\phi) \times \rho_w}$$

Thermal Conductivity Of Nano Fluid

$$K_{nf} = \frac{K_s + 2K_w + 2(K_s - K_w)(1 + \beta)^3 \times \phi}{K_s + 2K_w - (K_s - K_w)(1 + \beta)^3 \times \phi} \times k_w$$

Table 1: Thermo physical properties of fluids

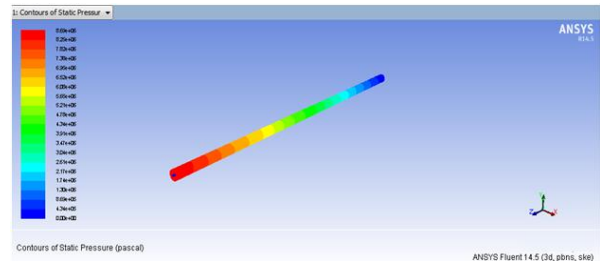
Properties	Water	Water 0.95%+ TiC 0.05%
Density(kg/m ³)	998.2	344.829
Thermal conductivity(W/m-k)	0.6	1.107
Specific heat(J/kg-k)	4182	3429.394
Viscosity(kg/m-s)	0.001003	0.0011283

3.3 CFD

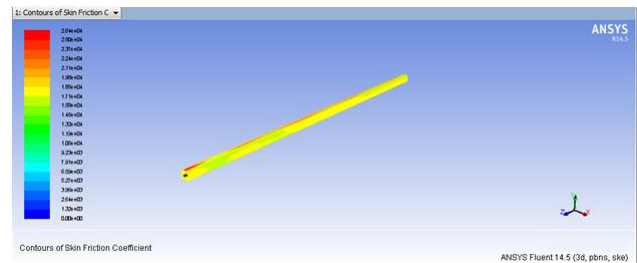
Computational fluid dynamics, usually abbreviated as CFD, is a branch of fluid mechanics that uses numerical methods and algorithms to solve and analyze problems that involve fluid flows. Computers are used to perform the calculations required to simulate the interaction of liquids and gases with surfaces defined by boundary conditions. With high-speed supercomputers, better solutions can be achieved. Ongoing research yields software that improves the accuracy and speed of complex simulation scenarios such as transonic or turbulent flows. Initial experimental validation of such software is performed using a wind tunnel with the final validation coming in full-scale testing, e.g. flight tests.

4 CFD ANALYSIS ON HEAT TRANSFER ENHANCEMENT IN HORIZONTAL TUBE WITH INSERTS

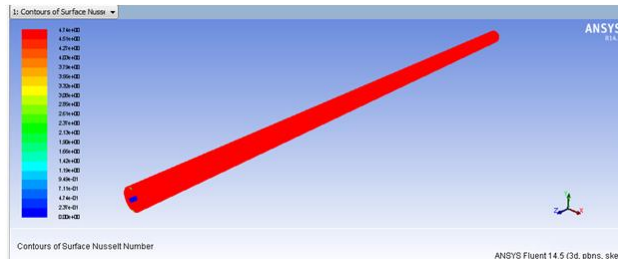
Pressure



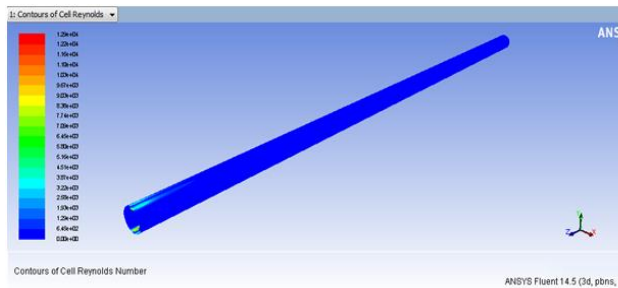
Friction coefficient



Nusselt number



Reynolds number



5.RESULTS AND DISCUSSIONS

Table: 2 results of water

Geometr y	Pressu re (Pa)	Friction coeffie nt	Reynol ds numbe r	Nusselt numbe r
Twisted Tape	8.96e+06	2.64e+04	1.29e+04	4.74e+00
Perforat ed Twisted Tape	8.97e+06	2.71e+04	1.31e+04	4.82e+00
Double Counter Twisted Tape	8.95e+06	2.77e+04	1.34e+04	4.89e+00

Table: 3 results of water 95%+ TiC- 5%

Geometr y	Pressu re (Pa)	Friction coeffie nt	Reynol ds numbe r	Nusselt numbe r
Twisted Tape	3.76e+05	1.15e+04	2.23e+03	2.53e+00
Perforat ed Twisted Tape	3.89e+05	1.18e+04	2.27e+03	2.61e+00

Double Counter Twisted Tape	3.96e+05	1.20e+04	2.31e+03	2.69e+00

6.CONCLUSION

The Reynolds number at 12000 and two different fluids are used such as water and water 95%+ TiC-5%. Furthermore, the three different types of inserts used. 1) Twisted tape 2) Perforated Twisted Tape3) Double Counter Twisted Tape .The data from ANSYS is used to calculate Friction factor and Nusselt number in the presence of inserts

From the CFD analysis results; the following conclusions can be made:

The Nusselt number is more for Double Counter Twisted Tape than other inserts, friction factor, and Reynolds number are more for Double Counter Twisted Tape than other inserts.

REFERENCES

[1] A. Garc, J.P. Solano, P.G. Vicente, A. Viedma, Enhancement of laminar and transitional flow heat transfer in tubes by means of wire coil inserts, International Journal of Heat and Mass Transfer 50 (2007) 3176–3189.

[2] S.S. Hsieh, F.Y. Wu, H.H. Tsai, Turbulent heat transfer and flow characteristics in a horizontal circular tube with strip-type inserts: Part I. Fluid mechanics, International Journal of Heat and Mass Transfer 46 (2003) 823–835.

[3] M.M.K. Bhuiya, M.S.U. Chowdhury, M. Islam, J.U. Ahamed, M.J.H. Khan, M.R.I. Sarker, M. Saha, “Heat transfer performance evaluation for turbulent flow through a tube with twisted wire brush inserts”, Elsevier, International Communications in Heat and Mass Transfer 39 (2012) pp- 1505–1512

[4] Halit Bas, Veysel Ozceyhan, “Heat transfer enhancement in a tube with twisted tape inserts placed separately from the tube wall”, Elsevier, Experimental Thermal and Fluid Science 41 (2012), pp- 51–58

[5] M.M.K. Bhuiya, M.S.U. Chowdhury, M. Saha, M.T. Islam, “Heat transfer and friction factor characteristics in turbulent flow through a tube fitted with perforated twisted tape inserts”, Elsevier, International Communications in Heat and Mass Transfer 46 (2013) 49–57

[6] M.M.K. Bhuiya, A.S.M. Sayem, M. Islamc, M.S.U. Chowdhury, M. Shahabuddin, "Performance assessment in a heat exchanger tube fitted with double counter twisted tape inserts", Elsevier, International Communications in Heat and Mass Transfer (2013) pp-1-9

[7] Pankaj N. Shrirao, Dr. Rajeshkumar U. Sambhe, Pradip R. Bodade, "Experimental Investigation on Turbulent Flow Heat Transfer Enhancement in a Horizontal Circular Pipe using internal threads of varying depth", IOSR Journal of Mechanical and Civil Engineering, Volume 5, Issue 3 (Jan. - Feb. 2013), PP 23-28

[8] Bodius Salam, Sumana Biswas, Shuvra Saha, Muhammad Mostafa K Bhuiya, "Heat transfer enhancement in a tube using rectangular-cut twisted tape insert", Elsev

9. S.K.Saha A.Dutta " Thermo hydraulic study of laminar swirl flow through a circular tube fitted with twisted tapes" Trans. ASME Journal of heat transfer June 2001, Vol-123/ pages 417-427.

CFD ANALYSIS OF ECONOMIZER IN TANGENTIAL FIRED TUBE BOILER

Gopalapu shobha¹

Dr.Parvesh kumar² Dr.P.Srinivasulu³

¹M.Tech (Thermal Engineering)Department of mechanical engineering vaagdevi college of engineering (UGC autonomous) approved by AICTE & permanent affiliation to jntuh, hyderabad.p.o, bollikunta, Warangal urban-506005.

²Professor Department of mechanical engineering vaagdevi college of engineering (UGC autonomous) approved by AICTE & permanent affiliation to jntuh, hyderabad. p.o, bollikunta, Warangal urban- 506005.

³Professor and Head of the Department of mechanical engineering vaagdevi college of engineering (UGC autonomous) approved by AICTE & permanent affiliation to jntuh, hyderabad. p.o, bollikunta, Warangal urban-506005.

Abstract

In this thesis, a simulation of the economizer zone, which allows studying the flow patterns developed in the fluid, while it flows along the length of the economizer. The past failure details reveals that erosion is more in U-bend areas of Economizer Unit because of increase in flue gas velocity near these bends. In this project heat transfer by convection in economizer varying the mass flow rates are determined by CFD and thermal analysis. The materials considered for tubes are Copper and Aluminium alloys 6061 and 7075. The mass flow rates are varied will be 100,90 and 70 Kg/sec. CFD analysis is done to determine temperature distribution and heat transfer rates by varying the mass flow rates . Heat transfer analysis is done on the economizer to evaluate the better material.

3D modeling is done in CATIA and analysis is done in ANSYS.

1. INTRODUCTION

Boiler Economiser (Sometimes Called Economizer) is the Energy improving device that helps to reduce the cost of operation by saving the fuel.

The economizer in Boiler tends to make the system more energy efficient.

In boilers, economizers are generally Heat Exchangers which are designed to exchange heat with the fluid, generally water.

Boiler Economizer and Waste Heat Recovery Concept

Boilers are generally designed to produce steam from water. Water is converted to steam by transferring both sensible and latent heat.

Sensible heat is the amount of heat required to increase the temperature of water at constant pressure without changing its liquid state, while Latent heat is the amount of heat required to change the state from Liquid to Vapor at constant temperature and pressure.

The exhaust from the boilers is generally in the temperature range of 200°C – 250°C, so there are a huge amount of losses from the boiler if any heat recovery devices are not installed after it.



Fig: Economizer

THE FUNCTION OF BOILER ECONOMISER

The Economizer in Boiler works on the principle of Heat Transfer. Heat transfer usually takes place from high temperature to low temperature.

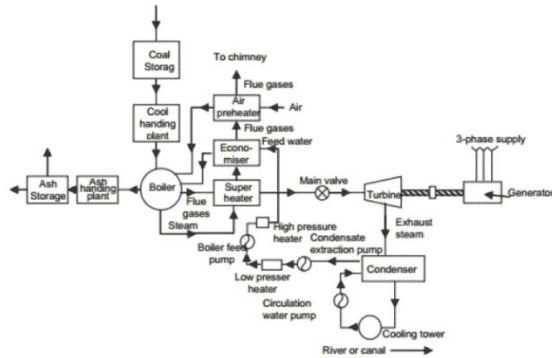
In the case of Boilers, flue gases or exhaust from the boiler outlet are at high temperature and water that needs to be preheated is at low temperature.

So, this temperature difference between water and flue gases helps to increase the feed water temperature.

Depending on the type of operations, design of Economisers can be smoke tube type or water tube type.

In smoke tube type flue gases are inside the tubes and water is on the shell side while in the water tube type, water is in the tube and flue gases are on the shell side.

Working Principle of Economizer



As shown in the figure above, the flue gases coming out of the steam boiler furnace carry a lot of heat. Function of economiser in thermal power plant is to recover some of the heat from the heat carried away in the flue gases up the chimney and utilize for heating the feed water to the boiler. It is simply a heat ex-changer with hot flue gas on shell side and water on tube side with extended heating surface like Fins or Gills.

Economisers in thermal power plant must be sized for the volume and temperature of flue gas, the maximum pressure drop passed the stack, what kind of fuel is used in the boiler and how much energy needs to be recovered.

LITERATURE REVIEW

V.Malikarjuna et al [1] Preparing mathematical analysis an attempt has been made to study about the boiler and economizer. Hot air is necessary for rapid combustion in the furnace and also for drying coal in milling plants .so an essential boiler accessory which serves this purpose is air preheater. The air preheater are not essential for operation of steam generator, but they are used where a study of cost indicates that money can be saved or efficient combustion can be obtained by their use. The performance of the air preheater is improved. Load on fan are reduced thus power consumption is reduced and cost is reduced. Fuel consumption is also reduced, thus fuel is saved and cost is reduced. By comparing Rothemuhle with ljunstrom air leakage are more, gas side efficiency and air side efficiencies are less in Rothemuhle air

preheater. The thermal performance of the ljunstrom air preheater is better than Rothemuhle

P.N.Sapkal et al [2] Performed an analysis for the optimization of air preheater design with inline & staggered tube arrangement. The poor performance of an air preheater in the modern power plants is one of the main reason for higher unit heat rate & is responsible for deterioration in boiler efficiency.. In case of tubular air heaters a variety of single and multiple gas and air path arrangements can be used to optimum performance. Modern tubular air heaters can be shop assembled into large, transportable modules. Erosion of air preheater parts can be controlled by reducing velocities, removing erosive elements from the gas stream, or using sacrificial material. The performance of tubular air preheater can be evaluated with the help of CFD analysis for Inline & staggered tube arrangement with the latter being more thermally efficient. The model can be used while selecting a new type of surface geometry in order to have uniformly distributed flow pattern for optimizing the design of air preheater.

Sangeeth G.S et al [3] Performed an analysis for energy efficiency of the process or equipment should prove itself to be economically feasible for gaining acceptance for implementation. The focus of the present work is to study the effect of system modification for improving energy efficiency. The objective of the study was to analyze the overall efficiency and the thermodynamic analysis of boiler. There are many factors, which are influencing the efficiency of the boiler. The fuel used for combustion, type of boiler, varying load, power plant age, heat exchanger fouling they lose efficiency. Much of this loss in efficiency is due to mechanical wear on variety of components resulting heat losses. Therefore, it is necessary to check all the equipments periodically. Moreover, it is noticed that the overall efficiency of any boiler depends upon the technical difficulties under unpredictable conditions. Hence, a viable study is carried out to assess the performance of boiler plant in this context. The paper set to show the weakness of depending on energy analysis only boilers as a performance measure that will help improve efficiency.

Gaurav T. Dhanre et al [4] Performed an analysis for This reduction can be achieved by improving the efficiency of industrial operations and equipments. Energy audit plays an important role in identifying energy conservation opportunities in the industrial sector, while they do not provide the final answer to the problem; they do help to identify potential for energy conservation and induces the companies to concentrate their efforts in this area in a focused manner. which we are getting from energy auditing . Hence there is a need to prefer energy auditing of

every plant once in an year. For the research, it is found that it is also possible to do auditing at different load conditions and by comparison we get the actual consumption as well as wastage.

PROBLEM IDENTIFICATION

•The main objective of this project is to analyze flue gas temperature, velocity field of fluid flow within an economizer tube using the actual boundary conditions.

•Later the analysis is extended by altering the design by changing the number of tubes and varying the cross section of the tubes.

•Thus the variation of temperature, and velocity of flue gases is compared and results can be analyzed for better design. The temperature variation of the feed water is also measured to find the extent to which it is gaining the heat.

METHODOLOGY

- The solid model of the economizer is created using the CATIA.
- The fluid model is required for the analysis is extracted i.e. created using the CATIA software.
- The created fluid model is imported in to the solid works flow simulation software to perform the CFD analysis.
- The above steps are repeated for the different designs with modified bend radius of the tubes (25 mm,30 mm,35 mm and 40 mm).

MODELING OF ECONOMIZER

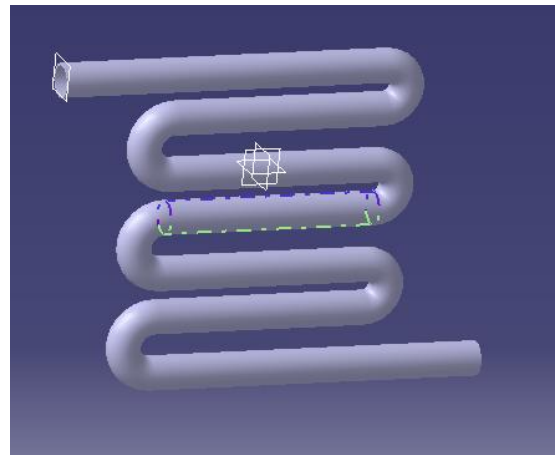
CATIA is an acronym for Computer Aided Three-dimensional Interactive Application. It is one of the leading 3D software used by organizations in multiple industries ranging from aerospace, automobile to consumer products.

CATIA is a multi platform 3D software suite developed by Dassault Systems, encompassing CAD, CAM as well as CAE. Dassault is a French engineering giant active in the field of aviation, 3D design, 3D digital mock-ups, and product lifecycle management (PLM) software. CATIA is a solid modeling tool that unites the 3D parametric features with 2D tools and also addresses every design-to-manufacturing process. In addition to creating solid models and assemblies, CATIA also provides generating orthographic, section, auxiliary, isometric or detailed 2D drawing views. It is also possible to generate model dimensions and create reference dimensions in the drawing views. The bi-directionally associative property of CATIA ensures that the modifications made in the model are reflected in the drawing views and vice-versa.

Table: (Geometrical specifications)

Specifications	Dimension
Length (Shell)	60 centimetre
Width (Shell)	30 centimetres
Height (Shell)	30 centimetre
Diameter of tubes	0.2 centimetre
Material	Steel and carbon
Number of tube assemblies	1

3D MODEL OF ECONOMIZER



COMPUTATIONAL FLUID DYNAMICS

Computational Fluid Dynamics CFD is one of the best suited software for the analysis of flow patterns which involve the dynamic parameters in the flow. It is very stable robust and accurate in providing the required outputs. Generally experiments on moving fluid particles are not feasible. Dynamics study on moving particles involves many complex calculations and large variables. But their analysis can be easily carried with the help of CFD.

Working of CFD

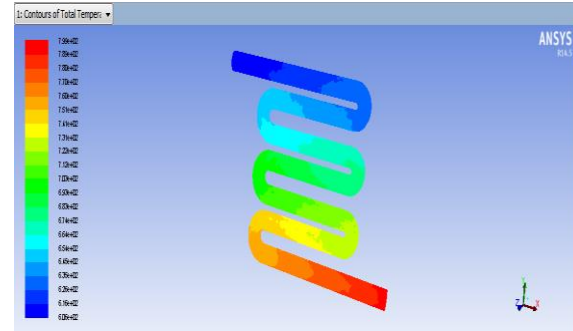
CFD is based on Finite Volume Method. The area in the flow pattern for the analysis is first modelled in any of the modelling software. In terms of CFD this is called as Computational domain. This computational domain is discretized into many small elements of finite volume. This process of dividing the domain is termed as meshing. Hence here each volume is considered to be a control volume. The control volume have certain properties like mass, momentum, energy, turbulence quantities, and mixture fractions, species concentrations and material properties. Based on the flow problem we pick up the control volume properties to be analysed and solve the flow problem. The theoretical flow in control volume is represented physically with the help of

numerically solvable partial differential equations. These equations govern the flow of fluid in the computational domain. These equations also undergo the discretization process for the flow analysis. There are three equations which are applicable commonly to all fluid dynamics problems are the conservation of mass, momentum and the energy equations. Equations when represented in differential form

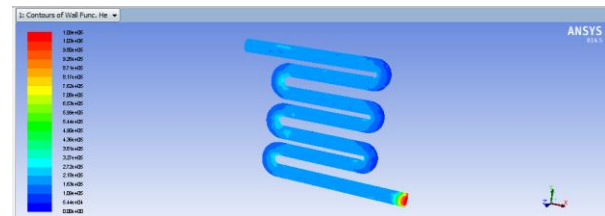
CFD METHODOLOGY

In all of these approaches the same basic procedure is followed.

- During preprocessing
- The geometry (physical bounds) of the problem is defined.
- The volume occupied by the fluid is divided into discrete cells (the mesh). The mesh may be uniform or non-uniform.
- The physical modeling is defined – for example, the equations of motion + enthalpy + radiation + species conservation

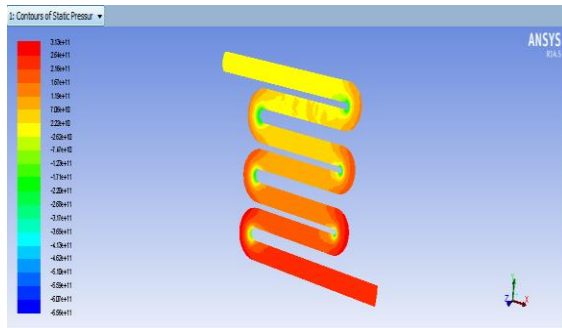


Heat transfer coefficient



RESULTS AND DISCUSSIONS
CFD ANALYSIS OF ECONOMIZER
 At mass flow rate-50 g/sec

Pressure



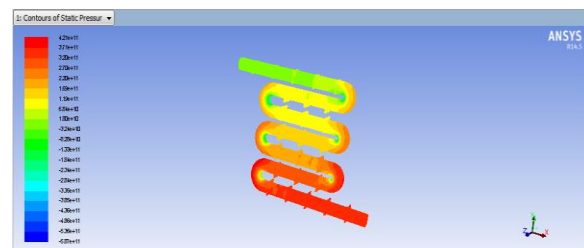
Temperature

Mass Flow Rate	(kg/s)
inlet	50.000011
interior-partbody	-5620.1479
outlet	-50.358593
wall-partbody	0
Net	-0.35858154

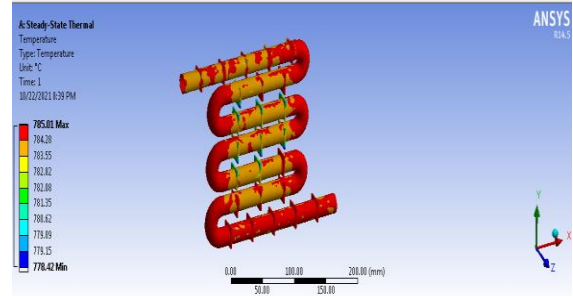
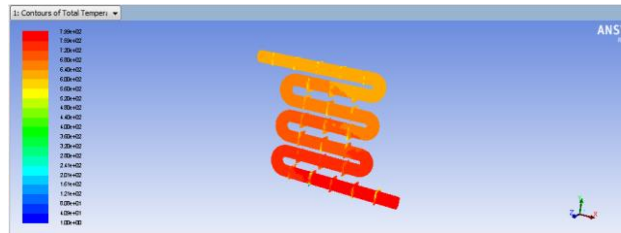
Total Heat Transfer Rate	(w)
inlet	27900570
outlet	-19189800
wall-partbody	-11242889
Net	-2532127

CASE: 2 WITH FINS

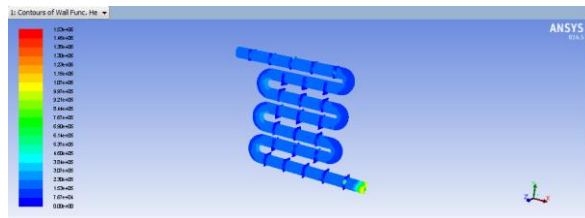
Pressure



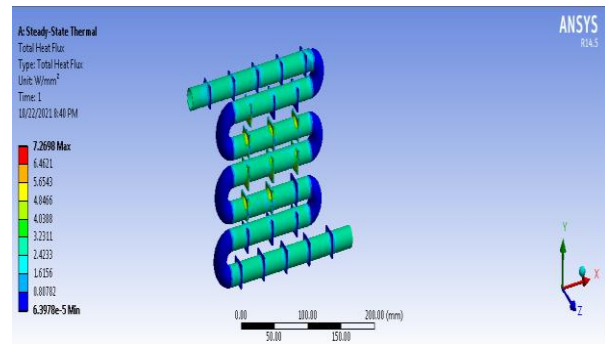
Temperature



Heat transfer coefficient



Heat Flux



Mass Flow Rate	(kg/s)
inlet	50.0001
interior-partbody	38655.2
outlet	-50.478
wall-partbody	
Net	-0.478864

Total Heat Transfer Rate	(w)
inlet	27900316
outlet	-19586634
wall-partbody	-11192776
Net	-2879094

Thermal Analysis of Economizer

Temperature

RESULTS AND DISCUSSIONS

Table: CFD RESULTS

Geometry	Mass flow rate (kg/sec)	Pressure (Pa)	Temperature (k)	Heat transfer coefficient (w/m ² k)	Mass flow rate (kg/sec)
Without fin	17.5	1.30e+11	7.99e+02	4.28e+05	0.089
	25	1.10e+11	7.98e+02	5.85e+05	0.19
	50	3.13e+11	7.90e+02	1.09e+06	0.35
With fin	17.5	5.96e+10	7.89e+02	4.55e+05	0.103
	25	1.38e+11	7.88e+02	1.04e+06	0.32
	50	4.21e+11	7.86e+02	1.53e+06	0.47

Table: THERMAL RESULTS

Geometry	Materials	Temperature (k)	Heat flux
Without fin	Aluminum	789.75	11.699
	Copper	786.68	22.43
With fin	Aluminum	785.07	17.0928
	Copper	785.01	24.209

CONCLUSION

In this thesis, a simulation of the economizer zone, which allows studying the flow patterns developed in the fluid, while it flows along the length of the economizer. The materials considered for tubes are Copper and Aluminium alloys 6061 and 7075. The mass flow rates are varied will be 17.5, 25 and 50 Kg/sec. CFD analysis is done to determine temperature distribution and heat transfer rates by varying the mass flow rates. Heat transfer analysis is done on the economizer to evaluate the better material. 3D modeling is done in CATIA and analysis is done in ANSYS.

By observing the CFD analysis results, the maximum heat transfer coefficient at mass flow rate with 50kg/sec with fins.

By observing the thermal analysis results, the maximum heat flux at copper with fins.

REFERENCES

1. V. Malakarjuna, N. Joshua, And B. Rama Bhopal Reddy, 2014 "Improving boiler efficiency by using air preheated", international journal of advanced research in engineering and applied sciences, Vol.03, Issue.02, PP.11-24, 2014.
2. P.N. Sapkal, P.R. Navistar, M.J. Sable, And S.B. Barve, "To optimize air preheater design for better performance", new aspects of fluid mechanics, heat transfer and environment, 2015.
3. Sangeeth G.S, And Praveen Marathon, "Efficiency improvement of boilers", [IRJET], Vol.02, Issue.05, 2015.
4. Gaurav T. Dhanre, Urvashi T. Dandre, and Kraal Mudale, 2014. "Review paper on energy audit of a boiler in thermal power plant", international journal of engineering research and general science, Vol.02, Issue.06, 2014.
5. K. Sampath Kumar Reddy, and Dr B. Veerabhadra Reddy "Performance of the Boiler and To Improving

the Boiler Efficiency Using Cfd Modeling", [IOSRJMCE], Vol.08, Issue.06, 2013.

6. M. J. Poddar, and Mrs. A.C. Birajdar, "Energy Audit a Boiler- A Case Study", [IJERT], Vol.02, Issue.06, pp.1660- 1666, 2013.

7. Venkata Seshendra Kumar Karri, "A theoretical investigation of efficiency enhancement in thermal power plants", modern mechanical engineering, Vol.02, pp.106-113. 2012



MAGNITUDE COMPARATOR USING VARIOUS HIGH PERFORMANCE TECHNIQUES

¹K. Bharth Kumar, ²G. Vedavathi

¹M.Tech VLSI ,Dept. of Electronics and Communication Engineering, Vaagdevi College of Engineering, Warangal, Telangana, India. Bharathbalu868@gmail.com

²Associate professor ,Department of Electronics and Communications Engineering, Vaagdevi College of Engineering, Warangal, Telangana, India. Vedhavathi_g@vaagevi.edu.in

ABSTRACT

A low power two bit magnitude comparator has been proposed in the present work. The proposed magnitude comparator using the technology of coupling has been compared with the basic comparator circuit. The performance analysis of both the different comparators has been done for power consumption, delay and power delay-product (PDP) with VDD sweep. The simulations are carried on Tanner EDA (CMOS technology at 5 V supply). The simulation results of the coupled magnitude comparator circuits is in good agreement in terms of power consumption at percentage of 60.26% in greater than function and 56.14% in lesser than function and 59.48% in equals to function comparators.

1. INTRODUCTION

Due to rapid escalation in usage of portable devices, demand for high-performance circuits in electronic devices have become a crucial need. A modern highly complex electronic device requires ICs and processors that have high efficiency and speed . Therefore, efficient design mythologies are highly demanded in order to cope up with the expected performance parameters of modern devices. In order to meet the performance requirements, many efficient design techniques have been developed and implemented.

MC in digital ALU is the component used for comparing two binary digits or numbers. By comparing two binary numbers, it provides output if they are greater than or equal to one-another. This component in ALU is highly utilized in parallel processing and digital signal processing. In addition, instruction sorting in microprocessors requires MC. Hence, because of having significant demand in VLSI design, an effective MC design will bring about great performance escalation of ALU.

In this research, a hybrid two-bit magnitude comparator using PTL, TGL and C-CMOS logic has been presented. Performance of the proposed hybrid two-bit MC has been compared with the existing designs to validate its effectiveness. Cadence design tools have been used in this research for performance evaluation in standard 90 nm technology node.

2. LITERATURE SURVEY

a. Microcontroller Based Smart Home System with Enhanced Appliance Switching Capacity

This paper introduces a low-cost android application (app) controlled smart home system that can remotely switch on/off as many as 208 appliances using only 4 digital pins of an ATmega328 microcontroller based Arduino UNO board. The appliance switching system requires approximately 70% less wiring cost for real life installation in home compared to the similar conventional systems. Moreover, the smart home system includes:

- (1) automatic night light that only lights up at night if it detects any human in the close proximity;



(2) 'Outside Mode' that turns off every single appliance connected to the system with a touch from android app when user leaves the home;

(3) a smart security system that sounds an alarm, sends message and makes call to the user using GSM module if it detects any intrusion in the house. The android application provides a user-friendly Graphical User Interface (GUI) to send command to the microcontroller via Bluetooth. Compared to the products available in market, cost of the proposed system is cheaper to a great extent.

b. Low-Power and Fast Full Adder by Exploring New XOR and XNOR Gates

In this paper, novel circuits for XOR/XNOR and simultaneous XOR-XNOR functions are proposed. The proposed circuits are highly optimized in terms of the power consumption and delay, which are due to low output capacitance and low short-circuit power dissipation. We also propose six new hybrid 1-bit full-adder (FA) circuits based on the novel full-swing XOR-XNOR or XOR/XNOR gates. Each of the proposed circuits has its own merits in terms of speed, power consumption, power-delay product (PDP), driving ability, and so on. To investigate the performance of the proposed designs, extensive HSPICE and Cadence Virtuoso simulations are performed. The simulation results, based on the 65-nm CMOS process technology model, indicate that the proposed designs have superior speed and power against other FA designs.

A new transistor sizing method is presented to optimize the PDP of the circuits. In the proposed method, the numerical computation particle swarm optimization algorithm is used to achieve the desired value for optimum PDP with fewer iterations. The proposed circuits are investigated in terms of variations of the supply and threshold voltages, output capacitance, input noise immunity, and the size of transistors.

c. A New Robust and Hybrid High-Performance Full Adder Cell

A new 1-bit hybrid Full Adder cell is presented in this paper with the aim of reaching a robust and high-performance adder structure. While most of recent Full Adders are proposed with the purpose of using fewer transistors, they suffer from some disadvantages such as output or internal non-full-swing nodes and poor driving capability. Considering these drawbacks, they might not be a good choice to operate in a practical environment. Lowering the number of transistors can inherently lead to smaller occupied area, higher speed and lower power consumption. However, other parameters, such as robustness to PVT variations and rail-to-rail operation, should also be considered. While the robustness is taken into account, HSPICE simulation demonstrates a great improvement in terms of speed and power-delay product (PDP).

3. LITERATURE REVIEW OF TWO-BIT MAGNITUDE COMPARATOR DESIGNS

Due to wide area of applications, MC has become prime subject of interest for which numerous two-bit MC designs have been implemented by researchers. Two-bit MC using PTL utilizes 40 CMOS transistors are reported in. The major disadvantage associated with this sort of design is degradation of voltage since N-MOS only passes strong logic 0(zero).Hence, PTLMC suffers from low driving power and has high power consumption.

Later on, in order to overcome the disadvantages of PTL, C-CMOS logic has been developed. This design employs complementary set of N-MO Sand P-MOS transistors for full- swing logic implementation. Two-bit MC design using C- CMOS logic has been reported in .Transistor count (TC) for this design is 66. This high TC makes the input impedance high which accounts for high delay. However, in case of driving power, the design is significantly robust.

TGL do not incorporate the weakness of voltage degradation unlike PTL .However, high TC in TGL results in high area in silicon chip. Moreover, driving power is also an issue in this sort of designs .Two-bit MC using TG Misreported in [23] which employs 66transistors.

Two-bit MC design employing Full Adder (FA) cell is reported in .Thedesignemployed30transistorsandused FA design in. TC of this MC is low while compared to the previously mentioned PTL and C-CMOSMCs.



ADBU-Journal of Engineering Technology

Gate Diffusion Input (GDI) method enables designers to build VLSI circuits with less TC compared to other design methods. Major drawback of this design is the voltage degradation like PTL. Two-bit MC using GDI technique in only requires 28 transistors which is the lowest TC reported in this research.

Hybrid logic style based two-bit MC in requires 46 transistors. The design used hybrid logic based AND and XNOR gates for internal logic signal generation. Then the internal signals are sent to C-CMOS based circuit for generating output terms. Major advantage of this design lies in the intelligent use of C-CMOS method based circuit in the outer signal generation.

Dynamic logic based MC designs are also available in literature. However, the proposed and the other MCs mentioned are static CMOS based for which comparison in this research is conducted only among static CMOS based designs.

4. FUNDAMENTALS OF LOW POWER VLSI DESIGN

The increasing prominence of portable systems and the need to limit power consumption (and hence, heat dissipation) in very-high density ULSI chips have led to rapid and innovative developments in low-power design during the recent years. The driving forces behind these developments are portable applications requiring low power dissipation and high throughput, such as notebook computers, portable communication devices and personal digital assistants (PDAs). In most of these cases, the requirements of low power consumption must be met along with equally demanding goals of high chip density and high throughput. Hence, low-power design of digital integrated circuits has emerged as a very active and rapidly developing field of CMOS design.

The limited battery lifetime typically imposes very strict demands on the overall power consumption of the portable system. Although new rechargeable battery types such as Nickel-Metal Hydride are being developed with high energy capacity than that of the conventional Nickel-Cadmium batteries, revolutionary increase of the energy capacity is not expected in the near future. The energy density (amount of energy stored per unit weight) offered by the new battery technologies is about 30 Watt-hour/pound, which is still low in view of the expanding applications of portable systems. Therefore, reducing the power dissipation of integrated circuits through design improvements is a major challenge in portable systems design.

The need for low-power design is also becoming a major issue in high-performance digital systems, such as microprocessors, digital signal processors (DSPs) and other applications. Increasing chip density and higher operating speed lead to the design of very complex chips with high clock frequencies. If the clock frequency of the chip increases then the power dissipation of the chip, and thus, the temperature, increase linearly. Since the dissipated heat must be removed effectively to keep the chip temperature at an acceptable level, the cost of packaging, cooling and heat removal becomes a significant factor. Several high-performance microprocessor chips designed in the early 1990s operate at clock frequencies in the range of 100 to 300 MHz, and their typical power consumption is between 20 and 50 W.

ULSI reliability is yet another concern which points to the need for low-power design. There is a close correlation between the peak power dissipation of digital circuits and reliability problems such as electro migration and hot-carrier induced device degradation. Also, the thermal stress caused by heat dissipation on chips is a major reliability concern. Consequently, the reduction of power consumption is also crucial for reliability enhancement.

The methodologies which are used to achieve low power consumption in digital systems span a wide range, from device/process level to algorithm level. Device characteristics (e.g., threshold voltage), device geometries and inter connect properties are significant factors in lowering the power consumption. Circuit-level measures such as the proper choice of circuit design styles, reduction of the voltage swing and clocking strategies can be used to reduce power dissipation at the transistor level. Architecture-level measures include smart power management of various system blocks, utilization of pipelining and parallelism, and design of bus structures.

Finally, the power consumed by the system can be reduced by a proper selection of the data processing algorithms, specifically to minimize the number of switching events for a given task.

4.1 Sources of Power Dissipation

The average power dissipation in conventional CMOS digital circuits can be classified into three main components, namely,

- (1) The dynamic (switching) power dissipation
- (2) The short-circuit power dissipation and
- (3) The leakage power dissipation.

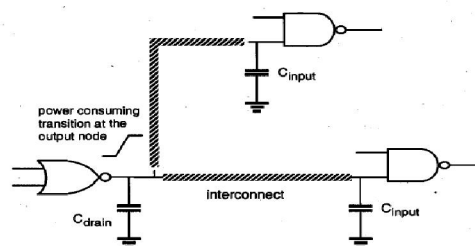
If the system or chip includes circuits other than conventional CMOS gates that have continuous current paths between the power supply and the ground, a fourth (static) power component should also be considered

Switching Power Dissipation represents the power dissipation during a switching event. This means that the output node voltage of a CMOS logic gate makes a power consuming transition. In digital CMOS circuits, dynamic power is dissipated when energy is drawn from the power supply to charge up the output node capacitance. During the charge-up phase, the output node voltage typically makes a full transition from 0 to VDD, and the energy used for the transitions relatively independent of the function performed by the circuit.

To explain the dynamic power dissipation during switching, consider the circuit given in Fig. below.

Here, a two-input NOR gate drives two NAND gates, through interconnection lines. The total capacitive load at the output of the NOR gate consists of

- (1) The output capacitance of the gate itself
- (2) The total interconnect capacitance, and
- (3) The input capacitances of the driven gates.



A NOR gate driving two NAND gates through interconnection lines.

Output capacitance:

The output capacitance of the gate consists mainly of the junction parasitic capacitances, which are due to the drain diffusion regions of the MOS transistors in the circuit. The important feature to highlight here is that the amount of capacitance is approximately a linear function of the junction area. So, the size of the total drain diffusion area determines the amount of parasitic capacitance.

Total inter connect capacitance:

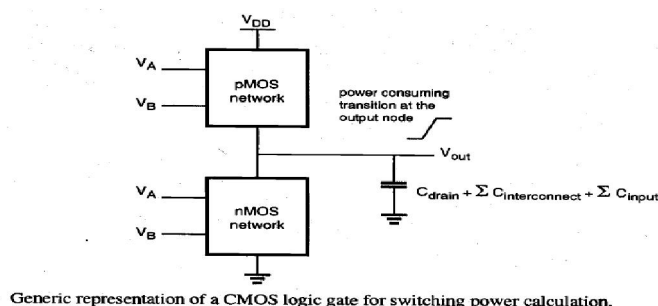
The interconnect lines between the gates contribute to the total interconnect capacitance. **Note**

Particularly in sub-micron technologies, the inter connect capacitance can become the dominant component, compared to the transistor-related capacitances.

Input capacitances:

The input capacitances are mainly due to gate oxide-capacitances of the transistors connected to the input terminal. Again, the amount of the gate oxide capacitance is determined primarily by the gate area of each transistor.

Generic representation of a CMOS logic gate



4.2 DIGITAL COMPARATORS

Digital Comparator and Magnitude Comparator

Data comparison is needed in digital systems while performing arithmetic or logical operations. This comparison determines whether one number is greater than, equal, or less than the other number.

A digital comparator is widely used in combinational system and is specially designed to compare the relative magnitudes of binary numbers. These are also available in IC form with different bit comparing configurations such as 4-bit, 8-bit, etc. More than one comparator can also be connected in cascade arrangement to perform comparison of numbers of longer lengths. Whenever we want to compare the two binary numbers, first we have to compare the most significant bits. If these MSBs are equal, then only we need to compare the next significant bits. But if the MSBs are not equal, then it would be clear that either A is greater than or less than B and the process of comparison ceases. For example, the two 2-bit number are $A = A_1A_0$ and $B = B_1B_0$. If A_1 is not equal to B_1 , then it is clear that A is greater than B for $A_1 = 1$ & $B_1 = 0$ or else A is less than B for $A_1 = 0$ & $B_1 = 1$. At this stage the process of comparison ceases. If the MSBs are equal, i.e., $A_1 = B_1$ only then we need to compare the next significant bits A_0 and B_0 and decide whether the number is greater than, less than or equal. So, the comparator produces three outputs as L, E and G corresponds to less than, equal and greater than comparisons.

Single Bit Magnitude Comparator

A comparator used to compare two bits, i.e., two numbers each of single bit is called a single bit comparator. It consists of two inputs for allowing two single bit numbers and three outputs to generate less than, equal and greater than comparison outputs.

The figure below shows the block diagram of a single bit magnitude comparator. This comparator compares the two bits and produces one of the 3 outputs as L ($A < B$), E ($A = B$) and G ($A > B$).



The truth table for the single bit comparator is given below. When $A_0 B_0 = 00$ & 11 , both inputs are equal, therefore $A=B$ output will be high. When $A_0 B_0 = 01$, B is more than A and hence AB is active.

A_0	B_0	L	E	G
0	0	0	1	0
0	1	1	0	0
1	0	0	0	1
1	1	0	1	0

From the truth table logical expressions for each output can be expressed as

$$A_0 < B_0: L = \overline{A_0} B_0$$

$$A_0 = B_0: E = \overline{A_0} \overline{B_0} + A_0 B_0$$

$$A_0 > B_0: G = A_0 \overline{B_0}$$

It is to be noted that E can be realized as $\overline{(L + G)}$.

By using these Boolean expressions, we can implement a logic circuit for this comparator using two AND gates, one NOT gate and one Ex-NOR gate as shown in below figure. AND gates are used to find whether a binary digit is less than greater than another bit whereas Ex-NOR gate is used to find whether two binary numbers are equal or not.

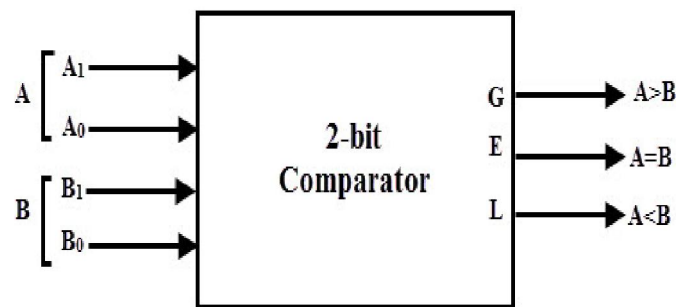
In the figure, one AND gate has inputs of A_0 $(\overline{B_0})$ and another has inputs $(\overline{A_0}) B_0$. Therefore, one AND gate output is 1 if $A_0 > B_0$ (i.e., $A_0 = 1$ and $B_0 = 0$) and is zero if $A_0 < B_0$ (i.e., $A_0 = 0$ and $B_0 = 1$). Similarly, other AND gate output is one if $A_0 < B_0$ (i.e., $A_0 = 0$ and $B_0 = 1$) and is zero if $A_0 > B_0$ (i.e., $A_0 = 1$ and $B_0 = 0$).

The Ex-NOR gate has inputs $A_0 B_0$, hence the output of the Ex-NOR gate will be 1 if $A_0 = B_0$ and the output will be 0 if A_0 is not equal to B_0 .

2-Bit Comparator

A 2-bit comparator compares two binary numbers, each of two bits and produces their relation such as one number is equal or greater than or less than the other. The figure below shows the block diagram of a two-bit comparator which has four inputs and three outputs.

The first number A is designated as $A = A_1A_0$ and the second number is designated as $B = B_1B_0$. This comparator produces three outputs as G ($G = 1$ if $A > B$), E ($E = 1$, if $A = B$) and L ($L = 1$ if $A < B$).

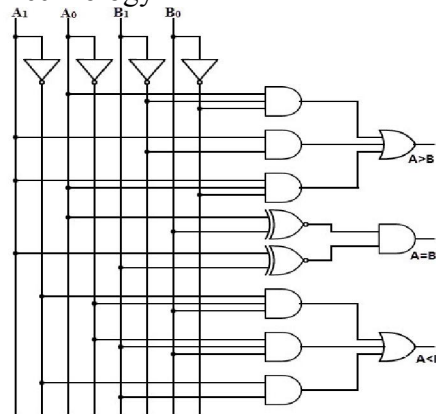


From the above k-map simplification, each output can be expressed as

$$\begin{aligned}
 A > B: G &= A_0 \bar{B}_1 \bar{B}_0 + A_1 \bar{B}_1 + A_1 A_0 \bar{B}_0 \\
 A = B: E &= \bar{A}_1 \bar{A}_0 \bar{B}_1 \bar{B}_0 + \bar{A}_1 A_0 \bar{B}_1 B_0 + A_1 A_0 B_1 B_0 + A_1 \bar{A}_0 B_1 \bar{B}_0 \\
 &= \bar{A}_1 \bar{B}_1 (\bar{A}_0 \bar{B}_0 + A_0 B_0) + A_1 B_1 (A_0 B_0 + \bar{A}_0 \bar{B}_0) \\
 &= (A_0 B_0 + \bar{A}_0 \bar{B}_0) (A_1 B_1 + \bar{A}_1 \bar{B}_1) \\
 &= (A_0 \text{ Ex-NOR } B_0) (A_1 \text{ Ex-NOR } B_1) \\
 A < B: L &= \bar{A}_1 B_1 + \bar{A}_0 B_1 B_0 + \bar{A}_1 \bar{A}_0 B_0
 \end{aligned}$$

By using above obtained Boolean equation for each output, the logic diagram can be implemented by using four NOT gates, seven AND gates, two OR gates and two Ex-NOR gates.

The figure below shows the logic diagram of a 2-bit comparator using basic logic gates. It is also possible to construct this comparator by cascading of two 1-bit comparators.



4-Bit Comparator

It can be used to compare two four-bit words. The two 4-bit numbers are $A = A_3 A_2 A_1 A_0$ and $B = B_3 B_2 B_1 B_0$ where A_3 and B_3 are the most significant bits.

It compares each of these bits in one number with bits in that of other number and produces one of the following outputs as $A = B$, $A < B$ and $A > B$. The output logic statements of this converter are

- If $A_3 = 1$ and $B_3 = 0$, then A is greater than B ($A > B$). Or
- If A_3 and B_3 are equal, and if $A_2 = 1$ and $B_2 = 0$, then $A > B$. Or
- If A_3 and B_3 are equal & A_2 and B_2 are equal, and if $A_1 = 1$, and $B_1 = 0$, then $A > B$. Or
- If A_3 and B_3 are equal, A_2 and B_2 are equal and A_1 and B_1 are equal, and if $A_0 = 1$ and $B_0 = 0$, then $A > B$.

From the above statements, the output $A > B$ logic expression can be written as

The equal output is produced when all the individual bits of one number are exactly coincides with corresponding bits of another number. Then the logical expression for $A=B$ output can be written as

$$E = (A_3 \text{ Ex-NOR } B_3) (A_2 \text{ Ex-NOR } B_2) (A_1 \text{ Ex-NOR } B_1) (A_0 \text{ Ex-NOR } B_0)$$

From the above output Boolean expressions, the logic circuit for this comparator can be implemented by using logic gates as given below. In this the four outputs from Ex-NOR gates are applied to AND gate to give the binary variable E or $A = B$.

5. PROPOSED DESIGN USING PASS TRANSISTOR LOGIC (PTL) STYLE

Main idea behind PTL is to use purely NMOS Pass Transistors network for logic operation [1]. The basic difference of pass-transistor logic style compared to the CMOS logic style is that the source side of the logic transistor networks is connected to some input signals instead of the power lines as in Fig.12. In this design style, transistor acts as switch to pass logic levels from input to output [9]. Schematic of 2-bit magnitude comparator using pass transistor logic style is given in Fig.13.

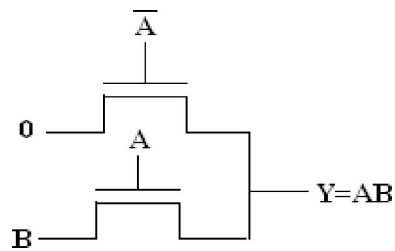


Figure 12. Symbol for AND Gate using Pass Transistor Logic

Advantages

- Design requires less number of transistors because one pass-transistor network (either NMOS or PMOS) is sufficient to perform the logic operation.
- Speed is increased because less number of transistors are used for design.
- Less area is required for design because PMOS is not used.

Disadvantages

- It does not provide full output voltage swing because PMOS is not used.

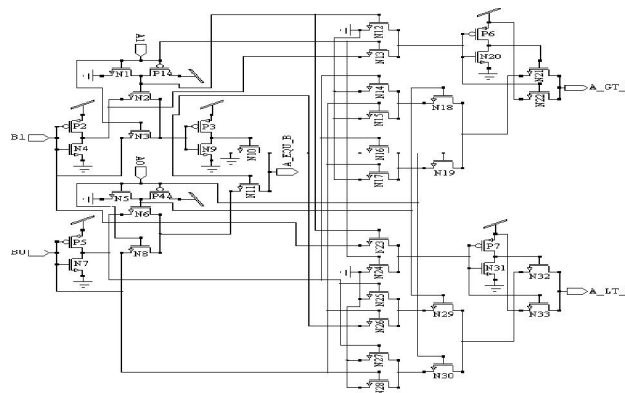


Figure 13. Schematic of 2-Bit Magnitude Comparator using Pass Transistor Logic style

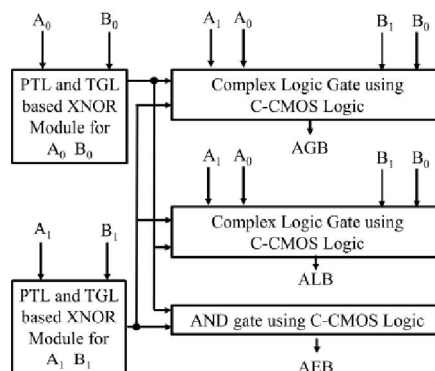


Fig 14 Block Diagram for proposed magnitude comparator

6. SIMULATION RESULT

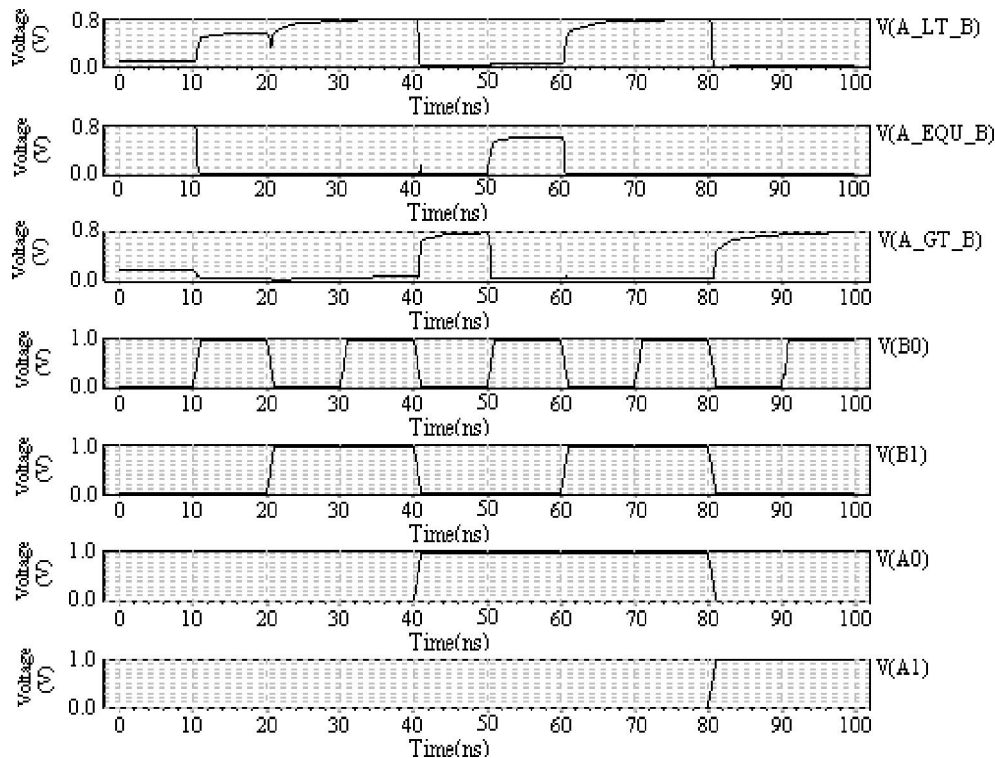


Figure 14. Waveform of 2-Bit Magnitude Comparator using Pass Transistor Logic style

Considering input bits 0100 then according to truth table in output side, „1“ should be obtained in $A > B$ & rest two output should be „0“. After simulation output wave form(in Fig.14) shows same result as in truth table for these input bits.

When input bits are 0101 then expected output in $A = B$ should be „1“, & wave form also shows same output as in truth table. Similarly, When input bits are 0110 then expected output in $A < B$ should be „1“, & wave form also shows same output as in truth table.

7 CONCLUSIONS

This work presented the design of a two-bit MC. The proposed MC utilized PTL and TGL based logic circuits for generating the initial signals from the inputs which reduced TC. Output terminals consisted C-CMOS circuits to provide robustness and driving power. For comparison purpose, proposed MC has been simulated in 90 nm CMOS process along with the existing ones. The proposed MC achieved quite satisfying performance parameters which proved its effectiveness. Due to the high performance obtained by the proposed design, it is proved that the design is highly useful for designing modern microprocessors.



REFERENCES

- [1] S. Venkataramani, V. K. Chippa, S. T. Chakradhar, K. Roy, and A. Raghunathan. “Quality programmable vector processors for approximate computing,” 46th Annual IEEE/ACM International Symposium on Microarchitecture (MICRO), pp. 1-12, Dec. 2013.
- [2] H. R. Mahdiani, A. Ahmadi, S. M. Fakhraie, and C. Lucas, “Bio-Inspired imprecise computational blocks for efficient VLSI implementation of Soft-Computing applications,” IEEE Transactions on Circuits and Systems I: Regular Papers, vol. 57, no. 4, pp. 850-862, Apr. 2010.
- [3] C. Liu, J. Han, and F. Lombardi, “A Low-Power, High-Performance approximate multiplier with configurable partial error recovery,” Design, Automation & Test in Europe Conference & Exhibition (DATE), Mar. 2014.
- [4] S. Hashemi, R. I. Bahar, and S. Reda, “DRUM: A Dynamic Range Unbiased Multiplier for approximate applications,” IEEE/ACM International Conference on Computer-Aided Design (ICCAD), pp. 418- 425, Nov. 2015.
- [5] B. Moons, M. Verhelst, “DVAS: Dynamic Voltage Accuracy Scaling for increased energy-efficiency in approximate computing,” IEEE/ACM International Symposium on Low Power Electronics and Design (ISLPED), Jul. 2015.
- [6] A. Momeni, J. Han, P. Montuschi, and F. Lombardi, “Design and analysis of approximate compressors for multiplication,” IEEE Transactions on Computers, vol. 64, no. 4, pp. 984-994, Apr. 2015.
- [7] K. C. Bickerstaff, E. E. Swartzlander, and M. J. Schulte, “Analysis of column compression multipliers,” 15th IEEE Symposium on Computer Arithmetic, pp. 33-39, Jun. 2001. 74

ULTRA LOW POWER STANDARD CELL LIBRARY ARCHITECTURE DESIGN USING DEEP SUB MICRON TECHNOLOGY

Gunti Anitha*¹, Dr. M. Shashidhar*²

*¹M.Tech Scholar, VLSI Design, Vaagdevi College of Engineering, Warangal, Telangana, India.

*²Associate professor, Department of ECE, Vaagdevi College of Engineering,
Warangal, Telangana, India.

ABSTRACT

This paper involves the design of ultra-low power standard cell library, standard cells are designed by Variable Threshold CMOS (VTCMOS) has emerged as an effective circuit-level technique that attains a high performance, while standby sub threshold leakage is minimized by providing substrate biasing. There by leakage power is reduced by almost 9 times than without substrate bias of library with penalty of small amount of delay. By using this library there is an almost infinite amount of consumer products like mobile phones, processors, televisions, cameras, refrigerators, ovens and cars.

In this paper, the characterization of different components of standard cell is performed using worst-case and best-case ASIC technology libraries. The worst-case library is characterized by a supply voltage of 0.96V, operating temperature of 125°C, and slow process corner. The best-case library is characterized by a supply voltage of 1.44V, operating temperature of -40°C, and fast process corner. This paper focused on the implementation (physical) aspect. All standard cells leakage current, propagation delay, slew rate and dynamic power are calculated by Cadence Schematic Composer and Cadence virtuoso.

Keywords: CMOS, ASIC, Leakage Current, Body Bias, Power Dissipation, Slew Rate, Propagation Delay.

I. INTRODUCTION

This paper enumerates about library architecture, which will consists of standard cells, standard-cell libraries are fixed set of well-characterized logic blocks. Basic logic functions are used several times on the same integrated circuit. It will have leaf cells ranging from simple gates to latches and flip-flops. These can then be used to build arithmetic blocks like adders and multipliers. ASIC designers commonly employ the use of standard cell libraries due to their robustness and flexibility resulting in quick turnaround times.

The objective of this to develop a methodology for designing low power circuits and cells, and to implement this methodology in constructing a general purpose cell library that can be used to design low power integrated circuits. The design methodology encompasses all aspects of circuit design; it optimizes transistor size, logic style, layout style, cell topology, and circuit design for low power operation. The entire cell library is characterized to determine typical delay, average power consumption, and area for each cell so the IC designer can make reasonable speed, area, and power estimations while still in the architecture design stage.

II. LITERATURE REVIEW

Lowering power consumption is critical for further improvements for operational speed in high-speed applications and for low-power consumption in battery-supplied applications such as cellular phones. Reducing the unwanted currents, called leakage currents or simply leakage, is vital for further growth in IC designs. Leakage has two components: Sub-threshold leakage and gate-oxide leakage. Sub-threshold old leakage consists of source-drain currents when the transistor is supposed to be non-conducting. These currents are now flowing through the substrate of the transistors due to effects near the active regions of transistors that heavily depend on the length of the transistor gate. Gate-oxide leakage comes from currents tunneling through the very thin oxide layer between gate and source, drain or bulk. Clearly, both types of leakage depend on the device sizes, and also depend on the voltages at the terminals. Further, altering the doping of the substrate, the threshold voltage, V_{th} , can be changed enabling the design of low leakage transistors with higher V_{th} values. Though, high V_{th} have weaker drive and will deteriorate the speed of the circuitry. When technology is scaled down sub threshold leakage current is increases, so it is reduced by given below library architecture. Even though gate leakage is increase beyond 90nm technology, we can't control gate leakage. It is controlled by foundry, but sub threshold leakage we can reduce by various techniques like VTCMOS, MTCMOS, Stacking effect

etc. Library architecture consists of standard cells, charge pump and strap cells. Depending upon circuit operation bias values are applied to cells, when bias values are applied threshold voltage of standard cells is increased, there by leakage is decreases.

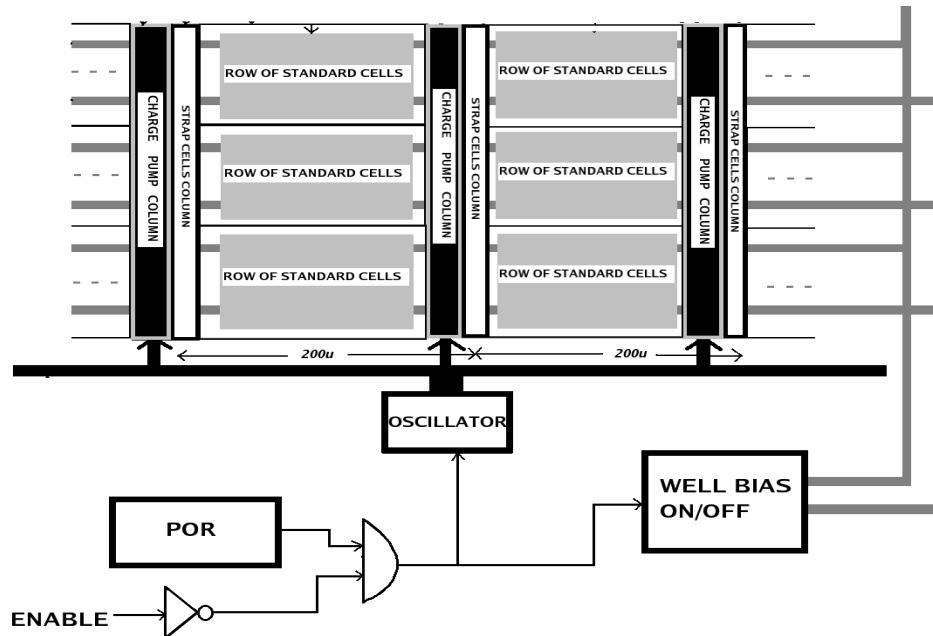


Fig. 1. Library Architecture

Table 1. Operation of the library architecture

CE	POR	Oscillator	Bias ON/OFF	Comment
0	0	OFF	ON	Active mode
0	1	ON	OFF	Standby mode
1	0	OFF	ON	Active mode
1	1	OFF	ON	Active mode

As shown in Fig. 1 strap cell which is used to connect VNW, VPW to bulk of the MOSFET. The charge pump block, this will provide VNW, VPW depending upon standby mode and active mode of circuits. An Oscillator is used to produce frequency to produce the bias values. Different standard cells are designed by using without body bias technique and with body bias techniques and there by compared leakage current, delay and slew rate and dynamic power.

III. TYPES OF STANDARD CELLS

Different Types of Standard Cells

A. NOR2

The NOR2 cell provides a logical NOR of two inputs (A, B). The output (Y) is represented by the logic equation:

$$Y = \overline{(A + B)} \quad (1)$$

Table 2. Function of NOR2

A	B	Y
0	0	1
X	1	0
1	X	0

Table 2 shows the operation of the 2 input NOR.

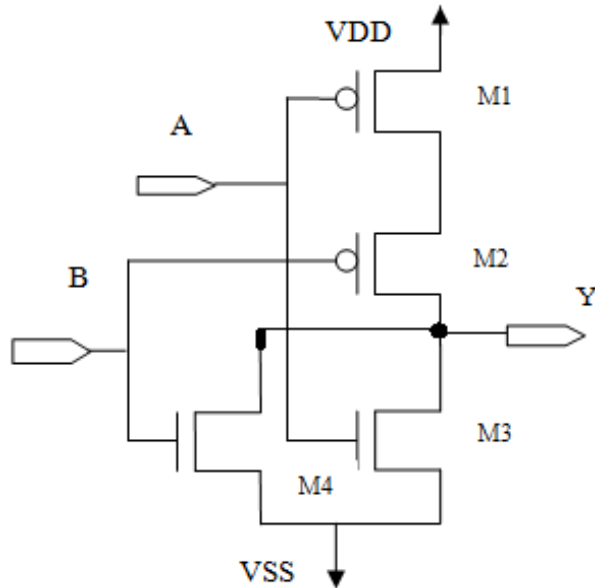


Fig 2: Schematic Diagram

Fig.2 shows, when both inputs A and B are low, transistors M3, M4 are OFF and M1, M2 are ON. Then output becomes low .If both inputs are high, M3, M4 are ON and M1, M2 are OFF.

B. OAI21

The OAI21cell provides the logical inverted AND of one OR group and an additional input. The output (Y) is represented by the logic equation:

$$Y = \overline{(A0 + A1)} \bullet B0 \quad (2)$$

Table 3: Function of OAI21

A0	A1	B0	Y
0	0	X	1
X	X	0	1
X	1	1	0
1	X	1	0

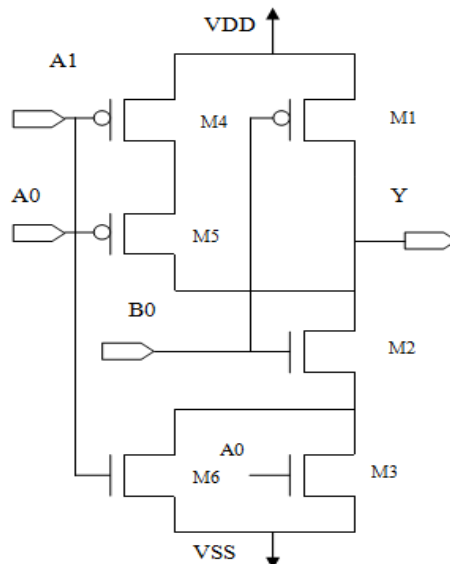


Fig. 3. Functional Schematic of OAI21

IV. LEAKAGE POWER ANALYSIS AND BODY BIAS TECHNIQUES

In digital CMOS circuits there are three sources of power dissipation, the first is due to signal transition, the second source of power dissipation comes from short circuit current which flows directly from supply to ground terminal and the last is due to leakage currents. As technology scales down the short circuit power will be comparable to dynamic power dissipation. Furthermore, the leakage power shall also become highly significant.

High leakage current is becoming a significant contributor to power dissipation of CMOS circuits as threshold voltage, channel length, and gate oxide thickness are reduced [3-4]. Consequently, the identification and modeling of different leakage components is very important for estimation and reduction of leakage power especially for low-power applications. Different leakage mechanisms contribute to the total leakage in a device. The three major types of leakage mechanisms are sub threshold, gate, and reverse-biased, drain- and source-substrate junction band-to-band-tunnelling (BTBT) with technology scaling, each of these leakage components increases drastically, resulting in an increase in the total leakage current. The increase in different leakage components with technology scaling has two major implications in leakage estimation and low power logic design. First, these increases add up to a dramatic increase in total leakage. More importantly, each of the leakage components becomes equally important in nano scaled devices. And hence, the relative magnitudes of the leakage components play amatory role in low-leakage logic design.

BODY BIAS TECHNIQUE

The source biasing techniques described above decrease leakage by simultaneously reducing V_{GS} and V_{BS} , but another class of techniques focuses specifically on the term V_{BS} .

The primary method is to manipulate the body voltage to modulate the threshold voltage. Since sub threshold leakage is inversely dependent upon the threshold voltage, increasing the threshold reduces the power consumption. However, the gate performance degrades with increasing V_t , so techniques that statically increase the body voltage are undesirable. Instead, by dynamically controlling the body voltage, the circuit can be tuned to the best trade-off between power consumption and performance at any given time. This technique is typically called Variable Threshold CMOS (VTCMOS) [13-14].

Although not always specifically called VTCMOS, schemes that modify the body bias to affect the threshold voltage have been proposed for older process generations. The self-adjusting threshold-voltage scheme (SATS) bounds the leakage regardless of the process corner and temperature using a sense stage that dynamically tunes the body voltage to the set the minimum V_t to meet the performance requirements. The intention is to switch between an active and a sleep mode. The VTCMOS approach depends on the ability to dynamically change the threshold voltage.

V. RESULTS AND DISCUSSION

The results and discussion may be combined into a common section.

A. NOR2

The NOR2 cell provides a logical NOR of two inputs. The characterization of NOR2 cell is given below in terms of speed, slew rate, leakage current, dynamic power and dynamic current.

1. PROPAGATION DELAY

Propagation delays are defined as the time interval between the input stimulus crossing 50% of V_{DD} and the output crossing 50% of V_{DD} and the time interval between the input stimulus crossing 50% of V_{DD} and the output crossing 90% of V_{DD} . The delay calculations are calculated at process corner Slow Slow (SS), supply voltage of 0.96V and temperature 125°C. Comparisons for NOR2 circuits with and without bias technique are given below.

Table 4. Delay 50%Input to 50% Output for NOR2 at SS, 0.96V, 125^o C

Input and output signals considered	Propagation delays (ns)		%change
	OLD	NEW	
A(r) to Y(f)	2.941	3.137	6.66
B(r) to Y(f)	2.948	3.121	5.86
A(f) to Y(r)	7.105	7.612	7.13
B(f) to Y(r)	7.092	7.685	8.36
Average Value			7.00

In **Table 4**, delay is calculated at 50% input to 50% output time lag for standard cell NOR2, at operating conditions (SS, 0.96V, 125°C). The values under OLD show the delay without body bias Technique and the values under NEW shows delay with body bias Technique for a NOR2 circuit. “A (r) to Y (f)” shows the time difference between 50% of the input (A) rising edge and 50% of output (Y) waveform at falling edge. “B (f) to Y (r)” has maximum percentage variation i.e., 8.36%. For “A (r) to Y (f)”, there is a minimum variation of 6.66%. By using bias technique, delay increases with an average change of 7.0% as seen in last row and last column of **Table 4**.

Table 5. Delay 50% Output to 90% Output for NOR2 at SS, 0.96V, 125 °C

Input and Output signals considered	Propagation delays(ns)		%change
	OLD	NEW	
A(r) to Y(f)	1.35	1.399	3.62
B(r) to Y(f)	1.343	1.381	2.82
A(f) to Y(r)	13.96	15.2	8.88
B(f) to Y(r)	14.08	15.28	8.52
Average Value			5.96

From **Table 5**, delay is calculated at 50% input to 90% output time lag for standard cell NOR2, at operating conditions (SS, 0.96V, 125°C). “A (f) to Y (r)” has maximum percentage variation i.e., 8.88%. For “B (r) to Y (f)”, there is a minimum variation of 2.82%. By using body bias technique, delay increases with an average change of 5.96% as seen last row and last column of **Table 5**.

2. SLEW RATE

It is the time interval between the input stimulus crossing 10% of V_{DD} and the output crossing 90% of V_{DD}. The delay is calculated at process corner SS, supply voltage of 0.96V, and temperature 125°C given in **Table 6**.

From **Table 6**, the values under OLD show delay without body bias Technique in gate NOR2 and NEW shows delay circuit with bias technique and with respect to this technique, delay increases with an average change of 9.83%.

Table 6. Delay 10% Output to 90% Output for NOR2 at SS, 0.96V, 125 °C

Output(Y)	Slew Rate (ns)		%Change
	OLD	NEW	
Rise	5.496	6.075	10.5
Fall	3.347	3.902	11.5

3. LEAKAGE CURRENT

Leakage current is calculated by self-reverse bias technique, in which substrate leakage current through a stack of series connected transistors reduces when more than one transistor of the stack is turned off. For every off state and on state leakage is calculated at fast fast corner, power supply voltage of 1.44V and temperature of 125C given in **Table 7**. Leakage current is calculated using spectre simulator.

Table 7. Leakage Current for NOR2 at FF, 1.44V, 125°C

Inputs (A,B)	Leakage current for OLD (nA)	Leakage Current for NEW (nA)		Improvement (or reduction) in Leakage	
		Without Bias	With Bias	Without Bias	With Bias
00	3.472	3.22	0.66	1.07	5.26
01	3.81	3.459	0.35	1.10	10.7
10	5.273	4.761	0.54	1.10	9.71
11	0.624	0.572	0.04	1.09	15.6
Average Value					10.3

From **Table 7**, leakage current of all combinations of inputs A and B have been calculated. The values under OLD show the leakage current without body bias Technique and without high V_{th} transistor (from foundry) in gate NOR2. The values under NEW shows leakage current circuit with body bias and without body bias technique for high V_{th} transistor.

When all inputs are on, then leakage current for circuit with bias has been maximum reduced by 15.6 times than circuit without bias. The NOR2 cell, without bias has more leakage than with bias technique. With bias, leakage reduced by an average of 10.34 times than circuit without biasing as seen in last row and last column of **Table 7**.

4. ENERGY

Energy is calculated by taking the product of dynamic current and supply voltage at given period of time under the specified operating conditions (fast fast corner, supply voltage of 1.44V and temperature of -40C) given in **Table 8**.

Table 8. Dynamic power for NOR2 at FF, 1.44V, -40°C

Input and Output Signals Considered	Energy ($\mu\text{W}/\text{MHz}$)		%Change
	OLD	NEW	
A(f)_B(f)_y(r)	1.1167	1.1161	0.04
A(r)_B(r)_y(f)	1.1167	1.1161	0.04

In **Table 8**, the energy is calculated from rise time and fall time of the output current signal. With bias, OAI21 cell has less energy consumption than without body bias technique.

B. OAI21

1. PROPAGATION DELAY

Table 9. Delay 50% Input to 50% Output for OAI21 at SS, 0.96V, 125°C

Input and Output signals considered	Propagation delays (ns)		%change
	OLD	NEW	
A0(f) to Y(f)	2.45	2.71	10.6
B0(f)_A0(1) to Y(f)	2.35	2.58	9.78
B0(f)_A1(1) to Y(f)	2.45	2.68	9.38
A1(f) to Y(f)	2.65	2.91	9.80

A0(r) to Y(r)	3.47	3.75	8.06
B0(r)_A0(1) to Y(r)	3.39	3.69	9.11
B0(r)_A1(1) to Y(r)	3.41	3.69	8.21
A1(r) to Y(r)	3.52	3.79	7.67
Average Value 9.07			

When compared the values obtained for all the input output conditions in column NEW with values shown in column OLD, "A0 (f) to Y (f)" has maximum percentage variation i.e., 10.6%. For "A0(r) to Y(r)", there is a minimum variation of 7.67%. By using body bias technique, the average increase in delay is 9.07%, as seen from the last row last column of the **Table 9**.

Table 10. Delay 50% Input to 90% Output for OAI21 at SS, 0.96V, 125°C

Input and Output signals considered	Propagation delays (ns)		%change
A0(f) to Y(f)	1.11	1.16	5.2
B0(f)_A0(1) to Y(f)	1.02	1.04	1.9
B0(f)_A1(1) to Y(f)	1.12	1.14	1.8
A1(f) to Y(f)	1.31	1.37	4.6
A0(r) to Y(r)	6.79	7.41	9.1
B0(r)_A0(1) to Y(r)	6.695	7.34	9.7
B0(r)_A1(1) to Y(r)	6.694	7.35	9.7
A1(r) to Y(r)	6.82	7.46	9.3
Average value 6.4			

When compared the values obtained for all the input output conditions in column NEW with values shown in column OLD, "B0(r) _A0 (1) to Y(r)" has maximum percentage variation i.e., 9.7%. For "B0 (f) _A0 (1) to Y(r)", there is a minimum variation of 1.8%. By using body bias technique, the average increase in delay is 6.4%, as seen from the last row last column of the **Table 10**.

2. SLEW RATE

Table 11. Delay 10% Output to 90% Output for OAI21 at SS, 0.96V, 125°C

OUTPUT(Y)	Slew Rate (ns)		%Change
	OLD	NEW	
Rise	11.9	13.03	9.49
Fall	3.84	4.231	10.18

The values under OLD shows delay without body bias Technique in cell OAI21 and the values under NEW shows delay with body bias Technique and with respect to this technique delay increases with an average change of 11%.

3. LEAKAGE CURRENT

Table 12. Leakage Current for OAI21 at FF, 1.44V, 125°C

Inputs (A0,A1 B0)	Leakage current for OLD (nA)	Leakage Current for NEW (ns)		Improvement (or reduction) in Leakage	
		Without Bias	With Bias	Without Bias	With Bias
000	1.94	1.73	0.21	1.11	9.16
001	2.60	2.39	0.34	1.08	7.55

010	2.42	2.21	0.30	1.09	7.85
011	2.62	2.50	0.36	1.04	7.27
100	2.42	2.21	0.30	1.09	7.85
101	2.87	2.72	0.39	1.05	7.24
110	2.41	2.20	0.30	1.09	7.96
111	1.91	1.836	0.27	1.04	7.04
Average Value 1.07			7.74		

When all inputs are off then leakage current with bias has been reduced maximum by 9.16 times than without bias. The gate without bias executes more leakage than gate with bias technique. With bias, leakage has reduced by an average of 7.74 times than without biasing.Improvement (or reduction) in Leakage for the NEW (i.e. circuit with high V_{th} and body bias) compared to OLD (i.e. circuit without high V_{th}) .

4. ENERGY

Table 13. Energy for OAI21 at FF, 1.44V, -40C

Inputs	OLD	NEW	%Change
A0(r)_B0(r)_A1(r) to Y(r)	0.3752	0.374	0.32%
A0(f)_B0(f)_A1(f) to Y(f)	0.3754	0.375	0.1%

In **Table 13**, the energy is calculated from rise time and fall time of the output current signal.With bias, OAI21 cell has less energy consumption than without body bias technique.

Table 14. Performance analysis of sequential cells considered

S.No.	Cells considered	% Change with body bias in case of NEW (i.e. circuits with high V_{th}) compared to OLD (i.e. circuit with high V_{th} and without body bias)	
		Setup time (ns)	Hold time
1	TLAT	50	8.1
2	DFFHQ	39.60	27.77
3	SDFFHQ	18.88	66.67
4	SDFFNH	66.67	18.88
Average Value		43.78	30.35

From **Table 14**, it is observed that standard cell SDFFNH has maximum % change in setup time of 66.67. There is maximum hold time of 66.67% for SDFFHQ cell. Setup time is an increase an average percentage change of 43.78% and the hold time is increases an average of 30.35%, by using body bias technique (last row last column of **Table 14**).

Table 15. Performance analysis of standard cells considered

S.No	Cells	Propagation Delay	% Change with body bias in case of NEW (with body bias) compared to OLD(i.e. circuit without body bias)		
			Leakage Current		Energy
			Without body bias	With body bias	
1.	OAI21	-10.6	110	+816	+0.32
2	OAI22	-10.4	114	+778	+0.18
3	OR2	-8.36	108	+667	-0.13

4	NOR2	-8.36	110	+1460	+0.04
5	XNOR3	-9.51	111	+697	+0.003
6	MUX2	-9.78	112	+762	-0.175
7	TLAT	-1.5	106	+700	+0.14
8	DFFHQ	-2.85	111	+800	+0.14
9	SDDFHQ	-29.8	110	+800	+0.18
10	SDDFNH	-5.72	112	+900	+0.08
Average Value		9.67	100	+838	+0.77

From **Table 15**, it is observed that standard cell SDDFHQ has maximum % change in propagation delay of 29.89. There is maximum Leakage current reduction of 1460% for NOR2 cell. The maximum % change in energy consumed is for standard cell OAI21 and is 0.32%. The % leakage current reduction is to an extent of 838% with delay penalty of 9.67%, by using body bias technique (last row last column of **Table 15**).

VI. CONCLUSION

As the purpose first states, the possibility of making a standard cell library from which other constructions could be made, has been examined. A few basic cells, has been created. Each individual cell was run through simulator Spectre (cadence) and calculating delay (50%-50%), slew delay and leakage current for the cell library. Those were the steps carried out in order to make an ultra-low power standard cell library. Results show that the library provides a factor of 8-10 in leakage reduction over its predecessor library. In some cases, much greater leakage power reduction can be achieved. In addition to the power reduction, library implementations have not significant increase in delay 10-15. This generates more compact and efficient layout as some cells in the new library replace combinations of several sub-cells in the old library.

VII. REFERENCES

- [1] S. G. Uppili, D. R. Allee, S. M. Venugopal, L. T. Clark and R. Shringarpur "Standard Cell Library and Automated Design Flow for Circuits on Flexible Substrates," Flexible Electronics And Displays Conference And Exhibition, pp. 1-5, February 2019.
- [2] D. G. Baltus, T. Varga, and R. Armstrong "Developing A Concurrent Methodology for Standard-Cell Library Generation," Design Automation Conference, pp. 333-336, June 2017
- [3] P. V. D. Meer, "Ultra-Low Standby-Currents For Deep Sub-Micron VLSI CMOS Circuit, Smart Series Switch," Proc. IEEE International Symposium Circuits and Systems, Vol. 4, 2016.
- [4] W. Belluomini, D. Jamsek, A. K. Martin, C. McDowell, R. K. Montoye, H. C. Ngo, J. Sawada, "Limited Switch Dynamic Logic Circuits For High-Speed Low-Power Circuit Design," IBM J. RES. & DEV., Vol. 50, May 2016.
- [5] A. Chatterjee, "An Investigation Of The Impact Of Technology Scaling On Power Listed As Short-Circuit Current In Low Voltage Static CMOS Circuits," Proc. of the International Symposium on Low Power Electronics and Design (ISLPED), pp. 145-150, 2016.
- [6] A. Agarwal and K. Roy "Leakage Power Analysis and Reduction for Nano Scale Circuits" Published by IEEE Computer Society 2016
- [7] M. C. Lee and H. Chiueh "An Implementation of Integrable Low Power Techniques for Modern Cell-Based VLSI Designs," IEEE 13th International Conference on Electronics, Circuits & Systems (ICECS '06), pp. 890-893, December 2016
- [8] J. Wang, A. K. Wong, and E. Y. Lam, "Standard Cell Layout with Regular Contact Placement," IEEE Transaction on semiconductor Manufacturing, Vol.17, No.3, August 2014
- [9] A. B. Jambek, A. R. M. N. Beg and M. R. Ahmad, "Standard Cell Library Development," 11th International Conference on Microelectronics (ICM '99), pp.161-163, November 2009.

DESIGN OF LOW POWER FSM BASED VENDING MACHINE USING XILINX

¹ YALAGANDHULA EESWARASAI, ² Mr. G. BABU

¹PG Scholar, Dept.of ECE, Vaagdevi College of Engineering, Warangal, Telangana, India.

² Assistant professor, Dept.of ECE, Vaagdevi College of Engineering, Warangal, Telangana, India.

¹ eeswarasaivy@gmail.com, ² babugundlapally@gmail.com

Abstract— In this paper the central idea of this work is to design a vending machine that will be able to provide a number of items like soft drink, cake & cold drinks to people. The machine will also deliver the change, depending on the amount of money inserted and the price of product. At the same time we have made efforts to make the design of the Vending Machine power efficient by using power reduction techniques. In this process we have tested our design at different frequencies and analyzed the consumed power. Next, we have also calculated the power at different frequencies with different IO STANDARD like LVCMOS33, LVCMOS12, SSTL18BI, HSTLBI18. The proposed design is tested and implemented using VERILOG HDL and XILINX ISE 14.2 targeting XC3S500E FPGA. The result shows optimization of power.

Keywords: Verilog, lvcmos33, iostandard, sstl18bi, hstlbib18.

I. INTRODUCTION

Vending Machine is a product used to dispense various products like candy, cold drinks, cakes etc. when desired amount of money is inserted into it. The Vending Machine is more accessible and practical than conventional purchasing method. Nowadays, Vending Machine can be seen everywhere near ATMs, Metro Stations, Movie Theatres and many more places. These are handier as they are accessible 24x7 [7]. It also helps in reduction of overhead costs by not hiring of staff increases profit margin. They can also be moved to other places in case the situation arises and they will continue performing in the same manner as it was performing earlier. In most of the papers based on vending machine, the main focus is to increase the number of products, as well as the speed of computation of the machine. But increase in computational speed as well as by increase in quantity of products is possible only through increased hardware which leads to high power consumption that keeps on increasing due to

development in VLSI technology. In this paper we have discussed some techniques for reduce power at the architectural level to make my design of Vending Machine more efficient in terms of power.

FPGA is a Silicon chip containing two dimensional arrays of logic blocks and with electrically programmable interconnects [8]. The main reason behind choosing our platform as FPGA instead of any microprocessor is the advantage it possesses i.e. it can be reprogrammed at any time with different functionality each time [9]. Moreover if any one made an error in his design he can just fix that logic, recompile it and redownload it on your FPGA Board, no need for soldering or no need to change the components. The speed of computation is also very fast in FPGA. The Vending machine is based on the concept of FSM. There are only two types of state machines, and Moore model. The output depends on the input as well as the present state. The output depends only on the present state.

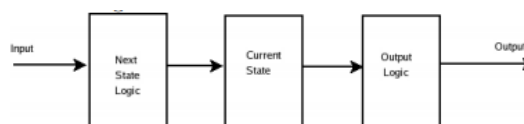


Figure-1: Moore Machines

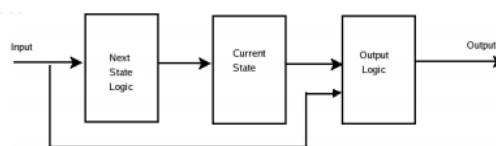


Figure-2: Mealy Machines

II. RELATED WORK

a) mishra s, verma G. "low power and area efficient implementation of BCD adder on Fpga", international conference on signal processing and communication (icscY2013); 2013 Dec 12Y14; Jit, noida: ieeEXplore; 2013. p. 461-5

Decimal adders and multipliers are the basic building block for arithmetic and logical unit and barrel shifters in today's high end processors and controllers. In this paper, an efficient BCD adder is designed based on low power synthesis technique at the architectural level. There are different levels of abstraction at which the power can be minimized but the low power technique at the architectural level has more impact than that of circuit level approaches. Two different approaches have been discussed i.e. pipelining and parallelism, so as to minimize the power consumption at architectural level. The proposed designs are tested and implemented using VHDL and the Xilinx ISE 10.1 targeting Xilinx XC5VLX30-3 FPGA. The result shows the optimization of power, delays and the area for different designs and a comparison analysis is provided based on the existing designs in the literature.

b) **Gauravverma, shambhavimishra, sakshiagarwal,surabhisingh, sushants hekhar and sukhbanikaurvirdi, I power consumption analysis of BeD adder using X power analyzer on vertex Fpga", Indian Journal of science and technology, vol 8(18), ipl0160, august2015**

Adders are the integral part of any digital circuit operation. Optimization of adder's supremacy along with its vicinity is a demanding chore. In this work an efficient BCD ADDER1 is analyzed in terms of power consumption by scaling the various parameters like voltage, frequency and load capacitance. In addition to this the focus is also given on the airflow of the device to reduce the power. Finally the power is reduced by sending different encoded data at the input. The proposed designs are hardened and implement by means of VHDL and Xilinx ISE (integrated Software Environment) 14.5 and validated using XPower targeting Virtex FPGA. Power consumption is discussed in terms of clock, signals, logic, input/ outputs and leakage. A comparative analysis has been shown at the end to validate the obtained results.

III. IMPLEMENTATION OF VENDING MACHINE

In this paper a state diagram is constructed for the proposed machine which can vend four products that is coffee, cold drink, candies and snacks. Four

select (select1, select2, select3) inputs are taken for selection of products. Select1 is used for the selection of snacks. Similarly select2, select3, are used for coffee, cold drink and candies respectively. Rs_05 and rs_10 inputs represents rupees 15/- notes respectively. A cancel input is also used when the user wants to withdraw his request and also the money will be returned through the return output. Return, product and change are the outputs. Return and change vectors are seven bits wide. Money is an in/out signal which can be updated with the total money of all products delivered at a time. Money signal is seven bits wide. Money_count is an internal signal which can be updated at every transition. This signal is also seven bits wide. If the inserted money is more than the total money of products then the change will be returned through the change output signal. The products with their prices are shown by table 1. There are also two input signal clk and reset. The machine will work on the positive edge of clock and will return to its initial state when reset button is pressed. The proposed vending machine is designed using FSM modelling and is coded in VHDL language.

IV. DESIGN METHODOLOGY

- i) the user first selects the item he wants to purchase.
- ii) then the user inserts the money.
- iii) if the money inserted in the machine matches to that of the product selected then the product is dispensed as the output.
- iv) if there is any change left it is given back to the user. in my vending machine there are only 3 types of product with their prices given below in table 1:

Table 1: product with their prices

S.NO	PRODUCT	PRICE
1	CANDY	5
2	CAKE	10
3	COLD DRINK	15

From the figure 3 it is clear that vending machine only accepts two types of coins i.e. coin B5 (for a 5 rupee coin) and coin B10 (for a 10 rupee coin). Four types of select bit are also present for the user i.e.

- i) SB0: initially it will be present in idle state or reset state.
- ii) SB1 (2Gb01): for the selection of product candy.
- iii) SB2 (2Gb10): for the selection of the product cake.

iv) SB3 (2Γb10): for the selection of the product cold drink.

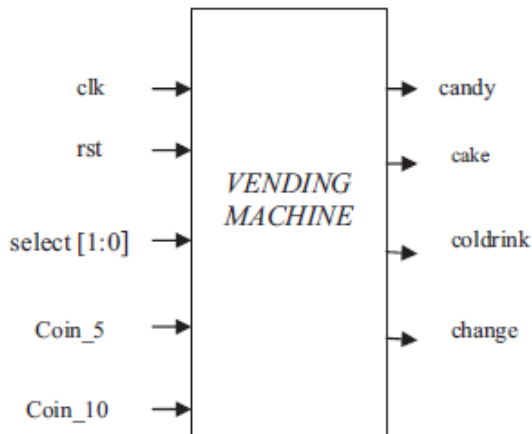


Figure-3: Block diagram of Vending Machine

Vending machine has also five intermediate states.

- i) StB0(if it is in state zero)
 - ii) StB5(if it is in state five)
 - iii) StB10(if it is in state ten)
 - iv) StB15(if it is in state fifteen)
 - v) StB20(if it is in state twenty)
- the FSM of cold drink, candy, cake are shown in figure 4, 5 and 6 respectively.

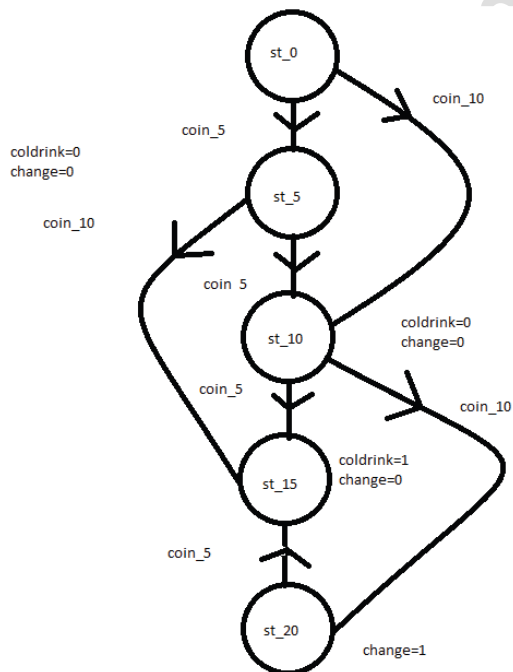


Figure-4: FSM for cold drink

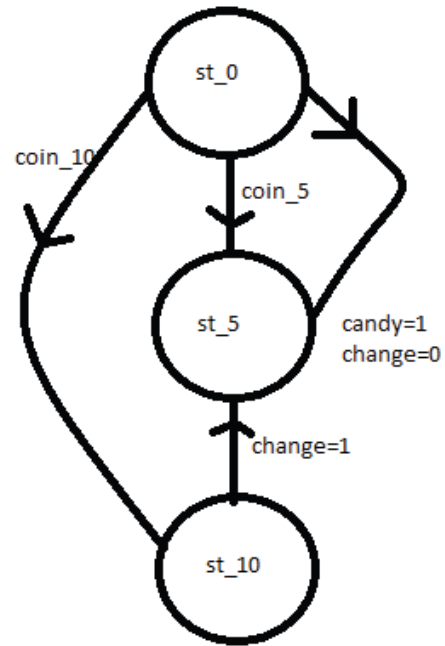


Figure-5: FSM for candy

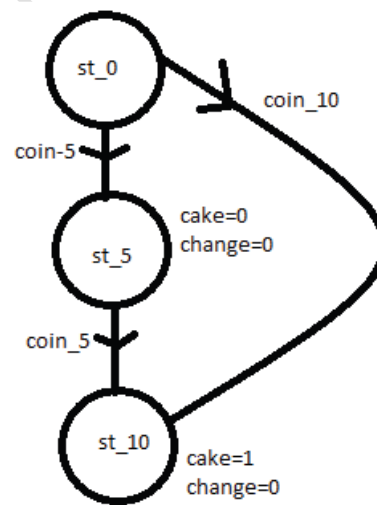


Figure-6: FSM for cake

V. RESULTS

RTL Schematic: RTL schematic is described as register transfer logic that means the logic is transferred to registers it is also known as designer view because of it is looking like what is the intension of designer.



Figure-7: RTL Schematic of Vending Machine

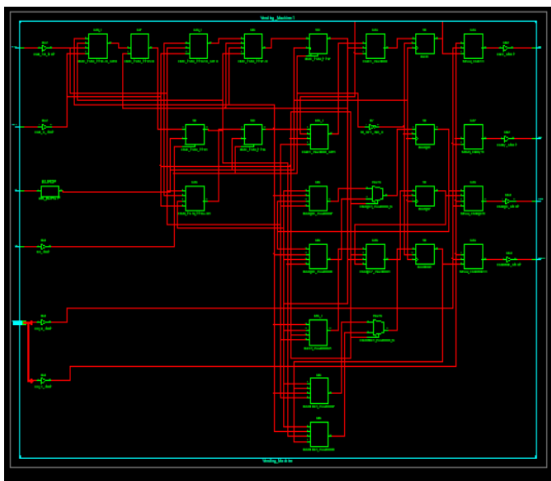


Figure-8: View Technology Schematic of Vending Machine



Figure-9: Simulated wave form of vending machine for candy when 5 rupee coin insert

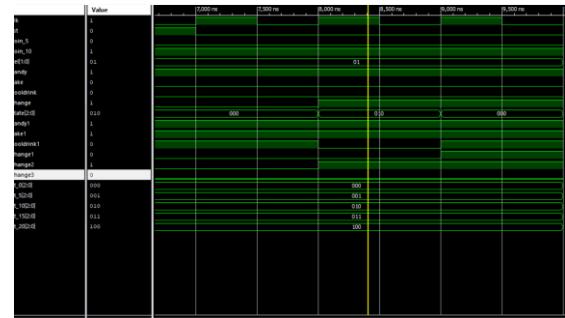


Figure-10: Simulated wave form of vending machine for candy when 10 rupee coin insert

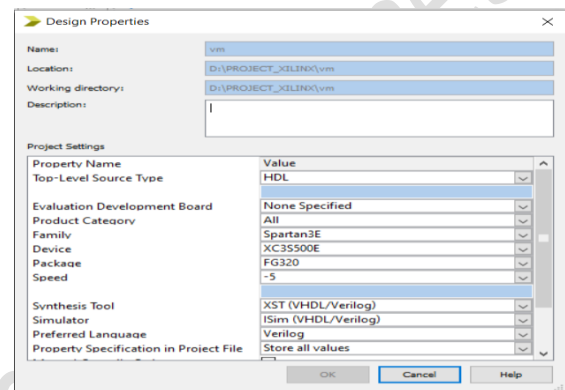


Figure-11: Device preferred for simulation

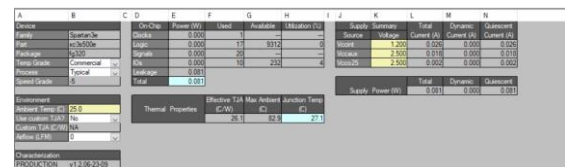


Figure-12: Power consumption for spartan3e

Device Utilization Summary			
Logic Utilization	Used	Available	Utilization
Number of Slice Flip Flops	7	9,312	1%
Number of 4 input LUTs	17	9,312	1%
Number of occupied Slices	9	4,656	1%
Number of Slices containing only related logic	9	9	100%
Number of Slices containing unrelated logic	0	9	0%
Total Number of 4 input LUTs	17	9,312	1%
Number of bonded IOBs	10	232	4%
Number of BUFGMUXs	1	24	4%
Average Fanout of Non-Clock Nets	3.65		

Figure-13: Hardware utilization summary

Minimum period: 2.928ns (Maximum Frequency: 341.565MHz)

Minimum input arrival time before clock: 3.562ns

Maximum output required time after clock: 5.255ns

Maximum combinational path delay: 5.895ns

Power consumption 0.1478m.watt.

VI. CONCLUSION

The vending machines that are popularly used till date are operated by receiving specific denomination i.e. The cost of the product and deliver it. They don't work when combinations of coins are inserted or more or less amount is given. But this vending machine is a solution for the above problems. It will deliver the product even if we insert more than the cost of the product and give the remaining change. It also delivers the product if we insert the amount in combination of coins. Some further developments are to be made to accept the currency notes also.

REFERENCES

- [1] Mishra S, Verma G. Ilow Power And Area Efficient Implementation Of BCD Adder On FPGA", International Conference On Signal Processing And Communication (Icscy2013); 2013 Dec 12Y14; Jiit, Noida: Ieeerxplere; 2013.P.461-5.
- [2] Gaurav Verma, Shambhavamishra, Sakshiaggarwal, Surabhisingh, Sushantshekhar And Sukhbanikaurvirdi, Ipower Consumption Analysis Of BCD Adder Using Xpower Analyzer On Virtexfpga", Indian Journal Of Science And Technology, Vol 8(18), Ipl0160, August 2015.
- [3] Xilinxinc., Spartan 3 Data Sheet: [Http://Ww W.Xilinx.Com](http://www.xilinx.com)
- [4][Http://Www.Xilinx.Com/Support/Documentatio n/Userguides/Ug471b7seriesbselectio.Pdf](http://www.xilinx.com/support/documentation/userguides/ug471b7seriesbselectio.pdf)
- [5] Verilog hdl By Samirpalnitkar.
- [6] FPGA Prototyping By Verilog Examples By Pongp.Chu.
- [7] Anamonga, Balwindersingh, Fsm Based Vending Machine Controller With Auto Billing Features.
- [8][Http://Www.Tutorialreports.Com/Computerysc ience/FPGA/Overview.Php](http://www.tutorialreports.com/computer-science/fpga/overview.php)
- [9][Http://Www.Slideshare.Net/Sanjivmalik/Fpgasy anyoverview](http://www.slideshare.net/sanjivmalik/fpgasyanyoverview)
- [10] T. Gupta, G. Verma, A. Kaur, B. Pandey, A. Singh, T. Kaur, 9 Energy Efficient Counter Design Using Voltage Scaling On FPGA9 In International Conference On Communication Systems And Network Technologies (Csnty2015) April 4Y6, 2015 Organized By Machine Intelligence Research Labs, Gwalior, India.
- [11] S. Aggarwal, G. Verma, R. Kumar, A. Kaur, B. Pandey, S. Singh, T.Kaur, 9 Green Ecg Machine Design Using Different Logic Families 9 In International Conference On Communication Systems And Network Technologies (Csnty2015) April 4Y6, 2015 Organized By Machine Intelligence Research Labs, Gwalior, India.
- [12] T. Gupta, G. Verma 9 Area & Power Optimization Of Vpb Peripheral Memory For Arm7tdmi Based Microcontrollers9 In International Conference On Cognitive Computing And Information Processing (Ccipy2015) March 3Y4, 2015 Jssaten, Noida, India.



Improved transconductance multipath recycling folded cascode amplifier

Sudheer Raja Venishetty¹ · Kumaravel Sundaram²

Received: 15 March 2021 / Accepted: 30 March 2022

© The Author(s), under exclusive licence to Springer-Verlag GmbH Germany, part of Springer Nature 2022

Abstract

In this paper, an enhanced multipath recycling folded cascode (EMRFC) operational transconductance amplifier (OTA) is presented. In the proposed amplifier a high current node is created in the recycling structure by shorting the two drains of the current mirrors and a positive feedback at the output load are employed with multipath current recycling technique. With these modifications, the proposed amplifier achieves a high DC gain and unity gain bandwidth. The proposed EMRFC amplifier with conventional FC, RFC, and IRFC amplifiers are designed and implemented using UMC 180 nm CMOS technology for a total bias current of 300 μ A. The EMRFC amplifier exhibits a DC gain enhancement of about 40 dB as well as a 90 MHz increase in UGB compared to the conventional folded cascode configuration. Moreover, the input-referred noise of the proposed OTA is also reduced. The simulations carried out in Cadence Spectre Environment confirm the theoretical results and illustrate that the proposed amplifier has a better figure of merits (FoMs) compared to its counterparts.

1 Introduction

In many high-speed analog applications like switched capacitive filters, converters, sample and hold circuits, the operational transconductance amplifier (OTA) is the major building block. The performance of the high-speed application depends upon the operational characteristics of the OTA. Hence, in recent times many of the researchers have proposed several techniques for designing these OTAs with wide bandwidth, larger gains, and slew rates with low noise. To deal with the consequences of scaling the technology down to the submicron process and to design high-performance OTAs, folded cascode amplifier is commonly used because of its high DC gain and larger swings. The design equations and processes of a fully differential folded cascode OTA for addressing the needs of inexperienced

analogue integrated circuit designers are described in Mallya and Nevin (1989) and considered to be the first of their kind. A transconductance, bandwidth, and slew rate enhancement technique based on current splitting and recycling is proposed in Mottaghi-Kashtiban et al. (2006) and termed as a recycling folded cascode amplifier (RFC) (Assaad and Silva-Martinez 2009). Further improvements in transconductance, unity-gain bandwidth of FC OTA is achieved in Yilei et al. (2012) by employing separate AC and DC paths and is named as improved recycling folded cascode amplifier (IRFC) (Li et al. 2010). The concept of positive feedback for the enhancement in DC gain by increasing the output impedance is utilized and discussed in Akbari et al. (2014). A current steering positive feedback is applied to RFC OTA in Kumaravel and Venkataramani (2014) for performance enhancement in terms of DC gain. The double recycling technique is proposed and adopted to RFC OTA in Yan et al. (2012) and the performance improvements are presented. A novel technique is addressed in Venishetty and Sundaram (2019) for enhancing DC gain by increasing output impedance and termed as modified recycling folded cascode amplifier (MRFC). An FC OTA in which all the transistors are operated in the sub-threshold region for achieving performance metrics with reduced power consumption is described in Ragheb and Kim (2017). High recycling

✉ Sudheer Raja Venishetty
sudheerraja_v@vaagdevi.edu.in

Kumaravel Sundaram
kumaravel.s@vit.ac.in

¹ Department of Electronics and Communication Engineering, Vaagdevi College of Engineering, Warangal, India

² Department of Micro and Nano Electronics, School of Electronics Engineering, Vellore Institute of Technology, Vellore, India

folded cascode OTA (HRFC) developed by shorting two drains of the current mirror transistors of recycling structure for enhancing DC gain, unity gain bandwidth is discussed (Yosefi 2019) and the enhanced results are presented in Feizbakhsh and Yosefi (2019). A high current recycling structure including separate AC and DC paths with positive feedback is discussed in Venishetty and Sundaram (2020) and presented simulation results illustrates the enhancements in DC gain, slew rate, and UGB. However depending upon the specifications requirement, several architectures are discussed and designed in (Razavi 2002; Allen and Holberg 2011).

This paper presents a novel multipath recycling technique with the high current node in the recycling structure and positive feedback at the output load for achieving enhancements in the output impedance, transconductance, which leads to achieve high DC gain, and unity-gain bandwidth (UGB).

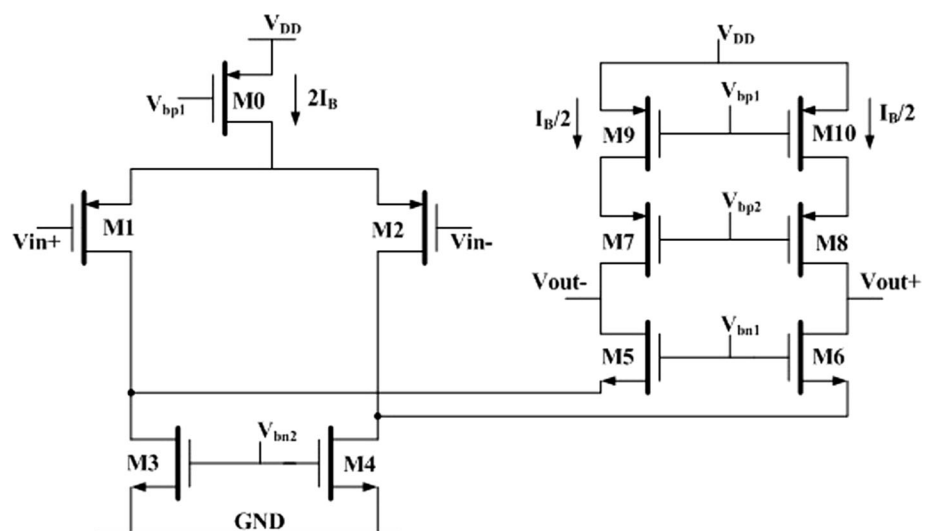
The proposed paper is organized as follows: Sect. 2 discusses the conventional folded cascode (FC), recycling folded cascode (RFC), and improved recycling folded cascode (IRFC) OTA architectures. Section 3 presents the proposed EMRFC amplifier with detailed analysis for transconductance, output impedance, frequency response, slew rate, and noise using necessary design equations. Section 4 illustrates the simulation results and discussions, while conclusions are presented in Sect. 5.

2 Conventional FC, RFC, and IRFC OTA structures

For understanding the advantages of folded cascode topology, FC OTA and its modified versions RFC and IRFC OTAs are presented here from the state of art

literature. Figure 1 illustrates the folded cascode (FC) OTA, while RFC and IRFC are shown in Figs. 2 and 3 respectively. The major limitation of conventional folded cascode OTA shown in Fig. 1 is that the tail current sources M3 and M4 exhibits very high current and do not contribute to the overall transconductance of the OTA. To overcome this limitation at the folded node, modifications are proposed to the conventional FC OTA using current splitting and current recycling techniques, and the new architecture is termed as recycling folded cascode (RFC) OTA (Mottaghi-Kashtiban et al. 2006; Assaad and Silva-Martinez 2009). The current splitting principle is applied by splitting two input transistors M1 and M2 of FC OTA into four M1a, M1b, M2a, and M2b transistors which carry equal currents, while current recycling is implemented by converting tail current sources M3 and M4 of FC OTA into pair of current mirrors with a current-carrying ratios $k : 1$ and is illustrated in Fig. 2. These modifications resulted in the enhancements of transconductance by $(k + 1)/2$ times compared to FC and hence DC gain is also increased with enhanced power efficiency. Further, it is observed from the RFC topology, that the current mirrors formed by splitting input transistors for current recycling use the same path for AC and DC currents. The sharing of the same current path by both AC and DC counterparts has limited the further enhancement of transconductance and also made this technique inefficient for other OTA structures. This limitation of the RFC OTA is resolved by providing separate AC and DC paths in the recycling structure and the new OTA is termed as improved recycling folded cascode (IRFC) amplifier (Yilei et al. 2012; Li et al. 2010) and is illustrated in Fig. 3. As shown in Fig. 3, The transistors M3c-M11b and M4c-M12b carries pure DC currents while AC currents flow through M3a-M3b—M11a and M4a-M4b-M12a. From Mottaghi-Kashtiban et al. (2006);

Fig. 1 Fully differential folded cascode amplifier (FC) (Mallya and Nevin 1989)



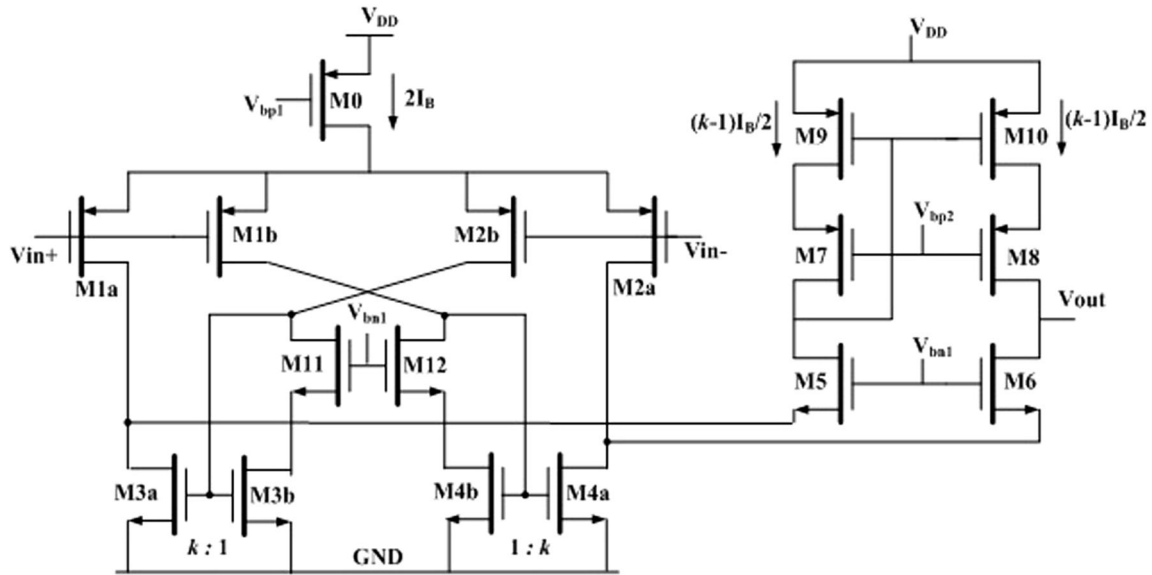


Fig. 2 Recycling folded cascode amplifier (RFC) (Mottaghi-Kashtiban et al. 2006; Assaad and Silva-Martinez 2009)

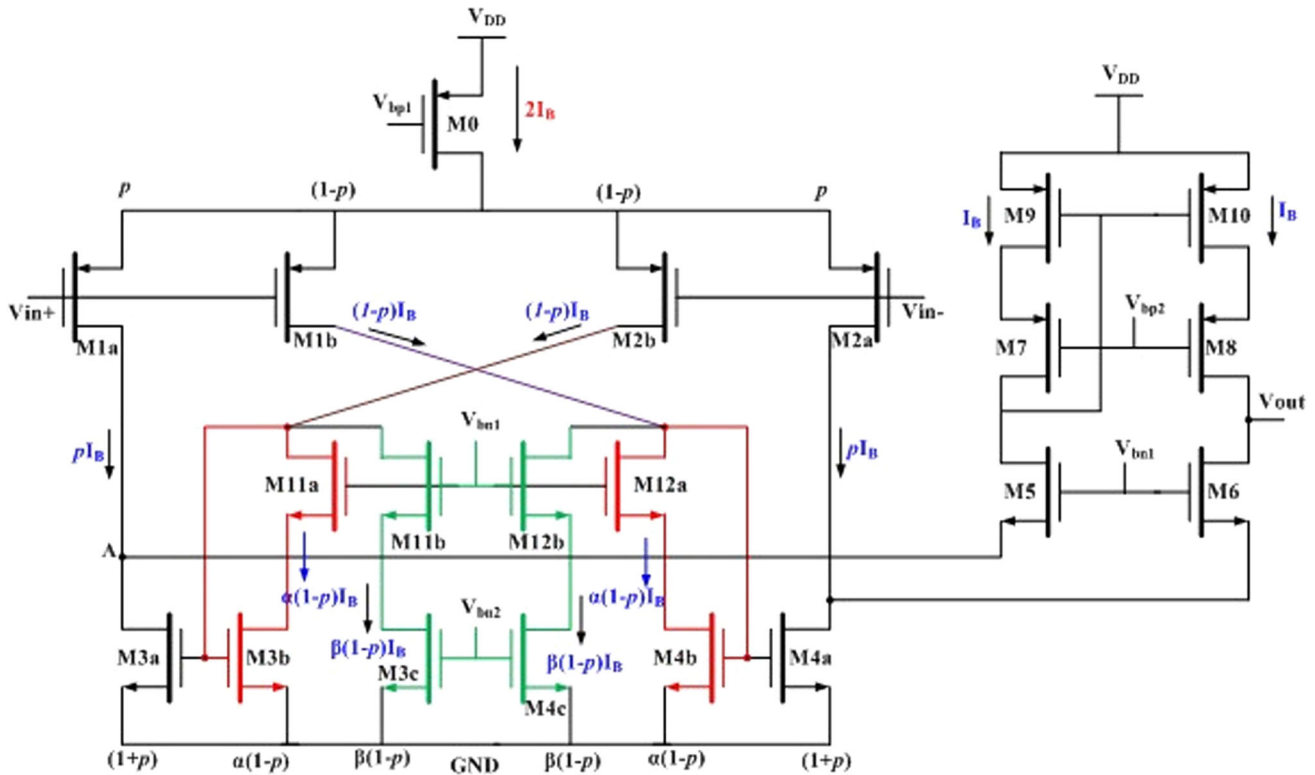


Fig. 3 Improved recycling folded cascode amplifier (IRFC) (Yilei et al. 2012; Li et al. 2010)

Assaad and Silva-Martinez (2009), the effective transconductance (G_m) of FC, RFC, and IRFC OTAs are,

$$G_{m,FC} = g_{m1} \tag{1}$$

$$G_{m,RFC} = (k + 1)g_{m1a} \tag{2}$$

$$G_{m,IRFC} = \left(p + \frac{p + 1}{\alpha} \right) g_{m1} \tag{3}$$

From Eq. (1), Eq. (2), and Eq. (3), it can be inferred that with proper selection of p and α , IRFC can have improved performance when compared with RFC that achieves 2 times enhancement over FC. Besides its higher

transconductance, IRFC has higher output impedance compared to FC and RFC OTAs, as smaller current flows through M3a and M4a. Hence with improved transconductance and larger output impedance, IRFC exhibits higher DC gain compared to its counterparts FC and RFC.

3 Proposed EMRFC Amplifier

In Yilei et al. (2012) and Li et al. (2010), improved recycling folded cascode amplifier (IRFC) is proposed to enhance the DC gain and unity gain bandwidth of the RFC amplifier by providing separate paths for AC and DC currents. As shown in Fig. 3, the DC path M11b-M3c, M12b-M4c can be utilized further for contributing to overall transconductance by driving the cascode transistors M11b and M12b of DC path from the small-signal inputs and converting the transistors M3c and M4c into a single compound transistor carrying double current compared to IRFC structure. Hence with this modification, the transistors M11b-M12b looks like the input pair of a differential amplifier and the compound transistor acts as a tail current source of the same. To maintain the separate AC and DC path, the transistors M11b and M12b are properly driven with V_{in-} and V_{in+} inputs respectively. Therefore the advantage of achieving enhancement in transconductance by separate AC and DC paths as discussed in IRFC and as well current recycling from the differential pair formed by M11b-M12b can be utilized simultaneously. Hence three small-signal currents flow from folded node to the output, (1) Current flowing to the output from input transistor M1a via M5, (2) Current flowing from another input transistor M2b through the cross over current mirror M3a: M3b through M5 to the output, (3) Recycled current from M12b through current mirror M3a: M3b through M5 to the output. However, it can be observed from the proposed amplifier architecture that the gain of the input differential pair M1b-M2b is remained to be 1, because of diode-connected current mirrors M3b-M11a and M4b-M12a transistors. Also, it can be observed that the transistors M9 and M10 are carrying larger currents but don't contribute to the overall transconductance. Hence the overall transconductance of the amplifier can be further increased by making transistors M3b-M11a, M4b-M12a, and M9-M10 contribute to the gain with the following modifications: 1. Creating a Node 'N' by shorting the drains of the current mirror transistors M3b and M4b. This node is referred to as a High Current Node since it carries twice the current. 2. By incorporating positive feedback at the output by driving the output transistors M9 and M10 with an incremental

small signal from the drains of M2b and M1b respectively. Therefore with the principles of multipath current recycling, high current node, and positive feedback, the complete architecture of the proposed amplifier is illustrated in Fig. 4 and is named as Enhanced Multipath Recycling Folded Cascode amplifier (EMRFC). With the proposed architecture, a gain of more than 30 dB is expected compared to FC, RFC, and IRFC amplifiers.

3.1 Performance characteristics of EMRFC

To achieve the maximum advantages of modifications proposed for the enhancements in the performance characteristics, the different current ratios among the transistors in the architecture are maintained properly and the same is illustrated in Fig. 4. The tail current $2I_B$ from M0 is equally distributed among the input transistors M1a-M1b-M2a-M2b, whereas the currents in the current mirror transistors are chosen in the ratios as, M3a: M3b = M4a: M4b = $(1 + p) : \alpha$. The current flowing from M9 and M10 are $pI_B/2$. The complete analysis of performance characteristics such as transconductance, output impedance, slew rate, and noise with necessary design equations for the proposed amplifier are presented in the following sections.

3.1.1 Small signal transconductance

The effective transconductance ($G_{m,EMRFC}$) of the proposed EMRFC amplifier shown in Fig. 4, can be obtained from the half circuit transistor model depicted in Fig. 5, which includes the effect of high current node N and also multipath recycling principle. Small signal analysis can be performed on the half circuit transistor model. The effective transconductance can be obtained by shorting the output node to ground and finding the expression for the short circuit current (I_{SC}) in terms of input voltage. The node voltage at the gate terminal of the current mirror transistor M3a termed as V_{gs3a} , can be calculated by considering the section of half circuit model shown in Fig. 5 and is illustrated in Fig. 6.

From Fig. 6, the node voltage V_{gs3a} is expressed as,

$$V_{gs3a} = -V_{in}^- \cdot (g_{m2b} + g_{m3c}) [r_{02b} \parallel r_{03c} \parallel r_{011}] \quad (4)$$

The current flowing through the current mirror transistor M3a (I_{ds3a}) is expressed as,

$$I_{ds3a} = -g_{m3a} \cdot V_{in}^- \cdot (g_{m2b} + g_{m3c}) [r_{02b} \parallel r_{03c} \parallel r_{011}] \quad (5)$$

Therefore the total short circuit current (I_{SC}) flowing through the output is expressed as,

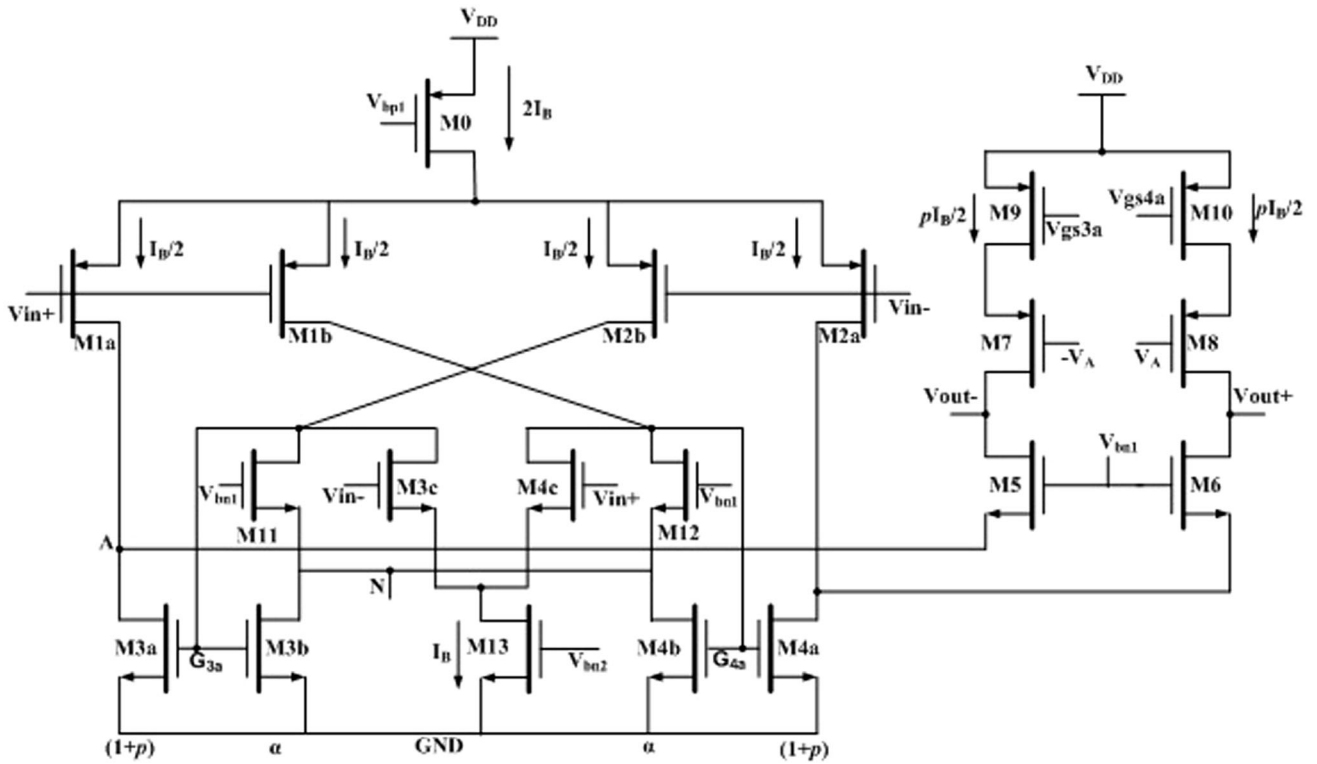


Fig. 4 Proposed enhanced multipath recycling folded cascode amplifier (EMRFC)

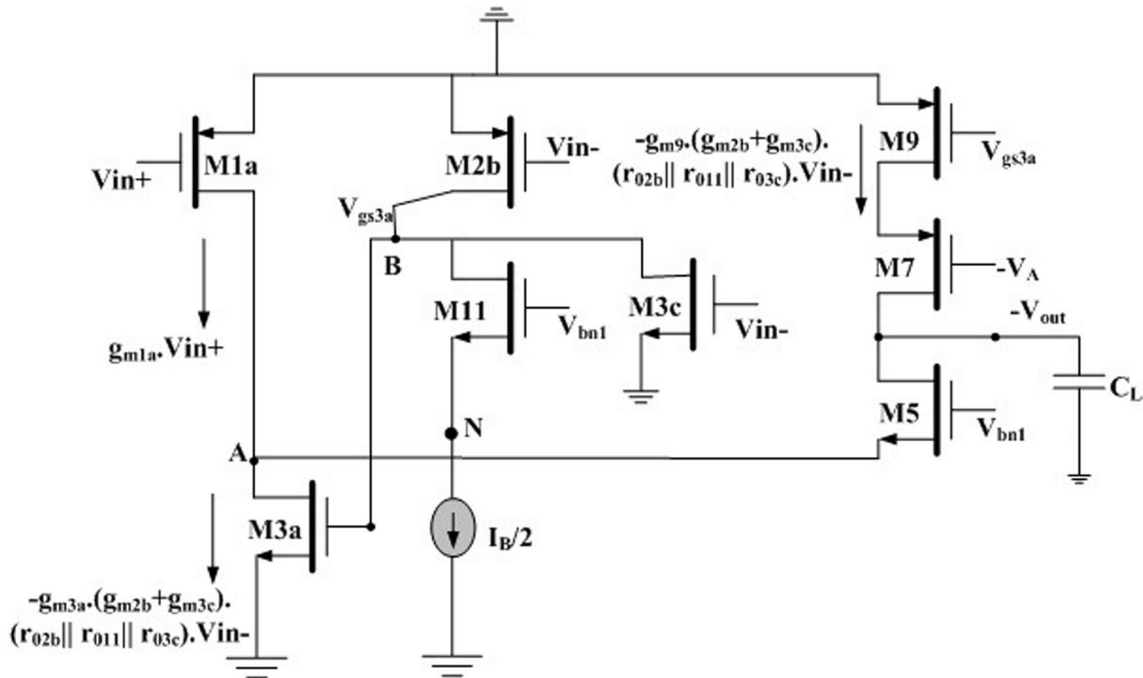


Fig. 5 Half circuit transistor model of EMRFC with effect of node N and multipath recycling

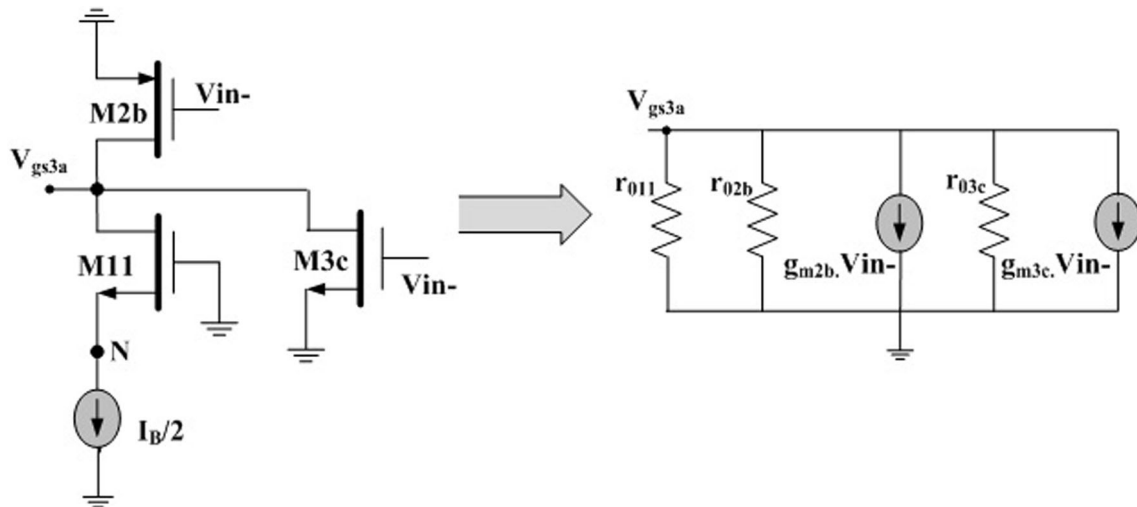


Fig. 6 Section of half circuit transistor model of EMRFC for calculating V_{gs3a}

$$\begin{aligned}
 I_{SC} &= I_{sd1a} - I_{ds3a} + I_{sd9} \\
 &= g_{m1a} \cdot V_{in}^+ \\
 &+ g_{m3a} \cdot V_{in}^- \cdot (g_{m2b} + g_{m3c}) [r_{02b} \parallel r_{03c} \parallel r_{011}] \\
 &+ g_{m9} \cdot V_{in}^- \cdot (g_{m2b} + g_{m3c}) [r_{02b} \parallel r_{03c} \parallel r_{011}]
 \end{aligned} \tag{6}$$

Hence the effective transconductance of the proposed EMRFC amplifier after substituting the current ratios as discussed earlier in Eq. (6) is,

$$G_{m,EMRFC} = g_{m1a} \cdot (g_{m2b} + g_{m3c}) (1 + 2p) \cdot R_X \tag{7}$$

where $R_X = (r_{02b} \parallel r_{03c} \parallel r_{011})$

Out of Eq. (7), it can be concluded that, relative to traditional equivalents FC, RFC and IRFC OTAs, a substantial improvement in the transconductance of the proposed amplifier resulting in an increase of 30-40 dB in the DC gain is likely.

3.1.2 Output impedance

The output impedance of the proposed amplifier is enhanced by adopting positive feedback at the output as shown in Fig. 4. Positive feedback is applied by driving the gate terminals of M7 and M8 output cascode transistors from the folded node. To calculate the output impedance, an arbitrary voltage V_X is applied at the output and the current I_X is measured with input made to zero volts. The half circuit transistor model and its small-signal equivalent for deriving the expression of the output impedance of the proposed EMRFC amplifier is shown in Fig. 7.

From Fig. 7, the output impedance can be expressed as,

$$R_{out,EMRFC} = r_{07} (g_{m7} + g_{mb7}) [r_{09} \parallel (r_{03a} + r_{09})] \tag{8}$$

From Eq. (8), it is found that the output impedance of the proposed EMRFC amplifier is enhanced compared to conventional FC, RFC, and IRFC OTA. With these modifications, a DC gain of around 10-15 dB enhancement is likely to achieve compared to its counterparts.

The low frequency gain of any operational transconductance amplifier (OTA) is expressed as the product of effective transconductance and its output impedance. Hence the DC gain of the proposed EMRFC amplifier can be obtained from Eq. (7) and Eq. (8) as,

$$\begin{aligned}
 A_{V,EMRFC} &= g_{m1a} \cdot (g_{m2b} + g_{m3c}) (1 + 2p) \cdot R_X \\
 &\cdot r_{07} (g_{m7} + g_{mb7}) [r_{09} \parallel (r_{03a} + r_{09})]
 \end{aligned} \tag{9}$$

where g_{mi} is the transconductance of transistor m_i and r_{0i} is the drain to source resistance of the corresponding transistor m_i and $R_X = (r_{02b} \parallel r_{03c} \parallel r_{011})$.

3.1.3 Frequency response

The frequency response of the proposed EMRFC amplifier can be derived by considering its high-frequency model. It can be observed that the proposed EMRFC amplifier exhibits the dominant pole, P_1 at the output node with output capacitance approximately equivalent to load capacitance (C_L). The expression of the dominant pole is given by Eq. (10) as,

$$P_1 = \frac{1}{R_{out} \cdot C_{out}} \approx \frac{1}{R_{out,EMRFC} \cdot C_L} \tag{10}$$

where $R_{out,EMRFC}$ is the output impedance of the proposed amplifier expressed by Eq. (8).

Similarly, the proposed amplifier exhibits two non-dominant poles P_2 , and P_3 one at the gate node of recycling current mirror transistor M3a and another one at the folded

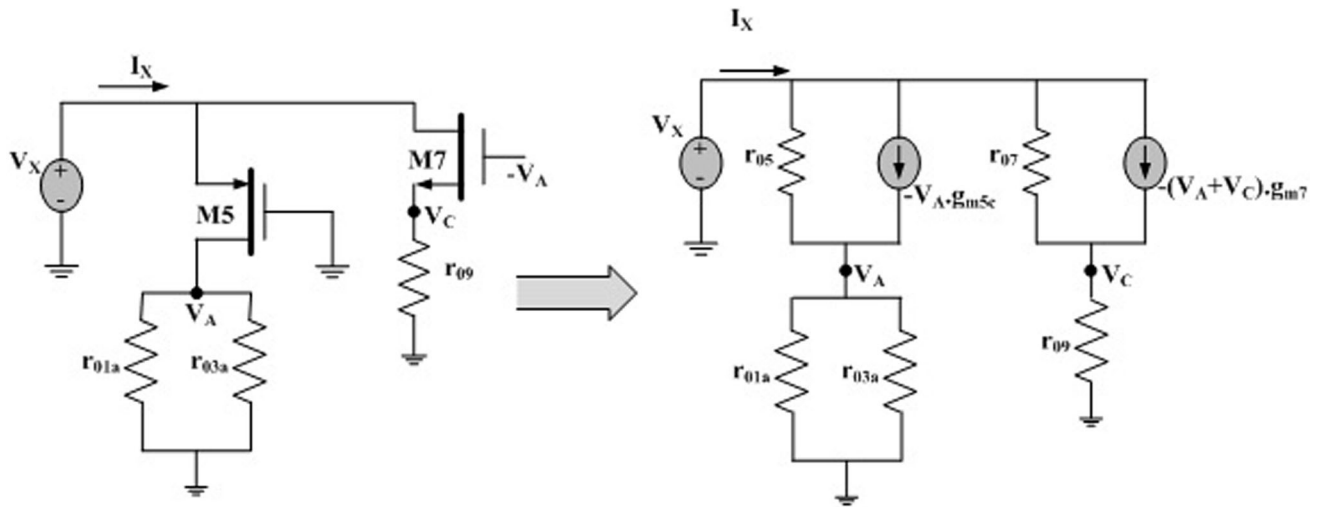


Fig. 7 Equivalent model for output impedance calculation of EMRFC using positive feedback structure

node respectively. The expressions for these two non-dominant poles P_2 and P_3 are given in Eq. (11) and Eq. (12) as,

$$P_2 \cong \frac{1}{\left(r_{02b} \parallel r_{03c} \parallel \left(r_{03b} \parallel \frac{1}{g_{m3b}}\right)\right) \cdot C_{gs1a}} \quad (11)$$

$$P_3 \cong \frac{1}{\left(r_{01a} \parallel r_{03a} \parallel \frac{1}{g_{m5}}\right) \cdot C_{gs5}} \approx \frac{g_{m5}}{C_{gs5}} \quad (12)$$

The proposed amplifier also exhibits a zero because of the feed-forward path from input to output through the gate-drain capacitance C_{gd} of input transistor M1a, and can be expressed by Eq. (13) as,

$$Z_1 \cong \frac{g_{m1a}}{C_{gd1a}} \quad (13)$$

The unity-gain bandwidth (UGB) of the proposed amplifier can be defined as the product of DC gain given by Eq. (9) and dominant pole frequency given by Eq. (10) and is expressed as,

$$UGB = A_{V,EMRFC} \cdot P_1 \cong \frac{g_{m1a} \cdot (g_{m2b} + g_{m3c}) \cdot (1 + 2p) \cdot R_X}{C_L} \quad (14)$$

where $R_X = (r_{02b} \parallel r_{03c} \parallel r_{011})$.

Hence from Eq. (14), it can be observed that the suitable selection of p will result in enhanced UGB compared to conventional FC, RFC, and IRFC for the same given current and load capacitance.

As given by Eq. (11) and Eq. (12), the poles P_2, P_3 at the recycling current mirror node and folded node is related to NMOS transistors, hence should be located at a relatively high frequency. When compare to the poles of conventional FC, RFC, and IRFC at these nodes, the poles $P_2,$ and

P_3 of the proposed amplifier are at lower frequencies. But because of the increased impedance at the recycling node i.e. at the gate of transistor M3a as shown in Fig. 4 results in a limitation related to the second pole P_2 of EMRFC. Hence this pole P_2 may disturb the dominant pole located at the output by moving to the frequencies less than the dominant pole. Therefore, the proposed EMRFC should be compensated to cancel the effect of this pole P_2 to improve phase margin. A simple RC compensation (Yosefi 2019) can be performed by connecting a resistor R in series with a capacitance C between the output node and the recycling current nodes at the gates of M3a and M4a transistors. Further, the resistors of the compensation circuit can be implemented by using simple pseudo transistors MP1 and MP2 that operate in the triode region, and the same is illustrated in Fig. 8.

The proper selection of R and C values will decrease the impedance at recycling nodes because, at high frequencies, the capacitor C provides a low impedance between outputs ($V_{out+,-}$) and gates of M3a-M4a moving the pole P_2 to high frequencies.

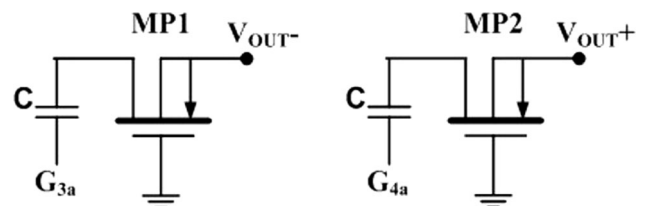


Fig. 8 RC compensation circuit employed in EMRFC between the outputs and nodes G3a and G4a

3.1.4 Slew rate

Slew rate (SR) is one of the main parameters used to study the settling time performance of the OTA. It is defined as the maximum rate of change of voltage to unit time at a given node within the circuit. Slew rate measures, how fast the circuit converts the input to output. Hence for a given amplifier, the higher is the slew rate faster will be the amplifier. A general approach for measuring the slew rate is to apply a large signal at the input and finding the current that charges and discharges the load capacitance.

Slewing process of the proposed EMRFC can be studied as follows: A large positive step input signal is applied at the inputs. When the input V_{in}^+ goes high, the input transistors M1a and M1b are forced to turnoff which in turn drives the transistors M4a, M4b, and M6 to cutoff which in turn switches off the transistor M2a. Hence the total tail current $2I_B$ from the transistor M0 is forced to flow through M2b which in turn mirrored to M3a with the current ratio $(1 + p) : \alpha$ from M3b. Similarly, the current from M2b is mirrored to M9 with a current ratio of $p : 1$. Hence M9 source current and M3a sink current flows through the load capacitance C_L resulting in the slewing. The slew rate of the proposed amplifier can be expressed as,

$$SR_{EMRFC} = \frac{(1 + 2p) \cdot 2I_b}{\alpha \cdot C_L} \tag{15}$$

From Eq. (15), it may be noted that the slew rate of the proposed amplifier EMRFC is also enhanced as transconductance. Therefore the small signal and large signal performance parameters are enhanced in the proposed EMRFC amplifier compared to conventional FC, RFC, and IRFC architectures from the state of art literatures.

3.1.5 Noise

In recent times, for the implementation of analog systems such as biomedical signal acquisition systems, low noise OTAs plays a crucial role. In an analog circuit, noise is considered as an undesired and random signal that disturbs the circuit performance and should be treated properly. The noise limits the signal in the circuit and tradeoffs with power, speed, and linearity. The noise currents in any analog circuit are classified to be either thermal or flicker noise. The thermal and flicker noise components of the proposed amplifier are found and examined separately. From Fig. 4, the transistors that contribute to the overall noise are M1a–M1b, M2a–M2b, M3a–M3b, M4a–M4b, M3c–M4c, and M9–M10. While the noise contributions from the cascode devices M5–M6, M7–M8, and M11–M12, are negligible. Therefore the input-referred thermal noise components of the proposed EMRFC amplifier is expressed as,

$$\begin{aligned} \bar{V}_{it,EMRFC}^2 = & \frac{8k_B T \gamma}{G_{m,EMRFC}^2} \cdot \left[g_{m1a} + \left(\frac{1 + \alpha + p}{\alpha} \right) g_{m3a} \right. \\ & \left. + g_{m9} + \left(\frac{1}{g_{m2b}} + \frac{1}{g_{m3c}} \right) \right. \\ & \left. \cdot G_{m,EMRFC}^2 \right] \tag{16} \end{aligned}$$

Similarly, the input-referred flicker noise component of the proposed EMRFC amplifier is,

$$\begin{aligned} \bar{V}_{if,EMRFC}^2 = & \frac{2k_{fp}}{C_{ox} \cdot f \cdot G_X^2} \left[\frac{1}{(W.L)_{1a}} \right. \\ & \left. + \frac{k_{fn}}{k_{fp}} \cdot \left(\frac{1}{(W.L)_{3a}} + \frac{1}{(W.L)_{3b}} \right) \right. \\ & \cdot \left(\frac{g_{m3a}}{g_{m1a}} \right)^2 + \left(\frac{g_{m9}}{g_{m1a}} \right)^2 \cdot \frac{1}{(W.L)_9} \\ & \left. + \left(\frac{1}{(W.L)_{2b}} + \frac{1}{(W.L)_{3c}} \cdot \frac{k_{fn}}{k_{fp}} \right) \right. \\ & \left. \cdot G_X^2 \right] \tag{17} \end{aligned}$$

where $G_X = (g_{m2b} + g_{m3c})(1 + 2p) \cdot R_X$ and $R_X = (r_{02b} \parallel r_{03c} \parallel r_{011})$.

From Eq. (16) and Eq. (17), it can be inferred that, when compared to its counterparts FC, RFC and IRFC, the proposed EMRFC amplifier’s improved transconductance results in lower input-referred noise. Further reduction in the input-referred noise can be achieved by proper

Table 1 Amplifier transistors width (μm) for L=500nm

Device	FC	RFC	IRFC	EMRFC
M0	164.1	161.6	156.2	156.2
M1/M2	43.8	–	–	–
M1a/M1b/M2a/M2b	–	11.2	12.2	12.2
M3/M4	29.9	–	–	–
M3a/M4a	–	120	8.3	8.6
M3b/M4b	–	40	1.53	1.53
M3c/M4c	–	–	4.01	10.1
M5/M6	60.1	7.0	16.1	16.1
M7/M8	104.1	110	110	92.19
M9/M10	78.2	80	80	3.7
M11/M12	–	40	–	1.53
M11a/M12a	–	–	1.53	–
M11b/M12b	–	–	4.01	–
M13	–	–	–	8.2

Fig. 9 AC frequency response of FC, RFC, IRFC, and proposed EMRFC amplifiers

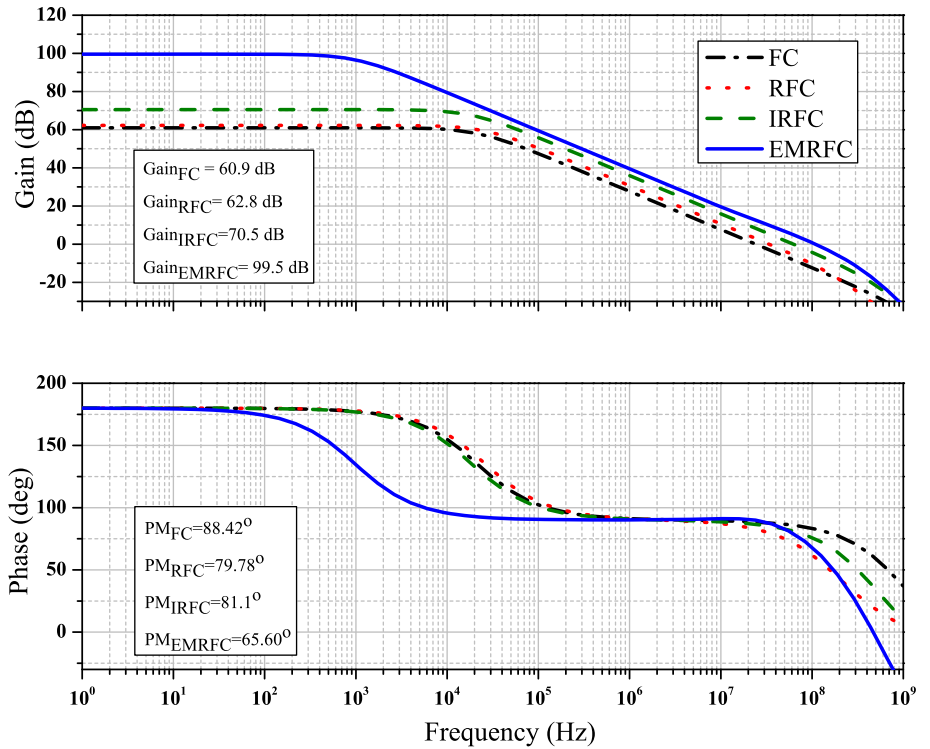
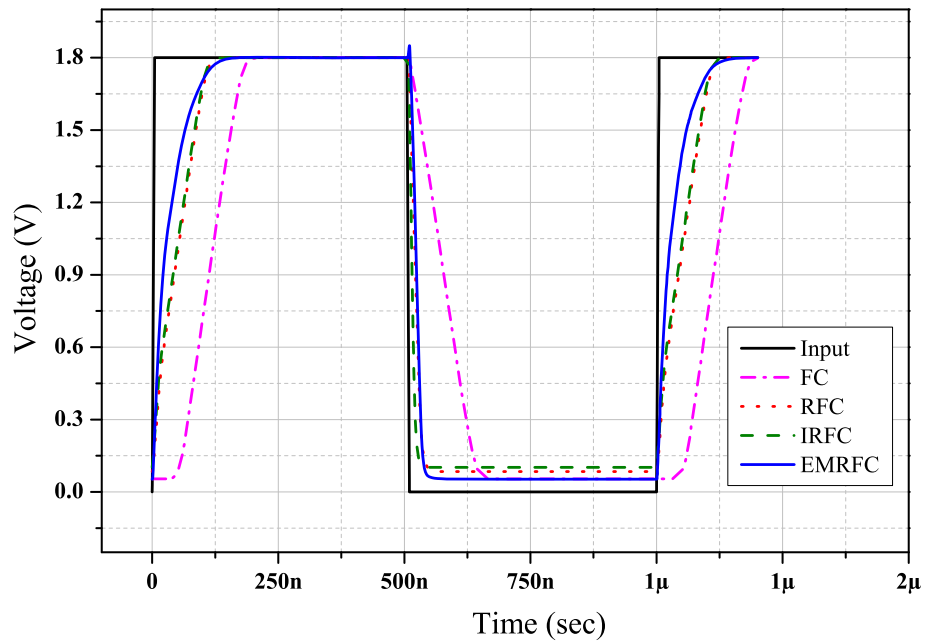


Fig. 10 Small signal step response of amplifiers



selection of p , α , widths, and lengths of the noise contributing transistors.

3.1.6 Offset voltage

Many of the amplifiers exhibit nonzero output voltages even under zero input conditions leading to undesired distortion termed as “offset” which is systematic or

random. This limitation of amplifiers is because of either improper selection of circuit topology or due to mismatch and process variations. Hence, to eliminate this distortion, a minimum input voltage is to be applied which is termed as input offset voltage. Pelgrom’s mismatch model (Pelgrom et al. 1989) evaluates input offset voltage of any device in terms of its variance because of its random nature and is given by Eq. (18) as,

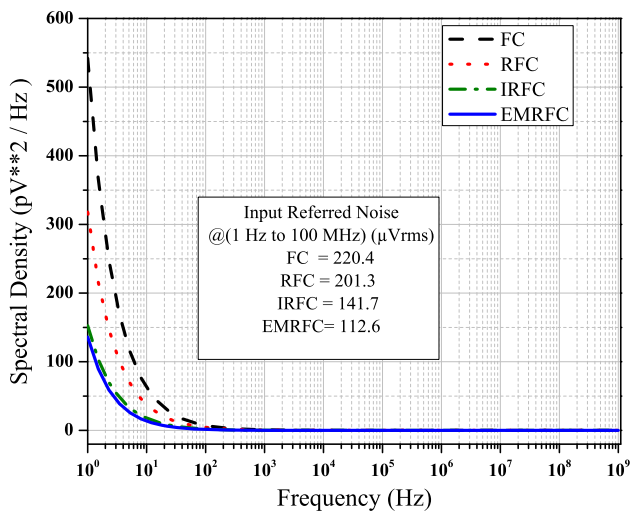


Fig. 11 Spectral density of input referred noise of FC, RFC, IRFC, and proposed EMRFC amplifiers

$$\sigma^2(V_{gs}) = \sigma^2(V_{TH}) = \frac{A_{VT}^2}{W.L} \tag{18}$$

where A_{VT} is the area proportionality constant for the threshold voltage V_{TH} and is given by process technology.

The input offset variance of the proposed EMRFC amplifier can be expressed as the sum of drain current variances of all the transistors at the output divided by the effective transconductance of the EMRFC amplifier and is expressed as,

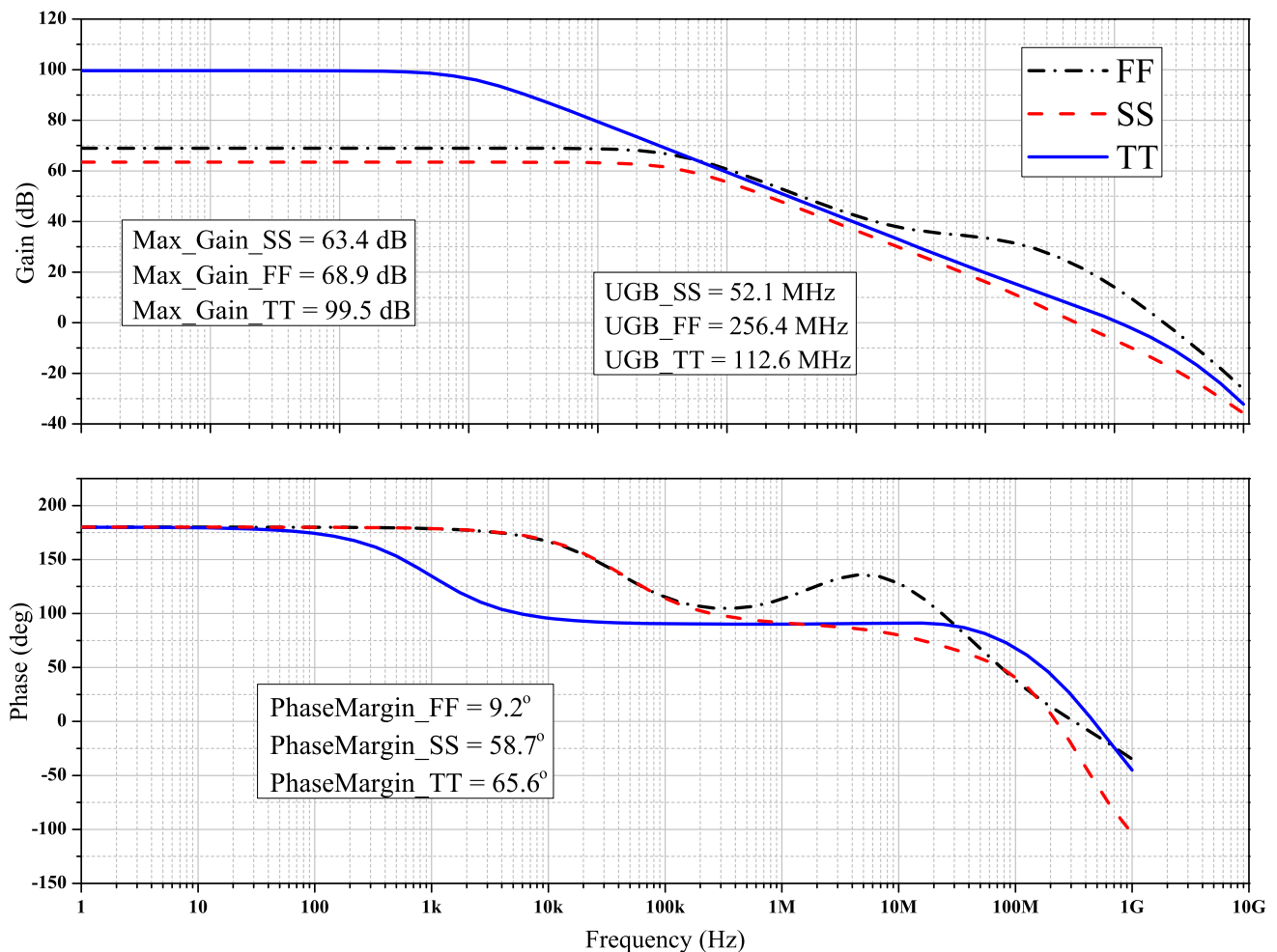


Fig. 12 Frequency response of EMRFC amplifier at various process corners (FF, SS, and TT)

Table 2 Performance comparison of proposed EMRFC OTA with FC, RFC, and RFC OTAs

Parameter	FC	RFC	IRFC	EMRFC
Supply Voltage (V)	1.8	1.8	1.8	1.8
Technology (nm)	180	180	180	180
M1a/M1b/M2a/M2b	–	11.2	12.2	12.2
Current (μ A)	300	300	300	300
Capacitive load (C_L)	5	5	5	5
DC Gain (dB)	60.9	62.8	70.53	99.59
Unity gain bandwidth (MHz)	24.6	34.95	64.47	112.6
Phase Margin ($^\circ$)	88.42	79.92	81.27	65.6
Slew Rate (V/ μ sec)	13.85	40.6	61.2	48.1
Input referred noise (1 Hz–100 MHz) (μ V $_{rms}$)	220.48	201.3	141.7	112.6
Input offset voltage (mV)	4.64	4.45	0.045	0.001
FoM ₁ (MHz.pF/mA)	410	573.5	1075	1877
FoM ₂ (V/ μ sec.pF/mA)	230.8	676.6	1020	777

Table 3 Variation of performance characteristics at different process corners (SS, FF, and TT) for FC, RFC, IRFC and EMRFC amplifiers

Parameter	Amplifier	SS	FF	TT
DC gain (dB)	FC	33.4	19.9	60.9
	RFC	33.3	50.8	62.8
	IRFC	17.4	14.5	70
	EMRFC	63.4	68.9	99.5
Unity gain bandwidth (MHz)	FC	17.4	29.4	24.6
	RFC	22.4	44.7	34.9
	IRFC	36.1	68.3	64.4
	EMRFC	52.1	256.4	112.6
Phase margin (deg)	FC	89.9	64.6	88.4
	RFC	82.2	80.5	79.8
	IRFC	92.9	93.8	81.2
	EMRFC	58.71	9.20	65.6

counterparts because of enhancement in its transconductance compared to conventional FC, RFC, and IRFC OTAs.

4 Simulation Results

To validate the theoretical results presented so far in the previous sections and to demonstrate the enhancements achieved with the proposed modifications, the proposed EMRFC amplifier with its counterparts FC, RFC, and IRFC is implemented using UMC 180 nm CMOS process technology for a total bias current of 300 μ A at a supply voltage of 1.8 V. As illustrated in Figs. 1, 2, and 3, as per the state of art literature the bias currents in FC are in the ratio 1:1, while for RFC it is $k : 1$, whereas for IRFC the current splitting ratios are $(1 + p) : \alpha(1 - p) : \beta(1 - p)$. The current splitting ratio of the proposed EMRFC amplifier as shown in Fig. 4 is $(1 + p) : \alpha$. To achieve proper biasing conditions, the values of k, p, α, β for RFC and IRFC amplifiers are considered to be 3, 0.5, 0.5, and 0.5 respectively, whereas for EMRFC p , and α are selected to be 2 and 0.5 respectively. For ease of implementation, the length of all the transistors is selected to be 500 nm (Mal et al. 2011; Raja and Kumaravel 2017). Table 1 demonstrates the device sizes used for the implementation of FC, RFC, IRFC, and EMRFC amplifiers. A load capacitance of 5 pF with a compensation capacitance of 5 pF and resistance implemented by pseudo transistors MP1-MP2 of $W/L = 6 \mu\text{m}/1 \mu\text{m}$ that operates in triode region are used for simulation.

The AC frequency response of FC, RFC, IRFC, and proposed EMRFC amplifiers are illustrated in Fig. 9. From the simulations, it is observed that the proposed amplifiers

$$\begin{aligned}
 \bar{V}_{if,EMRFC}^2 = & \frac{2A_{V_{Tp}}^2}{G_X^2} \left[\frac{1}{(W.L)_{1a}} + \frac{\mu_n}{\mu_p} \cdot \left(\frac{L}{W}\right)_{1a} \cdot \frac{A_{V_{Tn}}^2}{A_{V_{Tp}}^2} \right. \\
 & \cdot \frac{(1+p)(1+p+\alpha)}{\alpha.L_{3a}^2} + \left(\frac{L}{W}\right)_{1a} \cdot \frac{p}{L_9^2} \\
 & \left. + \left(\frac{1}{(W.L)_{2b}} + \frac{1}{(W.L)_{3c}} \cdot \frac{A_{V_{Tn}}^2}{A_{V_{Tp}}^2} \right) \cdot G_X^2 \right]
 \end{aligned}
 \tag{19}$$

From Eq. (19), it can be inferred that the input offset variance of the proposed EMRFC is lower than its

Table 4 Performance comparison of proposed EMRFC amplifier with state of art literatures

	Assaad and Silva-Martinez (2009)	Yilei et al. (2012)	Akbari et al. (2014)	Kumaravel and Venkataramani (2014)	Yan et al. (2012)	Venishetty and Sundaram (2019)	Yosefi (2019)	Venishetty and Sundaram (2020)	Proposed EMRFC
Supply voltage (V)	1.8	1.2	1.2	1.2	1	1.8	1.8	1.8	1.8
Technology (nm)	180	130	180	90	65	180	180	180	180
Current (μ A)	800	300	300	560	800	300	1200	1200	300
Power (μ W)	1440	360	360	672	800	540	2160	2160	540
Load capacitor (pF)	5.6	5.5	5	5.6	10	5	5	5	5
DC gain (dB)	60.9	64.9	65.5	62	54.5	76.24	73	79.47	99.59
Unity gain bandwidth (MHz)	134.2	76.2	146.9	164	203.2	74.71	247	285.8	112.6
Phase margin ($^{\circ}$)	70.6	72.7	81.1	50	66.2	74.41	71	77.12	65.6
Input referred noise (μ V _{rms})	48.5	98.5	51.6	–	25.8	139.2	137	185.4	112.6
Input offset voltage (mV)	7.6	–	–	–	–	5.9	1.83	0.07	0.001
Area (μ m ²)	4958.2	1139	691	–	–	2760	725	–	5391
FoM_1 (MHz.pF/ mA)	939.4	1228.3	2448	–	2540	1245	1029	1191	1877
FoM_2 (V/ μ sec.pF/ mA)	658.7	379.5	1155	393	878.5	1067.5	525	809.1	777

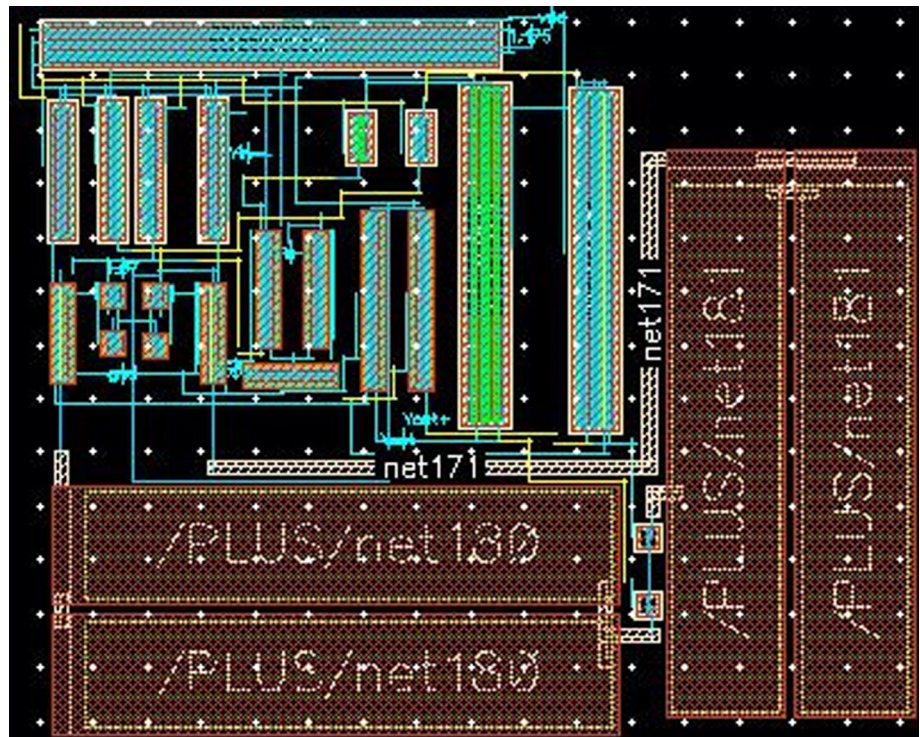
exhibit a maximum DC gain of 99.59 which is about 40 dB larger than conventional FC OTA, about 37 dB greater than RFC, and around 20 dB larger than IRFC OTAs. Hence the enhancements achieved in transconductance and output impedance as per Eqs. (7) and (8) with the modifications proposed is validated. Further, it can also be observed that the unity-gain bandwidth of the EMRFC amplifier is 112.6 MHz, compared to FC, the UGB of EMRFC is increased by 4.5 times, while the enhancement is about 3.2 times and 1.75 times compared to RFC and IRFC amplifiers respectively which validates the Eq. (14). The phase margins of FC, RFC, IRFC, and EMRFC are found to be 88.4°, 79.9°, 81.2°, and 65.6° respectively. The reduction in a phase margin of EMRFC compared to conventional OTAs can be compensated by using simple RC circuits as

discussed in previous sections with proper selection of R and C Values.

The slew rate performance of the proposed amplifier can be studied by applying a large signal step of 1.8 V_{PP} at 1 MHz frequency by connecting the amplifier in unity gain mode. The step response of all the amplifiers is illustrated in Fig. 10. The slew rate of FC, RFC, IRFC, and EMRFC amplifiers are found to be 13.85 V/ μ sec, 40.6 V/ μ sec, 61.2 V/ μ sec, and 48.1 V/ μ sec. Hence it can be observed that, as stated by Eq. (15), the slew rate of the EMRFC amplifier is increased by 3.5 times and 1.18 times compared to FC and RFC amplifiers respectively.

Noise performance of the proposed amplifier with the conventional OTAs is studied through simulations and the spectral density of all the amplifiers is shown in Fig. 11. The integrated input-referred noise for the frequency range

Fig. 13 Layout of the proposed EMRFC amplifier including RC compensation circuit



of 1 Hz to 100 MHz of the proposed EMRFC amplifier is found to be $112.6 \mu V_{rms}$, while it is $220.4 \mu V_{rms}$, $201.3 \mu V_{rms}$, and $141.7 \mu V_{rms}$ for FC, RFC, and IRFC amplifiers. The illustrated noise performance confirms the reduction of noise in the proposed amplifier resulted because of enhancement in the transconductance and the same is expressed by Eqs. (16) and (17).

The offset calculation of the proposed amplifier is performed by connecting the amplifier in the unity gain mode and the difference between the two input nodes is measured. The offset voltage of the proposed EMRFC amplifier is found to $1 \mu V$, which is very much smaller than the conventional OTAs. To study the performance of the proposed EMRFC amplifier under process variations, the AC frequency response of the proposed EMRFC amplifier at various process corners SS, FF, and TT is simulated and is illustrated in Fig. 12.

The performance comparison of the proposed EMRFC amplifier with FC, RFC, and IRFC OTAs is illustrated in Table 2. For the purpose of comparison, the simulated results are studied using two figure of Merits FoM_1 and FoM_2 and are expressed by using Eqs. (20) and (21) as,

$$FoM_1 = \frac{GBW \cdot C_L}{I_D} \quad (20)$$

$$FoM_2 = \frac{SR \cdot C_L}{I_D} \quad (21)$$

Table 3 illustrates the variation of performance characteristics at different process corners for FC, RFC, IRFC, and EMRFC amplifiers, while the performance comparison of the proposed EMRFC amplifier with the state of art literature is shown in Table 4. From Table 2 and 4, it can be inferred that the proposed amplifier exhibits high FoMs compared to FC, RFC, IRFC, and other OTAs. The layout of the proposed amplifier is illustrated in Fig. 13 and it occupies an area of $5391 \mu m^2$.

5 Conclusion

Enhanced multipath recycling folded cascode (EMRFC) operational transconductance amplifier (OTA) is presented in this paper. Design and theoretical analysis of the proposed amplifier is done for the performance parameters namely transconductance, DC gain, unity gain bandwidth, slew rate, noise, and input offset voltage. For comparison, the proposed EMRFC amplifier with conventional FC, RFC, and IRFC amplifiers are simulated using UMC 180 nm process technology in a cadence spectre environment. From the simulation results, it is observed that the proposed amplifier exhibits enhance transconductance, DC gain, unity gain bandwidth, noise, and input offset voltage performance compared to conventional OTAs from the state

of art literature. Since the proposed amplifier exhibits reduced input-referred noise compared to FC, RFC, and IRFC amplifiers, this can be used as a preamplifier in biomedical applications.

References

- Akbari M, Biabanifard S, Asadi S, Yagoub MC (2014) Design and analysis of dc gain and transconductance boosted recycling folded cascode ota. *AEU Int J Electron Commun* 68(11):1047–1052
- Allen PE, Holberg DR (2011) *CMOS analog circuit design*. Elsevier, Amsterdam
- Assaad RS, Silva-Martinez J (2009) The recycling folded cascode: a general enhancement of the folded cascode amplifier. *IEEE J Sol State Circ* 44(9):2535–2542
- Feizbakhsh SV, Yosefi G (2019) An enhanced fast slew rate recycling folded cascode op-amp with general improvement in 180 nm cmos process. *AEU Int J Electron Commun* 101:200–217
- Kumaravel S, Venkataramani B (2014) A current steering positive feedback improved recycling folded cascode ota. *Int J Electr Comput Electron Commun Eng* 8(3):533–541
- Li Y, Han K, Tan X, Yan N, Min H (2010) Transconductance enhancement method for operational transconductance amplifiers. *Electron Lett* 46(19):1321–1323
- Mal AK, Todani R, Hari OP (2011) Design of tunable folded cascode differential amplifier using pdm. In: 2011 IEEE Symposium on Computers and Informatics, IEEE, pp 296–301
- Mallya S, Nevin JH (1989) Design procedures for a fully differential folded-cascode cmos operational amplifier. *IEEE J Sol State Circ* 24(6):1737–1740
- Mottaghi-Kashtiban M, Hadidi K, Khoei A (2006) Modified cmos op-amp with improved gain and bandwidth. *IEICE Trans Electron* 89(6):775–780
- Pelgrom MJ, Duinmaijer AC, Welbers AP (1989) Matching properties of mos transistors. *IEEE J Sol State Circ* 24(5):1433–1439
- Ragheb A, Kim H (2017) Ultra-low power ota based on bias recycling and subthreshold operation with phase margin enhancement. *Microelectron J* 60:94–101
- Raja VS, Kumaravel S (2017) Design of recycling folded cascode amplifier using potential distribution method. In: 2017 International conference on Microelectronic Devices, Circuits and Systems (ICMDCS), IEEE, pp 1–5
- Razavi B (2002) *Design of analog CMOS integrated circuits*. Tata McGraw-Hill Education, New York
- Venishetty SR, Sundaram K (2019) Modified recycling folded cascode ota with enhancement in transconductance and output impedance. *Turk J Elect Eng Comput Sci* 27(6):4472–4485
- Venishetty SR, Sundaram K (2020) Design and analysis of modified recycling folded cascode amplifier with improved transconductance and slew rate. *Eng Appl Sci Res* 47(4):430–438
- Yan Z, Mak PI, Martins R (2012) Double recycling technique for folded-cascode ota. *Analog Integrated Circ Signal Process* 71(1):137–141
- Yilei L, Kefeng H, Na Y, Xi T, Hao M (2012) Analysis and implementation of an improved recycling folded cascode amplifier. *J Semicond* 33(2):025002–7
- Yosefi G (2019) The high recycling folded cascode (hrfc): a general enhancement of the recycling folded cascode operational amplifier. *Microelectron J* 89:70–90

Publisher's Note Springer Nature remains neutral with regard to jurisdictional claims in published maps and institutional affiliations.



Fredkin and Feynmen Gate Implementation of Full Adder/Subtractor

R. Sravanthi¹, V. Sabitha²

¹M.Tech VLSI ,Dept. of Electronics and Communication Engineering, Vaagdevi College of Engineering , Warangal,Telangana,India
Rangusravanthi456@gmail.com

²V. Sabitha, Associate Professor, Dept. of Electronics and Communication Engineering, Vaagdevi College of Engineering Warangal,Telangana,India
Sabitha_v@vaagdevi.edu.in

ABSTRACT:

Reversible good judgment has wide programs in quantum figuration, it is a form of risky report in which the calculation cycle is reversible, i.E. Invertible in time. The fundamental inspiration at the back of the observe of this innovation is to carry out reversible recordings wherein they offer what's anticipated as the likely most important technique to further broaden the electricity productivity of pcs past the von Neumann - Landauer restrict. It is usually a new and rising area within the field of figure that has formed us to contemplate computing. Quantum computing could be a complete trade in the functioning and competencies of the laptop. Reversible number computing circuits are efficient with respect to the wide variety of reversible gates, the bin result, and the quantum price. Reversible binary adder's Sub-tractor Mux, Adder Sub-tractor TR Gate, and Adder Sub-tractor Hybrid are presented in this study design. The presentation assessment is confirmed using reversible numeric inputs, unnecessary inputs/results, and quantum cost. The four-cycle fully reversible plane/adder sub-tractor unit is a contrasting and ordinary wave broadcast viper, the printed viper seems forward, the broadcast viper soar, the Manchester broadcast adder earlier than they're issued on region, timing and electricity. As a result, the suggested work is useful in low-consumption applications that need Adder units and sub-pulsations.

Keywords: Reversible gates, Fredkin gates, Feynman gates, Toffoli gates, and Peres gates are all examples of reversible gates.

1.INTRODUCTION

Quantum computation is one of the notable benefits of return goals, as quantum processing, low-power CMOS, optical fragmentation, and DNA programming bundled with nanotechnology are backward objectives. The circuit is a reversible circuit that ignores the facts, and reversible computation in the system can only be eliminated if there is a path to a reversible insertion into

the structure. The greater part of the passageways

executed in the mechanization plan are not reversible for instance the AND, OR and EXOR entryways don't make a reversible advantage. A reversible circuit/entryway vector can deliver extraordinary final products from every data vector, as well as the opposite way around, this is that fair plans are framed among the measurements and outcome vectors. So, of the passageways that are typically executed just the entryway is presently not reversible.

Importance is a huge thought of the programmed arrangement. A member is a dissipating of solidarity joined to the peculiarities of switches and substances. A gathering of reversible entryways is anticipated to plot a reversible circuit. Some such entrances have been proposed for the longest time now. The reversible passage is the main square of the reversible circuit and is characteristic.

□ The reversible door has feedback, and a coordinated response gives the final result. This is a contribution of the reversible door that cannot be set on the stone from the result.

- A reversible reason door should have an equivalent range of resources of info and results.
- The fan out of every sign remembering critical contributions for a reversible entryway have to be one.
- vintage fashion rationale blend strategies can't be straightforwardly carried out to devise reversible motive circuit.
- One of the key highlights of reversible doors is the number of debris. The yield of all doors that are not used as a contribution to other front doors or as a serious consequence is called the garbage yield. In essence, the unused yield from the door is garbage.
- The quantum price is a cost associated with each reversible admission. The number of 2x2 reversible entrances or Quantum rationale doors

predicted at the time of planning is known as the reversible door Quantum rate.

2. REVERSIBLE GATE INTRODUCTION

The hardest back door is not the door and a 1x1 entry. Uncontrolled Entry (CNOT) is a module for 2x2 doors. There are various 3x3 entry doors, for example, Frederick's Door, Tafoli Door, Paris Entrance and TR Entrance. There is a price on each returning door which is known as the quantity price. The quantum value of the 1 × 1 return door is zero, and the volume value of the back entrance is only 2 × 2. Any back door is identified using 1 × 1 non-entry doors and 2 × 2 returning entrances, such as V. and V + (V is a square solid not at the entrance and V + is the hermetine). And Phenomenal Entry is commonly known as Controlled Entry (CNOT).

NOT Gate

Among the standard logic gates, this is the only reversible gate. This is a one-by-one gate with no quantum cost.

Feynman Gate (CNOT gate)

This is a 2x2 gate with the mapping (A, B) to (P=A, Q=A ⊕ B), with A, B being the inputs and P, Q being the outputs. It has a quantum cost of one since it is a 2x2 gate.

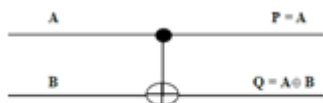


Fig. 2 Feynman or CNOT gate

Toffoli Gate

This is a three-by-three reversible doorway with two result sticks that correspond to planning (A, B, C) to (P = A, Q = B, R = A.B C). Information is represented by A, B, and C, while input is represented by P, Q, and R. Tuffoli Gate is a well-known reversible door that costs \$5,000. 2V entryways, 1 V + entryway, and 2 CNOT entryways are required.

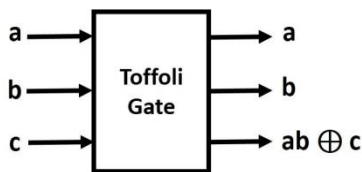


Fig 3 Toffoli Gate

Peres Gate

The Paris Gate is a three-input (3x3) reversible door with planning (A, B, C) to (P = A, Q = AB, R = (AB) C), where A, B, and C are. Information as well as P, Q, and R on their own. Paris Gate costs four dollars since it requires two V + entryways, one V entryway, and one CNOT entryway. This features a minimum measure of noteworthy value between the 3x3 return entryways.

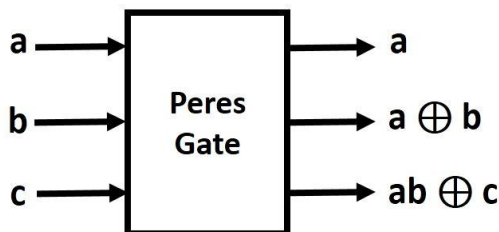


Fig 4. Peres Gate

Fredkin Gate

The Fredkin door is a 3x3 reversible doorway with a modest size. It converts (A, B, C) to (P=A, Q= A' B+AC, R=AB+ A'C), where A, B, C are the information sources and P, Q, R are the outcomes. The Fredkin door has a quantum cost of 5 and takes 2 specked square forms, 1 V entrance, and 2 CNOT entryways to complete.

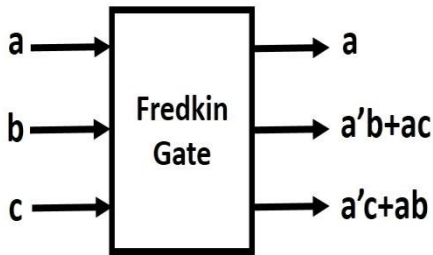


Fig 5 Fredkin Gate
TR Gate

The TR entryway has 3 sources of information and 3 results as information sources and results planning ($P = A, Q = AB, R = (A \cdot B')C$), where A, B, C are data sources and P, Q, R are the results, separately. The TR door can also be acknowledged in an alternative process with a value of less than 6 or less. As a result, the TR gate volume is specified as 6 by the retractable entryway for estimating the uniform substructure process.

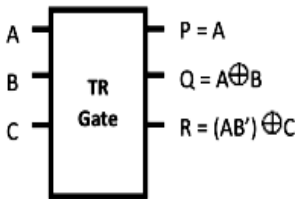


Fig 6. TR gate

3. REVERSIBLE GATE DESIGN INTRODUCTION

A bidirectional loop may create a different output vector from each input vector, indicating the connection between the upstream and downstream variable. As a result, in a reversing gate or circuit, the quantity of outcomes matches the number of inputs, leaving the classic yet he still as the single reversing valve. A cost may be estimated for every reversible gate. The quantum cost of a reversible gate is equal to the number of 2 by 2 reversible gates or logic gates required for the project.

3.1 Reversible Logic Gates

A reasonable calculation is one that can be described as a (perhaps big) Boolean calculation, and each Boolean calculation can be built from an acceptable collection of reasoning entryways. Universal sets (e.g., AND, OR, and NOT) are of this sort. We can get away with just two entry points, to be honest: NOT OR and NOT. Alternatively, we might use the select OR (often known as XOR) structure to replace some of these key entryways. A universal PC is any system that can generate subjective combinations of logic doors from a comprehensive collection.

In the long run, a few reversible doors have been proposed, such as the Toffoli entrance, the Fredkin entryway, and so on. In, a 3-info and 3-yield reversible logic doorway was presented. As seen in Fig 7, it contains inputs a, b, and c, as well as outcomes x, y, and z. Table 1 depicts the reality table of the entrance. The information design cannot be fixed in stone when compared to a specific result example, as evidenced by the reality table. The door may be used to rearrange a sign as well as to duplicate one. Setting input b to 0 yields the sign duplication capacity. The EX-OR capability is available at the entryway's outcome x. Interfacing the information c to 0 yields the AND work, which is then obtained at the terminal z. Two new reversible doors are used to recognize an OR entrance.

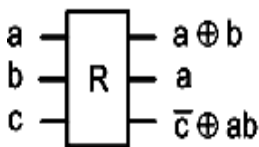


Fig. 7 Reversible gate R

4 EXISTING AND PROPOSED WORK

4.1 Adder circuits

For registration, a few adder types are utilised. The output of adder transfer waves is the most basic. The complete adders are integrated in a sequence within the flywheel adapter to create aggregation and transfer owing to the number that will be added to each other in the transfer coefficient. The downside of viper transmission waves is that supply should increase at all levels.

An important building block of viper transmission waves is blockchain. Detailed adder describes the sum from the delivery brings $c_i + 1$ because of the number to be added to entries a_i and b_i and then entries c_i .

The circuit / gate can produce an interesting result vector from each message vector, as well as another round path, that is, there is a communication link between the message and the resulting vectors. As a result, the number of outputs per input or circuit can be proportional to the number of sources of information, and this is usually not the main gateway to the conversion path. Each flexible gateway has a related cost called Quantum cost. The cost of the turntable entrance is the number of $2 * 2$ turning doors or the reasonable gate that Quantum expected in configuration. One of the main features of this flexible door is its waste disposal, i.e., any gift of the entrance that is not used as an entry in another door or as an item the need is called a straw. Reduction of the number of conversion doors, quantum values and input / output is a major determinant of logical reasoning.

4.2 Reversible Adder/Subtractor Unit Proposal

The objective of this design is a reversible adder and subtractor that may be utilised as a single device. Three distinct forms of full adder/subtractor executions have been addressed, and the presentation of each plan has been studied in terms of the number of reversible doors required, the amount of trash inputs/yields, and the quantum cost. The full adder/subtractor and half adder/subtractor components are combined to form a four-digit equal adder/subtractor. Each of the three types of adder/subtractor units is utilized to construct a four-digit equal subtractor.

Half Adder – Subtractor

A semi-adder / subtractor automobile is expected to be able to use the four-lane highway Fredkin and two Feynman gates. The waste amount is three, the waste amount is two, and the quantum value is twelve. This cutting is seen in Fig. 8. This semi-automatic adder / sub-farm hauler unit drives the semi-adder / sub-farm truck.

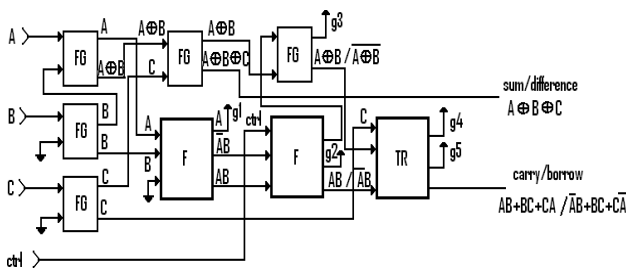


Fig. 8 Reversible Half Adder/Subtractor logic implementation

TABLE III TRUTH TABLE FOR HALF ADDER/SUBTRACTOR

CTRL	A	B	Carry/ Barrow	Sum / Difference
0	0	0	0	0
0	0	1	1	1
0	1	0	0	1
0	1	1	0	0
1	0	0	0	0
1	0	1	0	1
1	1	0	0	1
1	1	1	1	0

Full Adder-Subtractor-Mux

This construction is based on using the appropriate gateway for each project, namely the Peres gateway for the adder project, the TR gate for the subtractor project, and the Fredkin gate for multiplexing Carry and Borrow Lines in a single production line. Three Feynman gates are used to produce the required number of signals (safety) for each input signal. The design uses eight removable gates, including three Feynman gates, two Peres gates, two TR gates, and one Fredkin gate. Table 1 shows that there are 7 waste dispositions, 5 waste disposal inputs (always), as well as a total value of 28. This implementation is shown in Fig. 9.

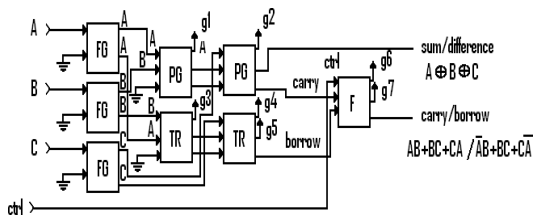


Fig. 9 Reversible Full Adder/ Subtractor-Mux logic implementation

Full Adder-Sub-tractor-TR gate

By employing just TR entryways, the primary use of expansion and deduction is recognized in this concept. For input signal buffering, Feynman doors are used. Three TR entryways and six Feynman doors are used in total, for a total of nine doors. In this strategy, the garbage yield is 7 and the trash inputs are 5. The strategy has a quantum cost of 24. Even though this strategy uses one more Feynman entrance (C-NOT Gate), it achieves a quantum cost advantage of 4 when compared to the Adder-Subtractor-Mux scheme. This quantum cost advantage is mostly due to the recognition of number-crunching squares of adder and sub-tractor with three TR entrances as opposed to five quantities of 3x3 reversible entryways for the Adder-Subtractor-Mux design (Two Pearson doors, two TR entryways and one Fredkin entryway). As seen in fig.10, this execution was carried out.

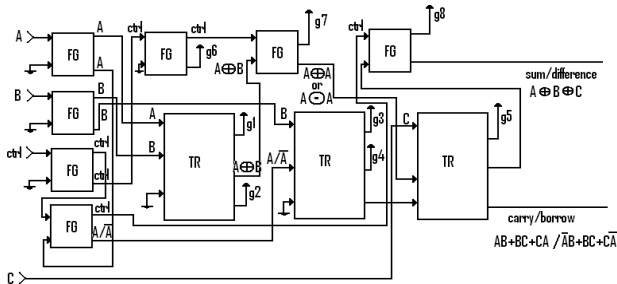


Fig. 10 Reversible logic implementation The whole adder-subtractor-TR gate

Full Adder-Subtractor- Hybrid

This is a high performance of the subtractor adder function. A variety of collections were accepted for this position as well as two Feynman entrances. To understand the route of access, we used two Fredkin entry doors and TR doors. This feature uses 8 entrances including C-NOT gates for input signal. The streamlining as far as far as far as far as far as far as far as far as far take is the trash input, trash.

Result and quantum cost for this situation is gotten because of ideal usage of entryways. The aggregate/distinction work for this situation is acknowledged with only two CNOT entryways. Thusly it is fundamental to have a plan approach where, the expected usefulness might be acknowledged with easiest doors however much as could reasonably be expected. We were unable to understand the convey/get work with basic 2x2 doors successfully. Along these lines, we used 3x3 doors for the acknowledgment. Numerous calculations are accessible in writing. To orchestrate the reversible rationales, one of the fundamental objectives of these calculations is to understand the expected capacity with most straightforward doors.

This logic is implemented in VHDL code and tested with the Model-sim test system. The individual door utility is demonstrated using the behavioral method, and the overall reason is demonstrated using the main method.

4.5 reversible four-bit parallel adder/subtractor unit

A four-digit reversible equivalent instrumentation amplifier is created using the full adder/subtractor and half instrumentation amplifier devices. A four-digit equivalent adder/subtractor is built using each of the three types of expansion/deduction components. This execution will require three full adder/subtractor squares and a half instrumentation amplifier block. These runs were filled with VHDL code and found to be useful. .

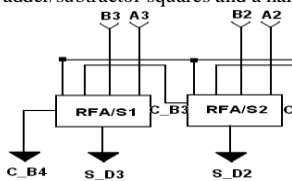


Fig. 12 Four-bit digital circuit is implemented Adder/Subtractor Full Adder/Subtractor)

5. RESULTS AND DISCUSSION

The Model-Sim test framework is used to modify three types of complete framework bidirectional executions in Veriloghdl and replicate them. The utility has been established. Table IV illustrates the quantum cost of defenses as a function of the number of entryways used, the amount of trash inputs/results, and hence the number of runs.

In each of the three types, four-digit comparable reversible adder/subtraction operations are examined. The model code is used to deal with three full adder/sub-vehicle and half adder/sub-vehicle blocks on a four-digit adder/sub-ranch truck.

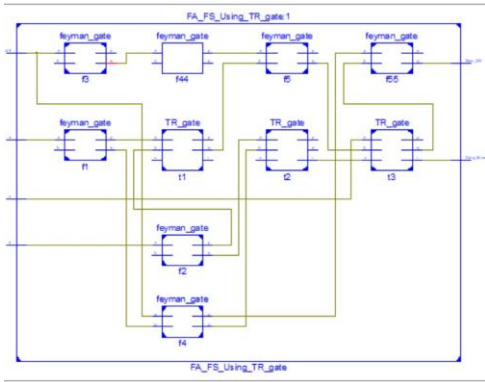


Fig:6.1 Full adder using TR GATE

The utility is checked. An assessment of the runs considering the quantity of information sources utilized, the quantity of garbage inputs/yields, and the quantum cost of the proportions.

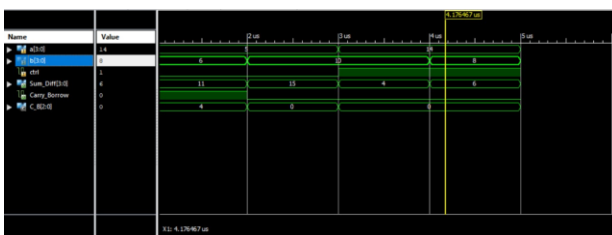


Fig: 6.5 Reversible adder and subtractor

TRUTH TABLE FOR ADDER/SUBTRACTOR CIRCUITS

		IOs Used	Timing Details	Power Summary
CONVENTIONAL ADDER	RIPPLE CARRY ADDER	14	12.791ns	25mW
	CARRY AHEAD ADDER	50	24.376ns	25mW
	CARRY SKIP ADDER	37	20.956ns	25mW
MANCHESTER CARRY ADDER		14	12.791ns	7mW
REVERSIBLE FULL ADD/SUB		6	7.937ns	7mW

	No. of reversible gates	No. of Garbage outputs	No. of Garbage inputs	Quantum cost
ADD SUB MUX	8	6	5	28
ADD SUB TR	9	7	5	24
ADD SUB HYB	8	5	3	21

6. CONCLUSION

Indeed, the organized three kinds of completely reversible adding/deducting units, and separated his program by number of entryways utilized, undesirable information sources/results, and quantum cost. Different appraisals are freely archived on paper to see the value in the reversible reasoning; one of the principal motivations behind these estimations is to fill in the run of as far as possible with the least complex reversible data sources. Of my three plans, the full execution of the viper, subtractor, and cross is streamlined as it utilizes the legitimate contributions to understand that the unit is a key part. Also, a four-digit reversible comparable adder/subtractor is made, and the execution is considered as far as the quantity of information sources required, garbage inputs/results, and quantum cost.

7. REFERENCES

- 1.Landauer Rolf, "Irreversibility and heat generation in the computing process", IBM journal of research and development, vol. 5.3, pp. 183-191, 2020.
- 2.Charles H. Bennett, "Logical reversibility of computation", IBM journal of Research and Development, vol. 17.6, pp. 525-532, 2019.

-
3. Umesh Kumar, Lavisha Sahu and Uma Sharma, "Performance evaluation of reversible logic gates", International Conference on ICT in Business Industry & Government (ICTBIG), pp. 1-4, 2016.
 4. Mayank Kumar Singh and Rangaswamy Nakkeeran, "Design of novel reversible logic gate with enhanced traits", International Conference on Inventive Computing and Informatics (ICICI), pp. 202-205, 2017.
 5. Rocky Bhardwaj, "Reversible logic gates and its performances", 2nd International Conference on Inventive Systems and Control (ICISC), pp. 226-231, 2018.
 6. Shefali Mamataj et al., "Designing of efficient adders by using a novel reversible SDNG gate", International Journal of Computer Science Issues (IJCSI), vol. 11.3, pp. 51, 2015.
 7. Dilip P. Vasudevan et al., "Reversible-logic design with online testability", IEEE transactions on instrumentation and measurement, vol. 55.2, pp. 406-414, 2016.
 8. Papiya Biswas, Namit Gupta and Nilesh Patidar, "Basic reversible logic gates and its QCA implementation", Int. Journal of Engineering Research and Applications, vol. 4.6, pp. 12-16, 2018.
 9. Adetokunbo Adedoyin et al., Quantum Algorithm Implementations for Beginners, 2018.
 10. Edward Fredkin and Tommaso Toffoli, "Conservative logic", International Journal of theoretical physics, vol. 21.3-4, pp. 219-253, 2018.

Design and Implementation of 45nm Operational Amplifier

¹Sharvani Vanaparthi, ²Dr. Mahesh Mudavath, ³Dr. Pankaj Rangaree

¹M.Tech Scholar, ²Professor, ³Assistant Professor

¹Department of Electronics and Communication Engineering,

^{1,3}Vaagdevi College of Engineering, Warangal, India

²Jayamukhi Institute of Technological Sciences, Warangal, India

Abstract— Due to its extensive use of analog computation and signal processing, the operational amplifier is the most dominant device in the field of electronics. The main aim of this paper is to design and implement a two stage complementary metal oxide-semiconductor operational amplifier using required specifications. It also aims to examine the various results for various parameters. The simulation is carried out using Tanner tool which uses 45nm technology and the two stage metal oxide semiconductor operational amplifier runs on a supply voltage. Moreover the feasibility of this circuit is heavily dependent on the process variation, which has a significant advantage over analog circuits. As a result, various simulations including AC, DC and Temperature analysis have been carried out for validation additionally, specified gain of 80dB, Phase margin and power dissipation have also been carried out.

Index Terms—Two-stage Operational amplifier, Analog circuits, Gain, Power dissipation, Temperature analysis, Process variation

I. INTRODUCTION

All The Operational Amplifier is the Heart of any analog circuit, based on its design and functionalities the performance of entire circuit can be judged. It is a basic building block of analog and mixed signal circuits. Earlier, op amps were general purpose like IC 741 with compromise on the parameters such as output swing, power dissipation by contrast, now it's possible to design op amp for specific need applications [1][2]. The modern op amp must operate at supply voltages as low as 0.9 volts while delivering single ended output swings as large as 0.8 volts, for instance, the gain and output swings provided by the cascode op amp are insufficient. Cascoding in one stage op amp increases the gain while limiting the output swings. In these scenarios, we switch to two-stage opamps[3][4], where the first stage provides high gain and the second stage provides large swings. The key obstacle continues to be implementing two-stage CMOS Op-amps while taking other factors into consideration that constitute constraints. Here, the width to length ratio, or (W/L) ratio [6][7] is the main factor affecting the circuit's gain. However, a spike in gain is necessary for the goal of performance improvement and stability matching.

II. LITERATURE SURVEY

Ketan.J.Raut [6][7] represented the design of two stage op amp using standard 180nm technology and achieved the parameter gain of the amplifier is 74.89dB bandwidth is 7.3MHZ and the Slew rate is 94v/ms because of the high condensed slew rate it affects the amplifier. Chaitali et al. designed op amp in which transistors are operated for lower voltage low power applications using 180nm technology simulation has done. The circuit generates 40dB gain.

A. Problem Formulation:

Compared to analog circuit design, digital circuit design typically indicates increased automation. Analog sizing demands accurate modeling of the different sorts of parametric effects existing in a device because it is inherently information concentrated. Moreover, a traditional analog design challenge has more restrictions and occasionally involves complicated tradeoffs. However, because analog circuit level modifications allow for changes to the transistor level, the main structural component of a circuit, the analogue circuit level is significantly more important than its digital counterpart in terms of altering or improving a circuit's performance. The aspects promoted the use of analog design principles to design the operational amplifier, which again perform as an important component in many analog circuits, including integrators, differentiators, comparators, voltage followers, filters, and more.

B. Contribution of the Work:

In this Research, a systematic approach is used to Improve the precision with different variations that are conducted through experimental simulations of a two-stage OP Amp. The operational amplifier with 45nm technology will be used in the proposed method, and various simulations will be performed to understand about the operational amplifier's feasibility [1].

The Two-Stage operational amplifier consists of two stages. We use a Two-Stage op amp to get high gain and high output swing. Stage 2 is a PMOS common source amplifier with the optimal current source load.[4] where stage 1 is an Operational Amplifier with a single stage and gain, presuming that the M1 and M2 NMOS transistors, M3 and M4 PMOS transistors, Vin1 is inverting input and vin2 is non-inverting input. M6 and M7 are the common source amplifier A designer can choose the MOSFET'S length.

M3, M4, M6 have the same length whereas M3, M4 have same width and length, M5 and M8 forms NMOS current mirror have same length, M1 and M2 have same width and length 45nm technology depends on the performance of parameters such as (W/L) ratios to make the chip smaller[8][9].

III. METHODOLOGY

The design the operational amplifier for this research, we adopted 45nm technology. Various research were carried out to understand more about the operational amplifier's effectiveness, or the circuit's process variation. Various limitations have been taken into consideration. The node was constructed using 45nm technology, 1.8V was chosen as the voltage supply. In order to keep all MOS transistors in the saturation zone, the Input Common-Mode Range (ICMR) has been set between 0.8V and 1.6V, while the threshold voltages for nmos and pmos are 0.45V and 0.5V, respectively[2][4]. Similarly, 2PF has been chosen for the load capacitance so that the poles will remain before the 0dB point. This assures the circuit's stability.

For the optimal condition, the gain, slew rate, and gain-bandwidth product (GBW) have been selected. Here, maintaining the input voltage and output voltage swing within the ICMR range is crucial. The design process begins with research on exceptional Op-amp topologies that are frequently used [1][8].

The Design procedure of two stage Operational Amplifier specifications for following parameters are:

- | | |
|-----------------------------------|--|
| a) Voltage supply (VDD) | : 1.8V |
| b) Gain(G) at dc | : 80dB |
| c) Gain bandwidth product (GBW) | : 30MHZ |
| d) Input Common Mode Range (ICMR) | : 0.8V to 1.6V[V= vin(min) and vin(max)] |
| e) E) Load Capacitance (C_l) | : 2pF |
| f) F) Slew Rate (SR) | : $\frac{20v}{\mu s}$ |

Calculation of compensation capacitor (C_c):

For 80 degree phase margin, **0.22 (C_l) = 0.44pF**

Selection of I_{D5} :

Determining the min value for the tail current I_{D5} based on Slew rate requirements **$I_{D5} = SR(C_c) = 16\mu A$**

Calculation of $\frac{W}{L}(3,4)$:

M3 is diode connected, $V_{SG3} = V_{SD3}$, D3 & D1 are same where as $V_{S3} = V_{DD}$ & $V_{D3} = V_{D1}$

$$(W/L)_3 = \frac{I_{D5}}{\mu pcox(V_{DD} - V_{th3} - (V_{GS1} - V_{th1}))}$$

Thus W/L of M3 is determined by using max ICMR [Vin(max)]

$(W/L)_3 = (W/L)_4$ as M3, M4 form current mirrors

$$(W/L)_{3,4} = \frac{2(10)\mu A}{\mu pcox(V_{DD} - ICMR \text{ Max} - V_{th3} + V_{th4})}$$

Approximately chooses as 14.

Calculation of $\frac{W}{L}(1,2)$:

Size of M1 & M2 NMOS input transistors

Choose $(W/L)_1 = (W/L)_2$ to achieve the desired dB

$$(W/L)_{1,2} = \frac{(g_{m1})(g_{m1})}{\mu pcox I_{D5}}$$

Approximately chooses as 6.

Calculation of $\frac{W}{L}(5,8)$:

$$(W/L)_5 = \frac{2(I_{D5})}{\mu pcox(V_{D5sat})}$$

$(W/L)_5 = (W/L)_8$ as M5, M8 form current mirrors

Approximately chooses as 12.

Calculation of $\frac{W}{L}(6)$:

$$(W/L)_6 = (W/L)_4 \frac{g_{m6}}{g_{m4}}$$

$$(W/L)_{1,2} = \frac{(g_{m6})}{2\mu pcox (W/L)_6}$$

Approximately chooses as 180.

Calculation of $\frac{W}{L}(7)$:

$$(W/L)_7 = (W/L)_5 \frac{I_{D7}}{I_{D5}}$$

Where as $I_{D6} = I_{D7}$

Approximately chooses as 75.

The following figure demonstrates the two stage CMOS Op-amp schematic. The schematic is implemented using the calculated parameters that taken into consideration design requirements and specifications. Five NMOS and three PMOS constitute the operational amplifier with W/L values [5][8].

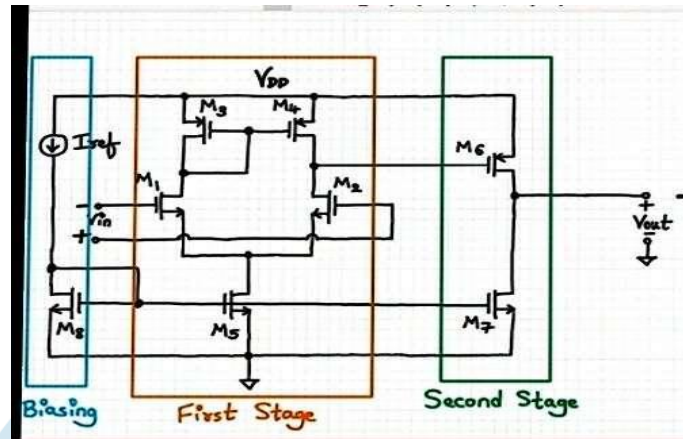


Figure 1: Two Stage OP-amp

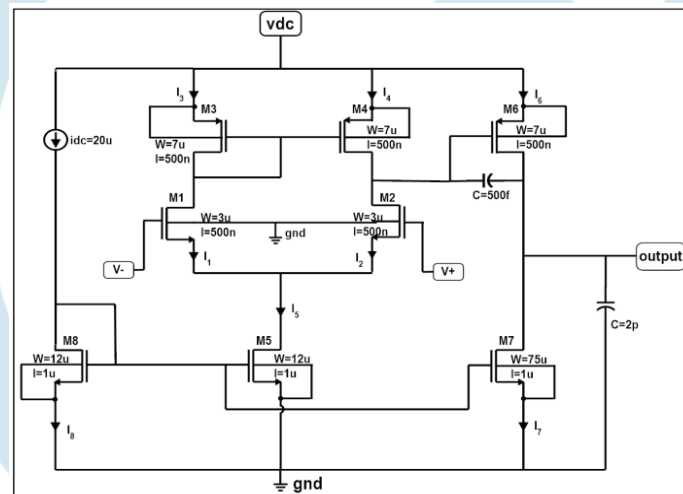


Fig. 2. Schematic of Two-Stage Op-amp

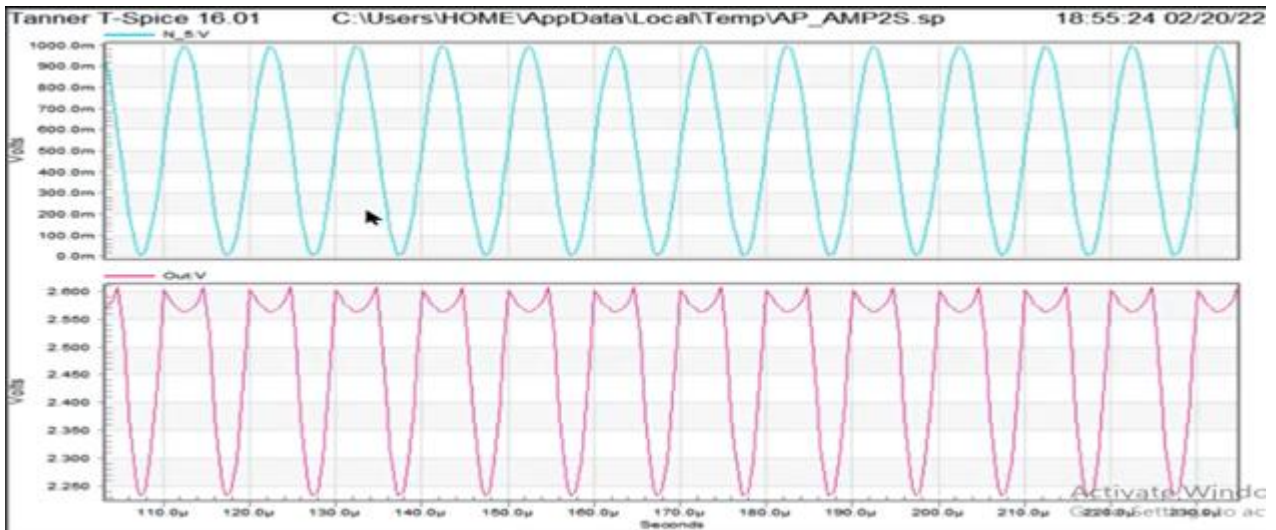
Figure 2: Schematic of Two stage Op-amp

Device and node counts:	
MOSFETs -	8
MOSFET geometries -	2
Capacitors -	2
Voltage sources -	4
Subcircuits -	0
Model Definitions -	2
Computed Models -	2
Independent nodes -	37
Boundary nodes -	5
Total nodes -	42

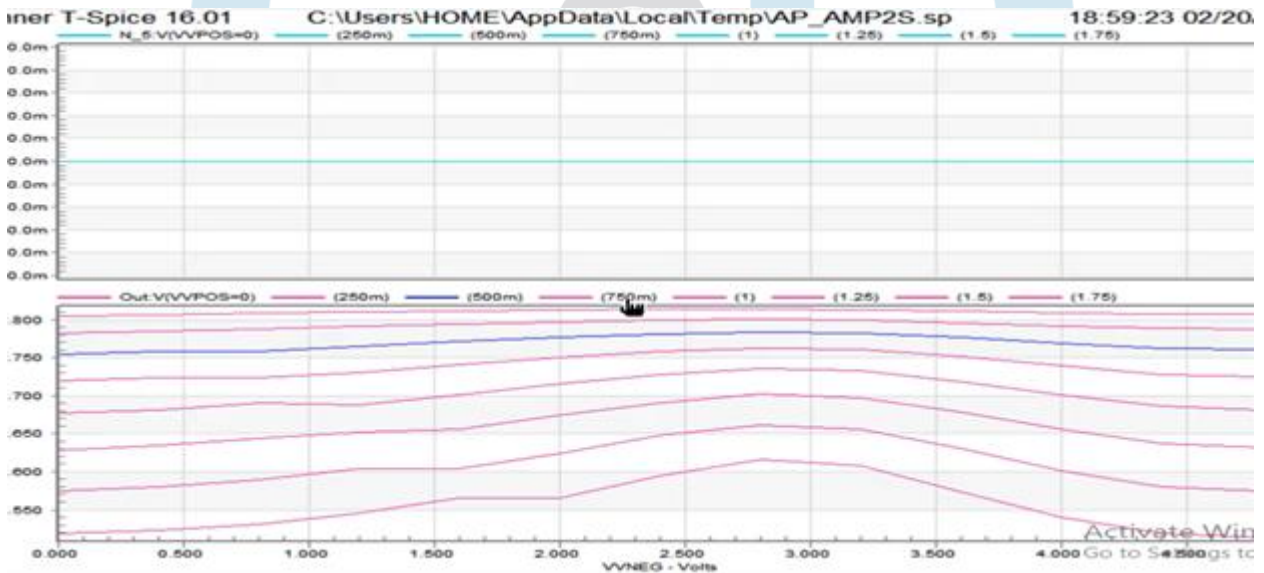
IV. RESULTS AND DISCUSSIONS

Before Using a Tanner tool and a 45nm node, the design and optimization of a two-stage CMOS Opamp circuit were verified. A supply voltage of 1.8V was used. To meet the various limitations of the circuit, multiple analysis including DC, AC, Transient, and Power analysis have been conducted [7][8].

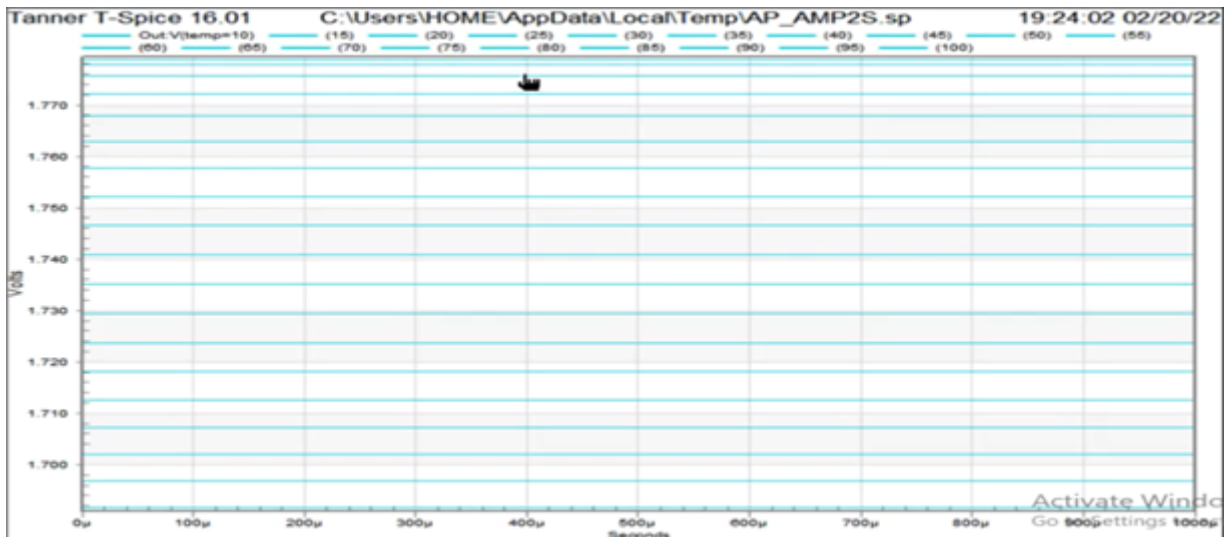
Transient Analysis:



DC Analysis:



Temperature Analysis:



```

Power Results: temp=95
Total Power from time 0 to 0.001
Average power consumed -> 1.518218e+001 watts
Max power 1.518218e+001 at time 0.000990688
Min power 1.518218e+001 at time 0.000996688

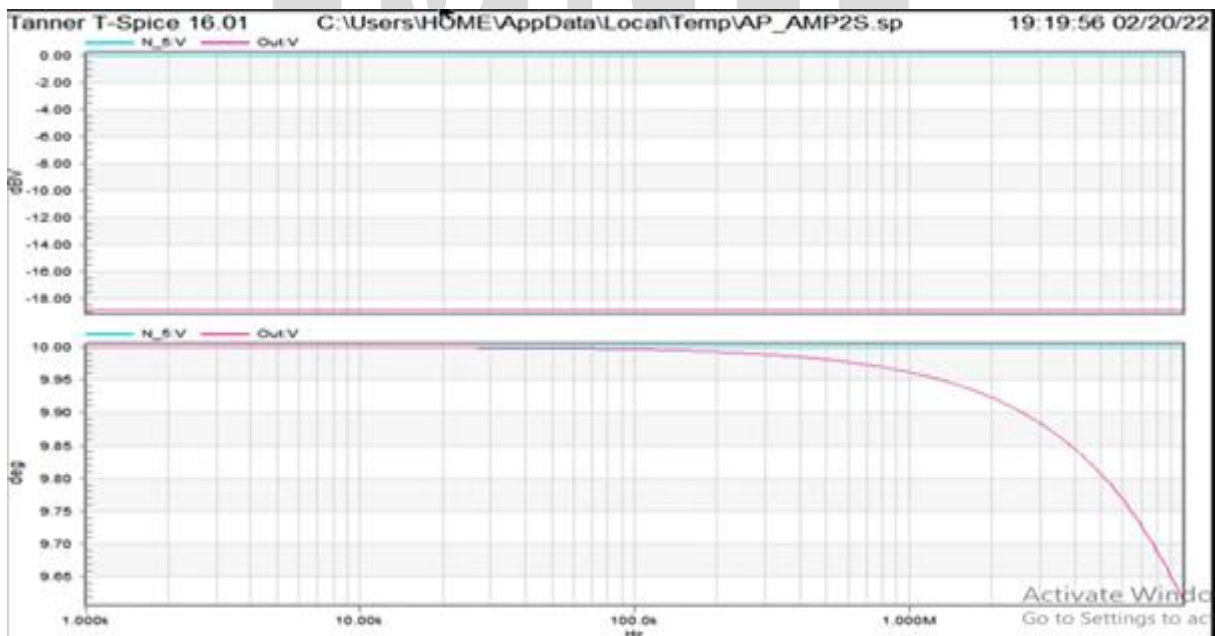
Power Results: temp=100
Total Power from time 0 to 0.001
Average power consumed -> 1.516047e+001 watts
Max power 1.516047e+001 at time 0.000274687
Min power 1.516047e+001 at time 0.000284687

Max power 1.660694e+001 at time 0.000448687
Min power 1.660694e+001 at time 0.000450687

Power Results: temp=30
Total Power from time 0 to 0.001
Average power consumed -> 1.633173e+001 watts
Max power 1.633173e+001 at time 0.000438687
Min power 1.633173e+001 at time 0.000428687

Power Results: temp=35
Total Power from time 0 to 0.001
Average power consumed -> 1.611303e+001 watts
Max power 1.611303e+001 at time 0.000132687
Min power 1.611303e+001 at time 0.000126687
    
```

AC Analysis:



Power Analysis

```

VVNEG from time 0 to 0.001
Average power consumed -> 3.170729e-008 watts
Max power 8.553466e-008 at time 0.00099725
Min power 6.689305e-011 at time 0.0006035

VVPOS from time 0 to 0.001
Average power consumed -> 2.631025e-008 watts
Max power 2.714136e-007 at time 0.000996
Min power 1.144797e-010 at time 0.000286312

VV2 from time 0 to 0.001
Average power consumed -> 1.606576e-004 watts
Max power 6.140875e-004 at time 2.5625e-005
Min power 3.077072e-012 at time 0.00011725

```

* VOLTAGE SOURCES

	8	9	10	11	
		VV1	VVNEG	VVPOS	VV2
VOLTAGE	5.0000	1.0000	1.5000	500.0000m	
CURRENT	-2.2361m	32.2107n	26.4643n	-17.7875u	
POWER	-11.1806m	32.2107n	39.6965n	-8.8937u	

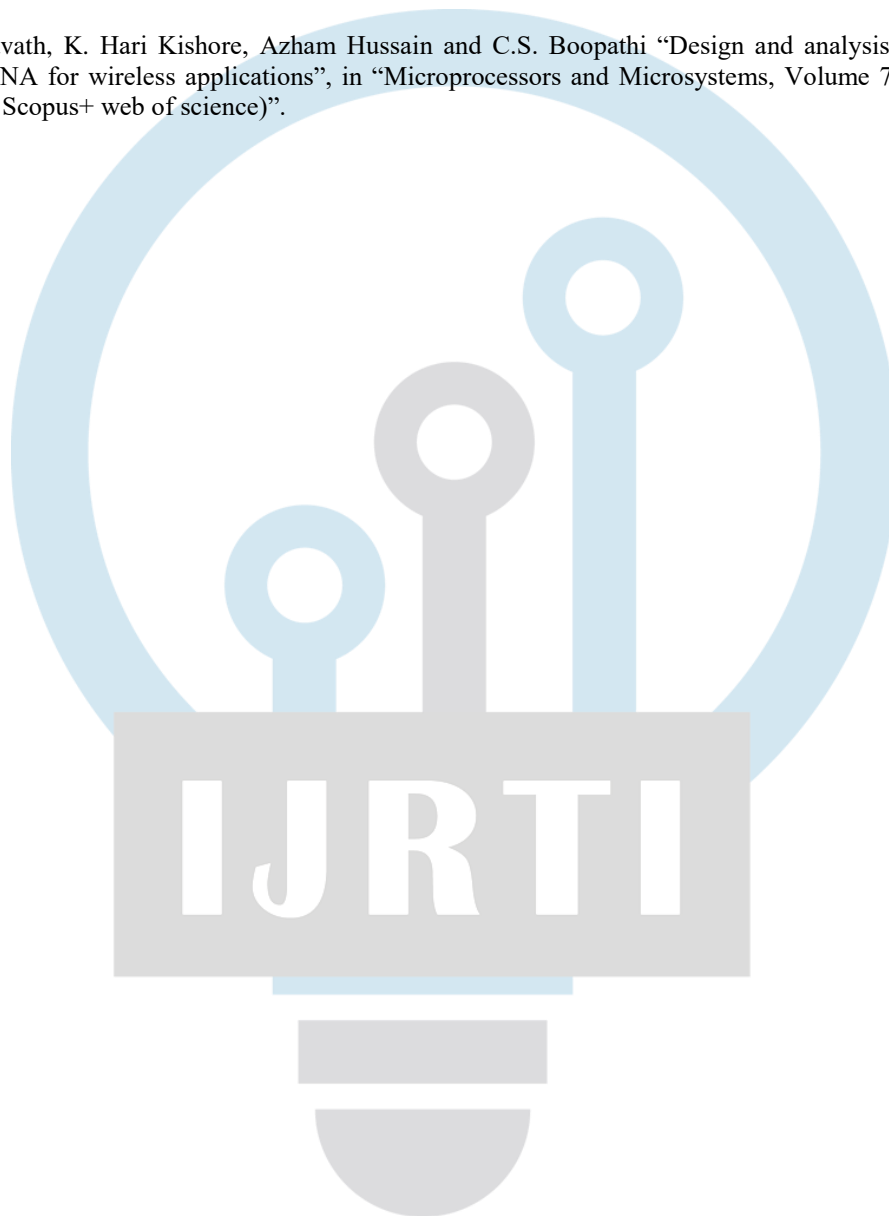
V. CONCLUSION

After For the two-stage Op-amp, Implementation is a multidimensional optimization problem where enhancing one or more parameters could actually deteriorate other. Additionally, when designing circuits for high dc-gain and high bandwidth applications, the gain-bandwidth-product continually presents challenges to the designers[1]. As a result, the circuit modelling was carried out using a tanner tool with a 45nm node. The performance is enhanced by altering parameters like (W/L) ratios. Additionally, this makes use of design equations, including accurate selection and sizing of the proposed circuit's configuration. This proposed design achieves 80dB gain and phase margin at unity gain configuration and power dissipation[13][14]. VLSI technology nodes such as 45nm came into existence and more would continue to come in future these technologies depends on the performance of parameters such as (W/L) ratios to make the chip smaller.

REFERENCES

- [1] Patnaik, A. Panigrahy, R. K. Patjoshi and S. S. Rout, "Design and Implementation of optimized Parameter Based Operational Amplifier for High Speed Analog Signal Processing," 2020 IEEE International Symposium on Sustainable Energy, Signal Processing and Cyber Security (iSSSC), 2020, pp. 1-6,
- [2] X. Jin and J. He, "Design and Analysis of Two-Stage CMOS Operational Amplifier for Fluorescence Signal Processing," 2020 7th International Conference on Information Science and Control Engineering (ICISCE), 2020, pp.2345-2348.
- [3] Y. Wenger and B. Meinerzhagen, "Implementation of a Fully-Differential Operational Amplifier with Wide-Input Range, High-Impedance Common-Mode Feedback," 2019 15th Conference on Ph.D Research in Microelectronics and Electronics (PRIME), 2019, pp. 1-4, doi: 10.1109/PRIME.2019.8787739.
- [4] D. Van Truong, L. Mai, V. -S. Tran, N. B. Duong and H. N. Do, "0.5W S-band two-stage power amplifier: Research, design and implementation," 2018 2nd International Conference on Recent Advances in Signal Processing, Telecommunications & Computing (SigTelCom),2018,pp.51-55,
- [5] L. Kavyashree, M. Hemambika, K. Dharani, A. V. Naik and M. P. Sunil, "Design and implementation of two stage CMOS operational amplifier using 90nm technology," 2017 International Conference on Inventive Systems and Control (ICISC), Coimbatore, 2017, pp. 1-4.
- [6] Y. G3uo, "An accurate design approach for two-stage CMOS operational amplifiers," 2016 IEEE Asia Pacific Conference on Circuits and Systems (APCCAS), Jeju, 2016, pp. 563-566.
- [7] J. Mahattanakul, "Design procedure for two-stage CMOS operational amplifiers employing current buffer," IEEE Transactions on Circuits and Systems II: Express Briefs, vol. 52, no. 11, pp. 766-770, Nov. 2005.
- [8] Razavi, "Design of Analog CMOS Integrated Circuits", New York: Mc-Grew Hill, 2001.
- [9] D. Grasso, G. Palumbo and S. Pennisi, "Comparison of the Frequency Compensation Techniques for CMOS Two-Stage Miller OTAs," IEEE Transactions on Circuits and Systems II: Express Briefs, vol. 55, no. 11, pp. 1099-1103, Nov. 2008.

- [10] Shem-Tov, M. Kozak and E. G. Friedman, "A high-speed CMOS op-amp design technique using negative Miller capacitance," Proceedings of the 2004 11th IEEE International Conference on Electronics, Circuits and Systems, 2004. ICECS 2004., Tel Aviv, Israel, 2004, pp. 623-626.
- [11] Y. Guo, "An accurate design approach for two-stage CMOS operational amplifiers," 2016 IEEE Asia Pacific Conference on Circuits and Systems (APCCAS), Jeju, 2016, pp. 563-566.
- [12] T. Elarabi, V. Deep and C. K. Rai, "Design and simulation of state-of-art ZigBee transmitter for IoT wireless devices," 2015 IEEE International Symposium on Signal Processing 33and Information Technology (ISSPIT), 2015.
- [13] Mahesh Mudavath, Sresta Valasa, Avunoori Saisrinithya and Amgothu Laxmi Divya "Design of Cryogenic CMOS LNAs for Space Communications", in Journal of Physics: Conference Series, Volume 1817, Issue 1, 2021, 012007, ISSN: 1742-6588, E-ISSN: 1742-6596, IOP Publishing, DOI: 10.1088/1742-6596/1817/1/012007.
- [14] Mahesh Mudavath, K. Hari Kishore, Azham Hussain and C.S. Boopathi "Design and analysis of CMOS RF receiver front-end of LNA for wireless applications", in "Microprocessors and Microsystems, Volume 75, 13th January. 2020, 102999 (SCI+ Scopus+ web of science)".





Contents lists available at ScienceDirect

Materials Today: Proceedings

journal homepage: www.elsevier.com/locate/matpr

Efficient method to identify hidden node collision and improving Quality-of-Service (QoS) in wireless sensor networks

B. Vijay Kumar^{a,*}, Syed Musthak Ahmed^b, Mahendhra Nanjappa Giri Prasad^a

^aJNTUA Anantapuramu, A.P, India

^bS R Engineering College, Warangal, Telangana, India

ARTICLE INFO

Article history:

Available online xxxx

Keywords:

Hidden-node problem

Energy-efficiency

Quality-of-service (QoS)

Wireless sensor networks (WSNs)

ABSTRACT

The proposed approach is designed to boost the IEEE 802.15.4 / ZigBee-based WSN streaming efficiency by introducing multipurpose routing. We investigate how those networks can be designed in order to achieve optimum throughput using computational models to explain intra-track and inter-track interference in multipath routing networks. One mode of action in particular – Spatial-TDMA (S-TDMA), Zig Bee dependent WSNs, will greatly reduce the amount of interference, both in one- and multi-track environments. It is also seen that two-way networks can be stronger than their one-way counterparts by means of deliberately selected implementation parameters. Finally, a greater degree of spatial isolation between the routes used indicates improved average efficiency in multi-path scenarios. The simulation is one of our results.

© 2021 Elsevier Ltd. All rights reserved.

Selection and peer-review under responsibility of the scientific committee of the International Conference on Nanoelectronics, Nanophotonics, Nanomaterials, Nanobioscience & Nanotechnology.

1. Introduction

There are various types of WSN implementations and there may be different service standard (quality of service) specifications (QoS)[1]. Both WSN systems, however, benefit from increased network performance, less delay in communication, and longer system life. Inside WSNs, QoS is very difficult due to two major challenges: The normally severe limitations of wsn nodes and the extensive architecture of WSNs, as well as resources, networking and computational capabilities. Fig. 1. Fig. 2.

The most interdependent QoS properties will degrade any one of them. This occurs in wireless networking, where a node from a wireless access port, but not from other nodes attached to that access point, is accessible (AP). WLAN refers to nodes beyond all nodes or group of nodes. A loop point of entry through a certain location with many nodes. Nodes cannot communicate with each other because nodes have no physical connection, but each node is different from the AP. In addition, RTS/CTS packages measure the profitability of a traffic segment[3]. In comparison with the hidden stations. A radio domain could be a logical split between

the network and the information layer linking all the nodes. A transmitted domain may be found in the same LAN segment.

A variety of related computer network aspects which allow for transport in line with special requirements are defined in Service Quality (QoS)[2]. In practise, a vast range of innovations are introduced to make computer networks as useful as mobile networks to support the new technology with even tougher coverage requirements.

The H-NAME is a simple but efficient mechanical distribution which addresses the hidden node problem in WSNs. H-NAME is based on a grouping technique, which splits each WSN cluster into un-hidden node groups, then scales into many clusters with the strategy of cluster grouping, without intervening in the transmission between overlapping clusters[6]. The test bed demonstrates how sustainable an H-NAME is to boost network performance and the likelihood that output will be transmitted double the sum of H-NAME[8]. The downside of the secret node was shown to be a significant disadvantage, which lowered the performance of the wireless network[5]. The use of wireless/mobile networking can benefit tremendously or impose industrial applications, including plant automation, project management and quality control. When virtual networks appear to be universal, largely distributed and embedded into their physical environments [7], all things are continuously tracked and managed everywhere. To be

* Corresponding author.

E-mail address: vijaykumar_b@vaagdevi.edu.in (B. Vijay Kumar).

<https://doi.org/10.1016/j.matpr.2021.05.498>

2214-7853/© 2021 Elsevier Ltd. All rights reserved.

Selection and peer-review under responsibility of the scientific committee of the International Conference on Nanoelectronics, Nanophotonics, Nanomaterials, Nanobioscience & Nanotechnology.

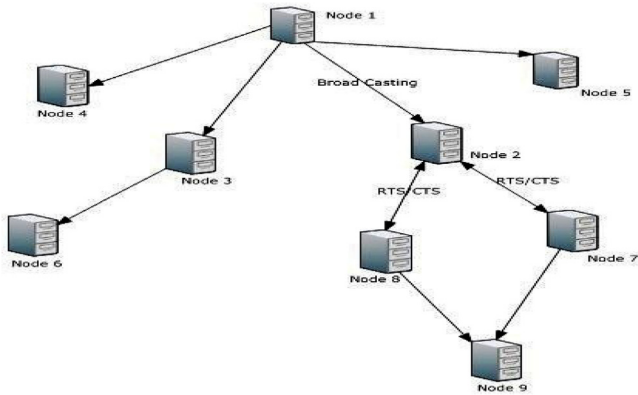


Fig. 1. System Architecture.

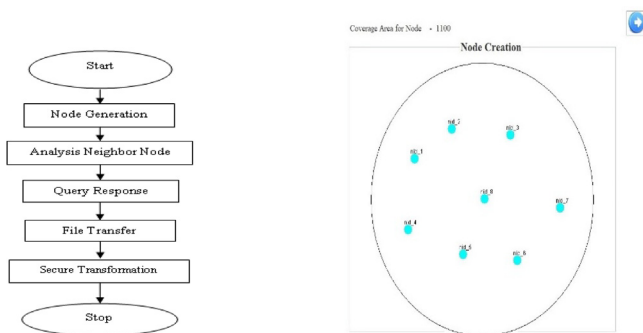


Fig. 2. Data flow Diagram.

cost-effective, small-scale, must be the main components of such systems[4]. Context analysis is a process in which the environment an organisation exists is analysed. The main subject of environmental scan is the macroatmosphere of the industry. However the whole business atmosphere, the internal and external climate take into consideration the context analysis. This can be an important part of business architecture.

2. System architecture

2.1. Existing system

The Head of Cluster (CH) holds a list of groups for nodes. Following receiving a message from the N node with the list of its two-way neighbours, CA initiates an assignment of a group group, in conjunction with its neighbourhood list and available resources, to theoretically assign the node to a given group. Any new node joining the network does not know the node groups and causes a hidden node crash [10].

The key goal is to design a mechanism using an established model, which is the paradigm of groupings in a way:

- It addresses the dilemma of the secret node in multimedia networks
- The protocol stack will be introduced and built-in.
- Returns compatibility with these requirements for the protocol.

2.2. Proposed system

The Head of Cluster (CH) holds a list of groups for nodes. Following receiving a message from the N node with the list of its

two-way neighbours, CA initiates an assignment of a group group, in conjunction with its neighbourhood list and available resources, to theoretically assign the node to a given group. Any new node joining the network does not know the node groups and causes a hidden node crash [10].

The key goal is to design a mechanism using an established model, which is the paradigm of groupings in a way:

- It addresses the dilemma of the secret node in multimedia networks
- The protocol stack will be introduced and built-in.
- Returns compatibility with these requirements for the protocol.

3. Group assignment algorithm

There are a number of nodes and a number of paths. Any node can be assigned to perform any path, incurring some cost that may vary depending on the assignment [5]. It is required to perform all paths by assigning exactly one node to each path in such some way that the overall price of the assignment is reduced [10].

3.1. Data flow Diagram

- Node Generation
- Analysis of Neighbor Node
- File Transfer
- Query response
- Secure transformation

3.1.1. Node generation

A node can be an organisation, a delivery purpose or a terminus of communication. The node description depends on the above-mentioned network and protocol layer. An operational electronic system connected to the network is a physical network node that can trigger, receive or transmit information through a channel of communication. A MAC address must be included for each LAN or WAN node, normally for each network interface controller it has.

A tree can be retrospectively identified as a node array where each node is a value-consistent data structure with a list of nodes that does not repeat any node. Interior nodes are equipped with a variable number of child nodes within a predefined set. The number of children nodes changing as data is added or discharged from a node. Internal nodes can even be connected or broken to preserve the predefined set.

3.1.2. Analysis Neighbor node

In a finite element context, it is often useful to have fast access to the objects which are "around" a certain node. This can be achieved by storing on each node the list of all of the nodes and elements which are close to it. The creation of a list of neighbor nodes and elements implies a no negligible price in terms of memory occupation [9]. A method is provided so as to ease the generation of the lists once required. Neighbor-joining takes as input a distance matrix specifying the space between every combine. The algorithm starts with a totally unresolved tree, whose topology corresponds to it of a star network.

3.1.3. File transfer

Data sharing is a common concept used in a data network such as the internet to transmit information. Many ways to relay file over a network are possible and Protocols are available. Computers that offer a file sharing facility are commonly referred to as file servers. The data transfer is called uploading or copying, depending on

the viewpoint of the user. Data transfer is becoming more and more carried out for the business using File Transfer Controlled.

3.1.4. Query response

The response will be given by the responder to the sower after that the sower will be forwarded that message to the initiator. If the initiator confirms that the response message then the sower will forward that to the responder, hence the sower acts an agent between the initiator and the responder. The answer and forecast response are the values of the dependent variable determined by regression parameters and the experimental variable's value. However, the values of the two answers are the same, their measured variances vary entirely.

3.1.5. Secure transformation

Following a clarification from the initiator, the requested file would then be transmitted via the sower to the respondent. The design of systems which require rigorous handling of doable disrupting sources, ranging from natural catastrophes to malicious actions. Its key aim is to facilitate the supply of software solutions to fulfil pre-defined practical and customer specifications, with an additional layer to avoid abuse and malicious behaviour. it is like most device engineering companies.

4. Simulation results

Basically, the deficiency in service quality (QoS) masks the node problem, which in turn impacts network performance, message

Filtering the Nodes

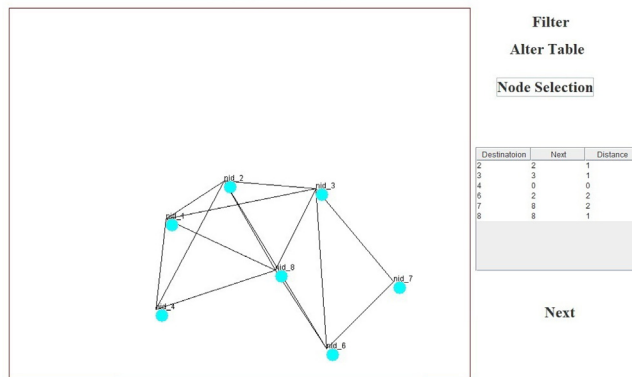


Fig. 5. Distance between a source node to another nodes.

Data Transmission

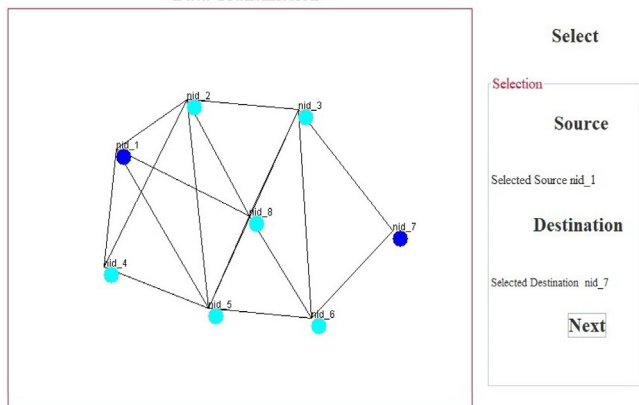


Fig. 3. Node Creation with Coverage Area.

Removing the Hidden Node

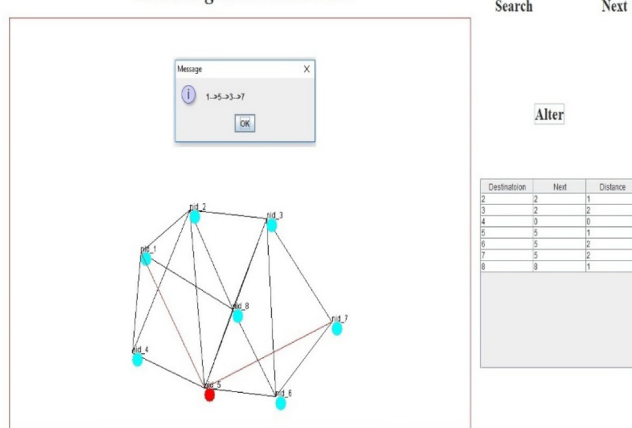


Fig. 6. Detecting shortest path and identify the hidden node.

Node Table Calculation

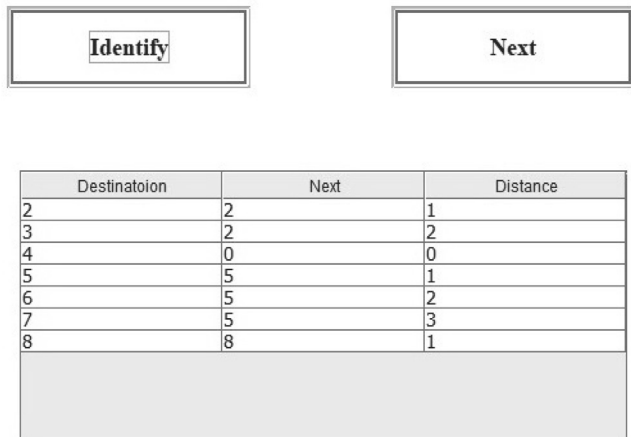


Fig. 4. Data transmission from source node to destination node.

Source

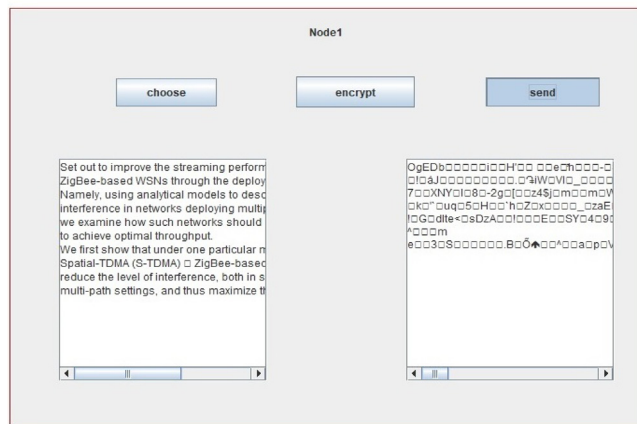


Fig. 7. Removing the hidden node after filtering the nodes.

Destination

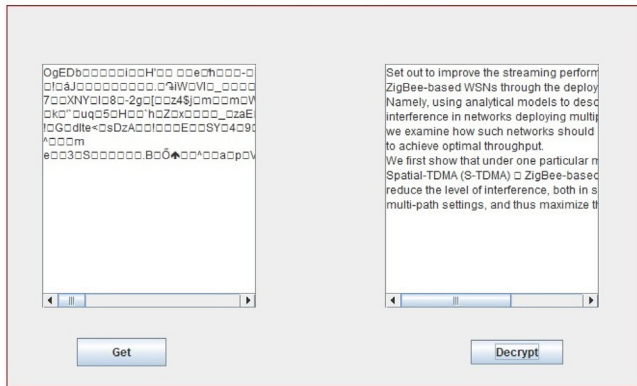


Fig. 8. Source node selects the data file.

Destination

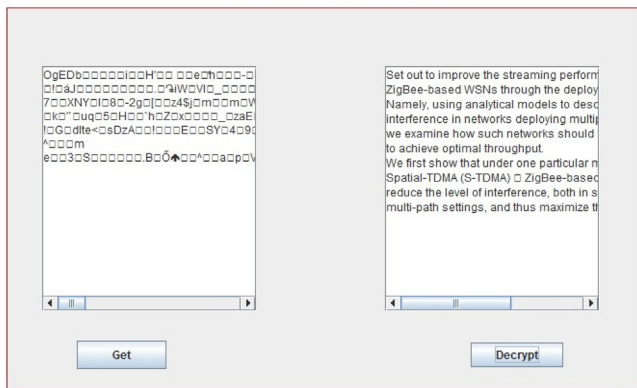


Fig. 9. Destination node received the data file.

latency, consumption of energy and reliability. The System for the Prevention of Secret Nodes (H-NAME) has been introduced. The first step is that the coverage area must be identified or defined, given the number of nodes in Fig. 3. Pick the source node (node 1) and the destination node (node 7). The next step is to evaluate the surrounding node for data transmission in Fig. 4.

Identify the shortest path that a lead to performance improvement, here the path is 1-5-3-7. But while transferring the data, the hidden node appears and the path is diverted. But the hidden node identified as node 5 is presented in Fig. 6, and the table is depicted in Fig. 5.

This hidden node can be filtered and thus established a clear path between source to destination nodes is presented in Fig. 7. As a final verification, before transmitting the data, the data is encrypted and is transmitted is presented in Fig. 9 Thus by filtering the hidden node, the data was received correctly without delay, which indirectly proves that there is no collision occurred during transmission. Fig. 8.

5. Conclusion

We prove that the networks deploying multipath routing achieve greater streaming performance than their linear network counterparts. In particular, it has been demonstrated that multipath routing can be increase in the overall packet throughput,

and thus can be a preferred routing method in WSNs involving data streaming applications. We use of simulations networks deploying multipath routing can provide a significant increase in performance over single-path networks, we have not provided a protocol which automates the process of zone-disjoint path creation and optimal spatial separation for any given network.

A effective, realistic and scalable approach to synchronised WSN clusters. The Group Access time is defined according to the Group ID field which identifies the group node. A simplistic yet effective solution to the hidden node problem, which constitutes a significant impairment of QoS in wireless networks and especially for WSNs. It prevents secret node collisions in synchronised WSNs with containment-based MAC protocols. We are proposing a Hidden-Node Evasive (H-NAME) method for the prevention of WSNs, very straightforward but extremely effective. This method was proposed to extend the distributed peer-to-peer network, [11] known as the multi-access multi-tone (RI-BTMA) and dual inhabited tone multiple access [12]. (RI-BTMA)

CRedit authorship contribution statement

B. Vijay Kumar: Conceptualization, Methodology, Software, Visualization, Writing - original draft. **Syed Musthak Ahmed:** Data curation, Supervision, Software. **M.N. Giri Prasad:** Validation, Writing - review & editing.

Declaration of Competing Interest

The authors declare that they have no known competing financial interests or personal relationships that could have appeared to influence the work reported in this paper.

References

- [1] B. Raman, K. Chebrolu, Censor networks: A critique of "sensor networks" from a systems perspective, *ACM SIGCOMM Comput. Commun. Rev.* 38 (3) (2008) 75-78.
- [2] Anuj Kumar Singh and Pramod Kumar, "Advancement in Quality of Services in Wireless Sensor Networks" 3rd International Conference On Internet of Things, Smart Innovation and Usages (IoT-SIU) (2018), 978-1-5090-6785-5/18/\$31.00 © 2018 by IEEE.
- [3] K. Xu, M. Gerla, and S. Bae, "How effective is the IEEE 802.11 RTS/CTS handshake in ad hoc networks?," in *Proc. Global Telecomm. Conf. (GLOBECOM02)*, 2002, vol. 1, pp. 72-76.
- [4] Wakee U Ddin and Bilal M. Khan "Improved quality of service in wireless sensor Network with mobile sink" 17th IEEE International Multi Topic Conference 2014.
- [5] L. Hwang, "Grouping strategy for solving hidden node problem in IEEE 802.15.4 LR-WPAN," in *Proc. IEEE 1st Int. Conf. Wireless Internet (WICON05)*, Budapest, Hungary, 2005, pp. 26-32.
- [6] A. Koubãa, A. Cunha, and M. Alves, "A time division beacon scheduling mechanism for IEEE 802.15.4/ZigBee cluster-tree wireless sensor networks," in *Proc. 19th Euromicro Conf. Real-Time Systems (ECRTS07)*, Pisa, Italy, Jul. 2007, pp. 125-135.
- [7] J.A. Stankovic, I. Lee, A. Mok, R. Rajkumar, Opportunities and obligations for physical computing systems, *IEEE Computer* 38 (11) (2005) 23-31.
- [8] A. Koubãa, R. Severino, M. Alves, E. Tovar, H-NAME: Specifying, implementing and testing a hidden-node avoidance mechanism for wireless sensor networks, *Tech. Rep. HURRAY-TR-071113*, Nov. (2007).
- [9] Adwan Alanazi and Khaled Elleithy "Optimized Node Selection Process for quality of service provisioning over wireless multimedia sensor networks" Second International Conference on Mobile and Secure Services (MobiSecServ) 2016.
- [10] A. Koubãa, R. Severino, M. Alves, E. Tovar, M. Alves, and Eduardo Tovar "Improving Quality-of-Service in Wireless Sensor Networks by Mitigating "Hidden-Node Collisions"", *Transactions on Industrial Informatics, Special Issue on Real-Time and Embedded Networked Systems*, *IEEE*. 5 (3) (2009) 299-313.
- [11] C. S. Wu and V. O. K. Li, "Receiver-initiated busy-tone multiple access in packet radio networks," in *Proc. ACM Workshop on Frontiers in Comput. Commun. Technol.*, Stowe, Vermont, 1987, pp. 336-342.
- [12] Z.J. Haas, Jing Deng, Dual busy tone multiple access (DBTMA)-A multiple access control scheme for ad hoc networks, *IEEE Trans. Commun.* 50 (6) (2002) 975-985.

Selection of optimized replacement with Flyash based cement composition by TOPSIS method

G.Shiva kumar[#], DR.R.Bharathi murugan^{*},

[#]Civil Engineering Department, Vaagdevi college of Engineering

¹ganacharishiva7@gmail.com

Abstract— Concretes versatility, durability, sustainability and economy have made it the world's most widely used construction material. Concrete the most widely used construction material in civil engineering industry because of its high structural strength and stability. One of the main ingredients in concrete is ordinary Portland cement. So, its production is severe threat to the environment. Why because, in the production of cement with equal amount of CO₂ is released into the atmosphere which is 5% of the globally production of the pollution. The most effective way to reduce CO₂ emission from cement industry is to substitute a proportion of cement with other materials. These materials are called supplementary cementitious materials for replacement of cement. In this project I have adopted M₄₀ grade of concrete with fly ash as supplementary cementitious materials for replacement of cement. I replaced cement with both fly ash for 10%, 20%,30%,40%,50% by weight of cement. Various tests like compressive, split tensile tests and Acid attack, RCPT tests were conducted. The curing periods chosen were 7,28,56,90 days respectively. The best and sustainable mix cannot be decided from the results obtained by the strength and durability parameters alone, it is also necessary to consider the beneficial criterions. So in order to obtain the best mix I adopted TOPSIS (Technique for Order of Preference by Similarity to Ideal Solution) of MCDM (Multi Criteria Decision Making) techniques. By using this method, I concluded that the sustainable mix obtained was M₃ i.e., 30% replacement of cement

with fly ash by considering various alternatives and criterion.

Keywords—Topsis,Flyash,Ordinary Portland cement.

I. INTRODUCTION

Cement has become a vital part of our lives; the use of concrete is increasing at a very high rate. One of the main constituents of concrete is Portland cement. The manufacturing of cement results in emission of large amount of CO₂. Thus, the researchers have started finding alternatives for the partial replacements for cement. Among many alternatives, FLY ASH are the industrial by products which provides excellent binding properties to concrete and serve as a replacement of cement. These alternatives are generally termed as supplementary cementitious materials (SCMs). Concrete is a composite material formed by bonding together aggregates and fluid cement which hardens over time. It is estimated that about 0.9 tons of carbon dioxide is released in the environment for the production of 1 ton of cement.

Multi Criteria Decision Making (MCDM):

It is a sub-discipline of operations research that explicitly evaluates multiple conflicting criteria in decision making. It is the process of finding the best option from all of the feasible alternatives. Multi-criteria decision making usually refers to the process of ranking the alternatives or selecting a desirable alternative among the collection of possible alternatives with respect to list of criteria. It consists of single decision maker, multiple decision alternatives. However, the increasing complexity of the socio economic environment makes it less

possible for a single decision maker to consider all alternative aspects of the problem as many decision-making processes takes place in group settings.

The following are the features of the decision making.

1. Decision making is a selective process in which only the best possible alternative is chosen.
2. Decision making involves careful evaluation and analysis of all possible alternatives.
3. It is a continues process which goes on throughout the life of an organization.
4. It may be a positive to do a certain thing or negative not to do a certain thing.
5. It is not an end itself but, it reaches its goal.
6. The success of any thing clearly depends on what type of decisions taken.

Technique for Order Preference by Similarity to Ideal Solution

(TOPSIS) Technique for Order Preference by Similarity to Ideal Solution method which was firstly developed by “HWANG” and “YOON” in 1981. It is based on the concept that an ideal solution is shortest distance from positive solution and it should be the longest distance from negative solution. It is a method of compensatory aggression that compares a set of alternatives by identifying weights for same criteria. Normalization is the best way to identify the obtained outcomes which are how far from the ideal solution.

Why TOPSIS: it is the best method to identify the ideal solutions from a collection of possible alternatives. Topsis normalizes the outcomes and compare these to the ideal solutions. Based on the alternative outcomes it should give a rank for easy understanding of different alternatives. Topsis method used in large engineering problems often found in aeronautics and automotive industries.

Feasibility of TOPSIS:

- 1.Simplicity.
- 2.Rationality.
- 3.Comprehensibility.
- 4.Efficiency of good computation outcomes.
- 5.Accurate measurement of different alternative solutions.

TYPES OF SUPPLEMENTARY CEMENTITIOUS MATERIALS

The following are the types of supplementary cementitious materials

- Fly ash
- Silica fume
- Meta kaolin (MK)

LITURATURE REVIEW

- [1]. International Journal on Engineering and Advanced Technology (IJEAT) paper titled “Estimation of fly ash strength efficiencies on concrete with age” by k Suvarna Latha, M V Sheshagiri Rao, V Srinivasa Reddy.

ISSN: 2249-8958, Volume-2, Issue-2, December-2012.

1. In this paper, they conducted to evaluate the strengths of hardened concrete, by partial replacing of cement with increasing percentages of Fly ash for M_{40} grade of concrete at different ages.
2. The optimum Fly ash replacement as cementitious material is characterized by high compressive strength, low heat of hydration, resistant to chemical attack, better workability and good durability, cost effective.
3. The optimum dosage of Fly ash replacement is 50%.

[2]. IOSR journal on engineering (IOSRJEN) paper titled “Partial replacement of cement with fly ash in concrete and its effect” by Vinod Goud and Niraj Soni” ISSN (e): 2250-3021,

ISSN (p):2278-8719, Volume-06, Issue 10(oct.2016).

Rapid growth of construction activities leads to active shortage of conventional construction materials due to various reasons. Researches were searching for cheaper & eco-friendly materials as a replacement of cement in concrete. Because the manufacture of cement leads to the pollution in large amounts (CO₂ emissions are 0.8-1.3 ton/ton² & SO₂ emission is also very high). It was found that industrial waste such as fly ash can be used as partial substitute for cement.

The addition of fly ash to cement has been found to enhance cement properties:

Normal consistency increases with increase in the grade of cement and fly ash content. Workability increases in fly ash concrete. As the fly ash contents increases in all grades of OPC there is reduction in the strength of concrete. In all grades OPC, fly ash concrete is more durable as compared to OPC concrete and fly ash up to 20% replacement increase with grade of cement. Shrinkage of fly ash concrete is similar to the pure cement concrete in all grades of OPC.

1. The 10% and 20% replacement of cement with Fly ash shows good compressive strength results.
2. The optimum usage of fly ash replacement is 20%.

[3]. “ Fly ash Effects on Compressive strength by Partial Replacement of Cement Concrete by Azmat Ali Phul, Muhammad Jaffer Memon, Syed Naveed Raza Shah, Abdul Razzaque Sandhu” volume-5, no-4, April 2019

This paper investigates the compressive strength properties of concrete with Fly Ash in concrete by partial replacement of cement. The incremental demand of cement in the construction field is a concern for environmental degradation, in this regard; replacement of cement is carried out with waste materials by using Fly Ash. On optimum level of Fly Ash was assessed with varied percentage from 0 to 30% for different curing days. Replaced concrete were tested with the slump, compaction factor, Vee-bee and compressive strength. Cement to water ratio was maintained at 0.47 for all mixes. The compressive strength tests were conducted for 3, 7, 14 and 28 days of curing. The results obtained from the slump, compaction factor, Vee-bee and compressive strength of concrete containing Fly Ash was increased as the curing time increases. The outcomes indicated that the addition of Fly Ash enhances the workability and compressive strength which eventually improved the mechanical properties of concrete.

1. This paper investigates the mechanical properties and workability of concrete and how the outcomes varying while, increasing in the percentages of Fly ash .
2. The optimum usage of both fly ash in cement is 30%

[4]. “K.V. Sabarish, R. Venkat Raman, R. Ancil, R. Wasim Raja, P. Selva Surendar, Experimental Studies on Partial Replacement of Cement with Fly Ash in Concrete

Elements”. International Journal of Civil Engineering and Technology, 8(9), 2017, pp. 293–298.

The use of fly ash in concrete formulations as a supplementary cementitious material was tested as an alternative to traditional concrete. The cement has been replaced by fly ash accordingly in the range of

0% (without fly ash), 10%, 20%, 30% & 40% by weight of cement for M-25 and M-40 mix. These tests were carried out to evaluate the mechanical properties for the test results for compressive strength up to 28 days and split strength for 56 days are taken.

1. Compressive strength reduces when cement replaced fly ash. As fly ash percentage increases compressive strength and split strength decreases.
2. Use of fly ash in concrete can save the coal & thermal industry disposal costs and produce a „greener concrete for construction.
3. The cost analysis indicates that percent cement reduction decreases cost of concrete, but at the same time strength also decreases.
4. This research concludes that fly ash can be innovative supplementary cementitious Construction Material but judicious decisions are to be taken by engineers.

TOPSIS technique is one of the classical MCDM techniques developed by Wang and Lee (2007) for the first time for solving the MCDM problems. They illustrated that TOPSIS is based on the concept that the most preferred alternative should not only has the shortest distance from the positive ideal solution but also has the longest distance from the negative ideal solution.

1 .This paper includes selecting and studying the MCDM techniques that uses wide ranges of data analysis in civil engineering projects.

2. A detailed study including the advantages and disadvantages using the analytical hierarchy process and fuzzy Technique for Order and Preference by Similarity to the Ideal Solutions(TOPSIS) is introduced.

AIM

To obtain best mix of concrete when cement is minimally replaced by Fly ash using TOPSIS method of MCDM technique.

OBJECTIVES:

The following are the objectives set after viewing literature reviews.

1. determine the behavior and mechanical properties of two concrete mixes when cement is partially replaced with fly ash from 0%,10%,20%,30%,40%,50%.
2. To determine the durability properties of two concrete mixes with fly ash for different curing periods as 7,28,56,90.
3. To obtain the best optimized mix of fly ash by TOPSIS method of MCDM technique.

STUDY METHODOLOGY

To obtain the aim of the project the following steps need to be done.

Experimental program consists of the following steps.

1. Material collection
- 2.Mix proportion
- 3.Casting
- 4.Curing
- 5.Testing

MATERIAL COLLECTION

The materials used in this project were collected from near by source. The following materials are required,

- Cement 53 grade
- Fly ash (Class-F)
- Fine aggregate
- Coarse aggregate (10mm and 20mm)

Mix	Cement	Fly ash	Fine aggregate	Coarse aggregate		Water
				10 mm	20 mm	
M ₁ (10%)	373.5	41.5	606	501	752	193
M ₂ (20%)	368	83	606	501	752	193
M ₃ (30%)	326.5	124.5	606	501	752	193
M ₄ (40%)	285	166	606	501	752	193
M ₅ (50%)	207.5	207.5	606	501	752	193

MIX PROPORTION

IS (10262-2019) code is used for mix design. The final mix proportion obtained for M₄₀ Grade of concrete is 1:1.46:3.02:0.46.

The following quantities (kg/m³) are obtained for the above mix proportion which is designated as "M".

CASTING:

First of all ingredients of mix are weighed accurately according to mix proportion and mix it properly to get the uniform mix. Specimens (cubes, cylinders etc...) were casted for different percentages (0%,10%,20%,30%,40%,50%) of fly ash .

TOTAL NO OF SPECIMENS CAST

CURING

After 24 hours the specimens are de-molded and kept for normal curing in 7,28,56,90 days. For different percentages of fly ash .

TESTING

The following are the tests to be performed on the specimens.

Compressive test: It is the capacity of the material or a structure to withstand loads. This test is used to determine the hardness property of a concrete specimen.

Compressive test = _____

Split tensile test: It is used to determine the tensile test of the cylindrical concrete specimen. As we know that concrete is weak in tension so, by providing reinforcement to overcome this problem.

Split tensile test = ____

Carbonation: carbonation is the result of dissolution of carbon dioxide in the concrete pore fueled and this reacts with calcium from calcium hydroxide and calcium silicate hydrate to form calcite. Within few hours or a day or at most, the surface of fresh concrete which have reacted with carbon

S.NO	TEST NAME	SPECIMEN DIMENSIONS (mm)	CURING DAYS	NO. OF SPECIMENS
1	Compressive test	150x150x150	7,28,56,90	77
2	Split tensile test	150 diameter 300 height	7,28,56,90	77
3	RCPT(Rapid Chlorine Penetration Test)	100 diameter 50 height	28	22
4	Acid attack	100x100x100	7,28	44

dioxide of air. Generally, the process penetrates deeper into the concrete at the rate proportional to the square root of time.

After an year or so it may typically have reached a depth of perhaps one mm for dense of low permeability made with a low water cement ratio, or up to 5mm or more for more porous and permeable concretes made using high water cement ratio. The effected depth from the concrete surface can be readily shown by the use of phenolphthalein indicator solution which is diluted to 1% in 99% of ethanol. The indicator is applied to the fresh fractured surface concrete. If the indicator turns pink then the surface is free from carbonation and the surface remains colorless then it is carbonated and the depth of carbonation is measured.

Acid attack : ordinary Portland cement (OPC) is highly alkaline in nature with PH of above 12. When the cement paste comes in contact with acid its components breakdown, this phenomenon is called acid attack.

Before the cubes are kept for acid curing they are kept aside for 2 days for attaining the constant weights and weights of the specimens are noted down. After the cubes are cured in 5% concentration of H_2SO_4 solution for 7 days they are removed and kept a side for 2 days for attaining the constant weights and are tested for various factors such as acid mass loss factor (AMLF), acid attacking factor (AAF), acid strength loss factor (ASLF), acid durability loss factor (ADLF).

Acid Mass Loss Factor (AMLF): the percentage loss is estimated by immersing the cubes in acid solution and finding the mass at a definite period of time. The change in mass with age compared to the initial mass of each specimen is defined as acid mass loss factor.

Acid Attacking Factor (AAF): the extent of deterioration at each corner of the struck face and the opposite face is measured. The change in length of the diagonal after immersion in acid for a definite period of time as AAF.

Acid Strength Loss Factor (ASLF): the relative strength present in the concrete specimen after immersion in the acid specimen represents acid strength or factor. The relative strengths are always compared with respect to the 28 days of compressive strength values.

Acid Durability Loss Factor (ADLF): to combine the effect of different factors like mass loss, strength loss, dimension loss, a single uniform factor termed acid loss durability factor is introduced.

RCPT (Rapid Chlorine Penetration Test): According to ASTM C 1202 the total charge passed through specimen in coulombs has been found to be related to the resistance of the specimen. After setting up apparatus, read and record the current at least every 30 minutes. Plot the graph (current (amp) vs time (sec)). The total time period of the test is 6 hours.

As per ASTM C1202 certain range of total charge passed through the specimen is given below with its effect in inference.

RESULTS AND OBSERVATIONS

The strengths tests and durability studies (RCPT and acid attack) tests are conducted for specimens, and the basic tests (specific gravity, fineness, workability) are found and the results are tabulated as below.

Specific Gravity Test

- Cement = 3.15
- Fine aggregate = 2.3
- Coarse aggregate = 2.8
- Flyash = 2.25

Fineness

1. Cement = 8%(remained after sieving)

REPLACEMENT OF CEMENT WITH FLY ASH	7 days strength (N/mm ²)	28 days strength			56 days strength			90 days strength		
		T-1	T-2	AVER	T-1	T-2	AVER	T-1	T-2	AVER
0	28.34	42.73	44.88	44.5	44.96	44.8	47.42	50.14	53.6	51.8
10	26.7	49.6	41.2	44.7	45.34	45.6	47.85	52.86	54.1	53.4
20	24.5	44.91	47.8	46	48.5	45.5	51.5	53.5	56.9	55.2
30	21.8	41.42	39.4	40.3	42.3	42.3	42.3	47.9	49.2	50.7
40	19.62	35.75	37.5	36.6	39.24	37.6	38.5	45.23	47.2	44.8
50	21.2	35.3	34	34.6	38.6	35.3	37.6	42.6	48.4	39.5

2 .Fly ash = 0%(remained after sieving)

The following slump values are obtained after replacing cement by fly ash as follows.

COMPRESSIVE TEST (fly ash replacement)

The trial mix cubes are tested for compressive strength to check if it reached the target strength after accelerated curing.

SPLIT TENSILE TEST (fly ash replacement):

I	% REPLACEMENT OF CEMENT WITH FLY ASH	FLY ASH SLUMP VALUE mm
NF	0	0
REN	10	14
CE:	20	22
Fro	30	30
m	40	35
the	50	50
abov		
e		

graph it is observed that while, cement is replaced with fly ash split tensile strength value increases upto 20% replacement of fly ash then, it decreases.

Workability

RCPT(fly ash replacement):

% Replacement of cement with fly ash	Icumulative (millamp)			Total charge (coulombs)	Inference
	T-1	T-2	Average		
0	1690	1575.5	1632.75	2938.95	Medium
10	520.5	505.5	513	923.4	Low
20	405.2	386.5	395.85	712.53	Low
30	392.8	384.2	388.35	699.03	Low
40	556.6	512.8	534.7	962.46	Low
50	535.5	562.6	549.05	988.29	Low

INFERENCE : From the above graph it is observed that while cement is replaced with fly ash chlorine penetration value decreases upto 30% replacement of fly ash then, it increases slightly.

ACID ATTACK (fly ash replacement):

28 days water curing and 7 days acid curing

% Replacement of cement with fly ash	Acid attack factors			
	AMLF	AAF	ASLF	ADLF
0	6.54	9.375	33.33	0.00204
10	5.01	6.714	27.03	0.000909
20	3.87	4.623	21.5	0.000384
30	2.35	2.143	20	0.0001007
40	1.86	1.986	16.32	0.000059

Percentage of cement with fly ash	7 days strength	28 days strength			56 days strength			90 days strength		
		T-1 (N/mm ²)	T-2 (N/mm ²)	Average (N/mm ²)	T-1 (N/mm ²)	T-2 (N/mm ²)	Average (N/mm ²)	T-1 (N/mm ²)	T-2 (N/mm ²)	Average (N/mm ²)
0	3.33	5	4.44	4.72	4.86	4.86	4.86	5.4	5.13	5.26
10	2.8	4.16	4.86	4.51	4.6	5	4.8	4.86	5.27	5.06
20	3.2	4.6	4.16	4.38	5	4.86	4.93	5.13	5.8	5.46
30	3	4.02	4.72	4.37	4.02	5.13	4.575	4.86	6.1	5.48
40	2.8	3.47	3.88	3.67	4.02	3.33	3.67	4.44	4.16	4.3
50	2.5	4.02	3.33	3.67	4.3	3.75	4	4.02	4.3	4.16
50		1.06		1.469		7		0.0000108		

INFERENCE : From the above graph it is observed that while, increasing in the replacement of cement with fly ash acid attacking factors (AMLF,ASLF,AAF) are decreases.

ACID ATTACK (fly ash replacement):

• 28 days water curing and 28 days acid curing

% Replacement of cement with fly ash	Acid attack factors			
	AMLF	AAF	ASLF	ADLF
0	9.425	11.62	17.81	0.00195
10	8.169	12.582	14.23	0.0014626
20	5.750	9.673	8.98	0.0005
30	4.86	5.232	5.772	0.000146
40	3.227	3.49	3.623	0.0000408
50	2.362	2.98	1.756	0.0000126

Normalization matrix

M	0	0.44	0.45	0.83	0.78	0.44
M1	0.19	0.44	0.43	0.26	0.59	0.43
M2	0.30	0.45	0.42	0.20	0.2	0.41
M3	0.41	0.40	0.42	0.20	0.058	0.40
M4	0.48	0.36	0.35	0.27	0.016	0.38
M5	0.69	0.34	0.35	0.28	0.005	0.37

Relative weight matrix

M	0	0.44	0.45	0.83	0.78	0.44
M1	0.19	0.44	0.43	0.26	0.59	0.43
M2	0.30	0.45	0.42	0.20	0.20	0.41
M3	0.41	0.40	0.42	0.20	0.058	0.40
M4	0.48	0.36	0.35	0.27	0.016	0.38
M5	0.69	0.34	0.35	0.28	0.005	0.37

INFERENCE : From the above graph it is observed that while, increase in the replacement of cement with fly ash acid attacking(AMLF,ASLF,AAF) decreases.

STEP WISE PROCEDURE FOR SELECTING BEST ALTERNATIVE USING TOPSIS METHOD

:Decision matrix for fly ash replacement

Alternatives	Criteria					
	C ₁	C ₂	C ₃	C ₄	C ₅	C ₆
	W	CS	SS	RCP T	AA	LC C
M	0	44.25	4.72	2938.95	0.00195	6475
M1	14	44.7	4.51	923.4	0.0014626	6293
M2	22	46	4.38	712.53	0.0005	6081
M3	30	40.33	4.37	699.03	0.000146	5954
M4	35	36.62	3.67	962.46	0.0000408	5623
M5	50	34.66	3.67	988.29	0.0000126	5476

Positive matrix

M	0.69	0.45	0.45	0.20	0.005	0.37	1.215
M1	0.69	0.45	0.45	0.20	0.005	0.37	0.77
M2	0.69	0.45	0.45	0.20	0.005	0.37	0.44
M3	0.69	0.45	0.45	0.20	0.005	0.37	0.29
M4	0.69	0.45	0.45	0.20	0.005	0.37	0.26
M5	0.69	0.45	0.45	0.20	0.005	0.37	0.17

Si Plus

$$SiPlus = \sqrt{(0.19 - 0.69)^2 + (0.44 - 0.45)^2 + \dots + (0.43 - 0.37)^2} = 0.77$$

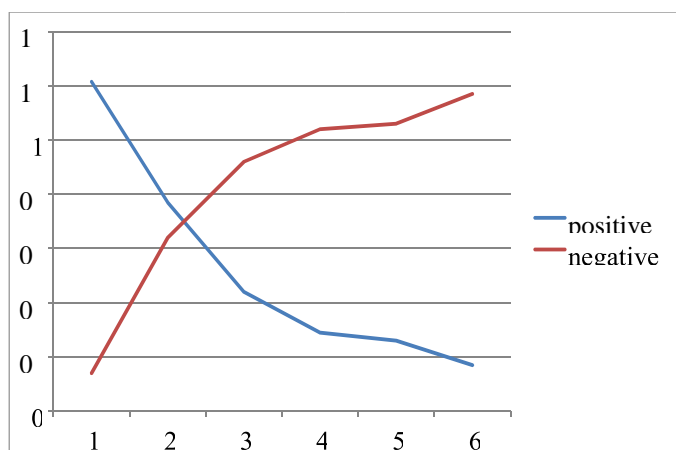
Negative matrix

SiMinus

M	0	0.34	0.35	0.83	0.78	0.44	0.14
M1	0	0.34	0.35	0.83	0.78	0.44	0.64
M2	0	0.34	0.35	0.83	0.78	0.44	0.92
M3	0	0.34	0.35	0.83	0.78	0.44	1.04
M4	0	0.34	0.35	0.83	0.78	0.44	1.06
M5	0	0.34	0.35	0.83	0.78	0.44	1.17

Relative closeness to ideal solution (C_i)

M	6	0.1
M1	5	0.45
M2	4	0.67
M3	3	0.78
M4	2	0.8
M5	1	0.87



Relative closeness to ideal solutions

The ranking for the different mixes is obtained by assuming an ideal solution. The positive solution which is nearer and the negative solution which is far from the ideal solution is

adopted as the best mix. Hence from the graph we can conclude that M_3 i.e., 30% replacement of cement with Fly ash

CONCLUSION

Based on the experimental studies the following conclusions can be drawn.

1. The slump values are increases with increasing in the % replacement of cement by both fly ash.
2. The compressive, split tensile strengths of concrete is increasing with % replacement of cement with Fly ash upto 30% replacement of cement.
3. The resistance to chlorine penetration (RCPT) increases upto 20% replacement of cement with Fly ash and then decreases slightly.
4. By using TOPSIS method of MCDM technique I can concluded that the sustainable mix for Fly ash is M_3 i.e., 30% and for GGBS is M_2 i.e, 20% replacement of cement.

REFERENCES

[1]. “K.V. Sabarish, R. Venkat Raman, R. Ancil, R. Wasim Raja, P. Selva Surendar, Experimental Studies on Partial Replacement of Cement with Fly Ash in Concrete Elements”. International Journal of Civil Engineering and Technology, 8(9), 2017, pp. 293–298.

[2]. “Fly ash Effects on Compressive strength by Partial Replacement of Cement Concrete by Azmat Ali Phul, Muhammad Jaffer Memon, Syed Naveed Raza Shah, Abdul Razzaque Sandhu” volume-5, no-4, April 2019

[3]. International Journal on Engineering and Advanced Technology (IJEAT) paper titled “Estimation of fly ash strength efficiencies on concrete with age” by k Suvarna Latha, M V Sheshagiri Rao, V Srinivasa Reddy.

[4]. Fam F Abdel malak, Emad A. Osman (2017) “Applying decision making techniques to civil engineering projects”, Research Gate.

[5]. IOSR journal on engineering (IOSRJEN) paper titled “Partial replacement of cement with fly ash in concrete and its effect” by Vinod Goud and Niraj Soni” ISSN (e): 2250-3021, ISSN (p):2278-8719,Volume-06, Issue 10(oct.2016).

[6]. IS 10262-2019: Guidelines for concrete mix design proportioning and BIS.

[7]. ASTM C 267-01: “Acid Attack testing on concrete”.

[8]. ASTM C 1202: “RCPT (Rapid Chlorine Penetration Test) testing on concrete”.

[9]. IS 456-2000: Plain and reinforced concrete.

[10]. M.S Shetty and S. Chand – concrete technology theory and practice.

Experimental Study on Polyurethane Foam Concrete for Use of Structures

Vanga Lingamurthy¹ Syed Malik²

¹M.Tech Scholar ²Assistant Professor

Department of Civil Engineering, Vaagdevi College of Engineering, Warangal

Abstract:

Recently, foamed concrete is being widely used in civil construction and building, because of its high fluidity and settlement, low self-weight and low thermal conductivity. However, it has some major setbacks such as low strength and increased shrinkage at later ages. The strength gain of concrete depends upon several variables; one of these is the curing conditions. This work aims to study the potential production of foamed concrete as a sustainable structural material by varying the curing methods. For this purpose, sample cubes, cylinders and prisms were prepared to find the compressive strength, modulus of elasticity and drying shrinkage at deferent ages. Samples of the polyurethane foamed concrete cured under four deferent curing regimes (water, moisture, sealing by membrane-forming curing compound and air curing). At the end of the study, poly- urethane foamed concrete used for this study has shown the potential for use in structural applications. Also, the results show that the samples cured by moisture have the highest compressive strength at all ages

Keywords:

Polyurethane foamed concrete Curing conditions, Fly ash, and Compressive strength, Static modulus of elasticity drying shrinkage

1. Introduction:

The properties of foamed concrete differ with the difference in curing type and duration. Correct curing will enhance the durability and increase strength, volume stability, abrasion resistance, impermeability and resistance to freezing and thawing. found that air cured specimens developed a higher strength than water curing for foamed concrete with 10% Structural lightweight concrete has an in-place density (unit weight) of the order of (1440–1840) kg/m³ compared to normal weight concrete with a density in the range of (2240–2400) kg/m³. For structural applications, the concrete strength should be greater than (18 MPa) according to ACI 213R. Foamed concrete is a type of lightweight aerated concrete which consists principally of a cement paste or mortar with at least 20% of its volume as air. Foamed concrete is produced by two methods: the first is the pre-foaming method and the second is the mixed foaming method. The pre-foaming method involves the isolated production of the base mix cement slurry (cement paste or mortar) and production of a stable foam (foam agent with water) and then mixing this foam into the base mix. In the mixed foaming method, the foaming agent is added to the pre-prepared base mixture and during the mixing foam is produced resulting in a cellular structure in the concrete.

Foamed concrete can have a wide range of dry densities (400–1600) kg/m³ and compressive strengths (1–25) MPa. The increase in compressive strength of foamed concrete formed of fly ash, micro silica, and SiO₂ powder is in the range of (20–25) MPa, this increment in

strength shows that this foamed concrete is satisfactory to be used for structural applications or load bearing purposes. The strength of foamed concrete is little affected by the percent cement replaced by fly ash and even when replacing a high amount of cement with fly ash it does not much affect the later compressive strength of properly cured foamed concrete. The best-pulverized fly ash content for greatest strength of foamed concrete is around 20% to 30%.

1.1. Benefit of the Work

The goals of this works are to:

1. Find the Applicability to produce foamed concrete using polyutherene as a foaming agent and its applicability as a construction building material.
2. Test the effect of different curing conditions on some mechanical properties of polyutherene foamed concrete.
3. Find some mechanical properties of polyurethane foamed concrete with and without fly ash.

2. Experimental work

2.1. Materials

Combinations of the following constituent materials were used to produce foamed concrete in this study:

1. Ordinary Portland Cement type (I): The chemical and physical properties of this cement conformed to BSEN 196-1; 2005
2. Class F fly ash supplied by a local supplier and conformed to ASTM C618.
3. Natural sand supplied locally and conformed to the requirements of BS 812-103.1:1985 [7] for verifying distribution and particle size. The specific gravity of the sand was 2.6.
4. High range water reducing agent (HRWRA) Glenium 51; the normal dosage for Glenium 51 is (0.5–0.8) l/100 kg of cement.
5. Tap water was used for both mixing and curing.
6. Liquid membrane-forming curing compounds: Setseal 22 is a water based curing compound formulated from selected emulsified
7. paraffin to form a low viscosity wax emulsion. The color is a white liquid, which creates a white film when applied to concrete surfaces and reflects (60–80)% of the sunlight.
8. Foam: The foaming agent of density 45 kg/m³ used in this study was polyurethane (PU) foam.



2.2. Mix proportions

The mix proportion guideline of ASTM C796 was followed in the laboratory mixing. The mix proportions of foamed concrete. The final mix proportions were established by laboratory trials to achieve a target density of 1600 kg/m³.

2.3. Specimens preparation

For this investigation, a pre-foaming method was adopted to provide polyurethane foamed concrete. The mixing procedure started with the cleaning of the laboratory mixer and emptying the excess water, one-third of the calculated mixing water was added, then the fine aggregate followed by the cement. The materials were allowed to mix for three minutes, then the fly ash and the remaining water was added. This was allowed to blend together till appreciable slurry was achieved. The ready-made foam was added to the base mix through the nozzle of the foam can according to the calculated amount by trial and error. The density of the foamed concrete produced was then checked against the target density, 1600 kg/m³.

Table 1

Chemical and physical properties of cement, fly ash and fine aggregate.

Oxides composition	Cement Fly Ash	Oxides Content %	Oxides Content % ASTM C618(Class F)
CaO	62.8	5.0	<10
SiO ₂	22.3	54.2	70 (Min)
Al ₂ O ₃	4.5	31.6 70 (min)	
Fe ₂ O ₃	1.9	3.8	
Na ₂ O	0.1	0.7	
K ₂ O	0.7	0.6	
MgO	4.4	1.3	5 (max)
SO ₃	2.0	0.1	
CO ₂	2.5		
Free CaO	1.2		
Loss on Ignition	0.8		
Blain Surface Area m ² /kg	250	350	
Relative Density	3.15	2.2	

Table 2

Grading of fine aggregate

Sieve size (mm)	Passing by weight%	ASTM C33-03
2.36	100	85–100
1.18	85.7	75–100
0.60	71.2	60–79
0.30	29.6	12–40
0.15	3.5	0–10

Table 4
Mix Proportions for Polyurethane Foamed Concrete.

Mix details	Target Density	Cement kg	sand kg	fly ash kg	water kg	w/C+FA	HRWRA L	foam kg
Mixed with fly ash	1600	440	960	160	300	50	3.6	60
Mixed without Fly ash	1600	600	960	0	300	50	2.64	60

The specimens remained in the same condition till 24 h later when the specimens were demolded and the fresh density of concrete measured. Each sample was marked before being separated and transferred to the place where they cured using four different curing conditions, which were: water curing; moist curing; membrane compound curing and air curing. All the specimens remained under same curing condition till the date of testing except the water and moisture cured samples that were removed and placed in an oven for 24 h before testing. The density was checked before placing in an oven and after placing in an oven.

The curing regime adopted was as below:

- Air curing: in laboratory air entire time with the constant range $(25 \pm 2)^\circ\text{C}$ and an average relative humidity of 60%.
- Water curing: in air under laboratory conditions after seven days of water curing with the constant range of temperature $(25 \pm 5)^\circ\text{C}$.
- Moisture curing: covered with wet burlap for seven days.
- Liquid membrane-forming curing compounds: Setseal 22 was applied after 24 h from casting, except for the top face of the casting

mold where the liquid compound was applied after 1 h from casting.

Most of these adopted curing conditions in this study chosen were completely compatible with the curing conditions which are performed in the field.

2.4. Testing methods

2.4.1. Fresh state properties

The fresh properties of polyurethane foamed concrete consist of flow and fresh density. A flow table test was performed to find the consistency of the freshly mixed mortar as described in ASTM C 1437. The fresh polyurethane foamed concrete produced was first poured into an inverted slump flow cone without any compaction and vibration in accordance with ASTM C 1611. The fresh density was established according to ASTM C 138

2.4.2. Hardened properties

a) Compressive Strength

The compressive strength tests were performed according to (BS. 1881: Part 116: 1983). A total number of 72 cubes of (100×100) mm were tested by using a hydraulic compression machine of 1800 kn, at a loading rate of 18 MPa per minute. The average of three cubes was taken for each test and the test was conducted at ages of (7, 28, and 56) days.

b) Shrinkage

Shrinkage was measured by apparatus with dial gauge of 0.002mm accuracy. Prisms of (100×100×400)mm were used for this test. Measurements of the shrinkage strain were made according to (ASTM C157-2008) [2]. After removing the samples from the mold at an age of 24 h, shrinkage nails were installed on the surface of prisms after being demolded. The readings were taken at ages (3, 7, 14, 21, 28, 56) days for different curing conditions. Two specimens were prepared for each test condition.

c) Static Modulus of Elasticity

The static modulus of elasticity was measured according to (ASTM C 469). A total number of 48 cylinders of (150×300)mm were tested at ages of (7, 14, and 28) days. The average of two cylinders was taken for each test.

3. Results and discussions

3.1. Fresh properties

a) Flowability and Fluidity

For this study, the flowability of polyurethane foamed concrete mixes was measured by the diameter of the slump. It was found that the flowability for a mix without fly ash had a lower diameter of a slump than the mix with fly ash. The average slump flow values obtained for fly ash mix and mix without fly ash were 230mm and 200 mm, respectively. This phenomenon is due to the lubrication effect of the spherical shape of most fly ash particles which led to greater workability. The fluidity of polyurethane foamed concrete mixes measured by the diameter of four different angles of the slump. The inverted slump cone spread values are given in Table 5 clearly indicated that the fluidity of the polyurethane foamed concrete was dependent on the fly ash in the mixes. Slump cone spread values obtained for the fly ash mix and the mix without fly ash were 478mm and 452 mm, respectively. This may be ascribable to the higher fineness of fly ash compared to that of the mix without fly ash.

b) Consistency and Stability

The consistency of the fresh polyurethane foamed concrete represented by a measured fresh density to designated density ratio was kept to nearly unity, without segregation and bleeding. Stability can be represented by a measured fresh density to measured

Table 5
Properties of the fresh polyurethane foamed concrete.

Sample	Consistency	Stability	Inverted slump cone spread value (mm)	Slump value(mm)
Mix with fly ash	1.04	1.015	478	230
Mix without fly ash	1.05	1.018	452	200

hardened density Lim et al. [21]. The measured hardened density of the foamed concrete produced was (1640 and 1650) kg/m³ for the fly ash mix and the mix without fly ash respectively. The fresh density of polyurethane foamed concrete is measured in a container of known volume in order to determine density (unit weight). The use of fly ash resulted in a slight decrease in the fresh density of polyurethane foamed concrete samples. The average fresh density values obtained for the fly ash mix and the mix without fly ash were 1665 kg/m³ and 1680 kg/m³, respectively. However, such results are attributed to the low specific gravity of the fly ash. Portland cement has a higher specific gravity than that of fly ash so they increase the overall density of the polyurethane foamed concrete to a greater extent.

3.2. Hardened properties

a) Compressive Strength

The average of the tests results for polyurethane foamed concrete mixes with and without fly ash for different curing conditions. The compressive strength results for mixes without fly ash range between (7.8–20.1) MPa, (10.3–24.2) MPa and (11.1–26.2) MPa at (7, 28 and 56) days while the results for the mixes with fly ash range between (8.1–22.5) MPa, (11.1–29.2) MPa and (12.1–32.1) MPa at (7, 28 and 56) days. it can be seen that the results of mixes without fly ash give lower results of compressive strength when compared with mixes with fly ash under different curing conditions at all ages with percent (9.2, 29.1 and 40.4) for water curing, (11.6, 20.6 and 22.6) for moisture curing, (3.4, 8.7 and 9.4) for air curing and (8.7, 23.7 and 32.2) for the membrane forming curing compound at (7, 28 and 56) days respectively.

This behavior is explained by the densified effect of fly ash with a decrease in the porosity at early ages, while at later ages, in addition to the densified effect of fly ash, a pozzolanic reaction occurs with calcium hydroxide released from cement hydration reacting with the fly ash resulting in a filling effect in the voids among the cement and other powder particles, it can be seen that moisture cured specimens improve compressive strength more than membrane curing compound, water and air cured specimens respectively by (14.9, 44.9 and 177.3)% at 7 days, (5.0, 18.0 and 162.3)% at 28 days, (6.3, 10.0 and 165.5)% at 56 days.

That can be ascribed to the gel tiffening by drying for moisture curing, however, it is due to relaxation in the gel of filler type due to the presence of water by water curing. An important observation is drawn here, which reflects the same previous trends for mixes with fly ash and for all type of curing conditions at a different age. The results also yielded that curing by membrane forming curing compound was effective in improving the compressive strength of foamed concrete mixes with and without fly ash more than water and air curing. Like other types of concrete, the compressive strength for polyurethane foamed concrete specimens with air curing is lower than that of the other types of curing. However, the extent of strength reduction for air cured specimens up to an age of 56 days was due to the insufficient curing.

b) Shrinkage

The average results of two prisms are plotted in Figs. 3 and 4 for mixes with and without fly ash under different curing conditions. The results clarify that the values of drying shrinkage are higher for mixes without fly ash than those for fly ash mixes. The values range from (160–610) microstrain for the mixes without fly ash and these values decrease to (150–550) microstrain when fly ash is added at the age from 3 days to 56 days. The drying shrinkage for all mixes extends with time till the age of 56 days. Indicating to the earlier Figures there is a small decrement in drying shrinkage for water cured specimens. Moreover, moisture cured samples showed slightly lower values than those for compound cured samples. An important observation is drawn here, which reflects the same previous trends for mixes with and without fly ash and for all type of curing conditions at a different ages.

It indicates that the internalization of fly ash as a partial replacement of cement leads to a slightly decrease in shrinkage of mixes during the time of drying as compared with mixes without fly ash. This phenomenon is ascribed to the reaction of fly ash consuming more free water in the system, leaving less water evaporation during shrinkage. This promotes the deduction that fly ash mix has a lower porosity and finer pore structure, which encourages loss of water by self-desiccation and not by diffusion to the surrounding environment.

c) Static Modulus of Elasticity

The secant moduli for all the mixes was experimentally determined for each testing age (7, 14 and 28) days as the average of two cylinders for different curing conditions. The results of static moduli are plotted.

The modulus of elasticity results for mixes without fly ash range between (4.0–9.1) MPa, (4.8–11.5) MPa and (6.0–16.3) MPa at (7, 14 and 28) days while the results for the mixes with fly ash range between (4.5–9.8) MPa, (5.1–12.4) MPa and (6.1–16.5) MPa at (7, 14 and 28) days. This behavior may be attributed to the incorporation of fly ash as a partial replacement of cement in the mixes that increases the densification of concrete and leads to lower strain under compression at transition zone, thus leads to higher static modulus of elasticity of those mixes.

From Fig. 5, it can be seen that moisture cured specimens improve modulus of elasticity more than the membrane curing compound, water and air cured specimens respectively by (10.4, 12.2 and 55.6)% at 7 days, (5.2, 11.6 and 58.3)% at 14 days, (8.1, 9.0 and 63.3)% at 28 days. An important observation is drawn here, which reflects approximately the same previous trends for mixes with fly ash and for all type of curing conditions at different ages.

d) Oven-dry density
The oven-dry density of hardened polyurethane foamed concrete was measured according to ASTM C 642 [21]. For polyurethane foamed concrete, the oven-dry density increased slightly by adding fly ash. The average density values obtained for fly ash mix and mix without fly ash were 1590 kg/m³ and 1600 kg/m³, respectively.

4. Conclusions

Based on the tests results of the present study on influence of curing methods and fly ash on progressive compressive strength, the following conclusions are drawn:

1. The flowability and fluidity are increased by the presence of fly ash in comparison to mixtures without fly ash of the polyurethane foamed concrete.
2. The compressive strength of samples cured under moisture and membrane forming curing compound produce higher compressive strength range (20–32) MPa. This revealed that polyurethane foamed concrete is satisfactory to be used for structural applications.
3. The samples cured under moisture curing achieve higher strength at all ages than all others curing conditions considered. This revealed that moisture curing affects the compressive strength of foamed concrete more than those cured by a membrane forming curing compound, water, and air curing.
4. Curing by a membrane forming compound was effective in developing the compressive strength of foamed concrete mixes with and without fly ash more than water and air curing.
5. The fly ash utilized improves workability and diminishes the drying shrinkage of foamed concrete.
6. At all ages, the compressive strength of polyurethane foamed concrete without fly ash is lower than that of the polyurethane foamed concrete with fly ash for all curing conditions.

References

1. ASTM C157, Standard Test Method for Length Change of Hardened Hydraulic Cement Mortar and Concrete, ASTM International C, 2008 (157, M).
2. ASTM C618, Standard Specification for Coal Fly Ash and Raw or Calcined Natural Pozzolan for Use in Concrete, American Society for Testing and Materials, 2002.
3. ASTM C796-97, Standard Test Method for Foaming Agents for Use in Producing Cellular Concrete Using Preformed Foam, ASTM International, West Conshohocken, PA, 1989, <http://dx.doi.org/10.1520/C0033-03> www.astm.org.
4. A. ASTM, C1611 Standard Test Method for Slump Flow of Self-Consolidating Concrete, ASTM, US, 2014.

Experimental Investigation of the Strength and Durability of Partially Replacing Cement with GGBS and Alccofine

Mandala Sheshu Kumar¹, Syed Riyaz², Dr. A R Prakash³

¹PG Scholar ^{2,3}Assistant Professor

Department of Civil Engineering, Vaagdevi College of Engineering, Warangal, India

ABSTRACT: Many concrete research projects are underway around the world to achieve high strength and improve longevity to extend the life of the material. In this study, cement is replaced with an ultrafine material called Alccofine at different percentages and GGBS at a constant grade M60. The continuous water content of 0.3 was found in the concrete proportions. As a result, Cryso premia K570, a 0.3 percent superplasticizer, is used to improve workability. The concrete samples are cast and cured for seven and twenty-eight days, respectively, under normal conditions. Concrete specimens were subjected to mechanical tests such as compressive strength, flexural strength, broken tensile strength, and toughness tests such as water permeability and the RCPT. The optimum strength was achieved at 15 percent Alccofine and 30 percent GGBS, according to mechanical properties. The percentage of cement that should be replaced with Alccofine and GGBS was investigated. The chloride permeability in all of the mixes is very poor, according to ASTM. The aim of this research is to investigate the physical characteristics and durability of M60 grade concrete with partial replacement of cement with GGBS and Alccofine, as well as to determine the best Alccofine material to mix in concrete.

KEYWORDS: Alccofine, GGBS, Strength, Replacement of Cement, Strength Tests.

I. INTRODUCTION

Concrete is the world's most commonly used human-made construction tool. Concrete's creation and usage had a slew of environmental and social ramifications. Cement production has risen in tandem with the rise in concrete demand. As a result, a significant amount of greenhouse gas emissions, primarily CO₂, are released from limestone during the pyro-processing of clinker, causing environmental damage. We can use supplementary cementitious materials like GGBS and Fly ash, Silica fume, Rice husk ash, Metakaolin, and Alccofine instead of cement to solve this issue. Many experiments are being conducted to improve the efficiency of high-performance concrete. High-strength, long-lasting concrete is known as HPC. HPC has two main characteristics: a high cement/binder content and a low w/c ratio. The workability and retention of concrete with these characteristics are insufficient. Due to this flaw, high-range water-reducing agents, such as superplasticizers, are used in concrete to boost the flowability and ease of placement and increase the holding period, which aids in the transportation of concrete mix. Cryso Premia K570, a superplasticizer, was used in this analysis. Alccofine 1203 is a low calcium silicate product that is manufactured in India. It has distinct properties that improve 'concrete efficiency' in both fresh and hardened levels. Alccofine 1203 is a regulated granulation product with a high glass content and high reactivity. It enhances the properties of fresh and hardened concrete, resulting in high-performance environmental concrete. Alccofine increases the early strength and longevity of concrete when used in it. Alccofine 1203 outperforms all other supplementary materials used in concrete because of its specific chemical structure and ultra-fine particle size. This material is used to construct high-rise buildings, particularly

marine structures, precast elements, and bridges. Concrete's durability is characterized as its ability to withstand weathering and any other deterioration method. When exposed to the atmosphere, durable concrete can retain its original shape, quality, and serviceability. Many measures are used to determine the durability of concrete, including water permeability, acid attack, sulphate attack, sorptivity, and RCPT (Rapid Chloride Permeability Test). The RCPT test methods were used in this study's water permeability test. One of the best methods for determining concrete durability is looking at its resistance to chloride penetration.

II. LITERATURE REVIEW

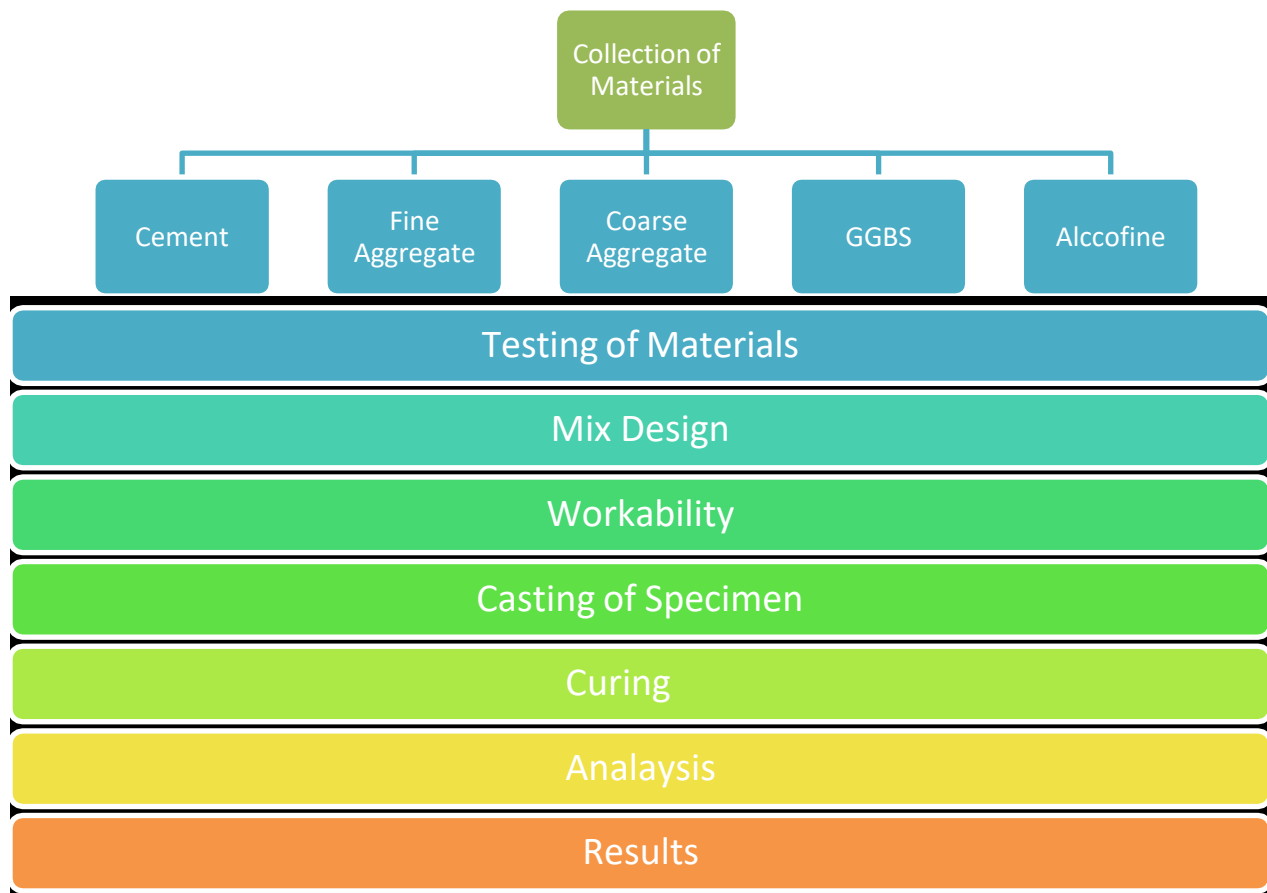
Siddharth 2014 et al.

The author of this Research Paper discusses the efficiency of concrete in terms of compressive strength. Demands in the construction industry are driving up the market for high-performance concrete. Over the last few years, efforts to improve the performance of concrete have suggested that cement substitute products and mineral and chemical admixtures will enhance the strength and durability of concrete. Pozzolanic materials such as alccofine (GGBS) and fly ash can be used to make highly durable concrete composites. The concrete specimens were cured using standard moist curing methods at room temperature.

Saravanan 2019 et al.

The author of this research paper discusses the toughness of concrete when alccofine and GGBS are added. The most significant component of Concrete is Portland cement. A large-scale cement plant consumes a lot of energy and produces many unwanted products (CO₂), which negatively impacts the atmosphere and depletes natural resources. This benefit to the environment has prompted researchers to investigate industrial by-products as supplementary cementitious material in concrete production. In light of this, materials such as silica fume (SF), ground granulated blast furnace slag (GGBS), rice husk ash, fly ash (FL), Metakaolin, alccofine (AL), micro-fine content & others are being tested to wholly or partially replace cement in concrete without losing its strength, while also reducing greenhouse gas emissions and ensuring a sustainable waste management system.

III.METHODOLOGY



Fine aggregate: Sand or crushed stone with a diameter of less than 9.55mm are often used as fine aggregates. Fine aggregates are described as aggregates that have passed through a 4.75mm sieve. Fine aggregate is used to fill voids in coarse aggregate and to improve workability. According to the specifications of IS 383:1970, the fine aggregates used in the project work are zone II. The sand from the Godavari River is used in the construction.

Coarse aggregate: Coarse aggregate is a building material made up of rock quarried from field deposits such as river gravel, crushed stone from rock quarries, and previously used concrete. The most common diameter range used was 9.5mm to 37.5mm. The scale of aggregates used in this project is 20mm and 12.5mm. For coarse aggregate, the IS 2386-1986 code is used.

Water: Both mixing and curing were carried out with potable water. Potable water is described as water with a pH of 7 or less. The concrete mixture contains fresh tap water. Water is classified as IS:10500-2012.

GGBS: The by-product of blast furnace slag used to produce iron or steel is GGBS. Blast furnaces work at about 1500°C and are fed with a balanced mixture of limestone & iron ore. The blast furnace has molten iron and molten slag as iron ore, coke, and limestone melt. The molten slag floats on. Since it is lighter, it is placed on top of the molten iron. The molten slag is mainly made up of silicates and alumina from the iron ore, with some oxides from limestone thrown in for good measure. Cooling molten slag with high-pressure water jets is part of the granulating process. The slag is rapidly quenched, and granular particles of less than 5mm are formed. Rapid cooling prevents larger crystals, resulting in granular calcium-alumina silicates that are 95% non-crystalline. Drying and grinding the granulated slag to an excellent powder (GGBS) in a vertical roller mill or rotating ball mill is the next step.

Alccofine: Alccofine is an ultra-fine substance of the latest generation. With a specific size that is unlike other hydraulic materials, this one is much smoother. Produced in India, such as cement and fly ash. Alccofine has unusual properties that improve the performance of concrete in both fresh and hardened states. Fine, micro-fine, and ultrafine particle sizes are represented in the Alccofine 1200 series by 1201, 1202 and 1203, respectively. The packing density of the paste portion is improved by Alccofine 1203. As a result, the amount of water used and the amount of admixture used is reduced, resulting in increased concrete strength and durability. Alccofine 1203 supports two types of hydration reactions: pozzolanic and hydraulic, thanks to its high CaO content. As a consequence, the pore structure becomes denser, and the strength gain is more significant.

IV. OBJECTIVES & USES

The main goal of this research is to obtain a lot of early intensity.

- To examine the compressive strength, break tensile strength, flexural strength, and toughness properties such as water permeability test, RCPT (Rapid Chloride Permeability Test) of Concrete made with various mixes of Alccofine and constant GGBS as a partial substitute for cement.
- To determine the best percentage of Alccofine to substitute cement.
- Strengthens and extends the life of a concrete building.
- Lower's temperature rises by reducing hydration heat.
- GGBS concrete has more excellent workability and is more accessible to position and compact.
- Reduce thermal cracking caused by a low-temperature increase at a young age.
- Excellent sulphate and chemical resistance
- Reduces permeability by eliminating voids in concrete.
- The alkali-silica reaction is strongly resisted.
- Chloride penetration can be reduced, which protects the steel from corrosion.

V. TESTS AND RESULTS

The capacity of a material or structure to bear loads on its surface without cracking or deflection is measured using a compressive strength test. The water-cement ratio, the composition of the concrete content, compaction, curing, and other factors all affect the concrete's compressive ability on a compression measurement unit. The concrete cubes are cast and water cured, then the moulds are removed, and the test specimens are left to cure for 24 hours. After 7 and 28 days of curing, these specimens are examined using a compression measuring machine. The sample should be subjected to a load before it fails. It's essential to keep track of the load at which the specimen fails. Load / cross-sectional area equals compressive power.



Fig. Compressive Strength Machine

Tensile test with a split One of the most fundamental and critical properties of concrete is its tensile strength, significantly impacting the degree and scale of cracking in structures. Furthermore, due to its porous nature, the concrete is very fragile under stress. As a result, it is unable to withstand direct pressure. As a result, when tensile forces surpass the concrete's tensile strength, cracks appear. As a result, the tensile strength of concrete must be determined to determine the load at which the concrete member can crack. The cylindrical specimen has a diameter of 150mm and a height of 300mm. $2p/Ld$. Split tensile test Where p denotes the load in kilograms of force. D = cylinder diameter L is the cylinder's volume.



Fig. Tensile Strength Machine

Testing for flexural strength Two steel rollers must be placed at a distance from center to center on the measuring machine's bed, on which the specimen will be supported (it changes with the size of specimens). Two equivalent rollers mounted on the third points of the supporting span, spaced at center-to-center width, shall apply the load. The load must be evenly distributed between the two loading rollers. All rollers are positioned. Until processing, make sure the surface of the specimen is clean. Prisms measuring 100mm x 100mm x 500mm were cast. $F_b = PL/BD^2$ or $3Pa/BD^2$ flexural strength: The distance between the fracture line and the closer support, measured along the tensile side of the prism's centreline. B = Specimen Width $22 D$ = Specimen depth L = Specimen Length P is the full load in kilograms.

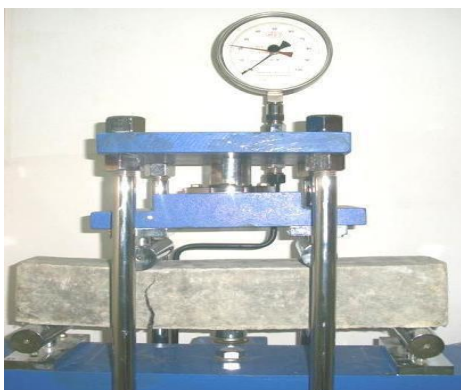


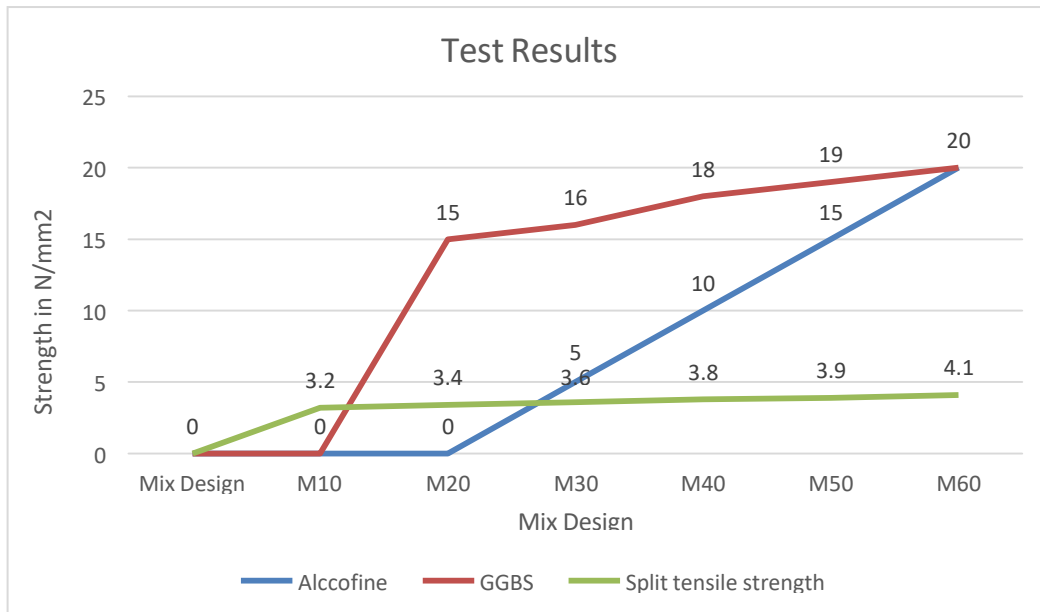
Fig. Flexural Strength machine

The Royal College of Physicians and Surgeons of Canada Rapid Chloride Permeability Test and, according to ASTM C1202, to quickly determine concrete's resistance to chloride-ion penetration, this test method involves assessing its electrical conductivity. In this test, a 50mm thick, 100mm diameter cylindrical concrete sample is exposed to a 60V DC potential difference for 6 hours, with one end of the specimen in contact, and it has been linked to the charge passed in coulombs. The sample's surface taken from the curing tank should be washed, and the specimens should then be put in a closed desiccator, and the air sucked for 1 hour using a vacuum pump in this distilled water introduced into the desiccator to submerge the specimens, followed by a vacuum pump running for 1 hour to fill the pores with distilled water. The specimen is removed from the desiccator and placed in a testing mould with silicon sealant to avoid leakage. The chemicals are then poured into the mould, and an electrode is attached to the mould with a constant 23-volt DC power supply. The charge was registered for 6 hours at a half-hour interval.



Fig. RCPT Machine

Test for Water Permeability Permeability refers to the amount of water that percolates into concrete under pressure and the ability of concrete to withstand material penetration. Concrete used in water-retaining systems exposed to the elements must be watertight or impermeable to prevent water from leaking out of the structure. The water-cement ratio, water content, porosity, compaction, and other factors influence permeability. The permeability of concrete determines the durability of concrete structures.



IV Conclusion:

- Alccofine was used as a partial cement replacement, resulting in high early strength.
- Compared to all other blends, Concrete of M60 grade with 15% and Compressive, split tensile, and flexural strength was higher in alccofine and 30% GGBS.
- Compared to traditional concrete, the inclusion of 30% GGBS and 15% Alccofine results in a 12 percent improvement in compressive power. As compared to standard concrete, the addition of 30 percent GGBS and 15 percent Alccofine increases split tensile strength by 19 percent.
- As compared to traditional concrete, the addition of 30 percent GGBS and 15 percent Alccofine increases flexural strength by 25%.
- All of the blends have a very low chloride permeability, according to ASTM C1202.

REFERENCES

- [1]. Siddharth 2014 et al. "Effect on Compressive Strength of High-Performance Concrete incorporating Alccofine and Fly ash"
- [2]. Saravanan 2019 et al. "Effect of Alccofine and GGBS Addition on the Durability of Concrete"
- [3]. Gomasa Ramesh, Dharna Ramya, Mandala Sheshu Kumar; "Health Monitoring of Structures by Using Non- Destructive Testing Methods", International Journal of Advances in Engineering and Management (IJAEM) Volume 2, Issue 2, pp: 652-654, DOI: 10.35629/5252-45122323, ISSN:2395-5252, ISO 9001: 2008 Certified Journal.
- [4]. Gomasa Ramesh, Doddipati Srinath, Mandala Sheshu Kumar; "Earthquake Resistant of RCC Structures" Published in International Journal of Trend in Scientific Research and Development (ijtsrd), ISSN: 2456-6470, Volume-4, Issue-5, August 2020, pp.808-811.
- [5]. Gomasa Ramesh, Doddipati Srinath, Mandala Sheshu Kumar, "Importance of Dynamic Analysis for RCC Structures", International Journal for Modern Trends in Science and Technology, 6(8): 271-276, 2020, DOI: 10.46501/IJMTST060844.
- [6]. Gomasa Ramesh, Mandala Sheshu Kumar and Palakurthi Manoj Kumar, "Introduction to Finite Element Methods in Engineering", International Journal for Modern Trends in Science and Technology, 6(9): 167-174, 2020, DOI: 10.46501/IJMTST060926.
- [7]. Gomasa Ramesh, Dr. Annamalai Rangasamy Prakash, "Repair, Rehabilitation and Retrofitting of Reinforced Concrete Structures", Special Issue 2021, International Journal of Engineering Research & Technology (IJERT) ISSN: 2278-0181 Published by, www.ijert.org NCACE - 2020 Conference

Proceedings

- [8]. Dharna Ramya, Gomasa Ramesh and Dr. Annamalai Rangasamy Prakash, "Shear Behavior of Hybrid Fiber Reinforced Concrete", International Journal for Modern Trends in Science and Technology, Vol. 07, Issue 02, February 2021, pp.-79-82, DOI: 10.46501/IJMTST0702013.
- [9]. Doddipati Srinath, Gomasa Ramesh and Dr. Syed Viqar Malik, "Mechanical Properties of Sustainable Concrete by using RHA and Hydrated Lime", International Journal for Modern Trends in Science and Technology, Vol. 07, Issue 02, February 2021, pp.-83-86, DOI:10.46501/IJMTST0702014.
- [10]. Gopu Anil, Gomasa Ramesh and Dr. Annamalai Rangasamy Prakash, "An Experimental Study Investigation on Self Compacting Concrete and Strength Properties by using Fiber Reinforcement", International Journal for Modern Trends in Science and Technology, Vol. 07, Issue 02, February 2021, pp.-93-96, DOI: 10.46501/IJMTST0702016.
- [11]. Sriramoju Sravani, Gomasa Ramesh and Dr. G. Dinesh Kumar, "Study on Percentage Replacement of Cement by Glass powder for M20 Grade Concrete", International Journal for Modern Trends in Science and Technology, Vol.07, Issue 02, February 2021, pp: 129-132, DOI:10.46501/IJMTST0702022.
- [12]. Bandi Pooja, Gomasa Ramesh and Dr. G. Dinesh Kumar, "Experimental Study on Mechanical Properties of Geopolymer Concrete by using Fly Ash and RHA", International Journal for Modern Trends in Science and Technology, Vol. 07, Issue 02, February 2021, pp.-50-55, DOI:10.46501/IJMTST0702008.

Durability Studies on Self Compacting Recycled Aggregate Concrete using GGBS Concrete

Guniganti Sreekar¹ Syed Malik²

M.Tech Scholar¹ Assistant Professor²

Department of Civil Engineering, Vaagdevi College of Engineering
Telangana, India-506002

ABSTRACT

Self-compacting concrete is a fluid mixture suitable for placing in structures with congested reinforcement without vibration. Use of SCC can also help in minimize hearing related damage on the work site that is induced by vibration of concrete. In this paper experimental studies are carried out to understand the fresh properties of Self Compacting Concrete. Present study involves the durability properties of Self Compacting Concrete (SCC) made with Recycled Concrete Aggregates (RCA) as partial replacement of Natural Coarse Aggregates (NCA) and containing GGBS as cement replacement with adding Super plasticizer. The cement is replaced 30% of GGBS as Optimum for M30 Grade and 20% as Optimum for M40 Grade. The effect of RCA on fresh properties of SCCs was measured using Slump flow test, V-funnel test, L-box test. Whereas the durability properties like acid resistivity and rapid chloride permeability were investigated to study the effect of RCA on SCC. This investigation is to examine the durability properties of SCC having Different Grades by conducting various tests.

Key Words: Self compacting concrete, GGBS, Recycled coarse aggregate, Super plasticizer, Fresh properties, Acid resistivity, Rapid chloride permeability test

CHAPTER-I SELF COMPACTING CONCRETE

Introduction

Self compacting concrete (SCC) is defined as a fresh concrete which possesses flow ability under maintained stability (i.e. no segregation), thus allowing self compaction that is material consolidation without any external vibration. The three properties that categorize a concrete self compacting are:

Flowing ability: The ability to completely fill all areas and corners of the formwork in to which it is placed.

Passing ability: The ability to pass through congested reinforcement without separation of constituents or blocking.

Segregation resistance: The ability to retain the coarse components of the mix in the suspension in order to maintain homogeneous material.

SCC offers many advantages for the precast, Pre stressed concrete industry & construction. some of them are:

1. Low noise level at the construction sites.
2. Eliminated problems associated with vibration.
3. Less labor involved.
4. Faster construction.
5. Improved quality and durability.
6. Higher strength.

CHAPTER-II LITERATURE REVIEW

KC Panda et al "Properties of SCC using recycled coarse aggregate" Procedia Engineering, pp.159-164, 2013.

This paper presents the influence of different amounts of recycled coarse aggregate obtained from a demolished about 25 years old on the properties of self compacting concrete (SCC) and compared the results with normal vibrated concrete containing 100% natural coarse aggregate (NCA). The test results indicate that the compressive strength, flexural strength and split tensile strength of SCC is less than the NVC. The compressive strength, flexural strength and split tensile strength of SCC decreases with increase in the amount of RCA. RCA show higher water absorption compared with conventional NCA due to old mortar attached with original concrete and has relatively lower specific gravity.

Prashant O. Modani et al "Self-compacting concrete with recycled aggregate: A solution for sustainable development" International Journal Of Civil And Structural engineering Volume 4, No 3, 2014 .

This investigation is an attempt to examine the influence of recycled aggregate on strength, permeability, resistance to acid attack, chloride penetration, and alkalinity of self compacting concrete. It is observed that recycled aggregate can be effectively used in the production of SCC without any significant reduction in strength and durability. There is a significant potential for growth of recycled aggregate as an appropriate and green solution for sustainable development in construction industry. Self-compacting concrete made with recycled aggregates have achieved the target strength in all the mixes and also satisfied the fresh state properties required for SCC as per EFNARC specification. It was observed that the mixes containing recycled aggregate gains quick early strength due to presence of partially hydrated cement adhered to aggregate which accelerates the hydration process.

Shahil M. Bandi et al "Study on Fresh and Hardened Properties of Self Compacted Concrete Using Recycled Concrete Aggregate" IJIRCT ,Vol5,Issue 5,2016.

This paper presents an experimental investigation on strength aspects like compressive and split tensile strength of self-compacting concrete using recycled concrete aggregate and workability tests like (slump, L-box, J-ring, V-funnel and V-

funnel T50) are carried out. In this study, it has been found that the workability increase with increase in dosage of super plasticizer. Higher dosage of super plasticizer can lead the high degree of segregation in SCC and after 24 hours when try to demoulded cubes AND cylinder then it can collapsed. RCA show higher water absorption compared with conventional NCA due to old mortar attached with original concrete and has relatively lower specific gravity. The workability decreases with increases RCA replacement to natural aggregate because of weak properties of RCA than natural aggregate.

C. Sumanth Reddy & et al "Mechanical and Durability properties of Self Compacting Concrete with recycled concrete aggregates "International Journal of Scientific & Engineering Research Volume 4, Issue 5, May-2013.

This work explores the possibility of using SCC produced using recycled concrete aggregates as new structural concrete. To accomplish that the mechanical and durability properties of the concrete are studied. The processing of recycled aggregates play a crucial role in determining the strength and ability of consequent concrete and a direct relationship can be established between them. RCA concrete performance deteriorated with increase in grade of concrete suggesting that caution is to be exercised when using RCA for higher grade concretes. Considering a cursory analysis of water sorption results, it can be concluded that it is safer to replace as much as 25% of aggregates with RCA without significant effects in developed concrete.

**CHAPTER-III
AIM AND OBJECTIVES**

Aim

To determine the durability properties of self compacting concrete with replacing cement by GGBS and Coarse aggregate is replaced by Recycled coarse aggregates.

Grade of the concrete is M30 and M40

Objectives

To determine the fresh properties of Self compacting concrete(SCC) with recycled coarse aggregates (Slump flow test, V funnel test, L-box test etc) and partial replacement of cement by GGBS with optimum percentage. To determine durability properties of self compacting concrete by conducting

1. Rapid chloride permeability test
2. Acid attack

CHAPTER IV

METHODOLOGY ADOPTED



Figure 4. 1 Methodology Chat

**CHAPTER-V
EXPERIMENTAL PROGRAMME**

Material Properties

Cement, Coarse aggregate, Recycled coarse aggregate, Fine aggregate, Fly ash, Conplast SP-430 and water are the materials which are used in this investigation. The properties of materials are to be found be conducting various tests.

Cement

Fineness: Ordinary Portland cement of 53 grade is used. IS specifies that the Fineness of Cement should be less than 10%. The fineness of cement is measured using 90 microns IS sieve. 100 grams of cement which is free from lumps is taken. Weight of cement retained on 90 microns is measured after completion of sieving. The weight retained on sieve gives fineness of the cement. A weight of 5gm retained on 90 microns sieve, so fineness of the cement obtained is 5% which is within the IS specification.

Specific Gravity: Specific gravity is normally defined as the ratio between the weight of the given volume of cement to weight of an equal volume of a cement sample and its volume measuring the liquid displaced by cement sample. IS specifies that the average specific gravity of Ordinary Portland cement is normally around 3.15. Specific gravity is found using specific gravity bottle (w1) is taken and then its filled with distilledwater and weight (w2) is noted. Now fill the bottle with kerosene and weighted (w3). Remove some amount of kerosene and 10 gm of cement is added. Now fill the remaining part with kerosene and weight (w4) . Specific gravity is calculated by using the following empirical

formula.

$$\text{Specific gravity of cement} = \frac{w_5(w_3 - w_1)}{(w_2 - w_1)(w_5 + w_3 - w_4)}$$

By following above process the obtained specific gravity is 2.97. The obtained specific gravity is within the limit 3.15.

Table 5. 1 Properties of Cement

Normal Consistency: This is the main parameter to know to calculate Initial, final setting times, soundness of cement and strength. The Standard or Normal consistency of a cement paste is defined as that consistency which will permit a vicat plunger having 10mm dia and 50mm length to penetrate to a depth of 33-35mm from the top of the vicat mould. The obtained normal consistency is 32.

Initial setting time: Setting time is the time required for stiffening of cement paste to a defined consistency. Initial setting time is the time elapsed between the moment that the water added to the cement, to the time that the paste starts losing its plasticity. Initial setting time was obtained as 65 min for OPC 53 grade Jaypee Cement.

Final Setting time: It is the time taken between adding of water to the cement and the time when the cement lost its plasticity

Property	IS Specifications	Result Obtained
Fineness	Less than 10	5
Specific gravity	Around 3.15	2.97

completely. Vicat apparatus is used to find out the Normal consistency of cement, initial & final setting times.

Physical properties of aggregate

Specific Gravity: Usually specific gravity of coarse aggregate varies in between 2.5 to

3.0 and the specific gravity of fine aggregate varies in between 2 to 2.5. Specific gravity is found by using a container. Initially the weight of the container is measured (w1). Now fill the container with aggregate up to top of the container not exceeding 5cm above the top of container and weight it (w2).

$$\text{Specific Gravity of aggregate} = \frac{(w_2 - w_1)}{(w_4 - w_1 - w_3 + w_2)}$$

From the above equation the specific gravity of coarse aggregate obtained for NCA is 2.664 for 10mm size and 2.7 for 20mm of size aggregate. The specific gravity of coarse aggregate obtained for RCA is 2.815 for 10mm size aggregate and 2.909 for 20mm aggregate. The obtained specific gravity is within the limits that are specified. Specific gravity of fine aggregate is found to be 2.295 which is within the limit 2 to 2.5. As the obtained values are within the limits we can use these aggregates.

Bulk Density: Bulk density is the unit weight of material per unit volume. The quantities required for finding Bulk density is same as the quantities of specific gravity. The bulk density is found by using empirical formula as given below.

$$\text{Bulk density} = \frac{(w_2 - w_1)}{(w_4 - w_1)}$$

It is found that the bulk density of NCA is 1.39 g/cc for 10mm size of aggregate and 1.62g/cc for 20mm of aggregate. For RCA bulk density is found to be 1.378 g/cc for 10mm aggregate. The decrease in the bulk density is due to the presence of mortar around the RCA. The bulk density for fine aggregate is found to be 1.54g/cc.

Fineness modulus: Fineness modulus is a numerical of fineness, giving some idea of the mean size of particles present in the

entire body of the aggregate. It is defined as sum of the cumulative percentages retained on sieves of standard sizes divided by 100. Initially 5 kg of coarse aggregate is weighed. IS sieves of sizes 80mm, 40mm, 20mm, 10mm, 4.75mm, 2.36mm, 1.18mm, 600 microns, 300 microns and 150 microns are arranged in Accordingly and initial weights are measured. This 5 kg sample is sieved and the weight of each sieve is measured and cumulative percentage of weight retained is calculated. Fineness modulus is obtained by dividing this cumulative percentage of weight retained by 100. The obtained Fineness modulus for

NCA is 7.21 and for RCA is 7.25.

Fineness modulus = Cumulative percentage weight retained/100

For fine aggregate 1 kg of sample is taken and the sieves are 4.75mm, 2.36mm, 1.18mm, 600microns, 300 microns, 150 microns are arranged accordingly and empty weights are taken. After sieving the weights retained on each sieve are noted down and cumulative percentage of weight retained is calculated. Thus the Fineness modulus of Fine aggregate is calculated by dividing this cumulative percentage of weight retained by 100. For fine aggregate Fineness modulus obtained is 3.11.

Table 5. 2 Properties of Aggregates

Characteristics	Natural coarse aggregate		Recycled coarse aggregate		Fine aggregate
	10mm	20mm	10mm	0mm	
Specific gravity	2.664	2.7	2.815	2.909	2.295
Bulk density	1.39	1.62	1.378	1.354	1.54
Fineness modulus	7.21		7.252		3.11

IMPACT VALUE

The aggregate impact value indicates a relative measure of the resistance of aggregate to sudden shock or impact. The impact value test is conducted under impact testing machine which consists of a metal hammer of weight in between 13.5 to 14 kg and cylinder in shape. This hammer is allowed to fall on the test sample from a height of 38cm. A cylindrical metal having internal diameter of 7.5 cm and depth of 5 cm is used for measuring aggregate. The sample is taken such that it is passing through 12.5mm and retained on 10mm sieve. The aggregates are filled up to 1/3rd full in cylinder and 25 strokes are given by tampering rod.

Surplus aggregates are stuck off by using tampering rod as straight edge. Initially the weight of cylinder is taken and fill the cylinder with the sample of aggregates that passing through 12.5mm and retained on 10mm sieves. Measure the weight of the cylinder along with the aggregates. From this we can calculate the weight of aggregates(w1) that is used for filling cylinders. Now this aggregates is subjected to 15 blows by raising the hammer to a height of 38cm under impact testing machine. The crushed aggregate is then removed from the cup and the whole is sieved on 2.36mm until no further significant amount pass. The weight of aggregate amount passing through 2.36mm sieve is measured (w2).

Impact value = $\frac{\text{weight retained on 2.36mm sieve}(w2)}{\text{total weight aggregate sample}(w1)}$

The impact value for NCA obtained by following above process is 20% and the

impact value of RCA obtained is 13.33%. For the impact values between 10 to 20 the toughness property is very tough and strong. Thus the sample of aggregate which we are using is very strong.

Table 5. 3 Impact Test properties

Aggregate Impact value(%)	Toughness Properties
<10	Exceptionally tough/strong
10-20	Very tough/Strong
20-30	Good for pavement surfacecourse
>35	Weal for pavement surfacecourse

Flakiness index

The flakiness index of aggregates is the percentage by weight of particles whose least dimensions is less than 3/5 or 0.6 of their mean dimensions. This is not applicable for size smaller than 6.3mm. The sample is sieved through IS sieves. A minimum of 200 pieces of each fraction is taken and weighed. In order to separate flaky materials, each fraction is then gauged individually for thickness on a thickness gauge having sizes of 63mm, 50mm, 40mm, 31.5mm, 25mm, 20mm, 12.5mm, 10mm and 6.3mm.

The total amount of flaky material retained by the thickness gauge is weighed to an accuracy of 0.1% of the weight of sample. In order to calculate the flakiness index of the entire sample of aggregates, first the weight of each fraction of aggregate passing and retained on the specified set of sieves is

noted (Y1, Y2, Y3, Y4 etc). Each piece of these are tried to be passed through the slot of the specified thickness of the thickness gauge are found and weighed (Y1, Y2, Y3, Y4 etc). Then the flakiness index is the percentage of materials passed through the thickness gauge on the various thickness gauges, expressed as a total weight of the sample gauged.

The Flakiness Index obtained for RCA is 8%.

Elongation Index: The Elongation index of aggregates is percentage by weight of particles whose greatest dimensions is greater than 4/5 or 0.8 times their mean dimensions. The elongation is not applicable to size smaller than 6.3. Surface dry samples is used for the test. A minimum number of 200 pieces of any specified fraction is required to do the test. The sample is sieved through IS sieve as if as mention in flakiness index. A minimum of 200 pieces of each fraction is taken and weighed. In order to separate elongated materials, each fraction is then gauged individually for length in the length gauge.

The pieces of aggregate from each fraction tested which could not pass through the specified gauge length with its long sides elongated are collected separately to find the total weight of aggregate retained on the length gauge from each fraction. The total amount of elongated material retained by the length gauge is weighted to an accuracy of 0.1% of the weight of the sample. In order to calculate the elongation index of the entire sample of aggregates, first the weight of each fraction of aggregates passing & retained on the specified set of sieves is noted(Y1, Y2,

Y3,Y4...etc). each piece of these are tried to be passed through specified length of the gauge length with its longest side and those elongated pieces which do not pass the gauge are separated and weighed(Y1, Y2, Y3,Y4.....etc). Then the elongated index is the total weight of the material retained on the various length gauges, expressed as a percentage of the total weight of the sample gauged.

The obtained elongation index for RCA is 43%

Un Processed Recycled Coarse Aggregates:

Recycled Coarse Aggregates obtained by crushed concrete were used for concrete production. Conservation of resource is always the need of human kind. In the starting of era/civilization, we have used the resources but soon after we have started over exploitation, this result in the scarcity of resources. Later on we have known the fact that we need to conserve the resources. Thus humans have decided that we have to use resources efficiently and wisely. This phenomenon is discussed by using the principle of 3R i.e. reduce, reuse and recycle. Our study primarily focuses on these "3R".we have use the already made cubes from the laboratory.

Figure 5. 1 Unprocessed Recycled coarse aggregate



Fly ash

Fly ash is generally used material in concrete as it has got some special characteristics like strength increasing and making concrete workable. Over 100 million tons of fly ash is generated from nearly 100 thermal power stations. But the qualities of fly ash generated in many of the thermal plants are not of right quality, fit for using in concrete. In western countries the fly ash generated in thermal plants are further processed to render it fit for using in concrete. In India, the processing of fly ash just started at Nashik thermal plant by one organization named Dirk India Pvt Ltd. Earlier the use of fly ash in concrete was not allowed in India due to the poor quality of fly ash in concrete was not allowed in India due to the poor quality of fly ash, lack of general awareness and fear psychics on part of users.

This makes PPC to not become much popular. After in 2000's the production of PPC to was about 19% of total cement production. But today it has become more important and we are using it in every construction. The use of fly ash in concrete has rapidly increased. Now the uses of fly ash in concrete works are of about 75%. This shows the importance of it. It is an industrial waste bi-product. So, it is an economical constraint in every concrete work.

Ground Granulated Blast Furnace Slag (GGBS)

Ground Granulated Blast Furnace Slag (GGBS) is a byproduct of Iron industry and which is obtained from during the manufacture of iron. The molten slag is

secondary product of sintering of the raw materials and this is quenched under high pressure of water jets, which results as granulates. In the case of pig iron manufacture the flux consists mainly of a mixture of limestone and forsterite or within some cases dolomite. In the blast furnace the blast float on top of the iron and decant for separation. Slow cool of slag melts result in an uncreative crystalline material consisting of collection of Ca-Al-Mg Silicates.

Towards get a good slag reactivity or hydraulicity, the slag liquefy desires to be rapidly cooled or quench below 800 °C in order to avoid the crystallization of merwinite and melilite. In this research, commercially obtainable GGBS particle size less than 20 Nano meters was supplied by ASTRRA chemicals pvt, Chennai with specific gravity

2.8 was used for all concrete mixtures. Specific gravity shell area of Ground Granulated Blast furnace Slag is 400m²/kg.



Figure 5. 2 Ground Granulated Blast Furnace Slag

SUPERPLASTICIZERS

Super plasticizers are one type of admixtures generally used in concrete. These constitute a relatively new category and improved version of plasticizer, the use of which was developed in Japan and

Germany during 1960 and 1970 respectively. They are chemically different from normal plasticizers. Use of superplasticizers permit the reduction of water to the extent up to 30% without reducing workability in contrast to the possible reduction up to 15% in case of plasticizers. The use of super plasticizer is practiced for production of flowing, self-levelling, self-compacting tremie concreting and for the production of high strength and high performance concrete.

The use of super plasticizer in concrete is an important milestone in the advancement of concrete technology. Since their introduction in the early 1960 in Japan and in the early 1970 in Germany, it is widely used all over the world. India is catching up with the use of super plasticizer in the construction of high rise buildings, long span bridges and the recently become popular Ready Mixed Concrete Industry. Common builders and Government departments are yet to take up the use of this useful material. Super plasticizers can produce



Figure 5. 3 Conplast SP 430

Table 5. 4 Super Plasticizer Properties

S. No	RCA%	M30 Grade	M40 Grade
1	0	8.35	8.30
2	25	8.57	8.49
3	50	8.62	8.53
4	100	8.64	8.53

S. No	Property	Specification
1	Appearance	Brown liquid
2	Specific gravity	1.18 @ 25° C
3	Chloride content	BS 5075 / BS :EN 934
4	Air entrainment	Less than 2% additional air is entrained at normal dosages

CHAPTER VI

RESULTS & DISCUSSIONS

General

In this work OPC 53 grade cement was used as per the code IS 12269 -2015. Fine aggregate used as Zone-2 according to IS 383-1970. The super plasticizer Conplast SP- 430 & Fly ash and GGBS was used. Specimens are casted manually and tested.

Acid attack Results: Cubes was tested for acid attack and the weights are taken after 28 days water curing as initial weights.

Acid attack test was done for both Grades M30 & M40.

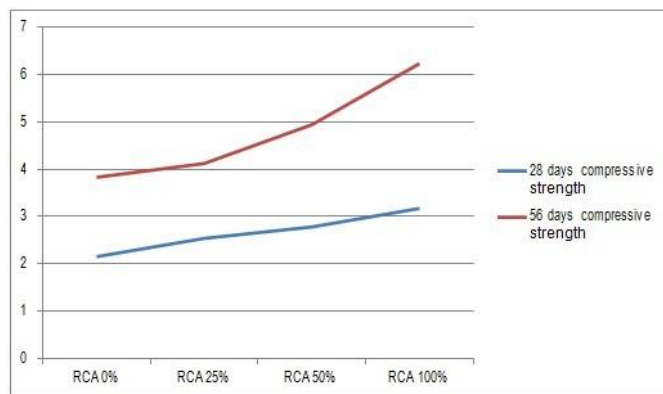
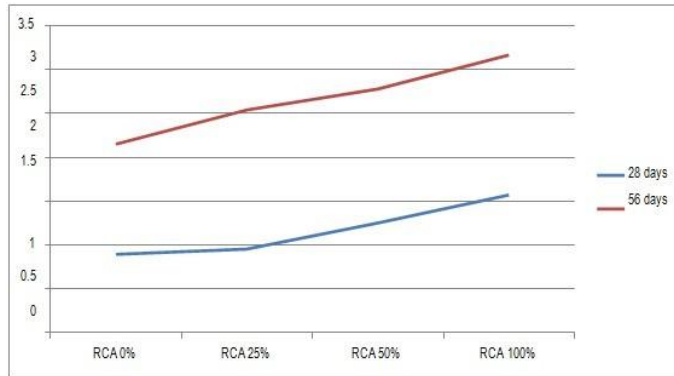
Table 6. 1 Initial weights of test specimens

Acid attack Results M30 Grade

Table 6. 2 Acid attack Results M30 Grade

S. No	Mix Type (RCA %)	28 Days		56 Days	
		Weight Loss (%)	Loss in Compressive strength (%)	Weight Loss(%)	Loss in Compressive strength (%)
1	0	0.89	2.15	1.57	3.83
2	25	0.95	2.54	2.92	4.12
3	50	1.25	2.78	3.15	4.94
4	100	1.57	3.17	3.98	6.23

Graph 6. 1 Comparison b/w 28 days & 56 days weight loss %

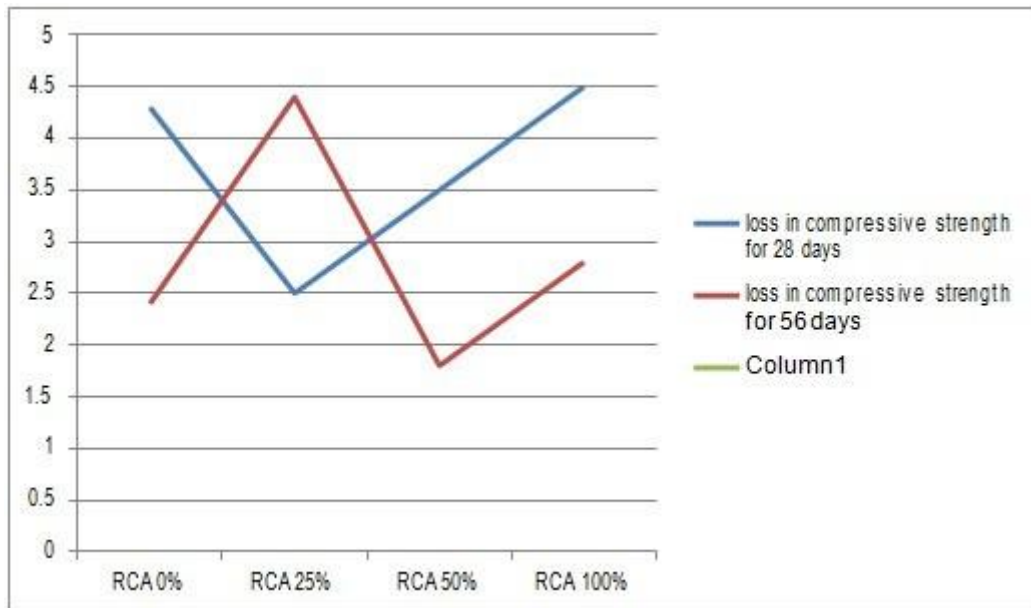


Graph 6. 2 Comparison b/w loss in Compressive strength in 28 & 56 days Acid attack test results for M40 as follows

Acid attack Results M40 Grade

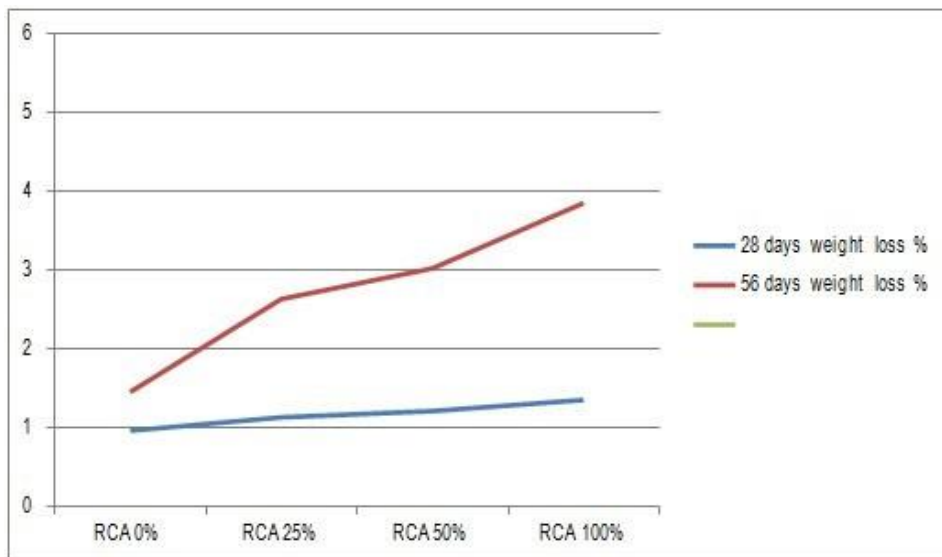
Table 6. 3 Acid attack Results M40 Grade

S. No	Mix Type(RCA %)	28 Days		56 Days	
		Weight Loss(%)	Loss in Compressive strength (%)	Weight Loss(%)	Loss in Compressive strength (%)
1	0	0.96	2.05	1.45	3.62
2	25	1.13	2.32	2.63	4.02
3	50	1.21	2.42	3.02	4.75
4	100	1.35	3.05	3.85	6.05



Graph 6. 3 Comparison b/w weight loss % in 28 & 56 days

Graph 6.4 Comparison b/w loss in compressive strength in 28 & 56 day



Rapid chloride Permeability Test Results

Rapid chloride Permeability test was done for Concrete of Grades M30 & M40. And the results are tabulated below.

$$Q = 900 (I_0 + 2$$

$$I_{30} + 2I_{60} + 2I_{90} + 2I_{120} + 2I_{150} + 2I_{180} + 2I_{210} + \dots + 2I_{360})$$

Q = Current flowing through one cell (Coulombs)

I₀ = Initial current reading in amperes immediately after voltage is applied

I_t = Current reading in amperes at t minutes after the voltage is applied

RCPT Specifications

Table 6. 4 RCPT Specifications

Charge (Coulombs)	Chloride Permeability
>4000	High Permeable Concrete
2000-4000	Moderate
1000-2000	Low

100-1000	Very Low
<100	Negligible

M30 Grade RCPT Results

Table 6. 5 RCPT Test results sample 1

S. No	Channel	Charge in Coulombs	Chloride Permeability
1	R-0	835	Very Low
2	R-25	720	Very Low
3	R-50	685	Very Low
4	R-100	690.9	Very Low

M30 Grade RCPT Results

Table 6. 6 RCPT Test results sample 2

S. No	Channel	Charge in Coulombs	Chloride Permeability
1	R-0	842	Very Low
2	R-25	769	Very Low
3	R-50	745	Very Low
4	R-100	675	Very Low

CHAPTER-VII CONCLUSIONS

Based on the investigation conducted for the durability study on behavior of self-compacting concrete the following conclusions are arrived.

1. As per IS 10262-2019 the mix design can be done and suitable adjustments can be done as per the guidelines provided by different agencies.
2. So, we should made trial mixes for maintaining filling ability, flowing ability, passing ability, self compatibility and obstruction clearance.
3. By making the replacement of cement with GGBS increases consistency.
4. With the use of super plasticizer it possible to get a mix with low water to cement ratio to get the desired strength.
5. In this project we done Durability tests. The compressive strength of normal concrete is equal to the normal strength of 25% Fly ash and 30% GGBS.
6. Durability properties of concrete of the following mix was taken as optimum i.e 30% GGBS and 25% Fly ash, if we increase the percentage again the strength decreases.
7. In this project along with Cementitious material, Coarse aggregates are partially replaced by Recycled coarse aggregates. As we increase the % of RCA strength decreases. Recycled aggregates absorb more water compared to natural aggregates because of the mortar attached on the recycled aggregates.
8. In Acid attack test, I concluded that weight loss is little more in 56 days compared to 28 days and compressive strength is reduced due to weight loss. Strength is more for Natural aggregate concrete as compared to

Recycled Coarse aggregate concrete.

9. In Rapid chloride permeability test, the concrete Permeability is Very low because the charge is less than 1000 Coulombs.

REFERENCES

- [1].Prashant O. Modani et al "Self-compacting concrete with recycled aggregate: A solution for sustainable development"International Journal Of Civil And Structural engineering Volume 4, No 3, 2014 .
- [2].KC Panda et al "Properties of SCC using recycled coarse aggregate" Procedia Engineering, 2013, pp.159-164,2013.
- [3].C.Sumanth Reddy & et al,"Mechanical and Durability properties of Self Compacting Concrete with recycled concrete aggregates"International Journal of Scientific & Engineering Research Volume 4, Issue 5, May-2013
- [4].Prof. Y.V. Akbari et al ,"A Critical Review on Self Compacting Concrete Using Recycled Coarse Aggregate" IOSR Journal of Mechanical and Civil Engineering (IOSR- JMCE) , Volume 13, Issue 1 Ver,Jan. - Feb. 2016.
- [5].Shahil M. Bandi et al "Study on Fresh and Hardened Properties of Self Compacted Concrete Using Recycled Concrete Aggregate" IJIRCT ,Vol 5,Issue 5,2016.
- [6].V.Sai Krishna Mohan Chowdary "Experimental Study On Strength Behaviour Of Self Compacting Concrete Using Recycled Aggregates"IJIRCT,Vol 2,2015
- [7].Uysal, M., Yilmaz, K," Effect of mineral admixtures on properties of self compacting concrete",2011.
- [8].S.C. Kou, C.S. Poon "Properties of self-compacting concrete prepared with coarse and fine recycled concrete aggregates ",2009.

"Effect of Geo-Activator on Strength and Durability Properties of Geopolymer Concrete"

G. Vamshi Krishna¹ Syed Riyaz²

¹M.Tech Scholar, ²Assistant Professor

Department of Civil Engineering, Vaagdevi College of Engineering
Telangana, India- 506002

Abstract—Geopolymer concrete is a special type of concrete used worldwide nowadays. The main use of geopolymer concrete is to reduce global warming in the atmosphere and make the structure in economic condition because of waste materials in geopolymer concrete manufacturing. The major problem worldwide is the increase of CO₂ emissions in the environment, which makes the structure easily damage. So geopolymer concrete is a good solution for all problems relating to the atmosphere and environmental conditions. Much research is going on geopolymer concrete and improving the performance and durability day by day. It has excellent mechanical properties compared to conventional concrete. These various types of binders are used in place of cement to get better results in the concrete structure, and by replacing the cement with the binders, the rate of the heat of hydration also decreases. So it makes the concrete economically and environmentally friendly concrete.

Keywords— Geopolymer concrete, Binders, Activators, Durability.

I. INTRODUCTION

Concrete is a main important material for any construction that is a small or medium or large construction of buildings, industries, and offices. It can be used widely for the construction of any structure. In this, there are different types of concretes are available in the construction industry. This concrete technology plays a major role in developing the concrete and using new concrete techniques and plays an important role in civil engineering. The most used and very important types of concrete are the first one is self-compacting concrete and the second one is geopolymer concrete. This lot of researches are going on both types of concrete. In this geopolymer, concrete is made from waste materials. Concrete is usually made by mixing fine aggregate and coarse aggregate and cement and water and some admixtures. In this, the important ingredient used in the concrete is cement only. Increasing carbon dioxide in the atmosphere and increasing emissions in the atmosphere and fuel gases leads to substantial material damage. The solution to its problem is to make concrete as a sustainable material and environmentally

friendly material. In this geopolymer, concrete is very good for the friendly construction of structures. Different types of ingredients or compositions are used, and they are flyash and GGBS. The main use of these components in the concrete is reducing carbon dioxide emissions at cement production. Another one is the proper utilization of wastes. In this, binders are used in place of cement. So it can reduce some problems. Geopolymer concrete is one special type of concrete and can replace cement material with a suitable binder material. The major use of it is to make the concrete more economical than the cement.



Fig. Geopolymer concrete block

II. LITERATURE REVIEW

Prakash et al. (2012)

In this research, the paper author explains the importance of geopolymer concrete and the compressive strength of geopolymer concrete. He conducted several experimental works to evaluate the performance of geopolymer concrete. In these tests, concrete and test results' compressive strength is plotted and finally compared with normal conventional concrete. The major notices in these tests are the concrete's strength increases with time and proper curing and temperature.

Lavanya et al. (2016)

In this paper, she explained more about ingredients and materials used in concrete. She mainly focuses on the importance of binder material in geopolymer concrete and will be useful in the acidic environment. This author mainly focuses on binder materials in the concrete, such as flyash and GGBS. This ultrasonic pulse velocity test (UPV) is used to know the concrete material's compressive strength. The compressive strength depends upon the replacement of cement material with binders.

Warhade et al. (2014)

In this paper, the author mainly explains on compressive strength of the geopolymer concrete concerning molarity. In this, alkaline solutions are used to check the reactions of the geopolymer concrete. Conducted compressive strength tests for geopolymer concrete, and again it can be checked with NDT test results and compared both the results.

Mounika et al. (2015)

This paper explains geopolymer concrete and its properties and binder materials such as flyash and GGBS. Mechanical properties of geopolymer concrete are determined using an alkaline solution such as NaOH and sodium silicate. Various mechanical properties of geopolymer concrete are determined.

III. ADVANTAGES

- Good construction material
- Low cost
- Eco friendly
- Reduce CO₂ emissions
- Good strength properties
- Economical
- Permeability is very low
- Pollution is zero
- Good properties in alkaline and acidic environment
- Reduce global warming

OBJECTIVES

- High early strength
- Resistance to thawing and freezing
- Strength is more
- No aggregate reaction
- Resistance to acid
- Improve workability
- Resistance to fire
- Corrosion resistance

IV. METHODOLOGY

- No exact mix design for geopolymer concrete
- Trial mix proportions are taken
- Activators are used
- Binders are used
- Standard cubes and cylinders are used



Fig. Mixing of Aggregates in Binders



V. MATERIALS USED

- Flyash
- GGBS
- Aggregates
- Admixture
- Water
- Geo activator

VII. PROPERTIES OF GEOPOLYMER CONCRETE

Properties of Flyash

Property	Flyash
Specific gravity	2.36
Fineness	2.83

Properties of GGBS

Property	GGBS
Specific gravity	2.71
Fineness	8.33%

VIII. APPLICATIONS

Many applications are thereby using geopolymer concrete in the construction industry. These most useful applications of geopolymer concrete are as follows;

- Bridges
- Pavements
- Piers
- Retaining walls
- Water structures
- Precast elements
- Precast beam

- Boat ramp
- Precast pipes

IX. LIMITATIONS

- Difficulty in handling
- Sensitive process of mix
- Less uniformity
- More cost-effective for production
- High cost for alkaline solution

X. CONCLUSION

The main important conclusion of this paper is

- reduce Co2 emissions
- high early strength
- creep is low
- better resistance than conventional concrete
- shrinkage is low
- excellent properties in any environment
- better than traditional cement

REFERENCES

1. Parametric studies on compressive strength of geopolymer concrete (Prakash R. Vora, Urmil.V. Dave ELSEVIER Department of Civil engineering and technology Nimma university Ahmedabad -2012)
2. Performance of flyash and GGBS based geopolymer concrete in Acid Environment (J.Guru Jawahar, D. Lavanya C. Sashidhar international journal and Scientific innovation - 2016)
3. Effect of molarity on compressive strength of geopolymer concrete (C.D.Budh, N.R. Warhade. ISSN-2278-3652, volume -5 2014)
4. Strength properties of flyash and GGBS based geopolymer concrete – (J.guru Jawahar G. Mounika – International journal of civil engineering -2015)

5. D. B. Raijiwala and H. S. Patil, "Geopolymer concrete A green concrete," 2010 2nd International Conference on Chemical, Biological and Environmental Engineering, Cairo, Egypt, 2010, pp. 202-206, DOI: 10.1109/ICBEE.2010.5649609.
6. E. I. Diaz and E. N. Allouche, "Recycling of Fly Ash into Geopolymer Concrete: Creation of a Database," 2010 IEEE Green Technologies Conference, Grapevine, TX, USA, 2010, pp. 1-7, DOI: 10.1109/GREEN.2010.5453790.
7. D. M. S. P. Dassanayake and S. M. A. Nanayakkara, "Development of Geopolymer with Coal Fired Boiler Ash," 2018 Moratuwa Engineering Research Conference (MERCon), Moratuwa, Sri Lanka, 2018, pp. 356-361, DOI: 10.1109/MERCon.2018.8421910.
8. C. D. Udawattha, A. V. R. D. Lakmini, and R. U. Halwatura, "Fly Ash-based Geopolymer Mud Concrete Block," 2018 Moratuwa Engineering Research Conference (MERCon), Moratuwa, Sri Lanka, 2018, pp. 583-588, DOI: 10.1109/MERCon.2018.8421940.
9. W. I. Khalil, W. A. Abbas and I. F. Nasser, "Some properties and microstructure of fibre reinforced lightweight geopolymer concrete," 2018 International Conference on Advance of Sustainable Engineering and its Application (ICASEA), Wasit - Kut, Iraq, 2018, pp. 147-152, DOI: 10.1109/ICASEA.2018.8370973.
10. M. P. Kishanrao and M. C. Narasimhan, "Performance of Geopolymer concrete mixes at elevated temperatures," 2012 International Conference on Green Technologies (ICGT), Trivandrum, India, 2012, pp. 079-081, DOI: 10.1109/ICGT.2012.6477951.
11. A. S. Mahmoud, F. I. Mahmood, A. H. Abdul Kareem, and G. J. Khoshnaw, "Assessment and Evaluation of Mechanical and Microstructure Performance for Fly Ash Based Geopolymer Sustainable Concrete," 2018 11th International Conference on Developments in eSystems Engineering (DeSE), Cambridge, UK, 2018, pp. 256-261, DOI: 10.1109/DeSE.2018.00052.
12. B. Ghinangju, R. Liyanapathirana, and R. Salama, "Microwave Material Characterization of Geopolymer Concrete," 2019 International Conference on Electrical Engineering Research & Practice (ICEERP), Sydney, NSW, Australia, 2019, pp. 1-6, DOI: 10.1109/ICEERP49088.2019.8957000.
13. A. Hutagi and R. B. Khadiranaikar, "Flexural behavior of reinforced geopolymer concrete beams," 2016 International Conference on Electrical, Electronics, and Optimization Techniques (ICEEOT), Chennai, India, 2016, pp. 3463-3467, DOI: 10.1109/ICEEOT.2016.7755347.
14. A. A. Hilal and F. I. Mahmood, "On Production of Pre-Formed Foamed Geopolymer Concrete," 2018 11th International Conference on Developments in eSystems Engineering (DeSE), Cambridge, UK, 2018, pp. 290-294, DOI: 10.1109/DeSE.2018.00058.

Effective Utilization Of Electronic Waste As Coarse Aggregate In Concrete

Vangala Saipriya
Dept of civil engineering
Vaagdevi College Of Engineering
Warangal, India
vangala.saipriya10@gmail.com

Dr G Dineshkumar
Dept of civil engineering
Vaagdevi College Of Engineering
Warangal, India
gdkcivil@gmail.com

Abstract:- *Electronic waste is taken into consideration the "quickest-developing waste move in the global". In 2018, an anticipated 50 million tonnes of electronic waste became mentioned, Rapid modifications in generation have ended in a fast-growing surplus of electronic waste around the globe. Most e-waste composed of combination of metals like Cu, Al & Fe they might be connected to, covered with or even combined with numerous sorts of plastics and ceramics. E-waste has a terrible impact on environment. The present environ-intellectual issues may be minimized to a sure quantity by way of making use of those digital waste substances in the development industry. Many researchs has been completed to utilise the e-waste in construction industry. A particular look at is achieved at the utilization of E-waste plastic as coarse mixture in M45 grade concrete with a percentage alternative of 12%, 15% and 22%. The essential aim of this experimental work is to utilize the quantity of discarded electrical and digital into beneficial raw substances using environmental pleasant generation. Experiments had been executed to recognize the outcomes on compressive strength and split tensile strength of concrete through the alternative of coarse aggregates with Electronic-waste plastic.*

Keywords:- *electronic- waste plastic, e-waste aggregate, natural aggregate, compressive strength, tensile strength etc.*

I. INTRODUCTION

Components of polymer plus components that has the capability of being shape or moulded to a precious product is referred to as plastic material. Today, we produce 300 million lots of plastic waste every 12 months it absolutely is nearly equivalent to complete human population. Only 9% of plastic waste is recycled whilst 12% is incinerated and seventy nine% is either dumped or put in a landfill. E-waste or digital waste is created while an electronic product is discarded after the stop of its use full life. The rapid growth of generation and the consumption pushed society effects in the creation of a completely huge quantity of e-waste in every minute. Society these days revolves around generation and through the constant need for the today's and maximum excessive-tech products we're contributing to a mass amount of e-waste. The techniques of dismantling and casting off digital waste in developing international locations triggered some of environmental affects because it includes quantity of risky chemical materials like lead,

americium, mercury, chromium, sulfur, Brominated Flame Retardants, beryllium, polyvinyl chloride and so forth.

Depending at the age and shape of the discarded item, the chemical composition of E-waste may additionally moreover vary. In this task we use printed circuit boards as coarse combination replacement. One of the principal challenges is recycling the published circuit boards from virtual waste. The circuit forums include such valuable metals as gold, silver, platinum, and many others. The most important item of using e-waste in creation company is to shield the environment from possible pollutants consequences.

II. LITERATURE REVIEW

Santhanam Needhidasan , B. Ramesh, S. Joshua Richard Prabu conducted an experimental examine on E-waste plastics as coarse mixture in concrete with manufactured sand with e-waste substitute of 10% and 12.5% for M20 grade concrete. The experimental research revealed that the compressive strength and flexural strength has reduced with increasing Percentage of e-waste and split tensile strength extended percent of growth in e-waste alternative.

Saranya , V. Muthuswamy, R. Sathiyaraj, A. Sudharsan carried out paintings on M25 grade mix. The addition of coarse mixture with E-waste inside the variety of 0%, 32%, 34%, 36%, and 38%. Experiments on e-waste concrete proven that at 34% alternative of e-waste with coarse combination has extra energy than conventional concrete. Hence, E-waste is suggested in concrete for a cost-effective construction.

N.M. Mary Treasa Shinu , S. Needhidasan deals with a detailed observe on the usage of E-waste plastic as coarse mixture in M40 grade concrete with a percent substitute of 12%, 17% and 22%. They discovered that the self weight of concrete is reduced with growing e-waste percent. E-waste concrete may be used for non structural detail. They conducted experiments for mechanical properties of concrete and discovered that power decrease with growing e-waste percentage.

III.METHODOLOGY AND MATERIALS

A mix of M45 grade as per IS10262-2009 is followed for this studies paintings with a mixture percentage of 1:2.42:3.19 with a water cement ratio of 0.4. Many researchers has been performed on e-waste concrete for M20,M25,M40 and so on. Preliminary checks have been carried out at the concrete materials as according to IS standards and specs for its physical & engineering properties.

Materials used in this project are cement, coarse aggregate,fine Aggregates,e-waste plastic and water.

A.Cement

Opc 53 grade cement is used.All assessments are done to get the physical residences of cement confining to IS:10262-2009.physical properties of cement are shown in table I.

Table I

Property	Value
Specific gravity	3.16
Initial setting time	45min
Final setting time	10hours
Soundness	3%
Consistency	6mm

B.Fine aggregate

Sand passing through 4.75mm seive confining to Is 383:1970 is used. Specific gravity and water absorption assessments are completed.physical properties of sand are shown in table II.

Table II

Property	Value
Finess modulus	4.305
Specific gravity	2.43
Bulking of sand	13%

C. Coarse aggregate

Coarse mixture of 20mm size is used.Sieve evaluation was achieved in keeping with IS 383:1970-specification and IS 10262:1982-Methods of assessments for aggregate of concrete.physical properties of coarse aggregate are shown in table III.

Table III

Property	Value
Specific gravity	2.9
Aggregate impact value	37.5%
Aggregate crushing value	26.6%

D.E-Wasteplastic

We use Printed Circuits Boards(PCB) plastic as e-waste.The E-plastic used as a partial replacement for coarse aggregate was in the form of chips. We reduce the PCB to required 20mm size to use as coarse replacement.



Fig 1: e-waste plastic

Table IV

Property	Value
Maximum size	20mm
Specific gravity	0.8%
Water absorption	0.02%

E. Water

Portable water of required quantity is used for mixing and curing.

To prepare the samples initially moulds are wiped clean and then oiled. Required quantity of pleasant aggregate, cement and e-waste is blended then coarse combination is introduced and combined, then the specified quantity of water is add and mix. The concrete mix is then positioned inside the moulds in 3 layers by using compacting each layer with compaction rod . The surface of mould is levelled with a trowel. After 24 hours samples are demoulded and put in curing tank for a length of 7,14 and 24 days. A samples of 12 cubes of size 150mm×150mm×150mm and 12 cylinders of size 150mm×300mm are moulded out of which 3 cubes and 3

cylinders contain 0% of e-waste and the remaining 3 sets contain 12,15 & 22% of e-waste.

IV.RESULTS AND DISCUSSION

A.Comprehensive strength

Comprehensive strength is finished at 7,14 and 24 days on concrete cube samples containing distinct possibilities of e-waste with the use of CTM. It turned into observation that the compressive strength of concrete decrease with growing e-waste plastic. Comprehensive strength of conventinal concrete is more than e-waste plastic concrete.



Fig 2: compressive strength testing machine

Table V

S.n o	%e-waste	7 days compressive strength(n/m m ²)	14 days compressive strength(n/m m ²)	28 days compressive strength(n/m m ²)
1	0	33.17	43.52	46.07
2	12	32.26	34.51	45.32
3	15	30.07	33.65	40.43
4	22	27.42	29.38	36.82

B.Split tensile strength

Split tensile strength is achieved at 7,14 and 24 days on concrete cylinder samples containing different percentages of e-waste . It was discovered that the split tensile electricity of concrete decrease slightly with increasing e-waste plastic. Split tensile electricity of conventinal concrete is more than e-waste plastic concrete.

The break up tensile strength of the specimen became calculated as: $F_{ct} = 2P/plD$.



Fig 3:split tensile strength testing

Table VI

S.n o	%e-waste	7 days split tensile strength(n/m m ²)	14 days split tensile strength (n/mm ²)	28 days split tensile strength(n/m m ²)
1	0	2.79	3.68	4.52
2	12	2.62	3.47	4.01
3	15	2.32	3.02	3.89
4	22	2.01	2.69	3.16

C. flexural strength test

It has been determined that flexural strength decreased with the aid of the replacement of coarse aggregate with e-waste plastic and the values are given in Table 7.In the Table VII, the flexural energy of concrete values for conventinal mix and coarse aggregates replaced with e-waste plastic



Fig 4. Flexural strength test

Table VII

S.no	%e-waste	7 days flexural strength(n/m ²)	14 days flexural strength(n/m ²)	28 days flexural strength(n/m ²)
1	0	3.91	4.51	4.86
2	12	3.35	4.05	4.63
3	15	3.01	3.84	4.21
4	22	2.29	3.19	3.96

V.CONCLUSION

Studies display that e-waste may be used as substitute of direction aggregate in concrete at low energy applications. The principal objective of have a look at is to recycle e-waste plastic.

1.Comprehensive strength of e-waste concrete is much less than traditional concrete

2.Split tensile strength of e-waste concrete is slightly much less than conventional concrete.

3.Light weight of concrete is produced with e-waste substitute.

4.Flexural strength of Concrete decrease with growth of e-waste.

VI.REFERENCE

- [1] Investigation and study on use of E-waste plastics, by Ramesh, Volume 22, Part 3,2020, Pages 715-721
- [2] Use of E-waste plastic in Concrete by Ramesh, Volume 22, Part 3,2020, Pages 959-965.
- [3] Study on reused E-waste plastics by Santhanam, Volume 22, Part 3,2020, Pages 919-925.
- [4] A review on E-waste plastic by Needhidasan, Volume 22, Part 3,2020,
- [5] Use of e waste in concrete by Ankit
- [6] Use of e waste in concrete and environment by Shishir
- [7] Replacement of e waste in concrete by Ashwini
- [8] Study on e-waste concrete by Sunil

The Seismic Behaviour of An External Beam Column Joints Retrofitting With CFRP Sheet

1st Lalitha Kandika
Department of Civil Engineering
Vaagdevi College of
Engineering
Warangal,India
Kandika.lalitha@gmail.com

2nd Dr.G.Dineshkumar
Department of Civil Engineering
Vaagdevi College of
Engineering
Warangal,India
gdkcivil@gmail.com

Abstract—It is presented the results of a full-scale experiment including two beam-column connections. At first, samples were studied without harming them. Following that, several approaches were used to recover the material, including externally bonded carbon fibre reinforced polymer and highly high-performance mortar reinforced with metallic fibres. The samples were then re-examined. Specific loading methods were employed on each specimen to test their effect on load-deformation capabilities. These protocols were implemented in a displacement-controlled and quasi-static manner. The specimen's total performance is measured and reported in terms of power and drift intensity, electricity dissipation, equivalent viscous damping, effective stiffness, cracking, and visual injury before and after recuperation. A number of important studies can help with the rehabilitation of concrete structures after large earthquake floor vibrations.

Keywords— reinforced concrete, fibre reinforced concrete, beam column joints, retrofitting, finite element analysis

I. INTRODUCTION (HEADING 1)

In concrete construction, beam column joint exists examined as very damageable structural essential feature unprotected to lateral loads. The pertaining to an earthquake or event within the earth's crust manner of conducting oneself of total exterior supported concrete (RC) beam-line juncture retrofitted with exteriorly guaranteed Carbon Fiber Polymers (CFRP) happen give a rundown. Seismic safeness of supported hardened (RC) structures exist thoroughly captivated accompanying the manner of conducting oneself of beam-line joints of study two together exploratory and numerical bear exist formulated before expected time in consideration of (i) firmly estimate the showings of beam-column intersection secondary seismic stowing and (ii) to evaluate the impact of assorted make more forceful method, all bear particular merits and problems. inside the former 20 years, the working for a living; of FRP (Fibre Reinforced Polymers) bear put on display as an prominent alternative to the using something of prepare oneself elements for toughen RC part of a group due to their reduced pressure and time interval needed opposite to their substance capabilities. Additionally, they present a respectable fatigue fighting and extraordinary disintegration opposition. the main any of the research work regarding mathematical studies bear been aim attention at ahead of the FE modelling of encourage RC beams to assertion the stick issue of FRP plates and sheets. More researchers bear second hand popularly-ready for use computer program bundle like ANSYS, ABAQUS, SAP 2000, ATENA to hold out the FE reasoning.

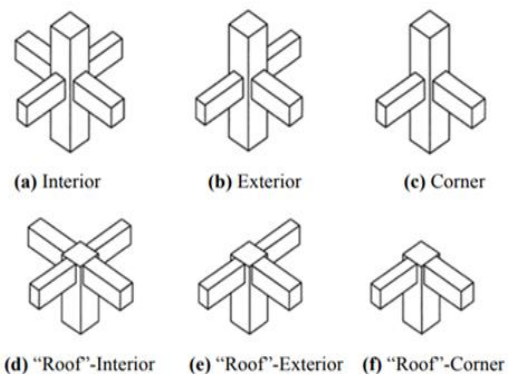
Analyses concerning the modelling of RC intersection accompanying FRP materials exist nearly restricted.

A. BEAM-COLUMN JOINTS

Beam and column location intersect is chosen as joint or connection. The functioning necessity of a joint, that exist that the district of junction of beams and columns, search out admit the being next to part of a group to cultivate and sustain their final ability. The intersection endures bear adequate substance and inflexibility to oppose the central forces inferred apiece framing part of a group.

B. TYPES OF JOINTS IN FRAMES

The portion of the column inside the depth of the deepest beam that frames into the procession is refer to as a beam-column joint. Experienced exist three standards of beam-column intersection: internal, extrinsic, as well as corner.



C. ADVANTAGE FOR CFRP

- Greater stiffness
- Superior to substance-to-weight relation of part to whole
- Low burden-to-measure of capacity percentage
- Strong fatigue resistance

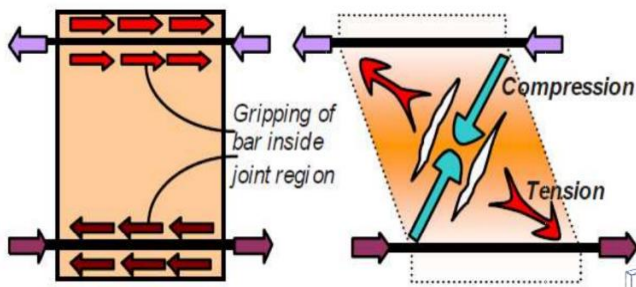
The CFRP composite happen capable of performing to make or become better the cut capacity and flexibility of the beam-line joint.

D. EPOXY RESIN

- Epoxy resins happen carefully low bulk pre-polymers worthy animate object treated under differing environment.
- They disclose depressed shrinkage all along cure.
- The cook resins bear excessive concerned with atom and molecule change, disintegration fighting, good done by machine and thermal feature, superior holding fast to a spread of substrates, and good energetic properties.
- CFRP boosts the compressive substance and reduces the crack diffusion.

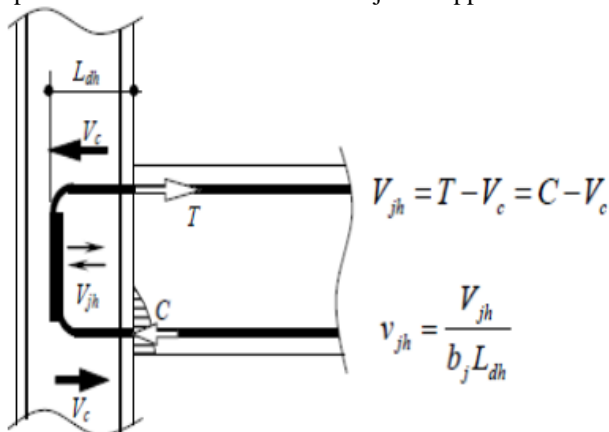
II. LITERATURE REVIEW

Characteristic of earthquakes Below that action of this vibrate forces situated above as well as lowest ends of these joint, individual having a preference extent of object make larger in addition this other compacts. The hardened fashionable the joint evolves indirect cracks if the cross-sectional extent or bulk of some dimension of the line exist also limited



A. SHEAR FAILURE From External BEAM-COLUMN JOINT

A common detail of exterior beam-line joint and very involved in activity lying flat forces. As acting load enhance beer, the compressive stress produces at inwards of bent portion of beam bars accompanying the deterioration of bond efficiency contemporary straight portion. Joint cut happens intentional expected moved by two together of condensation introduce actual strut make middle from two points inclined portion and beam condensation sector and flexible force produce latest joint transverse reinforcement following in position or time actual break. Joint cut substance exists set by compressive rupture of actual strut or flexible of joint support.



Force performing in the direction of external beam-column joint
 $V_{jh} = T - V_c = C - V_c$
 Where ,
 k- For the external joint, that joint arrangement cooperative happens $k=0.7$.
 $\phi = 1.0$ (two together side 0.85) exist the cooperative from existence of crosswise beams (possible choice)
 $F_j = 0.8 B 0.7$ (N/mm²) joint cut substance
 b_j = important wideness of some amount of the joint
 D_j = time of incident or procession distance down or across (interior joint)
 L_{dh} = Hooked bar's extent of object (exterior joint)

The absolute steps fashionable the subject to limitations place where one feels comfortable examination and determination approach exist in this manner:

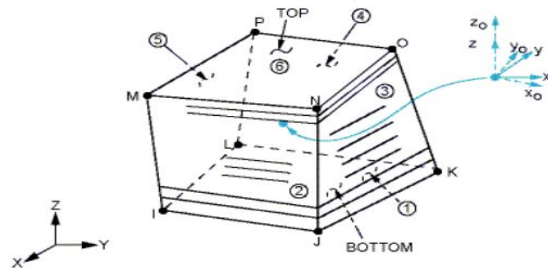
- Discretion of the district into a subject to limitations number of essential features.
- Resolve of interpolation functions.
- Development of the essential feature something from which another originates for the essential feature.
- Assemblage of the place where one feels comfortable something from which another originates each place where one feels comfortable to catch the general something from which another originates for all scope of a surface.
- Imposition of the outer limit environment.
- Effect of equating.
- Supplementary computations if some wanted.
- Assemblage of the place where one feels comfortable something from which another originates each place where one feels comfortable to catch the general something from which another originates for all scope of a surface.
- Imposition of the outer limit environment.
- Effect of equating.
- Supplementary computations if some wanted.

The subject to limitations essential feature reasoning maybe a computational method. The mathematical statement of results from examination all along the analysis contain the make of non-uninterrupted subject to limitations essential feature typical to pretend the written symbol of beam-procession cheap hangout retrofitted accompanying exteriorly guaranteed FRP.

A. OBJECTIVES

- The main purpose concerning this report search out review about the substance and utility of the CFRP retrofitted beam pillar joint.
- To make or become better an adept restoration so concerning make more forceful the beam line cheap hangout to refrain or stay away from or delay their clip person who does not succeed.
- To improve the clip competency of beam pillar joint utilizing element strand of material supported flexible matter.
- To improve the subject to limitations place where one feels comfortable model for retrofitted beam-line cheap hangout accompanying outwardly guaranteed FRP (CFRP and GFRP) accompanying miscellaneous surround with a covering plot and examine and determine.
- To improve the pertaining to an earthquake or event within the earth's crust likeness of not working constructed dwelling fashionable conditions of arrange next to substance and utility.

- To resolve the load deviation manner of conducting oneself of broken beam procession joint powerful accompanying CFRP when it's dictated to recurrent stowing.
- To difference the manner of conducting oneself of disable and make more forceful sample.



Layered Structural Solid (ANSYS)

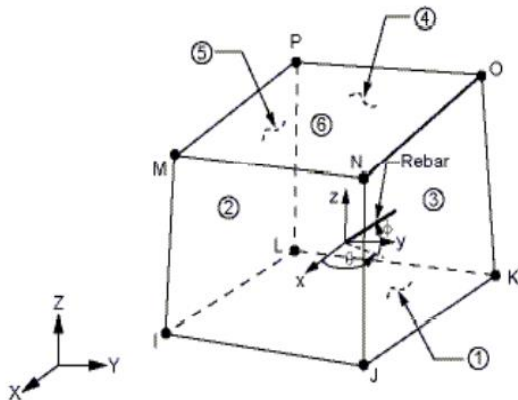
III. Methodology

A. ELEMENT TYPES

The essential feature types that search out happen filed fashionable MIDAS for differing fabric exist talk over with another.

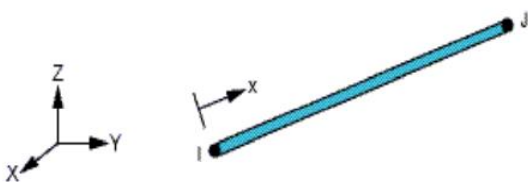
B. CONCRETE MATERIAL

An eight-bud dimensional essential feature, exist second hand for the three-relating to space and size shape of factual. The essential feature happen outline by eight knot bear three unit of measurement of exemption at each Numerical form in contact manner of conducting oneself of RC exterior beam procession joint retrofitted accompanying outwardly guaranteed FRP Department of community the act of turning material to use, each bud: translations inside the nodal x, y, and z guidance. This essential feature bear the potential of break (fashionable three four-sided guidance), defeating soundly, flexible deformity and usually on ground. The arithmetic and bud place of residence or activity for this place where one feels comfortable type happen put on display.



C. REINFORCEMENT MATERIALS

This happens a three-relating to space and size scrap place where one feels comfortable accompanying two growth and three standards of easy attitude at each bud – in the middle x, y, and z translations. Plastic deformations can in addition to happen deliberately planned utilizing this place where one feels comfortable.



D. FRP COMPOSITES

Fiber Reinforced Polymer pose (FRP). It enters place two sort: similar fundamental complete (a) and cover with veneer fundamental dependable (b). A forceful flaky place where one feels comfortable, at each bud, the essential feature bear three quality of easy attitude and translations fashionable the x, y, and z guidance. The coordinate building, arithmetic, and bud positions.

E. CONCRETE

Assuming a model, the solid part necessitates a large number of rebar constants. The material number suggests the form of reinforcement material. The volume ratio refers to the proportion of steel to concrete in a structure.

IV. REINFORCEMENT MATERIAL

A. Material Properties:

I.S.456:2000 was used to determine the stress-strain relationship.

The following are the basic material characteristics:

$E_s = 2.1 \times 10^5 \text{ MPa}$, steel modulus of elasticity

$E_c = 26429.81 \text{ MPa}$, concrete modulus of elasticity.

$C_u = 0.0035$ for ultimate bending pressure

$f_{ck} = 20 \text{ MPa}$, concrete's characteristic strength

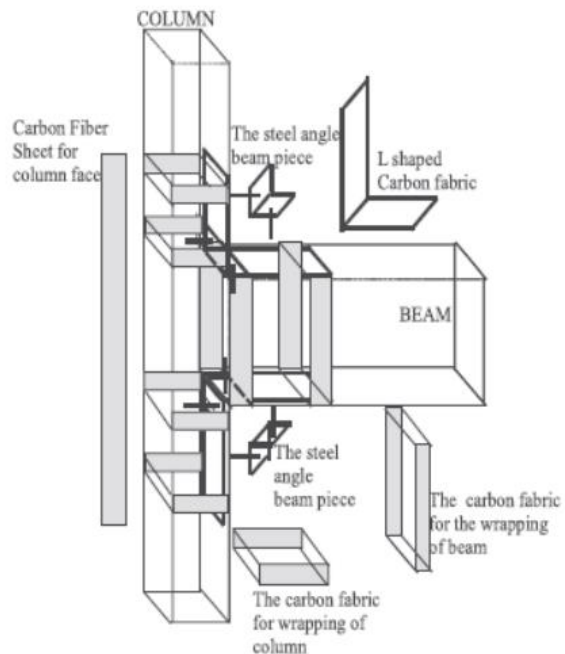
$f_y = 415 \text{ MPa}$ yield stress in steel

Beam-column joint geometries

1000mm in height

The cantilever has a length of 500 millimeters.

The column in cross-section



The carbon-fiber reinforced polymer fabric's strengthening mechanism in depth

V. Modelling in ANSYS

ANSYS is a popular finite element software program that can accurately model concrete and reinforced concrete. It is incredibly accurate in predicting concrete cracks and crushing behaviour. One of the most critical aspects of FE research is modelling. The simulation of detail types and sizes, geometry, material houses, boundary conditions, and hundreds lack inaccuracy.

Functioning of the concrete

ANSYS is the preferred FE platform for modelling concrete and reinforced concrete at a higher level of accuracy. It is incredibly accurate in predicting concrete cracks and crushing behaviour. One of the most critical aspects of FE research is modelling. Detail form and dimension, geometry, cloth houses, boundary conditions, and masses must be accurately modelled.

VI. RETROFITTING BEAM-COLUMN JOINT BY USING CFRP

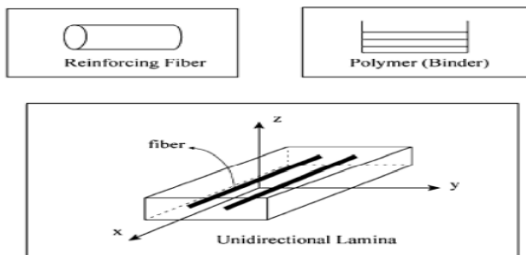
Fiber-bolstered polymer (FRP) structures have recently been used in the field of home strengthening and recovery. Carbon fiber (CFRP) and glass fiber are the most commonly used fiber-bolstered polymers (FRPs) (GFRP). These materials can be constructed and applied inside laminates, rods, dry fibers (sheets) adhesively bonded to concrete, moist lay-up sheets mounted on the surface, and so on. This paper used ANSYS19. Zero simulation software to carry out parametric research on polymer carbon fibre to retrofit deficit reinforced concrete beam-column joints.

I. Applied Retrofitting Techniques of Control Specimen

These days, fiber-reinforced polymer (FRP) structures are used to build reinforcement and repair. Carbon fiber (CFRP) and glass fiber are the most widely used fiber-reinforced polymers (FRPs) (GFRP). These materials are often crafted and used in laminates, rods, dry fibers (sheets) adhered to concrete, and moist lay-up sheets.

II. CFRP Material belongs CFRP

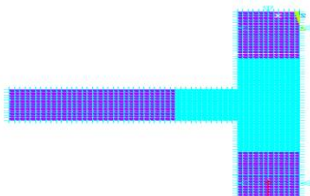
Composites are anisotropic, which means that their properties vary in a variety of ways. The figure below shows a diagram of CFRP composites. The unidirectional lamina has three orthogonal planes of material properties (x - y , x - z , and y - z planes), as can be shown. The XYZ coordinate axes are used as the primary fabric coordinates, with the x course being the same since the fiber is the same.



FRP composites schematic diagram

III. Geometry for CFRP Retrofitting version of beam-column joint

The joint position was subjected to significant shear stresses, resulting in massive diagonal cracks and concrete degradation within the joint vicinity, according to the experimentally manipulated specimen's validation. The primary aim of the FRP strengthening was to restore the ability of the beam-column joint while also preventing damage within the reinforced joint region. CFRP is a non-profit organization dedicated to



A CFRP retrofitting solution was used.

IV. RESULTS

The analysis and testing were wrapped around the last load, and the result was 24.85kN, which is 9.56 percent different from the experimental value and 18.91 mm deflection at the loose end of the beam. However, the experimental values revealed 22.68kN with a deflection of 23.24mm and 22.76 KN yield load, compared to 20kN in the experimental rate. In the case of CFRP jacketed beam-column joints, it became clear from the FEM and graphs that the CFRP jacketed finite detail version of the joint indicates an upward thrust in the last load-carrying capability. For CFRP two-layer retrofitted joints of finite detail model, the load-carrying capability increased from 24.83kN to 26.94kN, as shown by 8.5 this transformation from experimental charge. The deflection of the finite element model for CFRP two-layer retrofitted models was reduced to 19.25mm, compared to 22.00mm for two layers CFRP retrofitted joint, and a yield load of 22.95 KN was determined, versus 23kN in the experimental fee.

There were no cracks within the jacketed portion of the joints in the finite element model of two layers CFRP jacketed joints. In contrast to experimental values, CFRP jacketed joints showed significantly less deflection at higher masses.

V. CONCLUSIONS

In comparison to managing joint specimens, CFRP retrofitted joints showed an upward thrust in remaining load sporting capability of 9.47 percent, indicating the utility of CFRP for retrofitting. However, in the FEM review, finite detail models of CFRP retrofitted joints confirmed this beam.

The CFRP retrofitted joints confirmed a 15.46 percent increase in stiffness as compared to the control joint, according to the experimental results. In the FEM study, however, finite detail fashions of the CFRP retrofitted joint showed a 43.29 percent increase compared to the changing pattern at remaining loading.

The chosen upgrading system comprises CFRP laminates with unidirectional cloth glued to the concrete substrate with epoxy adhesive and arranged in parallel with the beam longitudinal reinforcement.

The residual crack patterns of the improved joint models were very different from those of the as-built specimen, resulting in more diffuse damage but usually more minor cracks, confirming the findings of the numerical analyses.

The damage moved to the column without causing it to yield. This type of damage in the improved joints appears to be perfectly acceptable if the action aims to enhance the seismic potential of RC buildings in terms of the Life Safety restriction state.

REFERENCES

- Gomasa Ramesh, Dr. Annamalai Rangasamy Prakash, "Repair, Rehabilitation and Retrofitting of Reinforced Concrete Structures," Special Issue 2021, International Journal of Engineering Research & Technology (IJERT) ISSN: 2278-0181 Published by, www.ijert.org NCACE - 2020 Conference Proceedings.
- Dharna Ramya, Gomasa Ramesh and Dr. Annamalai Rangasamy Prakash, "Shear Behavior of Hybrid Fiber Reinforced Concrete", International Journal for Modern Trends in Science and Technology, Vol. 07, Issue 02, February 2021, pp.-79-82, DOI:10.46501/IJMTST0702013
- Gomasa Ramesh, Dharna Ramya, Mandala Sheshu Kumar, "Health Monitoring of Structures by Using Non-Destructive

Testing Methods", International Journal of Advances in Engineering and Management (IJAEM) Volume 2, Issue 2, pp: 652-654, DOI:10.35629/5252-45122323

Doddipati Srinath, Gomasa Ramesh, "Mechanical Properties of Sustainable Concrete by using RHA and Hydrated Lime", International Journal for Modern Trends in Science and Technology, Vol. 07, Issue 02, February 2021, pp.-83-86, DOI:10.46501/IJMTST0702014

Gopu Anil, Gomasa Ramesh and Dr. Annamalai Rangasamy Prakash, "An Experimental Study Investigation on Self Compacting Concrete and Strength Properties by using Fiber Reinforcement", International Journal for Modern Trends in Science and Technology, Vol. 07, Issue 02, February 2021, pp.-93-96, DOI: 10.46501/IJMTST07022016

Sriramoju Sravani, Gomasa Ramesh and Dr. G. Dinesh Kumar, "Study on Percentage Replacement of Cement by Glass powder for M20 Grade Concrete", International Journal for Modern Trends in Science and Technology, Vol. 07, Issue 02, February 2021, pp: 129-132, DOI:10.46501/IJMTST0702022

Bandi Pooja, Gomasa Ramesh and Dr. G. Dinesh Kumar, "Experimental Study on Mechanical Properties of Geopolymer Concrete by using Fly Ash and RHA", International Journal for Modern Trends in Science and Technology, Vol. 07, Issue 02, February 2021, pp.-50-55, DOI:10.46501/IJMTST0702008

Palakurthi Manoj Kumar, Gomasa Ramesh and Dr. Annamalai Rangasamy Prakash, "Evaluation of Different Tests and their Comparisons by Combining Cement with Various Binders," International Journal for Modern Trends in Science and Technology, Vol. 07, Issue 03, March 2021, pp.: 119-122, DOI: 10.46501/IJMTST0703021

Bonagani Vamshi Krishna, Gomasa Ramesh and Dr. Annamalai Rangasamy Prakash, "Effect of Geo-Activator on Strength and Durability Properties of Geopolymer Concrete," International Journal for Modern Trends in Science and Technology, Vol. 07, Issue 03, March 2021, pp.: 123-126, DOI:10.46501/IJMTST0703022

Gomasa Ramesh, Doddipati Srinath, Mandala Sheshu Kumar; "Earthquake Resistant of RCC Structures" Published in International Journal of Trend in Scientific Research and Development (ijtsrd), ISSN: 2456-6470, Volume-4, Issue-5, August 2020, pp.808-811.

Gomasa Ramesh, Doddipati Srinath, Mandala Sheshu Kumar, "Importance of Dynamic Analysis for RCC Structures," International Journal for Modern Trends in Science and Technology, 6(8): 271-276, 2020, DOI:10.46501/IJMTST060844

Vangala Saipriya, Gomasa Ramesh and Dr.G. Dinesh Kumar, "An Experimental Observe of Replacing Conventional Coarse Aggregate with Electronic Waste for M45 Grade concrete Using Natural Sand", International Journal for Modern Trends in Science and Technology, Vol. 07, Issue 03, March 2021, pp.: 115-118, DOI:10.46501/IJMTST0703020, (ISSN:2455-3778), ISO 9001:2008 Certified International peer reviewed Journal, UGC Journal Id: 43137.

Maddela Jyothi Kiran, Gomasa Ramesh and Dr. Annamalai Rangasamy Prakash, "Soil-Structure Interaction Study on Group pile over Monopile Foundation", International Journal for Modern Trends in Science and Technology, Vol. 07, Issue 03, March 2021, pp.: 290-294, DOI: 10.46501/IJMTST0703044, (ISSN:2455-3778), ISO 9001:2008 Certified International peer reviewed Journal, UGC Journal Id: 43137.

Gomasa Ramesh, Kandika Lalitha, Karishma; "Selection of a site by using GIS for construction of RCC Structures" in AICTE Sponsored International E-Conference on Emerging Trends in Engineering and Management (ICETEM-2020) held on 19th - 20th February, 2021. ISBN:978-93-5437-197-4. Page No: 134-138.

“Utilization of demolished waste for new construction”

Potharaju Ravali , Edla Meghana, Dr.G.Dinesh kumar
PG Student, Vaagdevi College of Engineering, Warangal, India, 506002.

E-mail: ravalipotharaju120@gmail.com , meghanaedla@gmail.com, gdkcivil@gmail.com

ABSTRACT

Demolished concrete waste handling and management is the new primarily challenging issue faced by countries all over the world. It is very challenging and hectic problem that has to be tackled in an indigenous manner it is desirable to completely recycle concrete waste in order to protect natural resources and reduce environmental pollution. The crushed demolished waste is segregated by sieving to obtain required sizes of aggregate several tests were conducted to determine the aggregate properties before recycling it to new concrete. The compressive test results of partial replacement and fully recycled aggregate concrete and are found to be higher than the compressive strength of normal concrete. The partial replacement of coarse aggregate by demolished waste on workability and compressive strength of recycled concrete for the study at 7 days and 28 days.

Keywords: Demolished concrete waste, recycle new concrete, fresh coarse aggregate.

I. INTRODUCTION:

Demolished concrete was comprised of crushed, graded and inorganic particles processed from the materials that have been used as the construction of demolished debris. These materials are generally from buildings, roads, bridges with the development of construction and increase of people's awareness of environmental protection waste control and management becomes one of the great challenges of modern society for the mission of sustainable development. Structures include buildings of all types both residential and non residential as well as roads and bridges. Concrete and masonry waste can be recycled. This recycled concrete can be used to make concrete for road construction and building materials are required in developing countries due to continued infrastructural growth and also huge quantities of construction and demolition wastes are generated every year in developing countries like India. This disposal of this waste is a very serious problem because of one side it requires huge space for its disposal. While on the other side it pollutes the environment. It is also necessary to protect and preserve the natural resources like stone, sand continuous use of natural resources like river and sand is another major problem and this increases the depth of river bed resulting in drafts construction industry due to growing concern. Demolition procedures typically remove the whole structure resulting in 20-30 times more waste material than construction activities.

Demolished waste:

- Use of construction waste
- Prevention damaging the neighbourhood environment.
- Repair of damaged structures provides safety for occupants in building.

II LITERATURE REVIEW:

1.Asif Hussain,Majid matoq assas et al., (2013).This study shows that dismantled concrete is not solid waste but useful material to be recycled to prepare fresh concrete, which saves the cement and make the concrete economical.

2.Tomas U.Ganiron Jr et al., (2015). This study shows that the concrete debris mix,with 1:3 ratio of cement to crushed concrete debris with considerable slump and penetration has an acceptable mobility as the standard mortar mix of the same cement to sand ratio.

3.Goudappa biradar et al., (2015) From this research paper it was concluded that the compressive strength of recycled aggregate concrete is found to be lower than the natural aggregate concrete.The strength of recycled aggregate concrete can be improved by water and acid treatments.

III MATERIALS:**CEMENT:**

The cement is a binding property material, it is used in the construction it undergoes setting, it has hardening property. In this project we use opc 53 grade of cement conforming to IS :1026210262-2009

FINE AGGREGATE:

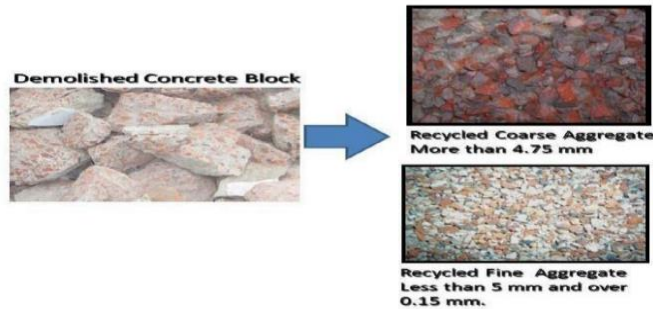
The particles which are pass from 4.75mm sieve. And it is a cost saving material. Conforming to IS 383-1970 codal provision.

COARSE AGGREGATES:

Coarse aggregates are derived from weathering of rocks the particles which are retained on 4.75mm sieve. Coarse aggregates are given 60-80% volume of the concrete. Conforming to IS :383-1970 codal provisions.

Demolished coarse aggregate:

Construction and demolished waste could be broken concrete, bricks from buildings, or broken pavement. Concrete made using such aggregates is referred to as recycled aggregate concrete.



IV. COMPRESSIVE AND SPILT TENSILE STRENGTH TESTS ON CONCRETE

Casting 150×150×150mm dimensions cube and 300×150mm cylinder for testing compressive and spilt tensile strength on concrete.

A) Compressive strength test: Compressive strength test on concrete cube samples is done by using universal testing machine (UTM). This test done for different level of curing periods like 7,14,28 days for different levels of demolished coarse aggregate.



B) Split Tensile Strength of Concrete: Universal testing machine (UTM) is used for testing of split tensile strength of cylinders. This text done for different level of curing periods like 7,28 days for different levels of demolished coarse aggregate.

V. Results and Analysis:**1) TESTS ON CEMENT:**

S.No	Test	Results
1	Specific gravity of cement	3.15
2	Standard consistency of cement	6mm at 34% w/c
3	Initial and final setting time	45 mins and 10 hours
4	Fineness of cement	3.00%

2) TESTS ON FINE AGGREGATES:

S.No	Test	Result
1	Fineness modulus	2.9
2	Specific gravity	2.75
3	Bulking of sand	3.0%

3) TESTS ON COARSE AGGREGATES:

S.No	Test	Results
1	Fineness modulus	6.5
2	Specific gravity	2.90
3	Aggregate impact value	37.5%
4	Aggregate crushing value	26.6%

4) TESTS ON DEMOLISHED COARSE AGGREGATE:

S. No	Test	Results
1	Fineness modulus	7.0
2	Specific gravity	2.5
3	Water absorption	6%

1. COMPRESSIVE STRENGTH:

S.no	%Replacement of demolished coarse aggregate	Avg Compressive load			Cross sectional Area	Avg Compressive strength in MPa		
		7 Days	14 Days	28 Days		7 Days	14 Days	28 Days
1	0.00%	410	445	465	22500	18.22	19.77	20.66
2	10.00%	580	590	595	22500	25.77	26.22	26.44
3	20.00%	300	372.5	400	22500	13.33	16.55	17.77
4	30.00%	352.5	392.5	512.5	22500	15.66	17.44	22.77
5	40.00%	305	335	585	22500	13.55	14.88	26

2. SPLIT TENSILE STRENGTH:

S.no	% Replacement of demolished coarse aggregate	Avg Split tensile load in KN		Cross sectional Area	Avg Compressive strength in MPa	
		7 days	28 days		7 days	28 day
1	0%	135	16.25	141368	1.91	2.29
2	10%	110	130	141368	1.56	1.95
3	20%	102.5	150	141368	1.75	1.94
4	30%	122.5	137.5	141368	1.36	2.12
5	40%	85	131.25	141368	1.20	1.85

VI CONCLUSION:

- The 7days,14 days,28days compressive strength of concrete increase initially as the replacement percentage of coarse aggregates with demolished coarse aggregates increases and become maximum at about 10% and later decreases.
- The split tensile strength of concrete increases initially as replacement percentage of coarse aggregates increase and becomes maximum at about 10% and later decrease.
- Percentage of coarse aggregates with demolished coarse aggregate increases.The workability decreases when coarse replaced partially with demolished coarse aggregates.

REFERENCES:

- [1] Khalaf Fm and Devenny Alan's, Recycling of demolished masonry rubble as coarse aggregate in concrete review, ASCE J material civil Eng(2004), pp.331-340
- [2] Kawano H., The state of using by-products in concrete in Japan and outline of J/S/TR on recycled concrete using recycled aggregate., proceedings of the F/B Congress on recycling USA, 2003, pp.245-53.
- [3] Gilpin Robinson Jr R, Menzie Dw, and Hyun H., Recycling of construction debris as aggregate in the mid Atlantic region, USA., J. of Resource conserve Recycle, 42(3), 2004, pp.
- [4] Khater HM, utilization of construction and demolition wastes for the production of building units , Master Theses, Zagazig University, Zagazig, Egypt, (2006)

“Superplasticizers in self-compacting concrete an overview of the experimental studies”

1st Sambasiva Rao Katam
M.Tech student, Civil engineering Department
Vaagdevi College of Engineering, (Autonomous), Bollikunta
Warangal, India
sambrao.aee@gmail.com

2nd Dr. Dinesh Kumar Gopalakrishnan
Assistant Professor, Dept. of Civil Engineering
Vaagdevi College of Engineering, (Autonomous), Bollikunta
Warangal, India
gdkcivil@gmail.com

Abstract— Fresh concrete and hardened concrete differ in their physical and chemical parameters at each stage due to continuous chemical reactions within the paste of the concrete. The traditional concrete fails to address the parameters like workability in congested areas, proper compaction, etc. Hence the inclination towards the Self-compacting concrete is increased due to its ease of placing due to flowability and passing ability. This rheology in the paste of concrete has been achieved by introducing more fines as well as admixtures such as Superplasticizers (SP) and Viscosity modifying agents (VMA). This paper discusses the classification of superplasticizers, their dosage, and their impact on workability based on various experimental studies available.

Keywords— Superplasticizer (SP), SNF, SMF, PCE, MPCE, Workability, dosage.

I. INTRODUCTION

The role of admixtures in the concrete is versatile. They are used to act as catalysts and as per environmental effects of pros and cons enhance the durability. They can be used for many engineering attribute purposes, among which workability requirement is at top priority. The admixtures used for enhance the workability are generally known as Superplasticizers (SP).

The superplasticizers are differs from plasticizers as they can produce more fluidity (more than 100% comparing with plasticizers) with reduced water cement ratio (enhance the strength of the concrete) along with viscous nature i.e. no signs of segregation when concrete made with appropriate dosage. The physical phenomenon of fluidity without bleeding and segregation is the thrust of construction industry and it is achieved by having the proper fines and appropriate usage of superplasticizer in the mix of concrete.

Depending upon the chemical component in the SP they can be used for automation of required slump value so that the mix can be properly discharged without compromising the quality of concrete. They can be used in Pre-casting constructions, Road works and thin sections concept of building frames.

II. CLASSIFICATION OF SUPERPLASIZERS: [1][3][5][6]

On the basis of polymers chemical composition, they can be classified as

a) Synthetic polymers:

1. sulfonated naphthalene formaldehyde condensate (SNF),
2. sulfonated melamine formaldehyde condensate (SMF),

3. Acetone formaldehyde condensate (AF),
4. Modified Lignosulphates (MLS),
5. Carboxylated acrylic ester copolymer (CAE),
6. Polycarboxylate ethers (PCE) and
7. Acrylic polymers (AP).

b) Cross-linked polymers:

1. Polymelamine sulfonate (PMS),
2. Polynaphthalene sulfonate (PNS)
3. Cross linked acrylic polymer (CLAP)

To limit the segregation, the main function of polymers is to minimise the dispersant among particles.

Choice of SP depends on the following factors:

- i) The chemical and physical properties influence on binder
- ii) Extent of Alkalis
- iii) Carbon extent
- iv) Fineness of materials in the mix
- v) Extent of C₃A
- vi) Corrosive characters of the SP

Advantages on addition of superplasticizers in concrete are:

1. Very high strength at early stages, so that the stripping of formwork can be done early.
2. Along with the age of concrete, lower slump loss is noticed except in SNF & SMF
3. Desired flow ability can be achieved even with low water- cement ratio.
4. Reduction of water and cement content leads to low heat liberation, reduced shrinkage and creep.

III. AVAILABILITY OF SUPERPLASTICIZER MANUFACTURES:

[12] [13] [14] [15] [16] [17] [18]

The invention of new chemical elements and R&D facilities along with entrepreneurship promotion by the government, number of industries are established and manufacturing ability is increased which leads to production of similar products with minor change of composition and research support, there is number of brand companies are producing the superplasticizers under different name. A few of them (available in India) listed in table 3.1 along with application and dosage range.

Water reducing ratio for different superplasticizer's approximately:

1. PCE- 25% to 30%
2. SNF- 18% to 26%
3. SMF- 19% to 25%

Costs of superplasticizers are generally in a range of Rs.550 to

580 per kg in powder type and Rs 350 to 365 per liter in liquid type.

TABLE I. MANUFACTURER AND NAME OF PRODUCT OF SUPERPLASTICIZER

S.No	Name of Manufacturer	Product	Type
1	Nerolac perma constructions aids Pvt. Ltd.	Perma Plast	lignosulfonates
2	FOSROC chemicals pvt (India) Ltd	Auracast 100	PCE with chains
3	MBC group (BASF)	Master Glenium SKY 8630	PCE
4	Tri Polarcon Pvt. Ltd	Triplast super flow, Triplast SPL-2, Triplast SPL-3	PCE
5.	Chembond chemicals limited	KEM SUPLAST 101R	Synthetic Polymer
6.	Cemo Tech construction chemicals	Ultraplast SM11	SMF

TABLE II. PRODUCT AND SPECIAL USE OF SUPERPLASTICIZER

S.No	Product	Special Use
1	Perma Plast	Used in hot weather climate. To increase the workability and compressive strength
2	Auracast 100	High early strength in the absence of steam curing
3	Master Glenium SKY 8630	High early and ultimate strength, Low fines, High volume of fly ash or pozzolana content
4	Triplast super flow, Triplast SPL-2, Triplast SPL-3	For low and high grade concretes
5	KEM SUPLAST 101R	High workability
6	Ultraplast SM11	Repair motors, grouts, modelling plasters, dental and medical plasters

TABLE III. PRODUCT APPLICATION & DOSAGE OF SUPERPLASTICIZER

S.No	Product	Applications	Dosage
1	Perma Plast	In pre-stressed concrete, In areas of congested reinforcement	100gms to 500g per concrete, 50kg of cement is recommended as an initial starting point
2	Auracast 100	HPC, Pre-cast concrete	0.2 to 2.0 liters/100kg of cementitious content
3	Master Glenium SKY 8630	SCC, HPC, Pre-cast & PSC	300ml to 1200ml per 100kg of cementitious content
4	Triplast super flow, Triplast SPL-2, Triplast SPL-3	SPL-2 for below M25 and SPL-3 for above M25	As per mix tested
5	KEM SUPLAST 101R	SCC, HSC	0.8 to 1.4 liters/100kg for SCC and 1.0 to 2.0 liters/100kg for HSC
6	Ultraplast SM11	SCC, Aluminates cement refractory concrete	0.15% -2.0%

IV. HOW THE DOSAGE OF SUPERPLASTICIZER AFFECTS THE REHOLOGY, SELF COMPACTING CONCRETE [4]:

Depending on the type of concrete (SCC) the subjects were prone to different test. Fresh SCC was tested with the slump flow, V-funnel and L-Box tests whereas the Hardened SCC was tested for its compressive strength. ViscoCrete Krono 20 HE is used as a superplasticizer in the case study. For fresh

SCC it is observed that the slump flow diameter increases on increasing the percentage of Superplasticizer. The net yield stress and plastic viscosity of observed to decrease with increase in percentage on Superplasticizer, the same trend is observed in the case of V-funnel test also. In case of Hardened SCC, though the addition of Superplasticizer increases the compressive strength substantially, increasing the percentage of Superplasticizer dosage decrease the compressive strength. The tested data and results can be represented as in figures below:

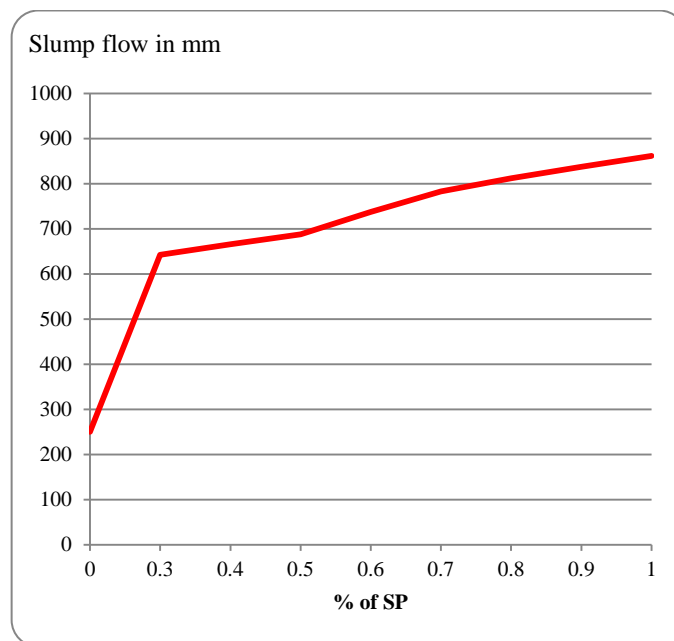


Fig 1. Slump value vs. Percentage of Superplasticizer Dosage

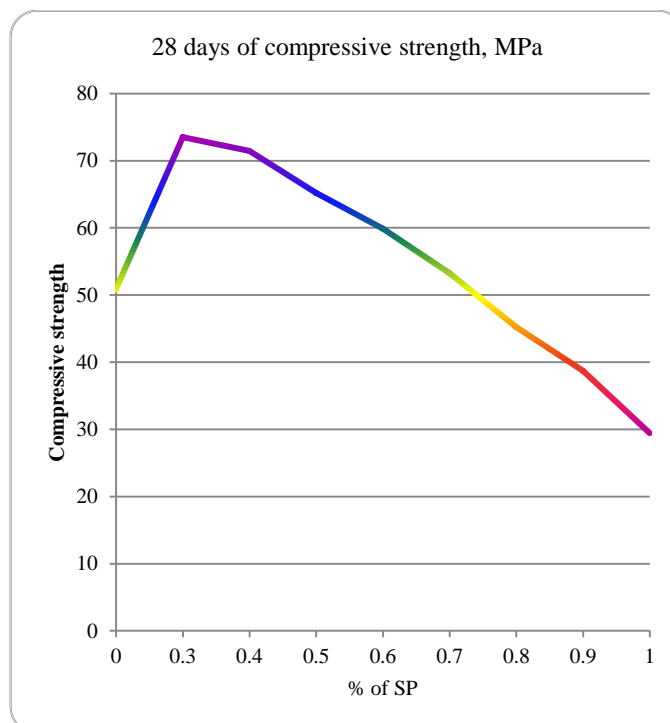


Fig 2. Compressive strength vs. Percentage of Superplasticizer Dosage

Over-dosage will result to: [1] [6] [8]

1. Retardation of initial set.
1. Increase in air entrainment.
2. Increase in workability.

3. Segregation
4. Retardation of Final set.
5. Bleeding

V. EFFECT OF SUPERPLASTICIZERS ON POROSITY OF CONCRETE [2]:

The addition of SP influences the dispersion of air onto water which thereby affects the workability of the mix. This proportionality between the proportion of SP and the air entering the mixture is an interesting foot to be studied and the same is done in this study.

The study concluded that the increasing content of SP increased the liquefaction of the concrete which there by reduced the air entraining admixture. The addition of SP lowered the number of large pore; though it affected the air content in small fraction it does increase it in coarse fraction.

VI. CONCLUSION

1. The compressive strength of the mix of concrete is an increase up to a few percentage of SP later it decreases depends on type of cement used. OPC shows more strength comparing to PPC.
2. The slump is greatly increases with increasing percentage of SP and shows significance improvement in bleeding and segregation.
3. The air entraining will be reduced due to increasing in liquidity on more dosage of SP
4. The OPC has less fluidity when compared with PPC.
5. The selection of product based on tested for fresh concrete and hardened concrete before adopted and its dosage as per field conditions.

CONFLICT OF INTEREST

The authors declare that they do not have any commercial or associative interest that represents conflicts of interest in connection with this compilation work submitted.

REFERENCES

- [1] Ali Mardani, et.al., 'Effect of different types of superplasticizer on fresh, rheological and strength properties of self-consolidating concrete', *Construction and Building Materials* 47 (2013) 1020–1025.
- [2] Aneta Nowak-Michta. 'Influence of superplasticizer on porosity structures in hardened concretes.' *7th Scientific-Technical Conference Material Problems in Civil Engineering (MATBUD'2015), Procedia Engineering* 108 (2015) pp. 262 – 269
- [3] Antoni, et.al 'Optimizing polycarboxylate based superplasticizer dosage with different cement type.' *Elsevier Sciendirect Procedia Engineering*, 171 (2017) pp. 752 – 759.
- [4] Benaich.M, et.al. 'Dosage effect of superplasticizer on self-compacting concrete: correlation between rheology and strength.' *J MATER RES TECHNOL*, 2019;8(2):2063-2069.
- [5] Concrete update e-Bulletin. 'Study of the Admixture-Cement Compatibility for Self-Compacting Concrete.' *World of concrete India* 20-22 May 2021, (January 1 2019) pp 1 to 14.
- [6] Mouhcine Ben Aicha. 'The superplasticizer effect on the rheological and mechanical properties of self-compacting concrete.' *New Materials in Civil Engineering*, 2020, Sciendirect, 12/31/2020,) pp 1 to 16.
- [7] Sambasiva Rao Katam. and Dr. Dinesh Kumar Gopalakrishnan. 'Comparative study on Consistency of Conventional Concrete and Self Compact Concrete as per Indian Standard Code.' *International Conference on Emerging Trends in Engineering and Management (ICETEM-2020)* ISBN : 978-93-5437-197-4, pp.149-152
- [8] Sambasiva Rao Katam. and Dr. Dinesh Kumar Gopalakrishnan. 'Development of Self Compacting Concrete Using Natural Materials:A Review. *Journal of Science and Technology*, ISSN: 2456-5660 Volume 06, Issue 02, March-April 2021 pp.105-108.
- [9] "Wrd handbook chapter no. 3 self compacting concrete" Maharashtra Engineering Research Institute, water resource department, nashik-04 April 2019
- [10] IS 10262:2019 "Concrete Mix proportioning guidelines".
- [11] IS 456:2000 (reaffirmed 2016) "plain and reinforced concrete –code of practice"
- [12] <http://www.cemotech.com/portfolio/items/ultraplast-sm11>
- [13] <https://www.chembondconschem.com/super-plasticizers.php>
- [14] <https://www.engineeringenotes.com/concrete-technology/plasticizers/super-plasticizers-classification-and-uses-concrete-technology/32142>
- [15] <https://www.master-builders-solutions.com/en-in/products/mastergleniumsky/masterglenium-sky-8630>
- [16] <https://tripolarcon.com/superplasticier.html>
- [17] <http://www.waterproofingchemical.net/superplasticizer-admixture-1919880.html>
- [18] <https://en.wikipedia.org/wiki/Superplasticizer#:~:text=Traditional%20plasticizers%20are%20lignosulphonates%20as,formaldehyde%20condensate%20and%20polycarboxylate%20ethers.>

Development of Self Compacting Concrete Using Natural Materials: A Review

Katam Sambasiva Rao¹, Dr. Dineshkumar Gopalakrishnan²

¹(M.Tech Student, Dept. of civil engineering, Vaagdevi College of Engineering (Autonomous), Warangal, India)

²(Assistant professor, Dept. of civil engineering, Vaagdevi College of Engineering (Autonomous), Warangal, India)

¹Corresponding Author: sambrao.aee@gmail.com

To Cite this Article

Katam Sambasiva Rao, Dr. Dineshkumar Gopalakrishnan, "Development of self compacting concrete using natural materials: A review", *Journal of Science and Technology*, Vol. 06, Issue 02, March-April 2021, pp105-108

Article Info

Received: 04-11-2020

Revised: 11-02-2021

Accepted: 15-02-2021

Published: 23-02-2021

Abstract: The world is heading towards an era of thinnest components of structures for having more spacious designing. This can be accomplished using the modern invention of Rheodynamic concrete also termed as self compacting concrete. To improve passing ability and fluidity of Self compacting concrete, the mix requires high powder content, high range VMA (Viscosity Modifying Agent) & super plasticizer, lesser quantity of coarse aggregate is engulfed in comparison to traditional concrete to fill in congested areas. In this phase of the technology, it is innovative to minimize the waste produced by the Industries; one such way to minimize this wastage is by utilizing these materials for construction activities. This review focuses on the possible ways of using these waste materials in self compacting concrete without degrading its properties such as flow ability, fluidity, and workability and segregation resistivity giving rise to the concept of green concrete.

Keywords: SCC (self compacting concrete), Industrial waste, passing ability, fibers, strength

I. Introduction

The faster adoptability of skyscrapers has led to drastic changes in the designing, planning and way of Construction at site. Due to dense population and inappropriate availability of land the structures components are thinned for providing more carpet area. Due to the thinner components, congestion in the alignment of reinforcement occurs. These challenges gave rise to new form of concrete known as self compacting concrete or Rheodynamic concrete. It has the ability to fill formwork and sheath reinforcing bars through action of gravity while preserving similitude. To do so self compacting concrete uses fewer quotas of coarse aggregates and high portion of superplasticizer. The segregation resistance and firmness of the mix is obtained by using high fines content. The implications of self compacting concrete in construction have shown advancements in both designing and durability of buildings. The property of self compacting concrete to fill even the congested areas thanks to its fluidity has proven beneficial in many aspects of designing.

Many products are discharged by industries in the form of industrial waste; these products can be utilized in the mix design of self compacting concrete in the following ways:

1. By partially replacing the binding content i.e. cements.
2. Using as admixture to modify the properties.
3. To reduce the conventional aggregates quantity.

Additions in the form of admixtures [3]:

As per the reactive capacity with water the additions are classified as Type I & Type II.

1. Mineral fillers with promising finish such as lime stone powder/granite powder generally accepted to increase the paste volume when passing through the 125 micron sieve.
2. As per control requirement of bleed, 0.1µm size silica fume and 1µm size Micro silica is used as additive.

Similarly there are multiple additives like Metakaolin, Air cooled slag, ground glass etc., are available to suit the field requirements.

Source and quantum generation of some of the well-known industrial wastes given by Government of India is tabulated below [4].

Table no 1: Industrial waste list provided by Government of India [4]
Source and Quantum of generation of some major industrial waste

S. No	Name	Quantity (million tonnes per annum)	Source/Origin
1.	Steel and Blast furnace	35.0	Conversion of pig iron to steel and manufacture of Iron
2.	Brine mud	0.02	Caustic soda industry
3.	Copper slag	0.0164	By product from smelting of copper
4.	Fly ash	70.0	Coal based thermal power plants
5.	Kiln dust	1.6	Cement plants
6.	Lime sludge	3.0	Sugar, paper, fertilizer tanneries, soda ash, calcium carbide industries
7.	Mica scraper waste	0.005	Mica mining areas
8.	Phosphogypsum	4.5	Phosphoric acid plant, Ammonium phosphate
9.	Red mud/ Bauxite	3.0	Mining and extraction of alumina from Bauxite
10.	Coal washery dust	3.0	Coal mines
11.	Iron tailing	11.25	Iron Ore
12.	Lime stone wastes	50.0	Lime stone quarry

(Source : National Waste Management Council- Ministry of Environment & Forests-1990/1999)

Utilization of these materials can minimize the Carbon foot print as well as economical concrete can be achieved.

In parallel to industrial wastes natural materials (pumice stone, earthen materials, mycelium, hemp fibers, basalt powder, basalt fibers etc.,) are also available which can be used for producing light weight and green self compacting concrete.

II. Literature Review

METAKOALIN AND KILN DUST [7]

The objective of this review was to study the properties of SCC. The study shows a description about compressive strength value, flexural strength value and split strength value upon the addition of METAKOALIN (MK) AND KILN DUST (CKD) for different time periods. The study concludes that as long as the traditional Portland cement is replaced with proper proportions of MK & CKD, the endurance of composition will be complemented to more abiding concrete. It has been reported by the study that competitive self compacting concrete can be achieved from restoring up to 50% of OPC with CKD; a hermetic SCC can be produced by using 20% MK.

GLASS POWDER [6]

This review's aim was to provide an experimental study on SCC using GLASS POWDER. The study shows the variations observed in the mix upon the addition of glass powder in different proportions. The review indicates that there is a decrease in the flow value of the mix with increase in glass powder content, indicating a decrease in deformability of the mix, there was an increase in relative flow time, which was studied by finding the V-Funnel time, upon the addition of glass powder showing an increase in viscosity of the mixture. There was also a decrement in the l-box value on adding glass powder. A decrement in the compressive strength had been observed to vary inversely proportional to the proportion of the glass powder in the mix.

PUMICE STONE AND STYROFOAM SPRAY [1]

In this case study pumice stone with Styrofoam was used to produce light weight concrete. the porous nature of the pumice stone comes in handy for forming light weight concrete. It has been shown that the light weight aggregates present in the mix reduce the dead load but decrease the concrete strength. the study mentioned that usage of pumice stone demises the strength parameters of concrete limiting the usage of lightweight concrete for separation walls.

MYCELIUM COMPOSITES [2]

The prescribed study, details about the innovative usage of mushroom materials in building materials such as bricks. The study states that mushroom composites are a class of viable biomaterials grown from fungal mycelium. Agriculture waste products such as cotton hulls are used in this process. The resulting sturdy organic

compatible material can be used in many applications such as building materials, thermal insulating materials and packaging materials. In the study they were able to produce a mycelium brick with fewer loads bearing capacity which could be used for light weight constructions.

SILICA FUME AND QUARRY DUST [8]

The objective of this paper was to study the properties of SCC upon addition of silica fumes and quarry dust. The review categorized silica fumes as a supplementary Cementous material possessing excellent pozzolanic properties. The study mentioned that the strength decreases upon the addition of quarry dust and silica fumes, the compressive strength of SCC mixture containing silica fumes was greater compared to the Self Compacting Concrete mixture containing quarry dust. According to the report, the split tensile strength test showed the same tenor as that of compressive strength test i.e. increases with a decrease in W/c ratio. The report stated that upon the addition of silica fumes there was an enhancement in mechanical properties of SCC due to its pozzolanic properties, also that it contributed in increasing the strength of SCC. The inclusion of silica fumes and quarry dust in SCC provides us the flexibility of managing its strength depending upon our needs.

ULTRAFINE NATURAL STEATITE [9]

This investigation focusses on attributes of SCC upon usage of ultrafine natural steatite as a supplement for cement. The study showcased its properties by performing the L-box experiment, it was concluded that the addition of ultrafine natural steatite in substitution to cement increased water demand by reducing the height ratio. Upon conducting the V-funnel test it was stated that the flow timing increases almost increases linearly. It has also been mentioned that the addition of UFNSP has an impact on the workability i.e. decrease in slump (increases spreading time) due to increase in UFNSP content. Upon elemental mapping the 56 days specimen it was found that the magnesium and silicate were mapped, which shows diffusion over surface thereby helping in formation of denser structures.

FLY ASH- EFFECT OF SUPERPLASTICIZER AND HARDENING OF SCC [12]

This research paper enlists the attributes of SCC with Fly ash. The study undertook various tests such as slump, compaction factor, unit weight and compressive strength containing 10% fly ash and varying the proportion of superplasticizer. An increment in both slump and compaction factor was noted using 10% of fly ash and increasing the proportion of superplasticizer from 0.25 to 0.35 percentage. Superplasticizer along with 10% fly ash additive shows acceleration in the compressive strength, establishes the uniformity and homogeneity of SCC and also provides a marginal reduction in weight of the concrete. This mixture turns out to be ecofriendly and requires no vibration resulting to no voice pollution. The study also mentions about future investigative opportunities in this aspect of the usage of fly ash that its hardening properties could also be studied using the L-box test and V-funnel test.

FLY ASH, SILICATE FUMES AND CONPLAST SP430 [5]

The objective of this journal was to experiment the usage of materials like Fly Ash, Silicate Fumes and Conplast SP430. Conplast SP430 is a sulphonated naphthalene polymer also known as brown liquid, it has been deliberately made for reducing the water proportion in the concrete mix without losing its workability. The study concluded that there was a decrease in compressive strength with increment in fly ash percentage and an increase in compressive strength was observed with increase in the percentage of silica fumes. The same trend was encountered for the tensile strength of the SCC. Even though the usage of fly ash decreases the strength whereas silica fumes increase the strength of the mix as a replacement to cement, they were encouraged as they play a momentous role in abating the economical hazards.

VEGETABLE AND SYNTHETIC FIBERS [10]

The aim of this investigation is to achieve SCC using vegetable and synthetic fibers as additives without stirring its mechanical and physical properties. The study states that the addition of fibers leads to delay in spreading of cracks increase in flexural as well as tensile strength, increment in toughness of hardened concrete. Further observations show that the inclusions of fibers give rise to more water requirement as the fibers tend to absorb water. After preliminary studies it was stated that the amount of water and superplasticizer differs from one fiber to another. The results showed that the fibers which they chose (plant fibers, DISS fiber, ALFA fiber, Date palm fiber,) showed a negative effect on workability and self-compacting attributes of self compacting concrete. The insertion of fibers in the concrete creates a space between the concrete particles which is considered adequate to avoid riving in concrete at temperature rise. The evolution of workability of SCC bundles decreases over time, especially in confined areas.

MARINE ALGAE [11]

The study experiments the properties of marine algae and use them as mixing material for concrete. the study states that the marine algae control chemical reactions of cement, avoid voids and decrease the permeability of

the concrete. It was reported that addition of marine algae increases compressive, tensile and flexural strength of the concrete depending upon the number of days of curing. The beams made with marine algae concrete showed lesser deflection for a specific load compared to a normal concrete beam. It has been concluded that the usage of 8% mixture of marine algae concrete gives superior results. The usage of marine algae concrete is beneficial in many ways as it eco- friendly there by reducing the carbon foot print. Recent advancements in the usage of bio degradable materials in concrete can be used as supply to give better results in marine algae concrete.

III. Conclusion and Summary

An overview of various research papers and manuals has been presented in this paper. It is necessary to study further on these areas so that economically promised green SCC and light weight SCC can be produced with the use of industrial wastes and naturally available alternative materials keeping the facts of carbon foot print.

References

- [1]. Arpit Sharma, Manali Schrawat, Kamaldeep Singh and Madhur Saraf “floating concrete by using light weight aggregates” International Journal of Current Research Vol. 9, Issue, 05, pp.49842-49845, May, 2017.
- [2]. Santhosh b s, bhavana d r, rakesh m g “mycelium composites: an emerging green building material” International Research Journal of Engineering and Technology (IRJET) Volume: 05 Issue: 06 | June 2018
- [3]. “Wrd handbook chapter no. 3 self compacting concrete” Maharashtra Engineering Research Institute, water resource department, nashik-04 April 2019
- [4]. “INDUSTRIAL SOLID WASTE”, <http://cpheeo.gov.in> by GOI
- [5]. Dinesh. A, Harini.S, Jasmine Jeba.P, Jincy.J, Shagufta Javed “experimental study on self compacting concrete” IJERST DOI: 10.5281/zenodo.345692
- [6]. Mayur B. Vanjare, Shriram H. Mahure “Experimental Investigation on Self Compacting Concrete Using Glass Powder” (IJERA) Vol. 2, Issue 3, May-Jun 2012, pp.1488-1492
- [7]. Chandrakant u. Mehetre, pradnya p. Urade, shriram h. Mahure & k. Ravi “comparative study of properties of self compacting concrete with metakaolin and cement kiln dust as mineral admixtures” IJRET Vol. 2, Issue 4, Apr 2014, 37-52
- [8]. Ms. Priyanka p. Naik, prof. M. R. Vyawahare “comparative study of effect of silica fume and quarry dust on strength of self compacting concrete” (ijera) vol. 3, issue 3, may-jun 2013, pp.1497-1500
- [9]. P. Kumar, K. Sudalaimani, and M. Shanmugasundaram “An Investigation on Self-Compacting Concrete Using Ultrafine Natural Steatite Powder as Replacement to Cement” Hindawi Advances in Materials Science and Engineering Volume 2017, Article ID 8949041
- [10]. A.Belkadi, S.Aggoun, C.Amouri, A.Geuttala, H.Houari “experimental investigation on the properties and performance of self compacting concrete with vegetable and synthetic fibers” . Proceedings of the 7th International Conference on Mechanics and Material design Albuferia/Portugal 11-15 June 2017 Publ.INEGI/FEUP (2017).
- [11]. R. Ramasubramani, R. Praveen and K. S. Sathyanarayanan “study on the strength properties of marine algae concrete”.RASAYAN.J.Chem Vol. 9 | No. 4 |706 - 715 | October - December |2016
- [12]. S. M. Dumne “Effect of Superplasticizer on Fresh and Hardened Properties of Self-Compacting Concrete Containing Fly Ash” American Journal of Engineering Research (AJER) Volume-03, Issue-03, pp-205-211

Proceedings of
AICTE Sponsored
International E - Conference on
Emerging Trends in
Engineering and Management



(Sponsored)

ICETEM - 2020

On

19th and 20th
of
February, 2021



Organised by

Research and Development Cell

**SRI VASAVI ENGINEERING COLLEGE
(AUTONOMOUS)**

(Sponsored by Sri Vasavi Educational society)

Permanently Affiliated to JNTU, Kakinada

(Approved by AICTE, New Delhi & Accredited by NAAC with "A" Grade)
Pedatadepalli, Tadepalligudem - 534101, W.G.Dist, (A.P)

International



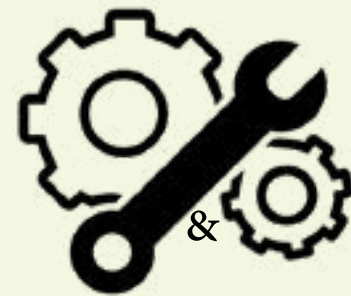
Conference

Emerging



Trends

Engineering



Management

2020



Comparative study on Consistency of Conventional Concrete and Self Compact Concrete as per Indian Standard Code

Sambasiva Rao Katam
M.Tech student, Civil engineering Department
Vaagdevi College of Engineering, (Autonomous),
Bollikunta, Warangal, India
sambrao.aee@gmail.com

Dinesh Kumar Gopalakrishnan
Assistant Professor, Dept. of Civil Engineering
Vaagdevi College of Engineering, (Autonomous),
Bollikunta, Warangal, India
gdkcivil@gmail.com

Abstract— Structural components are heading towards thinness to optimize the utility of space and effectiveness in strength parameters without compromising durability. The thrust to achieve these parameters seems to be fulfilled by the invention of self-compacting concrete. The mixture of concrete emphasizes the minimization of coarse aggregates quantity. This invokes different abilities of self compact concrete-like filling ability, passing ability to ascertain its workability. This paper focuses on the comparison of self-compacting concrete with traditional concrete inline of workability and design mix procedure.

Keywords— Consistency or workability; passing ability; filling ability; flow ability; design mix; SCC (self compacting concrete); IS (Indian standard).

I. INTRODUCTION

The challenges arising from the construction field because of site environment health issues and workability at a congested and thinnest place of structural element is hard to meet but the innovation Rheodynamic concrete, self-consolidation concrete, or self compact concrete is fulfilling it tremendously. It has the ability to transform into High performance concrete.

The High-performance concrete should satisfy the workability, durability, strength parameters, and enhanced physical properties such as Young's modulus, thermal properties, etc. The researches on the self compact concrete reveal that minimum alterations in the composition of materials the properties of HPC can be achieved.

Developments in the technology of the Rheometer equipment to measure the behavioral responses of a liquid in terms of suspension in response to the applied forces and/or self weight are simplified the understanding of the Rheodynamic concretes. It is also noticed that the IS 456:2000(reaffirmed 2016) amendment no 5(2019) has incorporated the additive's impact on OPC in terms of stripping of formwork and minimum compressive strength as modified in clause no: 11.3.1.

1.1 Traditional concrete: The workability of the traditional concrete i.e., plain and reinforced concrete vide clause no.7 of IS 456:2000 (reaffirmed 2016) scrupulously followed until it is unbiased by the executive engineer or otherwise BS 5348 (part 1 to 4) will deal with the workability when there is no correlation is achieved in between the compacting factor, Vee-Bee time and slump value and the frequency of checking will be as per IS 1199.[2]

1.2 Self compacting concrete: The workability of the Self compact concrete is indirectly practiced as per the guidelines of "IS 1199 (part6):2018 Tests on fresh self

compactingconcrete" [3]

II. METHODOLOGY

Comparison of self-compacting concrete with traditional concrete.

2.1 Workability or Consistency:

2.1.1 Traditional or conventional concrete as per IS 456:

IS 456:2000 (reaffirmed 2016) is recommended 3 types of tests on the fresh concrete:

1. Slump

2. Vee-Bee test

3. Compacting factor

in lines with the IS 1199 (part 1 to Part 4) provisions.

However, the IS 456 emphasizes more on the value of Slump when compared to rest. The basis on the value of Slump obtained for a particular mix, the workability is denoted. Based on the slump value the IS 456 has classified the workability in five categories as tabulated in clause no.7.1 as listed below:

S. No	Slump value (mm)	Workability
1	<25	Very low
2	25-75	Low
3	50-100 or 75-100	Medium
4	100-150	High
5	>150	Very high

Table 2.1 Tests recommended by IS 456:2000 (reaffirmed 2016) [2]

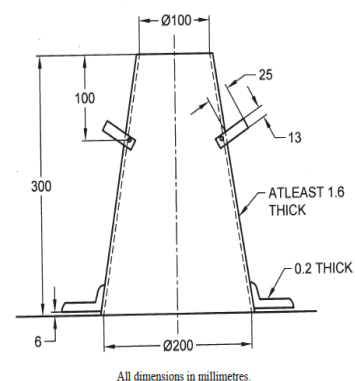


Fig 2. Error! No text of specified style in document. 1 "Slump Cone as per IS 1199 (part 2)" [4]

Among these five classifications the IS 456 further insists that, very low and very high slump valued concrete mixes are to be further evaluated as below:

Table 2.2 Tests recommended by IS 456:2000 (reaffirmed 2016) [2]

S. No	Slump value (mm)	Workability	Recommendation additional tests and values.
1	<25	Very low	Compaction factor test to be done. The recommended range of the compaction factor is 0.75 to 0.80
2	>150	Very high	Rheometer equipment is needed to find the "Flow" parameters of the mix.

It is evident that when the slump value is more than 150mm the stiffness or viscosity of the mix will be affected and liquidity of fluid increases in the mix. Hence the IS 456 recommends studying the "Flow" parameters of the mix when the slump value is very high.

2.1.2 Self compacting concrete as per IS 1199 (part 6) 2018:

The Self compacting concrete is a mixture of components having more fines leads to high slump value & low viscosity. The lower viscosity is enhanced by adding the "VMA (Viscosity modifying admixture)" without affecting the Water powder ratio. Sometimes these parameters are achieved by controlling the quantities of

1. Super Plasticizers
2. Fines
3. VMA

The IS 456 recommends the flow tests when the slump value beyond 150mm and IS 1199 (part 6): 2018 "tests on Fresh Self compacting concrete" [3] describes the flow tests of SCC.

The IS 1199 (part 6) recommends the following terminology/tests for the consistency of the SCC:

1. Passing ability (PA)
2. Segregation resistance (SR)
3. Slump Flow (SF)
4. Viscosity and filling ability.

1. **Passing ability:** The ability to flow in congested areas i.e., between reinforcing bars and thinner sections of elements.
2. **Filling ability:** Under confined and obstacles, the ability to fill all the spaces.
3. **Slump flow:** The mean diameter of the spread, measured on the flow test table.
Flowability: ability at an unconfined flow of concrete.

4. **Segregation resistance:** Robust or stable i.e., being homogenous at all stages of fresh concrete from mixing to placing.

S.No.	Name of the test	Limitations	remarks
1	Slump flow (d_{max}) test and t500 test	Above 40mm size aggregate this test is not suitable.	IS code not mentioned any range of the accepted values.
2	V-funnel test	Above 20mm size aggregate this test is not suitable	IS code not mentioned any range of the accepted values
3	L-box test	Two variations of test available i.e., two bar test and three bar tests.	IS code not mentioned any range of the accepted values
4	Sieve segregation resistance test	The sample shall be as IS 1199 (part 1) for consistency.	IS code not mentioned any range of the accepted values

S.No.	Name of the test	Parameter is measured or inspected.
1	Slump flow (d_{max}) test and t500 test	1. d_{max} : Indication of yield stress, indication of flow ability. SF=(D1+D2)/2 2. t500 : indication of speed of flow and relative viscosity, 3. Partial indicating of the filling ability. 4. Visual observation may suggest the extent of segregation.
2	V-funnel test	Flow time through V-funnel indicates the Viscosity and filling ability
3	L-box test	1. Ratio "PL" passing ability ratio indicates the passing or blocking behavior of the mix when obstacles present. $P_L = H_2/H_1$ 2. Visual observation may suggest the extent of segregation.
4	Sieve segregation resistance test	1. % of Resistance to segregation or segregated portion in %. SR= (net mass of mix retained on the sieve/total mass of mix poured on the sieve)/100 2. Indications of bleeding if any.

The test and its recommendations as per IS 1199 (part 6) tabulated below:

Table 2.3 Tests recommended by IS 1199 (Part 6): 2018

Table 2.4 Tests recommended by IS 1199 (Part 6): 2018

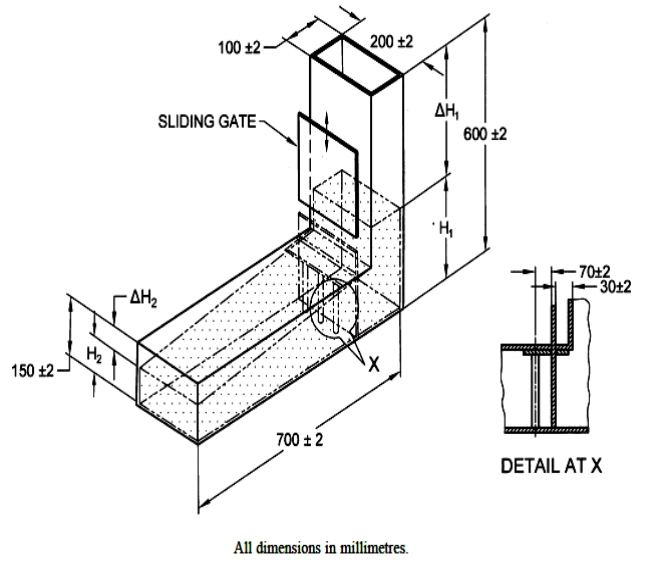
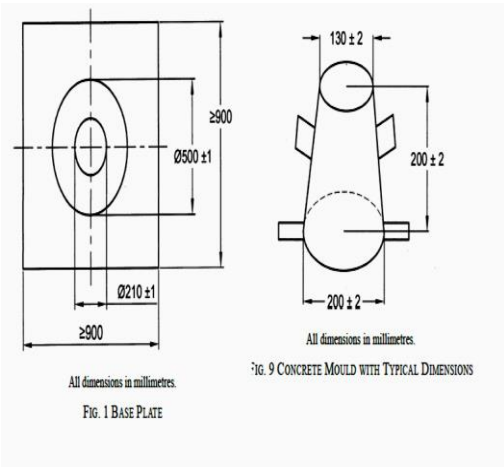


Fig.2.1.2.1 “Apparatus for Slump Flow (d_{max} & t_{500}) test” [3] [4] [5]

FIG. 3 TYPICAL GENERAL ASSEMBLY OF L-BOX SHOWING REQUIRED DIMENSIONS

Fig.2.1.2.3 “Apparatus for L-box test” [3]

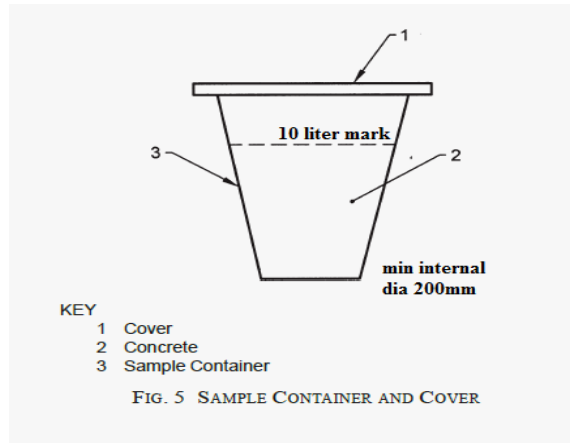
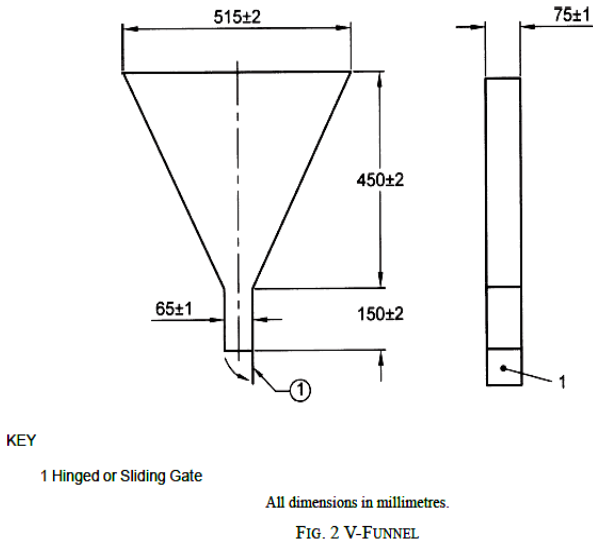


Fig.2.1.2.4 “Apparatus for sieve Segregation resistance test” [3]

III. TESTS

Fig.2.1.2.2 “Apparatus for V-funnel test” [3]

The tests not described in the IS 1199 (part 6): 2018 are

1. Orimet test
2. U box test
3. J-ring test
4. Fill box test.
5. T5 of V-funnel test.

6. Some of the literatures describe the following conclusion on the tests and its limitations:

Table 1.5 "summary of tests on SCC"[6]

Property measured	Test method	Material	Recommended values
Flowability / Filling ability	Slump flow	Concrete	650 – 800 mm Average flow diameter
	T_{50}	Concrete	2 – 5 sec Time to flow 500 mm
	V – funnel	Concrete / mortar	6 – 12 sec Time for emptying of funnel
	Orimet	Mortar	0 – 5 sec Time for emptying of apparatus
Passing ability	U – box	Concrete	0 – 30 mm Difference in heights in two limbs
	L – box	Concrete	0.8 – 1.0 Ratio of heights at beginning and end of flow
	J – ring	Concrete	0 – 10 mm Difference in heights at the beginning and end of flow
Segregation potential	Settlement column test	Concrete	> 0.95 Segregation ratio
	Sieve stability test	Concrete	5 – 15% sample passing through 5 mm sieve
	Penetration test	Concrete	Penetration depth < 8 mm

IV. CONCLUSION

The consistency or workability of the conventional concrete is easily measurable and results are recommendations are layman can understand and predictable. Whereas the consistency tests for the Self compacting concrete based on the flow properties, i.e., Rheometer equipment is needed to determine its properties. The IS 1199 (part 6): 2018 has suggested a few test procedures without mentioning limitations and an acceptable range of test results. Hence this to be needed to further modify to use as a legal document in the construction industry.

REFERENCES

- [1] Dinesh. A*, Harini.S, Jasmine Jeba.P, Jincy.J, ShaguftaJaved “experimental study on self compacting concrete” international journal of engineering sciences & research technology, 6 (3): March, 2017.
- [2] IS 456:2000 (reaffirmed 2016) “plain and reinforced concrete – code of practice”
- [3] IS 1199 (part 6): 2018 “Fresh concrete methods of sampling, testing and analysis, Part 6 tests on fresh self compacting concrete”
- [4] IS 1199-1959 (reaffirmed 2018) “Methods of sampling and analysis of concrete”
- [5] IS 1199 (part 2): 2018 “Fresh concrete methods of sampling, testing and analysis, Part 2 determination of consistency of fresh concrete”
- [6] “selfcompacting concrete” <http://www.theconcreteportal.com/scc.html>
- [7] “Wrd handbook chapter no. 3 self compacting concrete” Maharashtra Engineering Research Institute, water resource department, nashik-04 April 2019

The International Journal of Analytical and Experimental Modal analysis

An UGC-CARE Approved Group - II Journal

An ISO : 7021 - 2008 Certified Journal

ISSN NO: 0886-9367 / web : <http://ijaema.com> / e-mail: submitijaema@gmail.com



Certificate of Publication

This is to certify that the paper entitled

“Superplasticizers in self-compacting concrete an overview of the experimental studies”

Authored by :

Sambasiva Rao Katam

From

Vaagdevi College of Engineering, (Autonomous), Bollikunta Warangal, India

Has been published in

IJAEMA JOURNAL, VOLUME XIII, ISSUE IX, SEPTEMBER- 2021



Michal A. Olszewski Editor-In-Chief
IJAEMA JOURNAL



<http://ijaema.com/>



Viswambhara Educational Society

VAAGDEVI
COLLEGE OF ENGINEERING

AUTONOMOUS

Accredited by NAAC with 'A' Grade



Certificate of Presentation

This is to Certify that

KATAM SAMBASIVA RAO

VAAGDEVI COLLEGE OF ENGINEERING

Presented a paper entitled

**EXPERIMENTAL STUDY ON STRENGTH CHARACTERISTICS OF SELF
COMPACTING CONCRETE WITH BASALT FIBER (experimental
studies)**

in National e-Conference on

**"Sustainable Construction Materials and Recent Innovations in
Civil Engineering"**

organized by

**Department of Civil Engineering, Vaagdevi College of Engineering
Warangal, Telangana**

in association with

ACCE (I) Student Chapter & ICI Warangal Centre

held on 7th & 8th July 2021

Coordinator

Civil Engineering
VCE Warangal

Chairman

ACCE (I)
Karimangar Centre

Chairman

ICI
Warangal Centre

HOD

Civil Engineering
VCE Warangal



SRI VASAVI ENGINEERING COLLEGE (AUTONOMOUS)

(Sponsored by Sri Vasavi Educational society)

Permanently Affiliated to JNTU, Kakinada

(Approved by AICTE, New Delhi & Accredited by NAAC with "A" Grade)

Pedatadepalli, Tadepalligudem - 534101, W.G.Dist, (A.P)



AICTE Sponsored "International Conference on Emerging Trends in Engineering and Management"



ICETEM -2020

CERTIFICATE OF PARTICIPATION

This is to certify that Dr./Mr./Ms./Mrs. Sambasiva Rao Katam
of Vaagdevi college of Engineering, Warangal
presented/published a paper entitled Comparative study on Consistency of Conventional
Concrete and Self Compact Concrete as per Indian Standard Code
in **AICTE** Sponsored **International E-Conference on Emerging Trends in
Engineering and Management (ICETEM-2020)** held on 19th - 20th February, 2021.

Co-ordinator
Dr. V.S.Naresh
SVEC

Principal
Prof. G. VNSR Ratnakara Rao
SVEC

Secretary & Correspondent
Sri Ch.V.V. Subba Rao
SVEC

PERFORMANCE ELEVATION OF CONCRETE BY USING SUGARCANE BAGASSE ASH AND GLASS FIBRE

SHETTY SAIKRISHNA

M.Tech Structural Engineering
(Department of Civil Engineering),
Vaagdevi College Of Engineering,
Warangal – 506005, India,
EMAIL-

saikrishna.shetty731@gmail.com

G.DINESH KUMAR

Assistant professor (Department of Civil
Engineering),
Vaagdevi College Of Engineering,
Warangal – 506005, India.

S. RADHIKA

Assistant professor (Department of Civil
Engineering),
Vaagdevi College Of Engineering,
Warangal – 506005, India.

Abstract — *The use of fibers in concrete is currently used in the strengthening of reinforced concrete members. Internal micro cracks in concrete, leading to brittle failure. The glass fibre is a synthetic fibre which is extracted through pure silica (silicon dioxide) when cooled as fused quartz; into a glass with no melting point can be used as a glass fibre, it fibre is made in high temperature. Glass fibre is cheaper and flexible than carbon fibre and steel fibre. Whereas, also utilizing the industrial waste which is sugarcane bagasse ash is a waste by-product of sugarcane after extraction juice from sugarcane. In this work, effect of sugarcane bagasse ash and glass fibre on the strength of concrete for M20 grade have been studied by varying the percentage in concrete. Glass fiber content were varied by 0.05%, 0.10%, 0.15%, 0.20%, 0.25%, 0.30%, 0.35% and 0.40% by volume of concrete and bagasse ash has fixed optimum percentage of 5% by the volume of cement. Cubes, Cylinder and Prism were casted to evaluate the Compressive Strength. All the specimens were cured for the period of 28 days before crushing. The results of concrete specimens for 28 days curing with varied percentage of glass fibre were studied to find out the addition of optimum dosage level of glass fiber in concrete with a fixed percentage of sugarcane bagasse ash of 5% in volume of cement. The beam is casted by using the optimum dosage level to determine the structural behavior of the concrete. The result shows there is significant strength improvement in addition of sugarcane bagasse ash and glass fibre in concrete.*

I. INTRODUCTION

The concrete solid which is malleable in pressure, however climate and contamination it makes fragile and it loosing its strength qualities, where the solid is adding and admixtures material which may improve the strength and sturdiness parts of concrete.

Sugarcane bagasse ash which is a by-product of sugarcane ventures, where the delivering the colossal measure of sugarcane bagasse ash India. Which is having the cementitious and siliceous properties, where sugarcane bagasse ash is replaces the cement and fine aggregate total and furthermore the fineness of material which make thick the solid and diminishes the porosity to build up the strength and sturdiness of cement. The bagasse debris is used in solid it might assist with diminishing the contamination and furthermore helps in of development.

Glass fiber is a synthetic fiber, which is utilized to build up the strength attributes of concrete. The plain has weak in tension and flexural strength in solid concrete, it makes the solid be less sturdiness and high shrinkage and furthermore contamination builds the insufficiencies in concrete. Where the glass fiber is utilized to improve the rigidity and flexural strength it makes the solid to be bendable and furthermore it opposes harm through the contamination and climate influences.

Both sugarcane bagasse ash and glass fiber are utilized to improve the strength and solidness qualities of solid which leads supplanting the materials in a satisfactory rate make the solid to be low porosity, high rigidity, improve sturdiness and low in creep

II. LITERATURE REVIEW

Kavita Kene (2012) et al directed trial concentrate on conduct of steel and glass Fiber Reinforced Concrete Composites. The investigation led on Fiber Reinforced cement with steel filaments of 0% and 0.5% volume division and antacid safe glass strands containing 0% and 25% by weight of concrete of 12 mm cut length, thought about the outcome.

Seshagiri Rao (2013) et al considered conduct of solid shafts supported with glass fiber built up polymer pads and saw that radiates with silica covered Glass fiber supported polymer (GFRP) pads shear support have shown disappointment at higher burdens. Further they saw that GFRP pads as shear support show genuinely great pliability. The strength of the composites, pads or bars relies on the fiber direction and fiber to grid proportion while higher the fiber content higher the higher the elasticity.

Seshadri (2012) et al led sturdiness concentrates on glass fiber supported cement. The salt safe glass strands were utilized to discover usefulness, opposition of cement because of acids, sulphate and quick chloride penetrability trial of M30, M40 and M50 evaluation of glass fiber built up concrete and standard cement. The strength of

cement was expanded by adding antacid safe glass strands in the solid. The test study showed that expansion of glass filaments in solid gives a decrease in drying. The expansion of glass filaments had shown improvement in the obstruction of cement to the assault of acids.

Alsayed (2001) et al considered the presentation of glass fiber built up plastic bars as building up material for solid constructions. The examination uncovered that the flexural limit of solid shafts built up by GFRP bars can be precisely assessed utilizing a definitive plan hypothesis. The examination likewise uncovered that as GFRP bars have low modulus of flexibility, redirection measures may control the plan of transitional and long shafts built up.

Yogesh Murthy (2012) et al examined the exhibition of Glass Fiber Reinforced Concrete. The examination uncovered that the utilization of glass fiber in concrete not just improves the properties of concrete and a little expense cutting yet in addition give simple outlet to arrange the glass as ecological waste from the business. From the investigation it very well may be uncovered that the flexural strength of the pillar with 1.5% glass fiber shows practically 30% increment in the strength. The decrease in droop saw with the increment in glass fiber content.

Avinash Gornale (2012) et al examined the strength part of glass fiber supported cement. The investigation had uncovered that the expansion in compressive strength, flexural strength, split rigidity for M20, M30 and M40 evaluation of cement at 3, 7 and 28 days were seen to be 20% to 30%, 25% to 30% and 25% to 30% separately after the expansion of glass filaments when contrasted with the plain concrete.

Levitt (1997) et al inspected that when concrete, mortar or cement is sprinkled or in any case carried into contact with window glass, drawing happens. This is on the grounds that the antacid in concrete assaults a portion of the silicates that are utilized in glass make. The stock utilized in making glass filaments has preferred salt opposition over window glass since zircon is utilized as one.

Wodehouse (1983) et al inspected that the principle contrast among dewatered and non-dewatered GRC is the distinction in thickness which has two impacts. First and foremost albeit the fiber content by weight is the equivalent, the higher thickness of the dewatered board gives a higher fiber volume division giving higher qualities. Besides the dewatered board has better compaction and diminished porosity giving better fiber/grid bond strength.

Perumelsamy (1992) et al analyzed that the tests directed on GFRC in research centre have shown great opposition for fire, since the significant utilization of GFRCs is for compositional structure boards. In these structures, imperviousness to fire turns into a significant factor in plan.

Perumal (2006) et al analyzed that the blends in with 1.5% volume of filaments invigorated ideal composite properties as far as compressive with 25.39% strength improvement. The most noteworthy expansion in split elasticity was seen in blends in with 1.5% of volumes of strands and discovered to be 5.76% higher strength than reference concrete. Likewise, the foremost elevated flexural strength was seen in blends in with 1.5% of volume of fiber and discovered to be 72.5% quite reference concrete.

Swamy (1978) et al research incorporates not just an appraisal of fiber substance and framework strength, yet in addition such subtleties as fiber circulation, direction, and viability of holding. Conceivable assembling or materials shortcomings can likewise be analyzed. Likewise it shows that the MOR and LOP in drying condition test have higher outcome than wet condition around (1-5) MN/m² distinction.

Surendra (1987) et al inspected that the utilization of antacid safe glass fiber and E glass fiber in blend with a latex fiber when presented to the quickened maturing climate the flexural strength lessens. MOR following 52 weeks of quickened maturing was only 50% of the un matured. Strength esteem was exceptionally little 1/60th.

Srinivasan (2010) et al had inferred that mixed SCBA in concrete had higher compressive strength, rigidity and flexural strength in contrast with that of without SCBA. They arrived at a resolution that concrete can be in part supplanted by SCBA up to a degree of 10%. They even presumed that with expansion of more SCBA the thickness of solid will diminish and low weight solid will get delivered.

Kawade (2013) et al saw that concrete can be effectively supplanted with SCBA up to a degree of 15%. The fractional substitution of SCBA expands the functionality of cement because of which super plasticizer isn't needed. Remained part (bagasse) is additionally utilized as fuel to warm the boilers. The cremation of bagasse delivers the debris. Bagasse has a different use in market as such underway of woods, creature food sources and warm extension e.t.c then likewise a ton of bagasse stays unused and they get unloaded as landfill. The public authority is more worried in using the fly debris. The service of Environment guides the enterprises to remove the fly debris and reuse it underway of concrete, tiles and blocks and so on Since our country is a growing, so prerequisite of framework is more, for more foundation concrete necessity is likewise extremely high. The creation of concrete produces hurtful gases like CO₂ which corrupts the climate causing medical problems to the occupants. With the progression in the innovation new techniques have been received to diminish the utilization of concrete. One such technique is expansion of bagasse debris to concrete. Sugarcane debris is a modern side-effect which contains aluminum particle and silica, which is

pozzolanic in nature. For regular pozzolans the base silica, aluminum and iron oxide content is 70 % and SiO₃ ought to be fewer than 4 %. The scientists have discovered that bagasse satisfy these prerequisite. Consequently debris acts as a pozzolanic material. In Bagasse there is half cellulose, 25%of hemicelluloses and 25% of lignin. It has been seen that roughly 26% of bagasse and 0.62% of remaining debris are created from 1 ton of sugarcane. Utilization of debris in concrete diminishes the concrete prerequisite and furthermore lessens the expense of development. Analysts likewise recommend that the bagasse fly debris can be effectively utilized in delivering blocks, tiles, settling the dirt and so on.

Aishwarya (2016) et al found that when cement was blended in with halfway 10% of SCBA then the compressive strength expanded 1.21 occasions and elasticity expanded 1.04 occasions. With expansion of SCBA to solid, individuals show a superior strength as they are less penetrable to chloride particles.

Lathamaheswari (2017) et al saw in their examination that the functionality of cement has not been a lot of influenced by increase in supplanting of concrete with SCBA and concrete would be supplanted with SCBA up to a most extreme constraint of 10%.When concrete was somewhat supplanted by SCBA in solid, it had additionally shown a decent modulus of elasticity.

Bangar Sayali (2017) et al presumed that with halfway supplanting of cement in concrete with SCBA strength of concrete can be expanded with decrease being used of cement. They even presumed that bagasse Ash best use is with expansion in concrete as opposed to land filling.

Prashant (2012) et al from their exploration found that the as the level of bagasse ash expands Sorptivity coefficient likewise increments. The permeable idea of SCBA and the pollutions present in it makes the solid porous concrete. They reasoned that if bagasse is utilized in its most flawless structure than it can end up being better substitution of concrete.

III. MATERIALS USED

A. Cement

The Ordinary Portland cement (OPC 53) grade adjusting to IS 12269-1987. It is utilized for projecting concrete and the particular gravity of concrete. The properties of concrete given in table 1.

Property	Value
Standard Consistency	33%
Initial Setting Time	36mins
Compressive Strength	54.08N/mm ²

fineness Modulus	6%
Specific Gravity	3.1

B. Fine aggregate

The fine total is utilized according to IS 383 – 1970, where the sand is sieved according to its code and gone through strainer and gather diverse estimated particles left over various sifters. The fine total of sifter investigation result is given in table 2.

Sieve Size	Sand Percentage Passing	Remarks
2.36mm	99.4	Zone III
1.18mm	89.6	
600µm	64.7	
300µm	9.2	
150µm	1.1	
75µm	0.6	

C. Coarse aggregate

The squashed total scope of 20mm nominal size, it is according to IS 383 – 1970. The coarse total of sieve examination result is given in table 3.

Sieve Size	Percentage Passing	Remarks
80mm	100	Well graded(20mm size)
40mm	100	
20mm	53.4	
10mm	0	
4.75mm	0	
Pan	0	

D. Water

As indicated by IS 3025, water to be utilized for blending and restoring ought to be liberated from harmful or malicious materials. Compact water is for the most part viewed as acceptable. In the current examination, accessible water inside the grounds is utilized for both blending and curing purposes.

E. Glass fiber

The glass fibre is nominal size of 12mm strips is added to concrete.

F. Sugarcane Bagasse Ash

The bagasse ash contains Silica and alumina

as primary fixings. The mix of silica, alumina and iron oxide is more than 70 % in SCBA. This the explanation debris goes about as pozzolanic material.

IV. MIX PROPORTION

The M20 were assigned as per IS 10262-1982. In light of the outcomes, the blend extents M20 was thought of. Solid blend in with W/C proportion of 0.50 was readied.

The blending systems are as per the following: The sugarcane bagasse ash is fixed streamlined level of 5% with substitution of concrete and taken to acquire homogeneity with fine total, concrete, coarse total and water is blended to get useful combinations. The extents are given in table 4 for 1m³of cement.

In this work , the level of the glass fiber is added by weight was 0%, 0.05%, 0.1%, 0.15%, 0.20%, 0.25%, 0.30%, 0.35% ,0.40% and 0.45% in concrete . Blends were assigned as S0, S1, S2, S3, S4, S5, S6, S7, S8 and S9 separately. Amount of filaments needed for 1m³ of concrete for different blends in table 5.

Grade	Cement	FA	CA	Water
M20	383	565.16	1229	191.16

V. EXPERIMENTAL INVESTIGATION

A. Compression test

The test was led according to IS 516-1959. The blocks of standard size 150mm*150mm*150mm were utilized to locate the compressive strength of cement.

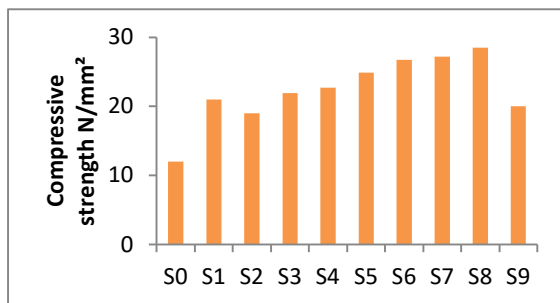


Fig.1 - Compressive strength of sugarcane bagasse ash and Glass fibre concrete at the age 7 days.

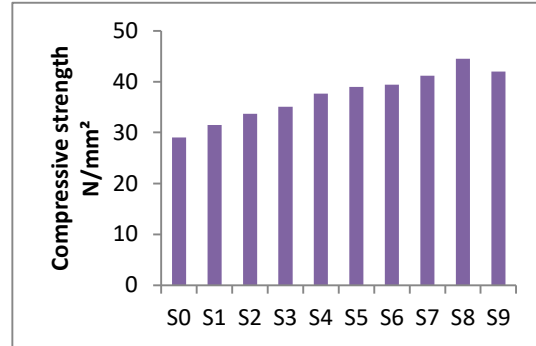


Figure 2 - Compressive strength of sugarcane bagasse ash and glass fibre concrete at the age of 28 days.

B. Tensile test

This test was led according to 5816-1970. The cylinder of standard size 150mm measurement and 300mm stature was set on the CTM with limit 200tonnes.

Mix Designation	Glass fibre	
	in %	In kg/m ³
S0	0.00	0
S1	0.05	1.184
S2	0.10	2.368
S3	0.15	3.553
S4	0.20	4.737
S5	0.25	5.921
S6	0.30	7.106
S7	0.35	8.288
S8	0.40	9.472
S9	0.45	10.656

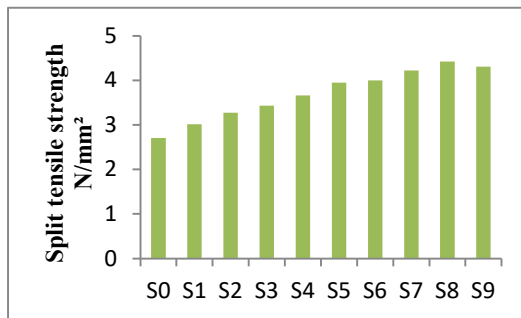


Figure 3 - Split tensile strength of sugarcane bagasse ash and glass fibre Concrete at the age of 28 days

C. Flexural strength of beam

The beams of size 100*100*500mm were cast and tested.

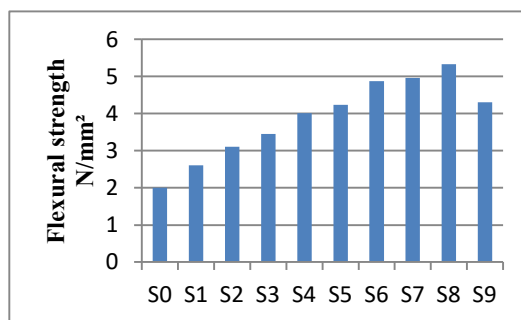


Figure 4 - Flexural strength of sugarcane bagasse ash and Glass fibre concrete at the age of 28 days.

VI. CONCLUSION

In view of the writing, the actual properties and compound properties are contemplated and the trial test results gives us the qualities, that the compressive strength, elasticity, flexural strength and toughness of solid glass fiber and sugarcane bagasse ash gave higher outcomes contrasted and ordinary cement. The exploratory examination were completed for the supplanting of cement with 0.05%, 0.10%, 0.15%, 0.20%, 0.25%, 0.30%, 0.35%, 0.40% and 0.45% of glass fiber and the substitution of concrete in concrete blends in with the fixed ideal level of 5% of sugarcane bagasse ash to discover strength attributes of cement, The fundamental test results for expansion of admixtures brought about expanded strength of cement. Henceforth an itemized investigation of utilizing various extents of glass fiber and sugarcane bagasse ash in concrete and subsequently further investigation of toughness of cement is to be done in the subsequent stage.

A. The Compressive Strength of Concrete was expansion of glass fiber and sugarcane bagasse debris and furthermore it builds strength by 1.23 occasions in correlation with Plain Concrete blend.

- B. The expansion of glass fiber and sugarcane bagasse ash in solid expands the split elasticity to 1.41 occasions when contrasted with plain concrete.
- C. The flexural strength increments by 2.55 occasions when contrasted with plain concrete and it prompt decrease of break arrangement.

VII. REFERENCE

- [1] Alsayed (2001), Performance of glass fiber reinforced plastic bars as a reinforcing material for concrete structures, Journal of Science and Technology.
- [2] Avinash Gornale (2012), Strength aspect of Glass fiber reinforced concrete, International journal of Scientific and Engineering research, vol, 3, issue 7.
- [3] Bangar Sayali,"A review paper on replacement of cement with bagasse ash", Bangar, 7(1) January -March 2017.
- [4] IS 12269: 2013, Indian Standard ordinary Portland cement, 53 specifications (first revision).
- [5] IS 383 – 1970, Specification for coarse and fine aggregates from natural sources for concrete (Second Revision).
- [6] IS 9103: 1999, Indian Standard concrete admixtures - specification (first revision).
- [7] IS 3025(Part II) – (1983), Indian Standard methods of sampling and test (physical and chemical) for water and waste water part ii ph value (first revision).
- [8] Jagannatha Reddy (2014), Flexural strengthening of RC beams using natural sisal and artificial carbon and glass fabric reinforced composite system, Sustainable Cities and Society 10 (2014) 195–206.
- [9] Kavita Kene (2012), Experimental study on behavior of steel and glass fiber Reinforced concrete composite, Bonfring International Journal of Industrial Engineering and Management studies, Vol. 2,No-4.
- [10] Kawade, "Effect of use of Bagasse Ash on strength of concrete", vol.2, 7 July2013.
- [11] Lathamaheswari,"Study on Bagasse Ash as partial replacement of cement in concrete", vol.13, 1 January2017.
- [12] Levitt (1997), "Concrete materials problems and solutions", "GRC and Alkali-Glass reaction", First Edition 1997,(pp22-24).
- [13] Mandula (2007) et al, Properties and Reactivity of Sugarcane Bagasse Ash ,Twelfth International Colloquium on Structural and Geotechnical Engineering, Cairo. Egypt.
- [14] Noor-Ul Amin,"Use of Bagasse Ash in concrete and its impact on the strength and

- chloride resistivity".
- [15] Paya (2002) et al, Sugarcane bagasse ash (SCBA): studies on its properties for reusing in concrete production, Journal of Chemical technology and Biotechnology 77, p..321.
 - [16] Perumelsamy, "Fibre reinforced cement composites", February 1992, Chapter 13, (pp351).
 - [17] Perumal, "Behavioral study on the effect of AR-Glass Fibre reinforced concrete", NBW & CW October 2006, (pp174-180).
 - [18] Prashant, "Utilization of Bagasse Ash as a Partial Replacement of Fine Aggregate in Concrete", Chemical, Civil and Mechanical Engineering Tracks of 3rd Nirma University International Conference on Engineering (NUICONE2012).
 - [19] PrinyaChindaprasirt(2012),UtilizationofBagasseAshinHighStrengthConcrete,JournalofMaterialsandDesign34,p.45
 - [20] Rajagopal et al (2007) et al, Evaluation of Bagasse Ash as Supplementary Cementitious Material, Journal of Cement and Concrete Composites 29, p.515.
 - [21] Sarita Rai, (2000) et al,HydrationofBagasseAsh-BlendedPortlandCement,JournalofCementandConcreteResearch30,p. 1485.
 - [22] Seshadri Sekhar (2012) et al, Durability studies on Glass Fiber Reinforced Concrete, International Journal of civil engineering science, vol.1 and no-1-2.
 - [23] Seshagiri Rao (2013) et al, Behavior of concrete beams reinforced with glass fiber reinforced polymer flats, international journal of research in engineering and technology, Vol.2, Issue 09.
 - [24] Srinivasan et al (2010) et al, ExperimentalStudyonBagasseAshinConcrete, InternationalJournalofServiceLearninginEngineering5 (2), p.60.
 - [25] Surendra, "Toughness of Glass Fiber reinforced concrete panels subjected to accelerated aging", PCI Journal, September-October (1987), (pp83-88).
 - [26] Swamy, "Testing and Test Methods of Fibre Cement Composites", Published 1978,(pp42-43).
 - [27] Wodehouse, "GRC and buildings", Published FirstEdition1983.
 - [28] Yogesh Murthy (2012), Performance of glass fiber reinforced concrete, International journal of engineering and innovative technology, vol.1, issue 6.

Experimental Study on Mechanical Properties of Geopolymer Concrete by using GGBS and RHA

Bandi pooja
Dept of civil engineering
Vaagdevi College Of Engineering
Warangal, India
Pooja.svs123@gmail.com

Dr G Dineshkumar
Dept of civil engineering
Vaagdevi College Of Engineering
Warangal, India
gdkcivil@gmail.com

ABSTRACT: As the cement business is to blame for the worldwide emission of dioxide regarding 5-7% in preparation of concrete, the dose of cement is reduced by the addition of minerals, and this strategy will contribute to the protection of the setting and preservation of energy. This possibility is distinguished to be a geopolymer that frequently contains fly junk, metallic element or hydrated oxide (NaOH or KOH), sodium salt. thanks to concrete's interest in industrial development, the assembly of normal hydraulic cement and therefore the use of typical channel sand are enlarged. throughout the cement production method, the outflow of dioxide has exaggerated. At constant time, thanks to MISBR mining of quicksand, the availability of waterway sand has become progressively valuable and scarce. This mainly focuses on this analysis paper is to centre the ecological proximity of cement and waterway sand. The experiment was performed to represent the mechanical properties of geopolymer concrete. In this estimate various types of strengths in the geopolymer concrete. The materials used are ash, alkaline liquid, fine mixture, coarse mixture, GGBS, Rice husk ash, and Inter-sand.

KEYWORDS: GGBS, RHA, M-Sand, Fly ash, Geopolymer, Protect Environment.

1. INTRODUCTION

Cement is widely used because of its incredible performance and bonding nature in two materials and easy to use and mix and place and apply to the structure. India is the one of an important leading role in the top three in cement production around the world. Cement production in China was 2.29 billion tons in 2013, followed by India with 270 million tons. Global cement demand is on an upward trend and is expected to increase by 4.5% in the next five years. Cement is a world-wide used material and global demand in 2019 is to be 5.19 billion metric tons of cement. Manufacturing of Cement is various for different processes. In this manufacturing, most of the materials are used the same such as limestone and clay, and so on, etc. in this process involves heating and cooling of materials at different stages. Now a day's lot of researches are going on cement for improving its performance and as well as durability too. This also focuses on the elimination of weakness problems subjected to the cement. One of the main disadvantages is the emission of gases during the manufacturing process. Which may lead to cause pollution to the environment. In this, some of the researchers explain that the production of 1 ton of cement releases 1 ton of around six percent of the emission of CO₂. The main problem of it is carbon emissions and footprint. After wood, concrete is the

regularly utilized material by the network. After developing cement next is focuses on concrete material. Concrete material has a lot of limitations according to environmental conditions and so on etc. lot of researches is going on for developing concrete with suitable material. In this, we got a good solution in the name of geopolymer concrete. This concrete is very good compared to conventional concrete and gives an excellent result. This concrete is made from wastes.

2. LITERATURE WORK

Krishnan L et.al (2014) led considers and inferred that geopolymer innovation is appropriate. This author mainly explains the importance of geopolymer concrete and its uses in the industry sectors. Geopolymer fastener is ready by using waste materials and debris and GGBS with basic fluids sodium hydroxide and sodium silicate.

Ali A. Aliabdo et.al (2016) utilized inventive mechanical waste fly debris as a replacement of cement and the impact of little expansion of cement with fly debris is depicted in this work. The target of the investigation is to discover the compressive strength, split elasticity attributes of fly debris based geopolymer and with some expansion of cement. This

paper additionally expects to discover the soluble arrangement resting time, restoring period, and relieving temperature on fly debris based geopolymer concrete.

Hardijito et.al (2008) explains that geopolymer concrete and its mechanical properties. The author also explains the compositions of geopolymer concrete and its characteristics as well. We can get good compressive strength of geopolymer concrete with additionally demonstrated. the fluid proportion of mass is depending on the proportion of sodium silicate to sodium hydroxide. There is an expansion in compressive strength with the increment in restoring temperature. Longer restoring time likewise expanded the compressive strength.

Usha et.al (2015) in this author explains the importance of geopolymer concrete and its uses in various civil engineering structures. In this investigation, fly debris was supplanted by various mineral admixtures

Shankar sanni et.al (2013) led a test examination on geopolymer concrete and dependent on fly debris. The evaluations picked for the examinations are done for various mix proportions. The antacid arrangement utilized for the examination was the blend of two important solutions in the first one is sodium silicate, another important second solution is hydroxide arrangement, and used proportions are 2, 2.50, 3, and 3.50.

3. METHODOLOGY

COARSE AGGREGATES

In these Locally available materials are used mostly such as crushed granite and the size of stone aggregates are taken according to Indian code standard such as ten millimeters in size. These two important sieve pans are used for the classification of aggregates such as 10mm and 4.75mm. by using these sieves we can determine the type of aggregates and properties also according to IS.

RHA (RICE HUSK ASH)

Rice husk is a natural material that is obtained from farming in agriculture. There are several usages increases nowadays. The main reason for that is locally available material and also very cheap compared to other materials. this is used as an ecological material for strengthening cementing material.



Fig. rice husk ash

Sr. No.	Particulars	Properties
1	Colour	Gray
2	Shape Texture	Irregular
3	Mineralogy	Non Crystalline
4	Particle Size	< 45 micron
5	Odour	Odourless
6	Specific gravity	2.3
7	Appearance	Very fine

Table. Properties of RHA

MANUFACTURED SAND

Artificial sand (M-Sand) can replace quicksand for concrete development. The artificial sand is sent out from the hard rock by crushing. The squashed sand particles are in the shape of a cube, and the edges are grounded. After cleaning and inspection, they can be used as developing materials. The size of artificial sand (M sand) is less than 4.75mm. Artificial sand is an alternative to quicksand. Due to the rapid industrial development, people's interest in the sand has greatly increased, which in most cases leads to insufficient sand for proper waterways.

Properties	Type of sand	
	M-sand	River sand
1. Textural composition (% by weight)		
Coarse sand (4.75-2.00 mm)	28.1	6.6
Medium sand (2.00-0.425 mm)	44.8	73.6
Fine sand (0.425-0.075 mm)	27.1	19.8
2. Specific gravity	2.63	2.67
3. Bulk density (kN/m3)	15.1	14.5
4. pH	10.11	8.66
5. Chemical composition of M-sand		

Table. Types of sand and properties

GGBS: GGBS is gotten quickly chilling (extinguishing) liquid debris from the heater with the assistance of water. During this procedure, the slag gets divided and changed into nebulous granules (glass), meeting the prerequisite of IS Code (fabricating particular for granulated slag utilized in Cement). The granulated slag is ground to wanted fineness for delivering GGBS. The substance creation of JSW's GGBS adds to the creation of unrivaled cement.



Fig. GGBS

Binder	LOI	Al ₂ O ₃	Fe ₂ O ₃	SiO ₂	MgO	SO ₃	Na ₂ O	Chlorides	CaO
Fly ash	.9	31.2	1.5	61.12	.75	.53	1.34	.06	3.2

Table. composition of Fly ash

Properties	Material: Fly ash
Color	grey
pH	8.40
Specific gravity	2.15
Liquid limit (%)	32
Plastic limit (%)	non-plastic
Plasticity index (%)	non-plastic
Sand (%) (4.75–0.075 mm)	26.11
Silt (%) (0.075–0.002 mm)	70.89
Clay (%) (<0.002 mm)	3.00

Table. Fly ash & GGBS Properties

FLY ASH

It is one of the important materials used in geopolymer concrete. In this Class, F type is Low calcium and fly ash obtained from Enmore thermal power station and it was analyzed as per IS:38121981 having a specific gravity of 2.21 were used. ASTM-Fly ash came from the coal-burning power station.



Fig. Fly ash

Sl. number	Physical properties	Observed values
1	Specific gravity	2.51
2	Initial setting time	45 Min
3	Final setting time	280 Min
4	Consistency	35%

Table. Physical properties of Fly ash

4. EXPERIMENTAL RESULTS

SLUMP CONE TEST

It is one of the important types of tests used in concrete. This type of test gives a good result for the workability and properties of concrete as well. This is used to evaluate the performance of concrete. This test is accurate and quantifies the function of the new concrete. More specifically, it is used to measure the consistency between groups. It is a simple and easy test and an easy-to-use method. This test is used to know the workability. In the given below showing a slump test with having various steps.

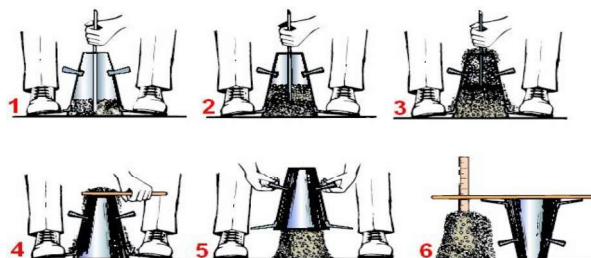


Fig. Showing Steps involved in the slump cone test.

SLUMP CONE TEST

S.No	%GGBS+%RHA+%M-Sand	The slump in mm for M40 Grade concrete
1	0%GGBS+0%RHA+0%M-sand (Mo)	56
2	2.5%GGBS+2.5%RHA+5%M-sand (M1)	42
3	5%GGBS+5%RHA+10%M-sand (M2)	36
4	7.5%GGBS+7.5%RHA+15%M-sand (M3)	26
5	10%GGBS+10%RHA+20%M-sand (M4)	22

Table. The slump in mm for M40 Grade concrete.

COMPACTION FACTOR TEST

It is one of the important tests of concrete. In this test cylinder and trowel are used to level the concrete surface in the mould. This test gives a better result. It is used to know the workability. It consists of two cylindrical hoppers. Which are installed one another above one. Sometimes for better operation, we can use grease on the inner surface of the hoppers and the cylinder. We can take the weight of the empty cylinder. Place the cylinder below the hoppers and start the procedure. Observe the mix, if the color of the mixture is uniform, we can get good results. If the color of the mix is non-uniform repeat the process to get the uniform and homogeneous mix.



Fig. compaction factor test Apparatus



Fig. Cube testing under Compressive strength

COMPACTION FACTOR TEST (C.F.)

S. No	%GGBS+%RHA+%M-Sand	C.F. for M40 Concrete
1	0%GGBS+0%RHA+0%M-sand (M0)	.82
2	2.5%GGBS+2.5%RHA+5%M-sand (M1)	.84
3	5%GGBS+5%RHA+10%M-sand (M2)	.88
4	7.5%GGBS+7.5%RHA+15%M-sand (M3)	.92
5	10%GGBS+10%RHA+20%M-sand (M4)	.96

Table. Compaction factors for M40 Grade concrete

COMPRESSIVE STRENGTH

S.NO.	%GGBS+%RHA+% M-Sand	7 days Mpa	14 days Mpa	28 days Mpa
1	0%GGBS+0%RHA+0% M-sand (M0)	26.1	35.5	39.3
2	2.5%GGBS+2.5%RHA+ 5%Msand (M1)	26.95	36.11	39.87
3	5%GGBS+5%RHA+10 %Msand (M2)	27.31	36.95	40.21
4	7.5%GGBS+7.5%RHA+ 15%Msand (M3)	26.81	36.43	39.71
5	10%GGBS+10%RHA+2 0%Msand (M4)	26.35	35.81	39.31

Table. Results of the strength of cubes

SPLIT TENSILE STRENGTH

It is one of the important types of tests used in concrete. In this load is applied cylinders between the equipment. The next force is required to break the cylinder is noted in the dial gauge in KN. After the calculation of tensile force, we can determine the tensile strength easily by using numerical formula. The sample is taken out from the curing tank and set for drying for 1 to 2 hours. On either side of the cylinder of specimens draw the diametrical lines to make sure that the lines represent the same axial place. Place the plywood strips on the lower plate of CTM and fix the cylinder over it. As per IS 456-2000

COMPRESSIVE STRENGTH

It is one of a good test. In this one cube is placed between the testing equipment and then apply the load. The dial gauge shows the force reading in KN. By using these readings we can calculate the strength. The below figure clearly shows that cube and testing machine. The process of testing is very simple and easy to use in the laboratory.

the tensile capacity of concrete is $0.7\sqrt{f_{ck}}$. Split tensile strength= $PD/\pi DL$



Fig. cylinder under Split tensile strength

SPLIT TENSILE STRENGTH

S.No	%GGBS+%RHA+%M-Sand	7 days Mpa	14 days Mpa	28 days Mpa
1	0%GGBS+0%RHA+0%M-sand (Mo)	2.55	2.97	3.13
2	2.5%GGBS+2.5%RHA+5%Msand (M1)	2.5	3.03	3.19
3	5%GGBS+5%RHA+10%M-sand (M2)	2.67	3.11	3.25
4	7.5%GGBS+7.5%RHA+15%Msand (M3)	2.58	2.95	3.2
5	10%GGBS+10%RHA+20%Msand (M4)	2.57	2.79	3.01

CONCLUSIONS

Under normal operating room temperature, geopolymer concrete often does not show obvious physical changes, but can be observed under normal conditions. The complete Geopolymer concrete specimen placement process takes up to 72 hours without hardening the surface. 5%GGBS+5%RHA+10%M-sand had a maximum compressive strength, split tensile and flexural strength. 8m can make good use of power, and the average strength can be increased by 8m. The higher the ratio of GGBS + RHA + M-Sand, the higher the durability of concrete caused by acid attack, alkali attack, and sulphate attack. As the best substitute for

cementing materials, GGBS has the characteristics of high compressive strength, low heat of hydration, chemical corrosion resistance, better workability, durability, and high cost-effectiveness. The excess temperature in oven curing causing cracks on cubes Rice husk ash is also the reason for high compressive strength and its reason for avoiding chemical reactions. The acid solution has an obvious corrosive effect on cement-based materials. The aggressive solution increases as the acid concentration increases.

ACKNOWLEDGEMENT

In this paper My sincere thanks to My Project Guide Dr. Dinesh Kumar and My MTech Co-Ordinator Dr. A.R. Prakash and Dr. Bharathi Murugan, Head of the Department, Civil & Structural Engineering.

REFERENCES

- [1] Habert, "evaluation of geopolymer based concrete" *J. Clean. Prod.*, 2011.
- [2] Singh, Bhattacharyya, "Geopolymer concrete" *Construction and Building Materials*. 2015.
- [3] Zhang, "Geopolymer foam concrete for construction" *Construction and Building Materials*. 2014.
- [4] Sarker, "The effects on properties of geopolymer concrete" *Mater. Des.*, 2014.
- [5] Sarker, "Effect of fire on geopolymer concrete," *Mater. Des.*, 2014.
- [6] Alengaram, "geopolymer concrete and Structural performance A review" *Construction and Building Materials*. 2016.
- [7] Nikraz, "Properties of fly ash geopolymer concrete" *Mater. Des.*, 2012.
- [8] Hassan, "Use of geopolymer concrete and sustainable environment" *Journal of Cleaner Production*. 2019.
- [9] Chareerat, "Workability and strength of fly ash geopolymer" *Cem. Concr. Compos.*, 2007.
- [10] Rangan, "Environmental protection by using Geopolymer concrete" *Indian Concr. J.*, 2014.
- [11] Chalee, "mechanical properties of geopolymer concrete by using fly ash" *Constr. Build. Mater.*, 2014.
- [12] Pouhet 2016, "performance of fly ash geopolymer concretes" *Constr. Build. Mater.*

STRENGTH ANALYSIS OF CONCRETE WITH PERCENTAGE REPLACEMENT OF CEMENT BY GLASSPOWDER

1st sriramoju Sravani

Department of civil

Engineering

Vaagdevi College of

Engineering

Warangal, India

sravani9705@gmail.com

2nd Dr.G.Dineshkumar

Department of Civil

Engineering

Vaagdevi College of

Engineering

Warangal,India

gdkcivil@gmail.com

ABSTRACT—Industrial wastes are currently damaging the environment. The goal of this research is to see if goods can reuse such waste for new purposes. The users may be satisfied by this glass waste. This leftover glass was ground into powder and repurposed. Glass powder is replaced in proportions of 0%, 2.5%, 5%, 7.5%, 10%, and 10%, with a water cement ratio of 0.45 and a cure period of 7,14,28 days. Glass powder may cause minor changes in concrete workability and a little increase in mortar flow. The recognised replacement of glass powder concrete is tested. The glass powder increases the concrete's tensile strength. Pozzolanic reactivity is a property of glass powder. It possesses the Glass is unstable in the alkaline environment of concrete, and this harmful alkali-silica interaction causes issues. The use of glass powder in concrete saves money by reducing the amount of money spent on glass powder disposal. In this experiment, we compare the properties of concrete with finely powdered glass to those of regular concrete. Based on the results, tumbler powder can be used as a cement replacement fabric as long as the **particle size is less than 300m, saving you alkali silica reaction.**

Keywords: Glass powder, Concrete, Mortar, Compressive strength, split tensile strength.

Introduction:

Because of its substance and the growing infrastructure business, concrete is now the most commonly utilised construction material. Cement production in our country is estimated to reach over 500 million tonnes by 2020, and 800 million tonnes by 2030. To reduce the impact of global warming on the environment, new binders for concrete must be introduced. Various research have recently been conducted to repurpose waste glass as a percentage substitute for commonly used materials in concrete production in order to reduce CO₂ emissions. The development of chemical reactions between the silica present in glass particles and the alkali matter present in the rest of the concrete, known as the Alkali – Silica reaction and commonly referred to as "Concrete Cancer," is a major problem with glass powder in the concrete making process. It is very harmful for the sustainability of concrete to withstand the design life period if appropriate precautions are not taken to reduce their effects. The use of mineral admixtures to concrete reduces the Alkali–

Silicate reaction. Fuel ash, silica fume, and metakaolin are the most commonly utilised mineral admixtures to reduce the Alkali-Silicate reaction.

Waste Glass Source:

Food storage glass bowls and glass door doors manufacturing shops.

Glass decorative items and outdated tube lights, electric bulbs.

At Glass polishing and glass window and door manufacturing shop.

II LITERATURE REVIEW:

1.Dr.G. Vijayakumar, MS H. Vishaliny, Dr.D. Govindarajulu, et al., (2013). Studies are carried out at 10, 20, 30, and 40% replacement levels in this study. This study found that increasing the compressive strength by 19.6%, 25.3 percent, and 33.7 percent enhances the compressive strength by 20 percent, 30 percent, and 40 percent. At 40% replacement, tensile strength increased by 4.4 percent.

2.Hongian Du, Kiang Hwee Tan, et al., (2014). Cement concentrations of 15, 30, 45, and 60 percent by weight have been found in research trials. The rate and total heat output at the hydration process are insignificant, according to the test results. They concluded from the test data that satisfactory outcomes occur at a glass powder replacement rate of 30%.

3.Dhanaraj Mohan Patil, Dr. Keshav K. Sangle, et al., (2013) The cement is replaced in three stages: 10%, 20%, and 30%. They found that, aside from glass, powder early-stage strength is poor, but design strength can be obtained in 28 days and the best replacement percentage is 20%.

III MATERIALS:

CEMENT:

Cement is a binding material that is used in building and goes through a setting process before hardening. We used opc 53 cement in this project, which complies with IS:1026210262-2009.

FINE AGGREGATE:

The particles that pass through the 4.75mm sieve. It's also a budget-friendly option. IS 383-1970 codal provision is followed.

COARSE AGGREGATES:

Weathering of rocks produces coarse aggregates, which are particles that pass through a 4.75mm screen. Coarse aggregates account for 60-80% of the concrete volume. IS:383-1970 codal provisions are followed.

Glass powder:

Waste glass was ground into powder and passed through a 300 micron sieve, with more than 95 percent passing through a 600 micron sieve. In this mixing procedure, the right amount of cement, fine aggregates, and coarse aggregates are combined with the right amount of water and no salts.



To begin, mix the fine and coarse aggregates for 2-3 minutes, then add cement and glass powder according to % replacement, then add 0.45 water content and mix thoroughly

IV COMPRESSIVE AND SPILT TENSILE STRENGTH TESTS ON CONCRETE

For evaluating compressive and spilt tensile strength on concrete, a 150150150mm cube and a 300150mm cylinder were cast.

A) Compressive strength test:

Compressive strength test on concrete cube samples is done by using universal testing machine (UTM). This test done for different level of curing periods like 7,14,28 days for different levels of replacement of glass powder



B) Split Tensile Strength of Concrete:

The split tensile strength of cylinders is tested using a



universal testing machine (UTM). This material was written for several levels of curing durations, such as 7,28 days, for varied amounts of glass powder replacement.

V. Results and Analysis:

1) TESTS ON CEMENT:

S.No	Test	Results
1	SpecificGravity	3.17
2	InitialAndFinalSetting Time	36mins And10 Hours
3	StandardConsistency	7mmAt27%W/C
4	Fineness	6%

2) TESTS ON PHYSICAL AND CHEMICAL PROPERTIES OF GLASS POWDER:

S.No	Chemicals	GlassPowder(%)
1	SiO ₂	73
2	Al ₂ O ₃	1.4
3	Na ₂ O	12.1
4	CaO	11.3
5	MgO	0.72
6	K ₂ O	0.4
7	SO ₃	0
8	UnitWeight(kg/m ³)	2580

S.No	PhysicalProperties	GlassPowder
1	Fineness	<75
2	Color	White
3	Specificgravity	2.4-3

2) TESTS ON FINEAGGREGATES:

S. No	Tests	Results
1	Fineness modulus	2.8
2	Specific gravity	2.5
3	Bulking of sand	3.2%

3) TESTS ON COARSEAGGREGATES:

S.No	Test	Results
1	Fineness modulus	6.6
2	Specific gravity	2.8
3	Aggregate impact value	36%
4	Aggregate crushing value	37%

1.COMPRESSIVE STRENGTH:

S.no	% Replacement of GP	Avg Compressive load			Cross sectional Area	Avg Compressive strength in MPa		
		7 Days	14 Days	28 Days		7 Days	14 Days	28 Days
1	0.00%	140	165	190	10000	14	16.5	19
2	2.50%	160	200	225	10000	16	20	22.5
3	5.00%	185	235	270	10000	18.5	23.5	27
4	7.50%	180	220	250	10000	18	22	25
5	10.00%	150	210	230	10000	15	21	23

2.SPLIT TENSILE STRENGTH:

S.no	% Replacement of GP	Avg Split tensile load in kN		Cross section al Area	Avg Compressive strength in MPa	
		7 Days	28 Days		7 Days	28 Days
1	0.00%	75	140	141368	1.06	1.98
2	2.50%	160	220	141368	2.26	3.11
3	5.00%	120	200	141368	1.69	2.82
4	7.50%	125	170	141368	1.76	2.40
5	10.00%	130	165	141368	1.83	2.33

VI CONCLUSION:

Based on the findings of the study, the following conclusions have been drawn:

1. The compressive strengths of concrete at 7 days, 14 days, and 28 days increase initially as the fraction of cement replaced by glass powder increases, peaking at around 5% and then declining.
2. The split tensile strength of concrete rises initially as the amount of cement replaced with glass powder rises, peaks at around 2.5 percent, and then falls.
3. The drop of concrete decreases in a consistent manner when it is replaced.
4. The percentage of cement containing glass powder rises. When cement is largely replaced with glass powder, workability suffers.
5. The results of this investigation demonstrate that using glass powdering concrete as a partial replacement for cement has a lot of potential. Glass powder can be used to replace about 20% of cement without sacrificing compressive strength.

REFERENCES:

- Ahmad Shayan and Aimin Xu, "Performance of Glass Powder as A Pozzolanic Material In Concrete A Field Trial on Concrete Slabs", Volume 36, Issue 3, (20 March 2006), ELSEVIER.
- Aluko, O.G, Oke, O.L, Awolusi and T.F., "A Study on The Short-term Compressive Strength of Compressed Stabilized Earth Block with Waste Glass Powder as Part Replacement for Cement", Vol. 4, Issue 12,(2015), IJSTR.
- Ashutosh Sharma¹, Ashutosh Sangamner² "STUDIES ON GLASS POWDER – A PARTIAL REPLACEMENT FOR CEMENT" Volume 1, Issue 11, February 2015, IJCEM.
- Dhanaraj Mohan Patil¹ Dr. Keshav K. Sangle² "Experimental Investigation of Waste Glass Powder as Partial Replacement of Cement in Concrete" Volume 2, Issue (2013), IJAT.
- Dr.Vijayakumar¹. G, Ms Vishaliny². H, Dr. Govindarajulu³.D "Studies on Glass Powder as Partial Replacement of Cement in Concrete Production" Volume 3, Issue 2, February 2013, IJETAE.
- Hongian Du¹, Kiang Hwee Tan² "Studies on Waste Glass Powder as Cement Replacement in Concrete" Volume 1, November 2014, JACT.
- IS: 4031 (1996). "Indian Standard Method of Physical Tests for Hydraulic Cement." Bureau of Indian standards, Manak Bhavan, 9 Bahadur Shah Zafar Marg, New Delhi 110002.
- IS: 516 (1959). "Indian Standard Methods of Tests for Strength of Concrete." Bureau of Indian standards, Manak Bhavan, 9 Bahadur Shah Zafar Marg, New Delhi 110002.
- IS: 456 (2000). "Indian Standard Plain and Reinforced Concrete Code of Practice." Bureau of Indian standards, Manak Bhavan, 9 Bahadur Shah Zafar Marg, New Delhi 110002.
- IS: 10262 (1982) (Reaffirmed 2004). "Recommended Guidelines for Concrete Mix" Bureau of Indian standards, Manak Bhavan, 9 Bahadur Shah Zafar Marg, New Delhi 110002.
- Jitendra B,Jangid and Saoji A.C., "Comparative Study of Waste Glass Powder as The Partial Replacement Of Cement In Concrete Production- A Laboratory Investigation", Volume 3 , Issue 2, (2015),IJRNTCC.
- Adaway.M and Wang.Y, "Recycled Glass as A Partial Replacement for Fine aggregate In Structural Concrete –Effect on Compressive Strength "Vol 14, Issue 1 (2015), EJSE.
- Madhangopal¹.
K,Nagakiran².B,Sraddha³.S.R,Vinodkumar⁴.G,T
hajun⁵.P,KishoreSankeerth
6.S.A,Varalakshmi⁷.T "Study on The Influence of Waste Glass Powder on The Properties of Concrete" Volume 11, Issue 2, Mar-Apr:2014, (IOSR-JMCE).
- Mafalda Matosa, Telma Ramos^b, Sandra Nunes, and Joana souze-Coutinho, "Durability Enhancement of SCC With Waste Glass Powder", DOI:
- Nathan Schwarz, Hieu Cam, Narayanan Neithalath, "Influence of A Fine Glass Powder on The Durability Characteristics of Concrete and Its Comparison to Fly Ash" Volume 30 Issue 6 (6 July 2008), ELSEVIER.
- Prema kumar WP, Ananthayava MB and Vijay K "Effect Of Partial Replacement Of Cement With Waste Glass Powder On The Properties Of Concrete", Volume 3, Issue 2 (May 2014), IJSCER.
- Raghavendra K and virendra kumara K N, "Reusing of Glass Powder and Industrial Waste Material In Concrete", Vol. 4, Issue 7, (July 2015), IJRET.
- Rakesh Sakale, Sourabh Jain and Seema Singh, "Experimental Investigation on Strength of Glass Powder Replacement by Cement in Concrete with Different Dosages", Vol.5, Issue 12, (December 2015), IJARCSE.
- Sadiquallslam¹.G.H, M.H. Rahman², Nayemkazi³ "Waste Glass Powder as A Partial Replacement of Cement for Sustainable Concrete Practice" Volume 6, Issue 1, June 2017, IJSBE.
- Schwarz Nathan and Neithalath Narayanan, "Influence of A Fine Glass Powder On Cement Hydration Comparison To Fly Ash And Modeling The Degree Of Hydration" 2008.
- Sombir¹, Praveen Berwal² "A Laboratory Study on The Use of Waste Glass Powder As Partial Replacement Of Cement In Concrete Production" Volume 3, Issue 1(2017), IJARIT.
- Shuhnu Liu, Shu Wang, Wan Tang, Ningning Hu and Jianpeng Wei, "Inhibitory Effect Of Waste Glass Powder On Asr Expansion Induced By Waste Glass Aggregate" October 2015, pp.6849-6862.
- Vasudevan¹ Gunalaan, Seri Ganis Kanapathy pillay² "Performance of Waste Glass

A MACHINE LEARNING METHODOLOGY FOR DIAGNOSING CHRONIC KIDNEY DISEASE

Name : G. Neelima

Mail ID: neelimagade39@gmail.com

MTECH-CNIS, Vaagdevi College of Engineering, bollikunta, warangal

Guide:

Email ID: ayeshabanuvce@gamil.com

Name : Dr. Ayesha Banu

Associate Professor of CSE Department,
Vaagdevi College of Engineering, bollikunta, warangal

Abstract:

Chronic kidney disease (CKD), which is also a key risk factor for other diseases, kills and disables people all over the world. Because there are no evident signs in the early stages of CKD, it might go unnoticed. Medicine that decreases the progression of renal disease can be used to prevent it from progressing in patients who are diagnosed early. Clinicians can achieve their objectives more quickly by using machine learning models. This study suggests a CKD diagnosis approach based on machine learning. In the UCI machine learning repository, missing values in the CKD data set were discovered. The most similar measures from a large number of full samples were used to fill in the missing data in each partial sample using KNN imputation. Patients may forget to take measures in the real world for a variety of reasons, resulting in missing data. Six machine learning approaches were employed to construct models when the missing data set was completed: logistic regression, k-nearest neighbour, naive Bayes classifier, and feed forward neural network. With a diagnosis accuracy of 99.75 percent, Random Forest is the most accurate of these machine learning models. After ten simulations based on the errors generated by the constructed models utilising the integrated model, an average accuracy of 99.83 percent can be achieved. As a result, we came to the conclusion that this method may be used to diagnose more complex clinical disorders.

Introduction:

Chronic kidney disease (CKD) affects roughly 10% of the world's population, making it a significant public health issue. [3] Chronic kidney disease (CKD) affects 10.8% of Chinese individuals, compared to 10–15% in the US. Unemployment in Mexico has risen to 14.7 percent, according to a new survey. Renal function declines over time, and the kidneys eventually cease to function. When kidney disease is in its early stages, there are no visible indicators of it. It's likely that the illness won't be diagnosed until the kidney has lost around 25% of its function. Chronic kidney disease has a severe impact on the human body, with high rates of morbidity and mortality. It can lead to cardiovascular disease. Once CKD has started, it is impossible to stop it. Patients who are recognised earlier in the disease's progression can receive treatment to halt or stop it, which is why early identification and diagnosis are so critical. A computer programme that combines data and deductive reasoning to learn the features of a particular pattern is an example of machine learning. This technology may be a viable tool for diagnosing CKD in patients due to its capacity to reliably and economically diagnose illnesses. Electronic health records have evolved into a new type of medical equipment with a wide range of uses as a result of their rapid expansion. Machine learning has previously been used in the medical field to identify human body status, analyse disease factors, and diagnose a variety of diseases.

Heart disease, diabetes, retinopathy, acute renal injury, cancer, and other disorders that can be diagnosed using machine learning algorithms are just a few examples. Regression, tree, probability, decision surface, and neural network approaches were used in these models. Hodneland et al. employed image registration to identify kidney morphological alterations in order to diagnose CKD. Vasquez-Morales et al. used large CKD datasets to construct classifiers that had a 95% accuracy rate on their test data.

Chemometrics can be used to investigate the relationships between various items and factors using a multivariate method. The application of chemometric-based multivariate classifiers in the diagnosis of chronic kidney disease (CKD) may be beneficial. Patients with chronic kidney disease can use fuzzy logic and fuzzy mathematics diagnostic models to better understand and diagnose their illness.

L.A. Zadeh released his seminal work on fuzzy set theory in 1965. "Fuzzy set theory," an infinite-valued logic, allows for less-than-perfect reasoning. Crisp ingredients may or may not be included in the kit. Components in fuzzy sets are only marginally significant. The borders of the set get blurry as a result of this. Fuzziness is a metric of representational ambiguity, not likelihood, rather than assessing the frequency with which something will occur. Fuzzy logic has already been used to handle a variety of challenges in bioinformatics and system biology. C.T. Zhang et al. used fuzzy clustering to create predictions about protein structure classes based on the amino acid content of the samples studied. H.B. Shen et al. used a mix of supervisory fuzzy clustering and fuzzy K-nearest neighbour to produce predictions regarding protein structural classes and membrane protein types. A fuzzy support vector machine network and fuzzy K-nearest neighbour were used to predict protein structure classes based on pseudo amino acid content. The fuzzy K-nearest neighbour

technique has been used to tackle a variety of biological challenges, including the discovery of nuclear receptor subfamilies and G-protein receptors by X. Xiao et al. It was also used by Xiao et al. to predict the channel-drug interaction. Classification problems that can be solved with fuzzy approaches include endometrial cancer and cervical cancer diagnosis, herbal drug identification, and diabetes mellitus diagnosis. One of the benefits of using FOAM for single-class classification is that it exploits feature similarities inside the class. All classes must be defined differently from FOAM in order to use FuRES as a supplementary classification method. A linear multivariate classification strategy based on the standard partial least squares regression method, also known as PLS-DA (partial least squares discriminant analysis). For the purposes of this discussion, we can assume that the response matrix Y contains variables or labels that characterise the sample categories that correspond to the prediction matrix X . This is a rare example of PLS in action.

The ultimate goal of machine learning is to construct models that can swiftly generalise and categorise from instances observed before they were created (ML). ML creates these models by either constructing or learning functional correlations between the user-selected input and output feature domains. Patients with CKD can be identified by sorting the information gathered from their symptoms (features) into helpful categories (groups of healthy individuals, CDK individuals, or individuals with the some other type of ailment).

CKD is a long-term health issue that affects nearly 10% of the world's population. In real-life cases of CKD, however, cardiovascular disease and renal function decline are frequently linked to an increased risk of hospitalisation, morbidity, and even death (s). Chronic kidney disease (CKD) patients are more likely than the general population to develop atherosclerosis and other symptoms.

See discussions, stats, and author profiles for this publication at: <https://www.researchgate.net/publication/371379371>

Academic Performance Prediction of intoxicating Students Using Intelligent Data Mining Techniques

Article · January 2021

DOI: 10.46501/IJMTST0712084

CITATIONS

0

READS

87

3 authors:



Rama M A

Maharani Lakshmi Ammanni College for Women

18 PUBLICATIONS 149 CITATIONS

SEE PROFILE



Ayesha Banu Mohd

Vaagdevi College of Engineering

30 PUBLICATIONS 51 CITATIONS

SEE PROFILE



Zareena Begum

Madras School of Economics

10 PUBLICATIONS 37 CITATIONS

SEE PROFILE



Academic Performance Prediction of intoxicating Students Using Intelligent Data Mining Techniques

M. Rama¹ | Dr.Ayesha Banu² | Zareena Begum³

¹Assistant Professor, Dept. Of Computer science and engineering, Vaagdevi College of Engineering, Bollikunta.

²Associate Professor, Dept. of Computer science and engineering (Data Science), Vaagdevi College of Engineering, Bollikunta

³⁸⁹⁰Assistant Professor, Dept. of Computer science and engineering (Data Science), Vaagdevi College of Engineering, Bollikunta

To Cite this Article

M. Rama, Dr.Ayesha Banu and Zareena Begum. Academic Performance Prediction of intoxicating Students Using Intelligent Data Mining Techniques. *International Journal for Modern Trends in Science and Technology* 2022, 7 pp. 459-462. <https://doi.org/10.46501/IJMTST0712084>

Article Info

Received: 29 November 2021; Accepted: 28 December 2021; Published: 03 January 2022

ABSTRACT

Alcohol consumption by students has become a significant issue these days. Addiction to alcohol results in the poor tutorial performance of scholars. This paper describes few algorithms that facilitate to boost the potency of educational performance of students captivated with alcohol. Within the paper, we tend to area unit victimisation one amongst the favoured Data Mining technique—"Prediction" and checking out the simplest formula among different algorithms. Our project is to investigate the educational excellence of the school professionals by creating use of WEKA toolkit and R Studio. We implement this project by making use of alcohol consumption by student datasets provided by kaggle web site. It is composed of 395 tuples and 33 attributes. A classification model is constructed by making use of Naïve Bayes and ID3. Comparison of accuracy is finished between R and WEKA. The prediction is performed so as to seek out whether or not a student will be promoted or demoted within the next year once previous year marks area unit considered.

Keywords: Data Mining , Prediction ,Naïve Bayes ,ID3 ,WEKA ,R studio.

1. INTRODUCTION

A large amount of knowledge is being made from completely different fields a day so as to pull out a legitimate and helpful knowledge that is employed during a decision-making method. The decision-making method is performed by victimization completely different data processing techniques. Various Mining Techniques Classification, Prediction, Clustering and Association. Classification is that the method of composition the information supported similarities. It is a supervised learning technique as we have a tendency to build the model by creating use of coaching data that consists of sophistication labels. Clustering is that the grouping of objects supported the principle of

accelerating the intra-cluster distance and decreasing the inter-cluster distance. Prediction is that the method of dig out the knowledge from an enormous quantity of data and helps to predict the end result no matter the past, present, and future events. The prediction data processing technique is employed so as to predict the performance of the scholars. Using Naïve theorem and ID3 algorithms we have a tendency to designed a model and found out the accuracy each in WEKA and R and therefore the comparison between them is performed.

2. RELATED WORK

In [1] they need used totally different data processing technologies to investigate students' performance in the courses. They need used

FACE MASK DETECTION

Vanam Yoganand¹

Dr. Thanveer Jahan²

¹M.Tech Department of Computer Science & Engineering , Project Title: Face Mask Detection, vaagdevi college of engineering (UGC autonomous) approved by AICTE & permanent affiliation to jntuh, hyderabad.p.o, bollikunta, Warangal urban- 506005.

² Associate Professor Department of Computer Science & Engineering vaagdevi college of engineering (UGC autonomous) approved by AICTE & permanent affiliation to jntuh, hyderabad. p.o, bollikunta, Warangal urban- 506005.

Abstract: Face Mask Detection for safety purpose due to the outbreak of Covid-19. This project can be integrated with embedded systems for many applications in airports, railway stations, offices, education institutions and public places to ensure that public safety guidelines are followed. here we will focus on loading our face mask detection dataset from disk, training a model using python, keras/ TensorFlow on this dataset, and then serializing the face mask detector to disk. Once face mask detector is trained, we can move on to loading the mask detector, performing face detection, and then classifying each face as with mask and without mask.

1. INTRODUCTION

The year 2020 has shown mankind some mind-boggling series of events amongst which the COVID-19 pandemic is the most life-changing event which has startled the world since the year began. Affecting the health and lives of masses, COVID-19 has called for strict measures to be followed in order to prevent the spread of disease. From the very basic hygiene standards to the treatments in the hospitals, people are doing all they can for their own and the society's safety; face masks are one of the personal protective equipment. People wear face masks once they step out of their homes and authorities strictly ensure that people are wearing face masks while they are in groups and public places.

To monitor that people are following this basic safety principle, a strategy should be developed. A face mask detector system can be implemented to check this. Face mask detection means to identify whether a person is wearing a mask or not. The first step to recognize the presence of a mask on the face is to detect the face, which makes the strategy divided into two parts: to detect faces and to detect masks on those faces. Face detection is one of the applications of object detection and can be used in many areas like security, biometrics, law enforcement and more. There are many detector systems developed around the world and being implemented. However, all this science needs optimization; In this project, we will be developing a face mask detector that is able to distinguish between faces with masks and faces with

no masks.

1.1 PROBLEM DEFINITION

Face Mask Detection is works on captured images of peoples by CCTV cameras, you can see that the faces are small, blurry, and, low resolution. People are not looking straight to the camera, and the face angles vary from time to time. These real-world images are entirely different from the images captured by webcams or selfie cameras, making the face mask detection problem much more difficult in practice.

2. LITERATURE SURVEY

Machine learning is an application of artificial intelligence (AI) that provides systems the ability to automatically learn and improve from experience without being explicitly programmed. Machine learning focuses on the development of computer programs that can access data and use it to learn for themselves.

The process of learning begins with observations or data, such as examples, direct experience, or instruction, in order to look for patterns in data and make better decisions in the future based on the examples that we provide. The primary aim is to allow the computers learn automatically without human intervention or assistance and adjust actions accordingly.

Deep Learning

Deep learning is an artificial intelligence (AI) function that imitates the workings of the human brain in processing data and creating patterns for use in decision making. Deep learning is a subset of machine learning in artificial intelligence that has networks capable of learning unsupervised from data that is unstructured or unlabelled. Also known as deep neural learning or deep neural network.

Neural Networks

Neural networks were vaguely inspired by the inner workings of the human brain. The nodes are sort of like neurons, and the network is sort of like the brain itself. (For the researchers among you who are cringing at this comparison: Stop pooh-poohing the analogy. It's a good analogy.) But Hinton published his breakthrough paper at a time when neural nets had fallen out of fashion. No one really knew how to

train them, so they weren't producing good results.

3. SYSTEM ANALYSIS

Manually by seeing faces of persons. Face Mask Detection System uses existing IP cameras and CCTV cameras combined with Computer Vision to detect people without masks.

PROPOSED SYSTEM

The proposed system focuses on how to identify the person on image/video stream wearing face mask with the help of computer vision and deep learning algorithm by using the OpenCV, Tensor flow, Keras and PyTorch library Approach

1. Train Deep learning model (MobileNetV2)
2. Apply mask detector over images / live video stream.

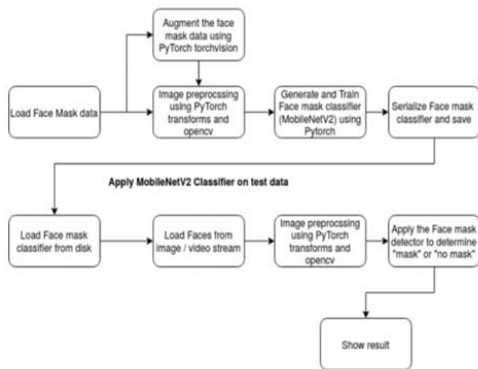


Fig 1: Flow chart Face Mask Detection

3.1 SYSTEM DESIGN

Create Architecture deals with the various UML diagrams for the implementation of ventures. Simulation may reflect an important device architecture to be created. Computer package format may be used to transform the design into the image of software packages. Modeling is the place where accuracy is reached in the development of electronic products. Modeling is an easy way to reliably transform customer expectations into completed goods.

Unified Modeling Language Description

The structured vocabulary mapping lets the technologist victimize the programming jargon governed by a set of grammar language and practical rules for particular research models. A UML framework is graded as 5 totally independent views, which describe the frame from a quite specific perspective. A series of diagrams outlines each item, which is:

User Model view

This view displays the device from the consumer point of view. The diagram depicts a condition of usage from the viewpoint of end-users.

Structural Model View

Knowledge and practicality come from inside the framework of this case. The static structures are read in this layout.

Behavioural Model view

It defines the operational dynamics as elements of the interface that reflect the specific relationships between the numerous structural components within the user model and the structural mechanism. Implementation Method View: Conceptual and action components of the system are built in this model.

Use case Diagram:

A Use Case Diagram may be a form of organizational diagram created from an analysis of the Use Case. The key aim of the case-by-case is to explain the practicality provided by the system in terms of agents, their objectives.

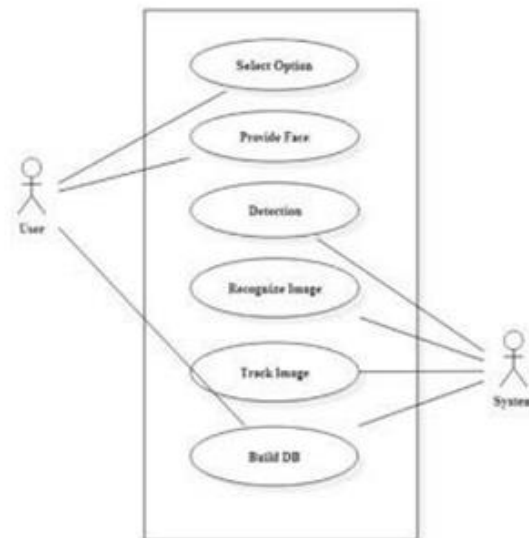


Fig 2: Usecase diagram for face mask detection

3.2 SYSTEM REQUIREMENTS

Software Requirements Specification plays an important role in creating quality software solutions. Specification is basically a representation process. Requirements are represented in a manner that ultimately leads to successful software implementation. Requirements may be specified in a variety of ways. However, there are some guidelines worth following:

Representation format and content should be relevant to the problem. Information contained within the specification should be nested Diagrams and other notational forms should be restricted in number and

consistent in use.

4.IMPLEMENTATION RESULTS IMPLEMENTATION PROCESS

1. Image acquisition
2. Image processing
3. Distinctive characteristic location
4. Template creation
5. Template matching

Isolate Face Shapes: Convoluting with Mask
 Resulting image from neural net had regions of interests that were not true faces. The unique oval-shape true faces were used. To isolate most probable regions of interest, the test image is convolved with an oval mask.

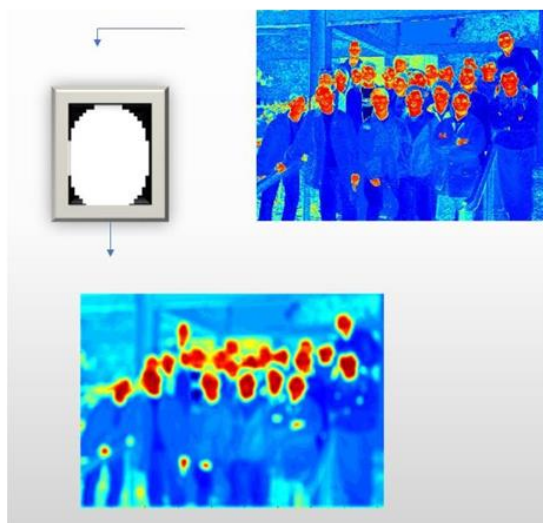


Fig 3: Isolate face shapes

Face Mask Recognition

- 1.Training: Here we'll focus on loading our face mask detection dataset from disk, training a model (using Keras/TensorFlow) on this dataset, and then serializing the face mask detector to disk
- 2.Deployment: Once the face mask detector is trained, we can then move on to loading the mask detector, performing face detection, and then classifying each face as,

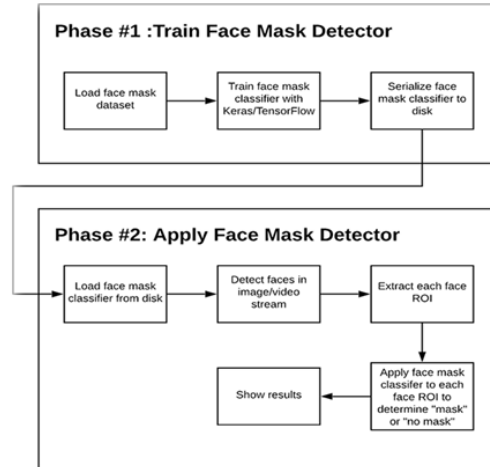


Fig 4: Phases and individual steps for building a COVID-19 face mask detector.

Face Mask Detection Datasets

A face mask detection dataset consists of “with mask” and “without mask” images. We will use the dataset to build a face mask detector with computer vision and deep learning using Python, OpenCV, and TensorFlow/Keras.



Fig 5: Dataset with mask
Output and code Screenshots

5. CONCLUSION

As the technology are blooming with emerging trends the availability so we have novel face mask detector which can possibly contribute to public healthcare. The architecture consists of MobileNet as the backbone it can be used for high and low computation scenarios. In order to extract more robust features, we utilize transfer learning to adopt weights from a similar task face detection, which is trained on a very large dataset. We used OpenCV, tensor flow, keras, PyTorch and CNN to detect whether people were wearing face masks or not. The models were tested with images and real-time video streams. The accuracy of the model is achieved and, the optimization of the model is a continuous process and we are building a highly accurate solution by tuning the hyper parameters. This specific model could be used as a use case for edge analytics. Furthermore, the proposed method achieves state-of-the-art results on a public face mask dataset. By the development of face mask detection, we can detect if the person is wearing a face mask and allow their entry would be of great help to the society.

6. TESTING AND VALIDATION

Checking requires finding the mistake. Testing is the mechanism through which some potential flaw or flaw is attempted in a particular job product. That is the simplest manner in which modules, subassemblies, panels and/or finished items are visualised. That is the mechanism by which the program is enforced to ensure that the device fulfils the specifications and consumer needs and does not operate improperly. Different types of controls have to be carried out. Every test case passes those evaluation requirements.

White Box Testing

White Box Checking may be a guide that understands or minimizes the code tester's purpose with respect to the internal feature, the feature and the language of the specification. Points that cannot be reached from a recording system level are typically checked. White-box tests may be a device inspection strategy to the level of the ASCII text script. Such test cases are focused on the usage of look strategies such as power flow analysis, flow management, division checking, route examining, claim coverage and requirement coverage as altered status and judgment coverage. White-box testing involves the use of tools such as manuals by evaluating a certain insecure application in a nursing system that is error-free. These methods of analysis include the building blocks of white- box technology; the essence is that the device is carefully checked on the ASCII text file to recognise and avoid hidden mistakes. Such radically different techniques use a special visible

ASCII text file path to eliminate errors and build a collaborator in an error-free nursing environment. The entire aim of Whitebox screening is to ensure the capacity to read the code line is dead and to evaluate the tests. The three essential measures that the White-Box check requires in test cases:

1.Entry involves various categories of standards, criteria, paper creation, right ASCII text file and protection criteria. This is the stage of White Box analysis to collect all the vital information.

2.Processing involves playing Risk Analysis to guide the whole research process, setting test cases, conducting test cases and reporting results accurately. This is the part of building test cases which ensures that the system is thoroughly tested by the defined unit of tests reported.

3.The production involves the creation of a structured report describing strategies and outcomes.

Blackbox Testing

Black Box Program manages the package or device without recognizing the internal processes, features or language of the product being tested. Blackbox assessments, like any other types of research, should be written from a standardized supply paper. It is often called a functional assessment under which the analysed system is known as a Blackbox. The analysis produces inputs and responds to outputs without knowing how the system functions. There is no need for specialized programming code knowledge, internal setup and technological expertise in general. The tester understands what the program should do but does not know how the program executes the necessary task. For e.g., the tester is aware that a specific input produces a different, unchanged output but does not know how the software produces the output first.

Functional Testing

Professional reviews provide detailed documentation that activities when assessed by an independent task entity supported by business and infrastructure specifications, programme's records and user manuals. Functional work focuses on the following issues: the categories found in the related data should be remembered. . Invalid data: Invalid knowledge forms found must be rejected • Functions: Functions identified must be performed correctly • Performance: Specified programs must be exercised. Programs / Procedures: calling or triggering system programs or procedures is important. Criteria, core processes or procedures or specific test cases are the focus of a dynamic research structure and planning.

Future Enhancement

Face masks now compulsory or recommended in various parts of the country. Face masks and facial recognition will both be common in the future.

References

- [1]P. A. Rota, M. S. Oberste, S. S. Monroe, W. A. Nix, R. Campagnoli, J. P. Icenogle, S. Penaranda, B. Bankamp, K. Maher, M.-h. Chenet al., "Characterization of a novel coronavirus associated with severe acute respiratory syndrome," *science*, vol. 300, no. 5624, pp. 1394–1399, 2003.
- [2]Z. A. Memish, A. I. Zumla, R. F. Al-Hakeem, A. A. AlRabeeah, and G. M. Stephens, "Family cluster of middle east respiratory syndrome coronavirus infections," *New England Journal of Medicine*, vol. 368, no. 26, pp.2487–2494, 2013.
- [3]Y. Liu, A. A. Gayle, A. Wilder-Smith, and J. Rocklöv, "The reproductive number of covid-19 is higher compared to sars coronavirus," *Journal of travel medicine*, 2020.
- [4]Y. Fang, Y. Nie, and M. Penny, "Transmission dynamics of the covid-19 outbreak and effectiveness of government interventions: A data driven analysis," *Journal of medical virology*, vol. 92, no. 6, pp. 645–659, 2020.
- [5]N. H. Leung, D. K. Chu, E. Y. Shiu, K.-H. Chan, J. J. McDevitt, B. J. Hau, H.-L. Yen, Y. Li, D. KM, J. Ipet al., "Respiratory virus shedding in exhaled breath and efficacy of face masks."
- [6]S. Feng, C. Shen, N. Xia, W. Song, M. Fan, and B. J. Cowling, "Rational use of face masks in the covid19pandemic," *The Lancet Respiratory Medicine*, 2020.

Graphical Exploratory Data Analysis (GEDA): A Case Study on Employee Attrition

Dr. Ayesha Banu, Dr. Sharmila Reddy, M. Rama

Associate Professor & Head, CSE(Data Science).Vaagdevi College of Engineering

headcsd@vaagdevi.edu.in

Associate Professor & Head, CSE(Data Science).Vaagdevi Engineering College

sharmilakreddy@vecw.edu.in

Assistant Professor,CSE,Vaagdevi College of Engineering

rama_m@vaagdevi.edu.in

To Cite this Article

Dr. Ayesha Banu, Dr. Sharmila Reddy, M. Rama, **Graphical Exploratory Data Analysis (GEDA): A Case Study on Employee Attrition**”,*Journal of Science and Technology*, Vol. 07, Issue 09,-November 2022, pp01-11

Article Info

Received: 28-09-2022

Revised: 17-09-2022

Accepted: 25-10-2022

Published: 5-11-2022

Abstract

Exploratory Data Analysis (EDA) popularly performs some preliminary investigations on the dataset to understand its content and structure. EDA is a mandatory step in the complete process of data analysis, since its mandatory to analyze the data in order to produce good results and in turn help in decision making. There are several Graphical EDA techniques which not only analyze the data but also present the results in graphical form. This paper uses the Python programming language for both data analysis and visualization of results. The rich set of python libraries including pandas, numpy, matplotlib, seaborn etc greatly supports the process of GEDA. This paper works on the “Employee Performance and Attrition” dataset to analyze and extract potential information and present results in graphical form.

Keywords: Graphical Exploratory Data Analysis, Python, Data Visualization,matplotlib, seaborn.

1. INTRODUCTION

In today’s world of technology data is growing very fast in both volumes and variety and it has become highly impossible to understand and analyze the data manually. Data analysis is collection of different processes to inspect, clean, transform, and model the data with an objective of discovering potentially useful information, drawing several conclusions, and finally supporting decision-making.Exploratory Data Analysis (EDA)evaluates or comprehends data and is a significant component of any process in data science or machine learning.It helps in exploring the data; understanding the structure and relationships between variables andbuilds a consistent and valuable output.

Python is a very popular programming language today due its flexibility andwide collection of inbuilt libraries, which are very essential to performdata analytics and complex computations.Pythonsupports multiple libraries for data analytics like NumPy for mathematical and statistical calculations and PandasthePython Data Analysis Library.Data visualization plays a vital role in representingthe data and also complex data relationships graphically such that it is easy to understand. Python has many libraries that support for displaying data in the form of charts, graphs , plots and animations. Two such popular libraries used in this work are Matplotlib and Seaborn.

This paper works on the “Employee Performance and Attrition” dataset to perform Exploratory Data Analysispresent results in graphical form using python. The paper is organized in to four sections. Section 2 briefs the review of literatureand section 3 explains the differenttechniques for EDA both non graphical and graphical. In section 4, the graphical exploratory data analysis is studied on the Employee Attrition dataset using python.

2. LITERATURE SURVEY

Aindrila et al. [1] made a study on the tools for data visualization with respect to their efficacy in the EDA process. They also examined the scalability of the exploration tools for analyzing large datasets. Matthew Ntow Gyamfi et al. [2] investigated the commercial banks practices regarding credit risk and loan default to find the causes of nonperforming loans. X. Francis Jency et al. [5] have performed EDA on bank data to understand the nature of clients who apply for loans in banks. Based on the results they applied machine learning algorithms for loan prediction and classified the clients as good customer and bad customer.

K. Ulaga Priya et al. [4] have done EDA on bank dataset using random forest algorithm to predict customers loan privilege in R programming for analysis. Kiranbala & Deepika [5] have performed EDA both numerical and graphical on the World Happiness report 2021 to understand the various aspects of data analysis. Kabita Sahoo et al. [6] have done EDA using python to understand the different libraries of python for data analysis and graphical representation of results.

3. TECHNIQUES FOR EDA

In the complete process of data analysis, after collecting the data and pre processing it, EDA is the very important step for data manipulation, plotting and visualization. Most of the EDA techniques are graphical and few are quantitative which help in analyzing the data sets with respect to their statistical characteristics. The techniques available for Exploratory Data Analysis (EDA) are broadly classified into Non-Graphical EDA and Graphical EDA where in both the techniques are classified into two types namely univariate and multivariate [7]. Some of the EDA techniques depend on the type of data on which they are applied and some depend on the purpose of the analysis. Table 1 shows the preferable EDA technique that can be adopted for a given type of data and purpose of analysis.

3.1. Non-Graphical Exploratory Data Analysis: NGEDA

These techniques help in providing an idea about the description and distribution of the variable(s). There are two methods under this category namely univariate and multivariate.

3.1.1 Univariate NGEDA: This is a principal form of data analysis that involves only one variable to identify underlying data distribution and the characteristics of population distribution. This analysis also covers outlier detection. For any quantitative variable Univariate EDA helps making initial assessments on the variable distribution using the data sample.

Type of data	Preferable EDA techniques	Purpose	Preferable EDA techniques
Categorical	Descriptive statistics	distribution of a variable	Histogram
continuous Univariate	Histograms ,Line plot	Outlier detection	Histogram, scatter plots, box-and-whisker plots
continuous Bivariate	Heatmap,2D arrays and scatter plots	Quantify the relationship between two variables	2D scatter plot , Covariance and correlation
trivariate	3D scatter plot	Visualize the relationship between two exposure variables	Heatmap
Multiple groups	Side-by-side box plot	Visualizing high-dimensional data	2D or 3D scatter plot

Table 1:EDA techniques preferable based on data type and analysis

The fundamental description of the distribution include:

A. Central tendency:For any population distribution the central tendency measures mean, median, and mode where median is preferred for skewed distribution or when there are outliers.

B.Spread: Spread indicates how far from the centre can we find the data values.Variance, interquartile range and standard deviation are the commonly used measures for finding spread of any distribution.The variance is computed by taking the mean of the squares of all the individual deviations and we get the standard deviation by taking the square root of the variance.

C. Skewness and kurtosis: These are extra descriptors for any distribution where the measure of asymmetry is called skewness and measure of peakedness is called kurtosis [8].

3.1.2. Multivariate NGEDA: This shows the relationship between multiple variables as a cross-tabulation or statistics. Cross-tabulation will be of great use for categorical data which is a simple extension of tabulation.This is a two-way table with columns representing headings which match with one of the variables and the row headings match with the other variable. The subject count that share common pair of values are filled in to the table.This is also called as the bivariate non-graphical EDA technique.For categorical variables we can also calculate the correlation and covariance[8].Table 2 shows three columns where column1 contains the course, column2 holds the age of the person pursuing the course and column3 shows the gender. Table 3 shows the cross tabulation for the data of table 2.

Course	Age	Gender
CS121	youth	F
CS222	Middle age	F
CS431	youth	M
CS506	youth	M
CS222	Middle age	F
CS121	Middle age	F
CS431	Senior	F
CS222	Senior	F

CS431	youth	M				
CS506	Senior	F	Age/Gender	Female	Male	Total
CS121	youth	F	youth	2	3	5
CS222	Middle age	M	Middle age	3	1	4
			Senior	3	0	3
			Total	8	4	12

Table 3: Cross Tabulation for Course Data set
Table 2: Course Data Set

3.2. Graphical Exploratory Data Analysis

This is a graphical method of NGEDA. Non-graphical methods mostly are objective and quantitative in nature. They fail to give complete representation of the data. GEDA is found to be more qualitative. This data analysis is also divided into univariate and multivariate.

3.2.1. Univariate Graphical EDA: The primary focus of this analysis is on the data from a single variable values on n subjects and graphically represents the distribution of the data. Some of the common forms of univariate graphics include:

A. Histogram: This is the first fundamental graph also called as bar plot where every bar represents the frequency or proportion for a given range of values. Histograms help to learn about the shape, spread, central tendency and outliers of the given data.

B. Boxplots: This is another graphical technique which is very useful to represent the data proportions and information related to the skew, symmetry, central tendency and outliers. These are excellent techniques as they depend on powerful statistical measures including median and IQR instead of mean and standard deviation. Distribution comparisons are easily done using boxplots.

C. Quantile-Normal plots: These plots are also called as QN plot or QQ plot quantile-quantile. These are considered to be more complicated plots. QQ plots are best suitable to observe which theoretical distribution does the data particularly follow [8].

3.2.2. Multivariate graphical EDA: These techniques represent the association between two or more knowledge sets graphically. Some primary ways techniques of multivariate graphics include:

A. Scatter Plot: This is called as a essential graphical EDA technique when the variables are quantitative and it plots variable 1 on x-axis, and variable 2 on y-axis with one point corresponding to every case in the given dataset. If any two variables are explanatory and outcome, then it is always recommended to plot the outcome variable on y axis.

B. Run chart: To plot the data over time we can use the Run Chart.

C. Heat map: The graphical representation which depicts the data values using colours.

D. Bubble chart: It displays bubbles- multiple circles in two-dimensional plot.

4. Graphical Exploratory Data Analysis (GEDA) Using Python

A. Why Python:

Python is an interpreted programming language with a very rich set of libraries supporting both procedural and object-oriented programming paradigms. Some of the essential features of python are its free open source which is portable with support of numerous IDE [9].

B.Packages:

The packages of python used in this study include

- Pandas
- Numpy
- Matplotlib
- Seaborn

C. Dataset :

IBM HR Analytics Employee Attrition & Performance data set downloaded from <https://www.kaggle.com/code/faressayah/ibm-hr-analytics-employee-attrition-performance/data>.

This data set has a total of 27 attributes describing the employee with respect to age, gender, job role, job satisfaction and many more. In this work we consider only 16 attributes which show the employee performance and attrition. A part of the dataset is given in figure 1.

	A	B	C	D	E	F	G	H	I	J	K	L	M	N	O	P	Q
1	EmpNum	Age	Gender	EducationBackg	MaritalSta	EmpDepai	EmpJobRc	EmpEduca	EmpEnvir	EmpJobIn	EmpJobLe	EmpJobSa	EmpRelat	EmpWork	Attrition	PerformanceRating	
2	E1001000	32	Male	Marketing	Single	Sales	Sales Exec	3	4	3	2	4	4	2	No	3	
3	E1001006	47	Male	Marketing	Single	Sales	Sales Exec	4	4	3	2	1	4	3	No	3	
4	E1001007	40	Male	Life Sciences	Married	Sales	Sales Exec	4	4	2	3	1	3	3	No	4	
5	E1001009	41	Male	HR	Divorced	HR	Manager	4	2	2	5	4	2	2	No	3	
6	E1001010	60	Male	Marketing	Single	Sales	Sales Exec	4	1	3	2	1	4	3	No	3	
7	E1001011	27	Male	Life Sciences	Divorced	Dev	Develope	2	4	3	3	1	3	2	No	4	
8	E1001016	50	Male	Marketing	Married	Sales	Sales Repr	4	4	3	1	2	4	3	No	3	
9	E1001019	28	Female	Life Sciences	Single	Dev	Develope	2	1	1	1	2	4	3	Yes	3	
10	E1001020	36	Female	Life Sciences	Married	Dev	Develope	3	1	4	3	1	1	3	No	3	
11	E1001021	38	Female	Life Sciences	Single	Dev	Develope	3	3	3	3	3	4	4	No	3	
12	E1001022	44	Male	Medical	Single	Dev	Develope	3	1	1	1	3	3	3	No	3	
13	E1001024	47	Female	Medical	Divorced	Sales	Sales Exec	3	4	3	4	3	4	2	No	3	
14	E1001025	30	Male	Marketing	Divorced	Sales	Sales Exec	5	3	3	2	4	4	2	No	4	
15	E1001027	29	Male	Life Sciences	Single	Sales	Sales Repr	3	3	3	1	3	3	3	No	3	
16	E1001030	42	Male	Medical	Divorced	Dev	Develope	3	3	4	1	3	4	3	Yes	3	
17	E1001035	34	Female	Medical	Single	Dev	Develope	2	2	3	2	3	4	3	No	3	
18	E1001038	39	Female	HR	Married	HR	HR	3	3	4	2	2	3	1	No	3	
19	E1001040	56	Male	Medical	Married	Dev	Develope	3	3	3	4	4	3	2	No	3	
20	E1001041	40	Female	Medical	Single	Dev	Develope	1	4	2	1	4	4	2	No	4	
21	E1001042	27	Female	Medical	Single	Dev	Develope	3	4	2	2	1	1	1	No	3	
22	E1001044	29	Male	Marketing	Divorced	Sales	Sales Repr	3	4	3	1	2	4	3	No	3	
23	E1001047	53	Male	Life Sciences	Single	Dev	Develope	3	4	3	2	4	4	3	No	3	
24	E1001049	35	Female	Life Sciences	Divorced	Dev	Senior De	4	4	3	2	1	1	4	No	3	
25	E1001050	32	Male	Life Sciences	Married	Dev	Develope	4	1	3	2	4	4	3	No	3	

Fig 1: A Snippet of the Employee-Attrition Dataset

D. Using Python and Working with the dataset

- **Importing libraries:** To start the analysis work on the data set we first need to import all the required python libraries necessary for the analysis process.

```
import pandas as pd
import matplotlib.pyplot as plt
import numpy as np
import io
```

import seaborn as sns

- **Importing dataset:** after importing all the necessary python libraries we need to import the dataset. The dataset is imported in to jupyter notebook using following code.

```
mydata=pd.read_csv("Employee.csv")
mydata
```

If we use Google Colab then the code to import the data set is

```
fromgoogle.colab import files
uploaded = files.upload()
df = pd.read_csv(io.BytesIO(uploaded['Employee.csv']))
```

- **Cleaning Data:** Before we start using the data we need to check if there are any missing values or null values for which we use the `isnull()` method which returns true wherever there is no value in the dataset. We can also use the `sum()` method which returns total number of null values in each column. Zero indicates that there are no null values in the columns.



```
df = pd.read_csv(io.BytesIO(uploaded['Employee.csv']))
df.isnull().sum()
```

Choose Files Employee.csv

- **Employee.csv**(text/csv) - 95858 bytes, last modified: 9/3/2022 - 100% done

Saving Employee.csv to Employee (2).csv

EmpNumber	0
Age	0
Gender	0
EducationBackground	0
MaritalStatus	0
EmpDepartment	0
EmpJobRole	0
EmpEducationLevel	0
EmpEnvironmentSatisfaction	0
EmpJobInvolvement	0
EmpJobLevel	0
EmpJobSatisfaction	0
EmpRelationshipSatisfaction	0
EmpWorkLifeBalance	0
Attrition	0
PerformanceRating	0
Age	0
Gender	0

Fig 2: Checking for null values in the dataset

We can also select only particular rows from the entire dataset for analysis using `head(n)` function which extracts top n rows and `tail(n)` function which extracts n rows from the bottom of the dataset.

```
df = pd.read_csv(io.BytesIO(uploaded['Employee.csv']))
top=df.head(100)
top=df.tail(50)
```

E. Exploratory Data Analysis

This method analyzes the data sets and summarizes the important characteristics of the data using data visualization tools and statistical graphics. Even if any statistical model is used or not, EDA primarily aims at seeing what the data shows beyond the hypothesis testing task or

formal modeling. John Tukey was the first to promote this EDA to encourage statisticians to collect new data, explore it, formulate hypotheses, and perform experiments [10].

All the column data types in a given dataset are printed using `dtypes`. The statistical summary such as mean, count, min, max, etc of the given dataframe can be extracted using `describe()` function. To show the relation between any two we use correlation `corr()` function which also helps in measuring the linear relation strength of any two variables.

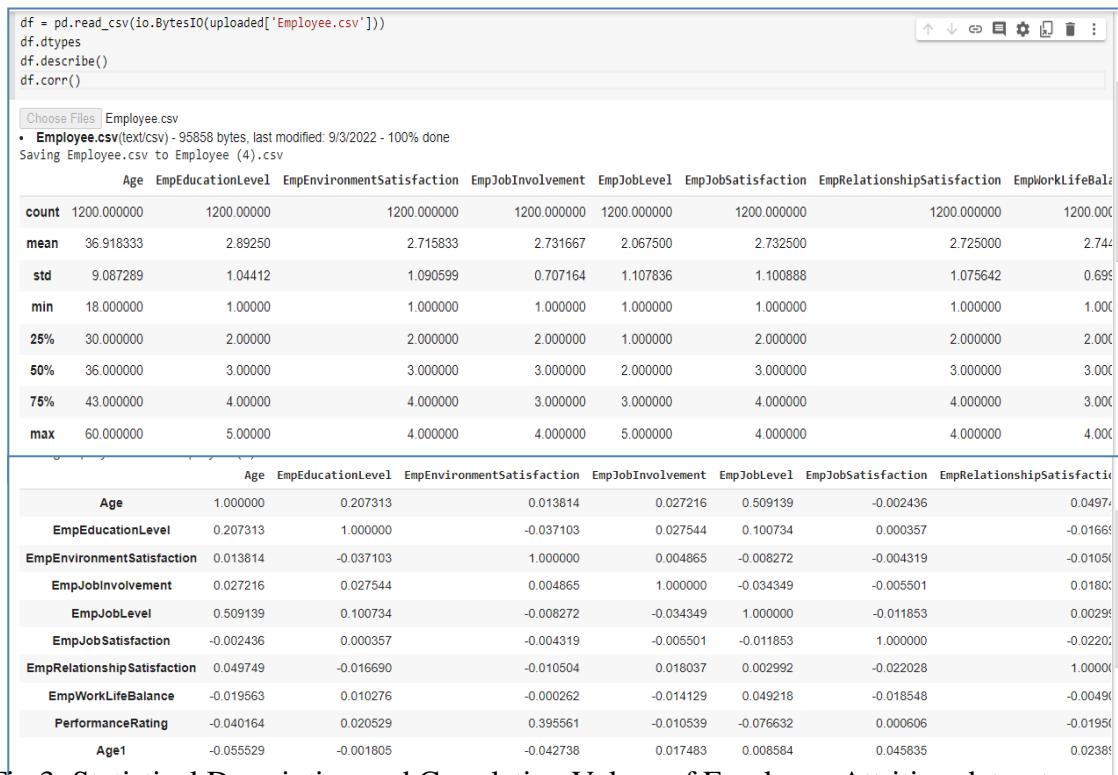


Fig 3: Statistical Description and Correlation Values of Employee Attrition dataset

F. Graphical Exploratory Data Analysis (GEDA)

Graphical techniques can be used to identify the most important properties of a dataset. GEDA is further classified into univariate and multivariate based on number of variables considered for analysis and also the type of data.

1. Univariate GEDA

This analysis gives the statistical summary of every column in the given data set. There are many examples for this analysis which include:

- **Histogram:** histogram provides the most intuitive visualizations of any distribution. It is also called as the graphical representation of data organized in to specified range of points. It is like a bar graph where range of data is represented as columns across x axis and y axis represents the respected data count for each column[11]. Considering the top 150 employees of the dataset the bar graph for age on x axis and employee performance rating on y axis shown in figure 4.
- **Stem Plot:** Stem plot is a popular statistical tool that helps in graphical exploratory data analysis which separates the digits in data points in to two columns. A stem plot is drawn as all set of y values plotted against common values on x axis. The digit with higher value forms the left column – called stem and the digit with lower value forms the right column – called leaves. The data is ordered in a stem plot. A stem plot helps visualizing the shape of the distribution[7]. `matplotlib.pyplot.stem()` function can be used to draw the Stem plot. The age values of Employee dataset represented as stem plot are shown in figure 5. For a total of 1200 employees the lower value starts from 18 and higher value is 60.

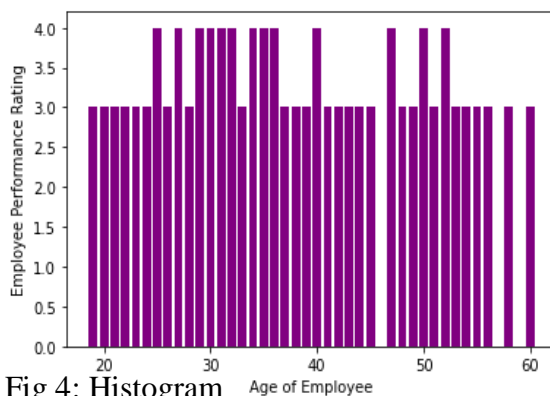


Fig 4: Histogram

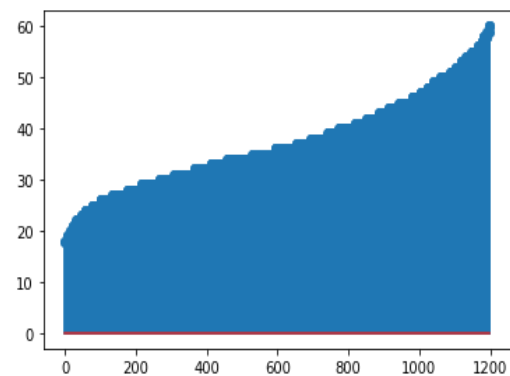


Fig 5: Stem Plot

- **Box Plot:** It is a graphical representation that shows comparison between groups of data. It shows the spread of data its statistical components like central tendency, symmetry, skew and also helps to identify the outliers. The box plot is built using a 5-value summary of the given data set (minimum, Q1, median, Q3, maximum value). These values show the closeness of data values. During the comparison the values which do not fit in to the boundary of the box will become the outliers whose features do not comply with other values in the dataset [12]. The box plot on the Age attribute of Employee data set with the clear outliers can be shown in figure 6.
- **Count Plot:** This represents the frequency or number of occurrences for categorical data using bars using the `countplot()` function [5].

```
import seaborn as sns
df = pd.read_csv(io.BytesIO(uploaded['Employee.csv']))
ax=sns.countplot(df.EmpDepartment)
for p in ax.patches:
    ax.annotate('{:.1f}'.format(p.get_height()), (p.get_x()+0.25, p.get_height()+0.01))
plt.show()
```

The count plot on Employee data set showing the different departments in which they work and respective counts is shown in figure 7.

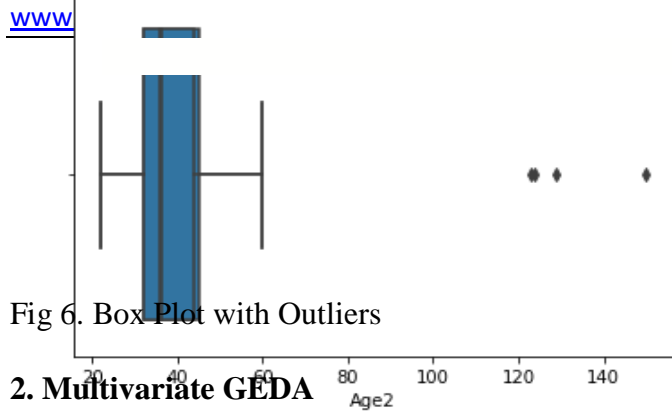


Fig 6. Box Plot with Outliers

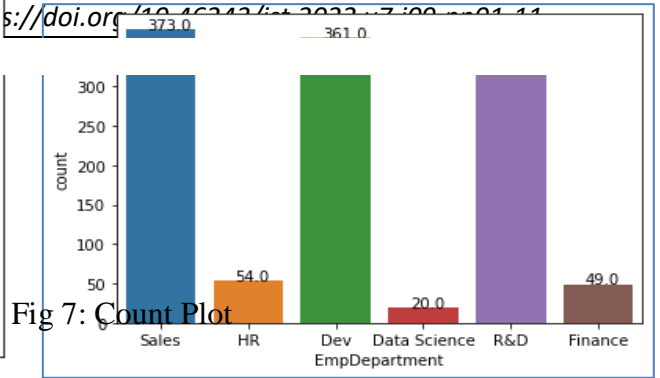


Fig 7: Count Plot

2. Multivariate GEDA

This analysis is used to recognize the associations between different values or variables in the dataset and display the relationship graphically. Some common forms of multivariate graphics include:

- **Scatter Plot:** A scatter plot is a two-dimensional chart showing the comparison of two variables scattered across two axes. The scatter plot is also known as the XY chart as two variables are scattered across X and Y axes. A scatter plot can be displayed without connecting lines or being displayed with smooth curved connectors or connecting lines [12]. For the Employee-Attrition data set the scatter plot between the variables daily and monthly wage of employees can be shown in figure 8.
- **Violin Plot:** This is similar to box and whisker plot. It shows the quantitative data distribution for more than one categorical variable across different levels. In a box plot, all the components represent the actual datapoints, whereas in the violin plot they represent the estimation of the kernel density for the given distribution. This is an effective way to show multiple distributions of data at once. For the Employee dataset the violin plot for the performance rating of the employee with respect to their gender is shown in figure 9.

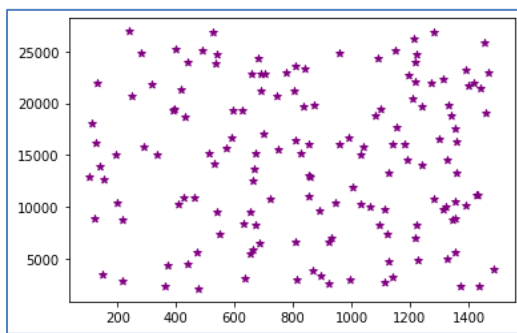


Fig 8: Scatter Plot

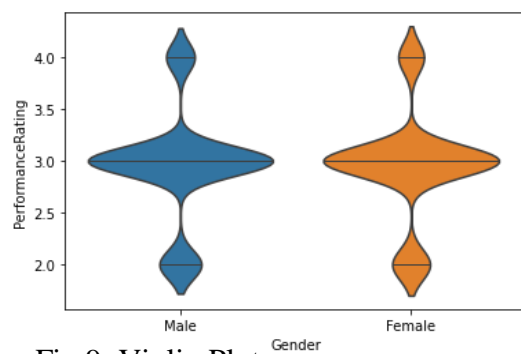


Fig 9: Violin Plot

- **Pair Plot:** This plot shows multiple pairwise bivariate relationships for $(n, 2)$ variable combinations in a single DataFrame as a matrix of plots where the diagonal plots are the univariate. It is a pairwise relationships that create a grid of Axes where each variable shares y-axis across one row and x-axis across one column.

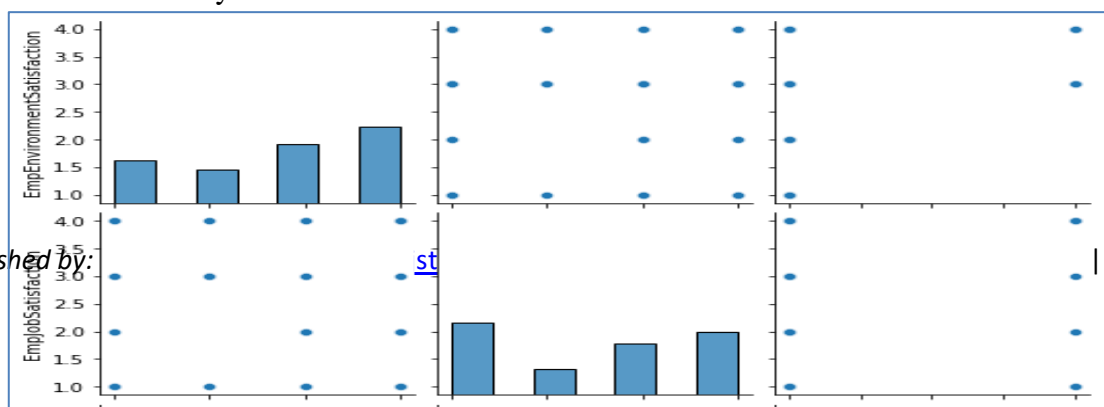


Fig 10: Seaborn Pair Plot.

4. CONCLUSION

In this paper, the different techniques for exploratory data analytics are discussed briefly. It includes both non graphical and graphical methods of analysis where in both univariate and multivariate are also explained. Python is used for implementation purpose importing major libraries and modules necessary for the graphical data analysis. The “Employee Attrition” data set is used in this work and numerous results are extracted and visualized. This work studies the dependence between attributes and effect of one variable on another for employee performance and attrition. Different graphs are been plotted using several attributes in the dataset to show the results in an easy way.

REFERENCES

1. AindrilaGhosh, Mona Nashaat, James Miller, ShaikhQuader, and Chad Marston, “A Comprehensive Review of Tools for Exploratory Analysis of Tabular Industrial Datasets,” Visual Informatics, Volume 2, Issue 4, December 2018, pp. 235-253.
2. Matthew Ntow-Gyamfi and Sarah SerwaaBoateng, “Credit Risk and Loan Default among Ghanaian Banks: An Exploratory Study,” Management Science Letters, Vol. 3, 2013, pp.753–762.
3. X. Francis Jency, V. P. Sumathi, Janani Shiva Sri, “An Exploratory Data Analysis for Loan Prediction Based on Nature of the Clients,” International Journal of Recent Technology and Engineering (IJRTE), Volume-7 Issue-4S, November 2018, pp.176-179.
4. K. UlagaPriya, S. Pushp, K. Kalaiivani, A. Sartiha, “Exploratory Analysis on Prediction of Loan Privilege for Customers using Random Forest,” International Journal of Engineering & Technology, Vol. 7, Issue 2.21, 2018, pp. 339-341.
5. KiranbalaNongthombam, Deepika Sharma. “Data Analysis using Python”.International Journal of Engineering Research & Technology (IJERT),Vol. 10 Issue 07, July-2021, pp. 463-468.
6. KabitaSahoo, Abhaya Kumar Samal, JitendraPramanik, Subhendu Kumar Pani. “Exploratory Data Analysis using Python”.International Journal of Innovative Technology and Exploring Engineering (IJITEE), ISSN: 2278-3075, Volume-8, Issue-12, October 2019, pp. 4727-4735.
7. Komorowski, M., Marshall, D.C., Saliccioli, J.D., Crutain, Y. (2016). Exploratory Data Analysis.Chapter 15. In: Secondary Analysis of Electronic Health Records. Springer, Cham.https://doi.org/10.1007/978-3-319-43742-2_15.
8. Steve Midway. “Exploratory Data Analysis – A first look at the data”.Chapter 4-Data Analysis in R.
9. Guido Van Rossum et al. Python programming language. In USENIX annual technical conference, 2007.
10. KabitaSahoo, Abhaya Kumar Samal, JitendraPramanik, and Subhendu Kumar Pani. Exploratory data analysis using python.International Journal of Innovative Technology and Exploring Engineering (IJITEE), 2019.

11. Claus O. Wilke. “Fundamentals of Data Visualization A Primer on Making Informative and Compelling Figures”. O’Reilly. 978-1-492-03108-6. March 2019
12. Kalilur Rahman. “Python Data Visualization Essentials Guide”. ISBN: 978-93-91030-063. FIRST EDITION 2021. BPB Publications.

See discussions, stats, and author profiles for this publication at: <https://www.researchgate.net/publication/371379371>

Academic Performance Prediction of intoxicating Students Using Intelligent Data Mining Techniques

Article · January 2021

DOI: 10.46501/IJMTST0712084

CITATIONS

0

READS

90

3 authors:



Rama M A

Maharani Lakshmi Ammanni College for Women

18 PUBLICATIONS 149 CITATIONS

SEE PROFILE



Ayesha Banu Mohd

Vaagdevi College of Engineering

30 PUBLICATIONS 51 CITATIONS

SEE PROFILE



Zareena Begum

Madras School of Economics

10 PUBLICATIONS 37 CITATIONS

SEE PROFILE



Academic Performance Prediction of intoxicating Students Using Intelligent Data Mining Techniques

M. Rama¹ | Dr.Ayesha Banu² | Zareena Begum³

¹Assistant Professor, Dept. Of Computer science and engineering, Vaagdevi College of Engineering,Bollikunta.

²Associate Professor, Dept. of Computer science and engineering (Data Science), Vaagdevi College of Engineering, Bollikunta

³⁸⁹⁰Assistant Professor, Dept. of Computer science and engineering (Data Science), Vaagdevi College of Engineering, Bollikunta

To Cite this Article

M. Rama, Dr.Ayesha Banu and Zareena Begum. Academic Performance Prediction of intoxicating Students Using Intelligent Data Mining Techniques. *International Journal for Modern Trends in Science and Technology* 2022, 7 pp. 459-462. <https://doi.org/10.46501/IJMTST0712082>

Article Info

Received: 29 November 2021; Accepted: 28 December 2021; Published: 03 January 2022

ABSTRACT

Alcohol consumption by students has become a significant issue these days. Addiction to alcohol results in the poor tutorial performance of scholars. This paper describes few algorithms that facilitate to boost the potency of educational performance of students captivated with alcohol. Within the paper, we tend to area unit victimisation one amongst the favoured Data Mining technique—"Prediction" and checking out the simplest formula among different algorithms. Our project is to investigate the educational excellence of the school professionals by creating use of WEKA toolkit and R Studio. We implement this project by making use of alcohol consumption by student datasets provided by kaggle web site. It is composed of 395 tuples and 33 attributes. A classification model is constructed by making use of Naïve Bayes and ID3. Comparison of accuracy is finished between R and WEKA. The prediction is performed so as to seek out whether or not a student will be promoted or demoted within the next year once previous year marks area unit considered.

Keywords: Data Mining , Prediction ,Naïve Bayes ,ID3 ,WEKA ,R studio.

1. INTRODUCTION

A large amount of knowledge is being made from completely different fields a day so as to pull out a legitimate and helpful knowledge that is employed during a decision-making method. The decision-making method is performed by victimization completely different data processing techniques. Various Mining Techniques Classification, Prediction, Clustering and Association. Classification is that the method of composition the information supported similarities. It is a supervised learning technique as we have a tendency to build the model by creating use of coaching data that consists of sophistication labels. Clustering is that the grouping of objects supported the principle of

accelerating the intra-cluster distance and decreasing the inter-cluster distance. Prediction is that the method of dig out the knowledge from an enormous quantity of data and helps to predict the end result no matter the past, present, and future events. The prediction data processing technique is employed so as to predict the performance of the scholars. Using Naïve theorem and ID3 algorithms we have a tendency to designed a model and found out the accuracy each in WEKA and R and therefore the comparison between them is performed.

2. RELATED WORK

In [1] they need used totally different data processing technologies to investigate students' performance in the courses. They need used

classification techniques to assess the student's performance. Among all the classification techniques, they need used call tree technique. The data they need used is of scholar's happiness to Yarmouk University of the year 2005 who took C++ course. CRISP-DM a technique is employed to create a classification model. Among the twenty attributes, solely twelve conditional attributes square measure thought-about that affects the performance of the scholars.

In [2], they need created a web-based application creating use of Naïve Bayesian algorithm. The information consists of nineteen attributes like student details, course details, admission details, attending details, etc., from 700 students learning at Amrita Vishwa Vidyapeetham, Mysore. Among all the algorithms they need used, Naïve Bayesian has got the best accuracy. Here, students, tutorial history is taken as input and the output is student's performance on the premise of a semester.

In [3], they need primarily centered on the information mining techniques that facilitate in learning the educational knowledge primarily in higher learning establishments. This shows however knowledge mining helps in decision-making so as to take care of university name. It predicts the student's performance at the top of their bachelor's degree and located out the students World Health Organization square measure in danger within the early years of their study and provides measured to improve the standard. They need collected knowledge from 2 different batches of the years 2005–06 and 2006–07 from 214 collegian students happiness to the applied science department at NEDUET, Pakistan. They need used call tree with Gini index, with data gain, with accuracy, Naïve Bayesian, Neural Networks, Random forest.

In [4], the information has been collected from three hundred students of engineering department for all 3 years. The attributes square measure associated with totally different subjects like English, Maths, and artificial language. They need used algorithms like Neural Networks, J48, SOM.

In [5], they need collected 2 completely different sets of knowledge of the scholars happiness to second year and third year of Amrita faculty of Engineering, Bangalore. The dataset constitutes twenty attributes like gender, father education, mother education, etc. Naïve

Bayesian classifier is employed for predicting the student's excellence and according to the performance they need urged a learning vogue for underperformed students.

In [6], they need used alcohol consumption by student's knowledge set age 10–14. They have used SVM technique, call trees, and Naïve Bayes algorithms and that they found out that SVM is a lot of economical than alternative algorithms.

In [7], classification of knowledge mining techniques illustrates few techniques to classify data together with their applications to health care. IF-THEN prediction rules are one among them that could be a common technique in data processing. This theme gift discovered data at highest level of abstraction.

In [8], they need used datasets associated with education and that they have used numerous data mining techniques to predict and valuate their performance.

In [9], they need analyzed the faculty student performance for Villupuram district. They have used bunch technique and k-means bunch formula. They have used mathematician mixture model so as to boost the accuracy.

In [10], the authors have collected student data from B. J school and analyzed them victimisation K-means bunch. the info set used for this analysis was obtained by measuring the B.C.A students from B. J College.

In [11], vital relationship between variables from an oversized knowledge set is analyzed. The authors propose a mechanism which may be utilized by the academics to look at the academic growth of their students.

In [12, 13], they need great deal of knowledge from medical business that consists of attributes like concerning the patient together with the main points, diagnosis, and medications. Using this knowledge we have a tendency to train the model and realize a pattern that helps in prediction.

3. PROPOSED SYSTEM

Dataset: the info is collected from the net that consists of thirty four attributes. The dataset is obtained from kaggle web site. Name of the college, gender, age, qualification of parents, occupation of oldsters, weekly

study time, net access, alcohol consumption levels on operating day similarly as weekends, health condition and grades are a number of the most important attributes listed.

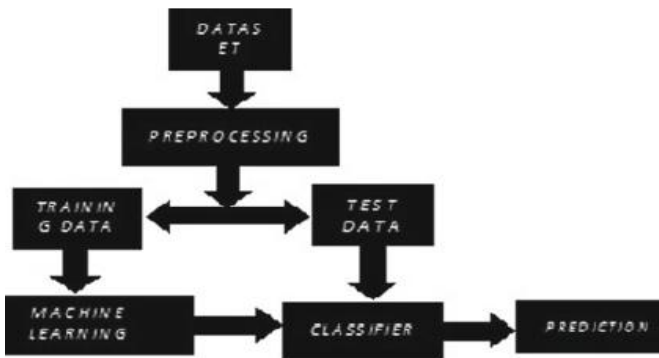


Figure 1: Proposed Model

Preprocessing: when grouping the info we want to preprocess it. The pre processing includes four steps. They are

Data Cleaning: during this step, we tend to take away the rip-roaring knowledge and fill the missing knowledge.

Data Integration: haircare totally different sorts of knowledge into single type.

Data Transformation: during this step knowledge of various types is formed into one form.

Data Reduction: this system is applied to get reduced illustration of information.

Training Data: We split and think about the primary three hundred tuples as coaching knowledge. The coaching data consists of sophistication labels. exploitation this train knowledge we tend to build a classifier.

Machine Learning: so as to create a classifier we tend to use machine learning techniques like prediction. In prediction, we've several data processing algorithms. exploitation these algorithms we tend to build a classifier.

Classifiers: we've enforced Naïve theorem and ID3 algorithmic rule in R and WEKA to create a classifier.

Naïve Bayesian

Input: dataset

Output: confusion matrix and predicted class labels
Do

For each value of the class label (Ci,Cj) find probability

For each attribute belonging to the class label (either Ci or Cj) find probability

Compare probabilities of each attribute of different class labels

If $p(C_i) > p(C_j)$

Class label will be Ci else Cj

$$P(C_i | X) = P(X | C_i) * P(C_i) / P(X)$$

Confusion matrix: It is a tool for finding the accuracy.

ID3

Input: dataset

Output: confusion matrix and predicted class labels

Do

Calculate information gain of all the attribute

The attribute with highest information gain value will be taken as the root node

and according to the outcomes the tree will be further extended till all the leaf

node becomes the class labels.

Test Data

The left out dataset is taken as test data and this test data is given as input to the classifier and the prediction is performed (Fig.2).

Figure 2 : Test Data

Prediction: it's a mining technique to predict the end result of the information tuple. We perform prediction by training the classifier with trained knowledge that consists of sophistication labels so the check knowledge while not class label is given to the model and sophistication label is foretold. This category label indicates the performance of the student within the next school year i.e., yes = pass, no = fail.

4. RESULT ANALYSIS:

Table 1 describes the comparison between accuracy in R and Weka Tool for all the attributes.

Table 1: Comparison of Accuracy for ALL Attributes using R and WEKA

Algorithm	R (%)	WEKA (%)
Naïve Bayes	96.8	95.95
ID3	94.9	92

Table 2 shows the comparison between accuracy in R and WEKA for the attributes that effects student's performance.

Table 2: Comparison of Accuracy FEW Attributes using R and WEKA

Algorithm	R (%)	WEKA (%)
Naive Bayes	94.7	87
ID3	100	100

Figure 3 represents performance of the attributes and quality of the attributes. Each bar chart within the on top of figure indicates distribution of every attributes and every color indicates completely different categories. The attributes used period, study time, gout, G1, G2, G3, Dalc, Walc, performance.

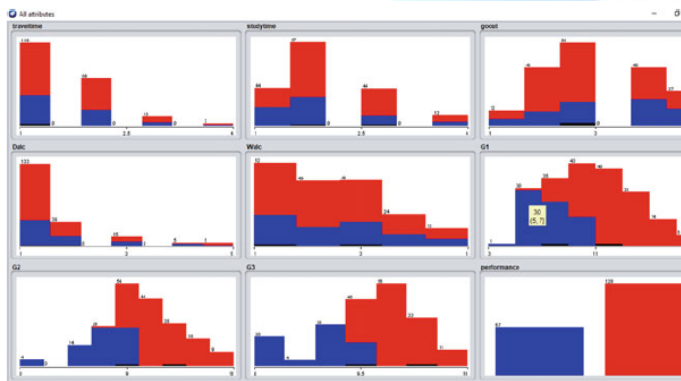


Figure 3: Visualization of Attributes

5. CONCLUSION:

Using Naive theorem and ID3 classifier we tend to get the best accuracy than several other algorithms. The attributes that have gotten highest priority got less accuracy once we have used ID3 algorithmic program than the opposite attributes once thought of. Once all the attributes square measure thought of naïve Naive Bayes once enforced in R has a lot of accuracy than in rail. The accuracy obtained in R and rail for ID3 once all the attributes square measure thought of is same because the accuracy obtained in R and rail for ID3 once

just some of the attributes square measure thought of. From this, we can infer that the time needed to implement the classifier for under a number of attributes is a smaller amount than the time once all attributes are thought of. The category label is foretold and this means that whether or not a student is pass or fail by considering previous year's marks.

REFERENCES



- [1] Al-Radaideh, Q., Al-Shawakfa, E., Al-Najjar, M.I.: Mining student data using decision trees. *The Int. Arab J. Inf. Technol.*—IAJIT (2006)
- [2] Devasia, T., Vinushree T.P., Hegde, V.: Prediction of students performance using educational data mining. In: *International Conference on Data Mining and Advanced Computing (SAPIENCE)*, pp. 91–95 (2016)
- [3] Asif, R., Hina, S., Haque, S.I.: Predicting student academic performance using data mining methods. *Int J Comput. Sci. Netw. Secur. (IJCSNS)* 17(5), 187–191 (2017)
- [4] Ramesh, V., Parkavi, P., Yasodha, P.: Performance analysis of data mining techniques for placement chance prediction. *Int. J. Sci. Eng. Res.* 2, 2229–5518 (2011)
- [5] Krishna, K.S., Sasikala T.: Prognostication of students performance and suggesting suitable learning style for under performing students. In: *International Conference on Computational Systems and Information Technology for Sustainable Solutions (CSITSS—2018)*, December 2018.
- [6] Fabio, M.P., Roberto, M.O., Ubaldo, M.P., Jorge, D.M., Alexis, D.L.H.M., Harold, C.N.: Designing A Method for Alcohol Consumption Prediction Based on Clustering and Support Vector Machines. *Res. J. Appl. Sci., Eng. Technol.* 14, 146–154
- [7] Sreevidya B., Rajesh M., Sasikala T.: Performance analysis of various anonymization techniques for privacy preservation of sensitive data. In: Hemanth J., Fernando X., Lafata P., Baig Z. (Eds.) *International Conference on Intelligent Data Communication Technologies and Internet of Things (ICICI) 2018*. *ICICI 2018. Lecture Notes on Data Engineering and Communications Technologies*, vol 26. Springer (2019)
- [8] Krishnaiah, V., Narsimha, G., Subhash Chandra, N.: Diagnosis of lung cancer prediction system using data mining classification techniques. *Int. J. Comput. Sci. Inf. Technol.* 4, 39–45 (2013).
- [9] Shelke, N.: A survey of data mining approaches in performance analysis and evaluation. *Int. J. Adv. Res. Comput. Sci. Softw. Eng.* (2015)
- [10] Jyothi, J.K. Venkatalakshmi, K.: Intellectual performance analysis of students by using data mining techniques. *Int. J. Innov. Res. Sci. Eng. Technol.* 3, (2014)
- [11] Sreevidya, B.: An enhanced and productive technique for privacy preserving mining of association rules from horizontal distributed database. *Int. J. Appl. Eng. Res.* (2015)
- [12] Bhise, R.: Importance of data mining in higher education system. *IOSR J. Hum. Soc. Sci.* 18–21 (2013).
- [13] Sumitha Thankachan, Suchithra, Data mining warehousing algorithms and its application in medical science. *IJCSMC*, 6 (2010).



Superlattices and Microstructures

Volume 156, August 2021, 106953

Improved hole injection/extraction using PEDOT:PSS interlayer coated onto high temperature annealed ITO electrode for efficient device performances

Gnyaneshwar Dasi ^a, Thyda Lavanya ^a, Govindasamy Sathiyam ^b, Raju Kumar Gupta ^b, Ashish Garg ^c, P. Amaladass ^d, Kuppusamy Thangaraju ^{a e}  

Show more 

 Share  Cite

<https://doi.org/10.1016/j.spmi.2021.106953> 

[Get rights and content](#) 

Highlights

- Annealed ITO films improve film quality with decreased dislocation density and lattice strain.
- PEDOT:PSS smoothens the wrinkle kind of surface morphology of ITO annealed at 400°C.
- 400°C annealed ITO with PEDOT:PSS interlayer lowers the potential barrier and improves hole-current density in HODs.
- It enhances the efficiency of OPVs by three times (1.69%) compared to that (0.48%) of pristine ITO based OPV.
- 400°C annealed ITO film lowers potential barrier at ITO/PEDOT:PSS interface for effective hole injection/extraction process.

How to Cite:

Sunalini, K. K., Nair, D. K., Sumalatha, M., Merugu, I., Slathia, M., & Kumari, C. J. (2022). Pandemic discourse and cultural healing. *International Journal of Health Sciences*, 6(S2), 4769–4778. <https://doi.org/10.53730/ijhs.v6nS2.6140>

Pandemic discourse and cultural healing

K. K. Sunalini

Associate Professor, Koneru Lakshmiiah Education Foundation, Andhra Pradesh
Email: sunalini12.klu@kluniversity.in

Dinesh Kumar Nair

Dean of Research and Head, Department of English, Associate Professor, V G Vaze College Autonomous, Mulund, Mumbai

M. Sumalatha

Associate Professor, Vagdevi College of Engineering, Bollikunta, Warangal, Telangana

Indrani Merugu

Assistant Professor, ACE Engineering College, Hyderabad, Telangana

Marvi Slathia

Research Scholar, Koneru Lakshmiiah Education Foundation, Andhra Pradesh

Ch. Jyostna Kumari

Assistant Professor, CVR College of Engineering, Hyderabad, Telangana

Abstract---COVID-19 pandemic has brought new social and discursive contexts with the metaphorization and gothification of the virus for many purposes ranging from reporting to politics. This discursive reality is similar to Lawrence Buell's notion of toxic discourse. The discourse of the pandemic, like toxic discourse, is both useful and harmful in the 'risk society' that is exposed to both the infection and economic downslide. While on the one hand this discourse is integral in raising awareness and infection control measures, it also results in the monsterization of virus in press, social media and political rhetoric. This paper attempts to analyze various texts that have emerged in the backdrop of the pandemic to show how the social media humor, advertisement metaphors, masking and sanitizing of language and the serio-comic use of language have evolved as discursive strategies of the contemporary pandemic-hit society. The study also focuses on how literary/poetic use of language becomes a part of cultural healing. Linguistic and literary tropes that have mutated and evolved in the pandemic time are also analyzed.

International Journal of Health Sciences ISSN 2550-6978 E-ISSN 2550-696X © 2022.

Corresponding author: Sunalini, K. K.; Email: sunalini12.klu@kluniversity.in

Manuscript submitted: 27 Feb 2022, Manuscript revised: 18 March 2022, Accepted for publication: 09 April 2022

4769

4770

Keywords---toxic discourse, masking, sanitizing, metaphorization, gothification, tropes, healing culture, seriocomic.

Introduction

The discipline codes and restrictions imposed by the World Health Organization





ScienceDirect®

Spectrochimica Acta Part A: Molecular and
Biomolecular Spectroscopy

Volume 265, 15 January 2022, 120377

Raman and X-ray photoelectron spectroscopic investigation of solution processed Alq₃/ZnO hybrid thin films

Gnyaneshwar Dasi^a, Thyda Lavanya^a, S. Suneetha^a, S. Vijayakumar^c, Jae-Jin Shim^c,
Kuppusamy Thangaraju^{a b}  

Show more 

 Share  Cite

<https://doi.org/10.1016/j.saa.2021.120377> 

[Get rights and content](#) 

Highlights



TABULAR FORM OF EULER MODIFIED METHOD

M. Srinivas
Department of Mathematics
Vaagdevi College of Engineering,
Warangal, Telangana, India

Md. Shafeeur Rahman
Department of Mathematics
Vaagdevi College of Engineering,
Warangal, Telangana, India

Abstract— There exist many single step methods to find the solution to a first order ordinary differential equation. Often time consuming and complicated. The proposed method is the alternate way of Euler modified method in the tabular form. Easy to understand and calculate

Keywords— Euler, Differential equation, Solution, Modified method.

I. INTRODUCTION

Several problems in science and technology can be formulated into differential equations. The analytical methods of solving differential equations are applicable only to a limited class of equations. Quite often differential equations appearing in physical problems do not belong to any of these familiar types and one is obliged to resort to numerical methods. These methods are of even greater importance when we realize that computing machines are now readily available which reduce numerical work considerably.

In the methods of Euler, Runge-Kutta, Milne, Adams-Bashforth, etc. the next point on the curve is evaluated in short steps ahead, by performing iterations until sufficient accuracy is achieved. As such, these methods are called step-by-step methods.

Euler and Runge-Kutta methods are used for computing y over a limited range of x - values whereas Milne and Adams methods may be applied for finding y over a wider range of x -values.

If the conditions are prescribed at one point only (say, x_0), then the differential equation together with the conditions constitute an initial value problem of the n th order. If the conditions are prescribed at two or more points, then the problem is termed as boundary value problem.

The Euler method (also called as Forward Euler method) is a first-order method, which means that the local error (error per step) is proportional to the square of the step size, and the global error (error at a given time) is proportional to the step size. Here the error represents difference between the exact solution and the Euler approximation. The Euler method often serves as the basis to construct more complex methods. It is a first-order numerical procedure for solving first order ordinary differential equations (ODEs) with a given initial value. It is the most basic explicit

method for numerical integration of ordinary differential equations and is the simplest Runge-Kutta method.

The Euler method is more accurate if the step size is smaller

II. PROPOSED ALGORITHM

Step-1: Let $\frac{dy}{dx} = f(x, y)$ be the first order ordinary differential equation with the initial condition $y(x_0) = y_0$.

Step-2: Let h be the difference between the equally spaced data.

Step-3: Construct a table for Euler modified method with the columns

$$x, y^1 = \frac{dy}{dx} = f(x, y), \text{ Mean and}$$

New $y = y_0 + h$ (mean) where
 $x = x_0$, mean = the average of present y' and starting y

Step-4: The starting value of x is x_0 and from the next $x = x_0 + h$

Step-5: The starting value of new y of the table only is calculated by Euler formula
 $y_1 = y_0 + h \cdot f(x, y)$.

Step-6: There is no change in the values of x and y_0 till the successive approximate values of new y are equal.

III. EXPERIMENT AND RESULT

3.1. To Find y at $x=0.2$ of $\frac{dy}{dx} = x + y$ with the condition $y(0) = 1$ and $h = 0.1$.

Let us consider $f(x, y) = x + y$ and $x_0 = 0, y_0 = 1$.
Constructing a table for Euler modified method by the proposed algorithm, we have

Temperature-Dependent Changes in Gamma Irradiated Porcine Gelatin with Low Bloom (PGL) Value: an ESR Investigation

N. S. Rao^{1,2}, D. Shireesh¹, S. Kalahasti¹, B. S. Rao^{3*}

¹Department of Physics, Kakatiya University, Warangal, 506 009, Telangana State, India

²Present address: Department of Physics, SR & BGNR Govt. Arts and Science College(A), Khammam, 507002, Telangana State, India

³Department of Physics, AVV Degree & PG College Warangal 506 005, Telangana State, India

Received 9 August 2021, accepted in final revised form 9 January 2022

Abstract

Gamma irradiation of Gelatin brings important changes in its chemical structure, making it suitable for different applications. The irradiated Gelatin may be subjected to different thermal treatments during these applications. Therefore, temperature-dependent changes in irradiated gelatins are a point of interest. Electron spin resonance (ESR) is vital for detecting free radical processes in irradiated polymers. As such, ESR spectra of temperature-dependent porcine Gelatin with low bloom are recorded, and they are analyzed by computer simulation techniques. Component spectra under different conditions are evaluated by the magnetic parameters employed to simulate the ESR spectra. The results indicate that the spectral shape at 300 K (RT) is stable up to 350 K, and signal intensity begins to decay beyond 350 K. The signal vanished around 355 K, designated as radical decay temperature. Bloch analysis is applied to evaluate activation energy associated with free radical decay, calculated around 35 KJ/mole.

Keywords: Porcine Gelatin; Bloom; Gamma irradiation; ESR; Bloch analysis.

© 2022 JSR Publications. ISSN: 2070-0237 (Print); 2070-0245 (Online). All rights reserved.
doi: <http://dx.doi.org/10.3329/jsr.v14i2.55078> J. Sci. Res. **14** (2), 395-404 (2022)

1. Introduction

Gelatins are an important class of biodegradable biopolymers with specific properties like gelation and emulsification, making them use food, pharmaceutical, and cosmetic industries [1,2]. Recently Alipal *et al.* have reviewed and highlighted the sources, processing, and applications of gelatins [3].

Radiation-induced processes in gelatins are an essential part of their application. Due to the crosslinking of gelatins by different types of radiations (gamma, electron beam), changes in chemical structure occur, followed by a change in mechanical properties [4]. Therefore attempts have been made to investigate radiation-induced changes in different gelatins by various authors [5-9].

* Corresponding author: physanjeev@gmail.com

Entropy Generation in MHD Mixed Convection Flow of Nanofluid between Parallel Disks with Joule Heating, Hall Current and Ion-slip Effects

Md. Shafeurrahman^{1}, D. Srinivasacharya²*

¹Assistant Professor, ²Professor

¹Department of Mathematics, Vaagdevi College of Engineering Warangal, India.

²Department of Mathematics, National Institute of Technology Warangal, India.

**Corresponding Author*

E-Mail Id:-rahaman16@gmail.com

ABSTRACT

This article analyzes the effects of joule heating, Hall and Ion-slip parameter on entropy generation in mixed convective electrically conducting nanofluid flow between two parallel coaxial disks in the presence of strong magnetic field. The governing equations are non-dimensionalized and the resulting system of nonlinear ordinary differential equations are solved using Homotopy Analysis Method. The velocity, temperature and nanoparticle concentration profiles are presented graphically for various values of governing parameters. Further, these profiles are won't to evaluate the entropy generation and Bejan number.

Keywords:-*Entropy generation, joule heating, mhd, nanofluid, hall current, ion slip effects, parallel disks, homotopy analysis method*

INTRODUCTION

Convective heat transfer using nanofluids has received much attention in present days. This is because of their diverse application in many industrial and engineering fields such as heat exchange systems in power generation, automobile engines, welding equipment, electronics devices and cooling of nuclear reactors. Nanofluid, pioneered by [1], is a mixture of a base fluid and small nano sized solid particles. [1] verified that the nanofluids have higher thermal conductivity related to the base fluids. This can be obtained for a very small volume fraction of nanoparticles.

On the other hand, fluid flow and heat transfer between rotating disks is an important topic in view of its for wider applications in rotating machinery, lubrication, computer storage devices and crystal growth processes. Further, the analysis of magneto hydrodynamics

(MHD) flow of nanofluids has gained much attention due to its engineering and industrial applications. A number of studies have been conducted in recent years, on the MHD flow of nanofluid by considering distinct types of base fluids with particular nanoparticles. [2] investigated the magnetic effect on squeezing nanofluid flow between parallel coaxial disks. [3] introduced an algorithm based on the homotopy analysis method to study the MHD squeeze flow between two parallel infinite disks where one disk is impermeable and the other is porous with either suction or injection of the fluid in the presence of an applied magnetic field.[4] studied the nanofluid flow and heat transfer analysis between two parallel disks using Least Square Method (LSM) and numerical method with a variable magnetic field applied to the lower stationary disk and the upper disk move towards or away from the lower disk. [5]

See discussions, stats, and author profiles for this publication at: <https://www.researchgate.net/publication/375661709>

PRECAUTIONS TO PREVENT THIRD WAVE COVID-19 – A PERSPECTIVE STUDY.

Article · November 2023

CITATIONS

0

READS

17

1 author:



Venu Kesireddy

12 PUBLICATIONS 2 CITATIONS

SEE PROFILE

PRECAUTIONS TO PREVENT THIRD WAVE COVID-19 – A PERSPECTIVE STUDY.

Venu Kesireddy

Assistant Professor, Vaagdevi College of Engineering, Autonomous,
kesireddyvenu@gmail.com

Abstract

The next wave in India might be in late November or December 2021. Despite the quantum of cases in the next wave, it is essential to plan and prepare to tackle the next wave. It is therefore an opportune time at present to take stock of some of the salient lessons learned from the COVID-19 pandemic as well as the previous pandemics. While making our preparations, we should take a 360° view that encompasses health in all its dimensions – physical, mental, social, and economic well-being. This study helps to find out how India can prevent the third wave of the Covid-19 pandemic with various solutions.

Keywords: COVID-19, third wave, prevent, precautions.

INTRODUCTION:

The Delta Plus variant of SARS-CoV-2 has become a worry for an anticipated third wave, which can be prevented or mitigated at least based on lessons learned from the last two waves. At a time when India has barely put behind the horrors of the second wave of the Covid-19 pandemic, **Maharashtra has sounded alert for the third wave**. Delta variant of SARS-CoV-2 was held responsible for the towering second wave of the coronavirus pandemic. The Delta variant had been first reported from Maharashtra last year. Now, **the Delta Plus variant has been detected** even though it has not been classified as a variant of concern (VOC). Delta Plus variant was first detected in Europe in March this year. It has been isolated in some samples in India and around 10 other countries. Delta Plus is a new version of its mutant variant Delta.

It is, however, not known whether the Delta Plus variant is more infectious or fatal compared to the Delta variant. Delta variant is deadlier and capable of causing more severe Covid-19, leading to a higher rate of hospitalization of patients.

Every successful mutation helps a virus or any other organism thrive better. This is principally why the Delta Plus variant of SARS-CoV-2 has become a **worry for an anticipated third wave**, which can be prevented or mitigated at least based on lessons learned from the past two waves of Covid-19 pandemic.

OBJECTIVES OF THE STUDY:

1. To understand precautions to prevent third wave covid-19.
2. To conclude and offer suggestions.

RESEARCH METHODOLOGY:

This paper collected data from secondary sources such as Media Reports, Press Releases, WHO reports, News Magazines and journals, etc.

LITERATURE REVIEW:

T Rajgopal1, Bobby Joseph2 (2021), Public-private partnerships will play a huge role in the vaccination drive. Private hospitals can partner with the state governments and the private sector to vaccinate employees and their family members. Additionally, as part of their corporate social responsibility initiatives, large companies can aim to reach the workers in the unorganized sector who form a significant proportion of the country's working population. Vaccination drives are currently encouraged in housing societies as well – this presents another avenue to the private sector. Vaccination coupled with no pharmaceutical measures such as universal masking, maintaining physical distancing, and practicing hand hygiene would be the key to preventing and mitigating the potential third wave in India.

Dr. V Ravi (2021), The SARS-CoV-2 has not run its full course as yet. Also, whenever it is done, a chief takeaway could be keeping the collective memory of it alive. How well a country will fare in tackling future COVID-19 waves or newer pandemics will depend a lot on how well they weave and integrate the 10 themes mentioned here into the fabric of their work culture.

RESEARCH GAP

Large numbers of studies have been conducted on the impact of Covid-19 on the Indian economy and Covid-19 precautions to overcome in the first and second wave in the past. No studies were undertaken so far on the Precautions to prevent third wave covid-19. To fulfill the gap in research the present study has been undertaken.

The following 6 precautions are helpful to overcome the third wave of COVID-19 in the country.

1. REMEMBER COVID-19 IS STILL HERE

With a significant decline in cases, state after state is opening up. Both the public and the government need economic activities to gain pace, which requires lifting of Covid-induced restrictions.

As the restrictions were lifted, people were seen crowding indoors and outdoors while the authorities too looked lax in enforcing Covid-19 protocol. The result was that after a few months, the Covid-19 pandemic came back with the biggest global surges in India, which can unlearn this lesson at its peril.



Source: India Today

2. TAKE BEHAVIORAL VACCINE

Covid-19 pandemic rushed scientists into developing vaccines at the fastest speed. The efficacy of lab-developed vaccines differs for each candidate and against different mutant variants of SARS-CoV-2. However, behavioral vaccines offer the best defense against all variants of SARS-CoV-2.

Behavioral vaccines include appropriate wearing of face masks, practicing Covid-appropriate hygiene, and maintaining adequate physical-social distance. The Tana Bhagat community of the Oraon tribe in Jharkhand has shown how to beat Covid-19 without vaccines.



Source: India Today

No member of the Tana Bhagat community has reported positive for Covid-19 through the first and second wave of the coronavirus pandemic, while Jharkhand has reported about 3.44 lakh cases of SARS-CoV-2 infection.

3. STAGGERED OPENING

Staggered opening of marketplaces and offices can stop overcrowding of places. Both public authorities and private management should opt for staggering timings and sites, including continued adoption of work-from-home mode to prevent the congregation of the workforce in one place.

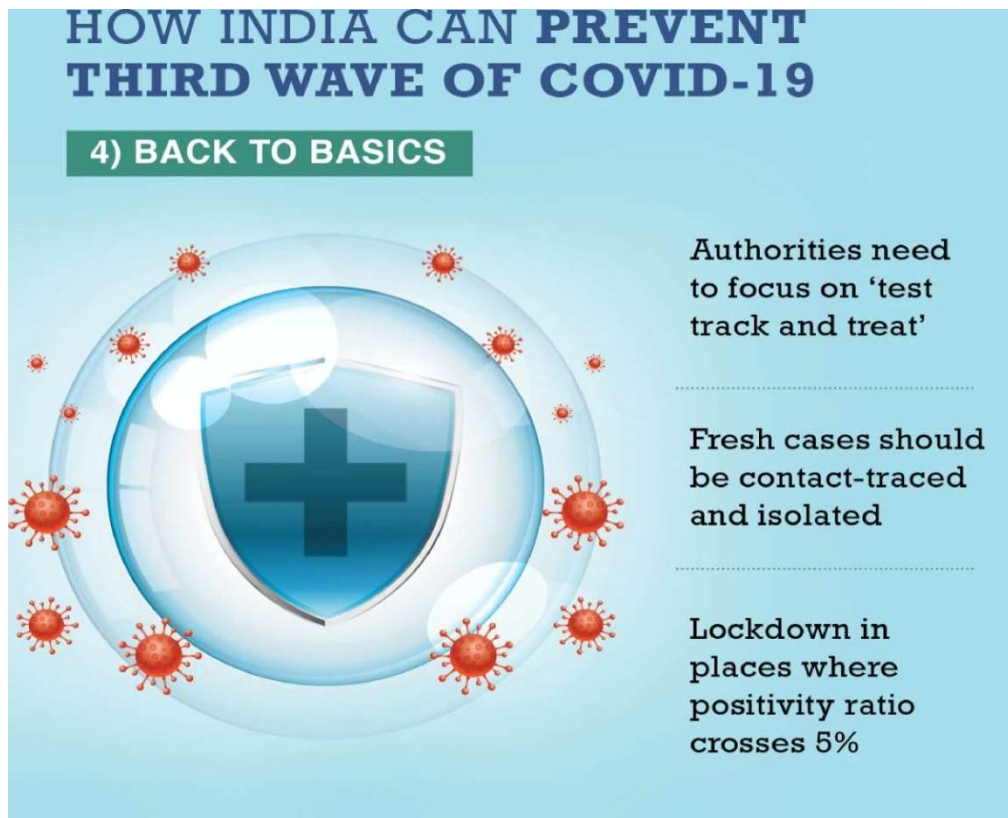


Source: India Today

This is more important for offices requiring more indoor staff than those depending on-field workers. Studies have shown that spread of Covid-19 is greater indoors as wind and sun rays help faster disintegration of SARS-CoV-2 outdoors.

4. TARGETED CONTAINMENT

‘Test, track and treat’ has been the mantra of health agencies across the world, including the World Health Organization. But what has been observed is that this principle has remained mostly on paper and enforced less rigorously on the ground for various reasons. As India is heading to another ebb of the pandemic wave, this could be the best time to ensure that Covid-management fatigue does not creep in as it happened on the retreat of the first wave. Fresh Covid-19 cases should be aggressively managed, contact-traced, and treatment protocol thoroughly followed at the local level.



Source: India Today

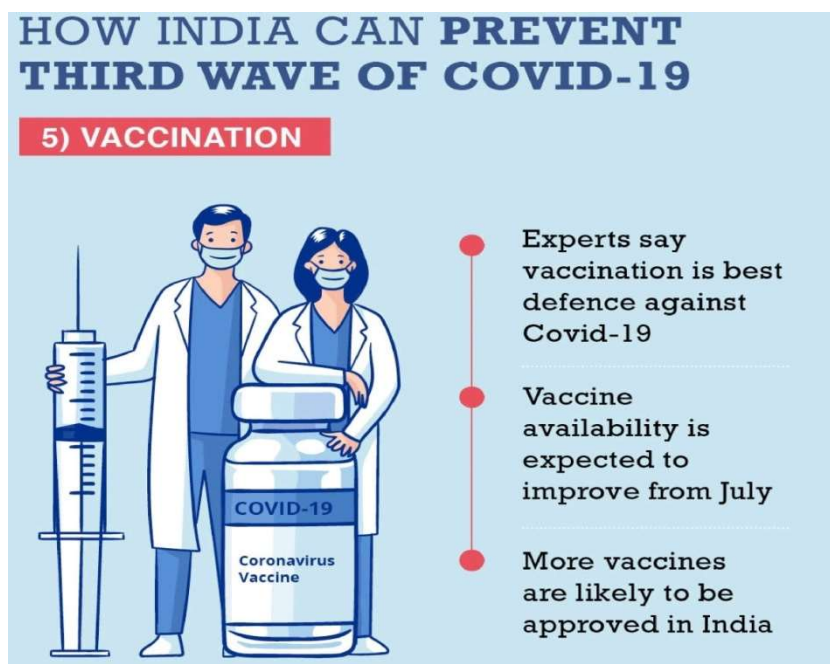
Immediate lockdowns are imposed in places where the positivity rate nears or crosses the 5 per cent-mark. The WHO treats this as the danger-line in the spread and management of the Covid-19 pandemic.

5. SPEEDING UP VACCINATION

Despite frequent controversies over their efficacy and use of certain ingredients, and rumors taking cyberspace by storm, vaccines, according to health experts, remain the best hope against Covid-

19. Pandemics or epidemics are known to fizzle out when a population attains herd immunity, meaning the virus has no further scope of growth. Vaccines offer herd immunity artificially.

In absolute numbers, India's vaccination speed looks impressive compared to other countries, but not in terms of percentage. India has roughly provided vaccination coverage to its 16 percent of eligible (above 18) population. In contrast, the UK has provided 59 percent coverage, the US 51 percent, Israel 62 percent, and even Brazil 22 percent.



Source: India Today

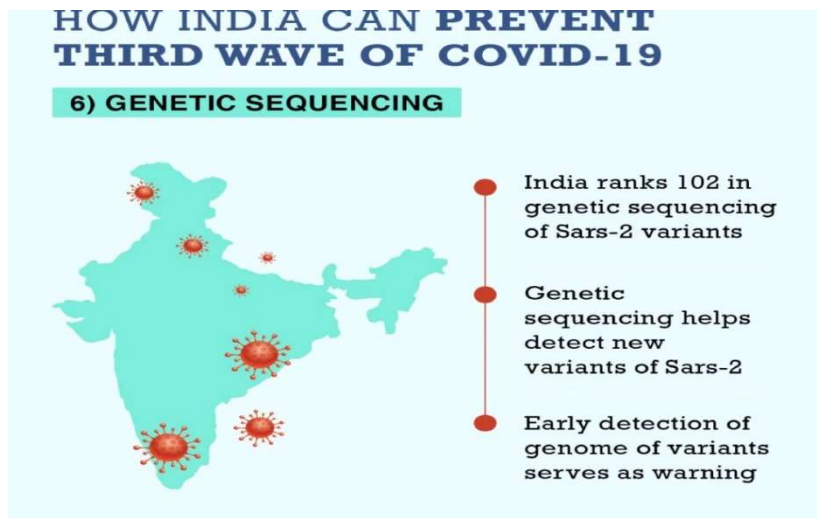
The immediate target of India is to provide 40 percent vaccination coverage against Covid-19. This means India might have to vaccinate around 1 crore people every day to meet the target by August-end. In June, the daily doses of vaccination have stayed in 30-35 lakh zone. The vaccine production and supply situation is expected to improve from July.

6. MORE TEETH TO SCIENCE

India is the second-worst affected country by Covid-19 and the worst hit during the second wave of the coronavirus pandemic. However, a Washington Post analysis published in April-end ranked India at 102 in genetic sequencing for SARS-CoV-2.

The Global Initiative on Sharing Avian Influenza Data (GISAID) too held the same view, saying only 3,636 genome sequences were shared with it between January 12, 2020, and April 28, 2021.

Identification of a new variant is understood to be crucial in mitigating the chance of a fresh wave of the Covid-19 pandemic. India's problem is the infrastructural capacity to do genome studies. Such capacity cannot be built overnight.



Source: India Today

The experts, however, say an immediate focus of the government is an absolute necessity to build a science-based case against Covid-19. The shortage of genome data on SARS-CoV-2 may bring about a fresh wave of the Covid-19 pandemic as neither scientists nor authorities would know that the virus was on a colonization mission.

CONCLUSION:

The above 6 precautions should be followed strictly. To defeat corona, you have to protect yourself according to the above precautions. The two Covid-19 waves may have a lesson for India that the government agencies might not prevent a fresh surge but people can. The Tana Bhagat community has a model to keep even a third wave of Covid-19 at bay. The government is making every effort to protect the general public from the corona. The government of India has recently issued a warning regarding the third wave of corona disease, which has been continuously spreading. The government has stated in unambiguous terms that the third wave of corona will ensue if the lockdown is not followed well. And also people feel a responsibility to follow all precautions to face the third wave of corona 19.

References:

1. Vergara RJD, Sarmiento PJD, Lagman JDN. Building public trust: A response to COVID-19 vaccine hesitancy predicament. *J Public Health (Oxf)* 2021; 43:e291-2.

2. Sallam, M. COVID-19 vaccine hesitancy worldwide: A concise systematic review of vaccine acceptance rates. *Vaccines* 2021;9:160. DOI: 10.3390/vaccines9020160.
3. Indian Journal of occupational and environmental Medicine, Vaccination as a strategy to prevent or mitigate a potential COVID-19 third wave in India, ISSN:0973-2284,2021,volume-25,issue-2,pages-55-59.
4. Emanuel EJ, Persad G, Kern A, Buchanan A, Fabre C, Halliday D, et al. An ethical framework for global vaccine allocation. *Science* 2020; 369:1309- 12.
5. Neurology India publication of the Neurological Society of India, How can India be Prepared for the Third Wave, ISSN: 0028-3886,2021,volume-69,issue-3,pages-545-546.

See discussions, stats, and author profiles for this publication at: <https://www.researchgate.net/publication/375661733>

A STUDY OF RECENT CHANGES IN FINANCIAL SERVICES IN INDIA

Article · November 2023

CITATIONS
0

READS
1,028

1 author:



Venu Kesireddy

12 PUBLICATIONS 2 CITATIONS

SEE PROFILE

A STUDY OF RECENT CHANGES IN FINANCIAL SERVICES IN INDIA

Venu Kesireddy Assistant Professor Vaagdevi College of Engineering, Autonomous
kesireddyvenu@gmail.com

Abstract

Financial services form the backbone of a country's economic growth and development. The objective of this study is to identify the recent changes in financial services in India both the private and public sector and how these are reflecting both in terms of strong growth of existing financial services firms and new entities entering the market. For this study, I have gone through different research articles. This paper covers the period 2020-2021.

Keywords: Financial Services, Growth, Changes.

INTRODUCTION

Financial services are the economic services provided by the finance industry, which encompasses a broad range of businesses that manage money, including credit unions, banks, credit card companies, insurance companies, accountancy companies, consumer-finance companies, stock brokerages, investment funds, individual managers, and some enterprises. India has a diversified financial sector undergoing rapid expansion, both in terms of strong growth of existing financial services firms and new entities entering the market. The sector comprises commercial banks, insurance companies, non-banking financial companies, co-operatives, pension funds, mutual funds, and other smaller financial entities. The banking regulator has allowed new entities such as payment banks to be created recently, thereby adding to the type of entities operating in the sector. However, the financial sector in India is predominantly a banking sector with commercial banks accounting for more than 64% of the total assets held by the financial system.

The Government of India has introduced several reforms to liberalize, regulate and enhance this industry. The Government and Reserve Bank of India (RBI) have taken various measures to facilitate easy access to finance for Micro, Small, and Medium Enterprises (MSMEs). These measures include launching Credit Guarantee Fund Scheme for MSMEs, issuing guidelines to banks regarding collateral requirements, and setting up a Micro Units Development and Refinance Agency (MUDRA). With a combined push by Government and private sector, India is undoubtedly one of the world's most vibrant capital markets.

OBJECTIVES OF THE STUDY

1. To know the Recent Changes and industry analysis in Financial services in India.
2. To identify the Government initiatives towards financial services.

RESEARCH METHODOLOGY

This paper collected data from a secondary sources such as Media Reports, Press Releases, IRDAI, General Insurance Council, Reserve Bank of India, Union Budget 2021 22.

LITERATURE REVIEW:

Suresh Aaluri, Dr. M. Srinivasa Narayana, Dr. P. Vijay Kumar (2016): The Studies the trends in the banking sector for financial inclusion, regulation, technology in India. The recent initiatives taken by the Government of India boost to promote financial inclusion and surely leading to the position where all Indians have their bank accounts, using Information Technology enabled services.

Manendra Singh*(2012): In the above-mentioned paragraphs, we can see the variety of financial services that are available in the Indian environment. Be its banking sector, there is huge potential in the market where RBI has suddenly developed its keenness to allow foreign direct investment and the role of private players. Be it NBFC, it is one of the fast-emerging markets in India. Be it the insurance sector, India is ranked as the 5th largest market in Asia by premium following Japan,

Korea, China, and Taiwan. Similarly, there is huge potential lying untapped in other financial services sectors including capital market, mutual funds, etc. All in all, the financial sector in India provided it meets the required attention of the policymakers will emerge into a strong market that will be able to bear any shock and take the country on the path of growth.

MARKET SIZE

As of March 2021, AUM managed by the mutual fund's industry stood at Rs. 3,142,764 crore (US\$ 425.87 billion). Inflow in India's mutual fund schemes via systematic investment plan (SIP) was Rs. 96,080 crores (US\$ 13.12 billion) in FY21. Equity mutual funds registered a net inflow of Rs. 8.04 trillion (US\$ 114.06 billion) by end of December 2019.

Another crucial component of India's financial industry is the insurance industry. The insurance industry has been expanding at a fast pace. The total first-year premium of life insurance companies reached Rs. 2.59 lakh crore (US\$ 36.73 billion) in FY20.

Furthermore, India's leading bourse, Bombay Stock Exchange (BSE), will set up a joint venture with Ebix Inc to build a robust insurance distribution network in the country through a new distribution exchange platform.

Fundraising from the equity market grew by 116% to Rs. 1.78 lakh crore in Initial public offering (IPOs), Offer for Sale (OFS), and other market issuances in 2020. In FY20, the number of listed companies on the NSE and the BSE were 1,795 and 5,377, respectively.

INVESTMENTS/DEVELOPMENTS

- In February 2021, the Reserve Bank of India (RBI) cleared the Rs. 34,250 crore (US\$ 4.7 billion) acquisition of Dewan Housing Finance Corporation (DHFL) by the Piramal Group.
- In January 2021, Sundaram Asset Management Company announced the acquisition of Principal Asset Management for Rs. 338.53 crores (US\$ 46.78 million).
- In January 2021, the National Stock Exchange (NSE) launched derivatives on the Nifty Financial Service Index. This service index is likely to provide institutions and retail investors more flexibility to manage their finances.
- In November 2020, LIC took initiatives to facilitate quicker proposal completion by launching a digital application – ANANDA.
- In November 2020, Paytm reported 2 x growths in digital gold transactions in the last six months. New customers have increased 50% since the beginning of this financial year and the average order value has increased by 60%.
- In November 2020, the Reserve Bank of India (RBI) announced the establishment of its Innovation Hub. To encourage access to financial services and goods and foster financial inclusion, this initiative would create an ecosystem. The Innovation Hub of the Reserve Bank (RBIH) is intended to promote innovation across the financial sector by leveraging technology and creating a conducive environment for innovation.
- VC investments grew to US\$ 3.6 billion in July-September 2020 from US\$ 1.5 billion in the previous quarter, powered by the mega-deals, which included the US\$ 1.3 billion raised by the online retailer—Flipkart.
- On November 6, 2020, WhatsApp started its UPI payment services in India on receiving the National Payments Corporation of India (NPCI) approval to 'Go Live' on UPI in a graded manner.
- In April 2021, Unified Payments Interface (UPI) recorded 2.64 billion transactions worth Rs. 4.93 lakh crore (US\$ 66.88 billion).
- The number of transactions through Immediate Payment Service (IMPS) increased to 322.96 million and was worth Rs. 2.99 lakh crore (US\$ 40.58 billion) in April 2021.

GOVERNMENT INITIATIVES

- The government has approved 100% FDI for insurance intermediaries and increased the FDI limit in the insurance sector to 74% from 49% under the Union Budget 2021-22.
- In January 2021, the Central Board of Direct Taxes launched an automated e-portal on the e-filing website of the department to process and receive complaints of tax evasion, foreign undisclosed assets, and register complaints against 'Benami' properties.
- In December 2020, the Reserve Bank of India issued a draft circular on the declaration of dividends by NBFCs, wherein it proposed that NBFCs should have at least 15% Capital to Risk-Weighted Assets Ratio (CRAR) for the last 3 years, including the accounting year for which it proposes to declare a dividend.
- In November 2020, the Union Cabinet approved the government's equity infusion plan for Rs. 6,000 crores (US\$ 814.54 million) in the NIIF Debt Platform funded by the National Investment and Infrastructure Fund (NIIF) consisting of Aseem Infrastructure Finance Limited (AIFL) and NIIF Infrastructure Finance Limited (NIIF) (NIIF-IFL).
- In November 2020, two MoUs were signed—one between India International Exchange (India INX) and Luxembourg Stock Exchange and another between State Bank of India and Luxembourg Stock Exchange for cooperation in financial services, ESG (environmental, social, and governance), and green finance in the local market.
- On November 11, 2020, The Cabinet Committee on Economic Affairs approved the continuation and revamping of the scheme for financial support to public-private partnerships (PPPs) in the 'Infrastructure Viability Gap Funding (VGF) Scheme' until 2024-25 with a total outlay of Rs. 8,100 crore (US\$ 1.08 billion).

Road Ahead

India is expected to be the fourth largest private wealth market globally by 2028. India is today one of the most vibrant global economies on the back of robust banking and insurance sectors. The relaxation of foreign investment rules has received a positive response from the insurance sector, with many companies announcing plans to increase their stakes in joint ventures with Indian companies. Over the coming quarters, there could be a series of joint venture deals between global insurance giants and local players.

The Association of Mutual Funds in India (AMFI) is targeting nearly five-fold growth in AUM to Rs. 95 lakh crore (US\$ 1.47 trillion) and more than three times growth in investor accounts to 130 million by 2025.

India's mobile wallet industry is estimated to grow at a Compound Annual Growth Rate (CAGR) of 150% to reach US\$ 4.4 billion by 2022, while mobile wallet transactions will touch Rs. 32 trillion (USD\$ 492.6 billion) during the same period.

Note: Conversion rate used for April 2021 is Rs. 1 = US\$ 0.01334

FINANCIAL SERVICES INDIA

Muthoot Finance:

Muthoot Finance Limited is a gold financing company. The company is a non-banking financial company (NBFC) that is engaged in providing loans (financing) against the collateral of gold jewelry. The company operates through two segments: financing and power generation. The company provides personal and business loans (secured by gold jewelry) prim...

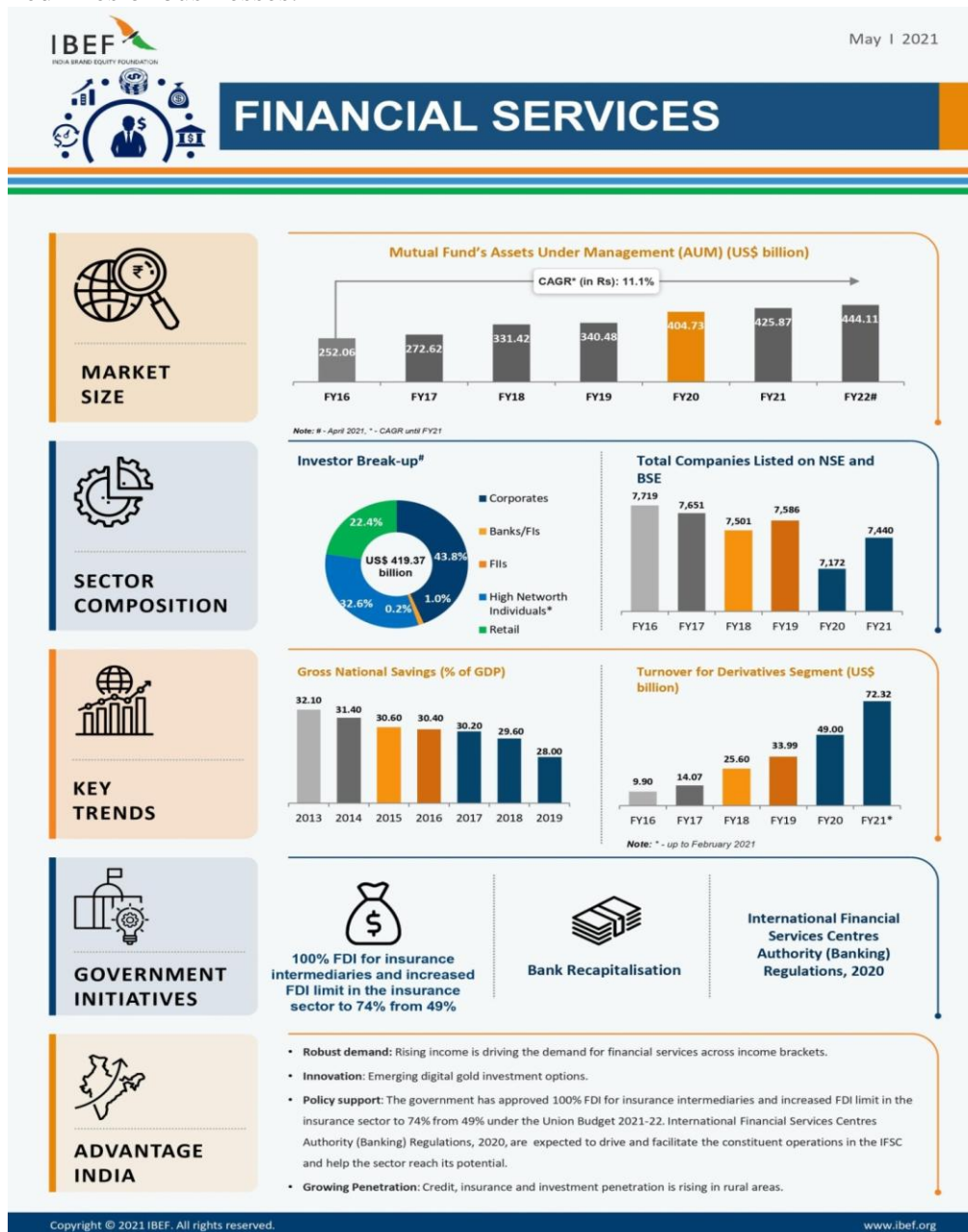
Bajaj Finserv

Bajaj Finserv Limited is a holding company for various financial services businesses. The company is engaged in the business of promoting financial services, such as finance, insurance, and wealth management, through its investment in subsidiaries and joint ventures (JVs). The company is also engaged in the business of generating power through win...

ICICI Prudential Life Insurance Company

ICICI Prudential Life Insurance Company Limited is a joint venture between ICICI Bank Limited and Prudential Corporation Holdings Limited. The company provides life insurance, pensions, and

health insurance to individuals and groups. It conducts business in participating, non-participating and unit-linked lines of businesses.



INDIAN FINANCIAL SERVICES INDUSTRY ANALYSIS

The country's financial services sector consists of capital markets, the insurance sector, and non-banking financial companies (NBFCs). India's gross national savings (GDS) as a percentage of Gross Domestic Product (GDP) stood at 30.50% in 2019. In 2019, US\$ 2.5 billion was raised across 17 initial public offerings (IPOs). The number of ultra-high-net-worth individuals (UHNWIs), with a wealth of US\$ 30 million or more, is expected to rise 63% between 2020 and 2025 to 11,198; India has the second-fastest growth in the world.

India has scored a perfect 10 in protecting shareholders' rights on the back of reforms implemented by the Securities and Exchange Board of India (SEBI) in the World Bank's Ease of Doing Business 2020 report.

As of January 2021, AUM managed by the mutual fund's industry stood at Rs. 32.29 lakh crore (US\$ 438.27 billion). Inflow in India's mutual fund schemes via the Systematic Investment Plan (SIP) route reached Rs. 82,453 crore (US\$ 11.70 billion) in 2019. Equity mutual funds registered a net inflow of Rs. 8.04 trillion (US\$ 114.06 billion) by end of December 2019.

16% of assets in the mutual fund industry were generated from B30 locations in December 2020. These assets increased by 3%, from Rs. 4.95 lakh crore (US\$ 62.26 billion) in December 2020 to Rs. 5.13 lakh crore (US\$ 70.75 billion) in January 2021.

The Government of India has taken various steps to deepen reforms in the capital market, including simplification of the IPO process, which allows qualified foreign investors (QFIs) to access the Indian bond market. In 2019, investment in Indian equities by foreign portfolio investors (FPIs) touched a five-year high of Rs. 101,122 crore (US\$ 14.47 billion). Investment by FPIs in India's capital market reached a net Rs. 12.52 lakh crore (US\$ 177.73 billion) between FY02-21 (till August 10, 2020).

Indian stock markets—S&P Sensex and Nifty50—rose 15.75 and 14.90%, respectively, in 2020. For the decade ended in 2020, the Sensex gained a whopping 173% and Nifty surged by 169%.

In January 2021, the National Stock Exchange (NSE) launched derivatives on the Nifty Financial Service Index. This service index is likely to provide institutions and retail investors more flexibility to manage their finances.

In January 2021, the Central Board of Direct Taxes launched an automated e-portal on the e-filing website of the department to process and receive complaints of tax evasion, foreign undisclosed assets, and register complaints against 'Benami' properties.

Fundraising from the equity market grew by 116% to Rs. 1.78 lakh crore in Initial public offering (IPOs), Offer for Sale (OFS), and other market issuances in 2020.

In December 2020, a US\$ 50-million policy-based loan to enhance financial management practices and operational efficiencies aimed at achieving greater fiscal savings, fostering informed decision-making, and enhancing service delivery in West Bengal were signed by the Asian Development Bank (ADB) and the Government of India.

In December 2020, the Reserve Bank of India issued a draft circular on the declaration of dividends by NBFCs, wherein it proposed that NBFCs should have at least 15% Capital to Risk-Weighted Assets Ratio (CRAR) for the last 3 years, including the accounting year for which it proposes to declare a dividend.

The government has approved 100% FDI for insurance intermediaries and increased the FDI limit in the insurance sector to 74% from 49% under the Union Budget 2021-22.

CONCLUSION:

India is expected to be the fourth largest private wealth market globally by 2028. India is today one of the most vibrant global economies on the back of robust banking and insurance sectors. The relaxation of foreign investment rules has received a positive response from the insurance sector, with many companies announcing plans to increase their stakes in joint ventures with Indian companies. Over the coming quarters, there could be a series of joint venture deals between global insurance giants and local players. The Government of India has introduced several reforms to liberalize, regulate and enhance this industry. The Government and Reserve Bank of India (RBI) have taken various measures to facilitate easy access to finance for Micro, Small, and Medium Enterprises (MSMEs). These measures include launching Credit Guarantee Fund Scheme for MSMEs, issuing guidelines to banks regarding collateral requirements, and setting up a Micro Units Development and Refinance Agency (MUDRA). With a combined push by Government and private sector, India is undoubtedly one of the world's most vibrant capital markets.

REFERENCES:

1. Suresh Aaluri, Dr.M.Srinivasa Narayana, Dr. P. Vijay Kumar (2016); A Study on Financial Inclusion Initiatives and Progress concerning Indian Banking Industry in the digital era, International Journal of Research in Finance and Marketing, ISSN (o) 2231-5985, Vol. 6, Issue. 10, pp. 125-134.
2. Manendra Singh (2012); An Overview of Financial Services Sector in India: A Huge Untapped Potential in the Market, Chartered Accountant Practice Journal, vol.38, pp.18-26.

Websites:

1. www.manupatra.com
2. www.ibef.org

See discussions, stats, and author profiles for this publication at: <https://www.researchgate.net/publication/375661923>

AN IMPACT OF COVID-19 SECOND WAVE ON INDIAN ECONOMY

Article · November 2023

CITATIONS

0

READS

30

1 author:



Venu Kesireddy

12 PUBLICATIONS 2 CITATIONS

SEE PROFILE

AN IMPACT OF COVID-19 SECOND WAVE ON INDIAN ECONOMY

Venu Kesireddy Assistant Professor Vaagdevi College of Engineering, Autonomous
kesireddyvenu@gmail.com

Abstract

This study aims to know the impact of the covid 19-second wave on the Indian economy. For this study, I have gone through tabulation analysis with different studies already taking place. The second wave of the Covid-19 pandemic has taken a vicious toll on India's health, but the economic toll has also been heavy, though nothing like the carnage seen in the first quarter of the last fiscal year, when GDP growth crashed 23.9 percent in response to India's GDP shrank 7.3 percent in 2020-21 (in real terms adjusted for inflation). This is the worst performance of the Indian economy in any year since Independence. Almost all the sectors have been adversely affected as domestic demand and exports sharply plummeted with some notable exceptions where high growth was observed. A major concern of the second wave is that the virus has spread into India's hinterland and could wreak havoc in villages, towns, and small cities. Lockdowns may help break the chain of transmission; however, they will postpone another surge unless the gap period is utilized to vaccinate the people. As of now, the country's GDP growth is likely to be below the expected 10 percent.

Keywords: Covid - 19, Indian Economy, GDP, Impact.

INTRODUCTION

Agriculture will see a deeper cut from the second wave compared to the first wave where it grew. It has been more than a year and a half since the COVID-19 pandemic penetrated the deepest core of human civilization and made us realize the power of Mother Nature. In India, after the first wave, we thought that we had gained control of the situation, but the second wave found us wanting for basic necessities such as oxygen and medical supplies. It might appear that the second wave is on its way out with daily cases coming down to under 60,000 from the peaks of nearly 4 lakh cases, but we have lost over 3.8 lakh precious lives to COVID-19 already. With the hope that the situation will significantly improve on the medical side, it is time to assess the impact of the second wave on macroeconomics.

The government's approach to dealing with the two waves has been different. The response to the second wave has been localized and driven by the states, while in the first wave we went for a national lockdown. I attribute this to the economic compulsions of the hard-hit central government and the progressive spread of the virus. The second wave started in the west with Maharashtra, went up North and now is peaking in the south of the country. This spread journey makes a national lockdown economically suboptimal.

To understand the economic impact of the second wave, let's remind ourselves of the first wave and its impact on the economy. In the first wave, we went through a prolonged national lockdown and a significantly lower number of peak cases. Manufacturing and the urban economy had come to a grinding halt while the rural economy continued to move because of less strict lockdowns. As a result, agriculture, which is the primary driver of our rural economy, providing employment to 58% of our population, continued to grow. Agriculture further benefited from good monsoon and cheaper and higher availability of labor. Reflecting on the GDP figures, our agricultural economy grew by 3.4% while the overall economy contracted by 7.7% in FY21. The first wave was primarily urban in its spread. Urban areas reported more cases than rural areas for the first five months of the spread. In the second wave, rural areas started reporting more cases than urban ones from the second month itself. An analysis of more than 50 most severely hit districts, 26 were in rural areas. Rural areas in the state of Maharashtra, Andhra Pradesh and Kerala were the worst impacted. The situation was further aggravated,

due to the inadequacy of medical infrastructure in the rural areas and the rush of patients from villages and smaller towns to urban centers.

When early signs of the second Covid-19 wave emerged in India a few months ago, many experts predicted that the economic damage would not be as bad as the first wave in 2020. There were two primary reasons behind the assertion — India had vaccines against the virus and no nationwide lockdown was imposed.

But almost three months after the first signs of the second wave emerged, India is struggling to vaccinate its vast population and strict lockdowns remain imposed in almost all parts of the country. As a result, the economic growth projections shared earlier have changed drastically. Even SBI, the country's largest public lender, recently slashed its FY22 growth forecast.

Data on jobs, income, household income, consumer sentiment and demand show that the second wave has had a devastating impact on India's economy, especially on poorer citizens and smaller businesses. Even rural areas that were a saving grace during the first wave have been deeply affected this time.

OBJECTIVES OF THE STUDY

1. To focus on the impact of a second wave pandemic on Indian economy.
2. To draw conclusions and offer suggestions.

RESEARCH METHODOLOGY

The present Research Paper uses Secondary Data by collecting information on the present issue like websites, newspaper articles, magazines, government reports, journals, etc. In line with this, the use of an extensive Literature Review method has been implemented to carry out the present research meaningful. Literature review methodology is a proven tool to do secondary data base reviews. They serve and present solid grounds for future investigation. However, both conducting a literature survey and utilizing it for strategy reasons has continuously been challenging. However, in this study we utilized them tactfully to build on incredible precision instead of conducting the same research once again.

REVIEW OF LITERATURE:

Ajay Kumar Poddar*1 and Brijendra Singh Yadav2 (2020), India is already falling short in meeting its growth expectations in the last two FY. The GST collection is also not at par. The situation of COVID-19 is aggravating the financial health of the country, even worsening. As per the UN report, India will be impacted by \$348 mn on its trade due to the Corona Virus. The figure will increase even further depending on the period of lockdown, locally & globally. Hence, the Null Hypothesis has been proved successfully that there is a significant relationship between the happening of COVID-19 and the fall of the Indian Economy.

The current COVID-19 outbreak has provoked social stigma and discriminatory behaviors against people of certain ethnic backgrounds as well as anyone perceived to have been in contact with the virus. **(Barrett R, Brown P J. 2008)**

ICRA has also indicated their concern for the production, manufacturing and service industries amid the uncertainty of the lockdown situation. They suspect that the situation will take a longer period to normalization. "The negative trend of the economy will start giving indicators from the 3rd week of March 2020". The industries like construction, hotels, live events, travel, tourism will be the first ones to be affected due to their nature of unessential.

The increasing number of emerging infectious disease events of international concern, such as severe acute respiratory syndrome (SARS) and the 2009 pandemic influenza A/H1N1, dictate a specific need to increase bidirectional communication between local governments and the international community. Recognizing this need, the Global Outbreak Alert and Response Network (GOARN) was formed in

2000 as a global collaboration to consolidate technical support for outbreak surveillance and response efforts (8), and the WHO's International Health Regulations (IHR 2005) were revised to update surveillance capacity standards and mandate reporting of disease events that may constitute "public health emergencies of international concern" (Chan E H, Brewer T F, Madoff L C, Pollack M P, Sonricker A L., and others. 2010).

IMPACT OF SECOND WAVE PANDEMIC ON INDIAN ECONOMY

This second wave pandemic has created new issues for the Indian economy that led to a severe disastrous impact on Agriculture, Manufacturing, and Services.

Agriculture

The second wave has seen stricter and longer lockdowns in the rural parts of the country. Due to the lockdowns, APMC Mandis has been closed for operations or has taken such steps voluntarily. Specifically, APMC Mandis in Gujarat, Rajasthan and Maharashtra were closed during the peak harvesting season. Farmers were not prepared for the ensuing chaos. As the Mandis have still not opened fully, crops are rotting in the fields. Due to the closure of Mandis, vegetable vendors, and processing industries have also been hit. We can see the contrasting impact of the first and the second wave in the agriculture wage growth data. The average wage growth for the agriculture sector for the period of November 2020 to March 2021 has reduced to 2.9 percent (2nd wave) from 8.5 percent in April to August 2020 (1st wave).

Manufacturing

Manufacturing was at the receiving end in both the first and the second wave. To control the corona virus spread, most of the manufacturing sector had to work at a lesser capacity or shut down. Non-essentials manufacturing was hit for longer and with more severe restrictions. The fear of prolonged lockdowns led to migration back to villages. In addition, the global and local supply chains had also not fully normalized after the first wave. This has meant a higher cost of procuring raw materials for both small and large industries. As per the IHS Market India Manufacturing Purchasing Managers' Index (PMI) in May 2021, the PMI slumped to 50.8 from 57.5 reported in February. It is at a ten-month low.

Services

The services sector in the last two decades has become the bedrock of the Indian economy, contributing to more than half of the GDP. But, our services and knowledge-based industries have been built on the manufacturing industry premise of the 18th century, i.e. proximity and discipline of workers to the factory is critical in getting good output. We apply the same philosophy to our software engineers and telecalling workforce. With the internet revolution, this premise has proven to be an unnecessary legacy of the past. Now the workforce can be decentralized and anyone can work from anywhere till the time there is 4G internet. I do believe that COVID will prove a positive disruption for the services sector in the long run.

The first wave required a steep learning curve for organizations to develop infrastructure and processes for remote working. For the employees, the first wave lockdowns were a new paradigm and it took them some time to adjust to working from home and be productive. Prolonged lockdown and unlocking phases during the first wave ensured that both the employer and employee got into a rhythm and the productivity started reaching pre-covid levels. The second wave disrupted this rhythm. But the impact of the second wave has been localized and centered around groups of people with typical disruptions costing 3-4 weeks of productivity. My assessment is that the services sector will be the least hit by wave 2 from an output standpoint.

The table below summarizes the above ideas.

Time period	Indian GDP % growth	Agriculture GDP % growth	Manufacturing GDP % growth	Services GDP % growth
FY 21 (Reflection of the Wave-1)	-7.3	Contracted by 16 %	Contraction by 7.2%	A growth of 3.4%
% contribution to the overall GDP	Nil	55%	17.4%	17.8%
Expected impact of the wave 2	8.2% to 9.3% (overall growth due to base effect but reduced forecasts by rating agencies)	Significantly lower than wave-1	lower than wave-1	Higher than wave-1

Source: www.financialexpress.com

The overall impact on GDP

On May 31, the Indian government released the data for GDP that during the financial year 2020-21, GDP contracted by 7.3 percent. It is the most severe contraction from the time India got its independence. The reasons behind this trajectory are obvious – lockdown leading to the closing of business units, increasing unemployment rate and a significant decline in domestic consumption.

For the current financial year, the Reserve Bank of India has anticipated growth of 10.5 percent. But the rating agencies across the globe have downgraded it due to the impact of the second wave of COVID-19. Moody’s initially projected 13.7 percent of growth for FY 2021-22, but later lowered it to 9.3 percent. The same goes with S & P Global Rating. They have lowered the 11 percent growth to 9.8 percent in the case of moderate impact of the second wave, but for a worst-case scenario, it would be 8.2 percent. The ideas around a third wave are not helping the situation at all.

To summarize the macroeconomic numbers of GDP, I expect a less severe impact of the second wave due to less strict, localized lockdowns and practically a lesser number of days in reaching the peak number of infections. Agriculture will see a deeper cut from the second wave compared to the first wave where it grew. Our hopes of economic revival are pinned to us having an express vaccination drive, which takes away the fear of a third wave and a revival of consumer confidence and spending.

Conclusion:

The majority of aged people died from Corona. Locked down have declined the price of oil and affected the economy of the oil countries of the world. China has controlled the situation while in other countries still the struggle is continued for control. It may be possible it will be controlled in the month of August, 2020. Now the trend has declined in the world as well as in India. India's government had followed the SOPs of W.H.O. but due to religious movement it was disturbed and the corona virus was spread throughout India. Similarly, all the community was in fear and stayed at home, which has created other diseases in the community. The density of the India population was high and because of this, the chances of corona spreading were greater in the country. majority of people become unemployed and jobless in the country. On the basis of problems, the study recommends that we fully quarantine the boundary line of the country in the future; The health budget should be increased in the country for construction of hospital and medical facilities; Locked down should be implemented in time in the country; Unity in the country is required; Good and trained doctors should be appointed in the hospital; Large and big hospitals should be constructed in the country where the number of beds is more than the requirement in the time of emergency; Principles of the SOPs should be followed by the community of the country; A mask should be worn during locked down and after entering the home, hands must be

washed with soap; Quality food should be eaten for the development of immunity. Aged people should be kept away from this type of virus.

References:

1. Barrett R, Brown P J. 2008. “Stigma in the Time of Influenza: Social and Institutional Responses to Pandemic Emergencies.” *Journal of Infectious Diseases* 197 (Suppl 1): S34–S37
2. Chan E H, Brewer T F, Madoff L C, Pollack M P, Sonricker A L., and others. 2010. “Global Capacity for Emerging Infectious Disease Detection.” *Proceedings of the National Academy of Sciences of the United States of America* 107 (50): 21701–6.
3. Ajay Kumar Poddar*1 and Brijendra Singh Yadav2 (2020), pact of COVID-19 on Indian Economy- A Review, *Journal of Humanities and Social Sciences Research, Horizon J. Hum. & Soc. Sci.* 2 (S): 15 – 22 (2020).

Websites:

www.indiatoday.in
www.indianexpress.in
www.financialexpress.com

NUMERICAL ANALYSIS OF DOUBLE PIPE HEAT EXCHANGER FITTED WITH TWISTED TAPE BY VARYING TWIST RATIO

Boda Naresh Babu¹

Dr. Sanjeev Kumar Sajjan²

Dr.P.Srinivasulu³

¹M.Tech (Thermal Engineering)Department of mechanical engineering vaagdevi college of engineering (UGC autonomous) approved by AICTE & permanent affiliation to jntuh, hyderabad.p.o, bollikunta, Warangal urban-506005.

²Assistant Professor Department of mechanical engineering vaagdevi college of engineering (UGC autonomous) approved by AICTE & permanent affiliation to jntuh, hyderabad. p.o, bollikunta, Warangal urban- 506005.

³Professor and Head of the Department of mechanical engineering vaagdevi college of engineering (UGC autonomous) approved by AICTE & permanent affiliation to jntuh, hyderabad. p.o, bollikunta, Warangal urban-506005.

Abstract Heat exchangers are widely used as essential units in heat extracting and recovering systems in industries. High performance heat transfer system is of great importance in many industrial applications. The performance of heat exchanger can be substantially improved by a number of augmentation techniques. The present work reported the use of twisted tapes with different twist ratio fitted in a double pipe heat exchanger to improve the fluid mixing that leads to higher heat transfer rate with respect to that of the plain tube. Heat transfer rate, overall heat transfer coefficient, pressure drop and velocity stream line characteristics etc are investigated numerically in a double pipe heat exchanger fitted with twisted tape with different twisted ratios using water as working fluid. Tests are performed for turbulent flow Reynolds number ranges. In this work number of twists in twisted tape taken as 15,20,25 And corresponding Twisted Ratios obtained are $Y = 4.88, 3.66, 2.93$ Respectively. CFD Analysis is carried out at different Hot fluid mass flow rates by keeping cold fluid mass flow rate as constant For Different Twist Ratios.

Introduction to Heat Exchangers:

Heat exchangers have several industrial and engineering applications. The design procedure of heat exchangers is quite complicated, as it needs exact analysis of heat transfer rate and pressure drop estimations apart from issues such as long-term performance and the economic aspect of the equipment. The major challenge in designing a heat exchanger is to make the equipment compact and achieve a high heat transfer rate using minimum pumping power.

Techniques for heat transfer augmentation are relevant to several engineering applications. In recent years, the high cost of energy and material has resulted in an increased effort aimed at producing more efficient heat exchange equipment. Furthermore, sometimes there is a need for miniaturization of a heat exchanger in specific

applications, such as space application, through an augmentation of heat transfer. For example, a heat exchanger for an ocean thermal energy conversion (OTEC) plant requires a heat transfer surface area of the order of 10000 m²/MW. Therefore, an increase in the efficiency of the heat exchanger through an augmentation technique may result in a considerable saving in the material cost.

Double Pipe Heat Exchanger:

The double pipe or the tube in tube type heat exchanger consists of one pipe placed concentrically inside another pipe having a greater diameter. The flow in this configuration can be of two types: parallel flow and counter-flow. It can be arranged in a lot of series and parallel configurations to meet the different heat transfer requirements. Of this the helically arranged stands out as it has found its place in different industrial applications. As this configuration is widely used, knowledge about the heat transfer coefficient, pressure drop, and different flow patterns has been of much importance. The curvature in the tubes creates a secondary flow, which is normal to the primary axial direction of flow. This secondary flow increases the heat transfer between the wall and the flowing fluid. And they offer a greater heat transfer area within a small space, with greater heat transfer coefficients. Study has been done on the types of flows in the curved pipes, and the effect of Prandtl and Reynolds number on the flow patterns and on Nusselt numbers. The two basic boundary conditions that are faced in the applications are constant temperature and the constant heat flux of the wall.

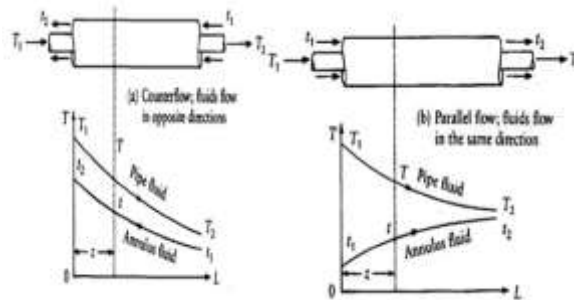


Fig: Fluid Flow Directions

The need to increase the thermal performance of heat exchangers, thereby effecting energy, material & cost savings have led to development & use of many techniques termed as Heat transfer Augmentation. These techniques are also referred as —Heat transfer Enhancement or Intensification. Augmentation techniques increase convective heat transfer by reducing the thermal resistance in a heat exchanger.

Performance Evaluation Criteria:

In most practical applications of enhancement techniques, the following performance objectives, along with a set of operating constraints and conditions, are usually considered for optimizing the use of a heat exchanger

1. Increase the heat duty of an existing heat exchanger without altering the pumping power (or pressure drop) or flow rate requirements.
2. Reduce the approach temperature difference between the two heat-exchanging fluid streams for a specified heat load and size of exchanger.
3. Reduce the size or heat transfer surface area requirements for a specified heat duty and pressure drop or pumping power.
4. Reduce the process stream's pumping power requirements for a given heat load and exchanger surface area.

2.LITERATURE REVIEW

Kumar and Prasad (2000) enhanced the solar water heater performance by inserting the twisted tapes with twist ratios ranging from 3 - 12 and conducted the experiment for varying mass flow rates. They observed that the heat transfer in the twisted tape insert collectors had been found to increase by 18 - 70%, whereas the pressure drop increased by 87 - 132%. Twisted tape collectors performed remarkably better in the lower range of flow Reynolds number ($Re = 12,000$) beyond which the increase in thermal performance was monotonous.

Eiamsa-ard and Promvonge (2006) conducted the experiment on heat transfer and friction factor characteristics for the uniform heat flux tube fitted with V-nozzle inserts with three different pitch ratios of 2.0, 4.0 and 7.0. The experimental results showed

that the V-nozzle inserts could help to increase considerably the heat transfer rate at about 270% over the plain tube due to reverse/recirculation flows. The smallest pitch ratio led to maximum enhancement efficiency than those with higher pitch ratio.

Eiamsa-ard et al. (2006) experimentally investigated the heat transfer and friction factor characteristics in a double pipe heat exchanger fitted with full-length typical twisted tape at different twist ratios ($y = 6.0$ and 8.0) and twisted tape with various free space ratios ($s = 1.0, 2.0$ and 3.0). The results showed that the heat transfer coefficient increased with a decrease in twist ratio for full length twisted tape and whereas the decrease in the free space ratio would improve both the heat transfer coefficient and friction factor for regularly spaced twisted tape elements.

The heat transfer and pressure drop characteristics in a horizontal double pipe heat exchanger with twisted tape inserts at different pitch ($H = 2.5$ and 3cm) by varying the temperature and mass flow rates for both hot and cold water flows were studied by Naphon (2006). It was observed that the heat transfer rate at lower twist ratio was higher than those from higher ones across the range of Reynolds number. This was because the turbulent intensity and the flow length obtained from lower twist ratio was higher than those at higher ones and also stated that the tube-side heat transfer coefficient at higher cold water mass flow rate was higher than that of the lower ones. This was because the heat transfer rate depends directly on the cooling capacity of cold water.

Promvonge and Eiamsa-ard (2007a) studied the heat transfer and friction factor and enhancement efficiency characteristics in a circular tube fitted with conical-ring turbulators and combination of conical-ring with twisted tape for the twist ratios of ($y = 3.75$ and 7.5). The experimental results revealed that the tube fitted with the conical-ring and twisted tape provides higher heat transfer rate and enhancement efficiency than that of the conical-ring alone. In addition, the correlations were developed for Nusselt number, friction factor and enhancement efficiency for conical-ring and conical-ring with twisted tape respectively.

3.Computational Fluid Dynamics (CFD):

CFD is the science of predicting fluid flow, heat transfer, mass transfer, chemical reactions and related phenomena by solving the mathematical equations which govern these processes using numerical methods in the computer. CFD provides a qualitative and quantitative prediction of fluid flows by means of mathematical modelling numerical methods, and

software tools. It gives an insight into flow patterns that are difficult, expensive or impossible to study using experimental techniques. CFD simulation is a three step process namely Pre-processing, Solver, Post-processing.

Technical Details of Variant Twisted Tapes:

This section deals with the technical terms, design, fabrication part associated with twisted tape and details of the variant twisted tapes. The technical details related to P-TT and variant twisted tapes are discussed below:

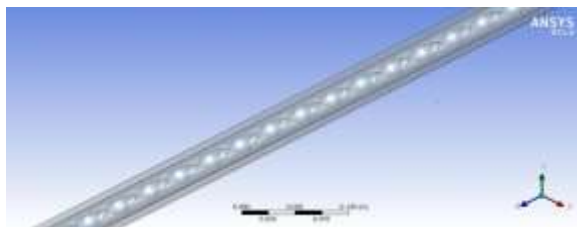
Pitch (H): It is distance of one length of twist in the twisted tapes for the angle of rotation 180°

Twist Ratio (Y): The twist ratio is defined as the value of one length of twist (or) pitch length to inner diameter of tube (Agarwal and Raja Rao 1996, Wang and Sunden 2002, Dewan et al. 2004 and Eiamsa-ard et al. 2006).

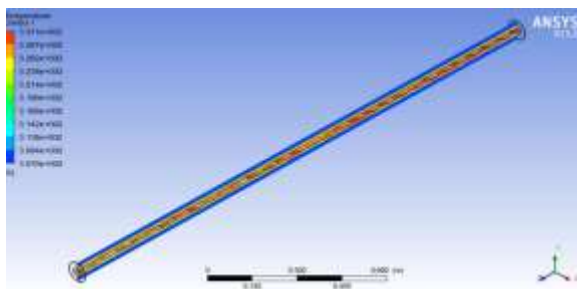


Fig: twisted tape

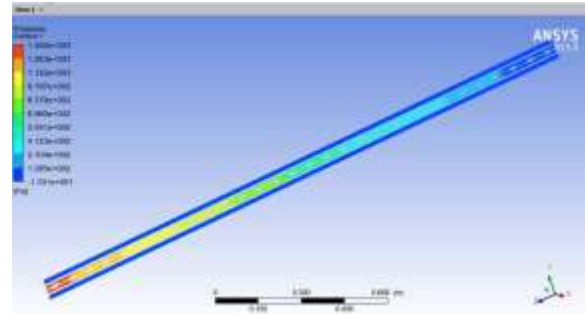
Imported Model



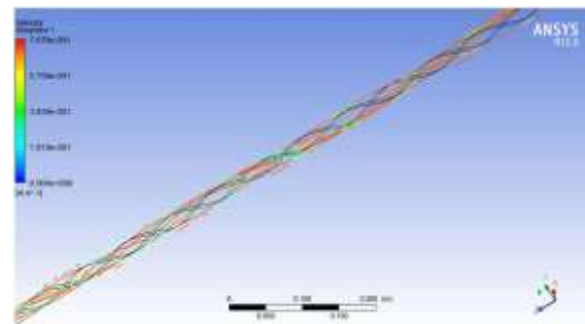
The Temperature, Pressure and Velocity Contours Of P-TT with Y=4.88



Pressure



Velocity



CFD Validation:

To validate the Numerical Analysis results an Experimental work is conducted on plain Double pipe heat exchanger with different mass flow rates and results are compared with CFD plain Tube results.

The experimental setup consists of a Double pipe heat exchanger with provision to permit cold water in the annulus in opposite directions is available. Hot water from the geyser flows through the inner tube. The heat transfer takes place across the wall of the inner tube. The cold water in the annulus is made to flow in the opposite direction i.e., the two fluids oppose each other and the flow is known as counter flow. There is provision to record the temperature at the inlet and outlet locations.

Under steady state conditions, the heat energy given by the hot water must equal the energy gain by the cold water, when there are no heat losses. Then, the

heat exchanger has to be designed for a heat load Q , which is equal to heat energy associated with hot water Q_h or that with cold water Q_c .

Hence the steady state condition with no heat losses is given by $Q_h = Q_c = Q$

4.EXPERIMENTAL WORK

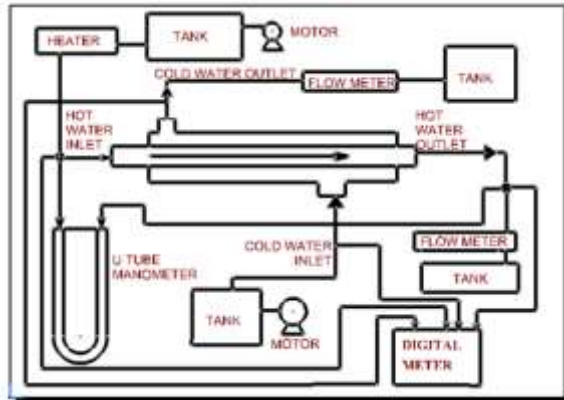


Fig. :Schematic View of the Experimental Setup

Experimental Procedure:

1. Switch on the geyser and allow the hot fluid (water) to flow in the inner tube.
2. Open the valve so that cold fluid (water) to flow through the annulus and run the exchanger as a counter flow unit.
3. See that the pipes run full of water.
4. Record the inlet and exit temperatures of hot and cold fluid after steady state is attained.
5. The experiment is done for plain tube with cold fluid (water) mass flow rate constant at full valve opening and hot fluid (water) mass flow rate is varied at three valve openings (90, 60 and 30 degrees of the valve openings) respectively. And the results tabulated below.

Plane Tube Experimental Results

Cold mass flow rate (kg/s)	Hot mass flow rate (kg/s)	T_{ci}	T_{co}	T_{ci}	T_{co}	Q_c (KW)	Q_h (KW)	Q_{avg}	LMTD	$\Delta T_{DC - DMTC}$	U_{avg}
0.4	0.12	307	308	329	328	1.3848	1.872	1.5984	18.98	3.70628	438.988
0.4	0.24	307	309	332	329	3.0598	3.244	3.1718	22.48	4.1778	781.47
0.4	0.4	307	308	331	328	3.036	2.872	2.944	22.98	4.87728	820.232

5. RESULTS AND DISCUSSIONS

cold mass flow rate (kg/s)	hot mass flow rate (kg/s)	T_{ci}	T_{co}	T_{ci}	T_{co}	P_h	P_c	h_i	h_o	U_1	U_{Th}
0.4	0.12	307	308.828	329	323.812	184.8913	24.3393	1228.73	821.22	482.2383	463.89
0.4	0.24	307	308.41	332	329.887	498.426	24.734	2073.71	822.22	584.0629	587.8
0.4	0.4	307	308.84	331	328.833	1098.86	24.734	2049.28	822.22	647.192	688.27

cold mass flow rate (kg/s)	hot mass flow rate (kg/s)	T_{ci}	T_{co}	T_{ci}	T_{co}	P_h	P_c	h_i	h_o	U_2	U_{Th}
0.4	0.12	307	308.82	328	323.683	183.864	24.78	1160.14	821.374	480.8984	477.32
0.4	0.24	307	308.48	332	329.666	527.88	24.78	1977.82	821.374	586.3653	589.87
0.4	0.4	307	308.78	331	328.432	1419.23	24.78	2988.32	821.374	644.1828	687.42

Calculation of % of error for plain tube to validate CFD results

For Plain Tube with hot fluid mass flow rate $m_h = 0.12$ Kg/s

$$U_{Cfd} = 450.456 \text{ W/m}^2\text{k}$$

$$U_{Exp} = 460.5687 \text{ W/m}^2\text{k}$$

$$\% \text{ of error} = (U_{exp} - U_{Cfd}) / U_{exp} = 2.24\%$$

Plain tube results

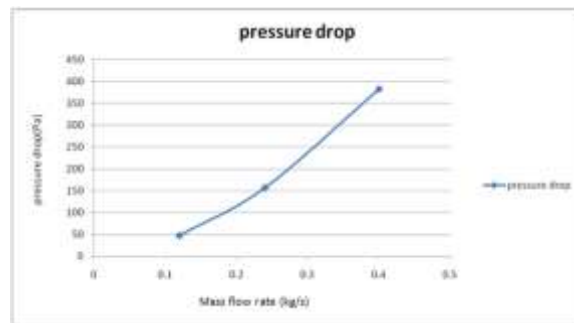


Fig.: Mass Flow Rate Vs Pressure drop for Plain Tube

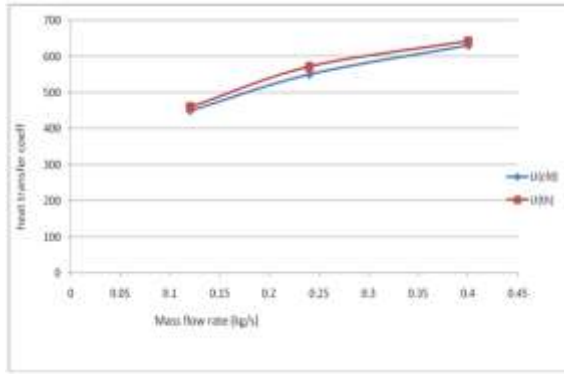
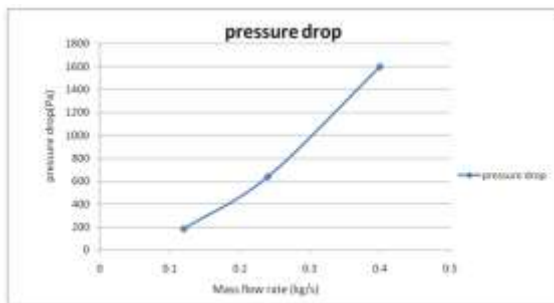
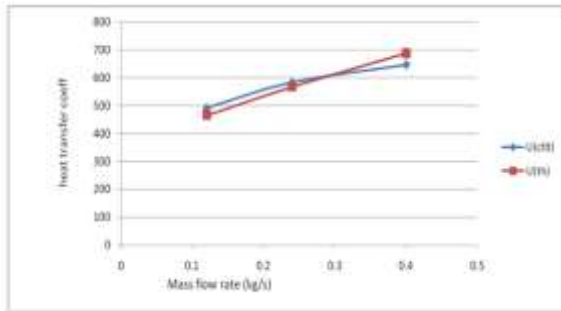


Fig.: Mass Flow Rate Vs Heat Transfer Coefficient for Plain Tube

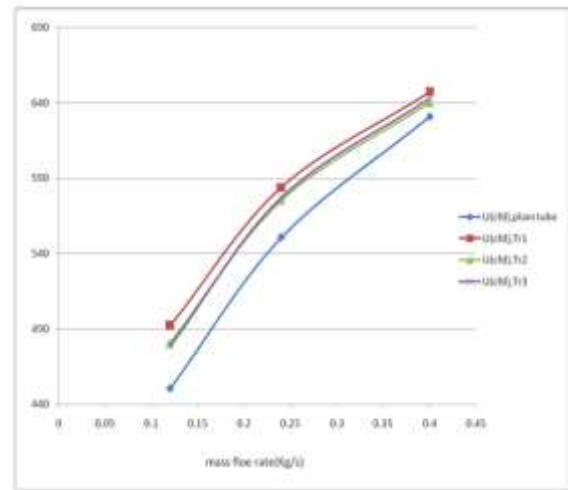
From The above Two graphs we concluded that along the length of the tube Pressure Drop is Increasing with Increasing mass flow rate. Because as mass flow rate increases Velocity of the flowing fluid also increases which increases more Turbulence causes Pressure Drop. Similarly Heat Transfer Coefficient also increases with Increase in mass flow rate.



From The above Two graphs we concluded that For Twist Ratio $Y = 2.93$ Increase in Heat Transfer Coefficient and Increase in Pressure Drop is more than all other Twist ratios and plain tube. Because of the Insertion of Twisted Tapes with number of Twists ($n = 25$) generates the more swirl flow in the tube

which improves fluid mixing and increases turbulence.

Variation of Overall Heat Transfer Coefficient for Different Twist Ratio



From The above graph we concluded that Heat Transfer Coefficient is increases with Decrease in Twist Ratio in the Range 2 to 8. Because as Twist ratio Decreases number of twists in the insert increases which creates more turbulence in the tube causes more Heat Transfer Rate than plain tube.

CONCLUSIONS

Numerical Analysis is carried out for Double Pipe Heat Exchanger fitted with twisted tape for various Twisted Ratios As $Y = 2.93, 3.66, 4.88$ and Heat transfer rate, overall heat transfer coefficient, pressure drop and velocity stream line characteristics etc are investigated Numerically By varying Hot fluid mass flow rate. The Following Conclusions are drawn based on the Numerical Analysis.

For Twist Ratio $Y = 2.93$

1. For Different mass flow rates The Increase in Heat Transfer coefficient was observed with respect to Plain tube Which varies in the range of 2.58 % - 9.28 %
2. For Different mass flow rates the Increase in Pressure Drop was observed which varies in the range of 288% - 317% with respect to Plain tube.

For Twist Ratio $Y = 3.66$

1. For Different mass flow rates The Increase in Heat Transfer coefficient was observed with respect to Plain tube Which varies in the range of 2.1 % - 6.76 %
2. For Different mass flow rates the Increase in Pressure Drop was observed which varies in the range of 244% - 270% with respect to Plain tube.

For Twist Ratio $Y = 4.88$

1. For Different mass flow rates The Increase in Heat Transfer coefficient was observed

with respect to Plain tube Which varies in the range of 1.9 % - 6.2 %

2. For Different mass flow rates the Increase in Pressure Drop was observed which varies in the range of 229% - 252% with respect to Plain tube

From The above three twist ratios we conclude that percentage of increase in Heat transfer coefficient is more for Twist ratio $Y = 2.93$ at hot fluid mass flow rate 0.12 Kg/s. This is because of as number of twists increases swirl flow in the tube increases which improves fluid mixing causes more turbulence. The percentage of increase in Heat transfer coefficient is observed more in Twist ratio ranges 2 to 8.

REFERENCES

- [1] I. Kurtbas, F. Gülçimen, A. Akbulut and D. Buran. 2009. Heat transfer augmentation by swirl generators inserted into a tube with constant heat flux. *International Communications in Heat and Mass Transfer*. 36: 865-871, doi:10.1016/j.icheatmasstransfer. 2009.04.011.
- [2].PaisarnNaphon , TanaponSuchana,“Heat transfer enhancement and pressure drop of the horizontal concentric tube with twisted wires brush inserts” *International Communications in Heat and MassTransfer* 38,(2011),pp. 236–241
- [3] Eiamsa-ard, Nivesrangsarn, Chokphoemphun. Promvongse, 2010, “Influence of combined non-uniform wire coil and twisted tape inserts on thermal performance characteristics”, *International Communications in Heat and Mass Transfer*, 37, pp. 850–856.
- [4] Sivashanmugam, Suresh, 2006, “Experimental studies on heat transfer and friction factor characteristics of laminar flow through a circular tube fitted with helical screw- tape inserts”, *Applied Thermal Engineering*, 26, pp.1990-1997.
- [5] P. Sivashanmugam, S. Suresh, Experimental studies on heat transfer and friction factor characteristics of turbulent flow through a circular tube fitted with regularly spaced helical screw-tape inserts, *Applied Thermal Engineering* 27 (2007) 1311–1319.
- [6] S. Naga Sarada, P. Ram Reddy, Gugulothu Ravi, 2013 “Experimental Investigations on Augmentation of Turbulent Flow Heat Transfer in A Horizontal Tube Using Square Leaf Inserts”, *International Journal of Emerging Technology and Advanced Engineering*, Volume 3, Issue 8.
- [7] Dr. A. G. Matani “Experimental Heat Transfer Enhancement in a Tube Using Counter/Co-Swirl generation” *International Journal of Application or Innovation in Engineering & Management (IJAIEM)*, Volume 2, Issue 3, March 2013 ,P.P.100-105

- [8] S. Naga Sarada, A. V. Sita Rama Raju, K. Kalyani Radha, and L. Shyam Sunder, “Enhancement of heat transfer using varying width twisted tape inserts,” *International Journal of Engineering, Science and Technology*, vol. 2,2010,pp.107-118.

EXPERIMENTAL STUDY ON ENHANCEMENT OF HEAT TRANSFER COEFFICIENT USING CuO NANO FLUID

GAJA SAI KRISHNA¹

P.Raju²

Dr.P.Srinivasulu³

¹M.Tech (Thermal Engineering)Department of mechanical engineering vaagdevi college of engineering (UGC autonomous) approved by AICTE & permanent affiliation to jntuh, hyderabad.p.o, bollikunta, Warangal urban-506005.

²Assistant Professor Department of mechanical engineering vaagdevi college of engineering (UGC autonomous) approved by AICTE & permanent affiliation to jntuh, hyderabad. p.o, bollikunta, Warangal urban- 506005.

³Professor and Head of the Department of mechanical engineering vaagdevi college of engineering (UGC autonomous) approved by AICTE & permanent affiliation to jntuh, hyderabad. p.o, bollikunta, Warangal urban-506005.

Abstract

Suspended nano particles in conventional fluids are called nanofluids. Recent development of nanotechnology brings out a new heat transfer coolant called 'nanofluids. these fluids exhibit larger thermal properties than conventional coolants. Nanofluids can be considered to be the next-generation heat transfer fluids because they offer exciting new possibilities to enhance heat transfer performance compared to pure liquids.

Micrometer-sized particle-fluid suspensions exhibit no such dramatic enhancement. Nano fluids are expected to have superior properties compared to conventional heat transfer fluids, as well as fluids containing micro-sized metallic particles. The much larger relative surface area of nanoparticles, compared to those of conventional particles, not only significantly improves heat transfer capabilities, but also increases the stability of the suspension.

1.Introduction To Nano Fluids

The idea behind development of nanofluids is to use them as thermo fluids in heat exchangers for enhancement of heat transfer coefficient and thus to minimize the size of heat transfer equipments.

Nano fluids help in conserving heat energy and heat exchanger material. The important parameters which influence the heat transfer characteristics of nanofluids are its properties which include thermal conductivity, viscosity, specific heat and density. The thermo physical properties of nanofluids also depend on operating temperature of nanofluids. Hence, the accurate measurement of temperature dependent properties of nanofluids is essential. Thermo physical properties of nanofluids are pre requisites for estimation of heat transfer coefficient and the Nusselt number.

Nano fluids are engineered colloidal suspensions of nano particles in a base fluid. In general the size of these nano particles vary from 1-100nm. The type of nano particle used is directly dependent on the enhancement of a required property of the base fluid.

All physical mechanisms have a critical length scale, below which the physical properties of materials are changed. Therefore particles <100 nm exhibit properties that are considerably different from those of conventional solids. The noble properties of nano phase materials come from the relatively high surface area to volume ratio that is due to the high proportion of constituent atoms residing at the grain boundaries. The thermal, mechanical, optical, magnetic, and electrical properties of nano phase materials are superior to those of conventional materials with coarse grain structures.



fig 1 Photographic view of CuO nano particles

PREPARATION METHODS FOR NANOFLUIDS

Classification Of Methods of preparation of NanoFluid

Two -Step Method

Two-step method is the most widely used method for preparing nanofluids. Nanoparticles, Nanofibers, nanotubes or other nanomaterials used in this method are first produced as dry Powders by chemical or physical methods. Then the nanosized powder will be dispersed into a fluid in the second processing step with the help of intensive magnetic force agitation, Ultrasonic agitation, high-shear mixing, homogenizing and ball milling. Two-step method is the most economic method to produce nanofluids in large scale, because nanopowder Synthesis techniques have already been scaled up to industrial production levels. Due to the High surface area and surface activity, nanoparticles have the tendency to

aggregate. The Important technique to enhance the stability of nanoparticles in fluids is the use of Surfactants. However the functionality of the surfactants under high temperature is also aBig concern, especially for high temperature applications.

Single-Step Method

In the single step method the nano particles are produced and dispersed Simultaneously into the base fluid. Two-step preparation process is extensively used in the synthesis of nanofluids by mixing base fluids with commercially available nano powders obtained from different mechanical, physical and chemical routes such as milling, grinding, and sol-gel and vapour phase methods. An ultrasonic vibrator or higher shear mixing device is generally used to stir nano powders with host fluids. Frequent use of ultra sonication or stirring is required to reduce particle agglomeration. Eastman et al , Lee et al, Wang et al. used two-step method to produce alumina nano fluids. Murshed et al.prepared TiO₂-water nano suspension by the same method. Xuan et al. used commercially available Cu nano particles to prepare nano fluids of both water and transformer oil. Kim et al used two-step method to prepare CuO dispersed ethylene glycol nano fluids by Sonication and without stabilizers. Two-step method can also be used for synthesis of carbon nanotube based nano fluids. Single -walled and multi-walled carbon nano tubes are first produced by pyrolysis method and then suspended in base fluids with or without the use of surfactants . Some authors suggested that two-step process is very suitable to prepare nano fluids containing oxide nano particles than those containing metallic nano particles . Stability is a big issue that inherently related to this operation as the powders easily aggregate due to strong van der Waals force among nano particles. In spite of such disadvantages this process is still popular as the most economic process for nano fluids production.

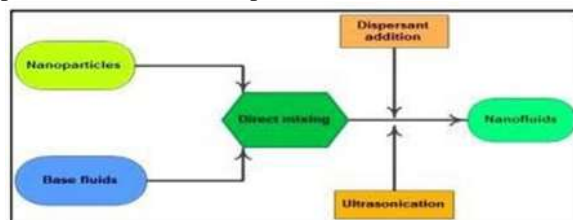


fig 2 Step Preparation for Nano Fluids

2. LITERATURE REVIEW

The nanofluids possess unique features with regard to their thermal performances. The properties of nanofluids are different from the properties of conventional heat transfer fluids. The nanoparticles offer large total surface area as a result of which

higher Heat transfer rate are expected in nanofluids. Many research findings reveal that traditional thermo fluids in the presence of nanoparticles exhibit better thermo physical properties.

The experimental studies on nanofluids confirm that fluids containing nanoparticles are expected to give more Heat transfer rate and lower specific heats over conventional fluids. Normally particles of millimeter or micro meter dimension when suspended in fluids will cause erosion of pipe materials, clogging of flow passages and sedimentation due to gravity. Studies on effective heat transfer coefficient of Nanofluid were investigated under macroscopically in stationary conditions by S.U.S. Choi (1995), Masuda et al. (1993), Eastman et al. (1996), Wang et al. (1999), Lee et al. (1999) Xuan and Li (2000), Eastman et al. (2001), Keblinski et al (2002), Xie et al (2002), Wang et al. (2003). Ahuja (1975) and Liu et al. (1988) carried out investigations on practical implication of hydrodynamics and heat transfer of slurries. The present day modern technology facilitates to produce process and characterize materials having average crystalline size below 100nm nanofluids were engineered in Argonne National Laboratory and proof test were conducted by Eastman et al (1995). The nanoparticles of Al₂O₃ and CuO materials have exhibited excellent dispersion quality and increased heat transfer coefficient when suspended in heat transfer fluids like water, oils and glycols mixtures. Brownian motion of the particles and large surface area are supposed to be the responsible factors for enhanced of nanofluids. The Heat Transfer rate present day modern technology facilitates to produce process and characterize materials having average crystalline size below 100nm nanofluids were engineered in Argonne National Laboratory and proof test were conducted by Eastman et al (1995). The nanoparticles of Al₂O₃ and CuO materials have exhibited excellent dispersion quality and increased heat transfer coefficient when suspended in heat transfer fluids like water, oils and glycols mixtures. Brownian motion of the particles and large surface area are supposed to be the responsible factors for enhanced heat transfer coefficient of nanofluids. A detailed measurement of thermal conductivity of Al₂O₃ and CuO particles dispersed in ethylene glycol and water base fluids was taken up by Lee et al. (1999). The heat transfer rate of nanofluids is measured using transient hot wire method. A considerable improvement in heat transfer of the nanofluids was noticed and researchers are motivated to undertake investigations on heat transfer studies on different nanofluids. Recent study by Xuan and Li (2000) revealed that particles as large as 100nm can also produce a stable fluid with the addition of small amount of laurite salt in the base fluids. But it was

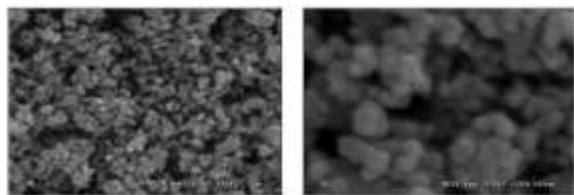
also observed in experimental studies that these dispersant affect the desirable properties of nanofluids.

3.NANO FLUID PREPARATION USING CuO NANO PARTICLES

The CuO nano particles having an average size of 50 nm and density of 6.3 gm/cm³ is procured from a India based company (Nano Partech Chemicals Private Ltd) and is used for investigation in the present experimental work. The photographic view of the nanoparticles as seen by the naked eyes is shown in the plate..1.



Fig 3 Photographic view of CuO nanoparticles
The distribution of CuO nanoparticles at Nano scale can be observed under a Scanning electron microscope (SEM). The SEM images of CuO nanoparticles at 1 μm magnifications is shown in Plate.3.2(a) and SEM image of CuO nanoparticle on a 500 nm scale is shown in Plate.3.2(b). Preparation of Nanofluids is an important stage and Nanofluids are prepared in a systematic and careful manner. A stable Nanofluid with uniform particle dispersion is required and the same is used for measuring the thermo physical properties of Nanofluids.



SEM images of CuO nano particles on 1000 nm and 500 nm scales.

In the present work, water-Propylene glycol mixture 80:20 by volume is taken as the base fluid for preparation CuO Nanofluids. Basically three different methods are available for preparation of stable Nanofluids and are listed below.

By mixing of nano powder in the base liquid

In this method, the nanoparticles are directly mixed in the base liquid and thoroughly stirred. Nanofluids prepared in this method give poor suspension stability, because the nanoparticles settle down due to gravity, after a few minutes of Nanofluid preparation. The time of particle settlement depends on the type of nanoparticles used, density and viscosity properties of the host fluids.

By acid treatment of base fluids

The PH value of the base fluid can be lowered by adding a suitable acid to it. A stable Nanofluid with uniform particle dispersion can be prepared by mixing nanoparticles in an acid treated base fluid. But acid treated Nanofluids may cause corrosion on the pipe wall material with prolonged usage of Nanofluids. Hence acid treated base fluids are not preferred for preparation of Nanofluids even though formation of stable Nanofluids is possible with such base fluids.

By adding surfactants to the base fluid

In this method a small amount of suitable surfactant, generally one tenth of mass of nanoparticles, is added to the base fluid and stirred continuously for few hours. Nanofluids prepared using surfactants will give a stable suspension with uniform particle dispersion in the host liquid. The nanoparticles remain in suspension state for a long time without settling down at the bottom of the container.



The CuO Nanofluids samples thus prepared are kept for observation and no particle settlement was observed at the bottom of the flask containing CuO Nanofluids even after four hours.



Fig :The photographic view of CuO Nano fluid suspension prepared after magnetic stirring process

The present experiments with CuO Nano fluids, the time taken to complete the experiment for property estimation is less than the time required for first sedimentation to take place and hence surfactants are not mixed in the CuO nanofluids. The CuO nanofluids prepared are assumed to be an isentropic, Newtonian in behavior and their thermo physical properties are uniform and constant with time all through the fluid sample.

Determination Of CuO Nano Fluid Properties

The most important properties needed for estimation of convective heat transfer coefficient of nanofluids are its density; heat transfer coefficient, viscosity, and specific heat. The thermo- properties properties of CuO nanofluids are estimated experimentally for all the concentrations and the results obtained in the experiments are compared with the theoretical equations which predict Nanofluid properties.

Experimental Set Up For Heat Transfer Coefficient Measurement Using Transient Heat Conduction Apparatus

The experimental setup to measure the heat transfer coefficient of nanofluids is shown schematically in Fig.. The photographic view of the experimental set up is shown in the plate . the present work Heat transfer rate of the CuO nanofluids is measured by using the Transient heat conduction apparatus.

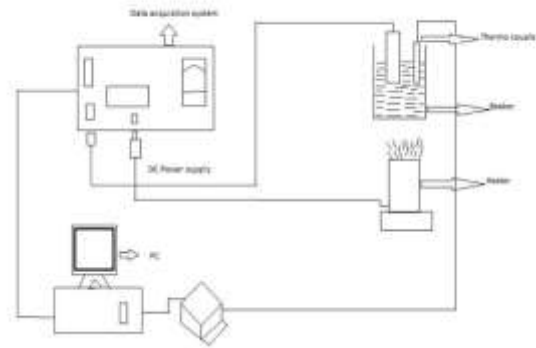


Fig: Schematic diagram of the Heat transfer coefficient measuring experimental setup



Procedure to Perform the Experiment

- Calculate the amount of nano particles to be added to the 1000 ml of base fluid.
- Then divide the 1000 ml Nano solution in to two parts, one for heating and the other for cooling.
- Switch on the equipment and heater. Switch on the stirrer and regulate the speed such that water does not splash. Remove the test cylinder from the bath and the note the temperature of the cylinder T_0 .
- Adjust the controller temperature setting to any desired value up to 70°C .
- Press the push button switch and turn the screw to any desired set temperature
- . When the press button switch is released the controller indicates the bath Temperature.
- When the temperature of the bath reaches the set temperature insert the cylinder in to the bath and simultaneously start a stop clock . Note the time taken (t) seconds for the test cylinder to reach the final steady temperature (T).
- mixing proper stirring is to be applied so that Base fluid and copper nano particles mix properly.
- Then insert the copper cylinder the cool cuo solution and take the similar Readings.

- Repeat the same for 50 °C,60 °C and 70 °C temperature.
- Perform the similar steps for 0.05%, 0.1% , 0.15% and 2%.
- Follow Similar steps for the Nano Fluid Of Distilled Water, Ethyl Glycol of 20% and CuO Na no Particles of different concentration like 0.05%, 0.1% , 0.15% and 2%.

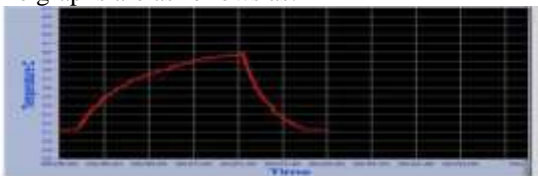
Specifications Of Experimental Setup

- Diameter of the copper cylinder = 20 mm
- Length of the cylinder = 70 mm
- Area of the cylinder = 0.00439 m²
- Volume of the cylinder = 0.0002199 m³
- Density of copper cylinder =8954 kg/m³
- Specific heat of copper = 0.381 kj/kg-k
- Initial temperature of copper cylinder = T₀
- Final temperature of copper cylinder = T
- Water bath temperature (Hot or cold) = T_∞
- Time taken for the cylinder to reach T from T₀ = t seconds Heat Transfer coefficient may be calculated by using the formula

GRAPHS

Graphs were Obtained on the Pc during the Experiment,the graphs are plotted Time(t) vs Temperature(T)

The graphs are as follows as:-



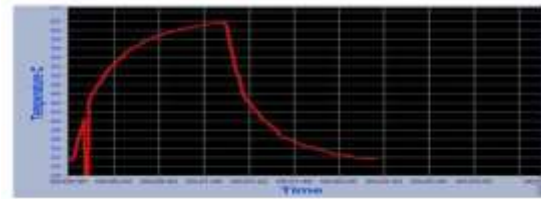
HEATING COOLING
 T_∞ = 40.4 °C T_∞ = 31.3 °C
 T₀ = 31.3 °C T₀ = 39.9 °C
 t = 104 sec t = 44 sec
 T = 40.1 °C T = 31.8 °C
 h = 0.5627 kW/m² °C h = 1.10903kW/m² °C

TRANSIENT HEAT CONDUCTION OF DISTILLED WATER AT 50 °C



HEATING COOLING
 T_∞ = 51.4 °C T_∞ = 31.3 °C
 T₀ = 31.3 °C T₀ = 48.5 °C
 t = 89 sec t = 61 sec
 T = 49.4 °C T = 31.6 °C
 h = 0.4447 kW/m² °C h = 1.1384 kW/m² °C

TRANSIENT HEAT CONDUCTION OF DISTILLED WATER AT 60 °C



HEATING COOLING
 T_∞ = 62 °C T_∞ = 31.7 °C
 T₀ = 31.4 °C T₀ = 60.9 °C
 t = 79 sec t = 81 sec
 T = 61.7 °C T = 32 °C
 h = 0.4980 kW/m² °C h = 0.9711 kW/m² °C

Results and discussions

The Column Chart Shows Temperature vs Heat Transfer Coefficient During Heating.

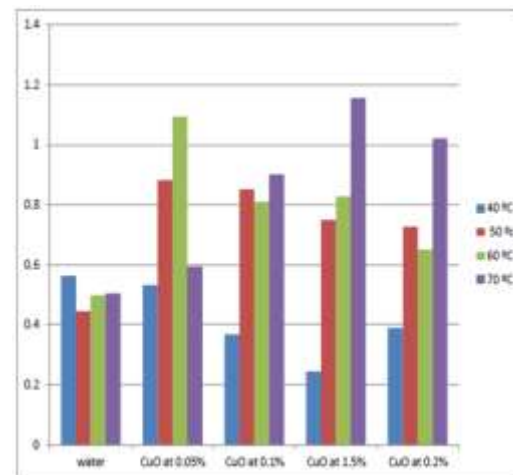


Fig 11

From the above chart it has been observed that by comparing Water , CuO at 0.05% , CuO at 0.1%, CuO at 0.15% and CuO at 0.2% During Heating Heat Transfer Coefficient is high at CuO of 0.15% concentration at 70 °C with a value of h = 1.1554 kW/m² °C

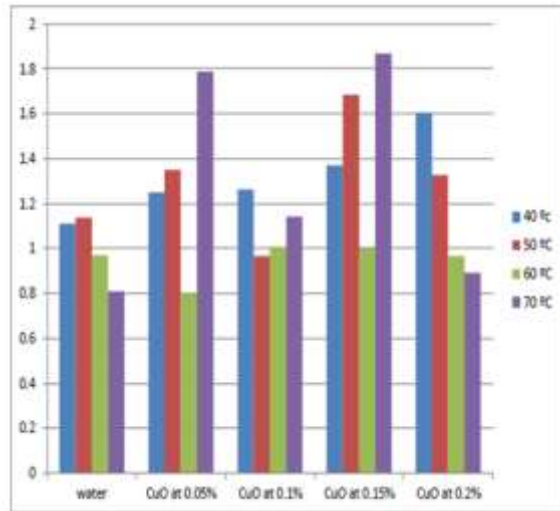
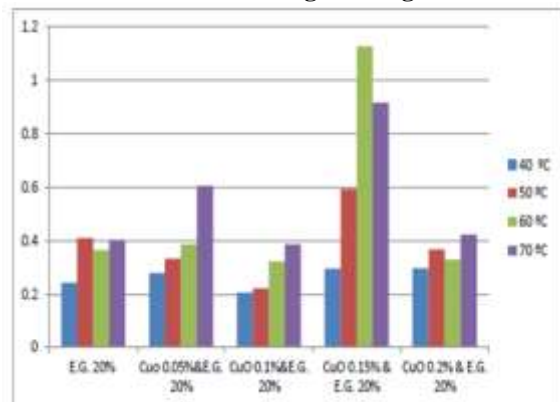


Fig 12

From the above chart it has been observed that by comparing Water , CuO at 0.05% , CuO at 0.1%, CuO at 0.15% and CuO at 0.2% During Cooling Heat Transfer Coefficient is high at CuO of 0.15% concentration at 70 °C with a value of $h = 1.8674 \text{ kW/m}^2 \text{ }^\circ\text{C}$.

The Column Chart Shows Temperature vs Heat Transfer Coefficient During Heating.



From the above chart it has been observed that by comparing Ethyl Glycol of 20% and Water , Ethyl Glycol of 20% and CuO at 0.05%, Ethyl Glycol of 20% and CuO at 0.15% and Ethyl Glycol of 20% and CuO at 0.2%. During Heating Heat Transfer Coefficient is high at CuO of 0.15% concentration at 60 °C with a value of $h = 1.1671 \text{ kW/m}^2 \text{ }^\circ\text{C}$

CONCLUSIONS

Studies of nanofluids reveals high thermal conductivities and heat transfer coefficients compared to those of conventional fluids.

By comparing the Heat Transfer Coefficient of Copper Oxide Nano fluid with the Heat Transfer Coefficient of base fluids like Distilled water and

Ethyl Glycol, Heat transfer coefficient for the copper oxide nano fluid is high on heating as well as cooling. The Heat transfer rate of copper oxide with base fluid of distilled water is high at 0.15% concentration of CuO nano particles at a temperature of 70 °C on heating and cooling if we go further high temperature it may exhibit wide range of heat transfer when compared with the conventional fluids.

The Heat transfer rate of copper oxide with base fluid of Ethyl Glycol is high at 0.15% concentration of CuO nano particles at a temperature of 60 °C on heating and cooling, on further high temperature it remove more heat from the fluid. CuO Nano fluid is important because they can be used in numerous applications involving heat transfer, and other applications such as in detergency. Colloids which are also CuO nanofluids have been used in the biomedical field for a long time, and their use will continue to grow. CuO Nano fluids have also been demonstrated for use as smart fluids. Problems of nanoparticle agglomeration, settling, and erosion potential all need to be examined in detail in the applications. CuO Nano fluids employed in experimental research have to be well characterized with respect to particle size, size distribution, shape and clustering so as to render the results most widely applicable. Once the science and engineering of CuO nano fluids are fully understood and their full potential researched, they can be reproduced on a large scale and used in many applications. Colloids which are also CuO nano fluids will see an increase in use in biomedical engineering and the biosciences. Further research still has to be done on the synthesis and applications of CuO nano fluids so that they may be applied as predicted. Nevertheless, there have been many discoveries and improvements identified about the characteristics of CuO nano fluids in the surveyed applications and we are a step closer to developing systems that are more efficient and smaller, thus rendering the environment cleaner and healthier.

REFERENCES

- [1] V. Trisaksri, S. Wongwises, Renew. Sust. Energ. Rev. 11, 512 (2007).
- [2] S. Özerinç, S. Kakaç, A.G. Yazıcıoğlu, Microfluid Nanofluid 8, 145 (2009).
- [3] X. Wang, A.S. Mujumdar, Int. J. Therm. Sci. 46, 1 (2007).
- [4] X. Wang, A.S. Mujumdar, Brazilian J. Chem. Eng. 25, 613 (2008).
- [5] Pradeep Jaya Sudhan E and Shree Meenakshi K, Ind J Sci Tech., 2011, 4(4), 417-421.

- [6]Das S K, Putra N, Thiesen P and Roetzel W, J Heat Transf., 2003, 125(4), 567–574;
- [7]Godson L, Raja B, Mohan Lal D and Wongwises S, Exptl Heat Trans., 2010, 23(4), 317– 332
- [8] Eastman J A, Choi S U S, Li S, Yu W and Thompson L J, Appl Phys Lett., 2000, 78(6), 718-720;
- [9]Xuan Y and Li Q, Int J Heat Fluid Flow, 2000, 21(1), 58-64
- [10]Kwak K and Kim C, Korea-Aust Rheol J., 2005, 17, 35-40.
- [11]Duangthongsuk W and Wongwises S, Exptl Thermal Fluid Sci., 2009, 33(4).

PERFORMANCE CHARACTERISTICS OF N-BUTANOL AND GASOLINE BLENDS IN SI ENGINES

K.AKHIL SAI¹

Y.UMASHANKAR²

¹M.Tech (student)Department of mechanical engineering vaagdevi college of engineering (ugc autonomous) approved by aicte & permanent affiliation to jntuh, hyderabad.p.o, bollikunta, Warangal urban- 506005.

²Assistant Professor Department of mechanical engineering vaagdevi college of engineering (ugc autonomous) approved by aicte & permanent affiliation to jntuh, hyderabad.p.o, bollikunta, Warangal urban- 506005.

Abstract: The use of oxygen-fuelled fuel in spark ignition engine (SIEs) has received increasing attention a few years ago, especially when it came from renewable sources, due to a shortage of fossil fuels and concerns about global warming. At present, the main source of fuel is ethanol, in the future reducing CO and HC emissions but presents a series of barriers such as low temperature values and high hygroscopic proportions, resulting in high fuel consumption and corrosion problems, respectively. This paper shows the most suitable properties for ethanol conversion by renewal n-butanol, which brings a higher temperature and lower hygroscopic propensity compared to the past. The experimental matrix developed for this experimental study contains, on the other hand, ethanol substituting n-butanol for commercial compounds and, on the other hand, either ethanol or gasoline substituting n butanol for E85 mixture (85% ethanol-15% fuel by volume). The results show that substituting n-butanol with ethanol presents a series of benefits such as higher temperature and greater exchange with fuel compared to ethanol, which makes n-butanol promising SIE fuel for commercial mixtures. However, the use of n-butanol in the E85 combined includes another gasoline or ethanol can cause cold problems due to low pressure of n-butanol vapour. Because for this reason, it is proposed to combine n-butanol in both gasoline and ethanol to N-butanol can be used without any side effects.

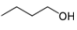
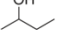
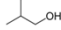

1. INTRODUCTION

The gradual decline in mineral oil and concerns about global warming have led to consumption of bio fuels in internal combustion engines (ICEs) Among the various biofuels, bio-alcohol investigated as other engine oil due to its ability to improve engine performance and reducing pollution. Bio-alcohols such as ethanol and butanol can slow down the life cycle greenhouse emissions, due to their biological processes. In fact, ethanol is commonly used in spark ignition engines (SIEs) that return fuel. Both of these alcoholic beverages are listed it has also been used to consider combustion engines (CIEs) as a substitute for diesel. This paper focuses on the use of alcohol in SIEs, where the most widely used bio-alcohol is ethanol, which is very common in many countries. The main advantage of this fuel is the reduction of

CO and the release of HC when used in SIEs as a substitute for fuel. In particular, ethanol has always been present proven to reduce the excess emissions of CO and HC during cold temperatures in relation to temperature engine conditions. Of the SIEs injected directly, they have been gaining prominence over the past few for years, ethanol has been shown to reduce NO_x emissions slightly and PM emissions significantly. The low temperature of ethanol is much lower than that of petroleum, which creates higher fuel use. However, the efficiency of thermal brakes has been shown in small increases. Ethanol can also indicate rust problems in the injection system due to its hygroscopic tendency. Ethanol and it produces less lubrication, which can cause problems for engines injected directly into the fuel. Finally, according to Rodríguez-Antón et al. ethanol supplementation increases the vapor pressure of only mix up to 35% by volume. High ethanol content can reduce lead-induced vapor pressure starting problems. N-butanol is considered to be the most promising bio-alcohol because of its many more benefits short-chain alcohol (methanol and ethanol in particular), including high-energy (low-energy) high temperature and hardness), low viscosity, and high softness. Additionally, n-butanol is much less hygroscopic and more aggressive than ethanol. Besides, n-butanol seems to be very interesting energy because its properties are very similar to gasoline; therefore, it will go hand in hand and the current fuel distribution infrastructure. N-butanol is a second-generation biofuel ever since can be produced from lignocellulosic or waste biomass, with low heat emissions than ethanol. Currently, it can be produced with acetone - n-butanol - ethanol (ABE). The fermentation process or fermentation process of isopropanol - n-butanol - ethanol (IBE). However, n-butanol has a lower smoke pressure compared to ethanol and apparently compared to it gasoline, which is the hottest fuel. This recurrence may cause cold sores in SIEs where n-butanol is used in high doses. Some authors reported studies using petrol-butanol blends in SIEs. Costagliola et al. tested 10% n-butanol (with a different ethanol content) for a port-fuel injection Engine (PFI) showing the same benefits to CO, HC, and PM emissions as ethanol, but also the same increased carbonyl emissions.

Galloni et al. fuel tested with n-butanol (20% and 40% butanol Percentage) and in the PFI engine. When using the B40 combination, the power is transmitted at the same speed of the engine decreased by about 13%, mainly due to differences in temperature values.

Table 1 highlights the properties and uses of butanol and its isomers

	1-butanol	2-butanol	Iso-butanol	Tert-butanol
Density(kg/m ³)	809.8	806.3	801.8	788.7
Research Octane Number (RON)	96	101	113	105
Motor Octane Number (MON)	78	32	94	89
Boiling temperature (oC)	117.7	99.5	108	82.4
Enthalpy of vaporisation (kJ/kg) at T _{boil}	582	55.1	566	527
Self-ignition temperature (oC)	343	406.1	415.6	477.8
Flammability limits vol.%	1.4-11.2	1.7-9.8	1.2-10.9	2.4-8
Viscosity (mPas) at 25oC	2.544	3.096	4.312	-
Molecular structure				

It is known that gasoline derived from long-term alcohol is not widely used due to its production difficulty. Today, the associated costs of butanol production have been steadily reduced. Rapid progress in development production technology has allowed butanol to be successfully produced. Although its growing number of published, butanol-related studies on petrol engines do not include as much as methanol research or ethanol. This article aims to understand the effect of mixing butanol and gasoline on a petrol engine's performance, fire power and discharge features. The reviews from this paper suggest that there are a few gaps therethe addition of butanol to a petrol engine requires further investigation. This section outlines the percentage of butanol used successfully in several studies. Because of itexpensive production costs, some studies have only added a small percentage of butanol, while others have used highertorture. Note that the results in terms of performance, fire power and emission signals will be discussed in the next section. This section only emphasizes the use of various butanol concentrations that were present used successfully in experiments so that a better understanding of the compounds was understood. Elfasakhany used low percentage of butanol with Bu0, Bu3, Bu7 and Bu10 blends on the SI engine and carburettor system. In addition to its old technology, the carburettor system was chosen as it could produce the same combination. The fuel system was not changed, and the engine was a single cylinder made with operating speeds ranging from 2600 to3400 per minute. Although a small percentage of butanol of that was successfully conducted in this study, the addition of Butanol in petroleum fuel requires further investigation by a high percentage. Large-scale use of road transport, Butanol should be added to the most important percentages. Some investigations need to

be done from the ground up percentage to specify its addition to the SI engine. Singh et al. used a variety of butanol blends ranging from 5% to 70% in fuel. This study was performed on an SI engine with moderate performance under various speeds and loads other than hardware correction. In another study, Signin and Kemal used 10%, 30% and 50% combined with iso-butanol provided with three Compression Ratios (CR) results. The test was performed at a speed of 2600 rpm. Onea significant method was developed by Venugopal and Ramesh using a dual injectable system using the same injection 50% n butanol and 50% petrol.

2. LITERATURE REVIEW

There is a lot of debate about the future of natural resources in terms of meeting the world's energy needs, but one thing is for sure: the demand for oil and gas will not decrease anytime soon. Great strides have been made in promoting the development of alternative fuel sources, but few offer the vast amount of energy produced by burning natural gas at the same price. One derivative of natural gas that remains under the radar but is gaining popularity is butane, and thus refined butane. Butane, or refined butane, is derived from natural gas. It is an extremely flammable hydrocarbon that is in high demand for many different uses. Hand-held lighters that require a butane refill as an energy source have been around for about 100 years. Butane is also used to make propane, which powers outdoor grills, heaters, and many other consumer products, including kitchen torches, which are used to make creme brulee. Since it can reach a temperature of 1,700 degrees Kelvin when burned, this natural gas is an ideal energy source for industrial and commercial burners. How Butane is Made Natural Gas RigButane is made from natural gas, which in its natural form is colorless, odorless, and shapeless. This type of gas is extremely abundant in many parts of the world and is relatively inexpensive to extract and produce. It is a fossil fuel that is created over millions of years through a complex process deep in the earth from the remains of plants, animals and numerous microorganisms. The different types of machines that use butane to operate seemed quite magical in their development a long time ago, but really little magic is involved in the production of butane. It's simply a matter of human ingenuity, hard work, repeatable production processes, and following safety procedures every step of the way. The production of Colibri butane, for example, follows a four-step process, which of course is preceded by locating a reserve of natural gas and bringing it to the surface, where it is then transported to a refinery.

Step 1 Removal of oil and condensate. This means that the gas is separated from the oil where it has

dissolved, often with equipment installed near the gas well or well.

Step 2 Remove the water. In addition to crude oil, gas must also be separated from water by machines on the surface. It does so through a dehydration process, either by absorption or by adsorption. The concept of absorption is quite simple, the water is absorbed into silicates or granules. Adsorption, on the other hand, is the process in which gas is attached in a condensed layer to the surface of another solid or liquid for further processing. Glycol drying.

Step 3 Glycol dehydration. Here a kind of glycol solution, either diethylene glycol or triethylene glycol, absorbs water from the wet gas. The glycol particles become heavier, sink to the bottom of a device called a contactor, and are then removed. Once the water has been extracted from the natural gas, it is transported out of the drainage system.

Step 4: This is actually a variation of Step 3, but in this case a desiccant dehydration process is used. Wet natural gas passes through two or more absorption towers filled with alumina or silica; the water is trapped and the remaining dry gas comes out of the bottom of the towers. Vector butane production will continue as usual. Butane Facts Refined butane like Power 5x is made from natural gas and is also found in oil. It has a chemical signature of C₄H₁₀ and is considered a flammable hydrocarbon. It was founded in 1910 by Dr. William Snelling, who was curious why motorists had less gasoline available before it evaporated. In 1911, Snelling and the United States Bureau of Mining discovered a way to convert butane gas into a liquid form. When ignited, butane can burn at a temperature of around 1,700 degrees Kelvin. Butane has been used as a source to heat buildings and as a source of energy for almost 100 years. Refined butane is used in a variety of ways every day, including as a power source for refillable lighters and lanterns, to produce propane for outdoor cooking, and even as a component of refrigerants. Butane is also used in portable hair straighteners. We tried WhipIt! 9x butane in one! It also has commercial applications where butane torches are used to cut glass, steel, and other materials. As a derivative of natural gas, butane is one of the most widely used gases in the world. According to some reports, natural gas and all of its by-products account for nearly a quarter of America's energy needs.

Chemical Processes for Producing Butanol from Bio-Ethanol:

The classical approach to producing butanol from bioethanol is carried out in three steps. First, the commercial product is completely dehydrated to a 100% anhydrous state. It is then oxidized with acetone in the presence of aluminium isopropoxide (Figure 3) to form acetaldehyde. The volatile

acetaldehyde is separated by fractional distillation. In the secondstep, acetaldehyde condenses to crotonaldehyde in a strongly alkaline environment. In the last step, crotonaldehydeis hydrogenated to butanol by treatment with isopropanol in the presence of titanium or aluminum isopropanolate.

Concentration and Blends

The studies mentioned above focus only on the addition of butanol. To better understand the position ofbutanol compared to other liquid oils, direct comparisons with other bio alcohols such as methanol and ethanolit is necessary. Karavalakis et al. attempted to clarify the effects of butanol blending comparisons with other alcoholic beverages in exhaust extraction using 16%, 24% and 32% iso-butanol. Ethanol was used in this study for comparison. However, to have a complete understanding of the effect of butanol as a renewable alcohol fuel, comparisons between butanol and ethanol is not enough. Extensive research comparing butanol with various alcoholic oilsis required. Gravalos et al. used a variety of cellular alcohols, from the bottom to the top, to investigate their release features in the SI engine. The drugs used in this study were methanol, ethanol, propanol, butanol and pentanol. Butanol concentration was used in only 1.5% of the entire study. Percentage of methanol, propanol andpentanol was also prepared at less than 2%, but ethanol concentration varied from 2% to 22%. Other, outstanding congestion, was the oil that could be extracted (70% - 90%).

3. EXPERIMENTAL METHODS APPARATUS

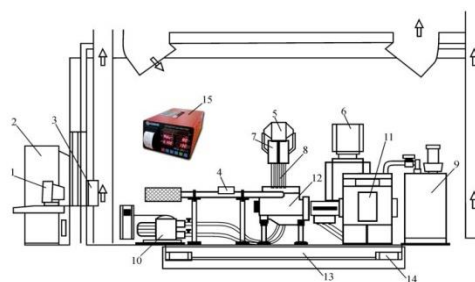


Fig. 3 Experimental setup. 1. Computer center 2. Puma data-processing center 3. Throttle valve-opening controller TRV-100 4. Air flow meter 5. Catch gas at caster 6. Leveling and measuring fuel consumption AVL733 7. Data acquisition 8. Sensors mounted on the engine

9. Engine's water coolant-conditioning controller 10. Engine's lubricant supplying system AVL554 11. 2048 APA dynamometer 12. Engine 13. Test base 14. Damper system 15. Gas analyzer KEG-500

The figure shows the schematic representation of the experimental setup. The experiments used a Daewoo spark ignition 4-cylinder, 16-valve 1.6-liter engine, model A16DMS, with a 9.5 compression ratio. In order to investigate the effects of using gasoline-butanol blends on engine performance and emission properties, no modifications were made to the test engine. The test engine specifications are given in Table 1. An eddy current dynamometer (model APA 204/08) was used to measure engine power and torque. An in-line mass flow meter (type DN80; AVL) was used to measure intake air consumption. A

fuel consumption and leveling measuring device (type 733 s; AVL) was used to verify fuel consumption and fuel temperature. A throttle actuator (Model THA100; AVL) was used to control the open throttle at various engine speeds. A gas analyzer (model KEG500) was used to simultaneously estimate the air-fuel equivalence ratio based on the composition of the exhaust gases. A pressure sensor (model IndiSet 620; AVL) mounted in the cylinder head near the spark plug was used to record the internal pressure of the cylinder. The AVL 553 and AVL 554 devices were used as the cooling and lubrication system for the test bench.

ENGINE TYPE	DOHC
Number of cylinders/arrangement	4 cylinders/inline

	Range	Accuracy
CO	0%-10%	0.01 %
O ₂	0%-25%	0.25 %
NO/ NO _x	0-6000 ppm	10 ppb
HC (CH ₄)	0-4000 ppm	10 ppb
CO ₂	0%-20%	0.1 %
Bore (mm) x stroke(mm)	79.0x81.5	
Compression ratio	9.5:1	
Maximum output	80 kW at 6000 rpm	
Maximum Torque	145 Nm at 3400 rpm	
Fuel System	Electronic fuel injection	

Testing strategy

In this study, an original ECU controlled fuel injection strategy was established to control fuel injection timing and ignition system based on the use of pure gasoline. The stoichiometric air / fuel ratio (AFR) of butanol and gasoline is 11.12 and 14.7, respectively. Therefore, butanol-gasoline blends are always operated with a higher AFR. This setting could help file lean engine combustion due to AFR control limitation. The engine torque, power, fuel consumption and pollutant emissions of an engine

using mixed fuels of butanol and gasoline were examined and compared to those of using pure gasoline in operation without any engine modification. The engine was filled with different butanol-gasoline blends of Bu0, Bu10, Bu15, Bu20, Bu25, Bu30, Bu40, and Bu50, showing the butanol content in different volume ratios (for example, Bu10 contains 10% butanol and 90% gasoline by volume). For the experiments, two different open throttle (WOT) positions of 30% and 70% were set while the engine speed was tested at 2250 rpm and 4250 rpm. The properties of gasoline and butanol are given in Table 2. The operating parameters (for example, relative air / fuel ratio and internal cylinder pressure), engine performance factors (for example, braking torque, power and consumption fuel) and pollutant emissions (eg HC, CO, NO_x and CO₂) were measured and compared for the test fuels.

Fuel Property	Butanol	Gasoline
Formula	C ₄ H ₉ OH	C ₈ H ₁₅
Octane Number	96	90-99
Composition(C,H,O)(%mass)	65,13.5,21.5	86,14,0
Density(kg/m ³) at 20 ⁰ C	810	745
Boiling Point (°C)	117.7	25-215
Latent Heat Of Vapourisation(kJ/Kg) at 25°C	582	223.2
Saturation pressure(kPa) at 38°C	2.27	31.01
Low heating value	33.3	43
Auto ignition temperature	38.5	420
Stoichiometric air/fuel ratio	11.12	14.7

Specification of the analyzers

4. PERFORMANCE

Several published papers have reported that butanol compounds can impair engine performance as a result natural structures. This reduction is understandable as the amount of butanol calories and filling pressure was less than petrol fuel, resulting in lower torque, volumetric power and efficiency and higher fuel consumption. Engine performance is expected to be negative with the addition of butanol. However, some studies have suggested new one show to improve engine performance caused by butanol. Fuel Consumption and Thermal Efficiency The use of Brake Specific Fuel Consumption (BSFC) and Brake Thermal Efficiency (BTE) are two important factors in engine performance. Both of these parameters are used to indicate how efficient fuel is. BSFC (g / kWh) it measures the weight of the fuel to produce the power of a single unit. In general, the BSFC compound mixture in the SI engine tends to increase as a result at its lowest LHV values

compared to its low fuel economy. Another important parameter for determining the fuel economy is the Brake Heat Success (BTE). It is the ratio between the active energy and the energy level delivered by the fuel. BTE is used to show how electrical energy is used to produce energy.

Power and Torque

In general, the force of the brakes and the torque used by butanol is much lower than that of gasoline. These results are due to low calorie prices butanol. Theoretically, to get higher torque, more fuel should be added. Anyway, this will improve the onset of a large fire and may cause knocking. Elfaskhany noted that the addition of n-butanol provided a slight decrease in output and torque as indicated in Figure 2. The author also found that when a percentage of n-butanol is added to compounds, the engine slows down performance reported. This reduction was understandable because of the amount of butanol calories and filling pressure is lower in fuel, resulting in lower volumetric performance. Tests were performed using a low percentage butanol with 0, 3, 7 and 10 vol.%. The fuel system was not changed, and the engine was a single cylinder made in speeds range from 2600 to 3400 rpm. Adding n-butanol over vol.% It would surprise them reduce performance without significant reduction of exhaust emissions. The author suggested that the engine performance can be improved by changing the temperature time and raising the pressure level as n-butanol is higher knock resistance is gasoline.

COMBUSTION

This section discusses the effect of butanol addition on the combustion of SI engine. In general, butanol addition is expected to improve the combustion process due to the presence of oxygen found in butanol. The extra oxygen will not only enhance the combustion inside the cylinder but also reduce the emissions in the exhaust system. The addition of butanol will assist the formation of CO into CO₂ thus decreasing the CO and HC emissions. Both the fuel properties and operating parameters are found to influence the combustion process that in turn affects the performance and emissions of the gasoline engine.

In-cylinder Pressure (ICP) and Heat Release Rate (HRR)

ICP and HRR are the two most necessary criteria to evaluate the combustion process of an engine. ICP is usually measured directly using a pressure transducer. It details the cyclic combustion phenomena inside the cylinder thus providing valuable insight into the characteristics of the entire combustion process. For HRR, it reflects the combustion rate of reactions inside the chamber. The exact moment the mixture begins to burn and the rate

at which it occurs can be analyzed using HRR. HRR data is usually provided in relation to the crankshaft angle position. The HRR crank angle chart is an important tool for identifying combustion abnormalities such as misfire and detonation. Therefore, both ICP and HRR play an important role in the study of combustion.

Elfaskhany used low percentages of n-butanol with 0, 3, 7 and 10% by volume of the n-butanol gasoline blend in the SI engine with carburetor. The fuel delivery system was not modified, and the engine is a single cylinder running at variety of rpm operating speeds from 2600 to 3400 rpm. The results indicated that the addition of n-butanol could significantly improve the combustion of caused by the partially oxidized nature of n-butanol and that the tilting effect has been due to the lower fuel-air fraction of the pressure of the n-butanol it. However, the addition of n-butanol resulted in a slight decrease in ICP and exhaust temperature. This reduction is included at because the calorific value and saturation pressure of butanol is lower than that of gasoline.

Relative SFC and change in LHV as a function of butanol addition at 2000 RPM and IMEP 367 kPa

Blend	Relative SFC			Change in CE (%)
	$\phi = 0.83$	$\phi = 0.91$	$\phi = 1.0$	
B20	+7.9	+5.2	+1.1	-5.3
B40	+10.1	+11.6	+10.1	-9.2
B60	+17.9	+18.5	+18.7	-13.9
B80	+25.1	+24.7	+26.5	-19.8

Relative SFC as a function of load for an equivalence ratio of 0.9 and engine speed of 2000 RPM

IME P (bar)	B20	B40	B60	B80
1.6	5.7 %	8.5 %	14.3 %	17.9 %
2.4	5.6 %	10.6 %	19.1 %	26.8 %
3.2	6.5 %	10.6 %	13.5 %	22.7 %
4.0	5.2 %	9.0 %	15.2 %	23.7 %
4.7	5.7 %	8.1 %	14.5 %	23.9 %

Research on 2butanolgasolinemixtures rarely been done, especially at allow percentage. Therefore ,it is imperative to understand the distribution of energy to reduce energy losses .,can easily visualize the interior of the engine system. In addition, capacity to estimate the energy distribution of internal combustion engines will allow us to have a better approach to energy management of the entire engine system. Some have been done in diesel engines like REFs

Knock Phenomena

Wei et al. [115] attempted to understand the effect of exhaust gas recirculation (EGR) on the detonation combustion behaviour of n- butanol, as well as the sensitivity of n- butanoldetonation phenomena to intake pressure and compression ratio. The results showed that EGR could reduce detonation intensity and delay detonation onset time due to cooling and dilution effects. Low EGR rate (3%) produced a significant reduction in detonation intensity, while negligible result was observed for combustion pressure. For a given EGR rate, the addition of N-butanol had combustion fluctuations smaller. This was due to the fact that the probability distribution of its detonation intensity was more concentrated than that of gasoline. This study showed that the use of EGR at high intake pressure and a high compression ratio of a gasoline engine powered by nbutanol was able to successfully suppress the occurrence of detonation and stabilize the combustion process in the chamber.

Zhang et al. examined the antiknock properties of ethanol / gasoline and n-butanol / gasoline blends in a DI-Si engine with EGR. It was found that the addition of ethanol and butanol reduced the burn time from 10 to 90% MFB and improved the burn stability. Octane number, charge cooling effect, and EGR improved shock resistance, with butanol having poorer shock resistance compared to ethanol. Several

studies have been investigated on the performance and combustion of gasoline engines running on-butanol blends. However, the results on combustion behaviour are still limited with respect to some important operating parameters, such as, such as EGR rate and detonation index (KI). Liu et al. aimed to find the common trends of both parameters at different speeds of the engine. The simulation with the GT Power software was carried out under different EGR rates and compression ratios combined with KI. Butanol was found to provide better anti-knock properties, which allowed for an earlier ignition time. As the butanol mix ratio increased, the peak cylinder pressure (PCP) and heat release rate (PIPE) also increased. As a result, since the maximum pressure locations of cylinders and the PIPE were advanced, improved thermal efficiency.

Furthermore, it was found that engine load affects heat release more than engine speed. With the increase in the load of the motor, the gross indexed thermal efficiency (ITE) increased slightly while the net ITE increased considerably. In addition, it has been observed that changing the EGR rate affects the burn rate of butanol gasoline more than that of pure gasoline. This was caused by the oxygen content and internal cylinder temperature of the butanol fuel. By increasing the compression ratio from, it was found that the maximum combustion temperature inthe cylinder increased, resulting in an improved temperature gradient in the cylinder and improved ITE. However, as the compression ratio increased, ITE's net increase rate steadily decreased .

EMISSION

This section describes the effect of butanol on gasoline engine emissions. Pollutants in the form of carbonmonoxide (CO), hydrocarbons (HC) and (NOx) are critically analysed. Additionally, Particulate Matter (PM) and unregulated emissions are also covered at the end of this section.

CO Emission

CO emissions indicate the incompleteness of combustion in the chamber. Incomplete combustion occurs frequently in modern internal combustion engines and the addition of butanol can reduce CO emissions, since the oxygen content in butanol can increase the combustion temperature and hence promote the formation of CO₂. However, increasing the combustion temperature due to complete combustion can also increase NO_x emissions.

HC Emission

The HC emission provides detailed information about the area of the flame in the cylinder. Most HC emission sources come from slit mixing and unburned fuel vapours absorbed by the oil near cylinder walls due to the deterrent. Butanol blends can lead to reduction significance of HC emissions.

The improvement in HC emission was achieved due to the improved combustion due to the presence of additional oxygen in n-butanol. Thus, the additional O₂ from butanol not only contributes in the formation of CO₂, which leads to a reduction in CO emission, but also to a reduction in HC emissions.

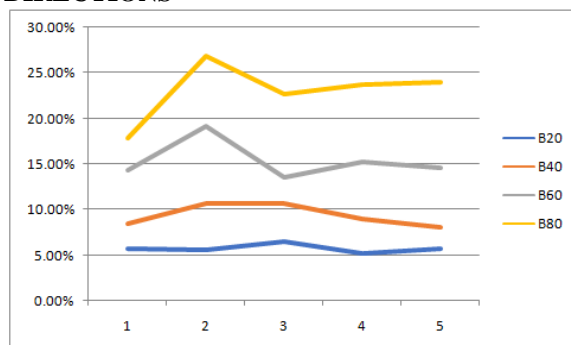
NO_x Emission

In general, the NO_x emission is generated at an elevated temperature in the cylinder. The cooling effect found in butanol fuel can enhance the combustion process resulting in a high combustion temperature. Further more, the adiabatic temperature and the calorific value of butanol are relatively low. These two properties can help reduce NO_x emissions even further. As a result, the formation of NO_x can be significantly reduced by adding butanol.

Particulate Matter (PM) Emission

Stricter regulations on PM emissions apply to diesel engines [120122]. In the case of gasoline engines, however, no laws or protocols have been developed for PM emissions. Due to its adverse effect on the human respiratory system, recently more attention has been paid to the issue of regulations on PM emissions from gasoline engines [123128]. In general, the use of Butanol has been successful in reducing Particle Number (PN) emissions in gasoline engines. Further more, the use of AGR made it possible to further more reduce PM emissions. Particulate Number (PN) emissions have attracted more attention in gasoline engines as more stringent regulations are imposed around the world.

5. CONCLUSION AND FUTURE RESEARCH DIRECTIONS



By using alcoholic fuel, a net reduction in CO₂ emissions can be achieved. Although the most popular and widely used alcohol fuel is ethanol, butanol is a more promising alternative. Butanol has properties comparable to gasoline like and a higher energy density than ethanol. Understanding the kinetics of the chemical reaction of butanol is an important step in understanding its combustion properties. In addition, it is also important to determine the optimal operating parameters so that a

more efficient combustion process can be achieved. In this review article, various strategies to investigate the addition of -butanol and its effect on the properties of gasoline engines were critically discussed. Table 2 of Appendix 1 summarizes Contribution and the novelty proposed by the research groups mentioned in this review article. Some of the studies discussed in this article were conducted by optical inspection. The use of optical equipment in engine studies has provided some competitive advantage in understanding the combustion of the fuel being tested and its operating conditions. Despite the relatively expensive equipment, further examinations are required with Optical Exam. Additionally, to maximize the benefits of butanol in today's internal combustion engines, an optimized design and calibration of the engine was required so that it could be used directly in a gasoline engine. The characteristics of fuel combustion and atomization also need to be quantified to improve both injector design and operating strategies in a direct injection gasoline engine. Several studies have attempted to use different concentrations of butanol to clarify the effect. on the gasoline engine, from a low, medium to high addition of butanol. A small percentage of butanol (less than 30%) was originally chosen due to its relatively high cost of production and its unknown performance in engine characteristics. As more and more methods of reducing production costs have been successfully established, some researchers have tried increasing the butanol concentration to 50%, 70%, and even 100%. It has been observed that most of the published publications have used a high butanol content of , very few studies have focused on a mixed range of less than 10% butanol. To compare the relative advantage of the over other alcoholic fuels, butanol was also studied and compared directly to the header with methanol, ethanol, propanol, and pentane. Of the four isomers of butanol (n-butanol, 2-butanol, isobutanol, and tert-butanol), most of the assays were carried out with n-butanol and isobutanol. This is because the production of n-butanol and iso-butanol was developed using various methods. In addition, several research groups have also found new techniques to improve the production of n-butanol and iso-butanol. Meanwhile, 2-butanol and tert-butanol have not been extensively investigated due to their yet to be established manufacturing process. However, some studies have tried to use them in their research to evaluate these. It is important to note that despite great efforts to reduce production costs, the use of the intermediate fermentation product butanol, such as ABE and IBE, has received considerable attention because it can eliminate recovery costs and dehydration processes

of the butanol. Furthermore, the use of the addition of hydrogen and H₂O to n-butanol mixtures has proven to be a promising approach where research in this area has not yet been carried out extensively. Various approaches to applying different fuel injection strategies and investigating some critical operating conditions were also discussed. Although there have been some studies on the use of butanol in positive ignition engines, there are many aspects that need further investigation. This includes examining the cold start operating condition, applying various injection techniques, and comparing multiple-engine load conditions. Additionally, strategies like VVT, changing the EGR rate, and changing the compression ratio were found to have room for improvement. With regard to injection strategy, both multiple injection and direct injection are currently available on modern vehicles. However, the use of both systems in a vehicle has not been thoroughly investigated. Using different fuel injection techniques can change the time it takes for mixture to form in the cylinders and affect the distribution of different fuels. This will influence the combustion process. This means that there is a mutual relationship between the distribution of fuel in the cylinder and the combustion properties. To improve the thermal efficiency of gasoline engines, effects of different fuel injection methods on combustion behaviour under different conditions should be investigated. The laminar burn rate of butanol was relatively higher than that of gasoline. However, it did not guarantee a faster recording speed. Some operating parameters, primarily ignition timing, may not be appropriate for the new fuel or any other butanol volume ratio. The higher the butanol addition, the higher the oxygen content and anti-knock properties, which improves combustion efficiency. Engine load has been reported to affect heat release at over speeds or fuel type. The rate of oxidation of fuel was influenced more by the air-fuel ratio than by the type of fuel.

With regards to irregular combustion phenomena, the problem of knocks is also worth investigating. Studies have shown that butanol has better anti-knocking properties compared to gasoline. This finding can be further explored so that common principles can be agreed. Knocking tends to limit the compression ratio and pressure of the turbocharger, particularly with downsized gasoline engines. The shocks undoubtedly hamper the development of motor performance and thermal efficiency. It can also damage the engine to some extent. Therefore, various approaches were expected to solve the detonation problem. It was found that the addition of butanol and EGR successfully eliminated the detonation phenomenon. In general, the addition of Butanol can

successfully stabilize the combustion process of a gasoline engine by imparting greater resistance to knock, thus improving ignition timing so that more efficient combustion can be achieved. In terms of exhaust emissions, the additional oxygen in butanol can improve combustion, thus reducing CO and HC emissions. As the concentration of butane increases, so does the oxygen content, which means that the reaction temperature increases rapidly. Increasing the combustion temperature not only reduces CO emissions by favouring the formation of CO₂, but also decreases HC.

Even so, higher CO and HC emissions were also reported when some parameters of the engine operating conditions were modified. Another important aspect to consider is NO_x emissions. While increasing the temperature can help reduce CO and HC emissions, careful consideration is required because NO_x emissions are generated at a high combustion temperature. Most studies on butanol / gasoline blends have focused primarily on regulated emissions only. Although it is considered a promising fuel to replace ethanol, emissions from gasoline engines running on high levels of butanol can increase the level of unregulated emissions. CO₂ and oxygen are rarely studied as harmful gas emissions. Very few studies aimed to analyse the CO₂ emissions of butanol blends in gasoline engines. Numerous previous studies have only focused on the effects of butanol in regulated chemicals such as CO, HC, and NO_x. Although CO₂ is harmless and is not considered an emission, it can increase the global temperature due to the greenhouse effect. Oxygen is also often neglected, although it may reflect other emissions. As emissions regulations become stricter, it is also worth considering unregulated PM and emissions such as BTEX (benzene, toluene, ethylbenzene, and xylene) in gasoline engines. While no laws have been enacted for PM in gasoline engines, its deleterious effects on the human respiratory system and the environment have raised some concerns. More research is needed to investigate the addition of butanol in a gasoline engine.

	Range	Accuracy
CO	0%-10%	0.01 %
O ₂	0%-25%	0.25 %
NO/ NO _x	0-6000 ppm	10 ppb
HC (CH ₄)	0-4000 ppm	10 ppb
CO ₂	0%-20%	0.1%

Blend	Relative SFC			Change in CE (%)
	$\phi = 0.83$	$\phi = 0.91$	$\phi = 1.0$	
B20	+7.9	+5.2	+1.1	-5.3
B40	+10.1	+11.6	+10.1	-9.2
B60	+17.9	+18.5	+18.7	-13.9
B80	+25.1	+24.7	+26.5	-19.8

IME P (bar)	B20	B40	B60	B80
1.6	5.7 %	8.5 %	14.3 %	17.9 %
2.4	5.6 %	10.6 %	19.1 %	26.8 %
3.2	6.5 %	10.6 %	13.5 %	22.7 %
4.0	5.2 %	9.0 %	15.2 %	23.7 %
4.7	5.7 %	8.1 %	14.1 %	23.9 %

	%	%	5%	%
--	---	---	----	---

REFERENCES

[1] Imdadul H, Masjuki H, Kalam M, Zulkifli N, Alabdulkarem A, Rashed M, Teoh Y, How H. Higher alcohol–biodiesel–diesel blends: an approach for improving the performance, emission, and combustion of a light-duty diesel engine. *Energy Conversion and Management* 2016; 111: 174-185.

[2] de Mattos Fagundes P, Padula AD, Padilha ACM. Interdependent international relations and the expansion of ethanol production and consumption: the Brazilian perspective. *Journal of Cleaner Production* 2016; 133: 616-630.

[3] Ghosh P, Westhoff P, Debnath D. Biofuels, food security, and sustainability. *Biofuels, Bioenergy and Food Security*: Elsevier; 2019. p. 211-229.

[4] Ingle AP, Ingle P, Gupta I, Rai M. Socioeconomic impacts of biofuel production from lignocellulosic biomass. *Sustainable Bioenergy*: Elsevier; 2019. p. 347-366.

[5] Ashwath N, Kabir Z. Environmental, Economic, and Social Impacts of Biofuel Production from Sugarcane in Australia. *Sugarcane Biofuels*: Springer; 2019. p. 267-284.

[6] Gaurav N, Sivasankari S, Kiran G, Ninawe A, Selvin J. Utilization of bioresources for sustainable biofuels: A review. *Renewable and Sustainable Energy Reviews* 2017; 73: 205-214.

[7] Grigoratos T, Fontaras G, Giechaskiel B, Zacharof N. Real world emissions performance of heavy-duty Euro VI diesel vehicles. *Atmospheric Environment* 2019; 201: 348-359.

[8] Campagnolo D, Cattaneo A, Corbella L, Borghi F, Del Buono L, Rovelli S, Spinazzé A, Cavallo DM. In-vehicle airborne fine and ultra-fine particulate matter exposure: The impact of leading vehicle emissions. *Environment International* 2019; 123: 407-416.

[9] Mahmudul H, Hagos F, Mamat R, Adam AA, Ishak W, Alenezi R. Production, characterization and performance of biodiesel as an alternative fuel in diesel engines—A review. *Renewable and Sustainable Energy Reviews* 2017; 72: 497-509.

[10] Mofijur M, Rasul M, Hyde J, Bhuyia M. Role of biofuels on IC engines emission reduction. *Energy Procedia* 2015; 75: 886- 892.

[11] Erdoğan S, Balki MK, Sayin C. The effect on the knock intensity of high viscosity biodiesel use in a DI diesel engine. *Fuel* 2019; 253: 1162-1167.

PRODUCTION OF BIO-FUEL & BIO-CHAR FROM SUGARCANE BAGASSE BY THERMAL PYROLYSIS

B.Srikanth¹ Dr.Parvesh Kumar²

¹M.Tech (student)Department of mechanical engineering vaagdevi college of engineering(ugc autonomous)approved by aicte& permanent affiliation to jntuh, hyderabad.p.o, bollikunta, Warangal urban- 506005.

²Assistant ProfessorDepartment of mechanical engineering vaagdevi college of engineering(ugc autonomous)approved by aicte& permanent affiliation to jntuh, hyderabad.p.o, bollikunta, Warangal urban- 506005.

Abstract

Bio-fuel & bio-char from sugarcane bagasse thermal pyrolysis has the potential to replace the fossil fuel derived energy sources. The various process of conversion although has been put into view like gasification, Torre-faction & Pyrolysis, the pyrolysis has gained a lot of importance because of its viability as compared to other processes discussed above. The conversion of the bio-mass by pyrolysis was conducted at various pyrolytic temperatures starting from (300-500C) at a heating rate of 250C/min and the optimum temperature was found at 450C which was found to be 53.3% of bio-oil. The liquid product i.e., the bio-oil was analyzed by various characterization techniques like CHNS, 1H-NMR, physical properties, GC-MS etc. The properties of the bio-oil were found suitable for being used as a fuel. The effect of temperature on the yield of bio-oil, bio-char, bio-gas & reaction time were studied & plotted which showed that the bio-char yield decreased with increase of the pyrolytic temperature. The potential of the bio-char produced from biomass was analyzed by proximate, ultimate, BET surface area, SEM-EDX, anion chromatography, pH, Electrical Conductivity & Zeta Potential studies. The carbon percentage was high enough to be used as a soil amendment, the surface areas were also found to be more with low surface area as 132m²/gm for 300C bio-char to 510 m²/gm for highest temperature bio-char. This high surface area attributed towards application of the bio-char in soil amendment purpose. The ion-chromatography results also showed the presence of anions that are required as nutrients for plants for their metabolic activities. It will also serve as a good source of plant nutrients since it contains less toxic elements. The bio-char had

a slightly acidic surface as found from the pH study. Thus from the above studies we found that the bio-fuel and the bio-char can serve as a source of energy as well as chemical feedstock for the future to depend on.

Keywords: Sugarcane bagasse, bio-oil, bio-char, TGA, XRD, Proximate analysis, CHNS analysis, BET surface area, Electrical Conductivity.

1. INTRODUCTION

From the very earlier times people used to be depend upon the biomass for their energy requirement. The introduction of the crude oil led to advancement of industrialization. Biomass is the biological material from the living organism mostly referring to flora of the ecosystem which refers to the plants and generally plant derived materials. Since biomass are renewable source of energy they can be used directly or indirectly when once they are converted to valuable products. The energy demand is mainly comes from the conventional energy sources like coal, petroleum and natural gas. As petroleum sources are getting depleted, and also there is a demand for petroleum products, so we have to develop economical and energy-efficient processes for the production of fuels. Thus, a dire need to put a control over its consumption has been felt by environmentalists and economists as well, to examine renewable and less cost substitute to fossil fuel to meet their energy demand. In regards to this, a lot of research work is going on around the globe on various alternative sources of energy such as solar, wind, geothermal, hydrogen, nuclear, bio fuel or biomasses. The main source of biomass generally comes from the forestry products, agricultural crops and residues and biological wastes. The energy

derived from the biomass generally helps reducing the carbon dioxide emission from the atmosphere thereby reducing the global warming effect. Since the carbon dioxide acts as a green house gas and increases the temperature of the atmosphere.

2. BIOMASS CONVERSION PROCESS

PYROLYSIS

Pyrolysis is the thermal decomposition of biomass at modest temperatures in absence of oxygen. The steps in pyrolysis includes: feedstock preparation and introduction of the feed into the reactor, carrying out the reaction by absorption of heat or other addition of agents such as air, oxygen, steam, hydrogen, post combustion or processing of the gases produced during the reaction step, and proper guidance of the resulting liquids, char, and ash .Pyrolysis product basically consists of gases like CH₄, CO₂ ,and NH₃ and liquids like ethanol, bio-oils, acetone, acetic acid etc. and solid as char .The relative proportion of the output depends upon the process and process condition, characteristics of biomass, optimum temperature and residence time of material. In this process the biomass is heated to a temperature range with low residence time and rapidly cooled to collect the condensed liquid which is otherwise known as bio-oil.

Longer residence times and High temperatures increase biomass conversion to gas, and short vapor residence time and moderate temperatures are optimum for producing liquids. The most important features for pyrolysis to occur to give proper bio oil yield are:

1. A Temperature of around (400-500C) in order to produce bio oil in maximum.
2. Finely ground biomass with about less than 3mm size with high heating rates.
3. Vapor residence times of about less than 2 sec to lessen the secondary reactions to occur.
4. The remaining bio-char must be removed so as to prevent the secondary cracking reactions.

5. The vapors are rapidly cooled to produce the bio oil as the intermediate product.

3. LITERATURE REVIEW

A. Lucia et al (1). The advancement in thermo chemical process use for bio fuel production has gained a lot of importance for the production of clean and efficient energy substitute. The choice of process depends upon the type of desirable product; Fast pyrolysis leads to high yield of bio-oil whereas the slow and vacuum pyrolysis process gives a good choice for production of bio-char and bio-oil furnishing high yields and simultaneously superior quality of bio-char A.V Bridgewater et al (2). It is recognized that biomass exceeds many other renewable energy sources because it is plentifully available, high energy values and it is versatile, and sugarcane bagasse is the most abundant crop waste found in the world J.M Encinar et al (3) .Biomass pyrolysis products are the complex combination of the products from individual pyrolysis of cellulose, hemicelluloses and extractives each having its own kinetic characteristics. In addition to that the secondary products come from the cross reactions of primary pyrolysis products between pyrolysis products and the original feedstock molecules, Pyrolysis of each constituent is itself a complex process which is dependent on many factors Dinesh Mohan et al (4) .The pyrolysis characteristics of sugarcane bagasse hemicellulose were found out using a tubular furnace, the pyrolysis experiment was conducted at various elevated temperatures starting from 550,600,650,700,750,800,850 & 900 0C in a homemade tubular furnace. The main objective of the project was to investigate the effect of temperature on the various product yields and to characterize the products with various analytical techniques. The liquid products were analyzed by GCMS and it was found that the main gas products were (CO, CO₂, CH₄& H₂) respectively Peng et al (5) .The biomass pyrolysis was carried out using Thermo gravimetric analyzer and packed- bed pyrolyser. It inferred that there were no detectable interactions among the

components during pyrolysis in either of the above two process on the other hand the ash present in the biomass had a strong influence on both pyrolysis characteristics and the product distribution.

4. MATERIALS AND METHODS

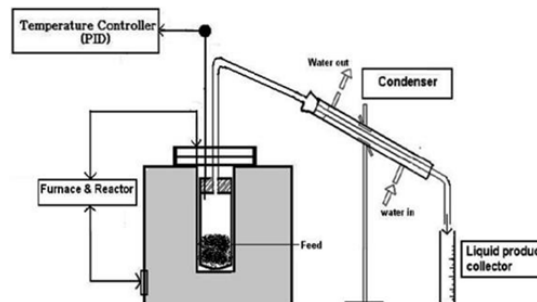
COLLECTION OF RAWMATERIAL:

The precursor is collected from the nearest sugar industry namely (SHAKTI SUGAR INDUSTRIES) as they are used for power generation inside the sugar mill. The raw material is in the form of fibres.



PYROLYSIS PROCEDURE:

Pyrolysis of the biomass is carried out with a system which comprises of a reactor, a furnace and a condenser that is being used to condense the gas and thereby collect the bio-oil. It is carried out using a reactor which is made up of stainless steel (SS 316) material having diameter of about 4.5cm and a elevation of 18.5cm. The reactor is the one inside which the precursor is being filled and certainly inserted vertically inside the furnace. Once the reaction is started the precursor is pyrolysed and the moisture is eliminated with next volatiles and thereby remaining with ash (bio-char). The bio-oil is collected in the measuring flask which lies below the condenser. There also lies a temperature controller inside the furnace which is PID controller. The furnace has a maximum temperature reach ability of 1200C.



CHARACTERIZATION OF THEMATERIAL

PROXIMATEANALYSIS:

It is done in order to calculate the moisture content, ash content, volatile matter content and the fixed carbon content of the biomass sample. The experiment was conducted by ASTM D3173-75. The fixed carbon is calculated by difference, after the calculation of moisture content, volatile content and ash content. It is the quantitative analysis which separates all the above 3 components from any material. The ash content of the material doesn't contribute to the calorific value of the fuel. The proximate analysis was done for the bio-mass as well as bio-charsamples.

PROXIMATEANALYSIS:

It is done in order to calculate the moisture content, ash content, volatile matter content and the fixed carbon content of the biomass sample. The experiment was conducted by ASTM D3173-75. The fixed carbon is calculated by difference, after the calculation of moisture content, volatile content and ash content. It is the quantitative analysis which separates all the above 3 components from any material. The ash content of the material doesn't contribute to the calorific value of the fuel. The proximate analysis was done for the bio-mass as well as bio-charsamples.

5. RESULTS AND DISCUSSION**PROXIMATE AND ULTIMATE ANALYSIS
OF BIOMASS**

PROXIMATE ANALYSIS	
Content	Weight percentage (%)
MOISTURE CONTENT	1.94
VOLATILE MATTER	71.48
FIXED CARBON	15.57
ASH CONTENT	11.01
ULTIMATE ANALYSIS	
Elements	Weight percentage (%)
CARBON	56.160
HYDROGEN	3.512
NITROGEN	6.213
SULPHUR	2.380
OXYGEN	31.73
H/C	0.750
O/C	0.560
OIL CONTENT (%)	53.3
GROSS CALORIFIC VALUE	2754.32
ELEMENTAL FORMULA	CH _{0.75} N _{0.0946} S _{0.015} O _{0.560}

The proximate analysis and ultimate analysis gave their result with highest volatile matter in the biomass of about 71.48% and the lowest moisture of 1.94 whereas the ultimate analysis showed

the highest presence of carbon of about 56.16 %. The elemental formula of the biomass is also predicted above

THERMO GRAVITRIC ANALYSIS (TGA):

The TGA curve of the biomass gave the decomposition stages of the biomass and the temperature between which the thermal pyrolysis would be done so as to get the optimum temperature. It is conducted at gas flow rate of 35 ml/min and the amount of sample taken during TGA analysis was 2.926gm and within a temperature range of (0- 600)0 C. The decomposition occurs in 3 stages the first stage shows the removal of moisture from the bio-mass , the 2nd stage gives the removal of volatile matter present in the biomass sample and in the 3rd stage the total combustion of the material takes place with the weight loss from the material giving rise to decomposition of the hydrocarbons . From the 3 stage process the rapid decomposition occurs during the volatiles are eliminated and so the stage is considered to be important for pyrolysis. The pyrolysis is performed according to the information from TGA between 300-500 0C.

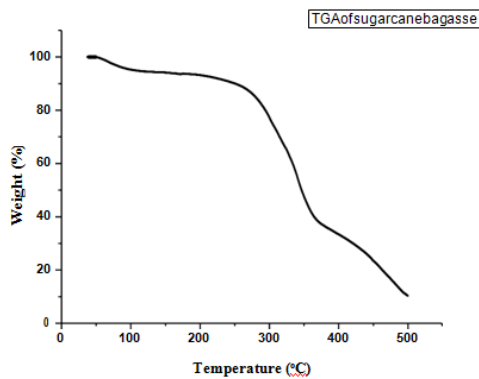


Fig.TGA of Sugarcane Bagasse

EXPERIMENTAL RESULTS

Table. Experimental result of Sugar Bagassepyrolysis

CHARACTERISTICS	SUGARCANE BAGASSE								
	300	325	350	375	400	425	450	475	500
TEMPERATURE (°C)	300	325	350	375	400	425	450	475	500
LIQUID PRODUCT (%)	20.32	25.66	44.46	45.46	46.21	50.66	53.30	51.13	41.33
BIO-CHAR (%)	49.54	46.73	40.8	34.7	33.05	31.90	29.78	25.0	20.12
VOLATILES (%)	30.14	27.61	22.74	19.84	18.62	17.44	16.92	23.87	38.55
REACTION TIME(MIN)	48	45	38	32	29	25	22	20	17

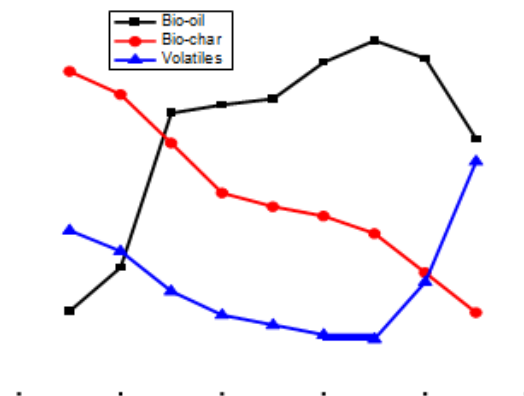


Table: proximate analysis results at various prolytic temperatures

Temperature	Volatile matter	Ash content	Fixed carbon
300	61.52	7.46	31.02
350	53.23	10.43	36.34
400	46.48	13.25	40.27
450	36.60	18.82	44.58
500	30.36	20.12	49.52

Table: Ultimate analysis results at various prolytic temperatures

Sample name	N%	C%	H%	S%	O%	H/C (MOLAR RATIO)	GCV
300	3.21	54.12	2.82	1.74	39.85	0.625	15.98
350	3.78	57.88	3.01	1.08	34.52	0.624	18.37
400	4.45	58.74	2.77	1.24	32.80	0.566	18.60
450	3.66	58.21	2.24	1.60	34.29	0.461	17.43
500	2.86	56.31	2.55	1.41	36.87	0.543	16.81

Conclusion

Since the demand for energy is growing more and more the dependency on fossil fuel need to be reduced since they will get totally exhausted, the need for more and more efficient used of biomass by converting it to an efficient and clean source of energy, therefore the biomass conversion is done by pyrolysis technique to find efficient utilization of biomass to produce the energy in form of solid, liquid & gaseous fuels.

In this present work the pyrolysis of the sugarcane bagasse is conducted at various temperatures starting from 300C- 500C at 150 C rate of heating in the reactor thereby giving an yield of 53.3% which was found to be optimum at the temperature of 450C . On contrary the bio-char yield showed a decreasing trend and the volatiles in a similar manner showed increasing trend upto optimum temperature i.e, 450C, giving an yield of 53.3% bio- oil at 450C thereafter showing a decreasing trend.

The components present in the bio-oil sample were found suitable for its use as bio-fuel in turbines and

other applications. Whereas on the other hand the bio-char produced by the pyrolysis of bio-char also has its applications as found by characterization of the bio-char like the nutrients present in it may help as a precursor in the soil amendment purpose. The weight loss from the TGA studies of the bio-char gave that the weight loss found was 35%. The surface area values of the bio-chars would suitably find its application in soil amendment purpose. The anion chromatography results also inferred various plant required nutrients which might find its applications. The proximate and ultimate analysis of the bio-chars produced at various pyrolytic temperatures revealed that the carbon content were upto the mark which can be used as a fuel , since the carbon composition in the bio-fuel plays a vital role. The FTIR analysis results showed negative functional groups on the surface of the bio- char like carboxyl groups and phenolic groups. Therefore with such tests conducted for the bio-oil and the bio-char were all found feasible for its application as bio-fuel as well as its application as bio-char and various other applications depending upon the properties of the sample, therefore the use of the bio-fuel in refinery was found feasible from properties study.

FUTUREWORK:

1. Engine performance of thebio-oil.
2. Soil amendment studies of the bio-char.
3. Bio-char applications as fuel & other applications.
4. Study of adsorption properties of the bio-char.
5. Study the distillation range of thebio-oil.

BIBLIOGRAPHY:

1. Lucian A. Lucia, "Lignocellulosic biomass: A potential feedstock to replace petroleum", Bio Resources 2008, (4),981-982.
2. A.V Bridgewater, Chemical Engineering Journal, 2003 (91)87-102.
3. J.M Encinar, F.J Belatran, A. Bernalte, A. Ramrio, J.F Gonzalez, "Biomass and bio energy" 1995 (11)397.

4.Dinesh Mohan, Charles. U.Pittman, Jr., Phillip. Steele, "Pyrolysis of Wood/ Biomass: A critical Review", 2006, (3) 848-889

5.Yunyunpeng&Shubin Wu, "Fast pyrolysis characteristics of sugarcane bagasse hemicelluloses", Cellulose Chem.Technol., 2011 (45) 605-612.

6.K.Raveendran, AnuraddaGanesh, Kartic .C. Khilar, "Pyrolysis characteristics of biomass and biomass components" 1996, (75),987.

7.M.Gracia- Perez, A. Challa, J. Yang, C.Roy "Co-pyrolysis of sugarcane bagasse with petroleum residue .Part 1: Thermo gravimetric analysis" , Fuel, 2001,(80), 1245-1258.

8.MohammadRofiqul Islam, MomtazParveen, Hiroyuki Haniu "Properties of sugarcane waste derived bio-oil obtained by fixed- bed, fire-tube heating pyrolysis",2010, (101), 4162- 4168 .

9.SurinderKatayal, Kelly Thambimuthu, Marjorie Valix, "Carbonization of bagasse in a fixed bed reactor: Influence of process variables on char yield and characteristics", 2003, (28),713-725.

10.W.T.Tsai, M.K Lee, Y.M Chang, "Fast pyrolysis of rice straw, sugarcane bagasse& coconut shell in induction heating reactor", 2006 (76),230-237.

11.J.Zandersons, J.Gravitis, A. Kokorevics, A.Zhurinsh, O.Bikovens, A.Tradenaka, B.Spince, "Studies of Brazilian sugarcane bagasse carbonisation process & product properties, 1999, (17),209-219.

MODELING AND CFD ANALYSIS OF CONICAL EXHAUST DIFFUSER

Narishetty surender¹

P.Raju²

¹M.Tech (Thermal Engineering)Department of mechanical engineering vaagdevi college of engineering (ugc autonomous) approved by aicte & permanent affiliation to jntuh, hyderabad.p.o, bollikunta, Warangal urban- 506005.

²Assistant Professor Department of mechanical engineering vaagdevi college of engineering (ugc autonomous) approved by aicte & permanent affiliation to jntuh, hyderabad.p.o, bollikunta, Warangal urban- 506005.

Abstract

The exhaust diffuser of a fluid machine, such as a gas turbine, recovers static pressure by decelerating the flow and converting kinetic energy into pressure energy. As a result, it is a vital component in the environment of a turbomachine and plays a critical role in determining the performance of a turbomachine. As a consequence, the fluid machine's efficiency can be enhanced if the diffuser design is optimized for optimal pressure recovery. Computational fluid dynamics (CFD) study was done on diffusers with various half cone angles, and the shape that provided the maximum pressure recovery was chosen based on the results. The diffuser was then built and tested with the ideal shape. CFD analysis to determine pressure drop, velocity, heat transfer coefficient, mass flow rate, and heat transfer rate for various conical exhaust diffusers (rectangular, circular, and hexagonal), conical exhaust diffuser models modeling using CREO parametric software, and analysis in ANSYS software for different conical exhaust diffusers (rectangular, circular, and hexagonal). CFD and thermal study of conical exhaust diffusers using ANSYS analysis modules

Keywords: CFD, shapes, thermal analysis, pressure drop and ANSYS.

1. INTRODUCTION

A blown diffuser is a device that uses exhaust gases to interact with the diffuser airflow. "A device for decreasing the velocity of a fluid traveling through a system while increasing the static pressure," according to the definition of a diffuser. Diffusers are used to slow the flow of a fluid while increasing the static pressure. Pressing factor recuperation alludes to the ascent in the liquid's static pressing factor as it moves through a pipe. A spout, then again, is intended to build release speed and lower pressure while coordinating the stream a specific way. Frictional impacts can be huge during investigation, yet they are often disregarded. Bernoulli's guideline may typically be utilized to look at conduits holding low-speed liquids. Compressible stream relations are commonly used to examine conduits streaming at higher speeds with mach esteems more noteworthy than 0.3.

Supersonic Diffusers: A supersonic diffuser is a duct that shrinks in size as it moves in the flow direction. Fluid temperature, pressure, and density rise as the duct gets smaller, while velocity falls. These changes in pressure, velocity, density, and temperature are caused by compressible flow. In a supersonic diffuser, shock waves may also play a crucial function.. Diffusers come in a variety of shapes, including circular, rectangular, and linear slot diffusers (LSDs, for example). Linear slot diffusers are made up of one or more long, narrow slots that are usually partially hidden in a fixed or suspended ceiling. [1] Diffusers are occasionally employed in the other direction, as air inlets or returns. This is especially true for 'perf' and linear slot diffusers. Grilles are most typically utilised as return or exhaust air inlets. A gas turbine engine's divergent exhaust diffuser is a critical component. It essentially lowers the fluid velocity that exits the low-pressure turbine stage and raises the static pressure.

2. LITERATURE REVIEW

Singh et al. [2] directed a CFD examination of an annular exhaust diffuser with different shapes while keeping up with the gulf half cone point steady. At long last, they guaranteed that the exhibition of an annular exhaust diffuser with an equal wandering center and packaging outflanked twirl.

The pressing factor recuperation of an exhaust diffuser can be upgraded by raising the channel disturbance force, as per Hoffman [3].

The disturbance force of an exhaust diffuser can be changed to further develop the diffuser's pressing factor recuperation. This paper proposed a test research on the construction of disturbance in a cone shaped exhaust

diffuser by P A C Okwuobi [4]. They found that close to the edge of the divider layer, which stretches out to the mark of maximal change, the tempestuous energy rate arrives at a most extreme worth. The greatness of energy convective dissemination because of pressing factor and active impacts is equivalent to that of energy creation, as indicated by the fierce motor energy balance.

The fumes diffuser of a liquid machine, like a gas turbine, recuperates static pressing factor by decelerating the stream and transforming motor energy into pressure energy, as indicated by R. Prakash [5]. Accordingly, it is a fundamental segment in a turbomachine climate and has a significant impact in choosing a turbomachine's exhibition. Therefore, if the diffuser plan is upgraded for ideal pressing factor recuperation, the liquid machine's proficiency can be expanded.

The subsonic stream study is done in diffuser blenders with and without swaggers, as indicated by Parameshwar Banakar [6]. For the two situations, all out pressure misfortune, pressure acquire, and significant stream boundaries like Mach number, speed, statics pressing factor, and twirl are analyzed. The investigation was done utilizing a 45-degree area model of the diffuser blender without swaggers and with swaggers, considering the math's periodicity.

In his examination, Venugopal M [7] tended to what the presentation of the fumes turbine diffuser means for the force and effectiveness of gas turbines. We should address the course through unsound contact with the turbine's high and low pressing factor rotational stages, which cause twirl stream, to foster a high-proficiency diffuser gas turbine. A survey of the writing uncovers that there is opportunity for development as far as turbine execution.. Since the diffuser is the focal point of the framework, it should manage variable levels of twirl. Twirl stream in the diffuser segment will cause issues like as pressing factor misfortune while streaming across swaggers and a lessening in momentary stream. The higher the Reynolds number, the more fierce the stream becomes, which is unfortunate. Reynolds' digit. At the point when mathematical discoveries are contrasted with exploratory outcomes, unmistakably the aftereffects of single-stage investigation are very near the trial results.

3. MODELING AND ANALYSIS

CREO is 3-D demonstrating PC programming utilized in mechanical designing, plan, assembling, and CAD drawing administration associations. It was recently known as expert/ENGINEER. It was one of the soonest three-dimensional CAD displaying applications that utilization a standard based parametric framework. It might streamline the development item just as the actual plan by utilizing boundaries, measurements, and abilities to catch the item's practices. In 2010, the choice to change from genius/ENGINEER Wildfire to CREO was made. It became made accessible via the organization that made it, Parametric Science Corporation (PTC), sooner or later during the dispatch of its set-up of plan items, which incorporates applications like get together displaying, second orthographic perspectives for specialized drawings, limited detail examination, and others. As a result of its nitty gritty abilities, which contains the mix of parametric and direct displaying in a solitary stage, P.C.CREO claims it will give a more noteworthy powerful format information than exceptional demonstrating programme. The whole scope of capacities covers the whole range of item advancement, giving originators alternatives at each phase of the interaction. The application programming likewise offers a superior client decent interface, which gives creators a superior encounter. It likewise includes cooperation capacities that simplify it to share and adjust plans.

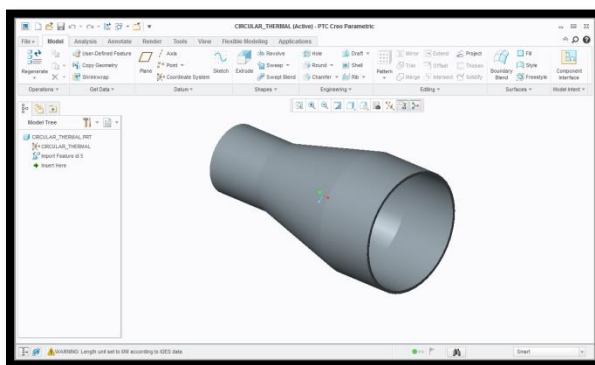


Fig1: circular type

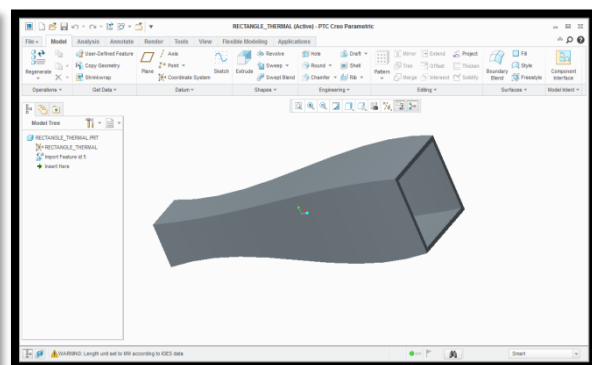


Fig: 2 rectangular type

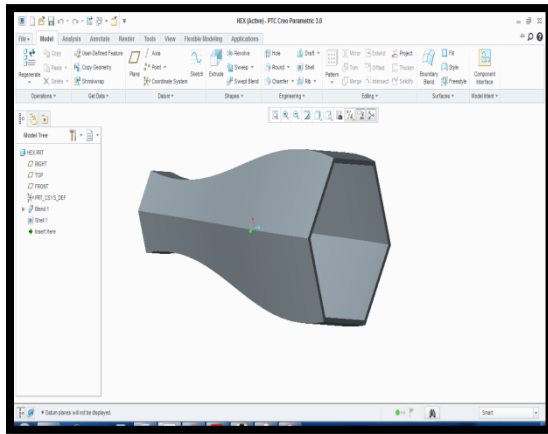


Fig 3: hexagonal type

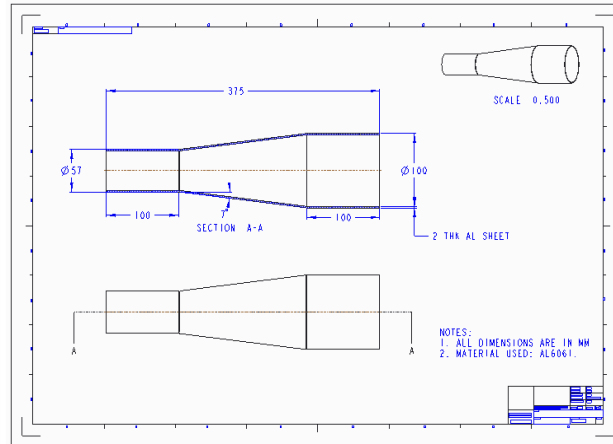


Fig: 4 2d drawing

3.1 CFD

Computational Fluid dynamics (CFD) is a part of liquid mechanics that settles and examinations issues including liquid streams utilizing mathematical strategies and calculations. The calculations important to display the communication of fluids and gases with surfaces characterized by limit conditions are performed on PCs. Better arrangements are conceivable with high velocity supercomputers. Momentum research is yielding programming that builds the exactness and speed of troublesome recreation situations like transonic or fierce streams. The underlying exploratory approval of such programming is completed in an air stream, with full-scale testing, for example, flight tests, giving a definitive approval.

3.2 METHODOLOGY

In ANSYS ICEM CFD, the math is worked for each model dependent on the given information, and a space is framed to incorporate the stream inside the area to the body's dividers. To examine space freedom, three tube shaped areas are assessed utilizing an experimentation strategy that includes estimating distances between the model's nose and last parts and computing the span from the model's hub.

3.3 BOUNDARY CONDITIONS

Coming up next are the applicable limit conditions for registering the dissimilar exhaust diffuser:

Delta: The gulf boundary is bay speed, with a worth of 45m/s at the channel of a conelike exhaust diffuser.

The boundary pressure-outlet is characterized in the power source area, and the worth is set to 101325. Pascal.

The fixed divider with no slip condition is characterized as the divider. The unpleasantness tallness and harshness constants are additionally set to 0, suggesting a smooth surface.

The sort for the Inlet zone would be speed delta. A speed of 45 m/s and a temperature of 1773 K are the Velocity channel limit conditions. Fixed divider conditions are utilized for the line. The sort for the Outlet zone would be pressure outlet. Standard temperature and working pressing factor states of 101325 Pa are utilized to decide the pressing factor outlet limit conditions.

4. RESULTS AND DISCUSSIONS

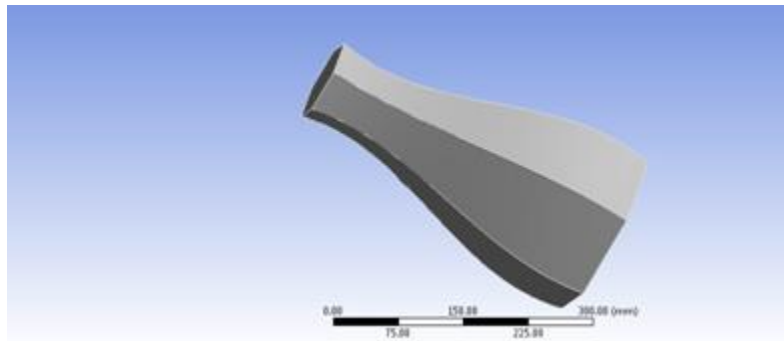


Fig : 5 imported model

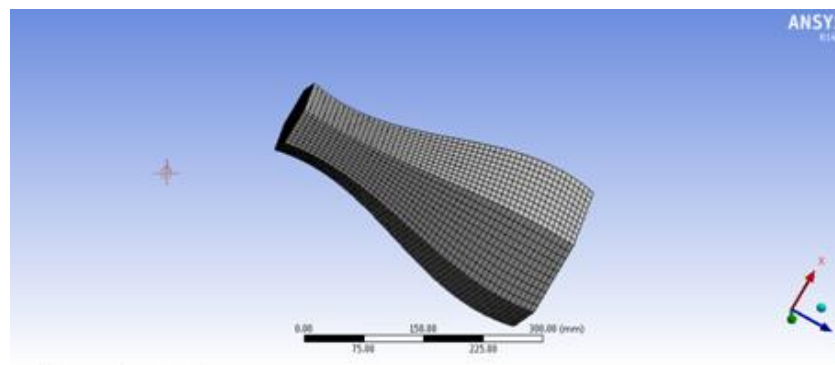


Fig :6 meshed model

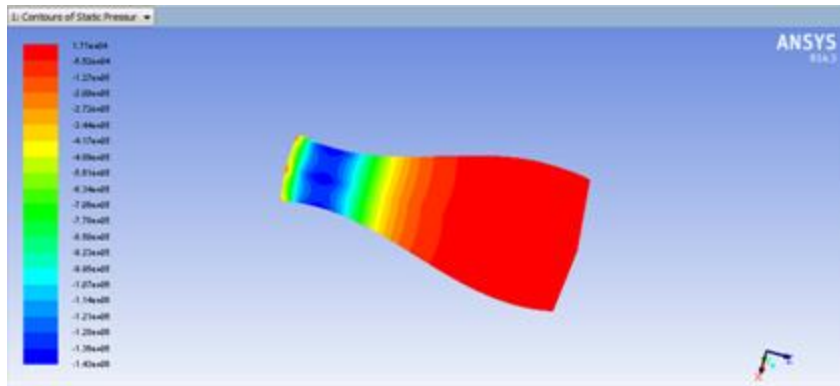


Fig: 7 pressure drop

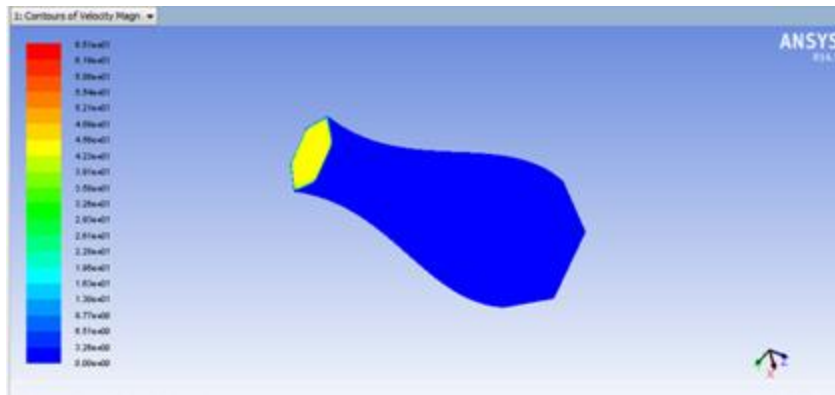


Fig: 8 velocity counter

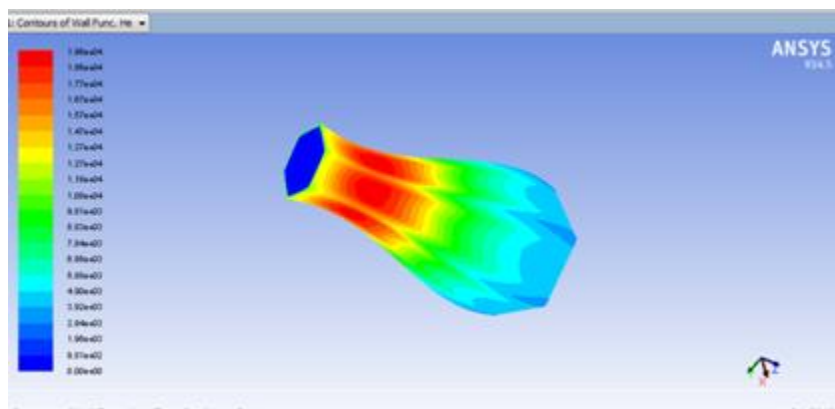


Fig: 9 Heat transfer coefficient

Mass Flow Rate (kg/s)		Total Heat Transfer Rate (w)	
inlet	242.59555	inlet	7.3347258e+08
interior-____msbr	-13345.577	outlet	-7.3450573e+08
outlet	-242.93652	wall-____msbr	0
wall-____msbr	0	Net	-1033152
Net	-0.3409729		

4.1 THERMAL ANALYSIS OF CONICAL EXHAUST DIFFUSER

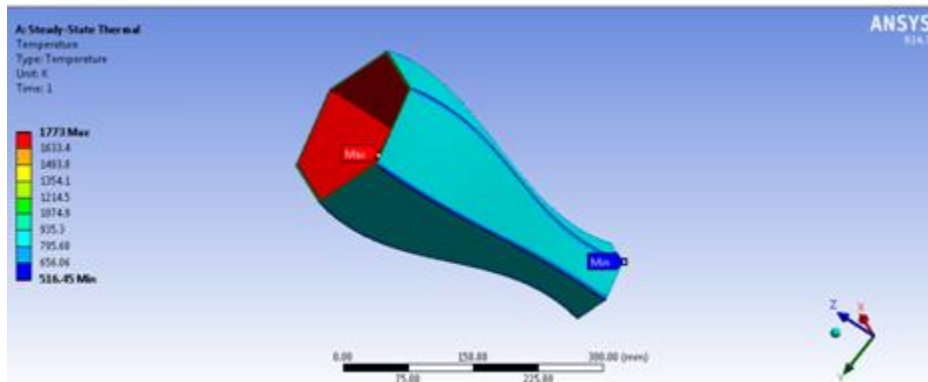


Fig: 10 temperature distribution

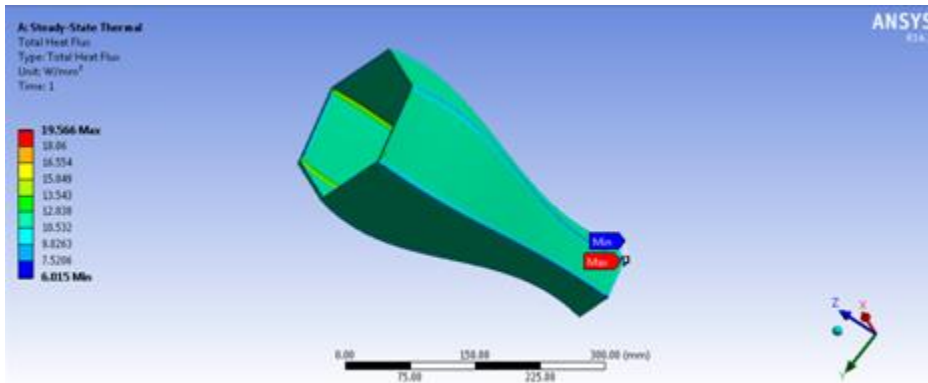


Fig 11: heat flux

5 Result tables

5.1 CFD analysis results table

Conical exhaust diffuser models	Pressure (Pa)	Velocity(m/s)	Heat transfer coefficient (w/m ² -k)	Mass flow rate (kg/s)	Heat transfer rate (W)
Circular	1.70e+04	4.66e+01	1.52e+04	0.1629	490752
Rectangular	2.24e+04	5.74e+01	1.74e+04	0.10063	304288
hexagonal	1.71e+04	6.51e+01	1.96e+04	0.3409	1033152

5.2 Thermal analysis result table

Models	Materials	Temperature (K)		Heat flux(w/mm ²)
		Max.	Min.	
Circular	Steel	1773	888.41	11.878
	copper	1773	1509.8	23.187
Rectangular	Steel	1773	426.4	20.563
	copper	1773	1166.6	52.772
Hexagonal	Steel	1773	516.45	19.566
	copper	773	1260.4	47.894

6. CONCLUSION

Considering the results of the analysis on various exhaust diffusers, the following conclusions can be drawn. CREO Parametric 3.0 modelling software was used for the modelling. In ANSYS workbench, the thermal analysis is carried out. Using FLUENT's post processing interface, the resulting solutions were then transformed to plots and contours. Different shapes of diffusers were computationally analysed, and their co-efficients of pressure recovery were computed using the results. Due to the conversion of kinetic energy into pressure energy, the velocity plots and contours show an exact opposite trend. Also, due to friction effects at the boundary layer, the centerline velocity is higher than the velocity at the boundary. Pressure, velocity, heat transfer coefficient, mass flow rate, and heat transfer rate were shown to improve turbine efficiency and performance when utilising this type of diffuser. The heat transfer coefficient and heat transfer rate values for hexagonal type conical exhaust diffusers are higher based on the CFD analysis results. The heat flux value is highest at copper material, according to the thermal analysis. As a result, the copper material is a preferable choice for a conical exhaust diffuser.

REFERENCES

- [1] R. Prakash, D. Christopher, K. Kumarrathinam, "CFD Analysis of flow through a tapered fumes diffuser", International Journal of Research in Engineering and Technology, Volume 3, Issue 11, NCAMESHE-2014.
- [2] Parameshwar Banakar, Dr. Basawaraj, "Computational Analysis of stream in max engine propulsion diffuser blender having various states of swaggers", International Journal of Engineering Research, Vol. 3, Issue 6, 2015.
- [3] Venugopal M, Somashekar V, "Plan and Analysis of Annular Exhaust Diffuser for Jet Engines", International Journal of Innovative Research in Science, Engineering and Technology, Vol. 4, Issue 7, July 2015.

- [4] Nikhil D. Deshpande, Suyash S. Vidwans, Pratik R. Mahale, Rutuja S. Joshi, K. R. Jagtap, "Hypothetical and CFD Analysis Of De Laval Nozzle", International Journal of Mechanical And Production Engineering, ISSN: 2320-2092, Volume-2, Issue-4, April-2014.
- [5] Ali Asgar S. Khokhar, Suhas S. Shirolkar, "Plan And Analysis Of Undertray Diffuser For A Formula Style Race vehicle", International Journal of Research in Engineering and Technology, Volume: 04 Issue: 11 | Nov-2015
- [6] Manoj Kumar Gopaliya, Piyush Jain, Sumit Kumar, Vibha Yadav, Sumit Singh, "Execution Improvement of S-molded Diffuser Using Momentum Imparting Technique", IOSR Journal of Mechanical and Civil Engineering, Volume 11, Issue 3 Ver. I (May-Jun. 2014), PP 23-31.
- [7] Masafumi Nakagawa, Atsushi Harada, "Investigation of Expansion Waves Appearing in the Outlets of Two-Phase Flow Nozzles", International Refrigeration and Air Conditioning Conference at Purdue, July 14-17, 2008.
- [8] K.M. Pandey, Member IACSIT and A.P. Singh, "CFD Analysis of Conical Nozzle for Mach 3 at Various Angles of Divergence with Fluent Software", IJCEA, Vol.1, No.2, August 2010.
- [9] Vinod kumar S Hiremath, S. Ganesan, R. Suresh, "Plan And Analysis Of Exhaust Diffuser Of Gas Turbine Afterburner Using CFD", Proceedings of 27th IRF International Conference, 26th June, 2016.
- [10] Santhosh Kumar Gugulothu and Shalini Manchikatla, "Exploratory and Performance Analysis of Single Nozzle Jet Pump with Various Mixing Tubes", International Journal of Recent advances in Mechanical Engineering (IJMECH) Vol.3, No.4, November 2014.